

JAERI - M  
85-151

ROSA-III 50% BREAK INTEGRAL TEST RUN 928  
(BREAK CONFIGURATION SENSITIVITY TEST)

October 1985

Taisuke YONOMOTO, Kanji TASAKA, Yasuo KOIZUMI  
Yoshinari ANODA, Hiroshige KUMAMARU  
Hideo NAKAMURA, Mitsuhiro SUZUKI and Hideo MURATA

日本原子力研究所  
Japan Atomic Energy Research Institute

JAERI-Mレポートは、日本原子力研究所が不定期に公刊している研究報告書です。  
入手の間合わせは、日本原子力研究所技術情報部情報資料課（〒319-11茨城県那珂郡東海村）あて、お申しこしてください。なお、このほかに財団法人原子力弘済会資料センター（〒319-11茨城県那珂郡東海村日本原子力研究所内）で複写による実費頒布をおこなっております。

JAERI-M reports are issued irregularly.

Inquiries about availability of the reports should be addressed to Information Division  
Department of Technical Information, Japan Atomic Energy Research Institute, Tokai-  
mura, Naka-gun, Ibaraki-ken 319-11, Japan.

©Japan Atomic Energy Research Institute, 1985

編集兼発行 日本原子力研究所  
印 刷 柳高野高速印刷

ROSA-III 50% BREAK INTEGRAL TEST RUN 928  
(BREAK CONFIGURATION SENSITIVITY TEST)

Taisuke YONOMOTO, Kanji TASAKA, Yasuo KOIZUMI  
Yoshinari ANODA, Hiroshige KUMAMARU, Hideo NAKAMURA  
Mitsuhiro SUZUKI and Hideo MURATA

Department of Reactor Safety Research,  
Tokai Research Establishment, JAERI

( Received September 10, 1985 )

This report presents the experimental data of RUN 928 conducted at the ROSA-III test facility. The facility is a volumetrically scaled (1/424) simulator for a BWR/6 with the electrically heated core, the break simulator and the scaled ECCS(emergency core cooling system). RUN 928 was a 50% split break test at the recirculation pump suction line with an assumption of HPCS diegel generator failure and conducted as one of the break configuration sensitivity tests. A long throat nozzle was used for a break plane. A peak cladding temperature (PCT) of 888 K was reached at 198 s after a break during the reflooding phase. Whole core was completely quenched by ECCS, and the effectiveness of ECCS was confirmed.

The primary test results of RUN 928 are compared in this report with those of RUN 916, which was a 50 % split break test with an orifice as the break plane. The initiation of core dryout in RUN 928 was slightly later than that in RUN 916 because of the smaller subcooled break flow rate. Duration of core dryout was, however, almost the same between the two tests. PCT in RUN 928 was 29 K lower than that in RUN 916.

Keywords: BWR, LOCA, Break Configuration, Nozzle, Orifice, ROSA-III,  
50% break, HPCS Failure, Break Area, Data Report, Effectiveness

ROSA-III 50%破断総合実験 RUN 928  
(破断形状感度実験)

日本原子力研究所東海研究所原子炉安全工学部

与能本泰介・田坂 完二・小泉 安郎

安濃田良成・熊丸 博滋・中村 秀夫

鈴木 光弘・村田 秀男

(1985年9月10日受理)

本報は、ROSA-III装置を用いて行われたRUN928の実験結果について記述したものである。本装置は、電気加熱ヒーター、破断模擬部及び緊急炉心冷却系(ECCS)を有する体積比(1/424)のBWR/6型原子炉模擬装置である。RUN928は、HPCSディーゼル発電機の故障を仮定した再循環ポンプ入口側配管における50%破断実験であり、破断口形状感度実験の一つとして行われた。のど部の長いノズルが破断口として用いられた。888Kの被覆管表面最高温度(PCT)が、破断後198秒の再冠水期に記録された。全炉心は、ECCSにより完全にクエンチされ、ECCSの有効性が確認された。

また、本報では、RUN928の実験結果と破断口としてオリフィスを用いた50%スプリット破断実験であるRUN916の実験結果とを比較している。RUN928の場合炉心の露出開始は、サブクール水の破断流量が少ないためRUN916の場合より少し遅くなった。しかしながら、炉心の炉出期間は、両実験においてほぼ同じであった。RUN928のPCTは、RUN916より29K低かった。

## Contents

Abbreviations .....	(15)
1. Introduction .....	1
2. ROSA-III Test Facility .....	2
3. Instrumentation .....	12
4. Test Conditions and Procedure .....	41
5. Data Processing .....	50
6. Test Results and Comparison with those of RUN 916 .....	208
7. Conclusions .....	215
Acknowledgments .....	216
References .....	216
Figures and Tables .....	(4)

## 目 次

略号 .....	(15)
1. 序 .....	1
2. ROSA-III 実験装置 .....	2
3. 計装 .....	12
4. 実験条件および手順 .....	41
5. 実験データ処理 .....	50
6. 実験結果およびRUN 916との比較 .....	208
7. 結論 .....	215
謝辞 .....	216
文献 .....	216
図表 .....	(4)

## List of Tables

- Table 2.1 Primary Characteristics of ROSA-III and BWR/6  
 Table 3.1 ROSA-III Instrumentation Summary List in RUN 928  
 Table 3.2 Measurement List for RUN 928  
 Table 3.3 Core Instrumentation Map  
 Table 4.1 Test Conditions of RUN 928  
 Table 4.2 Characteristics of Steam Discharge Line Valves  
 Table 4.3 Control Sequence for Steam Discharge Line Valves in RUN 928
- Table 5.1 Sequence of Events in RUN 928  
 Table 5.2 Maximum Cladding Temperatures Distribution in the Core
- Table 6.1 Comparison of initial conditions and major events in  
 RUN 928 and RUN 916

## List of Figures

- Fig. 2.1 Schematic diagram of ROSA-III test facility  
 Fig. 2.2 Internal structure of pressure vessel of ROSA-III  
 Fig. 2.3 ROSA-III piping schematic  
 Fig. 2.4 Pressure vessel internals arrangement  
 Fig. 2.5 Simulated fuel rod of ROSA-III  
 Fig. 2.6 Axial power distribution of heater rod  
 Fig. 2.7 Radial power distribution of core  
 Fig. 2.8 Piping layout of recirculation loops and jet pumps  
 Fig. 3.1 Instrumentation location of ROSA-III test facility  
 Fig. 3.2 Instrumentation location in pressure vessel  
 Fig. 3.3 Upper plenum instrumentation  
 Fig. 3.4 Lower plenum instrumentation  
 Fig. 3.5 Core instrumentation (cf. Table 3.3)  
 Fig. 3.6 Upper tieplate instrumentations  
 Fig. 3.7 Beam directions of three-beam gamma densitometer  
 Fig. 3.8 Beam directions of two-beam gamma densitometer  
 Fig. 3.9 Arrangement and location of drag disks

- Fig. 3.10 Location of two-phase flow measurement spool pieces
- Fig. 4.1 Break configuration details
- Fig. 4.2 Normalized power transient for ROSA-III test
- Fig. 4.3 Main steam line schematic
- Fig. 4.4 Feedwater line schematic
- Fig. 4.5 Feedwater line between valve av-112 and pressure vessel
- Fig. 5.1 Pressure in PV (pressure vessel)
- Fig. 5.2 Pressure in broken loop JP (jet pump)
- Fig. 5.3 Pressure near MRP (main recirculation pump)
- Fig. 5.4 Pressure at MRP side of break
- Fig. 5.5 Pressure at PV side of break
- Fig. 5.6 Pressure in MSL (main steam line)
- Fig. 5.7 Pressure in JP outlet spool
- Fig. 5.8 Differential pressure between lower plenum and upper plenum
- Fig. 5.9 Differential pressure between upper plenum and steam dome
- Fig. 5.10 DC (downcomer) head
- Fig. 5.11 Differential pressure between PV bottom and top
- Fig. 5.12 Differential pressure between JP-1,2 discharge and suction
- Fig. 5.13 Differential pressure between JP-1,2 drive and suction
- Fig. 5.14 Differential pressure between JP-3,4 discharge and suction
- Fig. 5.15 Differential pressure between JP-3,4 drive and suction
- Fig. 5.16 Differential pressure between MRP delivery and suction
- Fig. 5.17 Differential pressure between downcomer bottom and MRPI suction
- Fig. 5.18 Differential pressure between MRP delivery and JP-1,2 drive
- Fig. 5.19 Differential pressure between downcomer middle and JP-1,2 suction
- Fig. 5.20 Differential pressure between JP-1,2 discharge and lower plenum
- Fig. 5.21 Differential pressure between downcomer bottom and break B
- Fig. 5.22 Differential pressure between breaks A and B

- Fig. 5.23 Differential pressure between break A and MRP2 suction
- Fig. 5.24 Differential pressure between MRP delivery and JP-3,4 drive
- Fig. 5.25 Differential pressure between downcomer middle and JP-3,4 suction
- Fig. 5.26 Differential pressure between JP-3,4 discharge and confluence
- Fig. 5.27 Differential pressure between JP-3,4 confluence in broken loop and LP
- Fig. 5.28 Differential pressure between lower plenum and downcomer middle
- Fig. 5.29 Differential pressure between lower plenum and downcomer bottom
- Fig. 5.30 Differential pressure between downcomer bottom and downcomer middle
- Fig. 5.31 Differential pressure between downcomer middle and steam dome
- Fig. 5.32 Differential pressure between LP bottom and LP middle
- Fig. 5.33 Differential pressure across channel inlet orifice A
- Fig. 5.34 Differential pressure across channel inlet orifice B
- Fig. 5.35 Differential pressure across channel inlet orifice C
- Fig. 5.36 Differential pressure across channel inlet orifice D
- Fig. 5.37 Differential pressure across bypass hole
- Fig. 5.38 Liquid levels in ECCS tanks
- Fig. 5.39 Liquid levels in downcomer
- Fig. 5.40 Mass flow rate in MSL
- Fig. 5.41 ECC injection flow rate
- Fig. 5.42 Feedwater flow rate
- Fig. 5.43 JP-1,2 discharge flow rate (high range)
- Fig. 5.44 JP-3,4 discharge flow rate (high range)
- Fig. 5.45 JP-3,4 discharge flow rate (low range)
- Fig. 5.46 MRP discharge flow rate
- Fig. 5.47 Differential pressure across orifice flowmeter F-1
- Fig. 5.48 Differential pressure across orifice flowmeter F-2
- Fig. 5.49 Differential pressure across orifice flowmeter F-3
- Fig. 5.50 Differential pressure across venturi flowmeter F-17
- Fig. 5.51 Differential pressure across venturi flowmeter F-18



- Fig. 5.52 Differential pressure across orifice flowmeter F-19
- Fig. 5.53 Differential pressure across orifice flowmeter F-20
- Fig. 5.54 Differential pressure across orifice flowmeter F-21
- Fig. 5.55 Differential pressure across orifice flowmeter F-22
- Fig. 5.56 Differential pressure across venturi flowmeter F-27
- Fig. 5.57 Differential pressure across venturi flowmeter F-28
- Fig. 5.58 Electric core power
- Fig. 5.59 Valve operation signals
- Fig. 5.60 ECCS operation signals
- Fig. 5.61 MRP operation signals
- Fig. 5.62 Fluid density at JP-1,2 outlet, beam A
- Fig. 5.63 Fluid density at JP-1,2 outlet, beam B
- Fig. 5.64 Fluid density at JP-1,2 outlet, beam C
- Fig. 5.65 Fluid density at JP-3,4 outlet, beam A
- Fig. 5.66 Fluid density at JP-3,4 outlet, beam B
- Fig. 5.67 Fluid density at JP-3,4 outlet, beam C
- Fig. 5.68 Fluid density at MRP side of break, beam A
- Fig. 5.69 Fluid density at MRP side of break, beam B
- Fig. 5.70 Fluid density at PV side of break, beam A
- Fig. 5.71 Fluid density at PV side of break, beam B
- Fig. 5.72 Momentum flux at JP-1,2 outlet spool
- Fig. 5.73 Momentum flux at JP-3,4 outlet spool
- Fig. 5.74 Momentum flux at break A spool piece (low range)
- Fig. 5.75 Momentum flux at break A spool piece (high range)
- Fig. 5.76 Momentum flux at break B spool piece (high range)
- Fig. 5.77 Fluid temperatures in lower plenum and upper plenum
- Fig. 5.78 Fluid temperatures in steam dome and MSL
- Fig. 5.79 Fluid temperatures in downcomer
- Fig. 5.80 Fluid temperatures in intact recirculation loop
- Fig. 5.81 Fluid temperatures in broken recirculation loop
- Fig. 5.82 Fluid temperatures at JP-1,2 outlet
- Fig. 5.83 Fluid temperatures at JP-3,4 outlet
- Fig. 5.84 Fluid temperatures near breaks A and B
- Fig. 5.85 Feedwater temperature
- Fig. 5.86 Surface temperatures of fuel rod A11
- Fig. 5.87 Surface temperatures of fuel rod A12
- Fig. 5.88 Surface temperatures of fuel rod A13

- Fig. 5.89 Surface temperatures of fuel rod A14
- Fig. 5.90 Surface temperatures of fuel rod A22
- Fig. 5.91 Surface temperatures of fuel rod A24
- Fig. 5.92 Surface temperatures of fuel rod A33
- Fig. 5.93 Surface temperatures of fuel rod A34
- Fig. 5.94 Surface temperatures of fuel rod A44
- Fig. 5.95 Surface temperatures of fuel rod A77
- Fig. 5.96 Surface temperatures of fuel rod A85
- Fig. 5.97 Surface temperatures of fuel rod A87
- Fig. 5.98 Surface temperatures of fuel rod A88
- Fig. 5.99 Surface temperatures of fuel rod B11
- Fig. 5.100 Surface temperatures of fuel rod B22
- Fig. 5.101 Surface temperatures of fuel rod B77
- Fig. 5.102 Surface temperatures of fuel rod C11
- Fig. 5.103 Surface temperatures of fuel rod C13
- Fig. 5.104 Surface temperatures of fuel rod C22
- Fig. 5.105 Surface temperatures of fuel rod C33
- Fig. 5.106 Surface temperatures of fuel rod C77
- Fig. 5.107 Surface temperatures of fuel rod D22
- Fig. 5.108 Surface temperatures of water rod simulator A45
- Fig. 5.109 Surface temperatures of water rod simulator B45
- Fig. 5.110 Surface temperatures of water rod simulator C45
- Fig. 5.111 Surface temperatures of water rod simulator D45
- Fig. 5.112 Inner Surface temperatures of channel box A,  
location A1
- Fig. 5.113 Inner Surface temperatures of channel box A,  
location A2
- Fig. 5.114 Inner Surface temperatures of channel box B  
(position 1)
- Fig. 5.115 Inner Surface temperatures of channel box C
- Fig. 5.116 Inner Surface temperatures of channel box D
- Fig. 5.117 Outer surface temperatures of channel box A
- Fig. 5.118 Outer Surface temperatures of channel box C
- Fig. 5.119 Surface temperatures of fuel rod A15 at positions  
1 and 4
- Fig. 5.120 Surface temperatures of fuel rod A17 at positions  
1 and 4

- Fig. 5.121 Surface temperatures of fuel rod A26 at positions  
1 and 4
- Fig. 5.122 Surface temperatures of fuel rod A28 at positions  
1 and 4
- Fig. 5.123 Surface temperatures of fuel rod A31 at positions  
1 and 4
- Fig. 5.124 Surface temperatures of fuel rod A37 at positions  
1 and 4
- Fig. 5.125 Surface temperatures of fuel rod A42 at position  
1
- Fig. 5.126 Surface temperatures of fuel rod A48 at positions  
1 and 4
- Fig. 5.127 Surface temperatures of fuel rod A51 at positions  
1 and 4
- Fig. 5.128 Surface temperatures of fuel rod A53 at positions  
1 and 4
- Fig. 5.129 Surface temperatures of fuel rod A57 at positions  
1 and 4
- Fig. 5.130 Surface temperatures of fuel rod A62 at positions  
1 and 4
- Fig. 5.131 Surface temperature of fuel rod A66 at position 1
- Fig. 5.132 Surface temperatures of fuel rod A68 at positions  
1 and 4
- Fig. 5.133 Surface temperature of fuel rod A71 at position 1
- Fig. 5.134 Surface temperatures of fuel rod A73 at positions  
1 and 4
- Fig. 5.135 Surface temperatures of fuel rod A75 at positions  
1 and 4
- Fig. 5.136 Surface temperature of fuel rod A82 at position 1
- Fig. 5.137 Surface temperatures of fuel rod A84 at positions  
1 and 4
- Fig. 5.138 Surface temperatures of fuel rods B13,B31,B86 at  
position 4
- Fig. 5.139 Surface temperatures of fuel rods B33,B53,B66 at  
position 4
- Fig. 5.140 Surface temperatures of fuel rods B51,C15,D51,D77 at  
position 4

- Fig. 5.141 Surface temperatures of fuel rods C31,C68 at position 4
- Fig. 5.142 Surface temperatures of fuel rods C35,C66 at position 4
- Fig. 5.143 Surface temperatures of fuel rods D11,D13,D31,D86 at position 4
- Fig. 5.144 Surface temperatures of fuel rods D33,D53,D66 at position 4
- Fig. 5.145 Surface temperatures of fuel rods A11,A12,A13,A87,A88 at position 1
- Fig. 5.146 Surface temperatures of fuel rods A11,A12,A13,A87,A88 at position 2
- Fig. 5.147 Surface temperatures of fuel rods A11,A12,A13,A87,A88 at position 3
- Fig. 5.148 Surface temperatures of fuel rods A11,A12,A13,A87,A88 at position 4
- Fig. 5.149 Surface temperatures of fuel rods A11,A12,A13,A87,A88 at position 5
- Fig. 5.150 Surface temperatures of fuel rods A11,A12,A13,A87,A88 at position 6
- Fig. 5.151 Surface temperatures of fuel rods A11,A12,A13,A87,A88 at position 7
- Fig. 5.152 Surface temperatures of fuel rods A22,B22,C22,D22 at position 1
- Fig. 5.153 Surface temperatures of fuel rods A22,B22,C22,D22 at position 2
- Fig. 5.154 Surface temperatures of fuel rods A22,B22,C22,D22 at position 3
- Fig. 5.155 Surface temperatures of fuel rods A22,B22,C22,D22 at position 4
- Fig. 5.156 Surface temperatures of fuel rods A22,B22,C22,D22 at position 5
- Fig. 5.157 Surface temperatures of fuel rods A22,B22,C22,D22 at position 6
- Fig. 5.158 Surface temperatures of fuel rods A22,B22,C22,D22 at position 7
- Fig. 5.159 Surface temperatures of fuel rods A77,B77,C77 at position 1
- Fig. 5.160 Surface temperatures of fuel rods A77,B77,C77 at

- position 2
- Fig. 5.161 Surface temperatures of fuel rods A77,B77,C77 at position 3
- Fig. 5.162 Surface temperatures of fuel rods A77,B77,C77,D77 at position 4
- Fig. 5.163 Surface temperatures of fuel rods A77,B77,C77 at position 5
- Fig. 5.164 Surface temperatures of fuel rods A77,B77,C77 at position 6
- Fig. 5.165 Surface temperatures of fuel rods B77,C77 at position 7
- Fig. 5.166 Fluid temperatures at channel inlet
- Fig. 5.167 Fluid temperatures at channel A outlet
- Fig. 5.168 Fluid temperatures at channel C outlet
- Fig. 5.169 Fluid temperatures above UTP of channel A, openings 1 to 5
- Fig. 5.170 Fluid temperatures above UTP of channel A, openings 6 to 10
- Fig. 5.171 Fluid temperatures above UTP of channel A, openings 1 to 5
- Fig. 5.172 Fluid temperatures above UTP of channel A, openings 6 to 10
- Fig. 5.173 Fluid temperatures at UTP in channel A, opening 1
- Fig. 5.174 Fluid temperatures at UTP in channel A, opening 2
- Fig. 5.175 Fluid temperatures at UTP in channel A, opening 3
- Fig. 5.176 Fluid temperatures at UTP in channel A, opening 4
- Fig. 5.177 Fluid temperatures at UTP in channel A, opening 5
- Fig. 5.178 Fluid temperatures at UTP in channel A, opening 6
- Fig. 5.179 Fluid temperatures at UTP in channel A, opening 7
- Fig. 5.180 Fluid temperatures at UTP in channel A, opening 8
- Fig. 5.181 Fluid temperatures at UTP in channel A, opening 9
- Fig. 5.182 Fluid temperatures at UTP in channel A, opening 10
- Fig. 5.183 Fluid temperatures above UTP of channel C, openings 1 to 5
- Fig. 5.184 Fluid temperatures above UTP of channel C, openings 6 to 10
- Fig. 5.185 Fluid temperatures below UTP of channel C, openings 1 to 5
- Fig. 5.186 Fluid temperatures below UTP of channel C, openings 6 to 10
- Fig. 5.187 Fluid temperatures at UTP in channel C, opening 1
- Fig. 5.188 Fluid temperatures at UTP in channel C, opening 2
- Fig. 5.189 Fluid temperatures at UTP in channel C, opening 3
- Fig. 5.190 Fluid temperatures at UTP in channel C, opening 4
- Fig. 5.191 Fluid temperatures at UTP in channel C, opening 5

- Fig. 5.192 Fluid temperatures at UTP in channel C, opening 6
- Fig. 5.193 Fluid temperatures at UTP in channel C, opening 7
- Fig. 5.194 Fluid temperatures at UTP in channel C, opening 8
- Fig. 5.195 Fluid temperatures at UTP in channel C, opening 9
- Fig. 5.196 Fluid temperatures at UTP in channel C, opening 10
- Fig. 5.197 Inner and outer surface temperatures of channel box at pos.1
- Fig. 5.198 Inner and outer surface temperatures of channel box at pos.2
- Fig. 5.199 Inner and outer surface temperatures of channel box at pos.3
- Fig. 5.200 Inner and outer surface temperatures of channel box at pos.4
- Fig. 5.201 Inner and outer surface temperatures of channel box at pos.5
- Fig. 5.202 Inner and outer surface temperatures of channel box at pos.6
- Fig. 5.203 Inner and outer surface temperatures of channel box at pos.7
- Fig. 5.204 Fluid temperatures in lower plenum center
- Fig. 5.205 Fluid temperatures in lower plenum north
- Fig. 5.206 Fluid temperatures in lower plenum south
- Fig. 5.207 Liquid level signals in channel box A, location A1
- Fig. 5.208 Liquid level signals in channel box A, location A2
- Fig. 5.209 Liquid level signals in channel box B
- Fig. 5.210 Liquid level signals in channel box C
- Fig. 5.211 Liquid level signals in channel box D
- Fig. 5.212 Liquid level signals in channel A outlet location A1
- Fig. 5.213 Liquid level signals in channel A outlet location A2
- Fig. 5.214 Liquid level signals in channel A outlet, center
- Fig. 5.215 Liquid level signals in channel A inlet
- Fig. 5.216 Liquid level signals in channel B inlet
- Fig. 5.217 Liquid level signals in channel C inlet
- Fig. 5.218 Liquid level signals in channel D inlet
- Fig. 5.219 Liquid level signals in lower plenum, north
- Fig. 5.220 Liquid level signals in lower plenum, south
- Fig. 5.221 Liquid level signals in guide tube, north

- Fig. 5.222 Liquid level signals in guide tube, south
- Fig. 5.223 Liquid level signals in downcomer, D side
- Fig. 5.224 Liquid level signals in downcomer, B side
- Fig. 5.225 Estimated liquid level in pressure vessel
- Fig. 5.226 Dryout and quench transients in channel A
- Fig. 5.227 Dryout and quench transients in channel C
- Fig. 5.228 Average density at JP-1,2 outlet
- Fig. 5.229 Average density at JP-3,4 outlet
- Fig. 5.230 Average density at MRP side of break
- Fig. 5.231 Average density at PV side of break
- Fig. 5.232 Flow rate at MRP side of break (based on low range drag disk data)
- Fig. 5.233 Flow rate at PV side of break (based on low range drag disk data)
- Fig. 5.234 Flow rate at MRP side of break (based on high range drag disk data)
- Fig. 5.235 Flow rate at PV side of break (based on high range drag disk data)
- Fig. 5.236 Total discharge flow rate from break (based on low range drag disk data)
- Fig. 5.237 Total discharge flow rate from break (based on high range drag disk data)
- Fig. 5.238 Steam discharge flow rate through MSL
- Fig. 5.239 Flow rate at channel A inlet
- Fig. 5.240 Flow rate at channel B inlet
- Fig. 5.241 Flow rate at channel C inlet
- Fig. 5.242 Flow rate at channel D inlet
- Fig. 5.243 Flow rate at bypass hole
- Fig. 5.244 Total channel inlet flow rate
- Fig. 5.245 Flow rate at JP-1,2 outlet (high range)
- Fig. 5.246 Flow rate at JP-3,4 outlet (high range)
- Fig. 5.247 Flow rate at JP-3,4 outlet (low range)
- Fig. 5.248 Total JP outlet flow rate (high range)
- Fig. 5.249 Collapsed liquid level in downcomer
- Fig. 5.250 Collapsed liquid level inside core shroud
- Fig. 5.251 Fluid inventory in downcomer
- Fig. 5.252 Fluid inventory inside core shroud

- Fig. 5.253 Total fluid inventory in pressure vessel
- Fig. 5.254 Fluid mass increase by ECCS and FW and  
decrease by steam discharge flow
- Fig. 5.255 Discharged fluid mass from break
- Fig. 5.256 Discharged flow rate from break
- Fig. 6.1 Lower plenum pressures
- Fig. 6.2 Break flow rates
- Fig. 6.3 Total channel inlet flow rates
- Fig. 6.4 Mixture levels in the pressure vessel
- Fig. 6.5 Peak cladding temperatures



## ABBREVIATIONS

ADS	Automatic Depressurization System
AT	Air Tank
AV	Air Actuation Valve
(2)B	(2) inches pipe of Schedule 80
BN	Boron Nitride
BWR	Boiling Water Reactor
CA	Chromel-Alumel
CCFL	Counter Current Flow Limiting
CHV	Check Valve
CP	Conductivity Probe
CV	Control Valve
CWT	Cooling Water Tank
D	Differential Pressure
d	Diameter
DF	Density of Fluid
DL(+100)	Elevation (+100 mm) from the bottom of PV
ECCS	Emergency Core Cooling System
ESF	Engineered Safety Features
EX	Heat Exchanger
F	Flow Rate
Fig.	Figure
FS	Full Scale
FW	Feedwater
FWLF	Feedwater Line Flashing
FWP	Feedwater Pump
FWT	Feedwater Tank
HPCS	High Pressure Core Spray
HPCSP	High Pressure Core Spray Pump
HPCST	High Pressure Core Spray Tank

MW	Megawatt
N	Rotation Speed
OR	Orifice
P	Pressure
	Power
PCT	Peak Cladding Temperature
PV	Pressure Vessel
PWT	Pure Water Tank
QOBV	Quick Opening Blowdown Valve
QSV	Quick Shut-off Valve
RCN	Rapid Condenser
ROSA	Rig of Safety Assessment
rpm	Revolution per Minute
S	Signal
s	Second
Sch	Schedule
SUS	Stainless Steel
T	Temperature
T/C	Thermocouple
TC	Temperature of Fluid
TF	Temperature of Fuel
TS	Temperature of Structure Material
UTP	Upper Tie Plate
V	Valve
VF	Void Fraction
W	Watt
WL	Water Level
WSP	Water Supply Pump

HPWP	High Pressure Water Pump
ID	Inner diameter
INC 600	Inconel 600
JP	Jet Pump
K	Kelvin
kg	Kilogram
kPa	Kilopascal
kW	Kilowatt
L	Liter
LB	Liquid Level in Channel Box
LBWR	Large Boiling Water Reactor
LL	Liquid Level
LOCA	Loss-of-Coolant Accident
LOCE	Loss-of-Coolant Experiment
LP	Lower Plenum
LPCI	Low Pressure Coolant Injection
LPCIP	Low Pressure Coolant Injection Pump
LPCIT	Low Pressure Coolant Injection Tank
LPCS	Low Pressure Core Spray
LPCSP	Low Pressure Core Spray Pump
LPCST	Low Pressure Core Spray Tank
LPF	Lower Plenum Flashing
LTP	Lower Tie Plate
M	Momentum Flux
m	Meter
mm	Milimeter
MLHR	Maximum Linear Heat Rate
MPa	Megapascal
MRP	Main Recirculation Pump
MSIV	Main Steam Isolation Valve
MSL	Main Steam Line

## 1. Introduction

The Rig of Safety Assessment (ROSA)-III program was initiated in 1976 to study the thermal-hydraulic behavior of a Boiling Water Reactor (BWR) during a postulated Loss of Coolant Accident (LOCA) with the Emergency Core Cooling System (ECCS) actuation and to obtain the data base to evaluate the predictability of computer codes developed for reactor safety analysis. The ROSA-III test facility was fabricated in 1978 and consisted of the volumetrically scaled (1/424) primary system of a 3800 MW BWR/6-251 with the electrically heated core, the break simulator and the scaled ECCS<sup>(1)</sup>

Special emphasis is made on the following objectives in the ROSA-III program :

- (1) To provide the system data required to improve and evaluate the analytical methods currently used to predict the LOCA response of large BWRs. The performance of the Engineered Safety Features (ESFs), with particular emphasis on ECCSs, and the quantitative margins of safety inherent in performance of the ESFs are of primary interest.
- (2) To identify and investigate any unexpected event(s) or threshold(s) in the response of either the plant or the ESFs and develop analytical techniques that adequately describe and account for such unexpected behavior.

The information acquired from Loss of Coolant Experiments (LOCEs) is thus used for evaluation and development of LOCA analytical methods and assesment for the qualitative margins of safety of ESFs in response to a LOCA.

RUN 928 was conducted on November 12, 1981, as one of the break configuration sensitivity tests, and was simulated a 50 % split break at the recirculation pump suction line with the assumption of HPCS diesel generator failure. A long throat nozzle was used for a break plane.

The specific objectives of RUN 928 are as follows :

- (1) To obtain test data of a 50% break test at the recirculation pump suction line without HPCS actuation
- (2) To study the effect of the break configuration difference on the system thermal-hydraulic behavior under the 50 % LOCA condition comparing with the results obtained in the test using the other break configuration

In this report, all the data obtained in RUN 928 are presented. The processed data like mass inventory in the pressure vessel are also given.

## 2. ROSA-III Test Facility

The ROSA-III test facility is a volumetrically scaled (1/424) BWR system with an electrically heated core designed to study the response of the primary system, the core and the ECCS during the postulated LOCA. The test facility is instrumented such that various thermal-hydraulic parameters are measured and recorded during the test. Details of the instrumentation are described in section 3.

The test facility consists of four subsystems. These subsystems are : (a) the pressure vessel, (b) the steam line and the feedwater line, (c) the recirculation loops and (d) the ECCS. Figures 2.1 through 2.3 illustrate configuration of the test facility, the pressure vessel internals and the piping schematics, respectively. Table 2.1 compares the major dimensions of the ROSA-III test facility to the corresponding dimensions of the reference BWR system.

The ROSA-III pressure vessel includes various components in it simulating the internal structures of the reactor vessel in the BWR system as shown in Fig. 2.4. The interior of the vessel is divided into the core, the lower plenum, the upper plenum, the downcomer annulus, the steam separator, the steam dome and the steam dryer. The core is consisted of four model fuel assemblies of half length and a control rod simulator. Each fuel assembly contains 62 heater rods (Fig. 2.5) and 2 water rods spaced in a 8 x 8 square array and supported by spacers and upper and lower tie plates. The heater rod is heated electrically with chopped cosine power distribution along the axis as shown in Fig. 2.6. The effective heated length is 1880 mm, one half of the active length of a BWR fuel rod. The electric power supplied to the model fuel assembly "A" is 1.4 times larger than the power supplied to each of the other assemblies. The heater rods in each assembly are divided into three groups in terms of heat generation rate as shown in Fig. 2.7. The relative power generation rate of a heater rod in each group is 1.1, 1.0, and 0.875, respectively. The orifice plates are inserted at the core inlet to control the core inlet flow<sup>(1)</sup>.

The steam line is connected to the steam dome of the pressure vessel. A control valve is installed in the steam line to control the steam dome pressure in steady state before the initiation of the tests. The steam line has a branch in which the Automatic Depressurization System (ADS) is installed. The operation of valves in the steam line is described in Sec.

4. The feedwater is supplied from the feedwater tank (FWT) through the feedwater line and the feedwater sparger below the steam separator.

Figure 2.8 shows the recirculation lines consisted of two loops. Each line is furnished with a pump and two jet pumps. The jet pumps are installed outside the pressure vessel to simulate the relative volume and the relative height to the core. Two break simulators and a Quick Shut-off Valve (QSV) are installed in one of these loops to simulate the various break conditions. Each break simulator consists of a nozzle or an orifice to determine the break size and a Quick Opening Blowdown Valve (QOBV) to initiate the test. The break mode (double-ended or split), the break size and the break location can be changed. The diameter of the largest nozzle and orifice available is 26.2 mm. Figure 2.8 shows two QOBVs, a QSV and flow nozzles installed upstream of the QOBVs. Several flow nozzles and orifices of different size are prepared to vary the break size.

The ROSA-III test facility is furnished with all kinds of the ECCS available in the BWR system, i.e., the High Pressure Core Spray (HPCS), the Low Pressure Core Spray (LPCS), the Low Pressure Coolant Injection (LPCI), and the Automatic Depressurization System (ADS). The HPCS and the LPCS provide the cooling water from the top of the core. The LPCI injects the cooling water into the core bypass. Each ECCS consists of a pump, a tank, pipings, and a control system.

Reference (1) serves more detailed information on the facility.

Table 2.1 Primary Characteristics of ROSA-III and BWR/6

	BWR*	ROSA-III	BWR/ROSA-III
Number of Recirc. Loops	2	2	1
Number of Jet Pumps	24	4	6
Number of Separators	251	1	251
Number of Fuel Assemblies	848	4	212
Active Fuel Length (m)	3.76	1.88	2
Total Volume (m <sup>3</sup> )	621	1.42	437
Power (MW)	3,800	4.40	864
Pressure (MPa)	7.23	7.23	1
Core Flow (kg/s)	$1.54 \times 10^4$	36.4	424
Recirculation Flow (l/s)	2,970	7.01	424
Feedwater Flow (kg/s)	2,060	4.86	424
Feedwater Temp. (K)	489	489	1

\* BWR/6-251

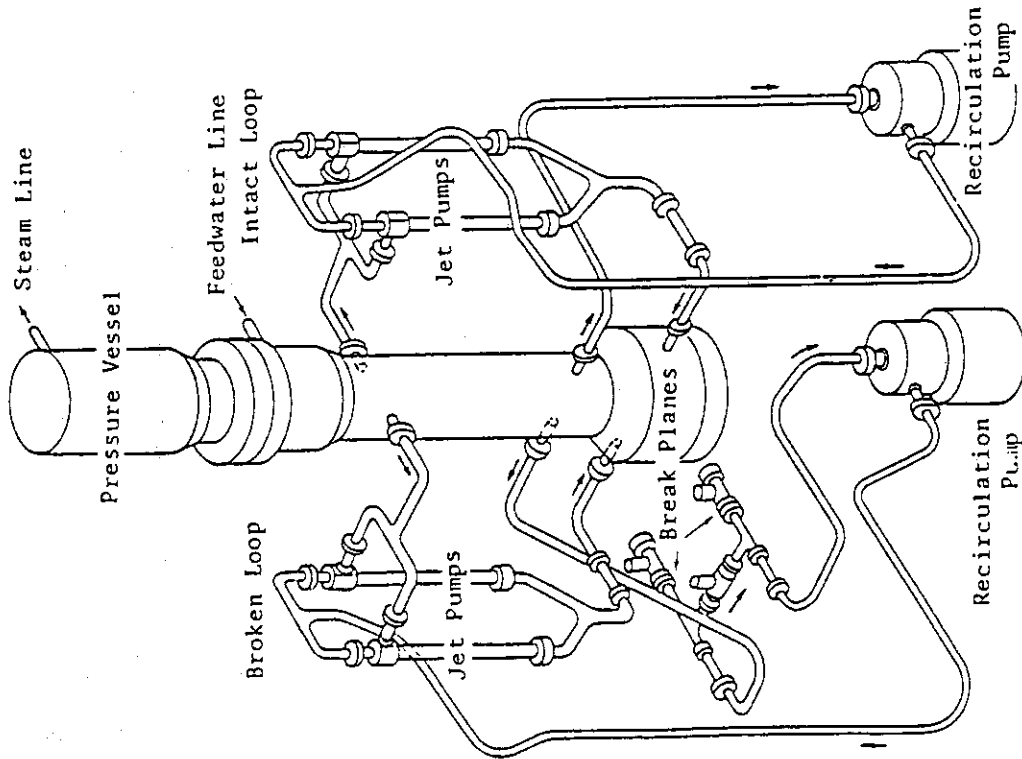
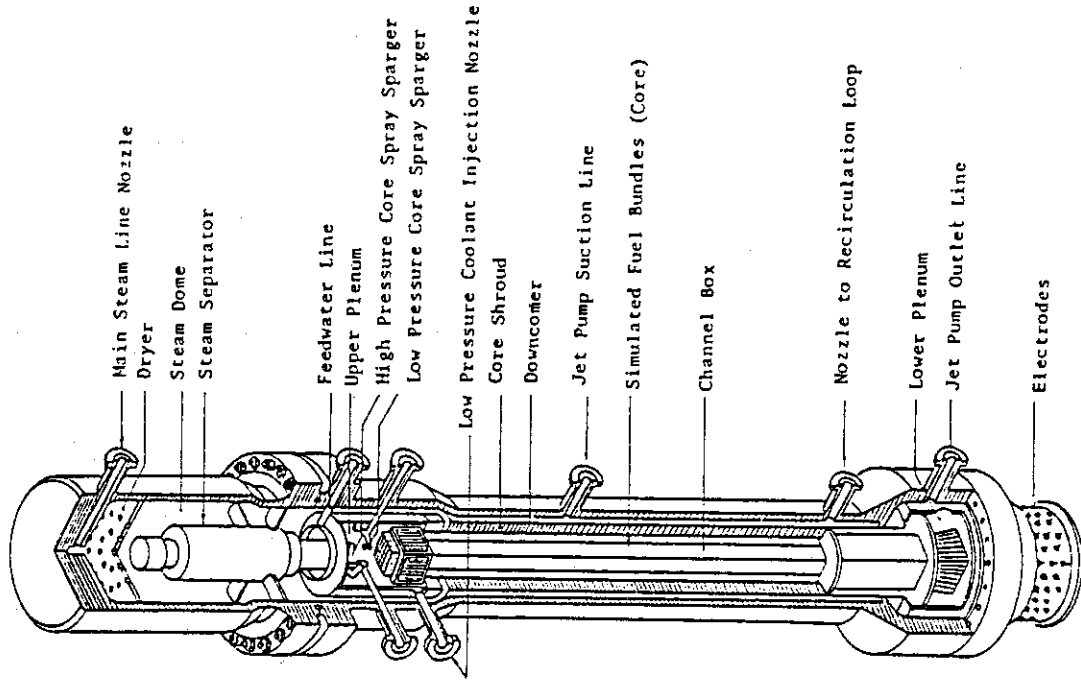


Fig. 2.1 Schematic Diagram of ROSA-III Test Facility Fig. 2.2 Internal Structure of Pressure Vessel of ROSA-III



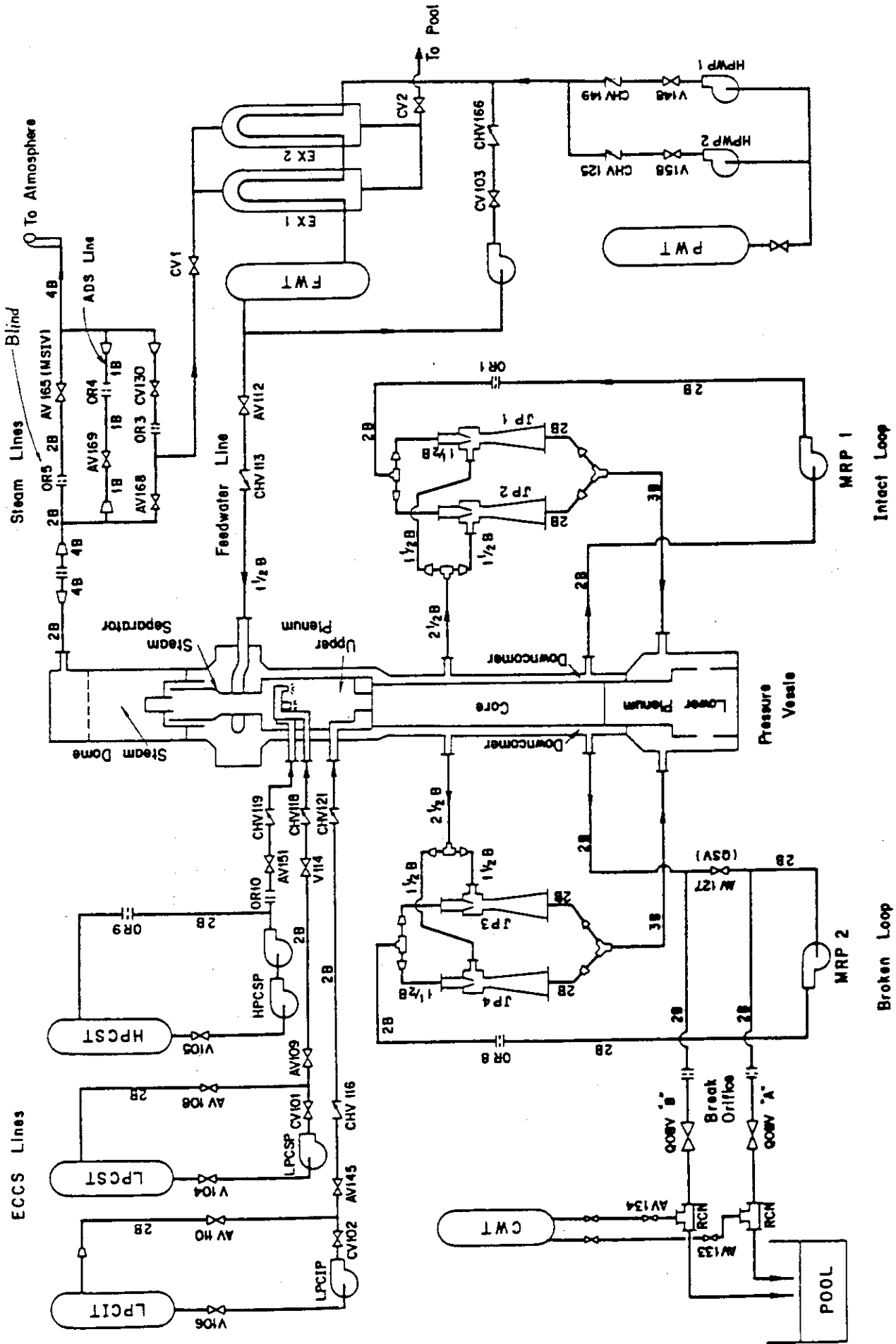


Fig. 2.3 ROSA-III Piping Schematics

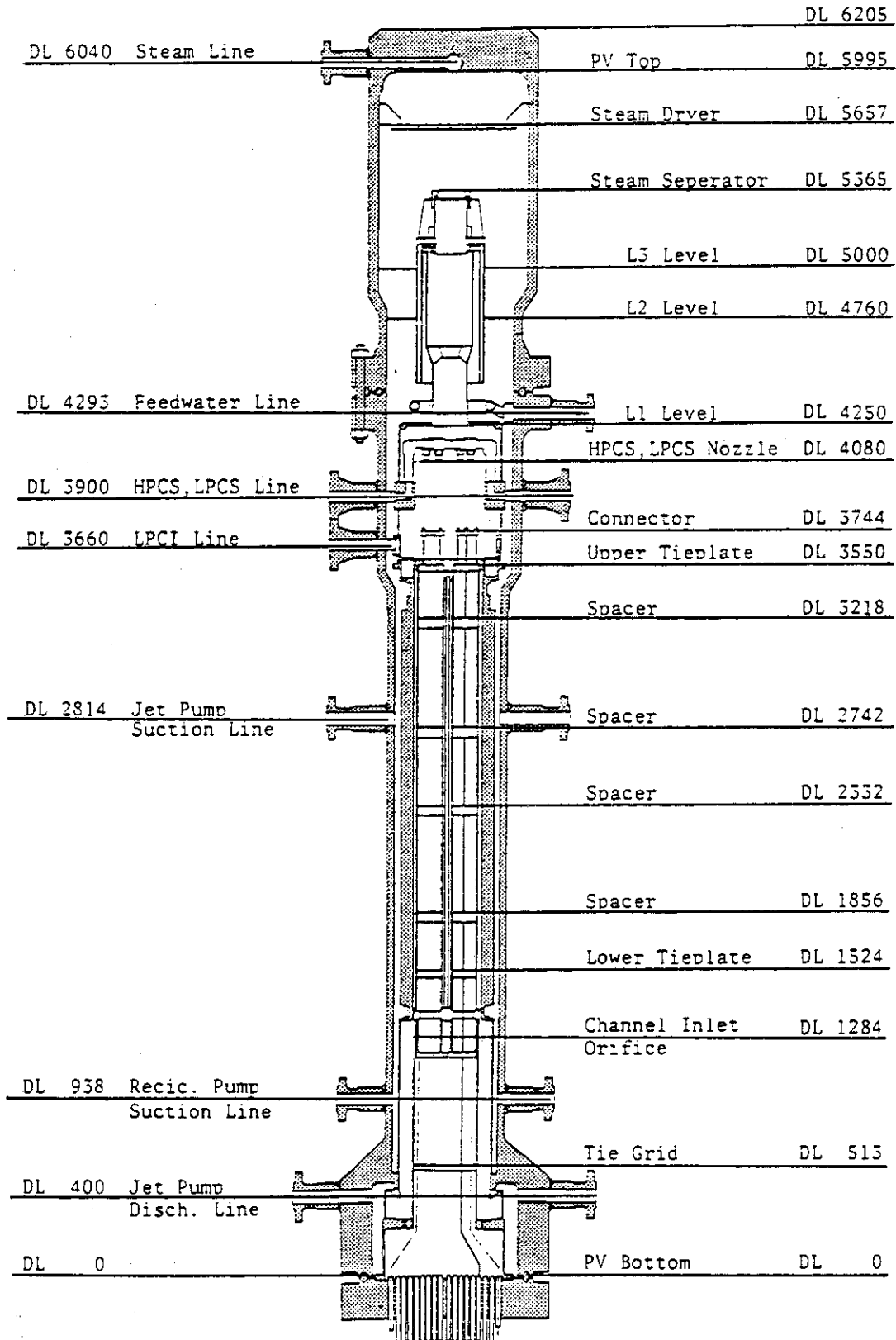


Fig. 2.4 Pressure Vessel Internals Arrangement

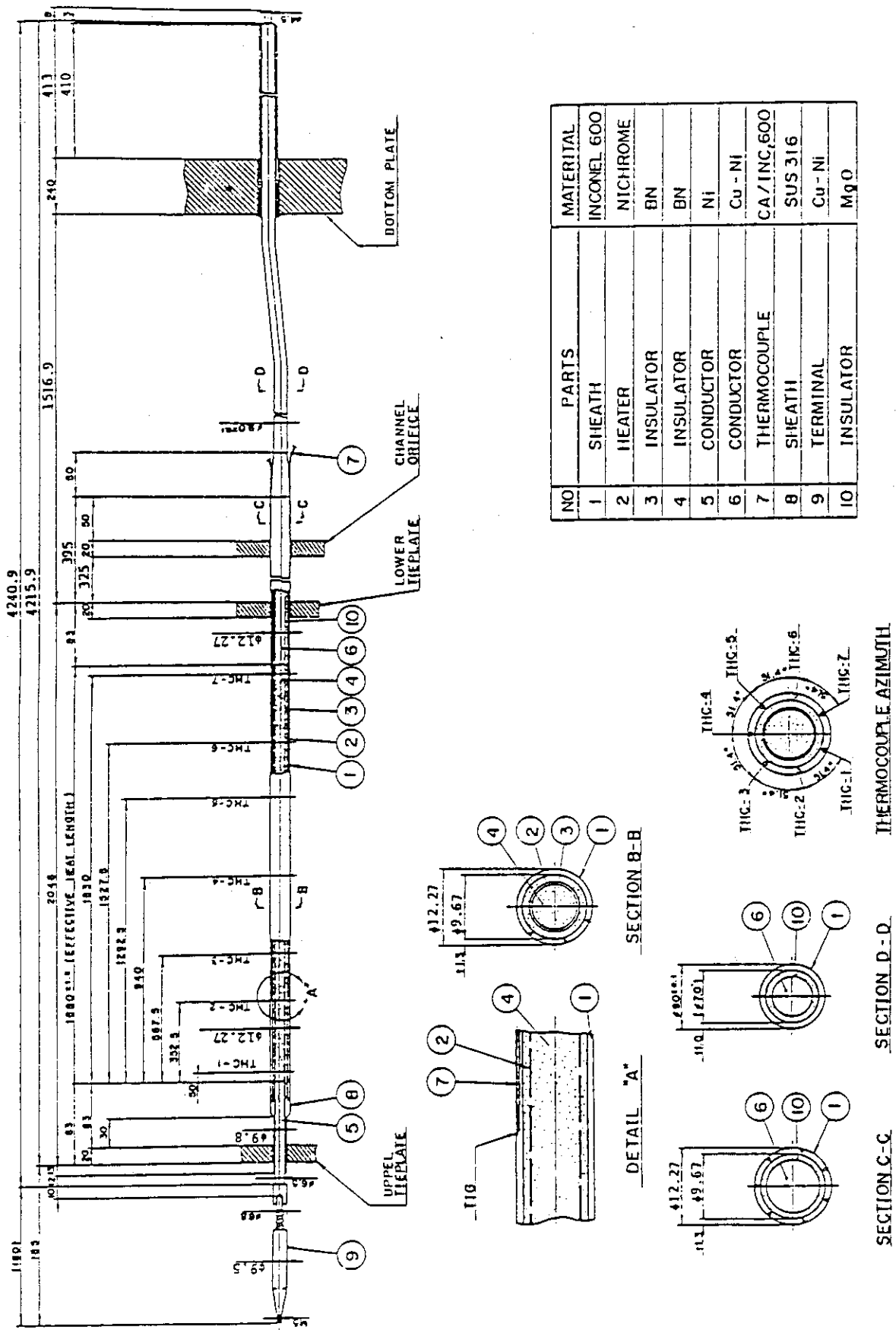
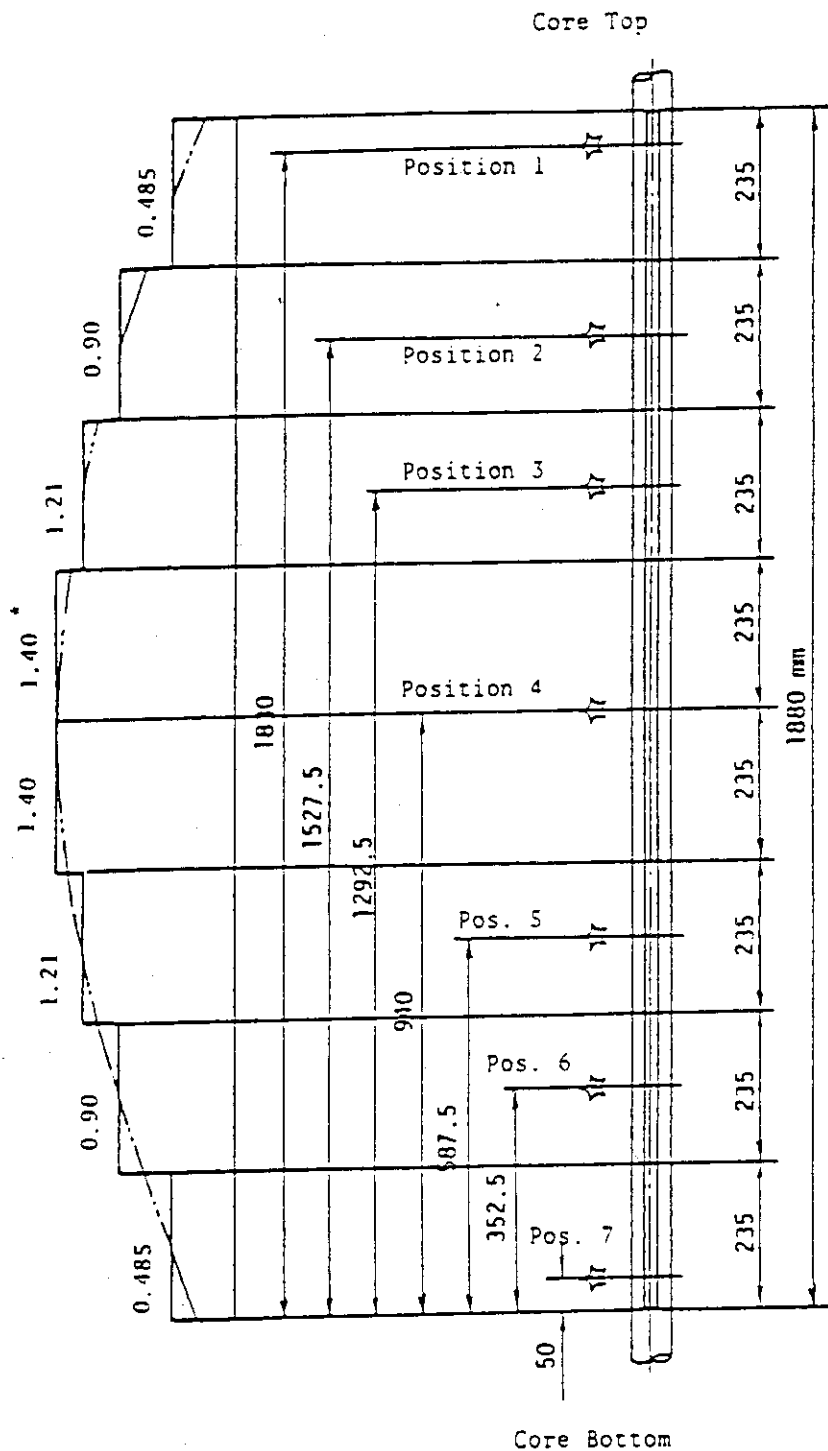
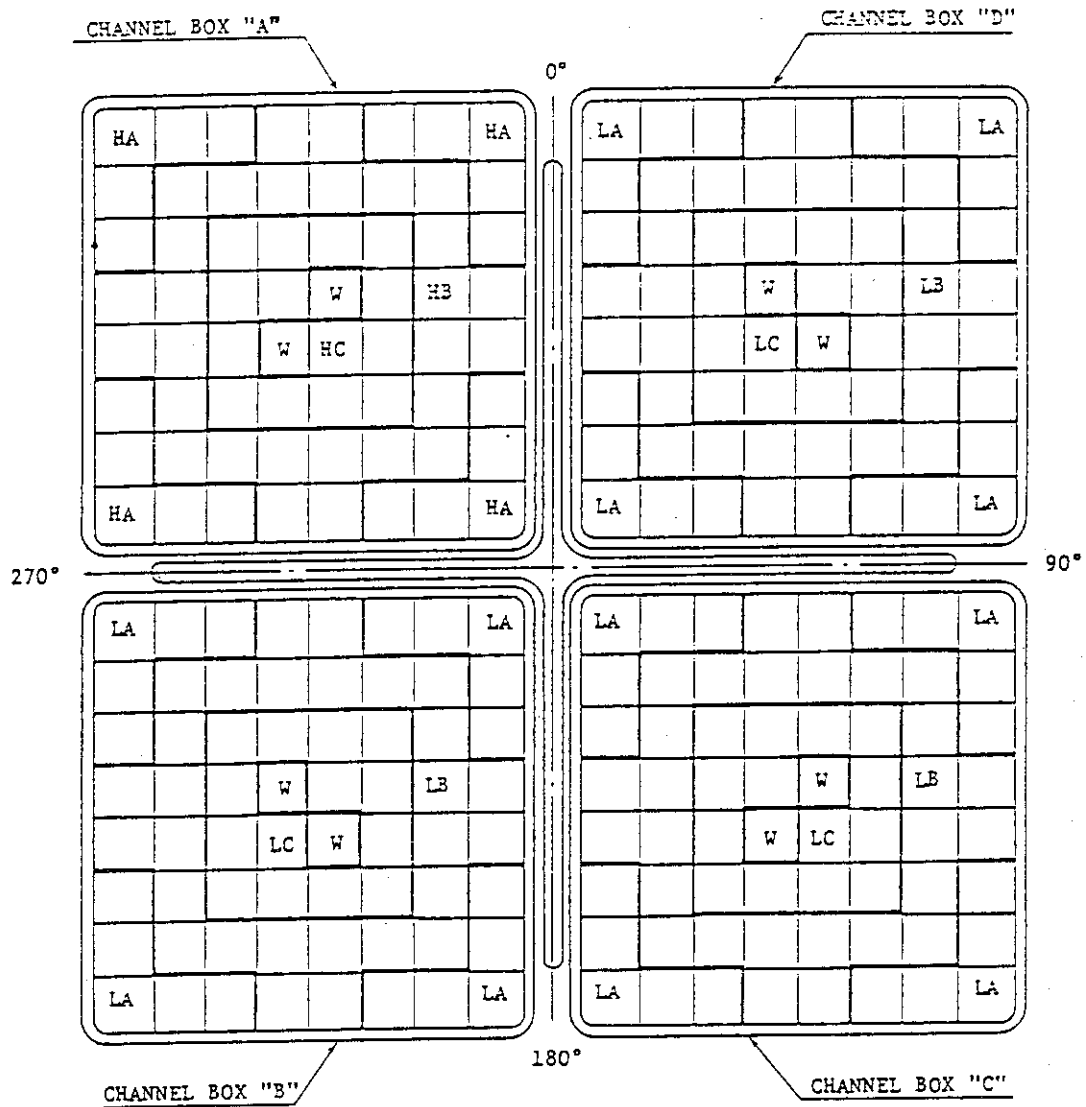


Fig. 2.5 Simulated Fuel Rod of ROSA-III



☆ Indicates position of thermocouple. \* Axial Peaking Factor

Fig.2.6 Axial Power Distribution of Heater Rod



Region	HA	HB	HC	LA	LB	LC	W
Linear Heat Rate (kW/m)	18.5	16.81	14.41	13.21	12.01	10.29	0.0
Local peaking factor	1.1	1.0	0.875	1.1	1.0	0.875	0.0
No. of Rods	20	28	14	60	84	42	8

\* note : Radial peaking factor is 1.4

Fig. 2.7 Radial Power Distribution of Core

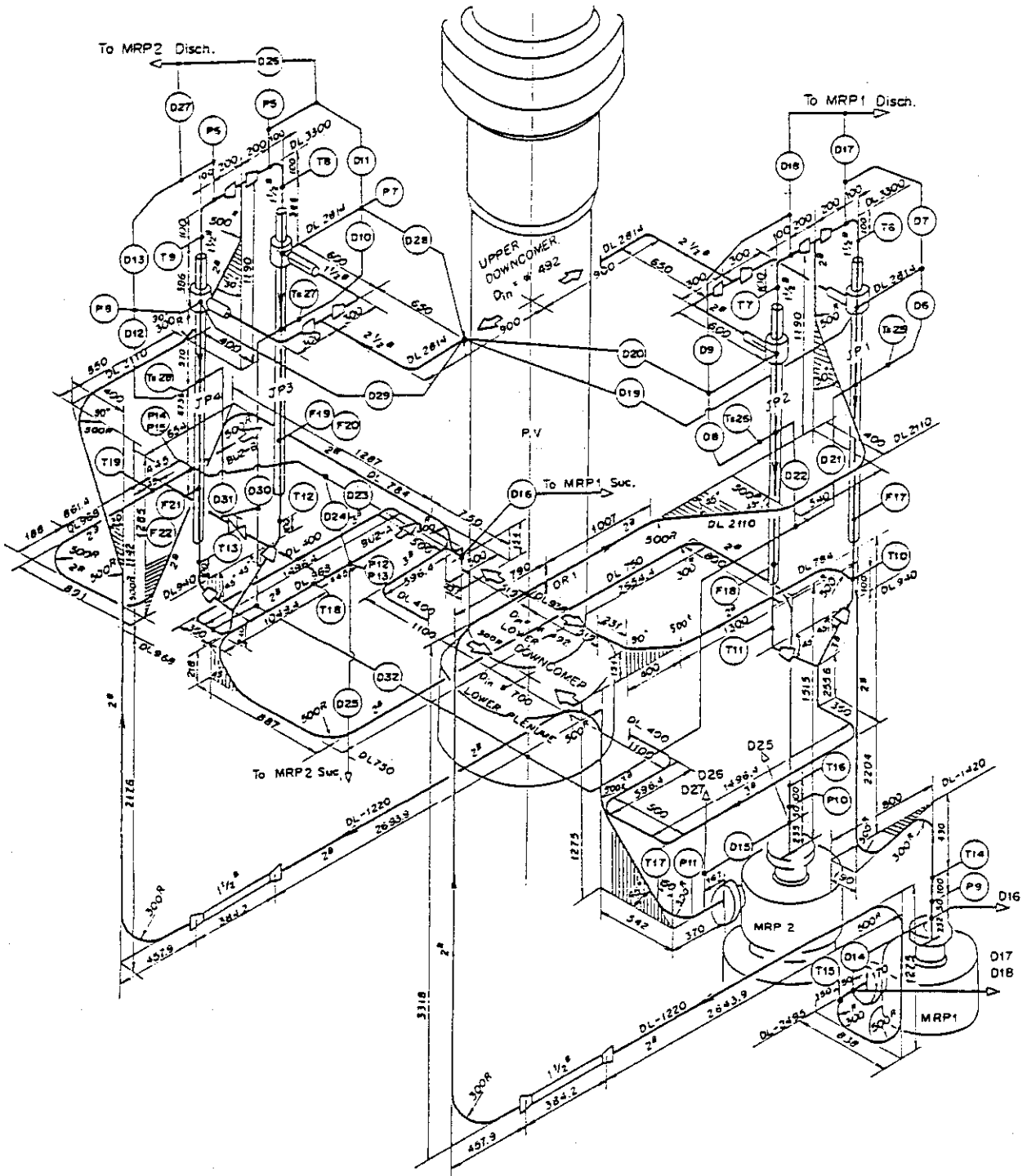


Fig. 2.8 Piping Layout of Recirculation Loops and Jet Pumps

### 3. Instrumentation

The instrumentation of the ROSA-III is designed to obtain thermal-hydraulic data during the simulated BWR LOCA. The data obtained from the experiments will contribute to the assessment of the analytical computer code. Table 3.1 summarizes instrumentation used in RUN 928.

Table 3.2 shows the measurement list of RUN 928, Table 3.3 shows the core instrumentation list. Instrumentation locations are shown in Figs. 3.1 through 3.7.

Typical measured parameters in the ROSA-III are pressure, differential pressure, flow rate, electric power, pump speed, fluid and metal temperature, collapsed liquid level, two-phase mixture level, coolant fluid density, on-off type signals and so on.

Pressure and differential pressure transducers are two-wire, direct-current type which convert diaphragm displacement to electric capacitance. The pressure lead pipes are either the standard single, cylindrical pipes used in conjunction with condensate pots, or dual concentric cylinders capable of the circulation of cooling water to prevent flashing of the fluid.

The flow rate is measured either by an orifice or a venturi type flow meter depending on the fluid condition and measurement location.

The temperatures of the fluid, structural material and fuel rod cladding are measured with chromel-alumel thermocouples (CA T/C) of 1.6 or 0.5 mm $\phi$ .

Liquid levels are measured by either differential pressure transducers, described above or needle type electrical conductivity probes (CP) developed in the ROSA-III program. The probes are distributed along the vessel height to detect the existence of water or vapor at different levels.

The electric power supplied to the simulated fuel rods is controlled to follow the predetermined function of time and measured by a fast response electric power meter.

Pump speed is measured by a pulse generator integral of the pump. On-off signals such as selected valve positions, decay heat and pump coast-down simulation initiations and so on are detected in order to record the exact actuation time.

Fluid density in the pipe is measured by means of gamma densitometers. Preliminary studies indicate that a three-beam densitometer should be used to determine the flow regime. Figures 3.7 and 3.8 show the beam directions of the three-beam and the two-beam gamma densitometers, respectively. The

gamma-ray source is  $^{137}\text{Cs}$  and the detector is a water cooled NaI(Tl) scintillation counter.

Momentum flux is measured by a drag disk as shown in Fig. 3.9. The combination of signals from a drag disk and a gamma densitometer is used to determine the two-phase flow rate as shown in Fig. 3.10.

The data acquisition system ( DATAAC 2000B, Iwasaki Tsushinki Co. ) scans all the 700 channels of signals with the frequency up to 30 Hz. The data recorded on magnetic tape are processed by the FACOM M200 system computer at JAERI by off-line control. After evaluation, for example by comparing the initial and final pressure values with standard values, the data is reprocessed using the correct conversion factors as determined from the consistency examination.

More detailed information on the instrumentation and the data processing procedure are available in reference (2).



Table 3.1 ROSA-III Instrumentation Summary List

ITEM	SENSOR	NUMBER	NOTE
Pressure	Pressure Transducer	20	
Differential Pressure	DP Cell	60	PV and Loop 44 Level Measurement 5 Flow Meter 11
Fluid Temperature	CA Thermocouple	129	Primary Loop 23 DTT 4 Tie Rod 28 Upper Plenum 10 Lower Plenum 10 Tie Plate 40 Bypass 14
Fuel Rod Temperature	CA Thermocouple	213	
Slab Surface Temperature	CA Thermocouple	70	Core Barrel 24 Pressure Vessel 3 Channel Box 35 Shroud Support 8
Slab Inner Temperature	CA Thermocouple	9	JP Diffuser 4 PV Wall 5
Volumetric Flow Rate	Turbine Flow Meter Venturi Flow Meter Orifice Flow Meter	3 4 6	ECCS Loop 3 Primary Loop 10
Mass Flow Rate	Turbine Flow Meter Orifice Flow Meter	4 3	Recirculation Loop 4 Main Steam Line 3
Liquid Level	Conductivity Probe Capacitance Probe	138 2	
Density	Gamma Densitometer	10	2 Beam GD 2 3 Beam GD 2
Momentum Flux	Drag Disk	4	JP Spool Piece 2 Break Spool Piece 4 Break Orifice 1
Signal	ON/OFF Switch	14	
Pump Speed	Revolution Counter	2	
Electric Core Power	VA Meter	2	
TOTAL		693	

Table 3.2 Measurement List for RUN 928

1Ch.- 50Ch.

Ch.	Item	Symbol	ID.	Location	Fig.No.	Range	Unit	Accuracy
1	Press.	P-1	PA	Lower Plenum	Fig.5. 1	0.100	MPa	1.08XFS
2	Press.	P-2	PA	Upper Plenum	Fig.5. 1	0.100	MPa	1.08XFS
3	Press.	P-3	PA	Steam Dome	Fig.5. 1	0.100	MPa	1.08XFS
4	Press.	P-4	PA	Downcomer Bottom	Fig.5. 1	0.100	MPa	1.08XFS
5	Press.	P-5	PA	JP-3 Drive	Fig.5. 2	0.100	MPa	1.08XFS
6	Press.	P-6	PA	JP-4 Drive	Fig.5. 2	0.100	MPa	1.08XFS
7	Press.	P-7	PA	JP-3 Suction	Fig.5. 2	0.100	MPa	1.08XFS
8	Press.	P-8	PA	JP-4 Suction	Fig.5. 2	0.100	MPa	1.08XFS
9	Press.	P-9	PA	MRP-1 Suction	Fig.5. 3	0.100	MPa	1.08XFS
10	Press.	P-10	PA	MRP-2 Suction	Fig.5. 3	0.100	MPa	1.08XFS
11	Press.	P-11	PA	MRP-2 Delivery	Fig.5. 3	0.100	MPa	1.08XFS
12	Press.	P-12	PA	Break A Upstream	Fig.5. 4	0.100	MPa	1.08XFS
13	Press.	P-13	PA	Break A Downstream	Fig.5. 4	0.100	MPa	1.08XFS
14	Press.	P-14	PA	Break B Upstream	Fig.5. 5	0.100	MPa	1.08XFS
15	Press.	P-15	PA	Break B Downstream	Fig.5. 5	0.100	MPa	1.08XFS
16	Press.	P-16	PA	Steam Line	Fig.5. 6	0.100	MPa	1.08XFS
17	Press.	P-17	PA	JP-1,2 Outlet Spool	Fig.5. 7	0.100	MPa	1.08XFS
18	Press.	P-18	PA	JP-3,4 Outlet Spool	Fig.5. 7	0.100	MPa	1.08XFS
19	Press.	P-19	PA	Break A Spool Piece	Fig.5. 4	0.100	MPa	1.08XFS
20	Press.	P-30	PA	Break B Spool Piece	Fig.5. 5	0.100	MPa	1.08XFS
21	Diff.P.	D-1	PD	Upper Pl.-Upper Pl.	Fig.5. 8	-50.0	kPa	0.63XFS
22	Diff.P.	D-2	PD	Lower Pl.-Steam Dome	Fig.5. 9	-10.0	kPa	0.63XFS
23	Diff.P.	D-3	PD	Lower Plenum Head	Not Measured			
24	Diff.P.	D-4	PD	Downcomer Head	Fig.5.10	0.0	kPa	0.63XFS
25	Diff.P.	D-5	PD	PV Bottom-Top	Fig.5.11	-100.	kPa	0.63XFS
26	Diff.P.	D-6	PD	JP-1 Disch.-Suction	Fig.5.12	-100.	kPa	0.63XFS
27	Diff.P.	D-7	PD	JP-1 Drive -Suction	Fig.5.13	0.0	MPa	0.63XFS
28	Diff.P.	D-8	PD	JP-2 Disch.-Suction	Fig.5.12	-100.	kPa	0.63XFS
29	Diff.P.	D-9	PD	JP-2 Drive -Suction	Fig.5.13	0.0	MPa	0.63XFS
30	Diff.P.	D-10	PD	JP-3 Disch.-Suction	Fig.5.14	-100.	kPa	0.63XFS
31	Diff.P.	D-11	PD	JP-3 Drive -Suction	Fig.5.15	-4.00	MPa	0.63XFS
32	Diff.P.	D-12	PD	JP-4 Disch.-Suction	Fig.5.14	-100.	kPa	0.63XFS
33	Diff.P.	D-13	PD	JP-4 Drive -Suction	Fig.5.15	-4.00	MPa	0.63XFS
34	Diff.P.	D-14	PD	MRP-1 Deliv.-Suction	Fig.5.16	-0.100	MPa	0.63XFS
35	Diff.P.	D-15	PD	MRP-2 Deliv.-Suction	Fig.5.16	-0.100	MPa	0.63XFS
36	Diff.P.	D-16	PD	DC Bottom- MRP-1 Suc.	Fig.5.17	-50.0	kPa	0.63XFS
37	Diff.P.	D-17	PD	MRP1 Deliv.-JP1 Drive	Fig.5.18	0.0	kPa	0.63XFS
38	Diff.P.	D-18	PD	MRP1 Deliv.-JP2 Drive	Fig.5.18	0.0	kPa	0.63XFS
39	Diff.P.	D-19	PD	DC Middle-JP1 Suction	Fig.5.19	0.0	kPa	0.63XFS
40	Diff.P.	D-20	PD	DC Middle-JP2 Suction	Fig.5.19	0.0	kPa	0.63XFS
41	Diff.P.	D-21	PD	JP1 Disch.-Lower Pl.	Fig.5.20	-100.	kPa	0.63XFS
42	Diff.P.	D-22	PD	JP2 Disch.-Lower Pl.	Fig.5.20	-100.	kPa	0.63XFS
43	Diff.P.	D-23	PD	DC Bottom- Break B	Fig.5.21	-60.0	kPa	0.63XFS
44	Diff.P.	D-24	PD	Break B- Break A	Fig.5.22	0.0	kPa	0.63XFS
45	Diff.P.	D-25	PD	Break A- MRP2 Suction	Fig.5.23	-500.	kPa	0.63XFS
46	Diff.P.	D-26	PD	MRP2 Deliv.-JP3 Drive	Fig.5.24	-500.	kPa	0.63XFS
47	Diff.P.	D-27	PD	MRP2 Deliv.-JP4 Drive	Fig.5.24	-500.	kPa	0.63XFS
48	Diff.P.	D-28	PD	DC Middle-JP3 Suction	Fig.5.25	-250.	kPa	0.63XFS
49	Diff.P.	D-29	PD	DC Middle-JP4 Suction	Fig.5.25	-250.	kPa	0.63XFS
50	Diff.P.	D-30	PD	JP3 Disch.-Confluence	Fig.5.26	-100.	kPa	0.63XFS

Table 3.2 Measurement List for RUN 928 (Continued)

51Ch.-100Ch.

Ch.	Item	Symbol	ID.	Location	Fig.No.	Range	Unit	Accuracy
51	Diff.P.	D-31	PD	JP4 Disch.-Confluence	Fig.5.26	-100.	kPa	0.63%FS
52	Diff.P.	D-32	PD	Confluence -Lower Pl.	Fig.5.27	50.0	kPa	0.63%FS
53	Diff.P.	D-33	PD	Lower Pl.-DC Middle	Fig.5.28	-250.	kPa	0.63%FS
54	Diff.P.	D-34	PD	Lower Pl.-DC Bottom	Fig.5.29	-250.	kPa	0.63%FS
55	Diff.P.	D-35	PD	DC Bottom-DC Middle	Fig.5.30	50.0	kPa	0.63%FS
56	Diff.P.	D-36	PD	DC Middle-Steam Dome	Fig.5.31	50.0	kPa	0.63%FS
57	Diff.P.	D-37	PD	Lower Pl.Mid-Upper Pl	Not Measured			
58	Diff.P.	D-38	PD	Lower Pl.Bottom-Mid.	Fig.5.32	0.0	kPa	0.63%FS
59	Diff.P.	D-39	PD	Upper Pl.-DC High	Not Used	-20.0	kPa	0.63%FS
60	Diff.P.	D-40	PD	Channel Orifice A	Fig.5.33	50.0	kPa	0.63%FS
61	Diff.P.	D-41	PD	Channel Orifice B	Fig.5.34	50.0	kPa	0.63%FS
62	Diff.P.	D-42	PD	Channel Orifice C	Fig.5.35	75.0	kPa	0.63%FS
63	Diff.P.	D-43	PD	Channel Orifice D	Fig.5.36	50.0	kPa	0.63%FS
64	Diff.P.	D-44	PD	Lower Plenum Head	Fig.5.37	100.	kPa	0.63%FS
65	Level	WL-1	LM	HPCS Tank	Not Used	0.0	m	1.00%FS
66	Level	WL-2	LM	LPCS Tank	Fig.5.38	2.30	m	1.00%FS
67	Level	WL-3	LM	LPCI Tank	Fig.5.38	4.25	m	1.00%FS
68	Level	WL-4	LM	Upper Downcomer	Fig.5.39	6.04	m	1.00%FS
69	Level	WL-5	LM	Lower Downcomer	Fig.5.39	3.90	m	1.00%FS
70	Mass.F.	F-1	FM	Steam Line (Low Range)	Fig.5.40	0.0	kg/s	0.92%FS
71	Mass.F.	F-2	FM	Steam Line(High Range)	Fig.5.40	3.00	kg/s	0.92%FS
72	Mass.F.	F-3	FM	Steam Line (Mid Range)	Fig.5.40	0.0	kg/s	1.40%FS
73	Vol.F.	F-7	FV	HPCS (Upper Plenum)	Not Used	0.0	m <sup>3</sup> /s	0.79%FS
74	Vol.F.	F-9	FV	LPCS (Upper Plenum)	Fig.5.41	0.0	m <sup>3</sup> /s	0.79%FS
75	Vol.F.	F-11	FV	LPCI (Core Bypass)	Fig.5.41	0.0	m <sup>3</sup> /s	0.79%FS
76	Vol.F.	F-15	FV	Feedwater	Fig.5.42	0.0	m <sup>3</sup> /s	0.79%FS
77	Vol.F.	F-16	FV	PWT Flow	Not Used	0.0	m <sup>3</sup> /s	0.79%FS
78	Vol.F.	F-17	FV	JP1 Discharge	Fig.5.43	0.0	m <sup>3</sup> /s	0.88%FS
79	Vol.F.	F-18	FV	JP2 Discharge	Fig.5.43	0.0	m <sup>3</sup> /s	0.88%FS
80	Vol.F.	F-19	FV	JP3 Disch. Positive	Fig.5.44	0.0	m <sup>3</sup> /s	0.92%FS
81	Vol.F.	F-20	FV	JP3 Disch. Negative	Fig.5.44	0.0	m <sup>3</sup> /s	0.92%FS
82	Vol.F.	F-21	FV	JP4 Disch. Positive	Fig.5.44	0.0	m <sup>3</sup> /s	0.92%FS
83	Vol.F.	F-22	FV	JP4 Disch. Negative	Fig.5.44	0.0	m <sup>3</sup> /s	0.92%FS
84	Mass.F.	F-23	FM	JP1,2 Outlet Spool	Fig.5.45	0.0	m <sup>3</sup> /s	0.92%FS
85	Mass.F.	F-24	FM	JP3,4 Outlet Spool	Not Measured	30.0	kg/s	1.40%FS
86	Mass.F.	F-25	FM	Break A Spool Piece	Not Measured	30.0	kg/s	1.40%FS
87	Mass.F.	F-26	FM	Break B Spool Piece	Not Measured	30.0	kg/s	1.40%FS
88	Vol.F.	F-27	FV	MRP-1	Fig.5.46	0.0	m <sup>3</sup> /s	0.88%FS
89	Vol.F.	F-28	FV	MRP-2	Fig.5.46	0.0	m <sup>3</sup> /s	0.88%FS
90	Diff.P.	D-F1	PD	F1 Orifice	Fig.5.47	4.90	kPa	0.63%FS
91	Diff.P.	D-F2	PD	F2 Orifice	Fig.5.47	34.9	kPa	0.63%FS
92	Diff.P.	D-F3	PD	F3 Orifice	Fig.5.48	14.6	kPa	0.63%FS
93	Diff.P.	D-F17	PD	F17 Venturi	Fig.5.49	98.1	kPa	0.63%FS
94	Diff.P.	D-F18	PD	F18 Venturi	Fig.5.51	98.1	kPa	0.63%FS
95	Diff.P.	D-F19	PD	F19 Orifice	Fig.5.52	147.	kPa	0.63%FS
96	Diff.P.	D-F20	PD	F20 Orifice	Fig.5.53	13.2	kPa	0.63%FS
97	Diff.P.	D-F21	PD	F21 Orifice	Fig.5.54	147.	kPa	0.63%FS
98	Diff.P.	D-F22	PD	F22 Orifice	Fig.5.55	13.2	kPa	0.63%FS
99	Diff.P.	D-F27	PD	F27 Venturi	Fig.5.56	200.	kPa	0.63%FS
100	Diff.P.	D-F28	PD	F28 Venturi	Fig.5.57	200.	kPa	0.63%FS

Table 3.2 Measurement List for RUN 928 (Continued)

Ch.	Item	Symbol	ID.	Location	Fig.No.	Range	Unit	Accuracy
101	Power	W-1	WE 101	2100 kW Power Supplier	Fig.5.58	0.0	0.210E+04 kW	1.00XFS
102	Power	W-2	WE 102	3150 kW Power Supplier	Fig.5.58	0.0	0.315E+04 kW	1.00XFS
103								
104	Rev.	N-1	SR 104	MRP-1 Revolution	Failure	0.0	0.500E+04 RPM	1.08XFS
105	Rev.	N-2	SR 105	MRP-2 Revolution	Failure	0.0	0.500E+04 RPM	1.08XFS
106	Signal	S-1	EV 106	Break Signal A	Fig.5.59			
107	Signal	S-2	EV 107	Break Signal B	Fig.5.59			
108	Signal	S-3	EV 108	QSV Signal	Not used			
109	Signal	S-6	EV 109	HPCS Valve	Fig.5.60			
110	Signal	S-7	EV 110	LPCS Valve	Fig.5.60			
111	Signal	S-8	EV 111	LPCI Valve	Fig.5.60			
112	Signal	S-9	EV 112	Feedwater Control	Fig.5.59			
113	Signal	S-10	EV 113	MSIV Signal	Fig.5.59			
114	Signal	S-11	EV 114	Steam Line Valve	Fig.5.59			
115	Signal	S-12	EV 115	ADS Valve	Fig.5.60			
116	Signal	S-13	EV 116	MRP-1 Power OFF	Fig.5.61			
117	Signal	S-14	EV 117	MRP-2 Power OFF	Fig.5.61			
118	Signal	RD-1	EV 118	MRP-1 Rev. Direction	Fig.5.61			
119	Signal	RD-2	EV 119	MRP-2 Rev. Direction	Fig.5.61			
120	Density	DF-1	DE 120	JP1,2 Outlet Beam A	Fig.5.62	0.0	0.100E+04 kg/m <sup>3</sup>	1.00XFS
121	Density	DF-2	DE 121	JP1,2 Outlet Beam B	Fig.5.63	0.0	0.100E+04 kg/m <sup>3</sup>	1.00XFS
122	Density	DF-3	DE 122	JP1,2 Outlet Beam C	Fig.5.64	0.0	0.100E+04 kg/m <sup>3</sup>	1.00XFS
123	Density	DF-4	DE 123	JP3,4 Outlet Beam A	Fig.5.65	0.0	0.100E+04 kg/m <sup>3</sup>	1.00XFS
124	Density	DF-5	DE 124	JP3,4 Outlet Beam B	Fig.5.66	0.0	0.100E+04 kg/m <sup>3</sup>	1.00XFS
125	Density	DF-6	DE 125	JP3,4 Outlet Beam C	Fig.5.67	0.0	0.100E+04 kg/m <sup>3</sup>	1.00XFS
126	Density	DF-7	DE 126	Break A	Fig.5.68	0.0	0.100E+04 kg/m <sup>3</sup>	1.00XFS
127	Density	DF-8	DE 127	Break B	Fig.5.69	0.0	0.100E+04 kg/m <sup>3</sup>	1.00XFS
128	Density	DF-9	DE 128	Beam A	Fig.5.70	0.0	0.100E+04 kg/m <sup>3</sup>	1.00XFS
129	Density	DF-10	DE 129	Beam B	Fig.5.71	0.0	0.100E+04 kg/m <sup>3</sup>	1.00XFS
130	Mo.Flux	M-1	MF 130	Beam B	Fig.5.72	0.0	0.220E+05 kg/ms <sup>2</sup>	1.00XFS
131	Mo.Flux	M-2	MF 131	JP1,2 Outlet Spool	Fig.5.73	0.0	0.220E+05 kg/ms <sup>2</sup>	1.00XFS
132	Mo.Flux	M-3	MF 132	JP3,4 Outlet Spool	Fig.5.73	0.0	0.220E+05 kg/ms <sup>2</sup>	1.00XFS
133	Mo.Flux	M-4	MF 133	Break A (Low Range)	Fig.5.74	0.0	0.220E+05 kg/ms <sup>2</sup>	1.00XFS
134	Mo.Flux	M-5	MF 134	Break B (Low Range)	NOT MEASURED	0.0	0.220E+05 kg/ms <sup>2</sup>	1.00XFS
135	Mo.Flux	M-6	MF 135	Break A (High Range)	Fig.5.75	0.0	0.220E+06 kg/ms <sup>2</sup>	1.00XFS
136	Mo.Flux	M-7	MF 136	Break B (High Range)	Fig.5.76	0.0	0.220E+06 kg/ms <sup>2</sup>	1.00XFS
137				Break Orifice	Not Measured	0.0	0.220E+05 kg/ms <sup>2</sup>	1.00XFS
138	Fluid T.	T-1	TE 138	Lower Plenum	Fig.5.77	273.	673.	0.64XFS
139	Fluid T.	T-2	TE 139	Upper Plenum	Fig.5.77	273.	673.	0.64XFS
140	Fluid T.	T-3	TE 140	Steam Dome	Fig.5.78	273.	673.	0.64XFS
141	Fluid T.	T-4	TE 141	Upper Downcomer	Fig.5.79	273.	673.	0.64XFS
142	Fluid T.	T-5	TE 142	Lower Downcomer	Fig.5.79	273.	673.	0.64XFS
143	Fluid T.	T-6	TE 143	JP-1 Drive	Fig.5.80	273.	673.	0.64XFS
144	Fluid T.	T-7	TE 144	JP-2 Drive	Fig.5.80	273.	673.	0.64XFS
145	Fluid T.	T-8	TE 145	JP-3 Drive	Fig.5.81	273.	673.	0.64XFS
146	Fluid T.	T-9	TE 146	JP-4 Drive	Fig.5.81	273.	673.	0.64XFS
147	Fluid T.	T-10	TE 147	JP-1 Discharge	Fig.5.82	273.	673.	0.64XFS
148	Fluid T.	T-11	TE 148	JP-2 Discharge	Fig.5.82	273.	673.	0.64XFS
149	Fluid T.	T-12	TE 149	JP-3 Discharge	Fig.5.83	273.	673.	0.64XFS
150	Fluid T.	T-13	TE 150	JP-4 Discharge	Fig.5.83	273.	673.	0.64XFS

Table 3.2 Measurement List for RUN 928 (Continued)

151Ch.- 200Ch.

Ch.	Item	Symbol	ID.	Location	Fig.No.	Range	Unit	Accuracy
151	Fluid T.	T-14	TE 151	MRP-1 Suction	Fig.5-80	273.	K	0.64%FS
152	Fluid T.	T-15	TE 152	MRP-1 Delivery	Fig.5-80	273.	K	0.64%FS
153	Fluid T.	T-16	TE 153	MRP-2 Suction	Fig.5-81	273.	K	0.64%FS
154	Fluid T.	T-17	TE 154	MRP-2 Delivery	Fig.5-81	273.	K	0.64%FS
155	Fluid T.	T-18	TE 155	Break A Upstream	Fig.5-84	273.	K	0.64%FS
156	Fluid T.	T-19	TE 156	Break B Upstream	Fig.5-84	273.	K	0.64%FS
157	Fluid T.	T-20	TE 157	RCN A Condensed Water	Not Used	273.	K	0.64%FS
158	Fluid T.	T-21	TE 158	RCN B Condensed Water	Not Used	273.	K	0.64%FS
159	Fluid T.	T-22	TE 159	Discharged Steam	Fig.5-78	273.	K	0.64%FS
160	Fluid T.	T-24	TE 160	JP-1,2 Outlet Spool	Fig.5-82	273.	K	0.64%FS
161	Fluid T.	T-25	TE 161	JP-3,4 Outlet Spool	Fig.5-83	273.	K	0.64%FS
162	Fluid T.	T-26	TE 162	Break A Spool Piece	Fig.5-84	273.	K	0.64%FS
163	Fluid T.	T-37	TE 163	Break B Spool Piece	Fig.5-84	273.	K	0.64%FS
164	Fluid T.	T-38	TE 164	Feedwater	Fig.5-85	273.	K	0.64%FS
165	Slab T.	TS-1	TE 165	Core Barrel C Pos.1	Not Measured	273.	K	0.64%FS
166	Slab T.	TS-2	TE 166	Core Barrel C Pos.2	Not Measured	273.	K	0.64%FS
167	Slab T.	TS-3	TE 167	Core Barrel C Pos.3	Not Measured	273.	K	0.64%FS
168	Slab T.	TS-4	TE 168	Core Barrel C Pos.4	Not Measured	273.	K	0.64%FS
169	Slab T.	TS-5	TE 169	Core Barrel C Pos.5	Not Measured	273.	K	0.64%FS
170	Slab T.	TS-6	TE 170	Core Barrel C Pos.6	Not Measured	273.	K	0.64%FS
171	Slab T.	TS-7	TE 171	Core Barrel A Pos.1	Not Measured	273.	K	0.64%FS
172	Slab T.	TS-8	TE 172	Core Barrel A Pos.2	Not Measured	273.	K	0.64%FS
173	Slab T.	TS-9	TE 173	Core Barrel A Pos.3	Not Measured	273.	K	0.64%FS
174	Slab T.	TS-10	TE 174	Core Barrel A Pos.4	Not Measured	273.	K	0.64%FS
175	Slab T.	TS-11	TE 175	Core Barrel A Pos.5	Not Measured	273.	K	0.64%FS
176	Slab T.	TS-12	TE 176	Core Barrel A Pos.6	Not Measured	273.	K	0.64%FS
177	Slab T.	TS-13	TE 177	Filler Block C Pos.1	Not Measured	273.	K	0.64%FS
178	Slab T.	TS-14	TE 178	Filler Block C Pos.2	Not Measured	273.	K	0.64%FS
179	Slab T.	TS-15	TE 179	Filler Block C Pos.3	Not Measured	273.	K	0.64%FS
180	Slab T.	TS-16	TE 180	Filler Block C Pos.4	Not Measured	273.	K	0.64%FS
181	Slab T.	TS-17	TE 181	Filler Block C Pos.5	Not Measured	273.	K	0.64%FS
182	Slab T.	TS-18	TE 182	Filler Block C Pos.6	Not Measured	273.	K	0.64%FS
183	Slab T.	TS-19	TE 183	Filler Block A Pos.1	Not Measured	273.	K	0.64%FS
184	Slab T.	TS-20	TE 184	Filler Block A Pos.2	Not Measured	273.	K	0.64%FS
185	Slab T.	TS-21	TE 185	Filler Block A Pos.3	Not Measured	273.	K	0.64%FS
186	Slab T.	TS-22	TE 186	Filler Block A Pos.4	Not Measured	273.	K	0.64%FS
187	Slab T.	TS-23	TE 187	Filler Block A Pos.5	Not Measured	273.	K	0.64%FS
188	Slab T.	TS-24	TE 188	Filler Block A Pos.6	Not Measured	273.	K	0.64%FS
189	Slab T.	TS-25	TE 189	JP-1 Diffuser Wall	Not Measured	273.	K	0.64%FS
190	Slab T.	TS-26	TE 190	JP-2 Diffuser Wall	Not Measured	273.	K	0.64%FS
191	Slab T.	TS-27	TE 191	JP-3 Diffuser Wall	Not Measured	273.	K	0.64%FS
192	Slab T.	TS-28	TE 192	JP-4 Diffuser Wall	Not Measured	273.	K	0.64%FS
193	Slab T.	TS-29	TE 193	PV Wall Inside 1-1	Not Measured	273.	K	0.64%FS
194	Slab T.	TS-30	TE 194	PV Inner Surface 1-2	Not Measured	273.	K	0.64%FS
195	Slab T.	TS-31	TE 195	PV Inner Surface 1-3	Not Measured	273.	K	0.64%FS
196	Slab T.	TS-32	TE 196	PV Wall Inside 2	Not Measured	273.	K	0.64%FS
197	Slab T.	TS-33	TE 197	PV Wall Inside 3	Not Measured	273.	K	0.64%FS
198	Slab T.	TS-34	TE 198	PV Wall Inside 4	Not Measured	273.	K	0.64%FS
199	Slab T.	TS-35	TE 199	L.P. Inner Surface	Not Measured	273.	K	0.64%FS
200	Slab T.	TS-36	TE 200	L.P. Wall Inside	Not Measured	273.	K	0.64%FS

Table 3.2 Measurement List for RUN 928 (Continued)

201Ch.- 250Ch.

Ch.	Item	Symbol	ID.	Location	Fig.No.	Range	Unit	Accuracy
201	Temp.	TF- 1	TE 201	A11 Fuel Rod Pos.1	Fig.5.86, 145	273.	0.147E+04 K	0.64%FS
202	Temp.	TF- 2	TE 202	A11 Fuel Rod Pos.2	Fig.5.86, 146	273.	0.147E+04 K	0.64%FS
203	Temp.	TF- 3	TE 203	A11 Fuel Rod Pos.3	Fig.5.86, 147	273.	0.147E+04 K	0.64%FS
204	Temp.	TF- 4	TE 204	A11 Fuel Rod Pos.4	Fig.5.86, 148	273.	0.147E+04 K	0.64%FS
205	Temp.	TF- 5	TE 205	A11 Fuel Rod Pos.5	Fig.5.86, 149	273.	0.147E+04 K	0.64%FS
206	Temp.	TF- 6	TE 206	A11 Fuel Rod Pos.6	Fig.5.86, 150	273.	0.147E+04 K	0.64%FS
207	Temp.	TF- 7	TE 207	A11 Fuel Rod Pos.7	Fig.5.86, 151	273.	0.147E+04 K	0.64%FS
208	Temp.	TF- 8	TE 208	A12 Fuel Rod Pos.1	Fig.5.87, 145	273.	0.147E+04 K	0.64%FS
209	Temp.	TF- 9	TE 209	A12 Fuel Rod Pos.2	Fig.5.87, 146	273.	0.147E+04 K	0.64%FS
210	Temp.	TF- 10	TE 210	A12 Fuel Rod Pos.3	Fig.5.87, 147	273.	0.147E+04 K	0.64%FS
211	Temp.	TF- 11	TE 211	A12 Fuel Rod Pos.4	Fig.5.87, 148	273.	0.147E+04 K	0.64%FS
212	Temp.	TF- 12	TE 212	A12 Fuel Rod Pos.5	Fig.5.87, 149	273.	0.147E+04 K	0.64%FS
213	Temp.	TF- 13	TE 213	A12 Fuel Rod Pos.6	Fig.5.87, 150	273.	0.147E+04 K	0.64%FS
214	Temp.	TF- 14	TE 214	A12 Fuel Rod Pos.7	Fig.5.87, 151	273.	0.147E+04 K	0.64%FS
215	Temp.	TF- 15	TE 215	A13 Fuel Rod Pos.1	Fig.5.88, 145	273.	0.147E+04 K	0.64%FS
216	Temp.	TF- 16	TE 216	A13 Fuel Rod Pos.2	Fig.5.88, 146	273.	0.147E+04 K	0.64%FS
217	Temp.	TF- 17	TE 217	A13 Fuel Rod Pos.3	Fig.5.88, 147	273.	0.147E+04 K	0.64%FS
218	Temp.	TF- 18	TE 218	A13 Fuel Rod Pos.4	Fig.5.88, 148	273.	0.147E+04 K	0.64%FS
219	Temp.	TF- 19	TE 219	A13 Fuel Rod Pos.5	Fig.5.88, 149	273.	0.147E+04 K	0.64%FS
220	Temp.	TF- 20	TE 220	A13 Fuel Rod Pos.6	FAILURE	273.	0.147E+04 K	0.64%FS
221	Temp.	TF- 21	TE 221	A13 Fuel Rod Pos.7	Fig.5.88, 151	273.	0.147E+04 K	0.64%FS
222	Temp.	TF- 22	TE 222	A14 Fuel Rod Pos.1	Fig.5.89	273.	0.147E+04 K	0.64%FS
223	Temp.	TF- 23	TE 223	A14 Fuel Rod Pos.2	Fig.5.89	273.	0.147E+04 K	0.64%FS
224	Temp.	TF- 24	TE 224	A14 Fuel Rod Pos.3	Fig.5.89	273.	0.147E+04 K	0.64%FS
225	Temp.	TF- 25	TE 225	A14 Fuel Rod Pos.4	Fig.5.89	273.	0.147E+04 K	0.64%FS
226	Temp.	TF- 26	TE 226	A14 Fuel Rod Pos.5	Fig.5.89	273.	0.147E+04 K	0.64%FS
227	Temp.	TF- 27	TE 227	A14 Fuel Rod Pos.6	Fig.5.89	273.	0.147E+04 K	0.64%FS
228	Temp.	TF- 28	TE 228	A14 Fuel Rod Pos.7	FAILURE	273.	0.147E+04 K	0.64%FS
229	Temp.	TF- 29	TE 229	A15 Fuel Rod Pos.1	Fig.5.119	273.	0.147E+04 K	0.64%FS
230	Temp.	TF- 30	TE 230	A15 Fuel Rod Pos.4	Fig.5.119	273.	0.147E+04 K	0.64%FS
231	Temp.	TF- 31	TE 231	A17 Fuel Rod Pos.1	Fig.5.120	273.	0.147E+04 K	0.64%FS
232	Temp.	TF- 32	TE 232	A17 Fuel Rod Pos.4	Fig.5.120	273.	0.147E+04 K	0.64%FS
233	Temp.	TF- 33	TE 233	A22 Fuel Rod Pos.1	Fig.5.90, 152	273.	0.147E+04 K	0.64%FS
234	Temp.	TF- 34	TE 234	A22 Fuel Rod Pos.2	Fig.5.90, 153	273.	0.147E+04 K	0.64%FS
235	Temp.	TF- 35	TE 235	A22 Fuel Rod Pos.3	Fig.5.90, 154	273.	0.147E+04 K	0.64%FS
236	Temp.	TF- 36	TE 236	A22 Fuel Rod Pos.4	Fig.5.90, 155	273.	0.125E+04 K	0.64%FS
237	Temp.	TF- 37	TE 237	A22 Fuel Rod Pos.5	Fig.5.90, 156	273.	0.125E+04 K	0.64%FS
238	Temp.	TF- 38	TE 238	A22 Fuel Rod Pos.6	Fig.5.90, 157	273.	0.125E+04 K	0.64%FS
239	Temp.	TF- 39	TE 239	A22 Fuel Rod Pos.7	Fig.5.90, 158	273.	0.125E+04 K	0.64%FS
240	Temp.	TF- 40	TE 240	A24 Fuel Rod Pos.1	Fig.5.91	273.	0.125E+04 K	0.64%FS
241	Temp.	TF- 41	TE 241	A24 Fuel Rod Pos.2	Fig.5.91	273.	0.125E+04 K	0.64%FS
242	Temp.	TF- 42	TE 242	A24 Fuel Rod Pos.3	Fig.5.91	273.	0.125E+04 K	0.64%FS
243	Temp.	TF- 43	TE 243	A24 Fuel Rod Pos.4	Fig.5.91	273.	0.125E+04 K	0.64%FS
244	Temp.	TF- 44	TE 244	A24 Fuel Rod Pos.5	Fig.5.91	273.	0.125E+04 K	0.64%FS
245	Temp.	TF- 45	TE 245	A24 Fuel Rod Pos.6	Fig.5.91	273.	0.125E+04 K	0.64%FS
246	Temp.	TF- 46	TE 246	A24 Fuel Rod Pos.7	Fig.5.91	273.	0.125E+04 K	0.64%FS
247	Temp.	TF- 47	TE 247	A26 Fuel Rod Pos.1	Fig.5.121	273.	0.125E+04 K	0.64%FS
248	Temp.	TF- 48	TE 248	A26 Fuel Rod Pos.2	Fig.5.121	273.	0.125E+04 K	0.64%FS
249	Temp.	TF- 49	TE 249	A28 Fuel Rod Pos.1	Fig.5.122	273.	0.125E+04 K	0.64%FS
250	Temp.	TF- 50	TE 250	A28 Fuel Rod Pos.4	Fig.5.122	273.	0.125E+04 K	0.64%FS

Table 3.2 Measurement List for RUN 928 (Continued)

251Ch. - 300Ch.

Ch.	Item	Symbol	ID.	Location	Fig.No.	Range	Unit	Accuracy
251	Temp.	TF-51	TE 251	A31 Fuel Rod Pos.1	Fig.5.123	273.	0.125E+04 K	0.64%FS
252	Temp.	TF-52	TE 252	A31 Fuel Rod Pos.4	Fig.5.123	273.	0.125E+04 K	0.64%FS
253	Temp.	TF-53	TE 253	A33 Fuel Rod Pos.1	Fig.5.92	273.	0.125E+04 K	0.64%FS
254	Temp.	TF-54	TE 254	A33 Fuel Rod Pos.2	Fig.5.92	273.	0.125E+04 K	0.64%FS
255	Temp.	TF-55	TE 255	A33 Fuel Rod Pos.3	Fig.5.92	273.	0.125E+04 K	0.64%FS
256	Temp.	TF-56	TE 256	A33 Fuel Rod Pos.4	Fig.5.92	273.	0.125E+04 K	0.64%FS
257	Temp.	TF-57	TE 257	A33 Fuel Rod Pos.5	Fig.5.92	273.	0.125E+04 K	0.64%FS
258	Temp.	TF-58	TE 258	A33 Fuel Rod Pos.6	Fig.5.92	273.	0.125E+04 K	0.64%FS
259	Temp.	TF-59	TE 259	A33 Fuel Rod Pos.7	Fig.5.92	273.	0.125E+04 K	0.64%FS
260	Temp.	TF-60	TE 260	A34 Fuel Rod Pos.1	Fig.5.93	273.	0.125E+04 K	0.64%FS
261	Temp.	TF-61	TE 261	A34 Fuel Rod Pos.2	Fig.5.93	273.	0.125E+04 K	0.64%FS
262	Temp.	TF-62	TE 262	A34 Fuel Rod Pos.3	Fig.5.93	273.	0.125E+04 K	0.64%FS
263	Temp.	TF-63	TE 263	A34 Fuel Rod Pos.4	Fig.5.93	273.	0.125E+04 K	0.64%FS
264	Temp.	TF-64	TE 264	A34 Fuel Rod Pos.5	Fig.5.93	273.	0.125E+04 K	0.64%FS
265	Temp.	TF-65	TE 265	A34 Fuel Rod Pos.6	Fig.5.93	273.	0.125E+04 K	0.64%FS
266	Temp.	TF-66	TE 266	A34 Fuel Rod Pos.7	Fig.5.93	273.	0.125E+04 K	0.64%FS
267	Temp.	TF-67	TE 267	A37 Fuel Rod Pos.1	Fig.5.124	273.	0.125E+04 K	0.64%FS
268	Temp.	TF-68	TE 268	A37 Fuel Rod Pos.4	Fig.5.124	273.	0.125E+04 K	0.64%FS
269	Temp.	TF-69	TE 269	A42 Fuel Rod Pos.1	Fig.5.125	273.	0.125E+04 K	0.64%FS
270	Temp.	TF-70	TE 270	A42 Fuel Rod Pos.4	Fig.5.125	273.	0.125E+04 K	0.64%FS
271	Temp.	TF-71	TE 271	A44 Fuel Rod Pos.1	Fig.5.94	273.	0.125E+04 K	0.64%FS
272	Temp.	TF-72	TE 272	A44 Fuel Rod Pos.2	Fig.5.94	273.	0.125E+04 K	0.64%FS
273	Temp.	TF-73	TE 273	A44 Fuel Rod Pos.3	Fig.5.94	273.	0.125E+04 K	0.64%FS
274	Temp.	TF-74	TE 274	A44 Fuel Rod Pos.4	Fig.5.94	273.	0.125E+04 K	0.64%FS
275	Temp.	TF-75	TE 275	A44 Fuel Rod Pos.5	Fig.5.94	273.	0.125E+04 K	0.64%FS
276	Temp.	TF-76	TE 276	A44 Fuel Rod Pos.6	Fig.5.94	273.	0.125E+04 K	0.64%FS
277	Temp.	TF-77	TE 277	A44 Fuel Rod Pos.7	Fig.5.94	273.	0.125E+04 K	0.64%FS
278	Temp.	TF-78	TE 278	A48 Fuel Rod Pos.1	Fig.5.126	273.	0.125E+04 K	0.64%FS
279	Temp.	TF-79	TE 279	A48 Fuel Rod Pos.4	Fig.5.126	273.	0.125E+04 K	0.64%FS
280	Temp.	TF-80	TE 280	A51 Fuel Rod Pos.1	Fig.5.127	273.	0.125E+04 K	0.64%FS
281	Temp.	TF-81	TE 281	A51 Fuel Rod Pos.4	Fig.5.127	273.	0.125E+04 K	0.64%FS
282	Temp.	TF-82	TE 282	A53 Fuel Rod Pos.1	Fig.5.128	273.	0.125E+04 K	0.64%FS
283	Temp.	TF-83	TE 283	A53 Fuel Rod Pos.4	Fig.5.128	273.	0.125E+04 K	0.64%FS
284	Temp.	TF-84	TE 284	A57 Fuel Rod Pos.1	Fig.5.129	273.	0.125E+04 K	0.64%FS
285	Temp.	TF-85	TE 285	A57 Fuel Rod Pos.4	Fig.5.129	273.	0.125E+04 K	0.64%FS
286	Temp.	TF-86	TE 286	A62 Fuel Rod Pos.1	Fig.5.130	273.	0.125E+04 K	0.64%FS
287	Temp.	TF-87	TE 287	A62 Fuel Rod Pos.4	Fig.5.130	273.	0.125E+04 K	0.64%FS
288	Temp.	TF-88	TE 288	A66 Fuel Rod Pos.1	Fig.5.131	273.	0.125E+04 K	0.64%FS
289	Temp.	TF-89	TE 289	A66 Fuel Rod Pos.4	Fig.5.131	273.	0.125E+04 K	0.64%FS
290	Temp.	TF-90	TE 290	A68 Fuel Rod Pos.1	Fig.5.132	273.	0.125E+04 K	0.64%FS
291	Temp.	TF-91	TE 291	A68 Fuel Rod Pos.4	Fig.5.132	273.	0.125E+04 K	0.64%FS
292	Temp.	TF-92	TE 292	A71 Fuel Rod Pos.1	Fig.5.133	273.	0.125E+04 K	0.64%FS
293	Temp.	TF-93	TE 293	A71 Fuel Rod Pos.4	Fig.5.133	273.	0.125E+04 K	0.64%FS
294	Temp.	TF-94	TE 294	A73 Fuel Rod Pos.1	Fig.5.134	273.	0.125E+04 K	0.64%FS
295	Temp.	TF-95	TE 295	A73 Fuel Rod Pos.4	Fig.5.134	273.	0.125E+04 K	0.64%FS
296	Temp.	TF-96	TE 296	A75 Fuel Rod Pos.1	Fig.5.135	273.	0.125E+04 K	0.64%FS
297	Temp.	TF-97	TE 297	A75 Fuel Rod Pos.4	Fig.5.135	273.	0.125E+04 K	0.64%FS
298	Temp.	TF-98	TE 298	A77 Fuel Rod Pos.1	Fig.5.95, 159	273.	0.125E+04 K	0.64%FS
299	Temp.	TF-99	TE 299	A77 Fuel Rod Pos.2	Fig.5.95, 160	273.	0.125E+04 K	0.64%FS
300	Temp.	TF-100	TE 300	A77 Fuel Rod Pos.3	Fig.5.95, 161	273.	0.125E+04 K	0.64%FS

Table 3.2 Measurement List for RUN 928 (Continued)

Ch.	Item	Symbol	ID.	Location	Fig.No.	Range	Unit	Accuracy
301	Temp.	TF-101	TE 301	A77 Fuel Rod Pos.4	Fig.5.95, 162	273.	0.125E+04 K	0.64%FS
302	Temp.	TF-102	TE 302	A77 Fuel Rod Pos.5	Fig.5.95, 163	273.	0.125E+04 K	0.64%FS
303	Temp.	TF-103	TE 303	A77 Fuel Rod Pos.6	Fig.5.95, 164	273.	0.125E+04 K	0.64%FS
304	Temp.	TF-104	TE 304	A77 Fuel Rod Pos.7	Failure	273.	0.125E+04 K	0.64%FS
305	Temp.	TF-105	TE 305	A82 Fuel Rod Pos.1	Fig.5.136	273.	0.125E+04 K	0.64%FS
306	Temp.	TF-106	TE 306	A82 Fuel Rod Pos.4	Failure	273.	0.125E+04 K	0.64%FS
307	Temp.	TF-107	TE 307	A84 Fuel Rod Pos.1	Fig.5.137	273.	0.125E+04 K	0.64%FS
308	Temp.	TF-108	TE 308	A84 Fuel Rod Pos.4	Fig.5.137	273.	0.125E+04 K	0.64%FS
309	Temp.	TF-109	TE 309	A85 Fuel Rod Pos.1	Fig.5.96	273.	0.125E+04 K	0.64%FS
310	Temp.	TF-110	TE 310	A85 Fuel Rod Pos.2	Fig.5.96	273.	0.125E+04 K	0.64%FS
311	Temp.	TF-111	TE 311	A85 Fuel Rod Pos.3	Fig.5.96	273.	0.125E+04 K	0.64%FS
312	Temp.	TF-112	TE 312	A85 Fuel Rod Pos.4	Fig.5.96	273.	0.125E+04 K	0.64%FS
313	Temp.	TF-113	TE 313	A85 Fuel Rod Pos.5	Fig.5.96	273.	0.125E+04 K	0.64%FS
314	Temp.	TF-114	TE 314	A85 Fuel Rod Pos.6	Fig.5.96	273.	0.125E+04 K	0.64%FS
315	Temp.	TF-115	TE 315	A85 Fuel Rod Pos.7	Fig.5.96	273.	0.125E+04 K	0.64%FS
316	Temp.	TF-116	TE 316	A87 Fuel Rod Pos.1	Fig.5.97, 145	273.	0.125E+04 K	0.64%FS
317	Temp.	TF-117	TE 317	A87 Fuel Rod Pos.2	Fig.5.97, 146	273.	0.125E+04 K	0.64%FS
318	Temp.	TF-118	TE 318	A87 Fuel Rod Pos.3	Fig.5.97, 147	273.	0.125E+04 K	0.64%FS
319	Temp.	TF-119	TE 319	A87 Fuel Rod Pos.4	Fig.5.97, 148	273.	0.125E+04 K	0.64%FS
320	Temp.	TF-120	TE 320	A87 Fuel Rod Pos.5	Fig.5.97, 149	273.	0.125E+04 K	0.64%FS
321	Temp.	TF-121	TE 321	A87 Fuel Rod Pos.6	Fig.5.97, 150	273.	0.125E+04 K	0.64%FS
322	Temp.	TF-122	TE 322	A87 Fuel Rod Pos.7	Fig.5.97, 151	273.	0.125E+04 K	0.64%FS
323	Temp.	TF-123	TE 323	A88 Fuel Rod Pos.1	Fig.5.98, 145	273.	0.125E+04 K	0.64%FS
324	Temp.	TF-124	TE 324	A88 Fuel Rod Pos.2	Fig.5.98, 146	273.	0.125E+04 K	0.64%FS
325	Temp.	TF-125	TE 325	A88 Fuel Rod Pos.3	Fig.5.98, 147	273.	0.125E+04 K	0.64%FS
326	Temp.	TF-126	TE 326	A88 Fuel Rod Pos.4	Fig.5.98, 148	273.	0.125E+04 K	0.64%FS
327	Temp.	TF-127	TE 327	A88 Fuel Rod Pos.5	Fig.5.98, 149	273.	0.125E+04 K	0.64%FS
328	Temp.	TF-128	TE 328	A88 Fuel Rod Pos.6	Fig.5.98, 150	273.	0.125E+04 K	0.64%FS
329	Temp.	TF-129	TE 329	A88 Fuel Rod Pos.7	Fig.5.98, 151	273.	0.125E+04 K	0.64%FS
330	Temp.	TF-130	TE 330	B11 Fuel Rod Pos.1	Fig.5.99	273.	0.125E+04 K	0.64%FS
331	Temp.	TF-131	TE 331	B11 Fuel Rod Pos.2	Fig.5.99	273.	0.125E+04 K	0.64%FS
332	Temp.	TF-132	TE 332	B11 Fuel Rod Pos.3	Fig.5.99	273.	0.125E+04 K	0.64%FS
333	Temp.	TF-133	TE 333	B11 Fuel Rod Pos.4	Fig.5.99	273.	0.125E+04 K	0.64%FS
334	Temp.	TF-134	TE 334	B11 Fuel Rod Pos.5	Fig.5.99	273.	0.125E+04 K	0.64%FS
335	Temp.	TF-135	TE 335	B11 Fuel Rod Pos.6	Fig.5.99	273.	0.125E+04 K	0.64%FS
336	Temp.	TF-136	TE 336	B11 Fuel Rod Pos.7	Failure	273.	0.125E+04 K	0.64%FS
337	Temp.	TF-137	TE 337	B13 Fuel Rod Pos.4	Fig.5.138	273.	0.125E+04 K	0.64%FS
338	Temp.	TF-138	TE 338	B22 Fuel Rod Pos.1	Fig.5.100, 152	273.	0.125E+04 K	0.64%FS
339	Temp.	TF-139	TE 339	B22 Fuel Rod Pos.2	Fig.5.100, 153	273.	0.125E+04 K	0.64%FS
340	Temp.	TF-140	TE 340	B22 Fuel Rod Pos.3	Fig.5.100, 154	273.	0.125E+04 K	0.64%FS
341	Temp.	TF-141	TE 341	B22 Fuel Rod Pos.4	Fig.5.100, 155	273.	0.125E+04 K	0.64%FS
342	Temp.	TF-142	TE 342	B22 Fuel Rod Pos.5	Fig.5.100, 156	273.	0.125E+04 K	0.64%FS
343	Temp.	TF-143	TE 343	B22 Fuel Rod Pos.6	Fig.5.100, 157	273.	0.125E+04 K	0.64%FS
344	Temp.	TF-144	TE 344	B22 Fuel Rod Pos.7	Fig.5.100, 158	273.	0.125E+04 K	0.64%FS
345	Temp.	TF-145	TE 345	B33 Fuel Rod Pos.4	Fig.5.138	273.	0.125E+04 K	0.64%FS
346	Temp.	TF-146	TE 346	B33 Fuel Rod Pos.4	Fig.5.139	273.	0.125E+04 K	0.64%FS
347	Temp.	TF-147	TE 347	B51 Fuel Rod Pos.4	Fig.5.140	273.	0.125E+04 K	0.64%FS
348	Temp.	TF-148	TE 348	B53 Fuel Rod Pos.4	Fig.5.139	273.	0.125E+04 K	0.64%FS
349	Temp.	TF-149	TE 349	B66 Fuel Rod Pos.4	Fig.5.139	273.	0.125E+04 K	0.64%FS
350	Temp.	TF-150	TE 350	B77 Fuel Rod Pos.1	Fig.5.101, 159	273.	0.125E+04 K	0.64%FS



Table 3.2 Measurement List for RUN 928 (Continued)

Ch.	Item	Symbol	ID.	Location	Fig.No.	Range	Unit	Accuracy
351	Temp.	TF-151	TE 351	877 Fuel Rod Pos.2	Fig.5.101, 160	273.	0.125E+04 K	0.64XFS
352	Temp.	TF-152	TE 352	877 Fuel Rod Pos.3	Fig.5.101, 161	273.	0.125E+04 K	0.64XFS
353	Temp.	TF-153	TE 353	877 Fuel Rod Pos.4	Fig.5.101, 162	273.	0.125E+04 K	0.64XFS
354	Temp.	TF-154	TE 354	877 Fuel Rod Pos.5	Fig.5.101, 163	273.	0.125E+04 K	0.64XFS
355	Temp.	TF-155	TE 355	877 Fuel Rod Pos.6	Fig.5.101, 164	273.	0.125E+04 K	0.64XFS
356	Temp.	TF-156	TE 356	877 Fuel Rod Pos.7	Fig.5.101, 165	273.	0.125E+04 K	0.64XFS
357	Temp.	TF-157	TE 357	886 Fuel Rod Pos.4	Fig.5.138	273.	0.125E+04 K	0.64XFS
358	Temp.	TF-158	TE 358	C11 Fuel Rod Pos.1	Fig.5.102	273.	0.125E+04 K	0.64XFS
359	Temp.	TF-159	TE 359	C11 Fuel Rod Pos.2	Fig.5.102	273.	0.125E+04 K	0.64XFS
360	Temp.	TF-160	TE 360	C11 Fuel Rod Pos.3	Fig.5.102	273.	0.125E+04 K	0.64XFS
361	Temp.	TF-161	TE 361	C11 Fuel Rod Pos.4	Fig.5.102	273.	0.125E+04 K	0.64XFS
362	Temp.	TF-162	TE 362	C11 Fuel Rod Pos.5	Fig.5.102	273.	0.125E+04 K	0.64XFS
363	Temp.	TF-163	TE 363	C11 Fuel Rod Pos.6	Fig.5.102	273.	0.125E+04 K	0.64XFS
364	Temp.	TF-164	TE 364	C11 Fuel Rod Pos.7	Fig.5.102	273.	0.125E+04 K	0.64XFS
365	Temp.	TF-165	TE 365	C13 Fuel Rod Pos.1	Fig.5.103	273.	0.125E+04 K	0.64XFS
366	Temp.	TF-166	TE 366	C13 Fuel Rod Pos.2	Fig.5.103	273.	0.125E+04 K	0.64XFS
367	Temp.	TF-167	TE 367	C13 Fuel Rod Pos.3	Fig.5.103	273.	0.125E+04 K	0.64XFS
368	Temp.	TF-168	TE 368	C13 Fuel Rod Pos.4	Fig.5.103	273.	0.125E+04 K	0.64XFS
369	Temp.	TF-169	TE 369	C13 Fuel Rod Pos.5	Fig.5.103	273.	0.125E+04 K	0.64XFS
370	Temp.	TF-170	TE 370	C13 Fuel Rod Pos.6	Fig.5.103	273.	0.125E+04 K	0.64XFS
371	Temp.	TF-171	TE 371	C13 Fuel Rod Pos.7	Fig.5.103	273.	0.125E+04 K	0.64XFS
372	Temp.	TF-172	TE 372	C15 Fuel Rod Pos.4	Fig.5.140	273.	0.125E+04 K	0.64XFS
373	Temp.	TF-173	TE 373	C22 Fuel Rod Pos.1	Fig.5.104, 152	273.	0.125E+04 K	0.64XFS
374	Temp.	TF-174	TE 374	C22 Fuel Rod Pos.2	Fig.5.104, 153	273.	0.125E+04 K	0.64XFS
375	Temp.	TF-175	TE 375	C22 Fuel Rod Pos.3	Fig.5.104, 154	273.	0.125E+04 K	0.64XFS
376	Temp.	TF-176	TE 376	C22 Fuel Rod Pos.4	Fig.5.104, 155	273.	0.125E+04 K	0.64XFS
377	Temp.	TF-177	TE 377	C22 Fuel Rod Pos.5	Fig.5.104, 156	273.	0.125E+04 K	0.64XFS
378	Temp.	TF-178	TE 378	C22 Fuel Rod Pos.6	Fig.5.104, 157	273.	0.125E+04 K	0.64XFS
379	Temp.	TF-179	TE 379	C22 Fuel Rod Pos.7	Fig.5.104, 158	273.	0.125E+04 K	0.64XFS
380	Temp.	TF-180	TE 380	C31 Fuel Rod Pos.4	Fig.5.141	273.	0.125E+04 K	0.64XFS
381	Temp.	TF-181	TE 381	C33 Fuel Rod Pos.1	Fig.5.105	273.	0.125E+04 K	0.64XFS
382	Temp.	TF-182	TE 382	C33 Fuel Rod Pos.2	Fig.5.105	273.	0.125E+04 K	0.64XFS
383	Temp.	TF-183	TE 383	C33 Fuel Rod Pos.3	Fig.5.105	273.	0.125E+04 K	0.64XFS
384	Temp.	TF-184	TE 384	C33 Fuel Rod Pos.4	Fig.5.105	273.	0.125E+04 K	0.64XFS
385	Temp.	TF-185	TE 385	C33 Fuel Rod Pos.5	Fig.5.105	273.	0.125E+04 K	0.64XFS
386	Temp.	TF-186	TE 386	C33 Fuel Rod Pos.6	Fig.5.105	273.	0.125E+04 K	0.64XFS
387	Temp.	TF-187	TE 387	C33 Fuel Rod Pos.7	Fig.5.105	273.	0.125E+04 K	0.64XFS
388	Temp.	TF-188	TE 388	C35 Fuel Rod Pos.4	Fig.5.142	273.	0.125E+04 K	0.64XFS
389	Temp.	TF-189	TE 389	C66 Fuel Rod Pos.4	Fig.5.142	273.	0.125E+04 K	0.64XFS
390	Temp.	TF-190	TE 390	C68 Fuel Rod Pos.4	Fig.5.141	273.	0.125E+04 K	0.64XFS
391	Temp.	TF-191	TE 391	C77 Fuel Rod Pos.1	Fig.5.106, 159	273.	0.125E+04 K	0.64XFS
392	Temp.	TF-192	TE 392	C77 Fuel Rod Pos.2	Fig.5.106, 160	273.	0.125E+04 K	0.64XFS
393	Temp.	TF-193	TE 393	C77 Fuel Rod Pos.3	Fig.5.106, 161	273.	0.125E+04 K	0.64XFS
394	Temp.	TF-194	TE 394	C77 Fuel Rod Pos.4	Fig.5.106, 162	273.	0.125E+04 K	0.64XFS
395	Temp.	TF-195	TE 395	C77 Fuel Rod Pos.5	Fig.5.106, 163	273.	0.125E+04 K	0.64XFS
396	Temp.	TF-196	TE 396	C77 Fuel Rod Pos.6	Fig.5.106, 164	273.	0.125E+04 K	0.64XFS
397	Temp.	TF-197	TE 397	C77 Fuel Rod Pos.7	Fig.5.106, 165	273.	0.125E+04 K	0.64XFS
398	Temp.	TF-198	TE 398	D11 Fuel Rod Pos.4	Fig.5.143	273.	0.125E+04 K	0.64XFS
399	Temp.	TF-199	TE 399	D13 Fuel Rod Pos.4	Fig.5.143	273.	0.125E+04 K	0.64XFS
400	Temp.	TF-200	TE 400	D22 Fuel Rod Pos.1	Fig.5.107, 152	273.	0.125E+04 K	0.64XFS

Table 3.2 Measurement List for RUN 928 (Continued)

Ch.	Item	Symbol	ID.	Location	Fig.No.	Range	Unit	Accuracy
401	Temp.	TF-201	TE 401	D22 Fuel Rod Pos.2	Fig.5-107, 153	273.	0.125E+04 K	0.64%FS
402	Temp.	TF-202	TE 402	D22 Fuel Rod Pos.3	Fig.5-107, 154	273.	0.125E+04 K	0.64%FS
403	Temp.	TF-203	TE 403	D22 Fuel Rod Pos.4	Fig.5-107, 155	273.	0.125E+04 K	0.64%FS
404	Temp.	TF-204	TE 404	D22 Fuel Rod Pos.5	Fig.5-107, 156	273.	0.125E+04 K	0.64%FS
405	Temp.	TF-205	TE 405	D22 Fuel Rod Pos.6	Fig.5-107, 157	273.	0.125E+04 K	0.64%FS
406	Temp.	TF-206	TE 406	D22 Fuel Rod Pos.7	Fig.5-107, 158	273.	0.125E+04 K	0.64%FS
407	Temp.	TF-207	TE 407	D31 Fuel Rod Pos.4	Fig.5-143	273.	0.125E+04 K	0.64%FS
408	Temp.	TF-208	TE 408	D33 Fuel Rod Pos.4	Fig.5-144	273.	0.125E+04 K	0.64%FS
409	Temp.	TF-209	TE 409	D51 Fuel Rod Pos.4	Fig.5-140	273.	0.125E+04 K	0.64%FS
410	Temp.	TF-210	TE 410	D53 Fuel Rod Pos.4	Fig.5-144	273.	0.125E+04 K	0.64%FS
411	Temp.	TF-211	TE 411	D66 Fuel Rod Pos.4	Fig.5-144	273.	0.125E+04 K	0.64%FS
412	Temp.	TF-212	TE 412	D77 Fuel Rod Pos.4	Fig.5-140	273.	0.125E+04 K	0.64%FS
413	Temp.	TF-213	TE 413	D86 Fuel Rod Pos.4	Fig.5-143	273.	0.125E+04 K	0.64%FS
414	Fluid T.	TW-1	TE 414	A45 Tie Rod Pos.1	Fig.5-108	273.	0.125E+04 K	0.64%FS
415	Fluid T.	TW-2	TE 415	A45 Tie Rod Pos.2	Fig.5-108	273.	0.125E+04 K	0.64%FS
416	Fluid T.	TW-3	TE 416	A45 Tie Rod Pos.3	Fig.5-108	273.	0.125E+04 K	0.64%FS
417	Fluid T.	TW-4	TE 417	A45 Tie Rod Pos.4	Fig.5-108	273.	0.125E+04 K	0.64%FS
418	Fluid T.	TW-5	TE 418	A45 Tie Rod Pos.5	Fig.5-108	273.	0.125E+04 K	0.64%FS
419	Fluid T.	TW-6	TE 419	A45 Tie Rod Pos.6	Fig.5-108	273.	0.125E+04 K	0.64%FS
420	Fluid T.	TW-7	TE 420	A45 Tie Rod Pos.7	Fig.5-108	273.	0.125E+04 K	0.64%FS
421	Fluid T.	TW-8	TE 421	B45 Tie Rod Pos.1	Fig.5-109	273.	0.125E+04 K	0.64%FS
422	Fluid T.	TW-9	TE 422	B45 Tie Rod Pos.2	Fig.5-109	273.	0.125E+04 K	0.64%FS
423	Fluid T.	TW-10	TE 423	B45 Tie Rod Pos.3	Fig.5-109	273.	0.125E+04 K	0.64%FS
424	Fluid T.	TW-11	TE 424	B45 Tie Rod Pos.4	Fig.5-109	273.	0.125E+04 K	0.64%FS
425	Fluid T.	TW-12	TE 425	B45 Tie Rod Pos.5	Fig.5-109	273.	0.125E+04 K	0.64%FS
426	Fluid T.	TW-13	TE 426	B45 Tie Rod Pos.6	Fig.5-109	273.	0.125E+04 K	0.64%FS
427	Fluid T.	TW-14	TE 427	B45 Tie Rod Pos.7	Fig.5-109	273.	0.125E+04 K	0.64%FS
428	Fluid T.	TW-15	TE 428	C45 Tie Rod Pos.1	Fig.5-110	273.	0.125E+04 K	0.64%FS
429	Fluid T.	TW-16	TE 429	C45 Tie Rod Pos.2	Fig.5-110	273.	0.125E+04 K	0.64%FS
430	Fluid T.	TW-17	TE 430	C45 Tie Rod Pos.3	Fig.5-110	273.	0.125E+04 K	0.64%FS
431	Fluid T.	TW-18	TE 431	C45 Tie Rod Pos.4	Fig.5-110	273.	0.125E+04 K	0.64%FS
432	Fluid T.	TW-19	TE 432	C45 Tie Rod Pos.5	Fig.5-110	273.	0.125E+04 K	0.64%FS
433	Fluid T.	TW-20	TE 433	C45 Tie Rod Pos.6	Fig.5-110	273.	0.125E+04 K	0.64%FS
434	Fluid T.	TW-21	TE 434	C45 Tie Rod Pos.7	Fig.5-110	273.	0.125E+04 K	0.64%FS
435	Fluid T.	TW-22	TE 435	D45 Tie Rod Pos.1	Fig.5-111	273.	0.125E+04 K	0.64%FS
436	Fluid T.	TW-23	TE 436	D45 Tie Rod Pos.2	Fig.5-111	273.	0.125E+04 K	0.64%FS
437	Fluid T.	TW-24	TE 437	D45 Tie Rod Pos.3	Not Measured	273.	0.125E+04 K	0.64%FS
438	Fluid T.	TW-25	TE 438	D45 Tie Rod Pos.4	Not Measured	273.	0.125E+04 K	0.64%FS
439	Fluid T.	TW-26	TE 439	D45 Tie Rod Pos.5	Not Measured	273.	0.125E+04 K	0.64%FS
440	Fluid T.	TW-27	TE 440	D45 Tie Rod Pos.6	Not Measured	273.	0.125E+04 K	0.64%FS
441	Fluid T.	TW-28	TE 441	D45 Tie Rod Pos.7	Not Measured	273.	0.125E+04 K	0.64%FS
442	Fluid T.	TC-1	TE 442	Channel Box A Inlet	Fig.5-166	273.	0.125E+04 K	0.64%FS
443	Fluid T.	TC-2	TE 443	Channel Box B Inlet	Fig.5-166	273.	0.125E+04 K	0.64%FS
444	Fluid T.	TC-3	TE 444	Channel Box C Inlet	Fig.5-166	273.	0.125E+04 K	0.64%FS
445	Fluid T.	TC-4	TE 445	Channel Box D Inlet	Fig.5-166	273.	0.125E+04 K	0.64%FS
446	Fluid T.	TC-5	TE 446	Channel Box Outlet A-1	Fig.5-167	273.	0.125E+04 K	0.64%FS
447	Fluid T.	TC-6	TE 447	Channel Box Outlet A-2	Fig.5-167	273.	0.125E+04 K	0.64%FS
448	Fluid T.	TC-7	TE 448	Channel Box Outlet A-3	Fig.5-167	273.	0.125E+04 K	0.64%FS
449	Fluid T.	TC-8	TE 449	Channel Box Outlet A-4	Fig.5-167	273.	0.125E+04 K	0.64%FS
450	Fluid T.	TC-9	TE 450	Channel Box Outlet A-6	Fig.5-167	273.	0.125E+04 K	0.64%FS

Table 3.2 Measurement List for RUN 928 (Continued)

Ch.	Item	Symbol	ID.	Location	Fig.No.	Range	Unit	Accuracy
451	Fluid I.	TC-10	TE 451	Channel Box Outlet C-1	Fig.5.168	273.	0.125E+04 K	0.64%FS
452	Fluid I.	TC-11	TE 452	Channel Box Outlet C-2	Fig.5.168	273.	0.125E+04 K	0.64%FS
453	Fluid I.	TC-12	TE 453	Channel Box Outlet C-3	Fig.5.168	273.	0.125E+04 K	0.64%FS
454	Fluid I.	TC-13	TE 454	Channel Box Outlet C-4	Fig.5.168	273.	0.125E+04 K	0.64%FS
455	Fluid I.	TC-14	TE 455	Channel Box Outlet C-6	Fig.5.168	273.	0.125E+04 K	0.64%FS
456	Fluid I.	TG-1	TE 456	Upper Tieplate A Up.1	Fig.5.169, 173	273.	0.125E+04 K	0.64%FS
457	Fluid I.	TG-2	TE 457	Upper Tieplate A Up.2	Fig.5.169, 174	273.	0.125E+04 K	0.64%FS
458	Fluid I.	TG-3	TE 458	Upper Tieplate A Up.3	Fig.5.169, 175	273.	0.125E+04 K	0.64%FS
459	Fluid I.	TG-4	TE 459	Upper Tieplate A Up.4	Fig.5.169, 176	273.	0.125E+04 K	0.64%FS
460	Fluid I.	TG-5	TE 460	Upper Tieplate A Up.5	Fig.5.169, 177	273.	0.125E+04 K	0.64%FS
461	Fluid I.	TG-6	TE 461	Upper Tieplate A Up.6	Fig.5.170, 178	273.	0.125E+04 K	0.64%FS
462	Fluid I.	TG-7	TE 462	Upper Tieplate A Up.7	Fig.5.170, 179	273.	0.125E+04 K	0.64%FS
463	Fluid I.	TG-8	TE 463	Upper Tieplate A Up.8	Fig.5.170, 180	273.	0.125E+04 K	0.64%FS
464	Fluid I.	TG-9	TE 464	Upper Tieplate A Up.9	Fig.5.170, 181	273.	0.125E+04 K	0.64%FS
465	Fluid I.	TG-10	TE 465	Upper Tieplate A Up.10	Fig.5.170, 182	273.	0.125E+04 K	0.64%FS
466	Fluid I.	TG-11	TE 466	Upper Tieplate A Lo.1	Fig.5.171, 173	273.	0.125E+04 K	0.64%FS
467	Fluid I.	TG-12	TE 467	Upper Tieplate A Lo.2	Fig.5.171, 174	273.	0.125E+04 K	0.64%FS
468	Fluid I.	TG-13	TE 468	Upper Tieplate A Lo.3	Fig.5.171, 175	273.	0.125E+04 K	0.64%FS
469	Fluid I.	TG-14	TE 469	Upper Tieplate A Lo.4	Fig.5.171, 176	273.	0.125E+04 K	0.64%FS
470	Fluid I.	TG-15	TE 470	Upper Tieplate A Lo.5	Fig.5.171, 177	273.	0.125E+04 K	0.64%FS
471	Fluid I.	TG-16	TE 471	Upper Tieplate A Lo.6	Fig.5.172, 178	273.	0.125E+04 K	0.64%FS
472	Fluid I.	TG-17	TE 472	Upper Tieplate A Lo.7	Fig.5.172, 179	273.	0.125E+04 K	0.64%FS
473	Fluid I.	TG-18	TE 473	Upper Tieplate A Lo.8	Fig.5.172, 180	273.	0.125E+04 K	0.64%FS
474	Fluid I.	TG-19	TE 474	Upper Tieplate A Lo.9	Fig.5.172, 181	273.	0.125E+04 K	0.64%FS
475	Fluid I.	TG-20	TE 475	Upper Tieplate A Lo.10	Fig.5.172, 182	273.	0.125E+04 K	0.64%FS
476	Fluid I.	TG-21	TE 476	Upper Tieplate C Up.1	Fig.5.183, 187	273.	0.125E+04 K	0.64%FS
477	Fluid I.	TG-22	TE 477	Upper Tieplate C Up.2	Fig.5.183, 188	273.	0.125E+04 K	0.64%FS
478	Fluid I.	TG-23	TE 478	Upper Tieplate C Up.3	Fig.5.183, 189	273.	0.125E+04 K	0.64%FS
479	Fluid I.	TG-24	TE 479	Upper Tieplate C Up.4	Fig.5.183, 190	273.	0.125E+04 K	0.64%FS
480	Fluid I.	TG-25	TE 480	Upper Tieplate C Up.5	Fig.5.183, 191	273.	0.125E+04 K	0.64%FS
481	Fluid I.	TG-26	TE 481	Upper Tieplate C Up.6	Fig.5.184, 192	273.	0.125E+04 K	0.64%FS
482	Fluid I.	TG-27	TE 482	Upper Tieplate C Up.7	Fig.5.184, 193	273.	0.125E+04 K	0.64%FS
483	Fluid I.	TG-28	TE 483	Upper Tieplate C Up.8	Fig.5.184, 194	273.	0.125E+04 K	0.64%FS
484	Fluid I.	TG-29	TE 484	Upper Tieplate C Up.9	Fig.5.184, 195	273.	0.125E+04 K	0.64%FS
485	Fluid I.	TG-30	TE 485	Upper Tieplate C Up.10	Fig.5.184, 196	273.	0.125E+04 K	0.64%FS
486	Fluid I.	TG-31	TE 486	Upper Tieplate C Lo.1	Fig.5.185, 187	273.	0.125E+04 K	0.64%FS
487	Fluid I.	TG-32	TE 487	Upper Tieplate C Lo.2	Fig.5.185, 188	273.	0.125E+04 K	0.64%FS
488	Fluid I.	TG-33	TE 488	Upper Tieplate C Lo.3	Fig.5.185, 189	273.	0.125E+04 K	0.64%FS
489	Fluid I.	TG-34	TE 489	Upper Tieplate C Lo.4	Fig.5.185, 190	273.	0.125E+04 K	0.64%FS
490	Fluid I.	TG-35	TE 490	Upper Tieplate C Lo.5	Fig.5.185, 191	273.	0.125E+04 K	0.64%FS
491	Fluid I.	TG-36	TE 491	Upper Tieplate C Lo.6	Fig.5.186, 192	273.	0.125E+04 K	0.64%FS
492	Fluid I.	TG-37	TE 492	Upper Tieplate C Lo.7	Fig.5.186, 193	273.	0.125E+04 K	0.64%FS
493	Fluid I.	TG-38	TE 493	Upper Tieplate C Lo.8	Fig.5.186, 194	273.	0.125E+04 K	0.64%FS
494	Fluid I.	TG-39	TE 494	Upper Tieplate C Lo.9	Fig.5.186, 195	273.	0.125E+04 K	0.64%FS
495	Fluid I.	TG-40	TE 495	Upper Tieplate C Lo.10	Fig.5.186, 196	273.	0.125E+04 K	0.64%FS
496	Slab I.	TB-1	TE 496	C.B. A1 Inner ,Pos.1	Fig.5.112, 197	273.	0.125E+04 K	0.64%FS
497	Slab I.	TB-2	TE 497	C.B. A1 Inner ,Pos.2	Fig.5.112, 198	273.	0.125E+04 K	0.64%FS
498	Slab I.	TB-3	TE 498	C.B. A1 Inner ,Pos.3	Fig.5.112, 199	273.	0.125E+04 K	0.64%FS
499	Slab I.	TB-4	TE 499	C.B. A1 Inner ,Pos.4	Fig.5.112, 200	273.	0.125E+04 K	0.64%FS
500	Slab I.	TB-5	TE 500	C.B. A1 Inner ,Pos.5	Fig.5.112, 201	273.	0.125E+04 K	0.64%FS

Table 3.2 Measurement List for RUN 928 (Continued)

501ch.- 550ch.

Ch.	Item	Symbol	ID.	Location	Fig.No.	Range	Unit	Accuracy
501	Slab T.	TB-6	TE 501	C.B. A1 Inner ,Pos.6	Fig.5.112, 202	273.	0.125E+04 K	0.64%FS
502	Slab T.	TB-7	TE 502	C.B. A1 Inner ,Pos.7	Fig.5.112, 203	273.	0.125E+04 K	0.64%FS
503	Slab T.	TB-8	TE 503	C.B. A2 Inner ,Pos.1	Failure		0.125E+04 K	0.64%FS
504	Slab T.	TB-9	TE 504	C.B. A2 Inner ,Pos.2	Fig.5.113, 198	273.	0.125E+04 K	0.64%FS
505	Slab T.	TB-10	TE 505	C.B. A2 Inner ,Pos.3	Fig.5.113, 199	273.	0.125E+04 K	0.64%FS
506	Slab T.	TB-11	TE 506	C.B. A2 Inner ,Pos.4	Fig.5.113, 200	273.	0.125E+04 K	0.64%FS
507	Slab T.	TB-12	TE 507	C.B. A2 Inner ,Pos.5	Fig.5.113, 201	273.	0.125E+04 K	0.64%FS
508	Slab T.	TB-13	TE 508	C.B. A2 Inner ,Pos.6	Fig.5.113, 202	273.	0.125E+04 K	0.64%FS
509	Slab T.	TB-14	TE 509	C.B. A2 Inner ,Pos.7	Fig.5.113, 203	273.	0.125E+04 K	0.64%FS
510	Slab T.	TB-15	TE 510	C.B. B Inner ,Pos.1	Fig.5.114, 197	273.	0.125E+04 K	0.64%FS
511	Slab T.	TB-16	TE 511	C.B. B Inner ,Pos.2	Fig.5.114, 198	273.	0.125E+04 K	0.64%FS
512	Slab T.	TB-17	TE 512	C.B. B Inner ,Pos.3	Fig.5.114, 199	273.	0.125E+04 K	0.64%FS
513	Slab T.	TB-18	TE 513	C.B. B Inner ,Pos.4	Fig.5.114, 200	273.	0.125E+04 K	0.64%FS
514	Slab T.	TB-19	TE 514	C.B. B Inner ,Pos.5	Fig.5.114, 201	273.	0.125E+04 K	0.64%FS
515	Slab T.	TB-20	TE 515	C.B. B Inner ,Pos.6	Fig.5.114, 202	273.	0.125E+04 K	0.64%FS
516	Slab T.	TB-21	TE 516	C.B. B Inner ,Pos.7	Fig.5.114, 203	273.	0.125E+04 K	0.64%FS
517	Slab T.	TB-22	TE 517	C.B. C Inner ,Pos.1	Fig.5.115, 197	273.	0.125E+04 K	0.64%FS
518	Slab T.	TB-23	TE 518	C.B. C Inner ,Pos.2	Fig.5.115, 198	273.	0.125E+04 K	0.64%FS
519	Slab T.	TB-24	TE 519	C.B. C Inner ,Pos.3	Fig.5.115, 199	273.	0.125E+04 K	0.64%FS
520	Slab T.	TB-25	TE 520	C.B. C Inner ,Pos.4	Fig.5.115, 200	273.	0.125E+04 K	0.64%FS
521	Slab T.	TB-26	TE 521	C.B. C Inner ,Pos.5	Fig.5.115, 201	273.	0.125E+04 K	0.64%FS
522	Slab T.	TB-27	TE 522	C.B. C Inner ,Pos.6	Fig.5.115, 202	273.	0.125E+04 K	0.64%FS
523	Slab T.	TB-28	TE 523	C.B. C Inner ,Pos.7	Fig.5.115, 203	273.	0.125E+04 K	0.64%FS
524	Slab T.	TB-29	TE 524	C.B. D Inner ,Pos.1	Fig.5.116, 197	273.	0.125E+04 K	0.64%FS
525	Slab T.	TB-30	TE 525	C.B. D Inner ,Pos.2	Fig.5.116, 198	273.	0.125E+04 K	0.64%FS
526	Slab T.	TB-31	TE 526	C.B. D Inner ,Pos.3	Fig.5.116, 199	273.	0.125E+04 K	0.64%FS
527	Slab T.	TB-32	TE 527	C.B. D Inner ,Pos.4	Fig.5.116, 200	273.	0.125E+04 K	0.64%FS
528	Slab T.	TB-33	TE 528	C.B. D Inner ,Pos.5	Fig.5.116, 201	273.	0.125E+04 K	0.64%FS
529	Slab T.	TB-34	TE 529	C.B. D Inner ,Pos.6	Fig.5.116, 202	273.	0.125E+04 K	0.64%FS
530	Slab T.	TB-35	TE 530	C.B. D Inner ,Pos.7	Fig.5.116, 203	273.	0.125E+04 K	0.64%FS
531	Fluid T.	TB-36	TE 531	C.B. A Outer ,Pos.1	Fig.5.117, 197	273.	0.125E+04 K	0.64%FS
532	Fluid T.	TB-37	TE 532	C.B. A Outer ,Pos.2	Fig.5.117, 198	273.	0.125E+04 K	0.64%FS
533	Fluid T.	TB-38	TE 533	C.B. A Outer ,Pos.3	Fig.5.117, 199	273.	0.125E+04 K	0.64%FS
534	Fluid T.	TB-39	TE 534	C.B. A Outer ,Pos.4	Fig.5.117, 200	273.	0.125E+04 K	0.64%FS
535	Fluid T.	TB-40	TE 535	C.B. A Outer ,Pos.5	Fig.5.117, 201	273.	0.125E+04 K	0.64%FS
536	Fluid T.	TB-41	TE 536	C.B. A Outer ,Pos.6	Fig.5.117, 202	273.	0.125E+04 K	0.64%FS
537	Fluid T.	TB-42	TE 537	C.B. A Outer ,Pos.7	Fig.5.117, 203	273.	0.125E+04 K	0.64%FS
538	Fluid T.	TB-43	TE 538	C.B. C Outer ,Pos.1	Fig.5.118, 197	273.	0.125E+04 K	0.64%FS
539	Fluid T.	TB-44	TE 539	C.B. C Outer ,Pos.2	Fig.5.118, 198	273.	0.125E+04 K	0.64%FS
540	Fluid T.	TB-45	TE 540	C.B. C Outer ,Pos.3	Fig.5.118, 199	273.	0.125E+04 K	0.64%FS
541	Fluid T.	TB-46	TE 541	C.B. C Outer ,Pos.4	Fig.5.118, 200	273.	0.125E+04 K	0.64%FS
542	Fluid T.	TB-47	TE 542	C.B. C Outer ,Pos.5	Fig.5.118, 201	273.	0.125E+04 K	0.64%FS
543	Fluid T.	TB-48	TE 543	C.B. C Outer ,Pos.6	Fig.5.118, 202	273.	0.125E+04 K	0.64%FS
544	Fluid T.	TB-49	TE 544	C.B. C Outer ,Pos.7	Fig.5.118, 203	273.	0.125E+04 K	0.64%FS
545	Fluid T.	TP-1	TE 545	Lower Pl. Center 1	Fig.5.204	273.	0.125E+04 K	0.64%FS
546	Fluid T.	TP-2	TE 546	Lower Pl. Center 2	Fig.5.204	273.	0.125E+04 K	0.64%FS
547	Fluid T.	TP-3	TE 547	Lower Pl. Center 3	Fig.5.204	273.	0.125E+04 K	0.64%FS
548	Fluid T.	TP-4	TE 548	Lower Pl. Center 4	Fig.5.204	273.	0.125E+04 K	0.64%FS
549	Fluid T.	TP-5	TE 549	Lower Pl. Center 5	Fig.5.204	273.	0.125E+04 K	0.64%FS
550	Fluid T.	TP-6	TE 550	Lower Pl. Center 7	Fig.5.204	273.	0.125E+04 K	0.64%FS

Table 3.2 Measurement List for RUN 928 (Continued)

Ch.	Item	Symbol	ID.	Location	Fig.No.	Range	Unit	Accuracy
551	Slab T.	TP-7	TE 551	Lower Pl. North 1	Fig.5.205	273.	0.125E+04 K	0.64%FS
552	Slab T.	TP-8	TE 552	Lower Pl. North 2	Fig.5.205	273.	673.	0.64%FS
553	Slab T.	TP-9	TE 553	Lower Pl. North 4	Fig.5.205	273.	673.	0.64%FS
554	Slab T.	TP-10	TE 554	Lower Pl. North 6	Fig.5.205	273.	673.	0.64%FS
555	Slab T.	TP-11	TE 555	Lower Pl. South 1	Fig.5.206	273.	673.	0.64%FS
556	Slab T.	TP-12	TE 556	Lower Pl. South 2	Fig.5.206	273.	673.	0.64%FS
557	Slab T.	TP-13	TE 557	Lower Pl. South 4	Fig.5.206	273.	673.	0.64%FS
558	Slab T.	TP-14	TE 558	Lower Pl. South 6	Fig.5.206	273.	673.	0.64%FS
559	Level	LB-1	LM 559	C.B.Liquid Level A1-1	Fig.5.207			
560	Level	LB-2	LM 560	C.B.Liquid Level A1-2	Failure			
561	Level	LB-3	LM 561	C.B.Liquid Level A1-3	Fig.5.207			
562	Level	LB-4	LM 562	C.B.Liquid Level A1-4	FAILURE			
563	Level	LB-5	LM 563	C.B.Liquid Level A1-5	Fig.5.207			
564	Level	LB-6	LM 564	C.B.Liquid Level A1-6	Fig.5.207			
565	Level	LB-7	LM 565	C.B.Liquid Level A1-7	Fig.5.207			
566	Level	LB-8	LM 566	C.B.Liquid Level A2-1	Fig.5.208			
567	Level	LB-9	LM 567	C.B.Liquid Level A2-2	Failure			
568	Level	LB-10	LM 568	C.B.Liquid Level A2-3	Fig.5.208			
569	Level	LB-11	LM 569	C.B.Liquid Level A2-4	Fig.5.208			
570	Level	LB-12	LM 570	C.B.Liquid Level A2-5	FAILURE			
571	Level	LB-13	LM 571	C.B.Liquid Level A2-6	Fig.5.208			
572	Level	LB-14	LM 572	C.B.Liquid Level B-1	Fig.5.208			
573	Level	LB-15	LM 573	C.B.Liquid Level B-1	Fig.5.209			
574	Level	LB-16	LM 574	C.B.Liquid Level B-2	Fig.5.209			
575	Level	LB-17	LM 575	C.B.Liquid Level B-3	Fig.5.209			
576	Level	LB-18	LM 576	C.B.Liquid Level B-4	Fig.5.209			
577	Level	LB-19	LM 577	C.B.Liquid Level B-5	Fig.5.209			
578	Level	LB-20	LM 578	C.B.Liquid Level B-6	Fig.5.209			
579	Level	LB-21	LM 579	C.B.Liquid Level B-7	Fig.5.209			
580	Level	LB-22	LM 580	C.B.Liquid Level C-1	Fig.5.210			
581	Level	LB-23	LM 581	C.B.Liquid Level C-2	Fig.5.210			
582	Level	LB-24	LM 582	C.B.Liquid Level C-3	Fig.5.210			
583	Level	LB-25	LM 583	C.B.Liquid Level C-4	Fig.5.210			
584	Level	LB-26	LM 584	C.B.Liquid Level C-5	Fig.5.210			
585	Level	LB-27	LM 585	C.B.Liquid Level C-6	Fig.5.210			
586	Level	LB-28	LM 586	C.B.Liquid Level C-7	Fig.5.210			
587	Level	LB-29	LM 587	C.B.Liquid Level D-1	Fig.5.211			
588	Level	LB-30	LM 588	C.B.Liquid Level D-2	Fig.5.211			
589	Level	LB-31	LM 589	C.B.Liquid Level D-3	Fig.5.211			
590	Level	LB-32	LM 590	C.B.Liquid Level D-4	Fig.5.211			
591	Level	LB-33	LM 591	C.B.Liquid Level D-5	FAILURE			
592	Level	LB-34	LM 592	C.B.Liquid Level D-6	Fig.5.211			
593	Level	LB-35	LM 593	C.B.Liquid Level D-7	Fig.5.211			
594	Level	LL-1	LM 594	Ch.Box Outlet A1-5	Fig.5.212			
595	Level	LL-2	LM 595	Ch.Box Outlet A1-6	Fig.5.212			
596	Level	LL-3	LM 596	Ch.Box Outlet A1-7	Failure			
597	Level	LL-4	LM 597	Ch.Box Outlet A2-5	Failure			
598	Level	LL-5	LM 598	Ch.Box Outlet A2-6	Fig.5.213			
599	Level	LL-6	LM 599	Ch.Box Outlet A2-7	Fig.5.213			
600	Level	LL-7	LM 600	Ch.Box Outlet A-1	Failure			

Table 3.2 Measurement List for RUN 928 (Continued)

601Ch.- 650Ch.

Ch.	Item	Symbol	ID.	Location	Fig.No.	Range	Unit	Accuracy
601	Level	LL-8	LM 601	Ch.Box Outlet A-2	Failure			
602	Level	LL-9	LM 602	Ch.Box Outlet A-3	Fig.5.214			
603	Level	LL-10	LM 603	Ch.Box Outlet A-4	Fig.5.214			
604	Level	LL-11	LM 604	Ch.Box Outlet A-6	Not measured			
605	Level	LL-12	LM 605	Ch.Box Outlet C1-5	Not measured			
606	Level	LL-13	LM 606	Ch.Box Outlet C1-6	Not measured			
607	Level	LL-14	LM 607	Ch.Box Outlet C1-7	Not measured			
608	Level	LL-15	LM 608	Ch.Box Outlet C2-5	Not measured			
609	Level	LL-16	LM 609	Ch.Box Outlet C2-6	Not measured			
610	Level	LL-17	LM 610	Ch.Box Outlet C2-7	Not measured			
611	Level	LL-18	LM 611	Ch.Box Outlet C-1	Not measured			
612	Level	LL-19	LM 612	Ch.Box Outlet C-2	Not measured			
613	Level	LL-20	LM 613	Ch.Box Outlet C-3	Not measured			
614	Level	LL-21	LM 614	Ch.Box Outlet C-4	Not measured			
615	Level	LL-22	LM 615	Ch.Box Outlet C-6	Not measured			
616	Level	LL-23	LM 616	Ch.Box Inlet A-1	Fig.5.215			
617	Level	LL-24	LM 617	Ch.Box Inlet A-2	Fig.5.215			
618	Level	LL-25	LM 618	Ch.Box Inlet B-1	Fig.5.216			
619	Level	LL-26	LM 619	Ch.Box Inlet B-2	Fig.5.216			
620	Level	LL-27	LM 620	Ch.Box Inlet C-1	Fig.5.217			
621	Level	LL-28	LM 621	Ch.Box Inlet C-2	Fig.5.217			
622	Level	LL-29	LM 622	Ch.Box Inlet D-1	Fig.5.218			
623	Level	LL-30	LM 623	Ch.Box Inlet D-2	Fig.5.218			
624	Level	LL-31	LM 624	Lower Pl. North 1	Fig.5.219			
625	Level	LL-32	LM 625	Lower Pl. North 2	Fig.5.219			
626	Level	LL-33	LM 626	Lower Pl. North 3	Fig.5.219			
627	Level	LL-34	LM 627	Lower Pl. North 4	Fig.5.219			
628	Level	LL-35	LM 628	Lower Pl. North 5	Fig.5.219			
629	Level	LL-36	LM 629	Lower Pl. North 6	Fig.5.219			
630	Level	LL-37	LM 630	Lower Pl. South 1	Fig.5.220			
631	Level	LL-38	LM 631	Lower Pl. South 2	Fig.5.220			
632	Level	LL-39	LM 632	Lower Pl. South 3	Fig.5.220			
633	Level	LL-40	LM 633	Lower Pl. South 4	Fig.5.220			
634	Level	LL-41	LM 634	Lower Pl. South 5	Fig.5.220			
635	Level	LL-42	LM 635	Lower Pl. South 6	Fig.5.220			
636	Level	LL-43	LM 636	Guide Tube North 0	Fig.5.221			
637	Level	LL-44	LM 637	Guide Tube North 1	Fig.5.221			
638	Level	LL-45	LM 638	Guide Tube North 3	Fig.5.221			
639	Level	LL-46	LM 639	Guide Tube North 6	Fig.5.221			
640	Level	LL-47	LM 640	Guide Tube South 0	Fig.5.222			
641	Level	LL-48	LM 641	Guide Tube South 1	Fig.5.222			
642	Level	LL-49	LM 642	Guide Tube South 3	Fig.5.222			
643	Level	LL-50	LM 643	Guide Tube South 6	Fig.5.222			
644	Level	L-1	LM 644	Downcomer D-Side 1	Fig.5.223			
645	Level	L-2	LM 645	Downcomer D-Side 2	Fig.5.223			
646	Level	L-3	LM 646	Downcomer D-Side 3	Fig.5.223			
647	Level	L-4	LM 647	Downcomer D-Side 4	Fig.5.223			
648	Level	L-5	LM 648	Downcomer D-Side 5	Not measured			
649	Level	L-6	LM 649	Downcomer B-Side 1	Fig.5.224			
650	Level	L-7	LM 650	Downcomer B-Side 2	Fig.5.224			

Table 3.2 Measurement List for RUN 928 (Continued)

Ch.	Item	Symbol	ID.	Location	Fig.No.	Range	Unit	Accuracy
651	Level	L-8	LM 651	Downcomer B-Side 3	Fig.5.224	0.0		
652	Level	L-9	LM 652	Downcomer B-Side 4	Fig.5.224	0.0		
653	Level	L-10	LM 653	Downcomer B-Side 5	Failure			
654	Void	VF-1	VD 654	A54 Tie Rod Pos.1	Not Measured	0.0	1.00	
655	Void	VF-2	VD 655	A54 Tie Rod Pos.2	Not Measured	0.0	1.00	
656	Void	VF-3	VD 656	A54 Tie Rod Pos.3	Not Measured	0.0	1.00	
657	Void	VF-4	VD 657	A54 Tie Rod Pos.4	Not Measured	0.0	1.00	
658	Void	VF-5	VD 658	A54 Tie Rod Pos.5	Not Measured	0.0	1.00	
659	Void	VF-6	VD 659	A54 Tie Rod Pos.6	Not Measured	0.0	1.00	
660	Void	VF-7	VD 660	A54 Tie Rod Pos.7	Not Measured	0.0	1.00	
661	Void	VF-8	VD 661	B54 Tie Rod Pos.1	Not Measured	0.0	1.00	
662	Void	VF-9	VD 662	B54 Tie Rod Pos.2	Not Measured	0.0	1.00	
663	Void	VF-10	VD 663	B54 Tie Rod Pos.3	Not Measured	0.0	1.00	
664	Void	VF-11	VD 664	B54 Tie Rod Pos.4	Not Measured	0.0	1.00	
665	Void	VF-12	VD 665	B54 Tie Rod Pos.5	Not Measured	0.0	1.00	
666	Void	VF-13	VD 666	B54 Tie Rod Pos.6	Not Measured	0.0	1.00	
667	Void	VF-14	VD 667	B54 Tie Rod Pos.7	Not Measured	0.0	1.00	
668	Void	VF-15	VD 668	C54 Tie Rod Pos.1	Not Measured	0.0	1.00	
669	Void	VF-16	VD 669	C54 Tie Rod Pos.2	Not Measured	0.0	1.00	
670	Void	VF-17	VD 670	C54 Tie Rod Pos.3	Not Measured	0.0	1.00	
671	Void	VF-18	VD 671	C54 Tie Rod Pos.4	Not Measured	0.0	1.00	
672	Void	VF-19	VD 672	C54 Tie Rod Pos.5	Not Measured	0.0	1.00	
673	Void	VF-20	VD 673	C54 Tie Rod Pos.6	Not Measured	0.0	1.00	
674	Void	VF-21	VD 674	C54 Tie Rod Pos.7	Not Measured	0.0	1.00	
675	Void	VF-22	VD 675	D54 Tie Rod Pos.7	Not Measured	0.0	1.00	
676	Void	VF-23	VD 676	D54 Tie Rod Pos.7	Not Measured	0.0	1.00	
677	Void	VF-24	VD 677	D54 Tie Rod Pos.7	Not Measured	0.0	1.00	
678	Void	VF-25	VD 678	D54 Tie Rod Pos.7	Not Measured	0.0	1.00	
679	Void	VF-26	VD 679	D54 Tie Rod Pos.7	Not Measured	0.0	1.00	
680	Void	VF-27	VD 680	D54 Tie Rod Pos.7	Not Measured	0.0	1.00	
681	Void	VF-28	VD 681	D54 Tie Rod Pos.7	Not Measured	0.0	1.00	
682	Void	VE-1	VD 682	Channel A Outlet 1	Not Measured	0.0	1.00	
683	Void	VE-2	VD 683	Channel A Outlet 2	Not Measured	0.0	1.00	
684	Void	VE-3	VD 684	Channel A Outlet 3	Not Measured	0.0	1.00	
685	Void	VE-4	VD 685	Channel B Outlet 1	Not Measured	0.0	1.00	
686	Void	VE-5	VD 686	Channel B Outlet 2	Not Measured	0.0	1.00	
687	Void	VE-6	VD 687	Channel B Outlet 3	Not Measured	0.0	1.00	
688	Void	VE-7	VD 688	Channel C Outlet 1	Not Measured	0.0	1.00	
689	Void	VE-8	VD 689	Channel C Outlet 2	Not Measured	0.0	1.00	
690	Void	VE-9	VD 690	Channel C Outlet 3	Not Measured	0.0	1.00	
691	Void	VE-10	VD 691	Channel D Outlet 1	Not Measured	0.0	1.00	
692	Void	VE-11	VD 692	Channel D Outlet 2	Not Measured	0.0	1.00	
693	Void	VE-12	VD 693	Channel D Outlet 3	Not Measured	0.0	1.00	
694	Void	VE-13	VD 694	Lower Plenum Bottom 1	Not Measured	0.0	1.00	
695	Void	VE-14	VD 695	Lower Plenum Bottom 2	Not Measured	0.0	1.00	
696	Void	VE-15	VD 696	Lower Plenum Bottom 3	Not Measured	0.0	1.00	
697	Void	VP-1	VD 697	Lower Plenum Inlet	Not Measured	0.0	1.00	
698	Void	VP-2	VD 698	Lower Plenum Inlet	Not Measured	0.0	1.00	

Table 3.3 Core Instrumentation Map

Item	Pos.	Core Outlet	Pos.1	Pos.2	Pos.3	Pos.4	Pos.5	Pos.6	Pos.7	Core Inlet
	DL									
	Rod NO.	3660	3417	3114.5	2879.5	2527	2174.5	1939.5	1637	1454
Surface Temp.	A11		TF 1	TF 2	TF 3	TF 4	TF 5	TF 6	TF 7	
	A12		TF 8	TF 9	TF 10	TF 11	TF 12	TF 13	TF 14	
	A13		TF 15	TF 16	TF 17	TF 18	TF 19	TF 20	TF 21	
	A14		TF 22	TF 23	TF 24	TF 25	TF 26	TF 27	TF 28	
	A15		TF 29			TF 30				
	A17		TF 31			TF 32				
	A22		TF 33	TF 34	TF 35	TF 36	TF 37	TF 38	TF 39	
	A23		TF 40	TF 41	TF 42	TF 43	TF 44	TF 45	TF 46	
	A24		TF 47	TF 48	TF 49	TF 50	TF 51	TF 52	TF 53	
	A26		TF 54			TF 55				
	A28		TF 56			TF 57				
	A31		TF 58			TF 59				
	A33		TF 60	TF 61	TF 62	TF 63	TF 64	TF 65	TF 66	
	A34		TF 67	TF 68	TF 69	TF 70	TF 71	TF 72	TF 73	
	A35		TF 74			TF 75				
	A37		TF 76			TF 77				
A42		TF 78			TF 79					
Fluid Temp.	A44	TC 1	TF180	TF181	TF182	TF183	TF184	TF185	TF186	TC 2
Surface Temp.	A45		TF 80			TF 81				
	A46		TF 82			TF 83				
	A48		TF 84			TF 85				
	A51		TF 86			TF 87				
	A53		TF 88			TF 89				
	A54		TF 90							
	A57		TF 91			TF 92				
	A62		TF 93			TF 94				
	A64		TF 95			TF 96				
	A66		TF 97			TF 98				
	A68		TF 99			TF100				
	A71		TF101			TF102				
	A73		TF103			TF104				
	A75		TF105			TF106				
	A77		TF107			TF108				



Table 3.3 Core Instrumentation Map (Continued)

Item	Pos.	Core Outlet	Pos. 1	Pos. 2	Pos. 3	Pos. 4	Pos. 5	Pos. 6	Pos. 7	Core Inlet
	DL Rod NO.									
		3660	3417	3114.5	2879.5	2527	2174.5	1939.5	1637	1454
Surface Temp.	A82		TF109			TF110				
	A84		TF111			TF112				
	A86		TF113			TF114				
	A88		TF115			TF116				
	B11					TF117				
	B13					TF118				
	B15		TF119	TF120	TF121	TF122	TF123	TF124	TF125	
	B31					TF126				
	B33					TF127				
	B35					TF128				
Fluid Temp.	B44	TC 3	TF187	TF188	TF189	TF190	TF191	TF192	TF193	TC 4
Surface Temp.	B51					TF129				
	B53					TF130				
	B85		TF131	TF132	TF133	TF134	TF135	TF136	TF137	
	C11					TF138				
	C13					TF139				
	C15					TF140				
	C31					TF141				
	C33		TF142	TF143	TF144	TF145	TF146	TF147	TF148	
C35					TF149					
Fluid Temp.	C44	TC 5	TF194	TF195	TF196	TF197	TF198	TF199	TF200	TC 6
Surface Temp.	C51					TF150				
	C53					TF151				
	C77		TF152	TF153	TF154	TF155	TF156	TF157	TF158	
	D11					TF159				
	D13					TF160				
	D27		TF161	TF162	TF163	TF164	TF165	TF166	TF167	
	D31					TF168				
	D33					TF169				
	D35					TF170				
Fluid Temp.	D44	TC 7	TF201	TF202	TF203	TF204	TF205	TF206	TF207	TC 8
Surface Temp.	D51					TF171				
	D53					TF172				
	D88		TF173	TF174	TF175	TF176	TF177	TF178	TF179	

Table 3.3 Core Instrumentation Map (Continued)

Item	Pos.	Core Outlet	Pos.1	Pos.2	Pos.3	Pos.4	Pos.5	Pos.6	Pos.7	Core Inlet
	Rod NO.									
		3660	3417	3114.5	2879.5	2527	2174.5	1939.5	1673	1454
Void	A55		VF 1	VF 2	VF 3	VF 4	VF 5	VF 6	VF 7	
	B55		VF 8	VF 9	VF 10	VF 11	VF 12	VF 13	VF 14	
	C55		VF 15	VF 16	VF 17	VF 18	VF 19	VF 20	VF 21	
	D55		VF 22	VF 23	VF 24	VF 25	VF 26	VF 27	VF 28	
Channel Box Surface Temp.	A1*		TB 1	TB 2	TB 3	TB 4	TB 5	TB 6	TB 7	
	A2*		TB 8	TB 9	TB 10	TB 11	TB 12	TB 13	TB 14	
	B*		TB 15	TB 16	TB 17	TB 18	TB 19	TB 20	TB 21	
	C*		TB 22	TB 23	TB 24	TB 25	TB 26	TB 27	TB 28	
	D*		TB 29	TB 30	TB 31	TB 32	TB 33	TB 34	TB 35	
Liquid Level in the Channel Box	A1*		LB 1	LB 2	LB 3	LB 4	LB 5	LB 6	LB 7	
	A2*		LB 8	LB 9	LB 10	LB 11	LB 12	LB 13	LB 14	
	B*		LB 15	LB 16	LB 17	LB 18	LB 19	LB 20	LB 21	
	C*		LB 22	LB 23	LB 24	LB 25	LB 26	LB 27	LB 28	
	D*		LB 29	LB 30	LB 31	LB 32	LB 33	LB 34	LB 35	

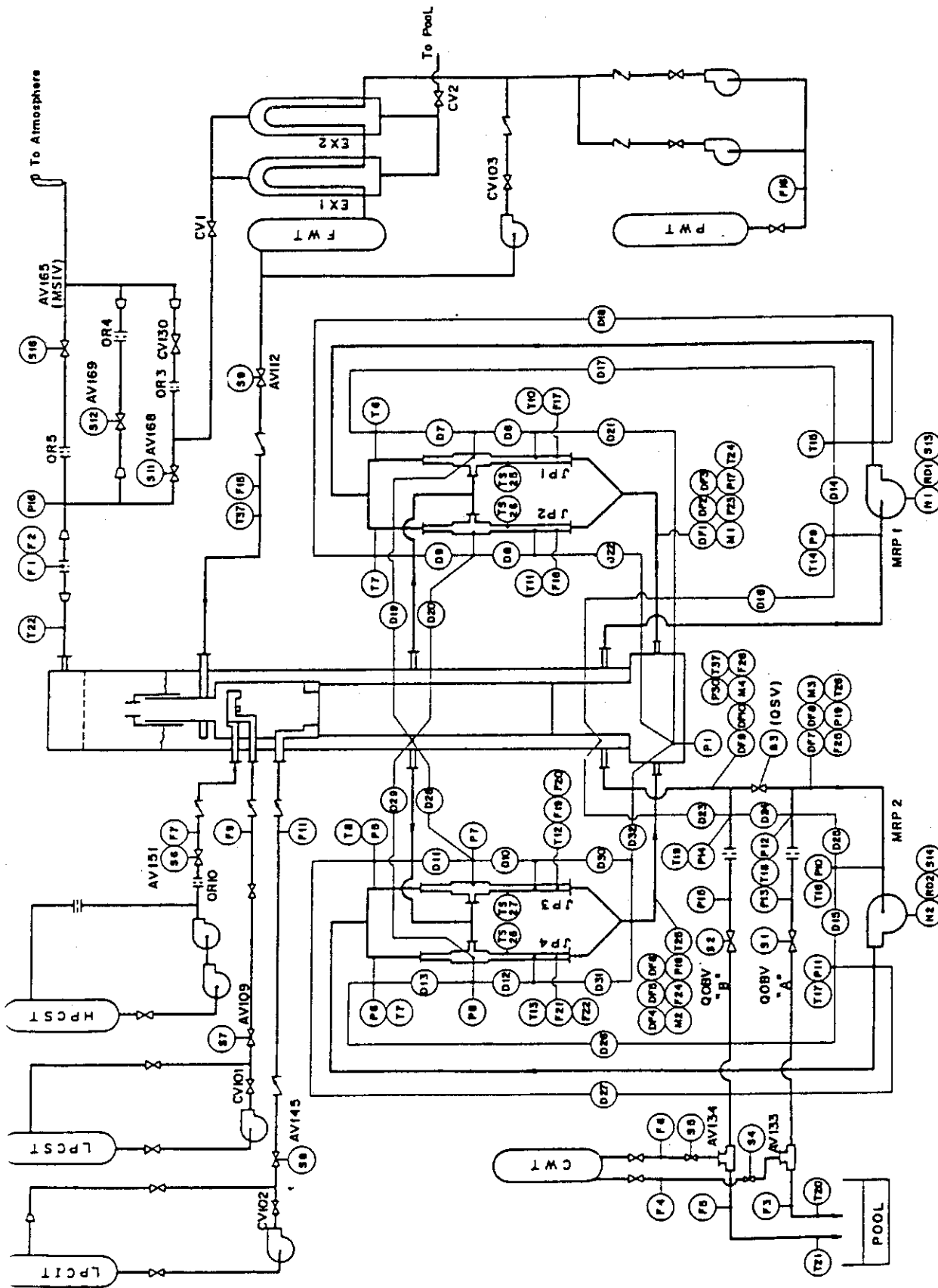


Fig. 3.1 Instrumentation Location of ROSA-III Test Facility

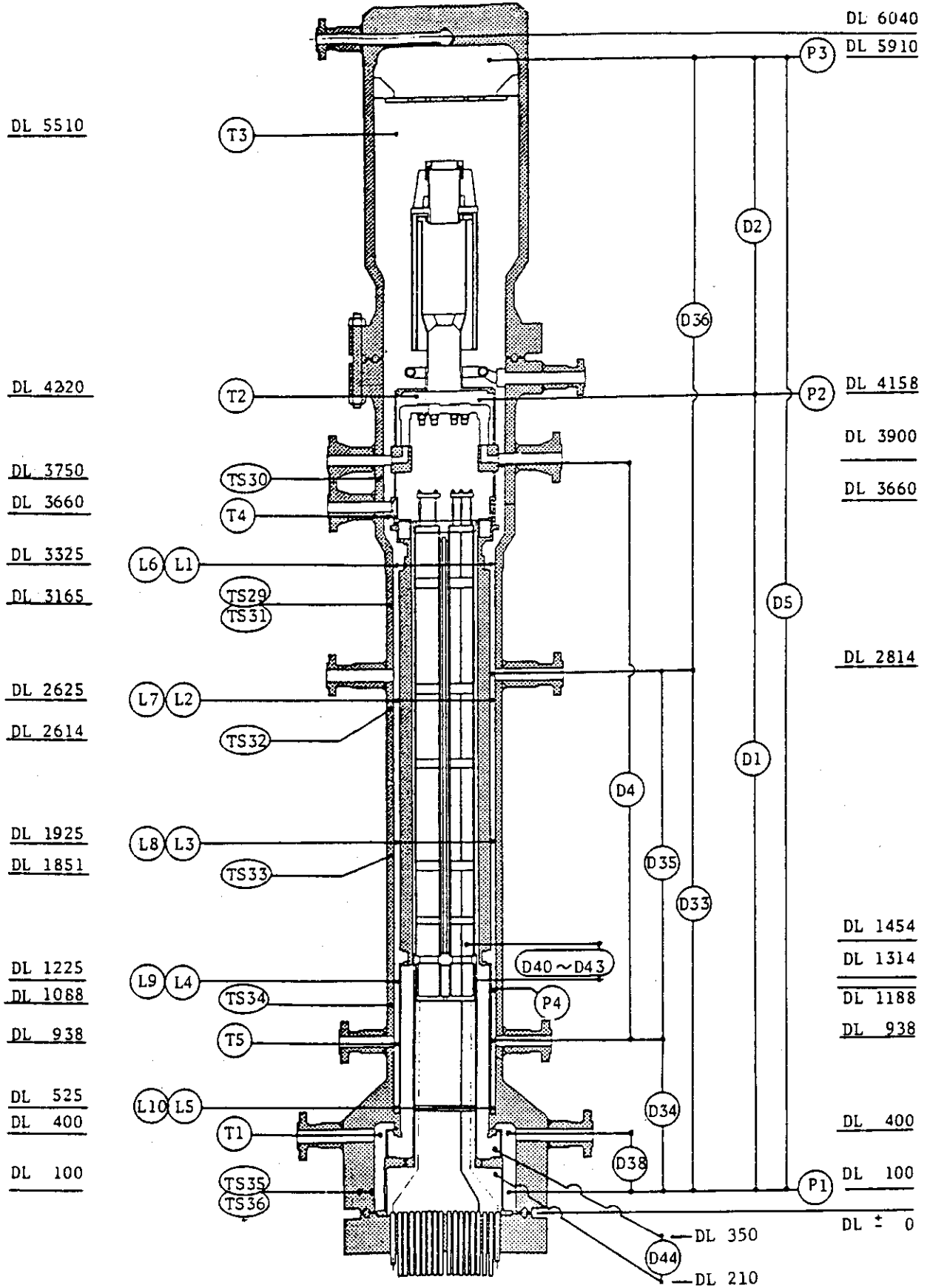


Fig. 3.2 Instrumentation Location in Pressure Vessel

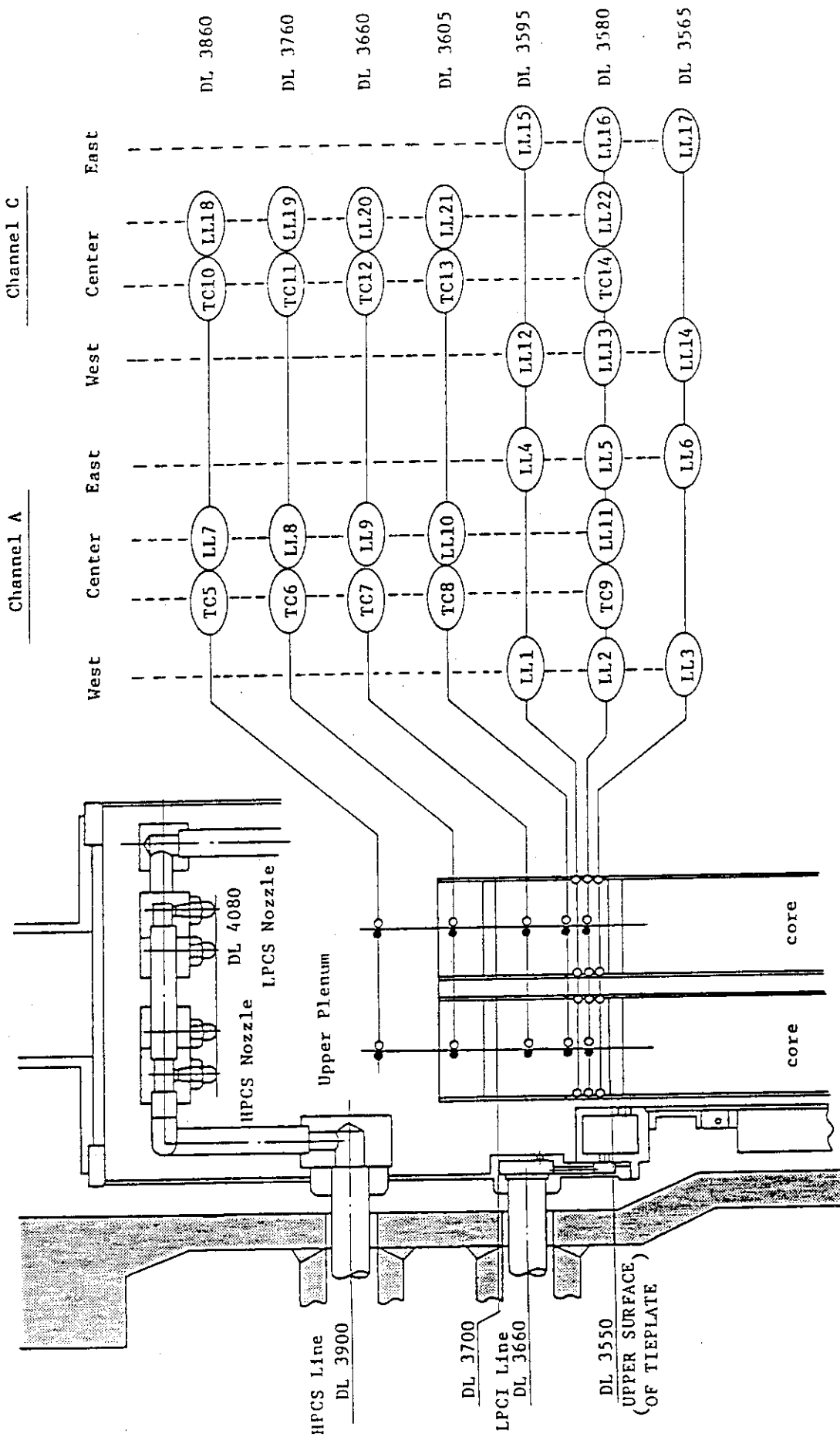


Fig. 3.3 Upper Plenum Instrumentation

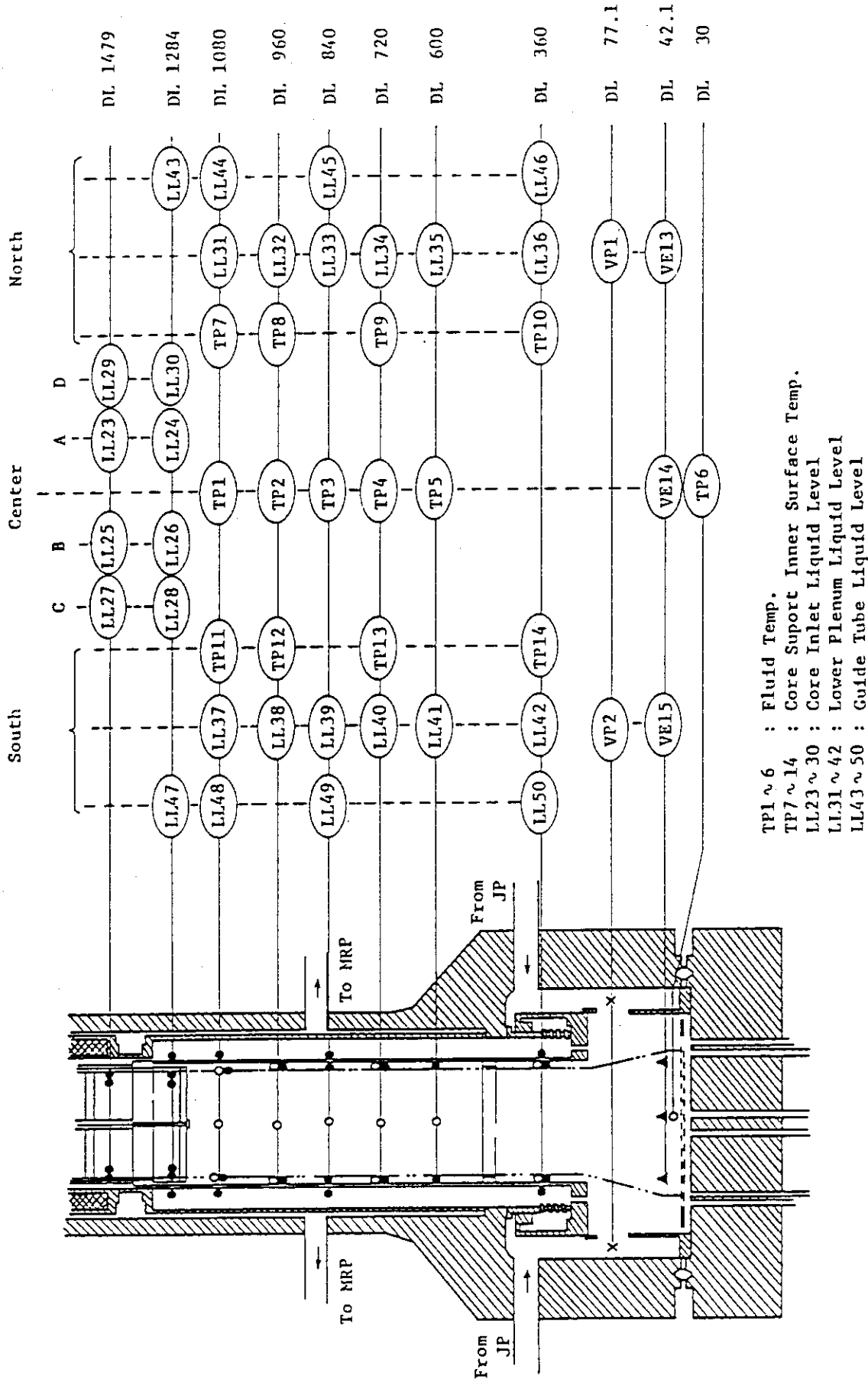
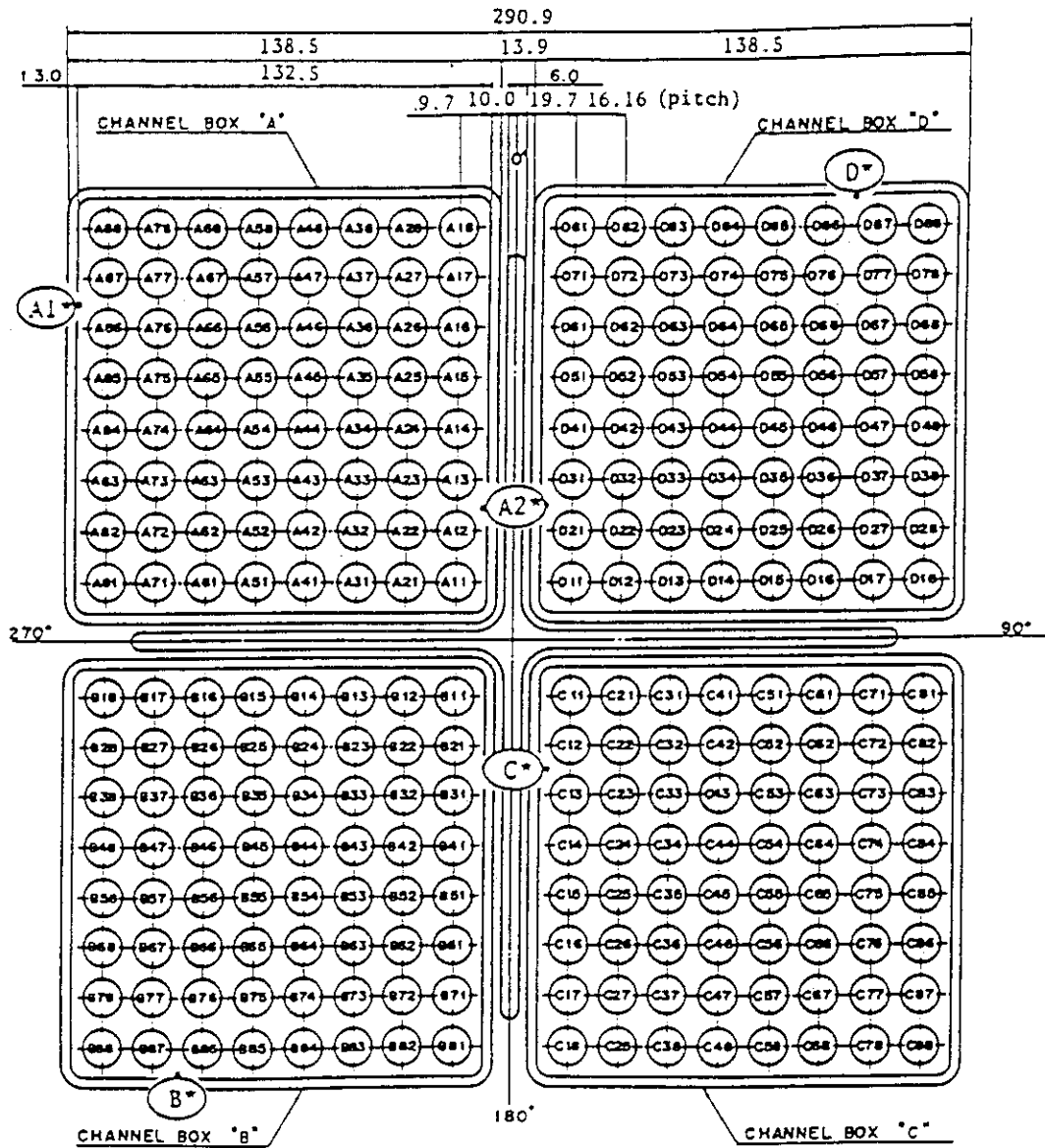
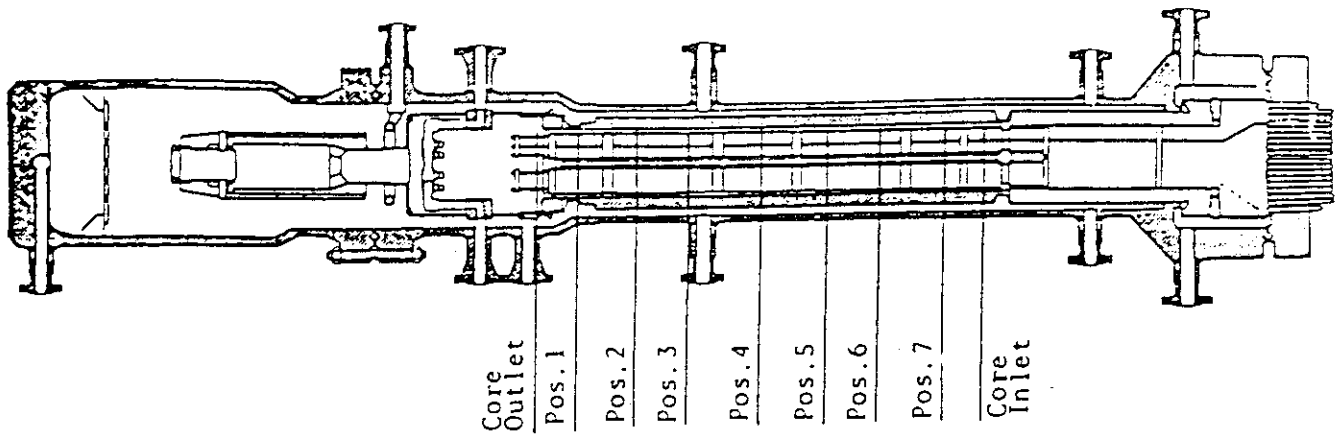


Fig. 3.4 Lower Plenum Instrumentation



Heater rod O.D. is 12.27mm

A54, B54, C54 and D54 are water rod simulators with void probes,  
O.D. = 15.01mm

A45, B45, C45 and D45 are water rod simulators with thermocouples,  
O.D. = 15.01mm

Fig. 3.5 Core Instrumentation (cf. Table 3.3)

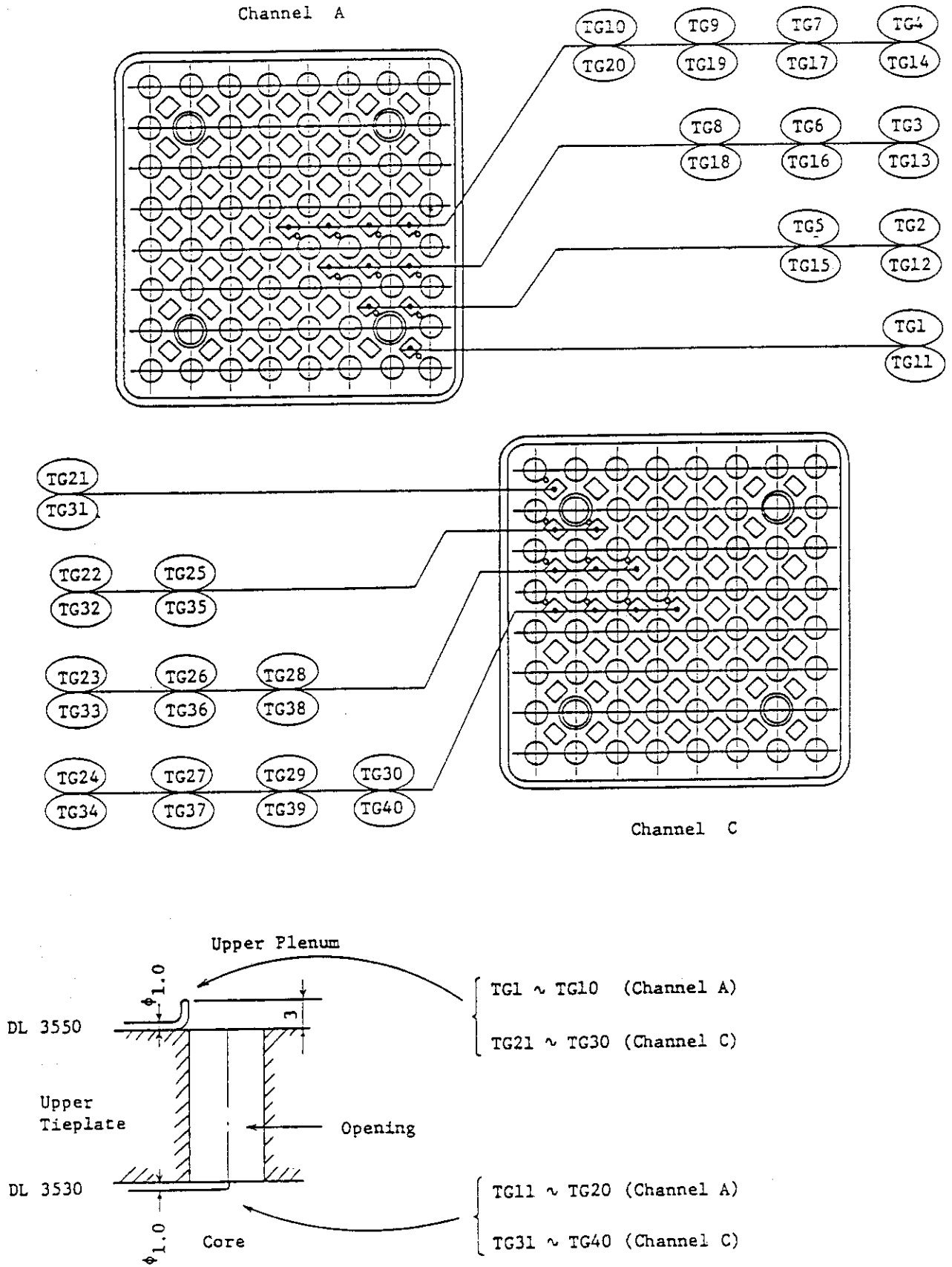


Fig. 3.6 Upper Tieplate Instrumentation



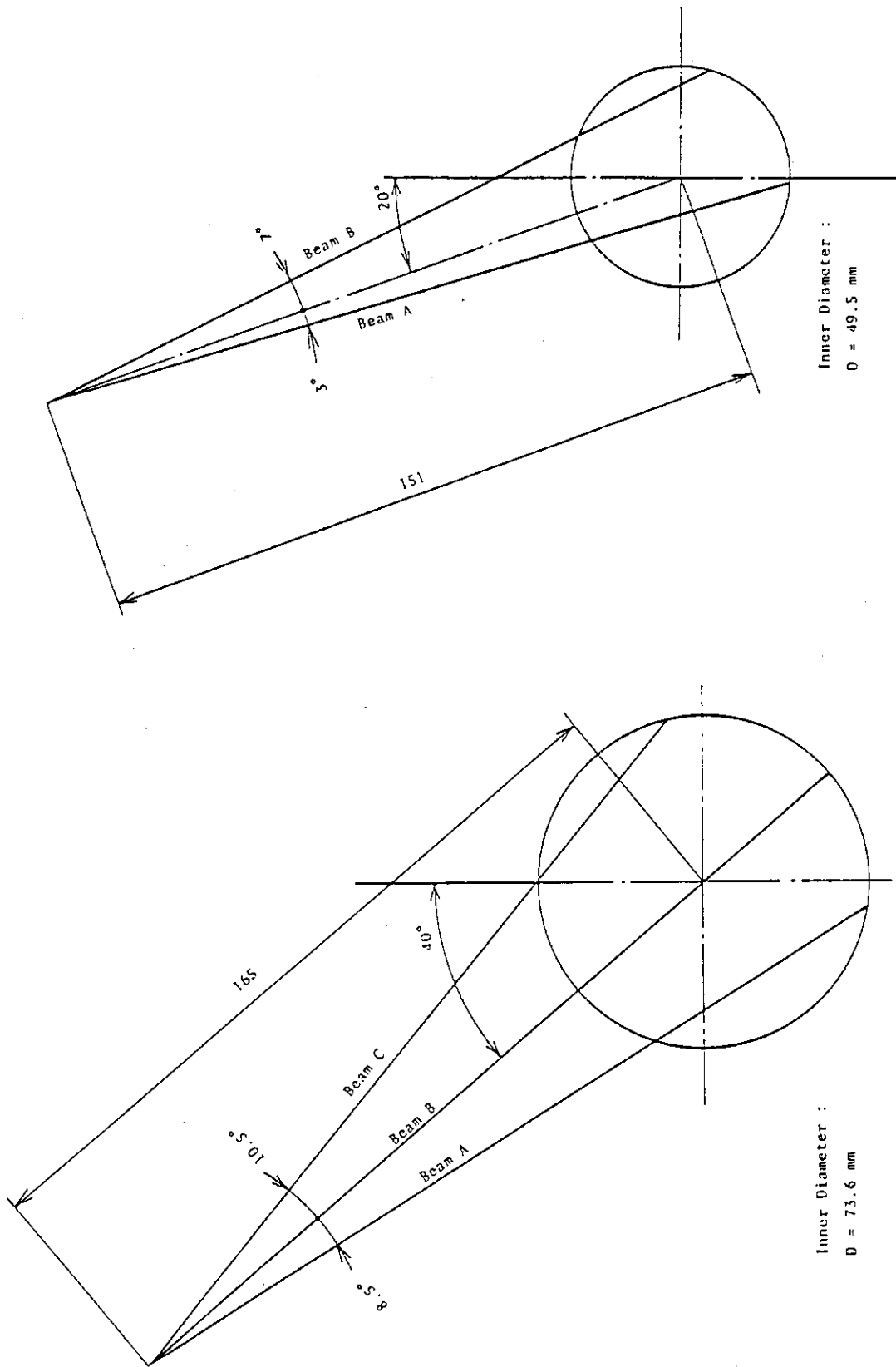
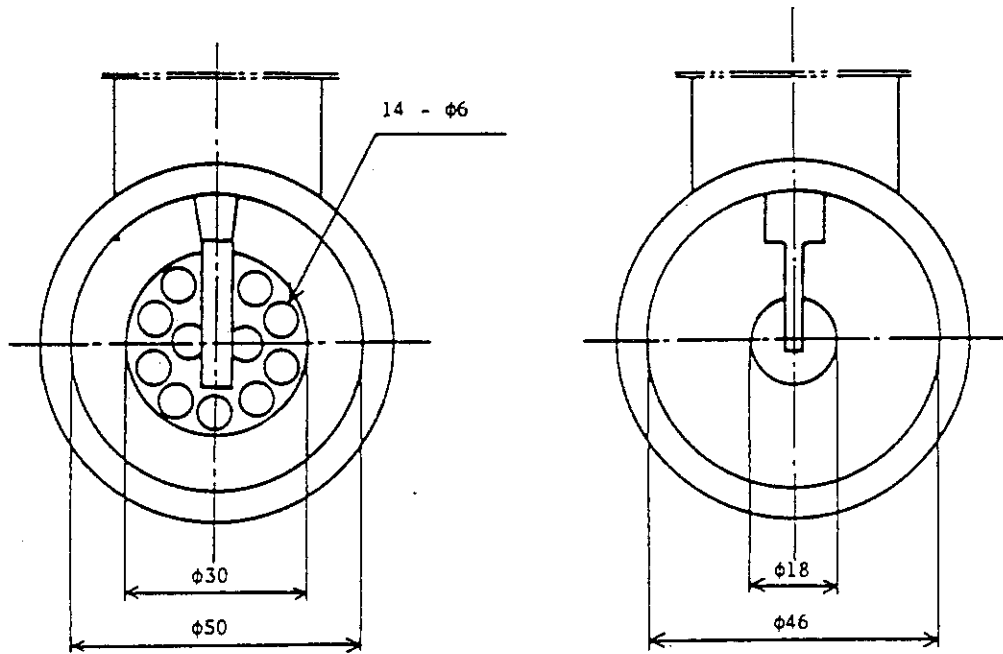


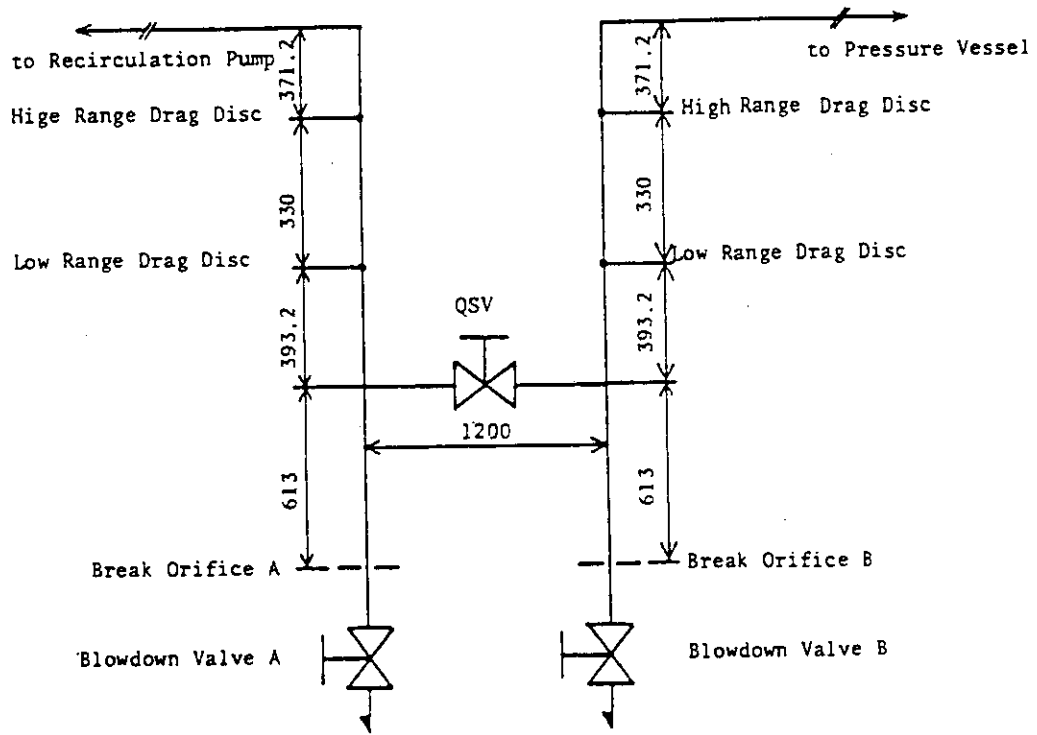
Fig. 3.8 Beam Directions of Two-Beam Gamma Densitometer

Fig. 3.7 Beam Directions of Three-Beam Gamma Densitometer



(a) High Range Drag Disc

(b) Low Range Drag Disc



(c) Location of Drag Discs

Fig. 3.9 Arrangement and Location of Drag Discs

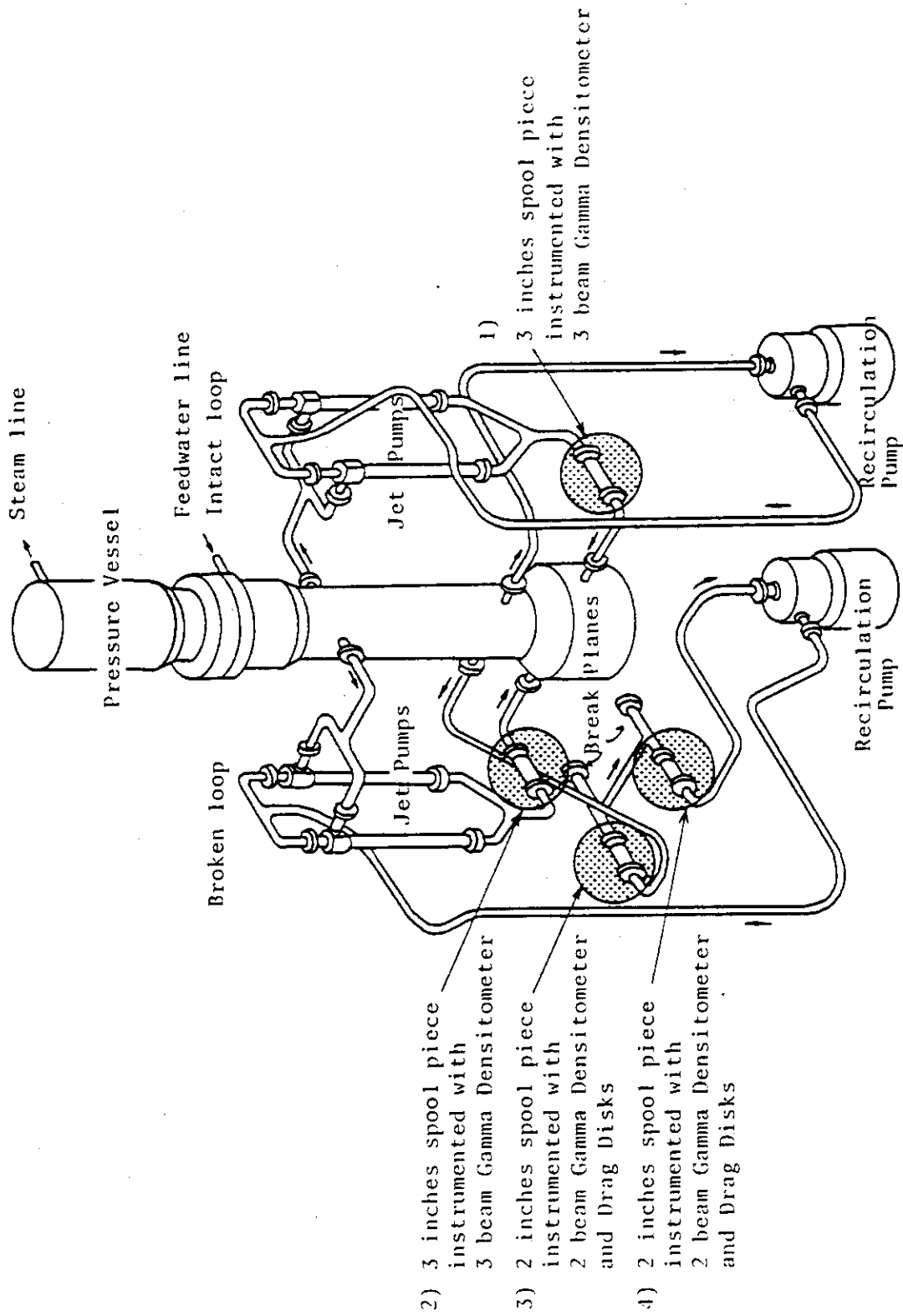


Fig. 3.10 Location of Two-Phase Flow Measurement Spool Pieces

#### 4. Test Conditions and Procedure

RUN 928 was a 50% break test at the recirculation pump suction in the recirculation line. A long throat nozzle was used in RUN 928 as a break plane. The break area was determined by inserting a nozzle upstream of the QOBV as shown in Figs. 4.1 and 3.9. Blowdown is initiated by opening the blowdown valve B. The initial conditions of RUN 928 are as follows: the steam dome pressure is 7.36 MPa, the lower plenum temperature is 554.2K giving the subcooling of 9.4 K, the core inlet flow rate is 16.4 kg/s, the core heat generating rate is 3.962 MW. The estimated quality at the core outlet is 17.2%. The detailed conditions are summarized in Table 4.1

To conduct the test, makeup water (pure water) is pumped into the primary system of the test facility and electric power is supplied to the core to heat the water in the system and to achieve the saturation condition in the upper portion of the pressure vessel. The core power is 3.962 MW in RUN 928 before the break initiation and is 44% of the steady state power 9 MW based on the conservation of the power to volume ratio in the reference BWR. The core power is changed during the transient after the break initiation as shown in Fig. 4.2. The power is kept constant for the first 9.0 seconds and reduced along the curve shown in the figure which simulated the total heat transfer rate in the core of the reference BWR (the delayed neutron fission power, the decay power of fission products and actinides and the stored heat in the nuclear fuel) neglecting the stored heat of ROSA-III heater rod<sup>(3)</sup>. The maximum linear heat rates of the peak power rod are 16.7 kW/m in RUN 928 before the break initiation.

The schematics of the main steam line and the feedwater line are shown in Figs. 4.3 and 4.4. The main steam line of the ROSA-III has three branches: (1) steady flow branch, (2) ADS branch and (3) transient branch. the transient branch was not used in RUN 928. Before the break initiation CV-130 in the steady flow branch controls the steam flow to maintain the steam dome pressure constant and CV-1 and CV-2 are opened to provide steam to the heat exchanger to heat the feedwater. At the break initiation, CV-1 and CV-2 are closed completely, and CV-130 is fully opened manually. Then the MSIV is simulated by CV-130 in the steady flow branch. The steam flow before MSIV closure is limited by an orifice OR-3 of 18.0 mm ID (inner diameter) installed upstream of CV-130. Tables 4.2 and 4.3 show the characteristics and the control sequence of steam discharge line valves in the present test, respectively.

The details of the feedwater line is shown in Fig. 4.5. The feedwater is terminated at 2 s after the break by closing AV-112 in the feedwater line. However, the feedwater remained in the piping between the valve AV-112 and the feedwater sparger below the steam separator in the pressure vessel.

The coolant recirculation pumps are tripped to start coasting down at the break initiation.

The liquid level signals in the downcomer are used to actuate the ECCS and to close the MSIV. The downcomer level in the steady state operation is set at the scram level L3 (5.00 meters above the bottom of the pressure vessel) and L1 and L2 levels are 4.25 meters and 4.76 meters, respectively. The L2 level signal is used to close the MSIV with a time delay of 3 s and to actuate HPCS with time delay of 27 s. The L1 level signal is used to actuate LPCS, LPCI and ADS with time delay of 40 s, 40 s and 120 s, respectively. The above lag times of 3 s, 27 s, 40 s and 120 s are used in a safety analysis of the reference BWR<sup>(4)</sup>. LPCS and LPCI could inject cooling water after the primary system pressure is reduced below 2.16 MPa and 1.57 MPa, respectively. Specified system pressures for actuating LPCS and LPCI were decided from the pump characteristics used in the safety analysis of the reference BWR<sup>(5)</sup>. The test was terminated after the whole core was quenched at 245 s after the break initiation.

Table 4.1 Test Conditions of RUN 928

Parameter	I	Specified Value	I	Measured Value
Break Conditions	I		I	
Location	I	MRP Suction	I	MRP Suction
Configuration	I	Nozzle	I	Nozzle
Break Nozzle Dia. (mm)	I	18.5	I	18.5
Initial System Conditions	I		I	
Steam Dome Press. (MPa)	I	7.36	I	7.36
Lower Plenum Temperature (k)	I	551.7	I	554.2
Lower Plenum Subcooling (K)	I	10.5	I	9.4
Core Inlet Flow Rate (kg/s)	I	16.0	I	16.4
Core Outlet Quality	I	13.8 <sup>(2)</sup>	I	17.2 <sup>(2)</sup>
Power Level (kw)	I	1260 + 2700	I	1261 + 2701
Maximum Linear Heat Rate (kW/m)	I		I	
Channel A P.F.=1.1	I	16.65	I	16.66
P.F.=1.0	I	15.13	I	15.15
P.F.=0.875	I	13.24	I	13.25
Channel B-D P.F.=1.1	I	11.89	I	11.90
P.F.=1.0	I	10.81	I	10.81
P.F.=0.875	I	9.46	I	9.46
Water Level in PV <sup>(1)</sup> (m)	I	5.0	I	5.0
Feedwater Conditions	I		I	
Temperature (K)	I	489.0	I	489.0
Flow Rate (kg/s)	I	2.39	I	Fig.5.1.42
Initiation of Line Closure (s)	I	2.0	I	1.4 - 3.4 s

(1) L3 Level for Scram : 5.0 m from PV Bottom

(2) not include core bypass flow  
core bypass flow is assumed to be 1.6kg/s

Table 4.1 Test Conditions of RUN 928 (contd.)

Parameter	I	Specified Value	I	Measured Value
-----				
Steam Discharge Conditions	I		I	
Steady State Flow Rate(kg/s)	I	2.39	I	2.03
Transient Flow Rate (kg/s)	I	keep steady value	I	Fig.5.40
Orifice Diameter (mm)	I	18.0	I	18.0
Initiation of Line Closure(s)	I	L2 +3 (s)	I	12.6
Safety Relief Valve	I	8.24 < P < 8.34	I	not-used
Setting Pressure (MPa)	I		I	
-----				
ECCS Conditions	I		I	
HPCS	I	not-used	I	not-used
LPCS	I		I	
Injection Location	I	Upper Plenum	I	Upper Plenum
Initial Conditions	I	L1 +40(s) and < 2.16(MPa)	I	147(s) at PV Press. 2.15(MPa)
Coolant Temperature (K)	I	313	I	313
Injection Flow Rate (m /s)	I	$1.13 \times 10^{-3}$	I	Fig.5.41
LPCI	I		I	
Injection Location	I	Core Bypass Top	I	Core Bypass Top
Initiation Conditions	I	L1 +40 (s) and < 1.57 (MPa)	I	186 (s) at PV Press. 1.59(MPa)
Coolant Temperature (K)	I	313	I	313
Injection Flow Rate (m /s)	I	$3.50 \times 10^{-3}$	I	Fig.5.41
-----				
ADS Conditions	I		I	
Initiation Time (s)	I	L1 +120 (s)	I	136 (s)
Flow Rate	I	BWR Scaled Flow	I	Fig.5.40
Orifice Diameter	I	15.5	I	15.5
-----				

note : Each trip level is as follows;  
 L3 Level for Scram : 5.0 m from PV Bottom  
 L2 Level for MSIV and HPCS : 4.76 m from PV Bottom  
 L1 Level for LPCS,LPCI and ADS : 4.25 from PV Bottom

Table 4.2 Characteristics of Steam Discharge Line Valves

Valve	Close to Open (sec)	Open to Close (sec)
AV165	Not Used	Not Used
AV168	-	0.1
AV169	0.3	2.0

Orifice	Diameter (mm)	Area (mm <sup>2</sup> )
OR3	18.0	254.5
OR4	15.5	188.7
OR5	Not Used (Blind)	Not Used (Blind)



Table 4.3 Control Sequence for Steam Discharge Line Valves

Time	$t < 0$ s	$t = 0$ s (Break)	$P \leq 6.67$ MPa	$L2 + 3$ s	---	$P \geq 8.14$ MPa	---	$L1 + 120$ s
CV-1	Open	Close (Manual)	Closed	Closed		Closed		Closed
CV-2 (see Fig.2.3)	Open	Close (Manual)	Closed	Closed		Closed		Closed
CV-130	Control to maintain steady state pressure	Open (Manual)	Control to maintain system pressure at 6.67MPa (Auto)	Close (Manual)		Control to maintain system pressure at 8.14MPa (Auto)		Closed
AV-168	Open	Open	Open	Open		Open		Close (Auto)
AV-169 (ADS Line)	Closed	Closed	Closed	Closed		Closed		Open (Auto)

$t = 0$  s : Break

$t = L2 + 3$  s : MSIV closure

$t = L1 + 120$  s : ADS valve opening

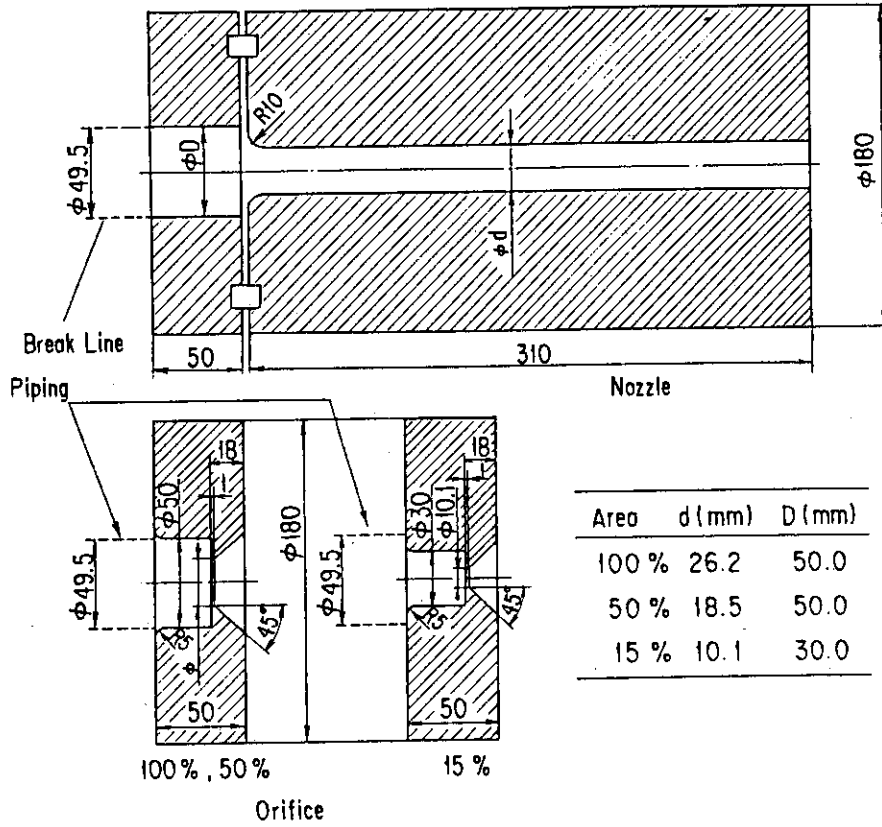


Fig. 4.1 Break configuration details

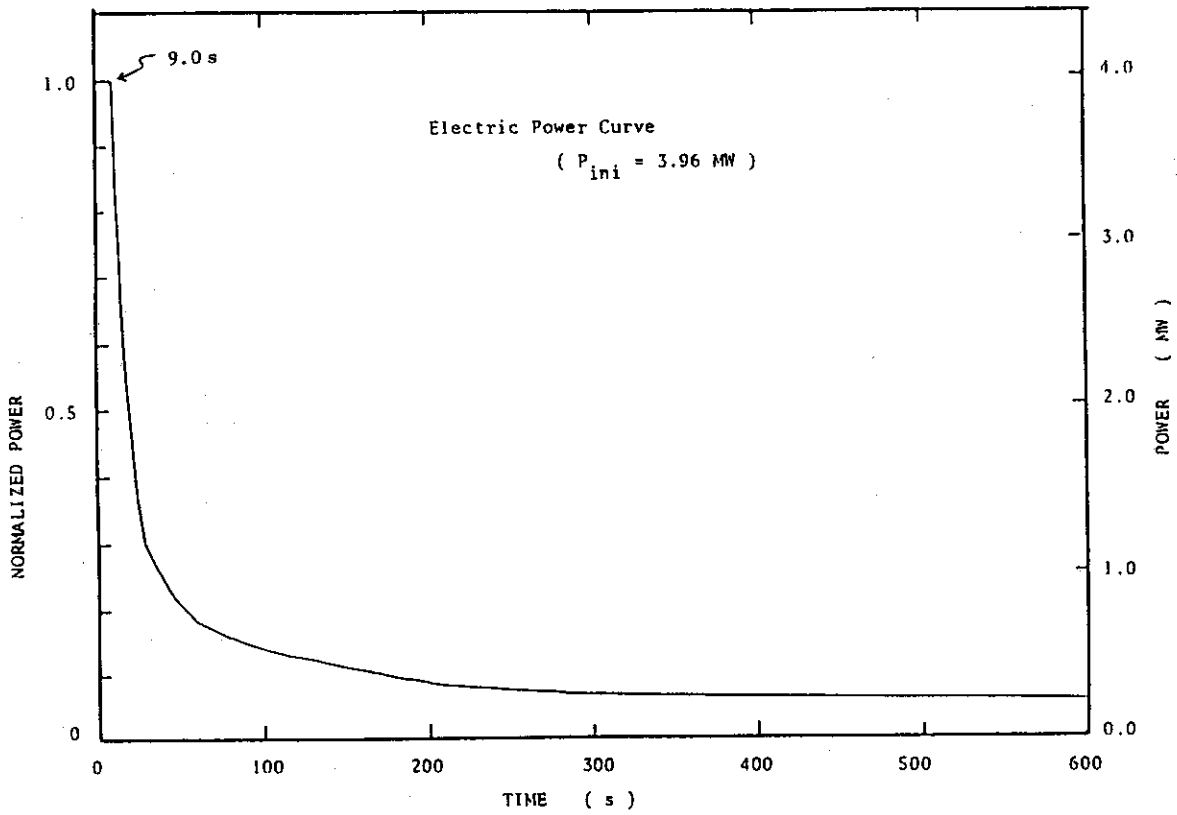


Fig. 4.2 Normalized Power Transient for ROSA-III Test

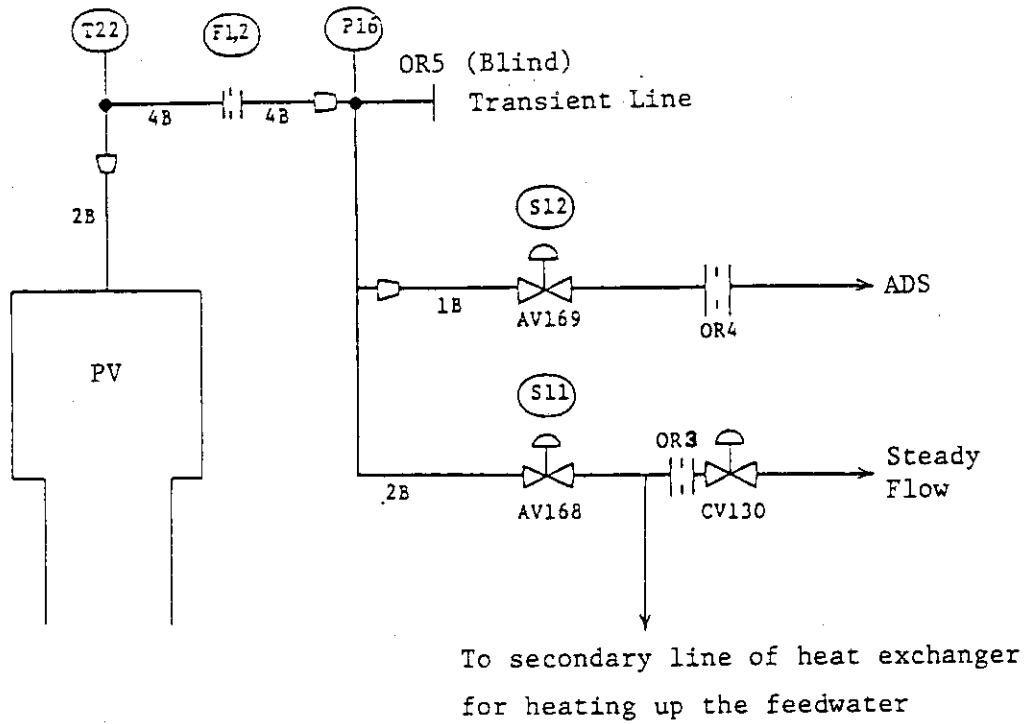


Fig. 4.3 Main Steam Line Schematic

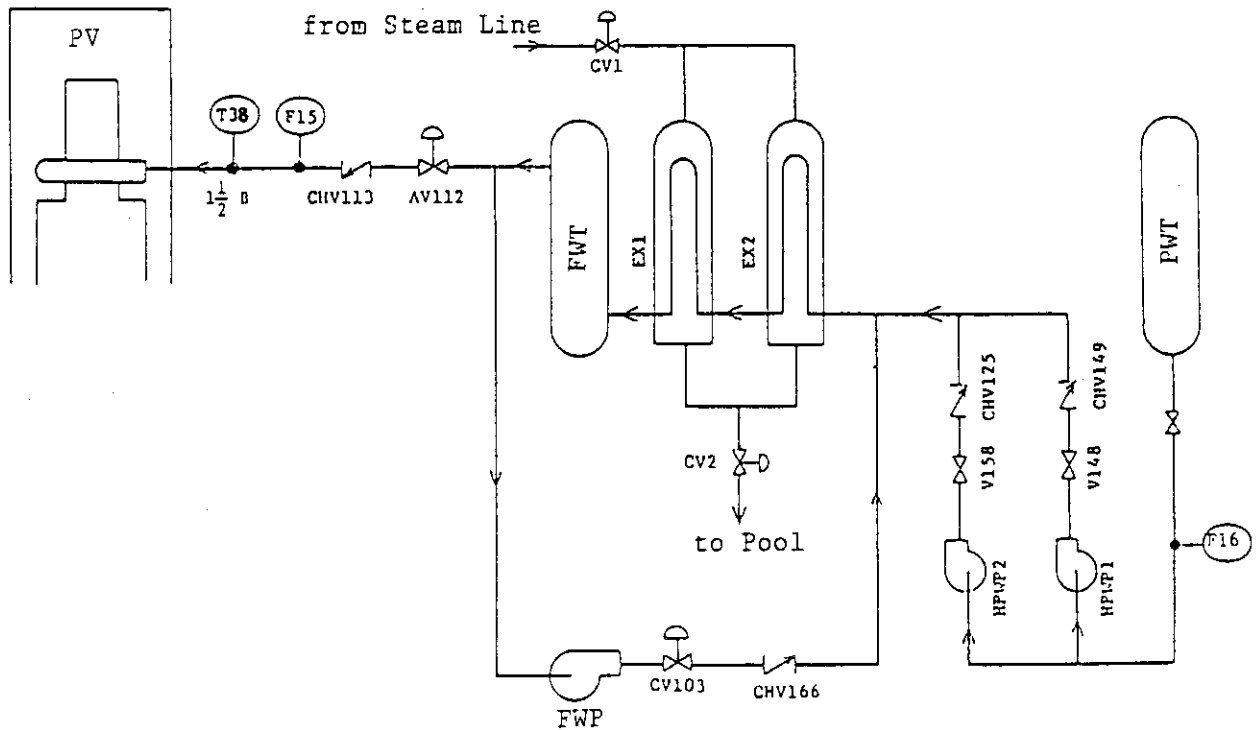


Fig. 4.4 Feedwater Line Schematic

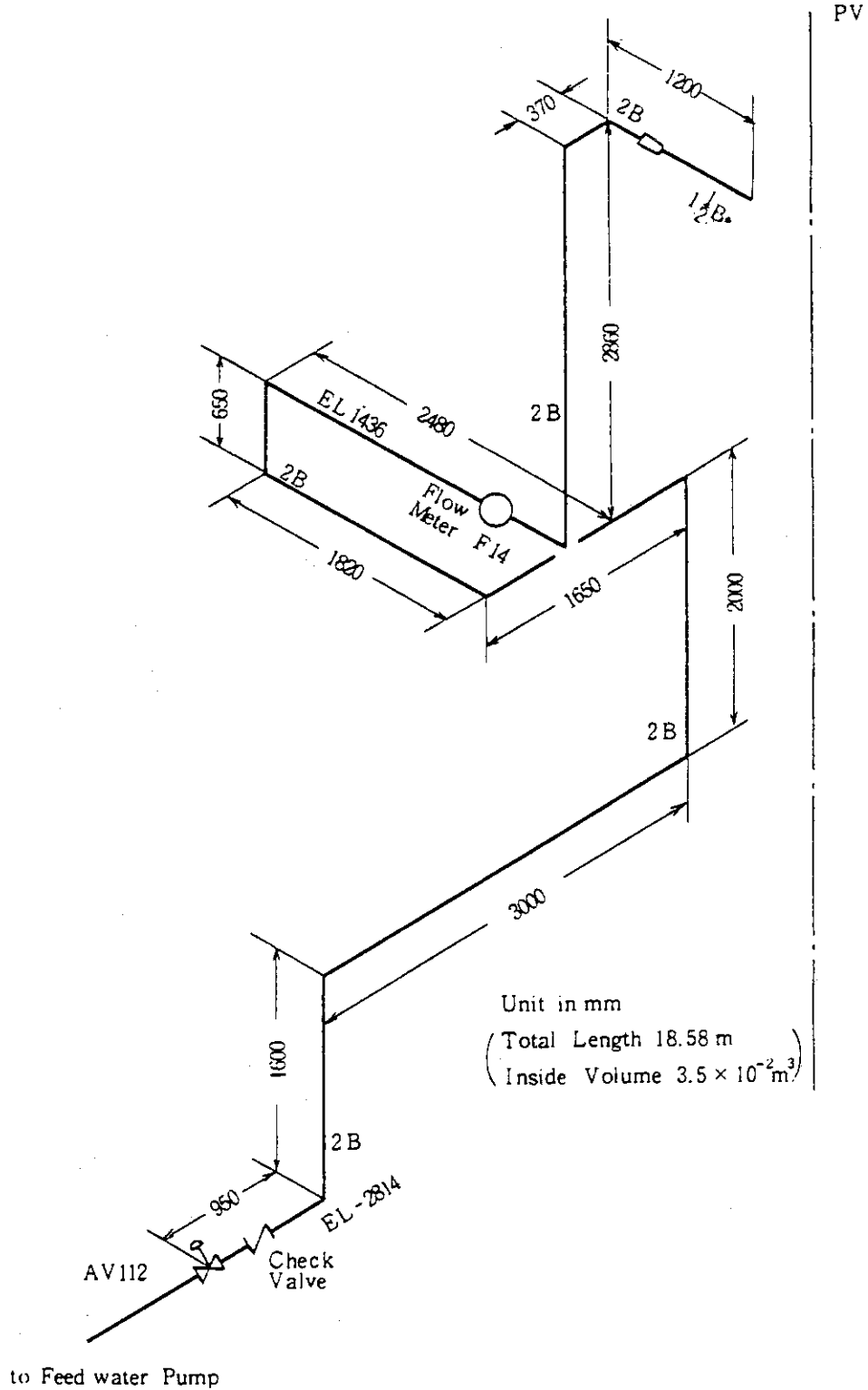


Fig. 4.5 Feedwater Line between Valve AV-112 and Pressure Vessel

## 5. Data Processing

The data acquisition by DATAC 2000B was started 118 s in RUN 928 before the break initiation and terminated 840 s after the break initiation. The data acquisition frequency was 10 Hz. The test data were processed and reduced to 1000 data points for computer plotting. The time span of the reduced data for plotting were 700 s in RUN 928. The test data are shown in Figs. 5.1 through 5.224 for RUN 928. In these figures, the measured quantity is identified by the channel number and the alphabetic characters (Ref. Tables 3.2)

The major test sequences and events observed in RUN 928 are summarized in Table 5.1.

Figures 5.1 through 5.7 show the pressure data in the pressure vessel and in the recirculation loop in RUN 928. Figures 5.8 through 5.37 show differential pressure data between various positions in the pressure vessel and the recirculation loop. Figures 5.38 and 5.39 show the liquid levels in the tanks and in the downcomer. Figures 5.40 through 5.46 show the flow rates. Differential pressures across orifices and venturies shown in Figs. 5.47 through 5.57 are useful to check out the flow rate instrumentation. Figure 5.58 shows the power supplies to the core with the maximum capacities of 2100 and 3150 kW. On-off signals such as the break initiation signal and the valve positioning signals are shown in Figs. 5.59 through 5.61. Figures 5.62 through 5.71 show the fluid densities measured by the gamma densitometer. Figures 5.72 through 5.76 show momentum fluxes measured by drag disks. Figures 5.77 through 5.85 show the fluid temperatures at various positions in the loops. The fuel rod cladding temperature and the surface temperatures of the water rods and the channel boxes measured at positions 1 through 7 are given in Figs. 5.86 through 5.118. Figures 5.119 through 5.165 show the fuel rod cladding temperatures in a different manner. Figures 5.166 through 5.168 show the fluid temperatures at the inlet and outlet of the channel box. The fluid temperatures at upper tieplate of Channel A are shown in Figs. 5.169 through 5.182. The fluid temperatures at upper tieplate of Channel C are shown in Fig. 5.183 through 5.196. The surface temperatures of the channel box are shown in Figs. 5.197 through 5.203, comparing the data at the same elevation. The fluid temperatures in the lower plenum are given in Figs. 5.204 and 5.206. The liquid level signals in the core, the upper and lower plena, the guide tube and the downcomer are shown in Fig. 5.207 through 5.224. The Peak Cladding Tempera-

ture (PCT) distributions in the core are given in Table 5.2 for RUN 928.

Quantities obtained from reduction of the test data are shown in Fig. 5.225 through 5.256. Figures 5.225 shows the estimated liquid level in the pressure vessel obtained by reducing the conductivity probe signals in Figs. 5.207 through 5.224. Figures 5.226 and 5.227 show transients of the dryout front and the quenching front. Figures 5.228 and 5.231 show the average density calculated from the data measured by the three-beam or two-beam gamma densitometers. The beam configurations of gamma densitometers installed in the ROSA-III facility are shown in Figs. 3.7 and 3.8. The average density is calculated as an arithmetic mean of the densities in multi directions with the weight of the cord length.

For the three beam densitometer at the jet pump outlet spool piece,

$$\rho_{av} = 0.3221\rho_A + 0.43\rho_B + 0.2479\rho_C \quad (5.1)$$

where,

$\rho_{av}$ : average density obtained from the three-beam gamma densitometer,

$\rho_A$ : density measured by beam A (bottom),

$\rho_B$ : density measured by beam B (middle),

$\rho_C$ : density measured by beam C (top).

For the two-beam densitometer at the break spool piece,

$$\rho_{av} = 0.5863\rho_A + 0.4137\rho_B \quad (5.2)$$

where,

$\rho_{av}$ : average density obtained from the two-beam gamma densitometer,

$\rho_A$ : density measured by beam A (bottom),

$\rho_B$ : density measured by beam B (top).

Figures 5.232 through 5.235 show the flow rates at upstream sides of the break in the recirculation loop. The flow rate is computed from the drag disk data and the gamma densitometer data using the following equation,

$$G = C_D \cdot A \cdot \sqrt{\rho_{av} \cdot \rho v^2} \quad (5.3)$$

where,

- $G$  : mass flow rate,  
 $C_D$  : drag coefficient ( = 1.13 ),  
 $A$  : flow area ( =  $1.923 \times 10^{-3} \text{ m}^2$  ),  
 $\rho_{av}$  : average density from gamma densitometer,  
 $\rho v^2$  : momentum flux from drag disk.

The break flow is derived from the flow rate in the recirculation loop as follows,

$$G_B = G_P - G_V \quad (5.4)$$

where,

- $G_B$  : break flow,  
 $G_P$  : flow rate at the pump side of the break,  
 $G_V$  : flow rate at the vessel side of the break,

The break flow rates are shown in Figs. 5.236 and 5.237

Figures 5.238 through 5.248 show the fluid flow rates at the main steam line, the channel inlet orifices, the bypass hole and the jet pump outlets. The fluid flow rates are calculated from the test data which are the pressure drop across the orifices or venturi flow meters and the liquid density obtained from the temperature and the pressure condition. The equation used for the calculation is as follows :

$$G = C_D \cdot A \cdot \sqrt{2g \cdot \rho_l \cdot \Delta P} \quad (5.5)$$

where,

- $G$  : flow rate,  
 $\Delta P$  : pressure drop across the orifice,  
 $C_D$  : discharge coefficient,  
 = 0.6552 ( the orifice to measure the steam discharge flow rate )  
 = 0.4761 ( the channel inlet orifice )  
 = 0.8032 ( the bypass hole )  
 = 0.7383 ( the orifice to measure the jet pump outlet flow rate )  
 = 1.1260 ( the venturi tube to measure the jet pump outlet flow rate )

- $A$  : flow area (  $\text{m}^2$  )  
 $= 2.875 \times 10^{-3}$  ( the orifice to measure the steam discharge flow rate )  
 $= 1.521 \times 10^{-3}$  ( the channel inlet orifice )  
 $= 1.758 \times 10^{-4}$  ( the bypass hole )  
 $= 1.133 \times 10^{-3}$  ( the orifice to measure the jet pump outlet flow rate )  
 $= 9.095 \times 10^{-4}$  ( the venturi tube to measure the jet pump outlet flow rate )
- $g$  : gravitational acceleration (  $= 9.807 \text{ m/s}^2$  ),  
 $\rho_l$  : density of the single-phase liquid (  $\text{kg/m}^3$  ),

This calculation method is not applicable for two-phase flow condition after the LPF initiation at the channel inlet orifice, the bypass hole and the jet pump outlet. The calculated value shows only a trend in two-phase flow condition. Total channel inlet flow rate presents the sum of four channel inlet flow rates.

Figure 5.249 and 5.250 show the collapsed water level outside and inside the shroud. The collapsed water level is obtained from the differential pressure in the pressure vessel. The differential pressure may include the flow resistance effect, however, the flow resistance becomes negligible after completion of the recirculation pump coastdown.

Figures 5.251 through 5.253 show the fluid mass inventories in the pressure vessel. The fluid mass inventory is determined from the density and the volumes of liquid outside and inside the shroud,

$$M = \rho_l \cdot Q \quad (5.6)$$

where,

$M$  : fluid inventory,

$\rho_l$  : liquid density estimated from the saturation temperature and/or pressure,

$Q$  : liquid volume calculated from the liquid level.

The volume  $Q$  (  $\text{m}^3$  ) outside the shroud is given below as a function of height.

$$Q = 0.0 \quad ( \quad L \leq 0.494 \quad )$$



$$\begin{aligned}
Q &= 0.0225L - 0.0111 & ( 0.494 < L \leq 1.384 ) \\
Q &= 0.0697L - 0.0769 & ( 1.384 < L \leq 1.519 ) \\
Q &= 0.0225L - 0.0048 & ( 1.519 < L \leq 3.355 ) \\
Q &= 0.0801L - 0.1980 & ( 3.355 < L \leq 4.250 ) \\
Q &= 0.2443L - 0.8959 & ( 4.250 < L \leq 4.413 ) \\
Q &= 0.2611L - 0.9700 & ( 4.413 < L \leq 4.578 ) \\
Q &= 0.2504L - 0.9211 & ( 4.578 < L \leq 4.654 ) \\
Q &= 0.2375L - 0.8610 & ( 4.654 < L \leq 4.815 ) \\
Q &= 0.2866L - 1.0974 & ( 4.815 < L \leq 4.915 ) \\
Q &= 0.3396L - 1.3580 & ( 4.915 < L \leq 5.143 ) \\
Q &= 0.3607L - 1.4665 & ( 5.143 < L \leq 5.365 ) \\
Q &= 0.3848L - 1.5960 & ( 5.365 < L \leq 5.955 ) \\
Q &= 0.7111 & ( 5.955 < L )
\end{aligned} \tag{5.7}$$

The volume  $Q$  ( $\text{m}^3$ ) inside the shroud is given below as a function of height.

$$\begin{aligned}
Q &= 0.0 & ( L \leq 0.0 ) \\
Q &= 0.2350L & ( 0.0 < L \leq 0.497 ) \\
Q &= 0.1245L + 0.0549 & ( 0.497 < L \leq 1.354 ) \\
Q &= 0.0698L + 0.1290 & ( 1.354 < L \leq 3.589 ) \\
Q &= 0.1648L - 0.2120 & ( 3.589 < L \leq 3.744 ) \\
Q &= 0.1963L - 0.3299 & ( 3.744 < L \leq 4.243 ) \\
Q &= 0.0196L + 0.4199 & ( 4.243 < L \leq 4.578 ) \\
Q &= 0.0186L + 0.4244 & ( 4.578 < L \leq 4.654 ) \\
Q &= 0.0410L + 0.3201 & ( 4.654 < L \leq 5.099 ) \\
Q &= 0.0196L + 0.4292 & ( 5.099 < L \leq 5.365 ) \\
Q &= 0.5344 & ( 5.365 < L )
\end{aligned} \tag{5.8}$$

The total fluid mass inventory in the pressure vessel is obtained as the summation of the mass inventory outside and inside the shroud.

Figure 5.254 shows the mass decrease by the fluid discharge from the break and the fluid mass recovery by the ECCS water and the feedwater injections. The variation of fluid mass inventory with time is calculated by the following equation,

$$M = \int_0^t \{ G + \rho_1 \cdot (W_H + W_L + W_I) + \rho_2 \cdot W_F \} dt \tag{5.9}$$

where,

- $M$  : mass accumulation,
- $G$  : steam discharge flow rate,
- $\rho_1$  : density of saturated liquid at 315 K,
- $\rho_2$  : density of saturated liquid at 489 K,
- $W_H$  : volumetric flow rate of the HPCS,
- $W_L$  : volumetric flow rate of the LPCS,
- $W_I$  : volumetric flow rate of the LPCI,
- $W_F$  : volumetric flow rate of the feedwater.

Figure 5.255 shows the fluid mass discharged from the break. The fluid mass discharge  $M_B$  is calculated as follows neglecting the change of the fluid mass inventory in the loops,

$$M_B = (M_P)_i - M_P + M_F \quad (5.10)$$

where,

- $M_B$  : fluid mass discharged from the break,
- $(M_P)_i$  : fluid mass inventory in the pressure vessel ( = 640 kg ),
- $M_P$  : fluid mass inventory in the pressure vessel,
- $M_F$  : net fluid mass increase by the ECCS, the feedwater flow and the steam discharge flow.

Figure 5.256 shows the break flow calculated from the fluid mass inventory in the pressure vessel. The break flow is estimated from the mass inventory as follows,

$$G_B = \frac{d}{dt} M_B \quad (5.11)$$

where,

- $G_B$  : break flow,
- $M_B$  : fluid mass discharged from the break.

Table 5.1 Sequence of Events in RUN 928

Time after break (s)	I	Events
0.0	I	Break
	I	Initiation of core power control
	I	Termination of MRP power input
1.4	I	Initiation of FW line valve closure
3.4	I	Closure of FW line valve
8.4	I	L2 level trip signal
14.5	I	L1 level trip signal
12.6-16.2	I	Main steam line valve closure
9.0	I	Initiation of core power reduction
19.6	I	Jet pump suction nozzle uncover
25.8	I	Recirculation line nozzle uncover
35	I	Dryout at the top of the core
45	I	Initiation of lower plenum flashing
120	I	Whole core uncover
136	I	ADS actuation
147	I	LPCS initiation ( at system pressure
148	I	Initiation of FW line flashing 2.26 MPa )
186	I	LPCI initiation ( at system pressure 1.68 MPa )
245	I	Whole core quench
248	I	Completion of core reflooding

Table 5.2 Maximum Cladding Temperature Distribution in the Core

	Pos.1	Pos.2	Pos.3	Pos.4	Pos.5	Pos.6	Pos.7
A-11 rod	TE 201	TE 202	TE 203	TE 204	TE 205	TE 206	TE 207
PCT (K)	615.1	719.5	859.9	886.3	825.1	715.9	585.1
Time (s)	109.9	128.1	198.1	193.2	197.4	195.3	190.4
A-12 rod	TE 208	TE 209	TE 210	TE 211	TE 212	TE 213	TE 214
PCT (K)	610.3	753.1	835.9	867.1	796.3	702.7	567.1
Time (s)	112.7	160.3	182.7	196.7	196.0	193.2	20.3
A-13 rod	TE 215	TE 216	TE 217	TE 218	TE 219	TE 220	TE 221
PCT (K)	615.1	759.1	826.3	863.5	795.1	-----	566.4
Time (s)	115.5	159.6	172.9	196.0	196.0	-----	0.0
A-14 rod	TE 222	TE 223	TE 224	TE 225	TE 226	TE 227	TE 228
PCT (K)	612.7	748.3	815.5	845.5	781.9	687.1	-----
Time (s)	116.9	162.4	183.4	196.7	193.9	194.6	-----
A-15 rod	TE 229			TE 230			
PCT (K)	617.5			847.9			
Time (s)	122.5			195.3			
A-17 rod	TE 231			TE 232			
PCT (K)	660.7			868.2			
Time (s)	151.2			196.0			
A-22 rod	TE 233	TE 234	TE 235	TE 236	TE 237	TE 238	TE 239
PCT (K)	649.9	769.9	828.7	865.1	799.4	708.2	568.1
Time (s)	151.2	159.6	175.0	196.0	196.7	195.3	19.6
A-24 rod	TE 240	TE 241	TE 242	TE 243	TE 244	TE 245	TE 246
PCT (K)	611.4	762.8	819.1	851.0	786.3	696.0	568.1
Time (s)	121.1	161.7	175.7	196.0	195.3	191.8	20.3

Table 5.2 Maximum Cladding Temperature Distribution in the Core (Continued)

	Pos.1	Pos.2	Pos.3	Pos.4	Pos.5	Pos.6	Pos.7
A-26 rod	TE 247			TE 248			
PCT (K)	669.5			858.5			
Time (s)	150.5			195.3			
A-28 rod	TE 249			TE 250			
PCT (K)	676.1			877.3			
Time (s)	153.3			194.6			
A-31 rod	TE 251			TE 252			
PCT (K)	629.6			870.9			
Time (s)	118.3			194.6			
A-33 rod	TE 253	TE 254	TE 255	TE 256	TE 257	TE 258	TE 259
PCT (K)	609.5	737.4	788.2	818.2	748.7	678.0	565.1
Time (s)	128.8	159.6	169.4	195.3	193.9	190.4	0.0
A-34 rod	TE 260	TE 261	TE 262	TE 263	TE 264	TE 265	TE 266
PCT (K)	652.4	741.2	791.0	822.9	754.4	675.2	566.2
Time (s)	151.2	163.8	175.7	195.3	195.3	190.4	18.9
A-37 rod	TE 267			TE 268			
PCT (K)	853.9			658.1			
Time (s)	195.3			156.8			
A-42 rod	TE 269			TE 270			
PCT (K)	640.0			867.9			
Time (s)	141.4			198.1			
A-44 rod	TE 271	TE 272	TE 273	TE 274	TE 275	TE 276	TE 277
PCT (K)	625.7	736.5	793.8	811.6	745.9	662.8	566.2
Time (s)	150.5	197.4	192.5	193.9	195.3	186.9	18.2

Table 5.2 Maximum Cladding Temperature Distribution in the Core (Continued)

	Pos.1	Pos.2	Pos.3	Pos.4	Pos.5	Pos.6	Pos.7
A-48 rod	TE 278			TE 279			
PCT (K)	696.0			846.3			
Time (s)	203.0			194.6			
A-51 rod	TE 280			TE 281			
PCT (K)	666.6			867.0			
Time (s)	152.6			196.0			
A-53 rod	TE 282			TE 283			
PCT (K)	650.5			818.2			
Time (s)	150.5			198.1			
A-57 rod	TE 284			TE 285			
PCT (K)	729.9			858.5			
Time (s)	205.8			194.6			
A-62 rod	TE 286			TE 287			
PCT (K)	678.0			871.7			
Time (s)	155.4			198.1			
A-66 rod	TE 288			TE 289			
PCT (K)	706.4			822.9			
Time (s)	208.6			194.6			
A-68 rod	TE 290			TE 291			
PCT (K)	720.5			876.4			
Time (s)	189.7			195.3			
A-71 rod	TE 292			TE 293			
PCT (K)	682.7			887.7			
Time (s)	158.9			198.1			

Table 5.2 Maximum Cladding Temperature Distribution in the Core (Continued)

	Pos.1	Pos.2	Pos.3	Pos.4	Pos.5	Pos.6	Pos.7
A-73 rod	TE 294			TE 295			
PCT (K)	686.5			873.6			
Time (s)	159.6			198.1			
A-75 rod	TE 296			TE 297			
PCT (K)	696.0			858.5			
Time (s)	207.9			193.9			
A-77 rod	TE 298	TE 299	TE 300	TE 301	TE 302	TE 303	TE 304
PCT (K)	745.0	827.6	862.3	856.7	790.0	682.7	-----
Time (s)	207.2	201.6	201.6	195.3	195.3	193.9	-----
A-82 rod	TE 305			TE 306			
PCT (K)	696.9			-----			
Time (s)	159.6			-----			
A-84 rod	TE 307			TE 308			
PCT (K)	681.8			861.0			
Time (s)	159.6			199.5			
A-85 rod	TE 309	TE 310	TE 311	TE 312	TE 313	TE 314	TE 315
PCT (K)	697.9	813.5	863.2	871.7	802.2	696.9	574.9
Time (s)	200.2	203.0	200.2	192.5	195.3	193.2	179.2
A-87 rod	TE 316	TE 317	TE 318	TE 319	TE 320	TE 321	TE 322
PCT (K)	732.7	821.0	868.9	875.5	806.0	700.7	573.0
Time (s)	202.3	202.3	195.3	193.9	193.2	193.9	174.3
A-88 rod	TE 323	TE 324	TE 325	TE 326	TE 327	TE 328	TE 329
PCT (K)	694.1	808.8	860.4	877.3	809.7	704.5	574.9
Time (s)	170.8	203.7	192.5	195.3	196.0	194.6	172.9

Table 5.2 Maximum Cladding Temperature Distribution in the Core (Continued)

	Pos.1	Pos.2	Pos.3	Pos.4	Pos.5	Pos.6	Pos.7
B-11 rod	TE 330	TE 331	TE 332	TE 333	TE 334	TE 335	TE 336
PCT (K)	607.6	720.5	795.7	804.1	743.1	654.3	500.6
Time (s)	113.4	151.2	193.2	196.0	196.0	193.2	198.8
B-13 rod				TE 337			
PCT (K)				796.6			
Time (s)				196.0			
B-22 rod	TE 338	TE 339	TE 340	TE 341	TE 342	TE 343	TE 344
PCT (K)	631.4	718.6	771.3	796.6	722.4	639.1	565.3
Time (s)	149.8	151.9	168.7	194.6	189.7	180.6	20.3
B-31 rod				TE 345			
PCT (K)				796.6			
Time (s)				195.3			
B-33 rod				TE 346			
PCT (K)				754.4			
Time (s)				195.3			
B-51 rod				TE 347			
PCT (K)				777.8			
Time (s)				193.2			
B-53 rod				TE 348			
PCT (K)				745.9			
Time (s)				195.3			
B-66 rod				TE 349			
PCT (K)				753.4			
Time (s)				192.5			

Table 5.2 Maximum Cladding Temperature Distribution in the Core (Continued)

	Pos.1	Pos.2	Pos.3	Pos.4	Pos.5	Pos.6	Pos.7
B-77 rod	TE 350	TE 351	TE 352	TE 353	TE 354	TE 355	TE 356
PCT (K)	714.8	785.4	814.4	809.7	742.1	647.6	567.2
Time (s)	205.8	204.4	193.9	195.3	193.9	192.5	20.3
B-86 rod				TE 357			
PCT (K)				817.2			
Time (s)				195.3			
C-11 rod	TE 358	TE 359	TE 360	TE 361	TE 362	TE 363	TE 364
PCT (K)	595.1	661.9	772.2	793.8	738.4	654.3	568.1
Time (s)	102.9	118.3	166.6	192.5	193.9	192.5	25.2
C-13 rod	TE 365	TE 366	TE 367	TE 368	TE 369	TE 370	TE 371
PCT (K)	595.1	715.8	768.5	792.8	736.5	652.4	567.2
Time (s)	103.6	152.6	161.7	197.4	195.3	186.9	21.0
C-15 rod				TE 372			
PCT (K)				791.9			
Time (s)				196.0			
C-22 rod	TE 373	TE 374	TE 375	TE 376	TE 377	TE 378	TE 379
PCT (K)	617.1	712.0	766.6	791.0	730.8	647.6	567.2
Time (s)	149.8	149.8	167.3	195.3	196.7	191.8	21.0
C-31 rod				TE 380			
PCT (K)				798.5			
Time (s)				191.1			
C-33 rod	TE 381	TE 382	TE 383	TE 384	TE 385	TE 386	TE 387
PCT (K)	582.6	686.5	729.0	755.3	696.9	621.9	565.3
Time (s)	102.9	151.2	162.4	198.1	195.3	186.2	22.4

Table 5.2 Maximum Cladding Temperature Distribution in the Core (Continued)

	Pos.1	Pos.2	Pos.3	Pos.4	Pos.5	Pos.6	Pos.7
C-35 rod				TE 388			
PCT (K)				766.6			
Time (s)				194.6			
C-66 rod				TE 389			
PCT (K)				755.3			
Time (s)				193.9			
C-68 rod				TE 390			
PCT (K)				815.4			
Time (s)				194.6			
C-77 rod	TE 391	TE 392	TE 393	TE 394	TE 395	TE 396	TE 397
PCT (K)	679.9	766.6	797.5	800.4	731.8	637.1	567.2
Time (s)	173.6	205.1	193.9	194.6	190.4	183.4	21.0
D-11 rod				TE 398			
PCT (K)				805.0			
Time (s)				214.9			
D-13 rod				TE 399			
PCT (K)				812.5			
Time (s)				213.5			
D-22 rod	TE 400	TE 401	TE 402	TE 403	TE 404	TE 405	TE 406
PCT (K)	644.8	732.7	776.9	803.2	736.5	655.2	567.2
Time (s)	149.1	155.4	168.7	214.2	195.3	190.4	20.3
D-31 rod				TE 407			
PCT (K)				813.5			
Time (s)				215.6			

Table 5.2 Maximum Cladding Temperature Distribution in the Core (Continued)

	Pos.1	Pos.2	Pos.3	Pos.4	Pos.5	Pos.6	Pos.7
D-33 rod				TE 408			
PCT (K)				759.1			
Time (s)				215.6			
D-51 rod				TE 409			
PCT (K)				787.2			
Time (s)				215.6			
D-53 rod				TE 410			
PCT (K)				761.9			
Time (s)				220.5			
D-66 rod				TE 411			
PCT (K)				753.4			
Time (s)				218.4			
D-77 rod				TE 412			
PCT (K)				802.3			
Time (s)				213.5			
D-86 rod				TE 413			
PCT (K)				804.1			
Time (s)				193.2			

Table 5.2 Maximum Cladding Temperature Distribution in the Core (Continued)

\*\* Order of PCT \*\*

No. 1	A-71 rod	Pos. 4	PCT = 887.7 (K)	Time = 198.1 (s)
No. 2	A-11 rod	Pos. 4	PCT = 886.3 (K)	Time = 193.2 (s)
No. 3	A-28 rod	Pos. 4	PCT = 877.3 (K)	Time = 194.6 (s)
No. 4	A-88 rod	Pos. 4	PCT = 877.3 (K)	Time = 195.3 (s)
No. 5	A-68 rod	Pos. 4	PCT = 876.4 (K)	Time = 195.3 (s)
No. 6	A-87 rod	Pos. 4	PCT = 875.5 (K)	Time = 193.9 (s)
No. 7	A-73 rod	Pos. 4	PCT = 873.6 (K)	Time = 198.1 (s)
No. 8	A-62 rod	Pos. 4	PCT = 871.7 (K)	Time = 198.1 (s)
No. 9	A-85 rod	Pos. 4	PCT = 871.7 (K)	Time = 192.5 (s)
No.10	A-31 rod	Pos. 4	PCT = 870.9 (K)	Time = 194.6 (s)



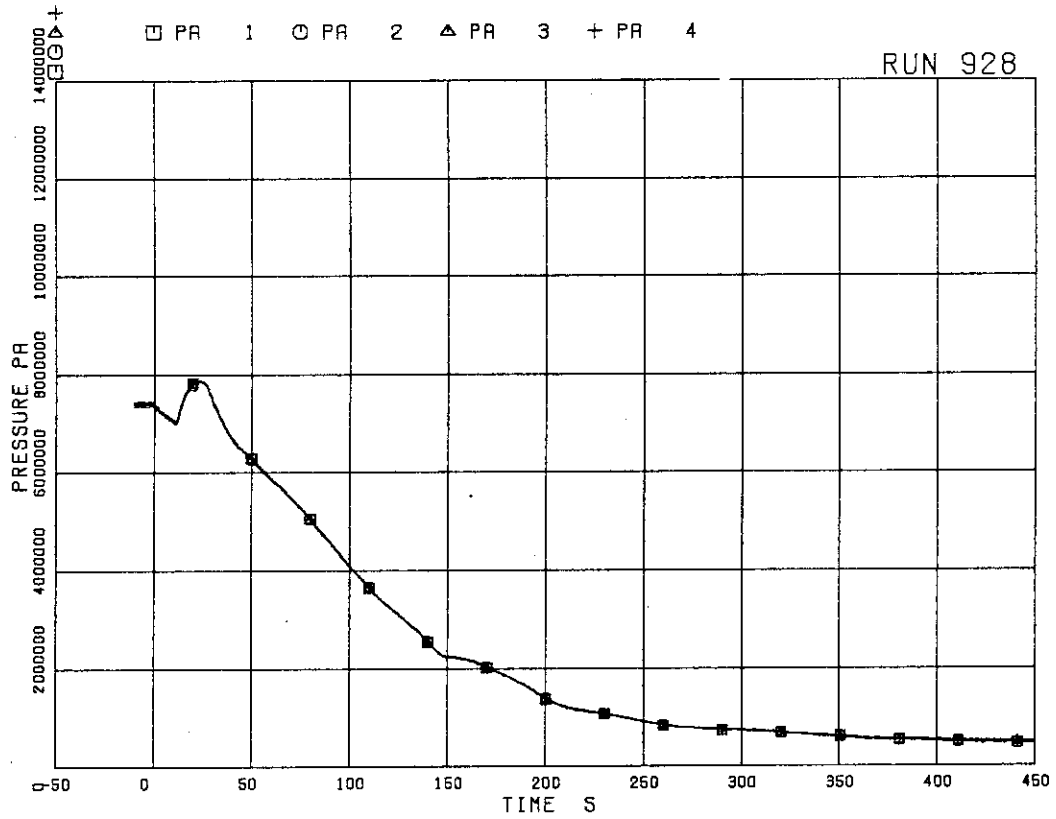


FIG.5. 1 PRESSURE IN PV (PRESSURE VESSEL)

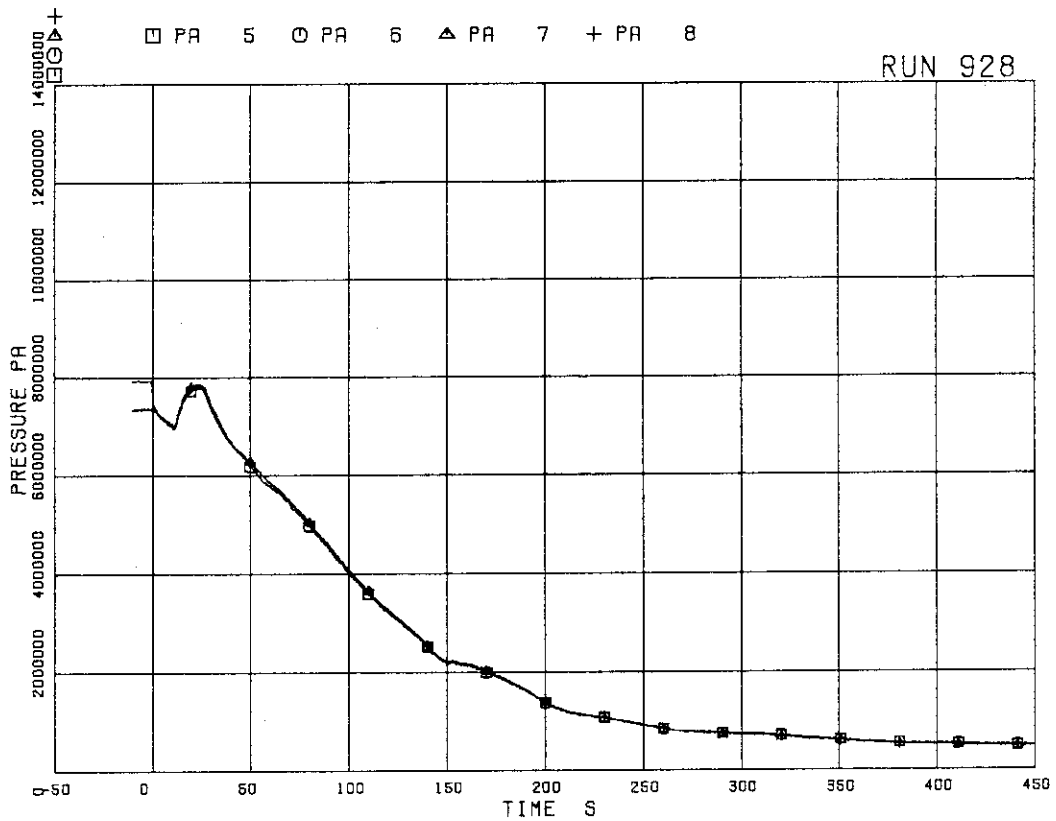


FIG.5. 2 PRESSURE IN BROKEN LOOP JP (JET PUMP)

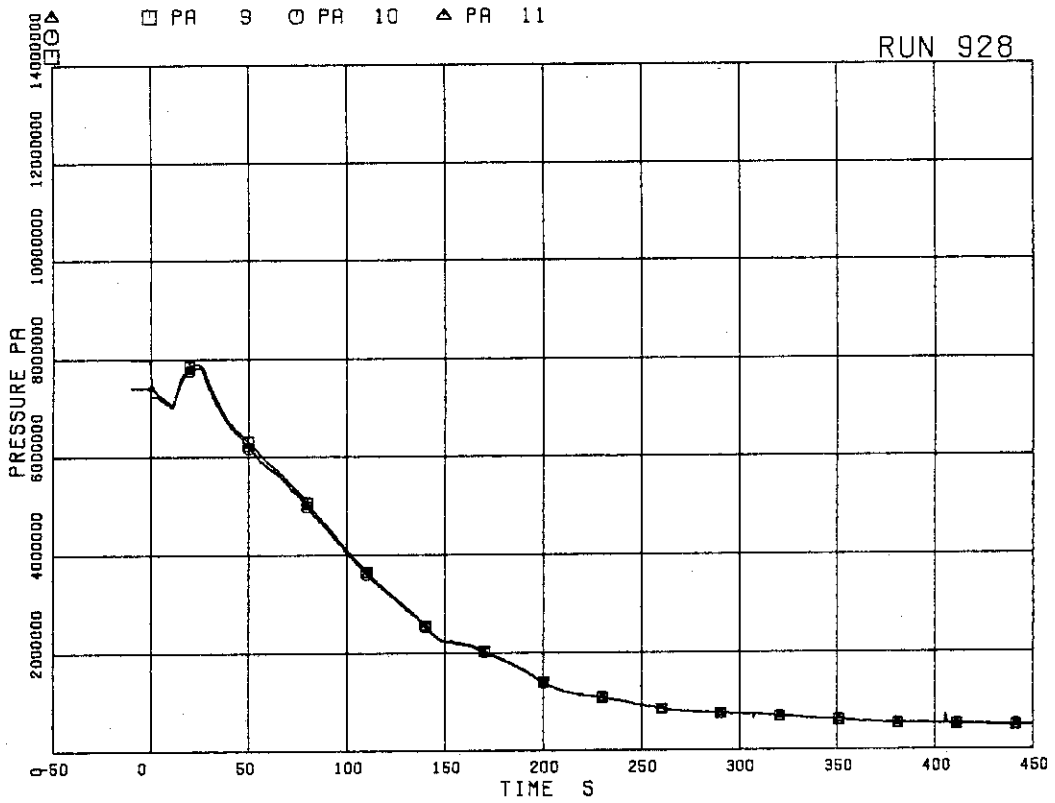


FIG.5. 3 PRESSURE NEAR MRP  
(MAIN RECIRCULATION PUMP)

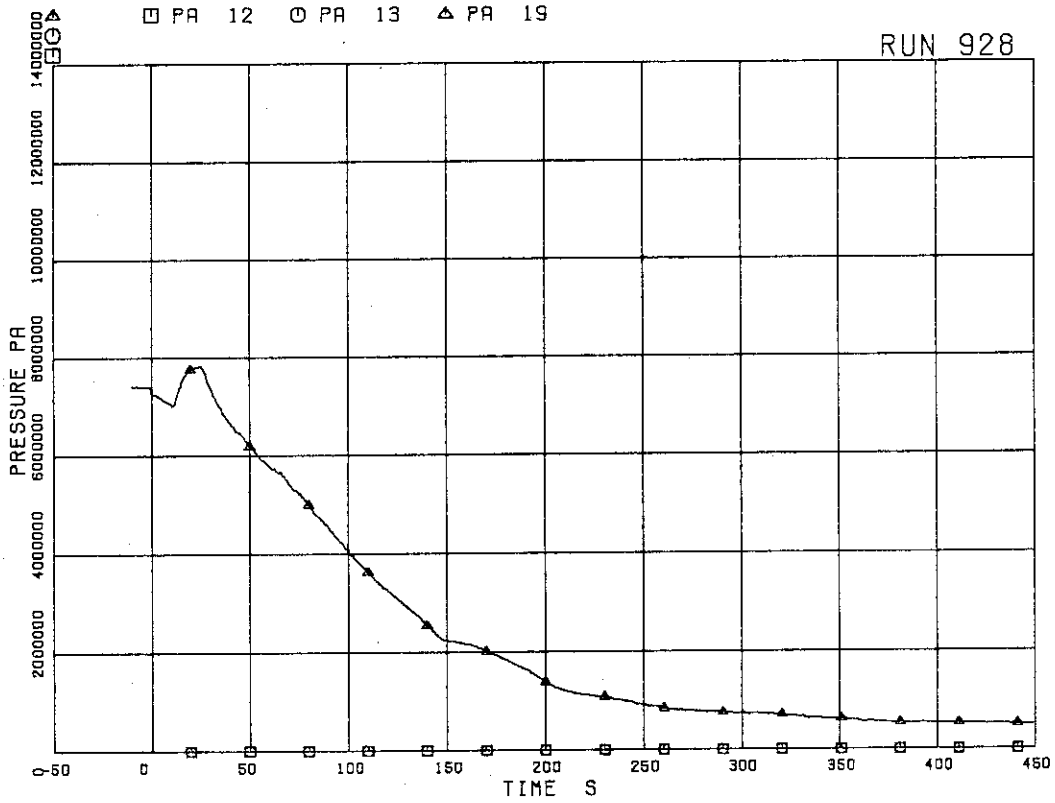


FIG.5. 4 PRESSURE AT MRP SIDE OF BREAK

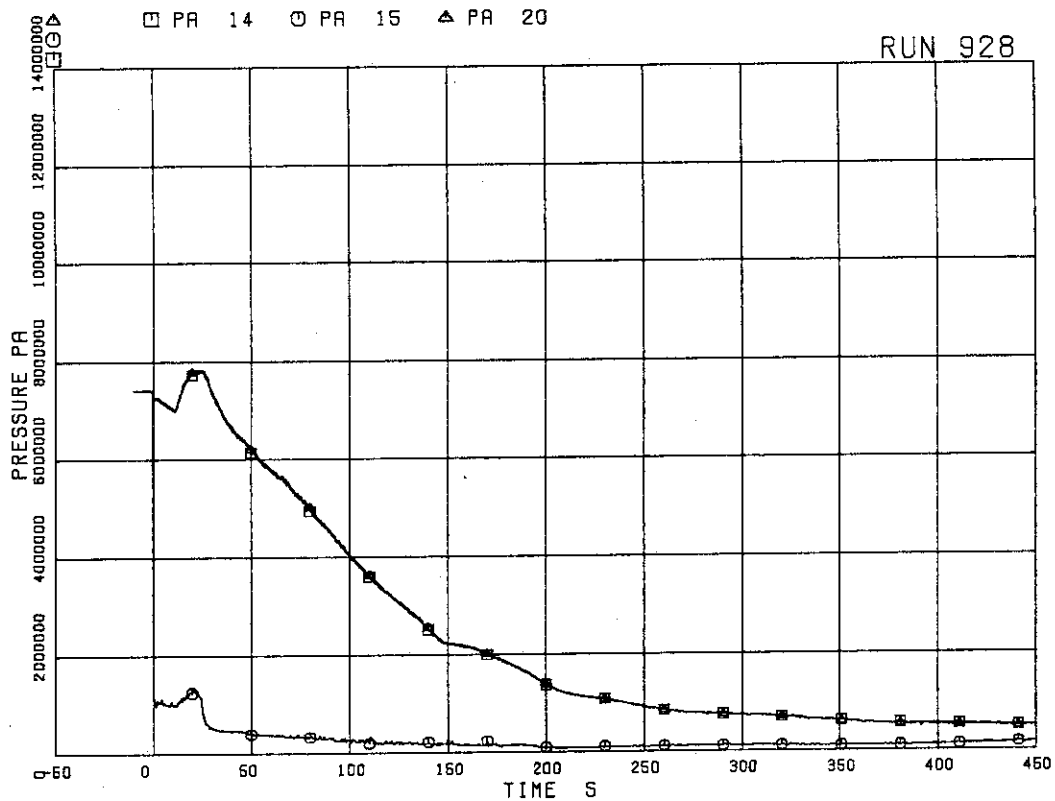


FIG.5. 5 PRESSURE AT PV SIDE OF BREAK

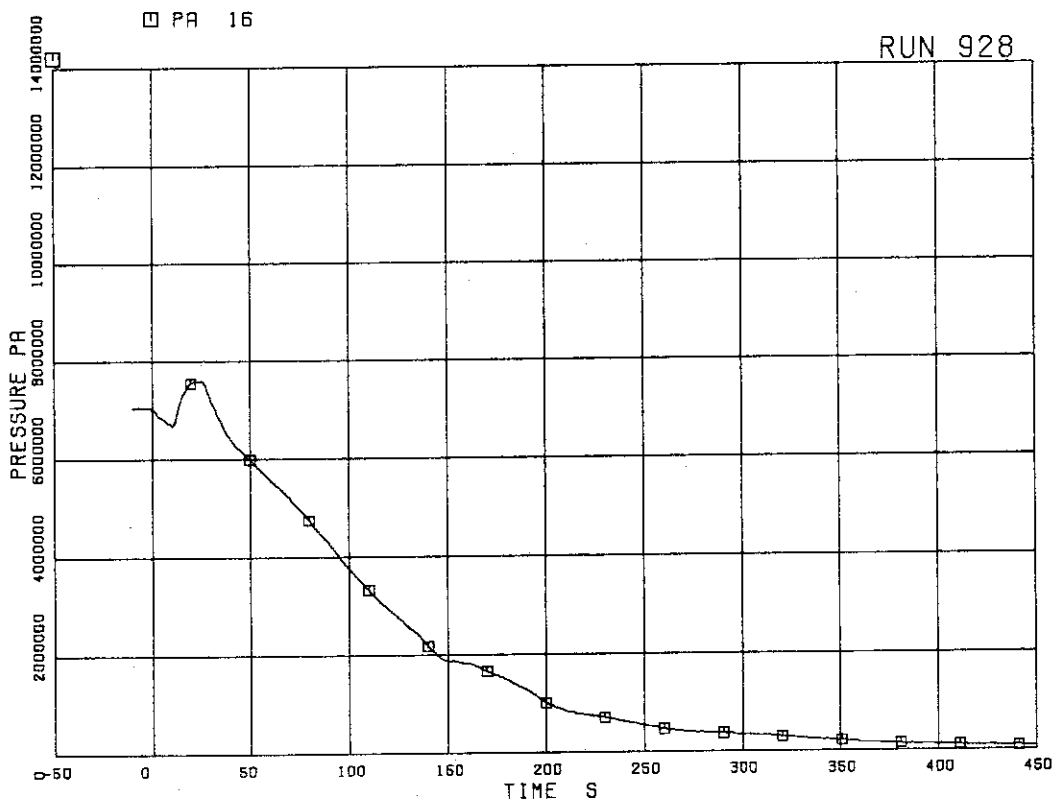


FIG.5. 6 PRESSURE IN MSL (MAIN STEAM LINE)

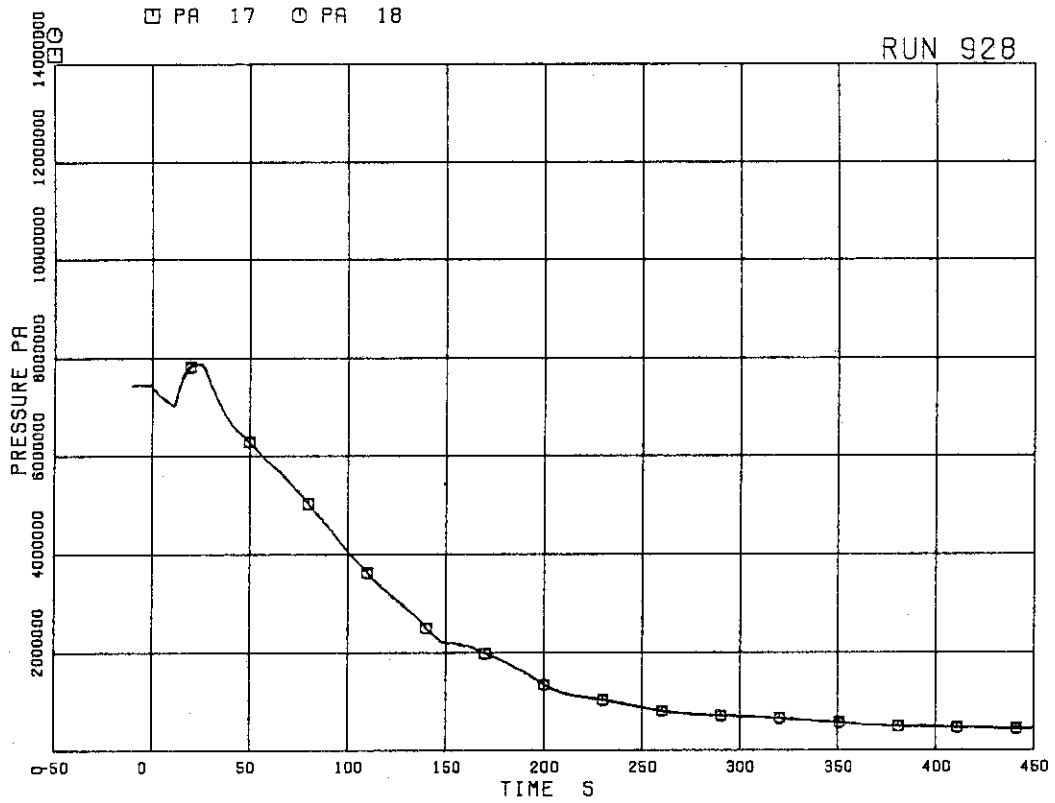


FIG.5. 7 PRESSURE IN JP OUTLET SPOOL

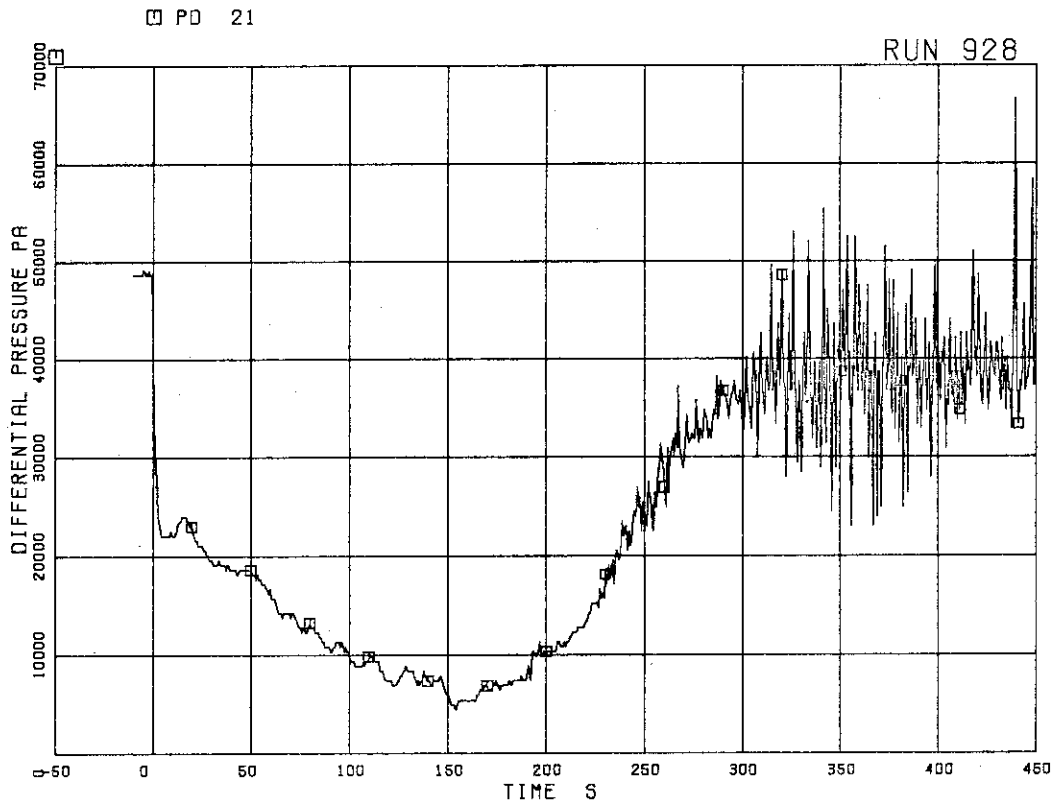


FIG.5. 8 DIFFERENTIAL PRESSURE BETWEEN LOWER PLENUM AND UPPER PLENUM

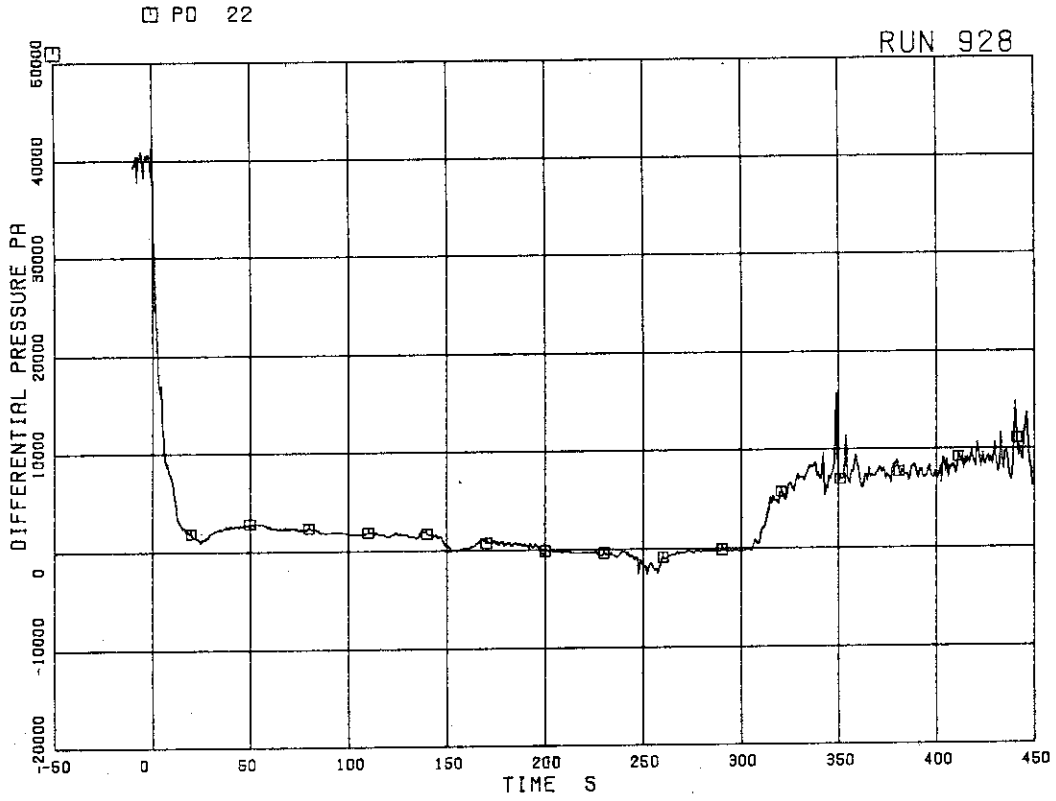


FIG. 5. 9 DIFFERENTIAL PRESSURE BETWEEN UPPER PLENUM AND STEAM DOME

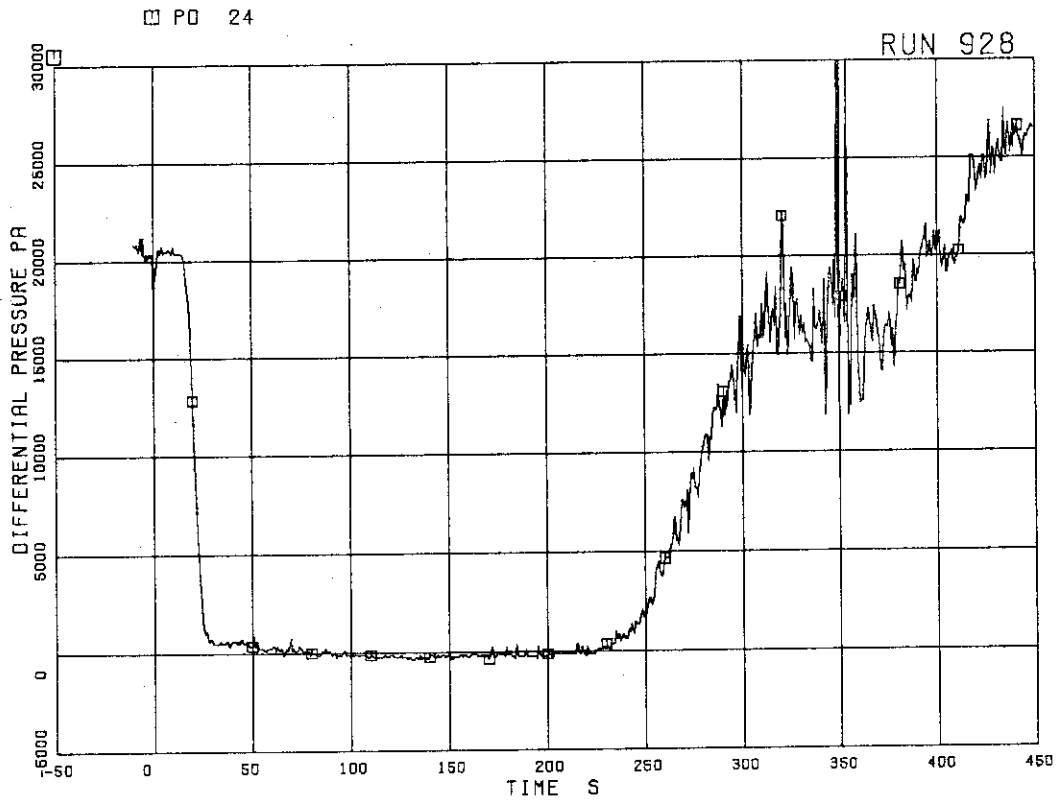


FIG. 5. 10 DC (DOWNCOMER) HEAD

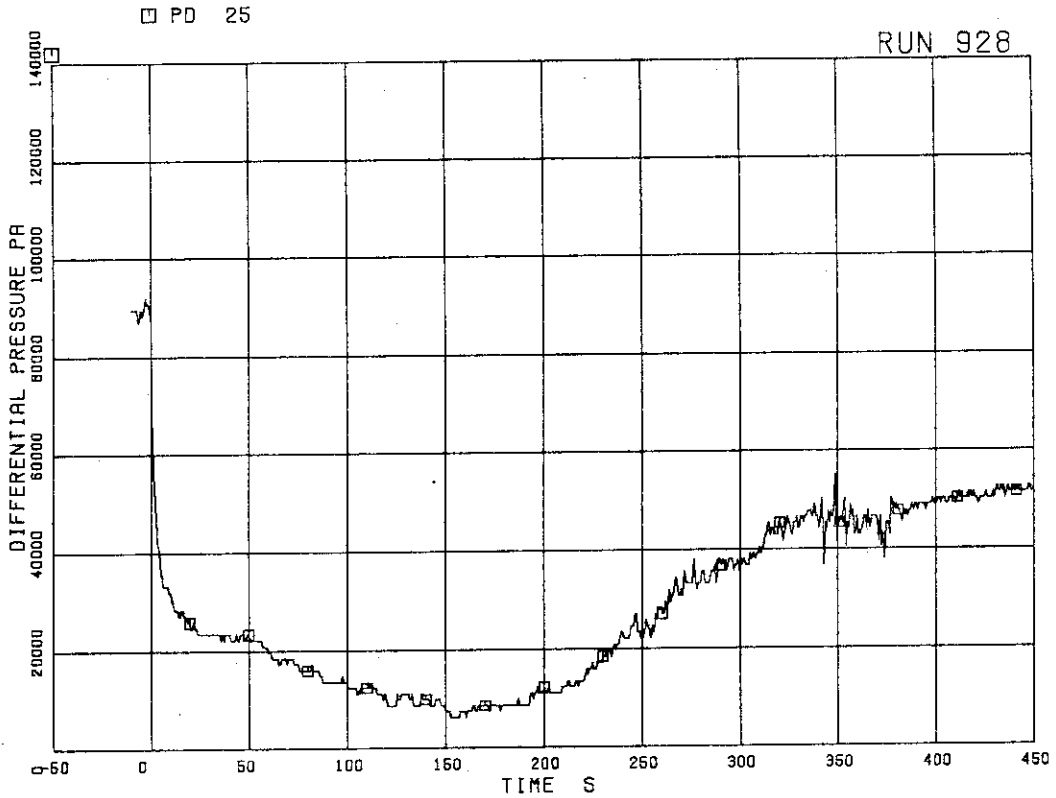


FIG. 5. 11 DIFFERENTIAL PRESSURE BETWEEN PV BOTTOM AND TOP

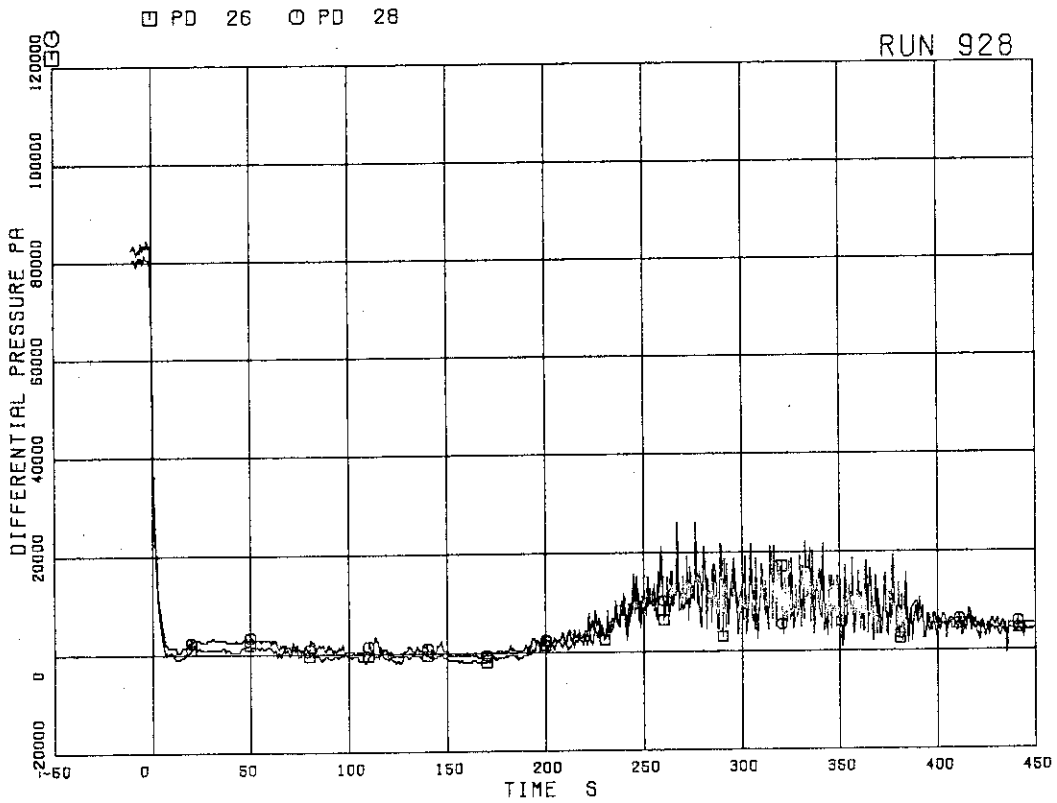


FIG. 5. 12 DIFFERENTIAL PRESSURE BETWEEN JP-1.2 DISCHARGE AND SUCTION

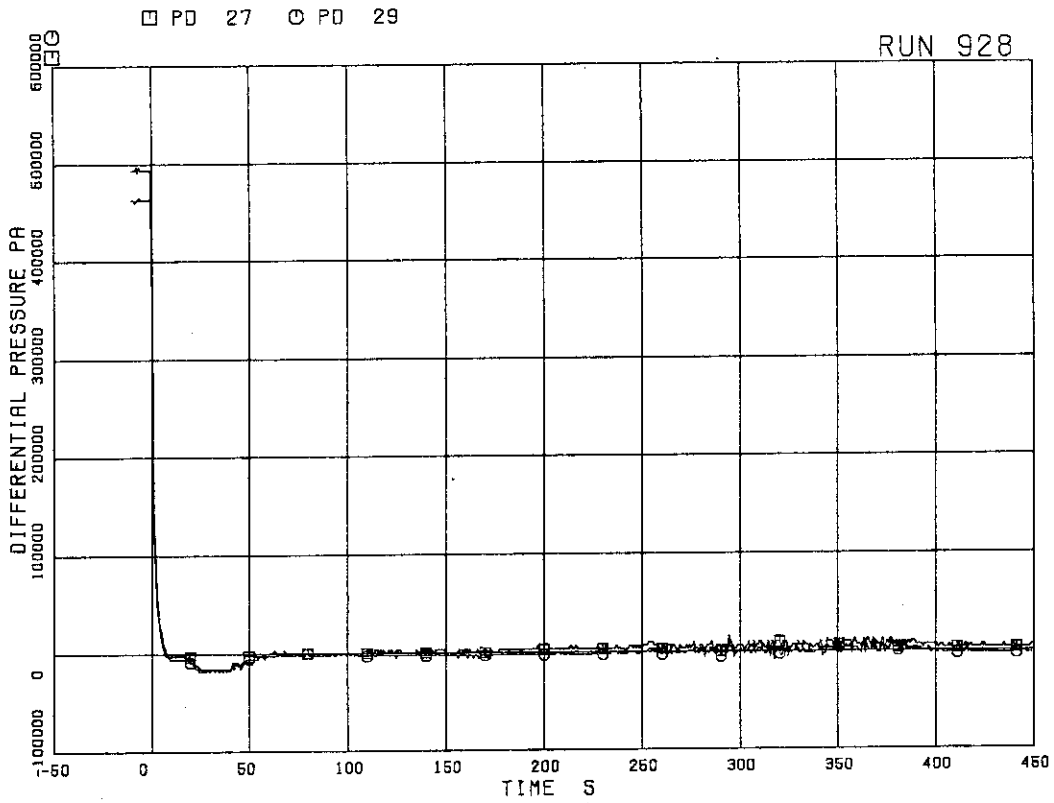


FIG.5. 13 DIFFERENTIAL PRESSURE BETWEEN JP-1,2 DRIVE AND SUCTION

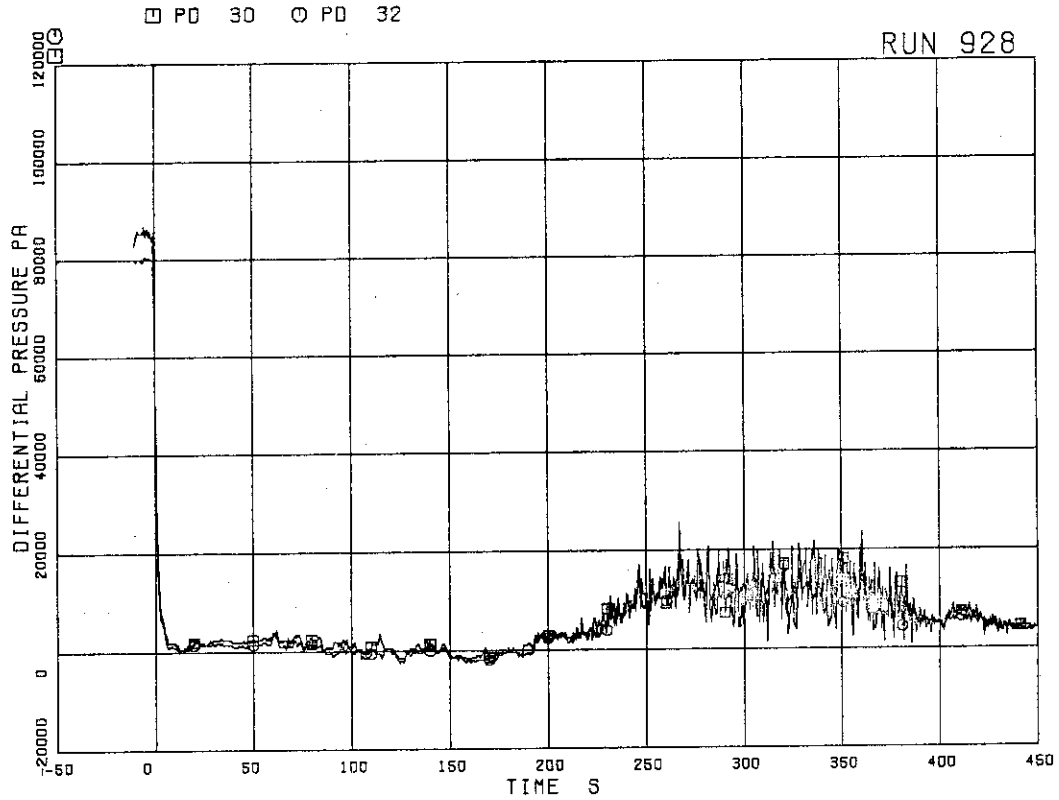


FIG.5. 14 DIFFERENTIAL PRESSURE BETWEEN JP-3,4 DISCHARGE AND SUCTION

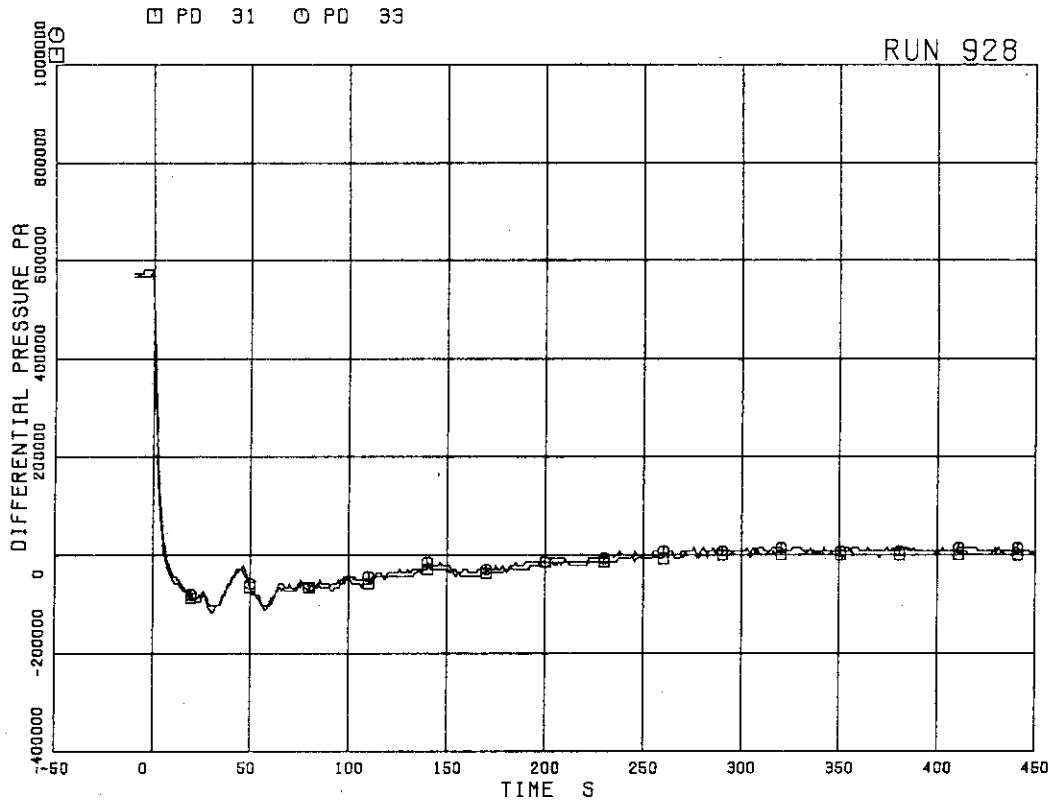


FIG.5. 15 DIFFERENTIAL PRESSURE BETWEEN JP-3,4 DRIVE AND SUCTION

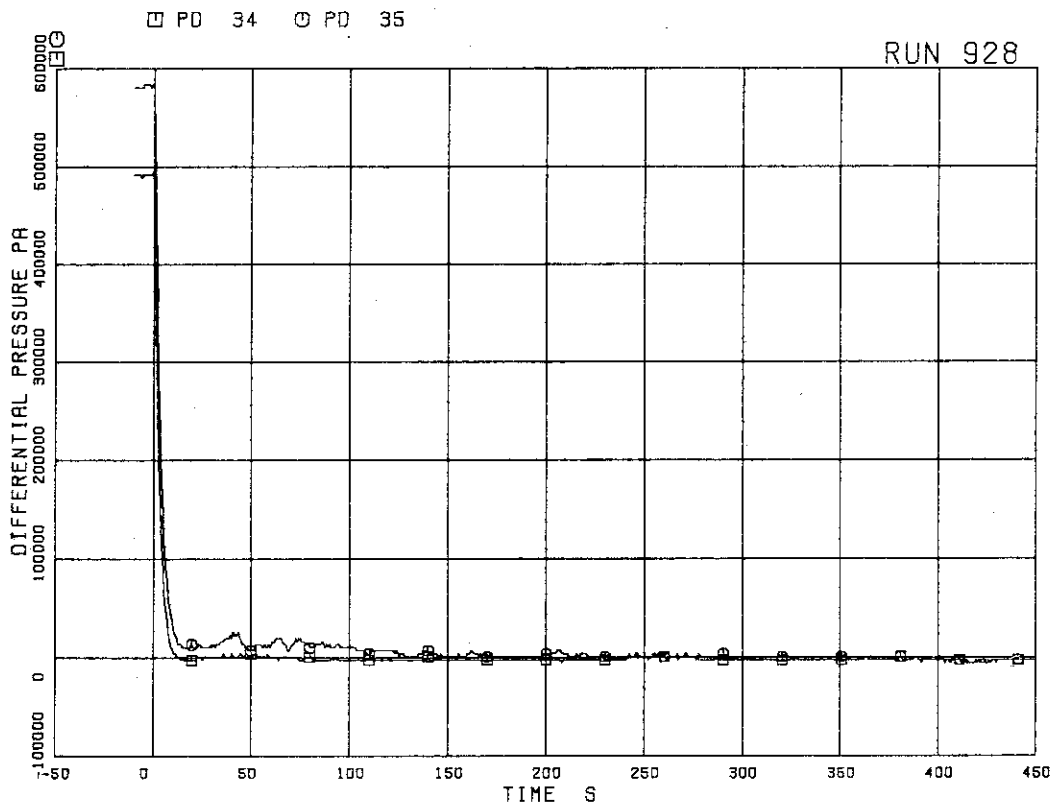


FIG.5. 16 DIFFERENTIAL PRESSURE BETWEEN MRP DELIVERY AND SUCTION



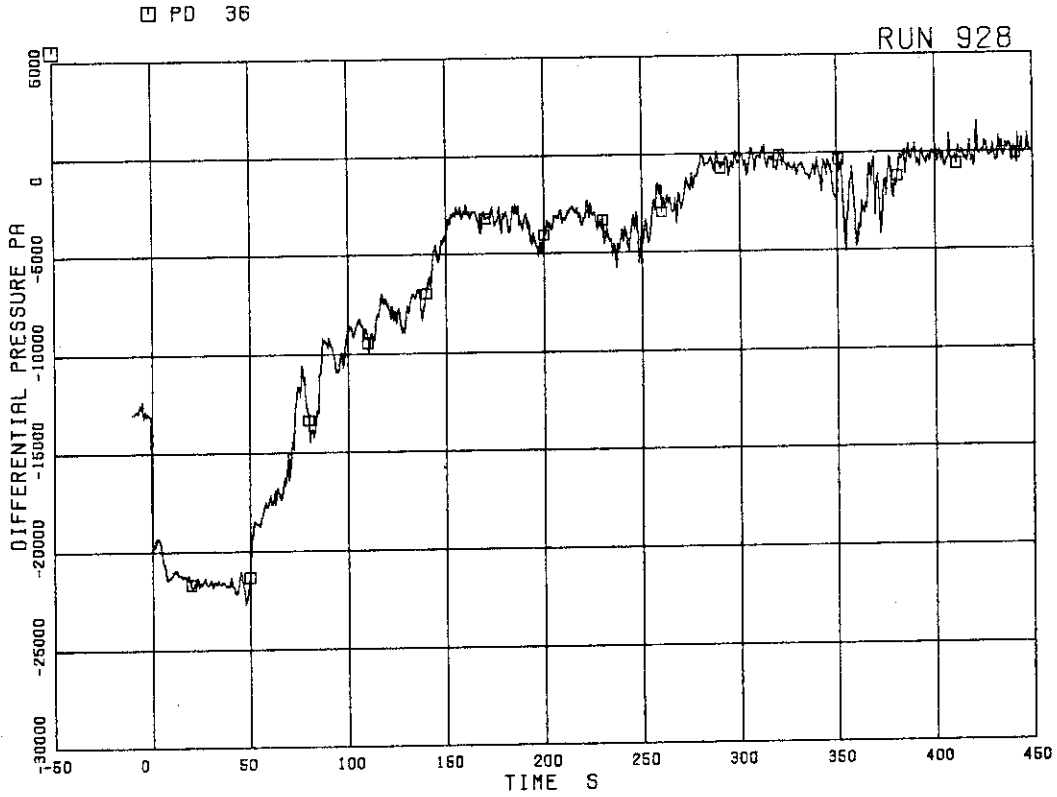


FIG.5. 17 DIFFERENTIAL PRESSURE BETWEEN DOWNCOMER BOTTOM AND MRP1 SUCTION

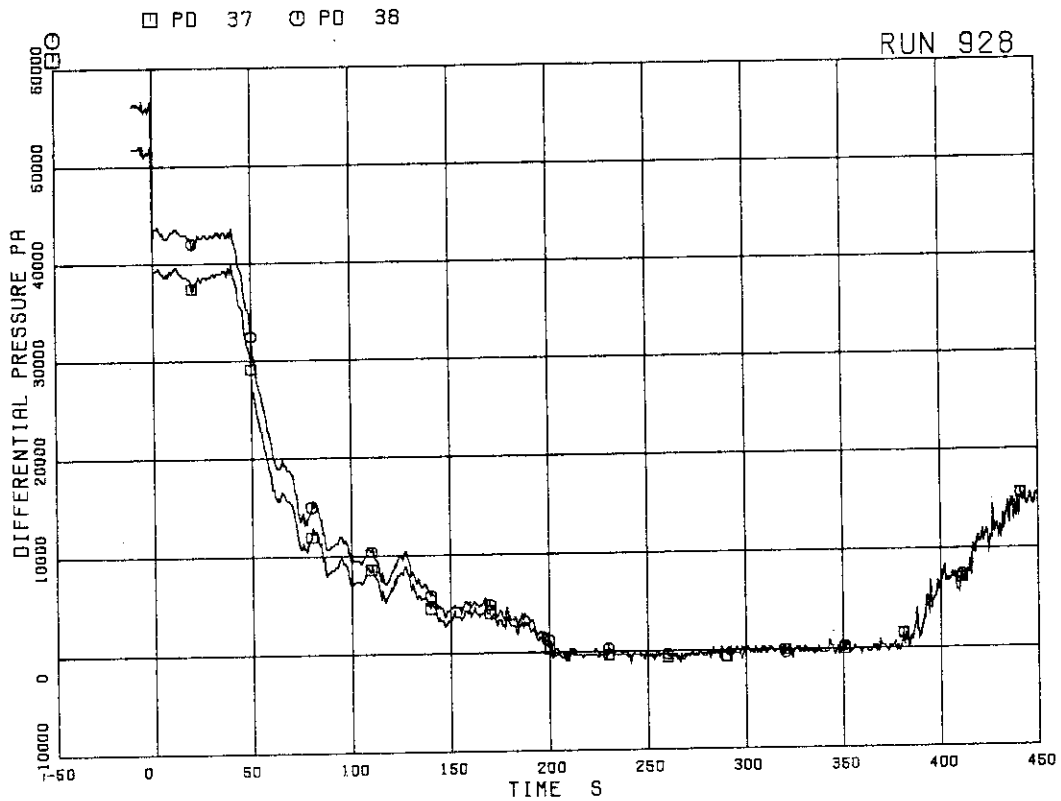


FIG.5. 18 DIFFERENTIAL PRESSURE BETWEEN MRP DELIVERY AND JP-1.2 DRIVE

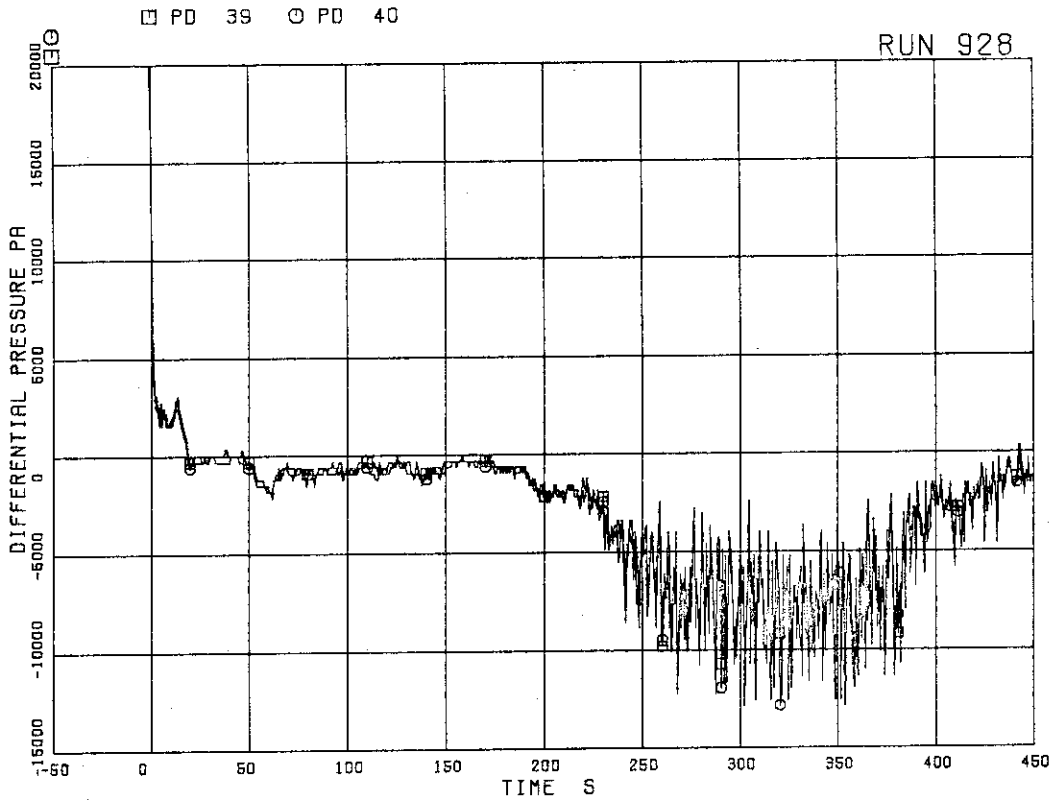


FIG.5. 19 DIFFERENTIAL PRESSURE BETWEEN  
DOWNCOMER MIDDLE AND JP-1,2 SUCTION

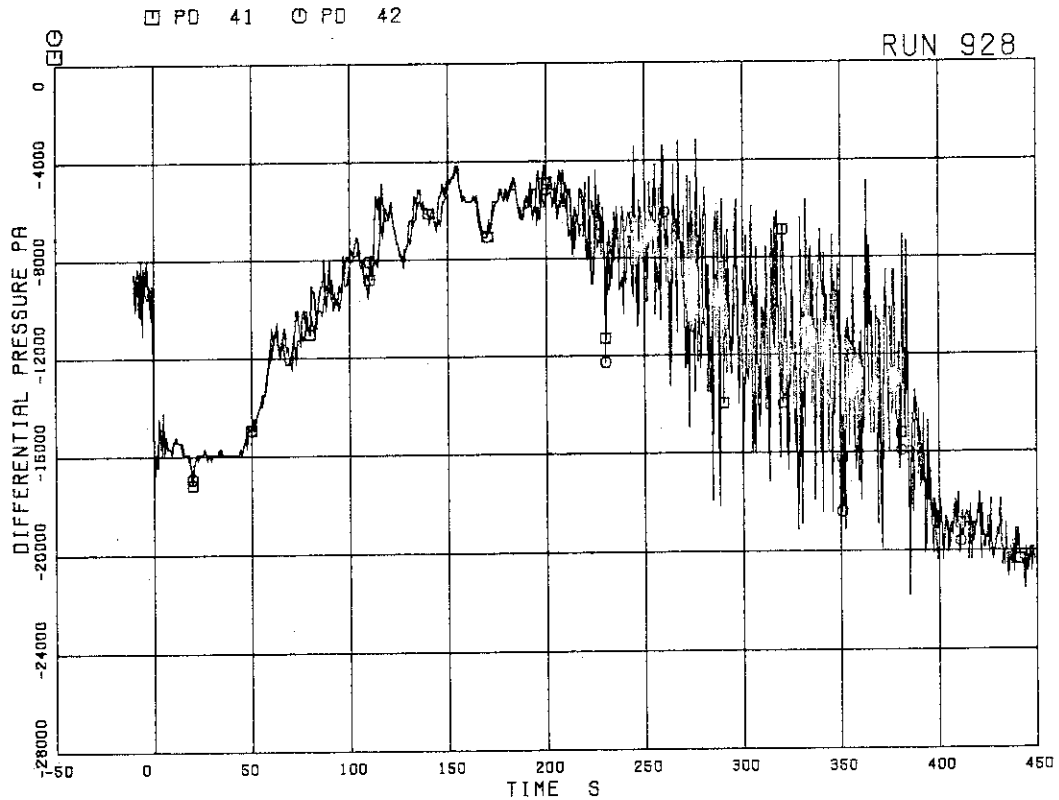


FIG.5. 20 DIFFERENTIAL PRESSURE BETWEEN  
JP-1,2 DISCHARGE AND LOWER PLENUM

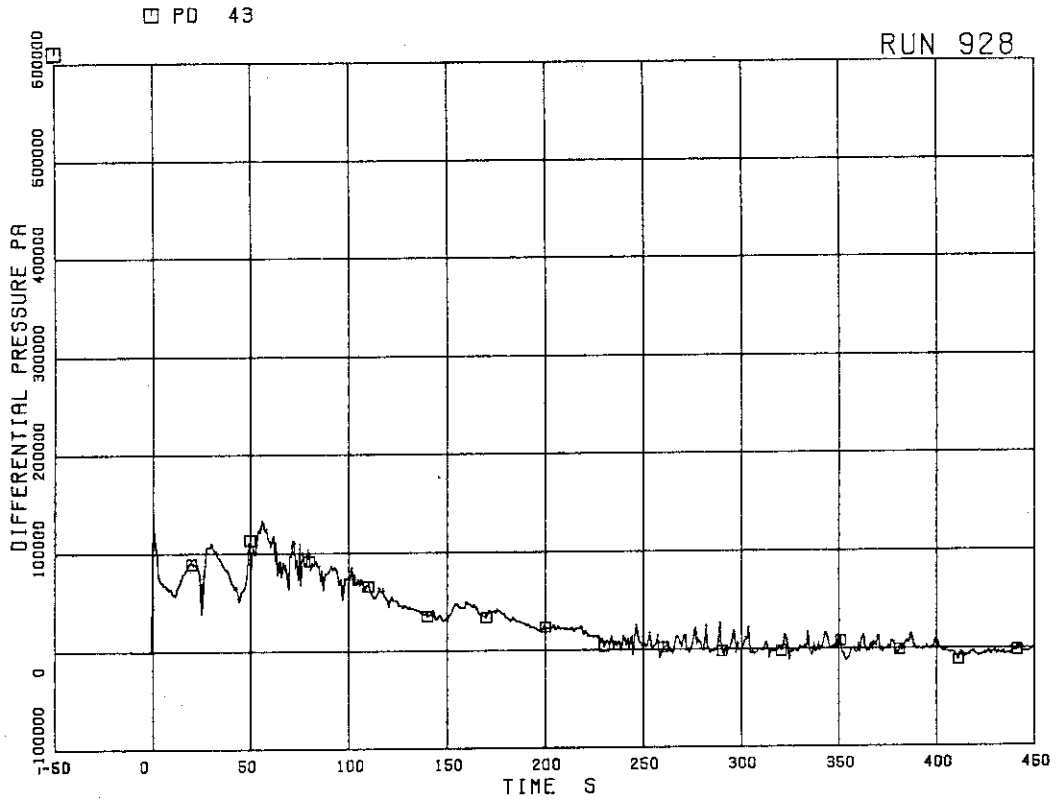


FIG.5. 21 DIFFERENTIAL PRESSURE BETWEEN  
DOWNCOMER BOTTOM AND BREAK B

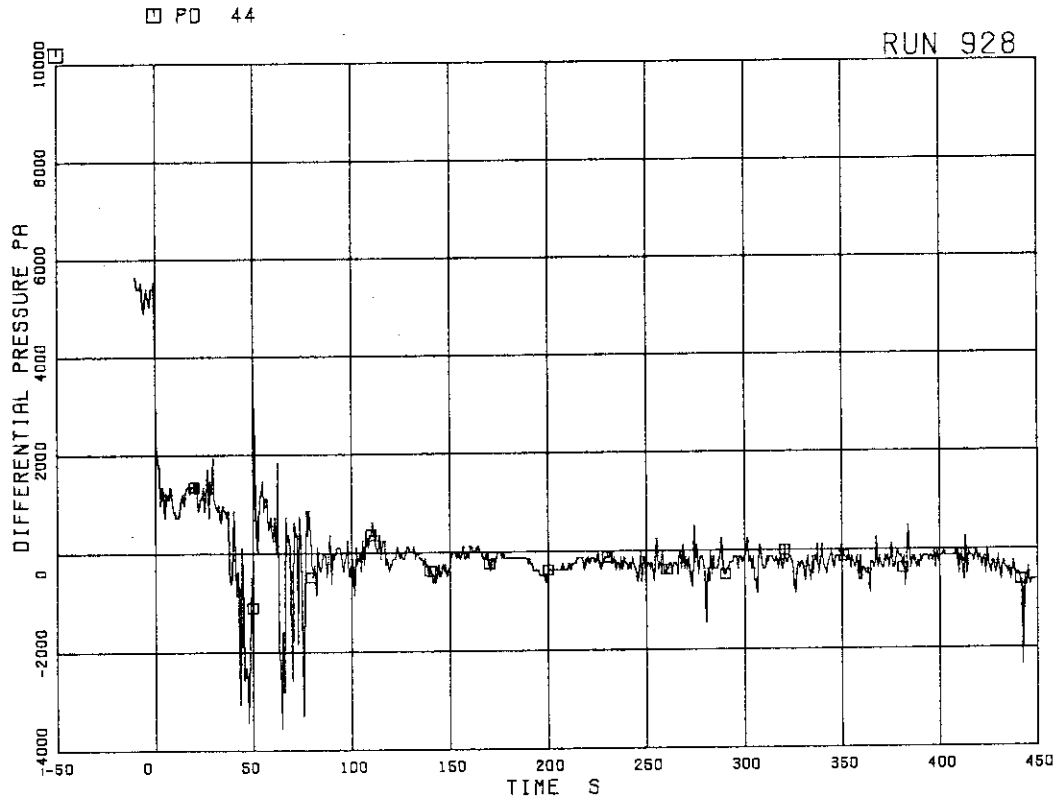


FIG.5. 22 DIFFERENTIAL PRESSURE BETWEEN  
BREAKS A AND B

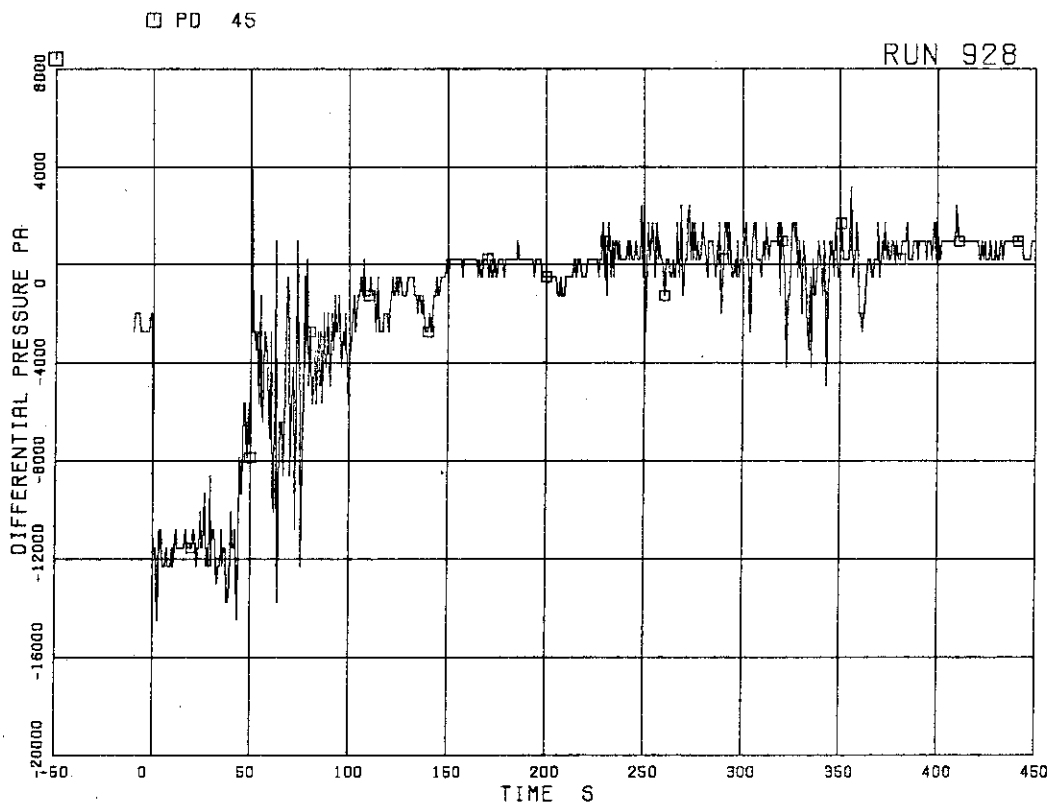


FIG.5. 23 DIFFERENTIAL PRESSURE BETWEEN  
BREAK A AND MRP2 SUCTION

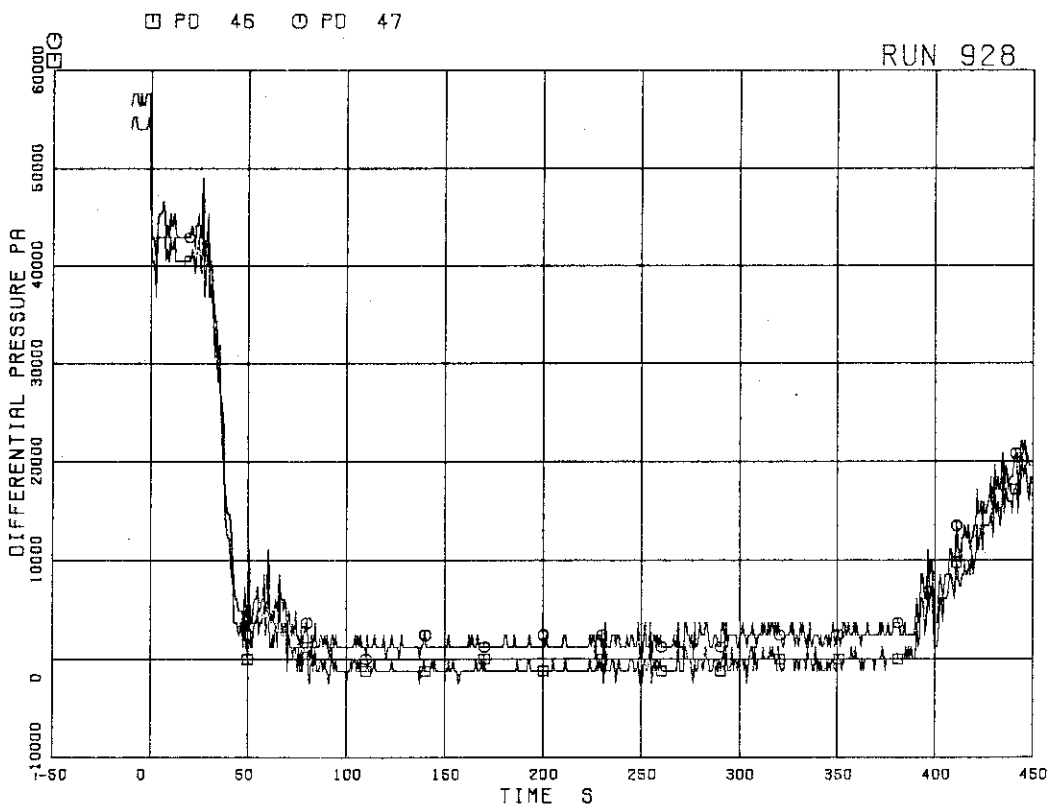


FIG.5. 24 DIFFERENTIAL PRESSURE BETWEEN  
MRP DELIVERY AND JP-3,4 DRIVE

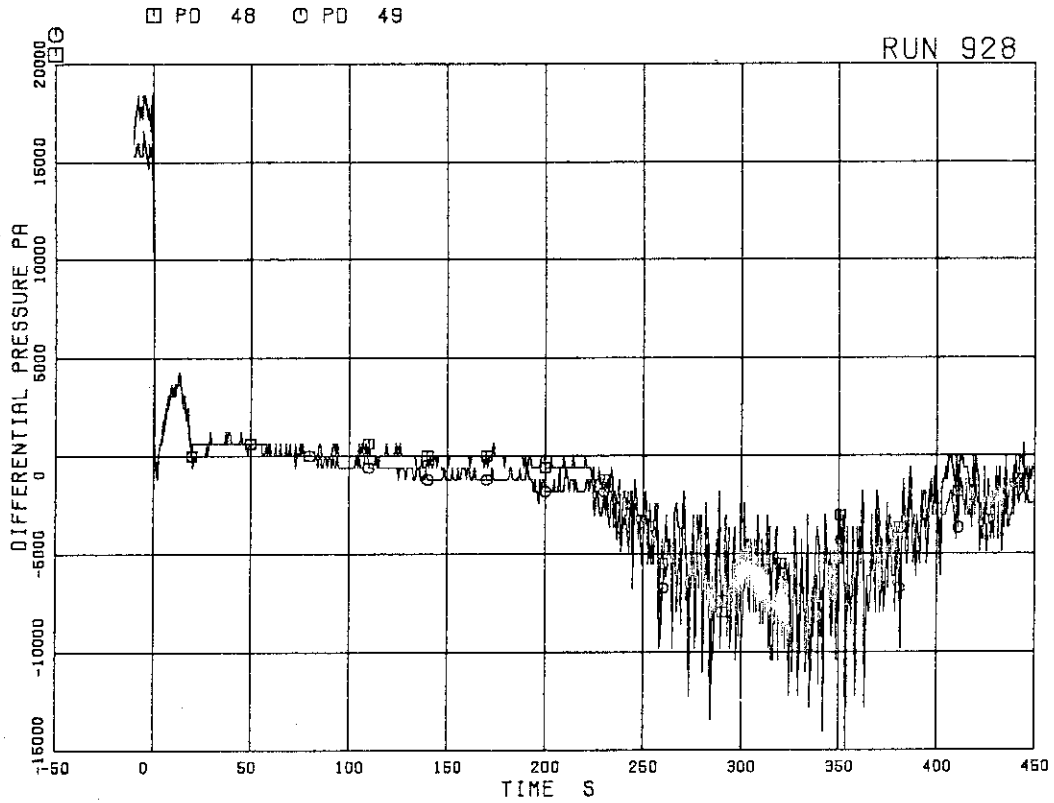


FIG.5. 25 DIFFERENTIAL PRESSURE BETWEEN  
DOWNCOMER MIDDLE AND JP-3,4 SUCTION

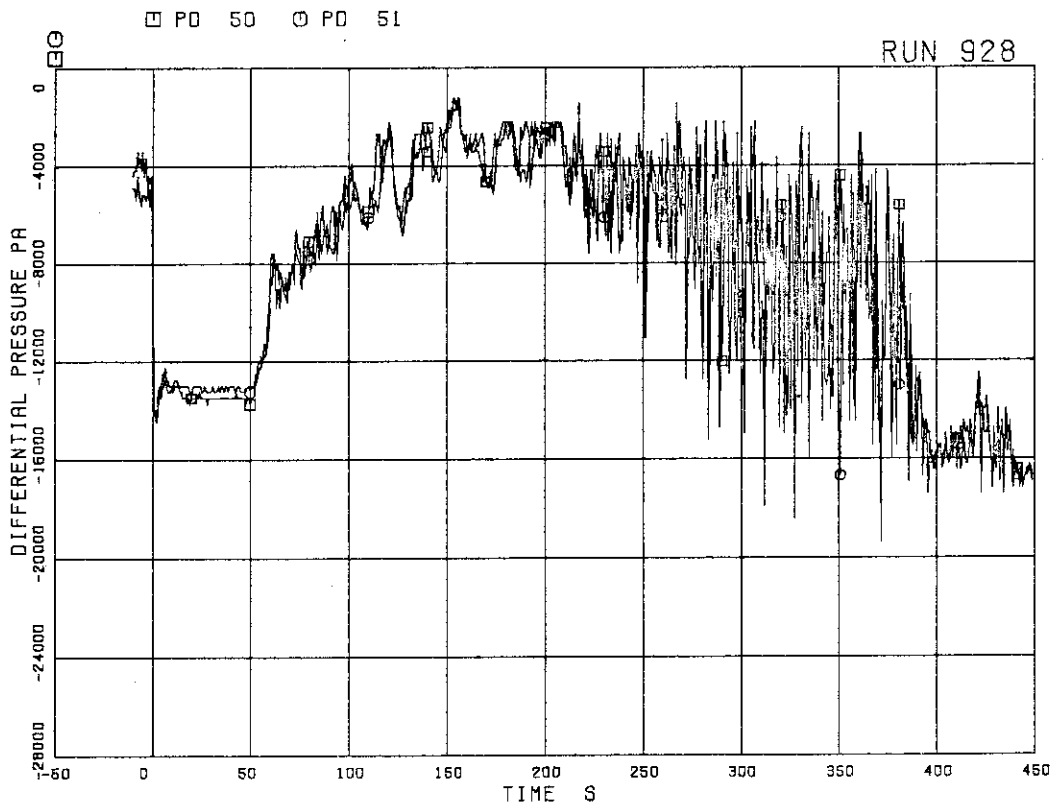


FIG.5. 26 DIFFERENTIAL PRESSURE BETWEEN  
JP-3,4 DISCHARGE AND CONFLUENCE

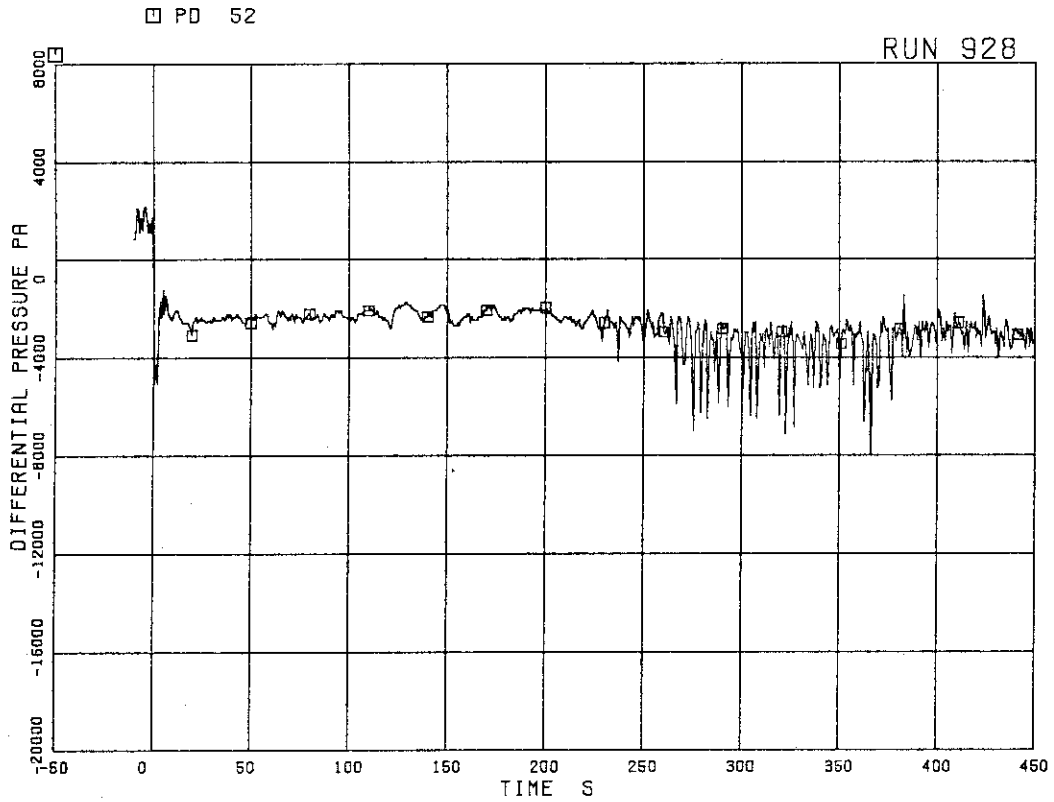


FIG.5. 27 DIFFERENTIAL PRESSURE BETWEEN JP-3,4  
CONFLUENCE IN BROKEN LOOP AND LP

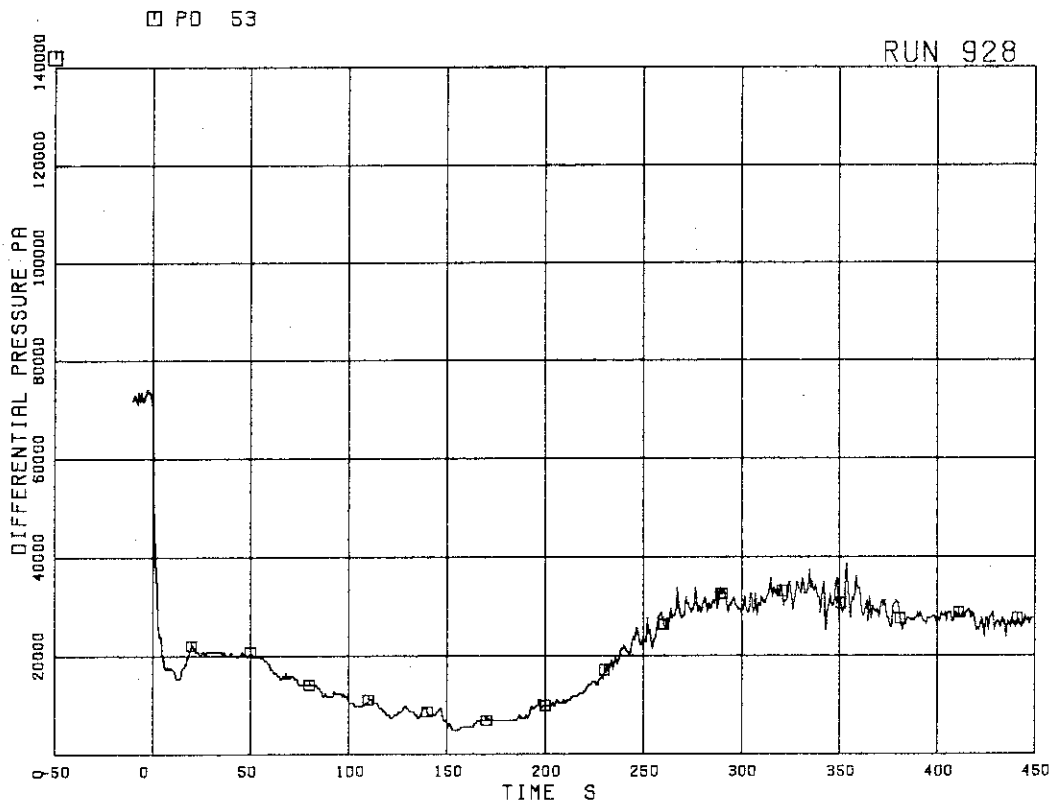


FIG.5. 28 DIFFERENTIAL PRESSURE BETWEEN  
LOWER PLENUM AND DOWNCOMER MIDDLE

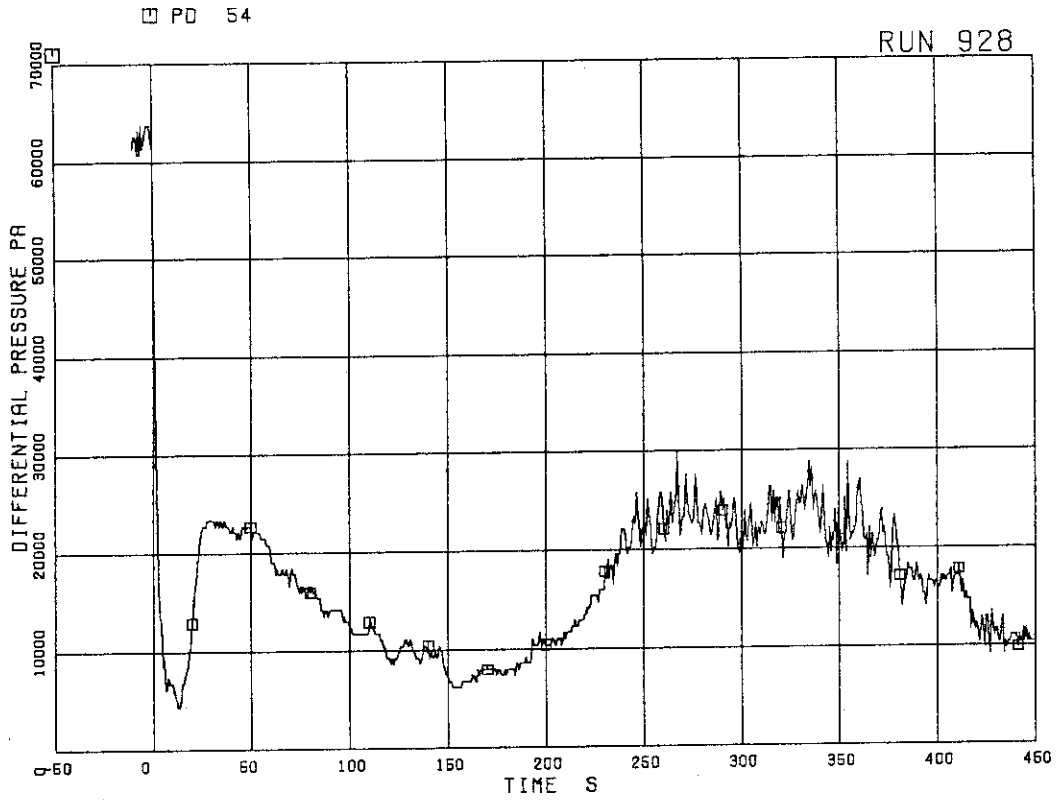


FIG.5. 29 DIFFERENTIAL PRESSURE BETWEEN  
LOWER PLENUM AND DOWNCOMER BOTTOM

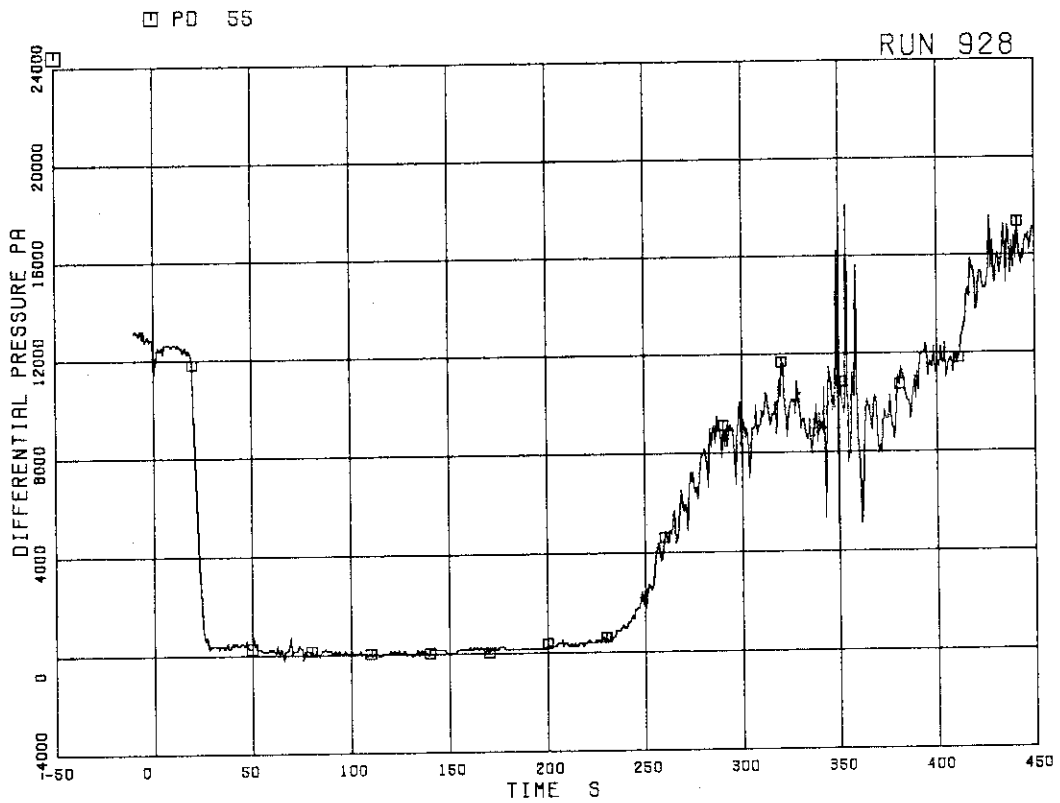


FIG.5. 30 DIFFERENTIAL PRESSURE BETWEEN  
DOWNCOMER BOTTOM AND DOWNCOMER MIDDLE

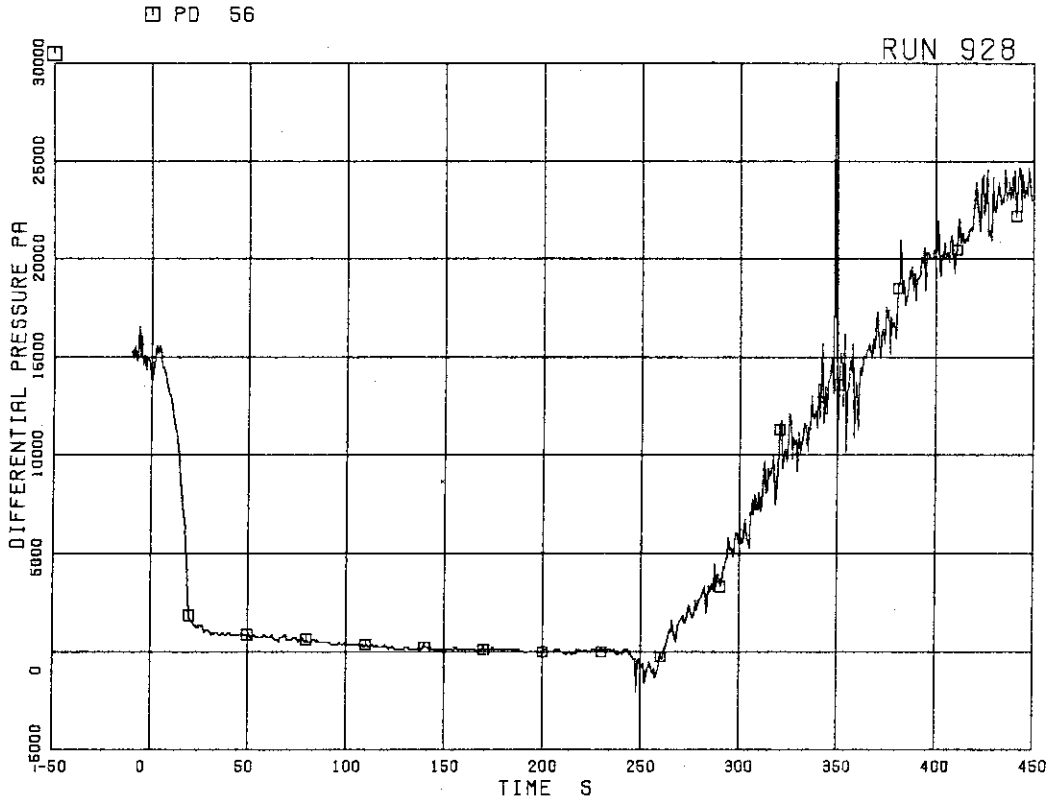


FIG.5. 31 DIFFERENTIAL PRESSURE BETWEEN  
DOWNCOMER MIDDLE AND STEAM DOME

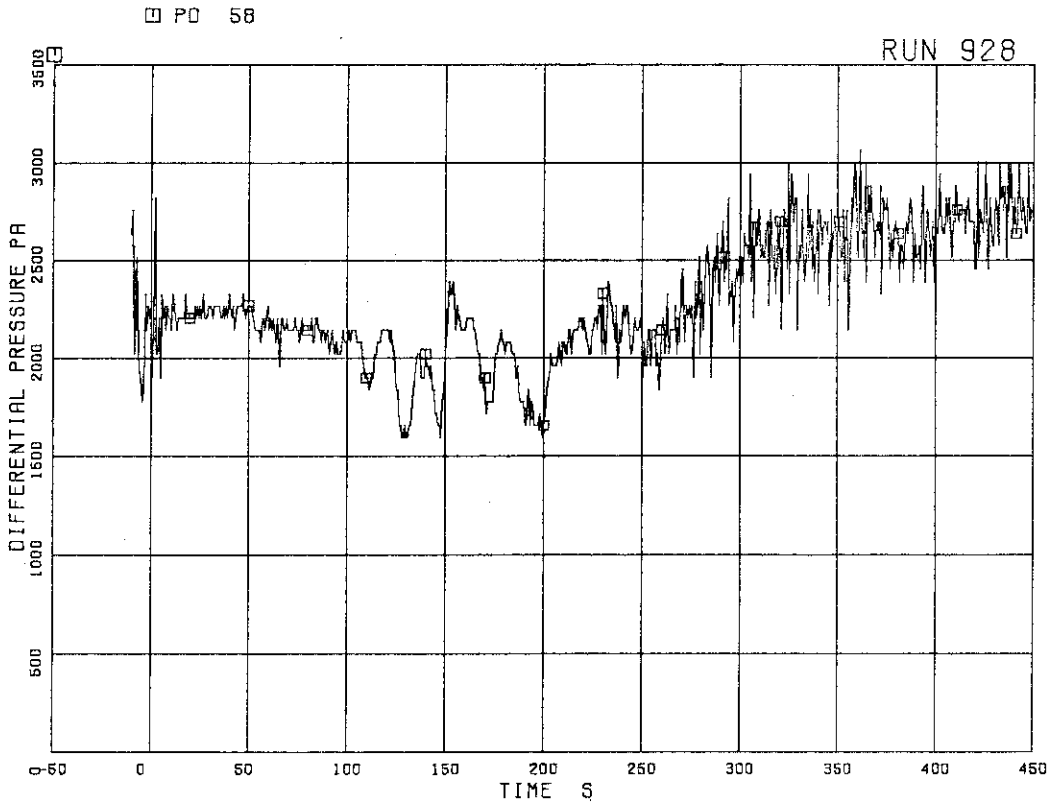


FIG.5. 32 DIFFERENTIAL PRESSURE BETWEEN  
LP BOTTOM AND LP MIDDLE



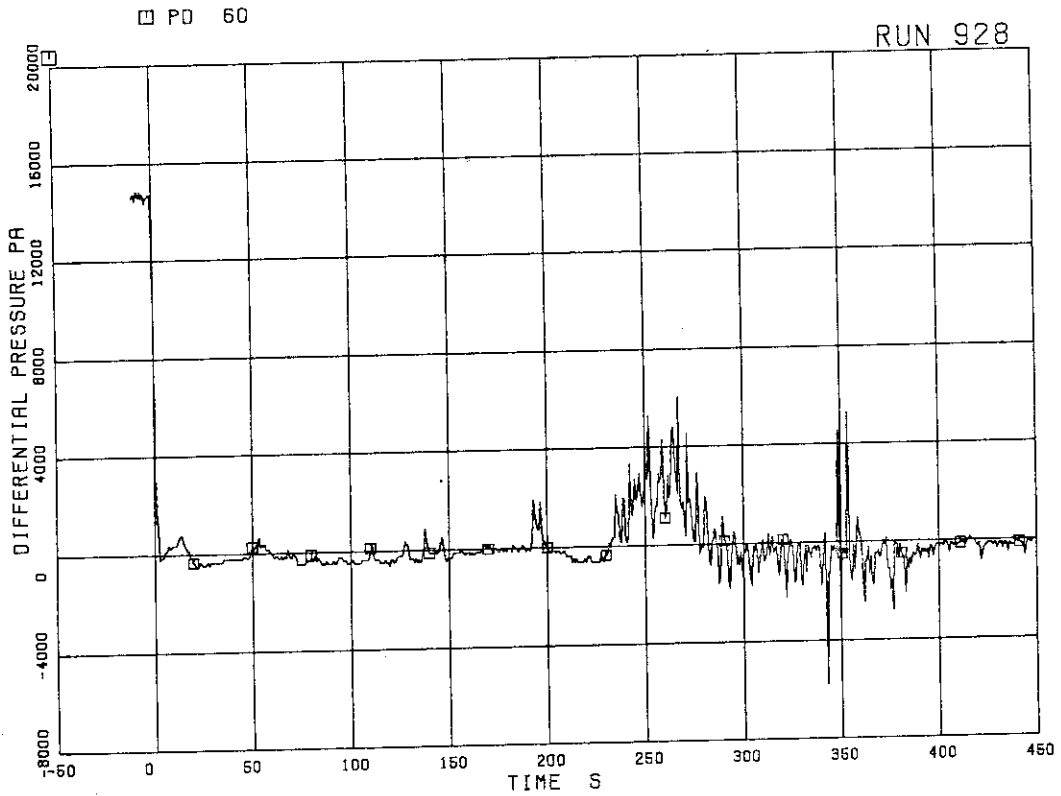


FIG.5. 33 DIFFERENTIAL PRESSURE ACROSS  
CHANNEL INLET ORIFICE A

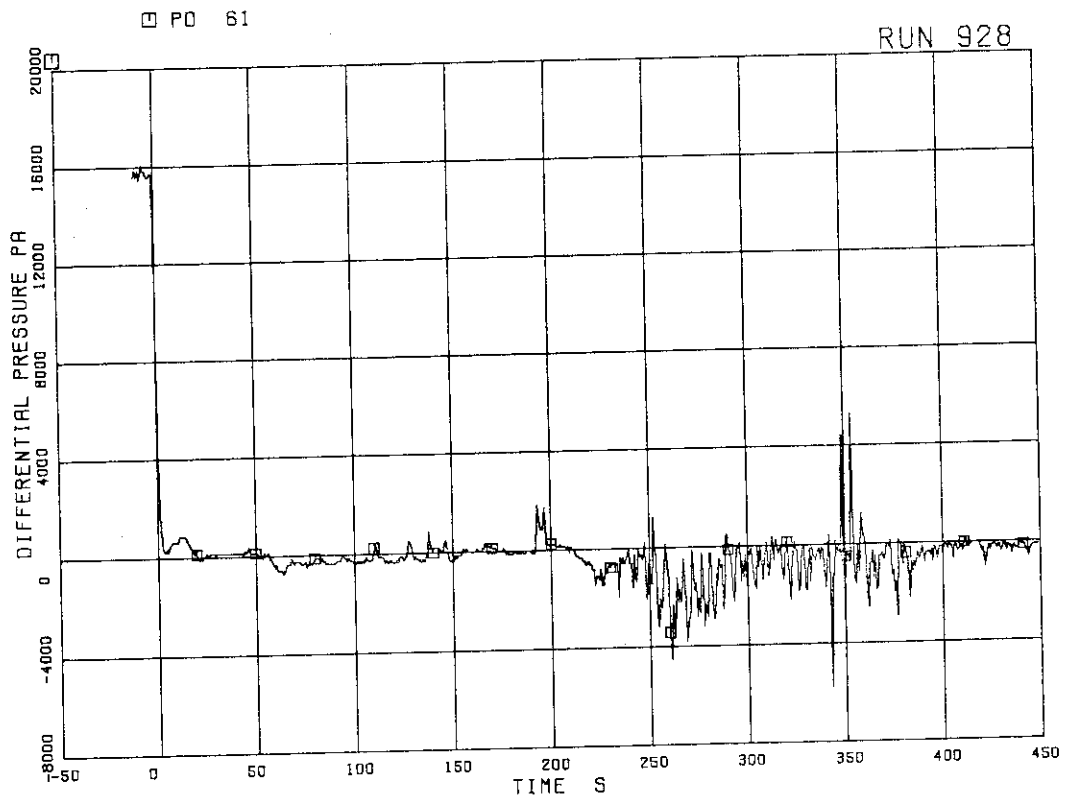


FIG.5. 34 DIFFERENTIAL PRESSURE ACROSS  
CHANNEL INLET ORIFICE B

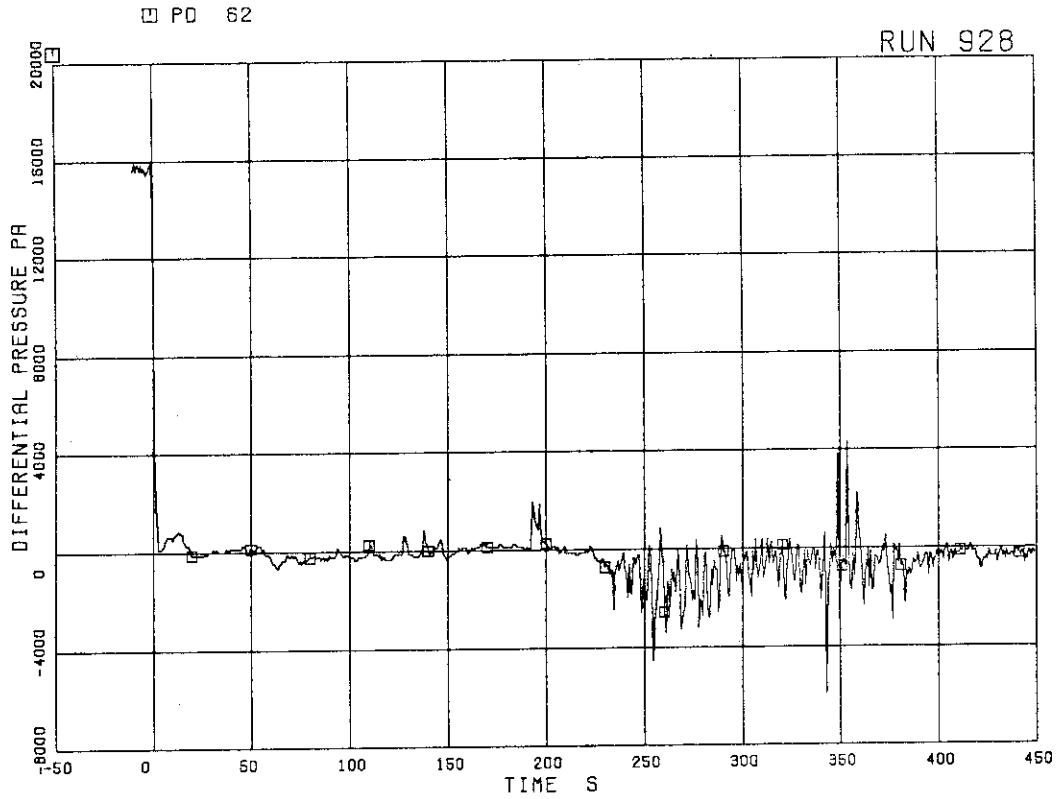


FIG.5. 35 DIFFERENTIAL PRESSURE ACROSS  
CHANNEL INLET ORIFICE C

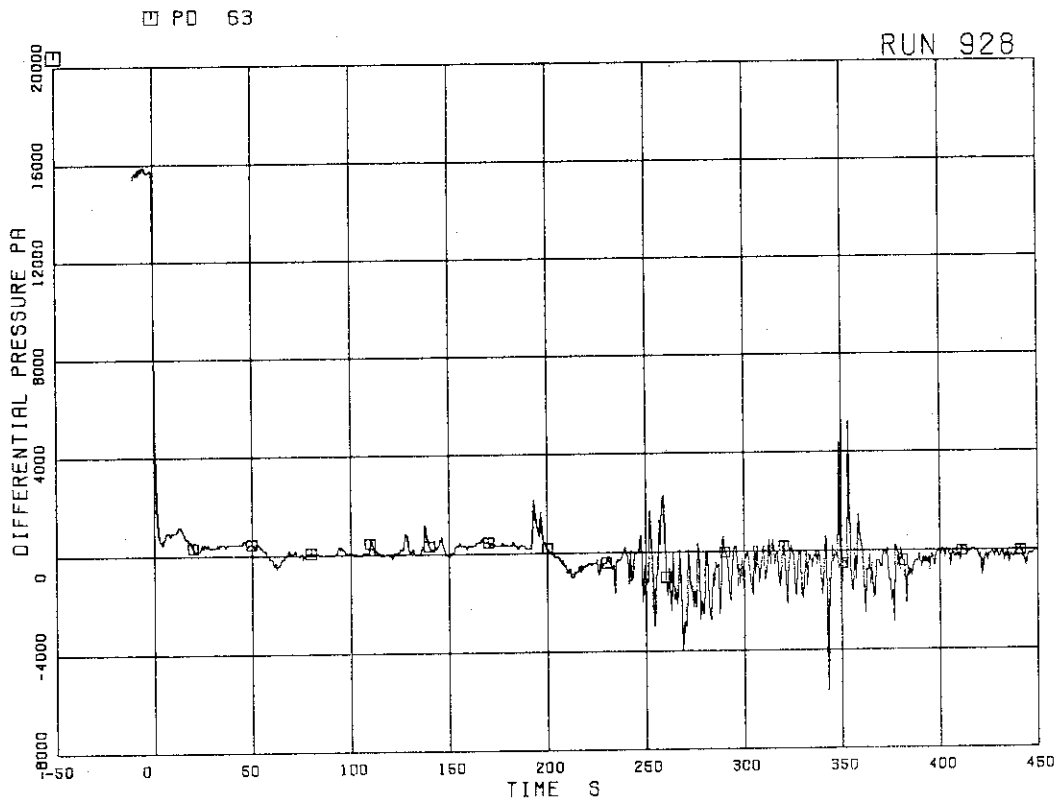


FIG.5. 36 DIFFERENTIAL PRESSURE ACROSS  
CHANNEL INLET ORIFICE D

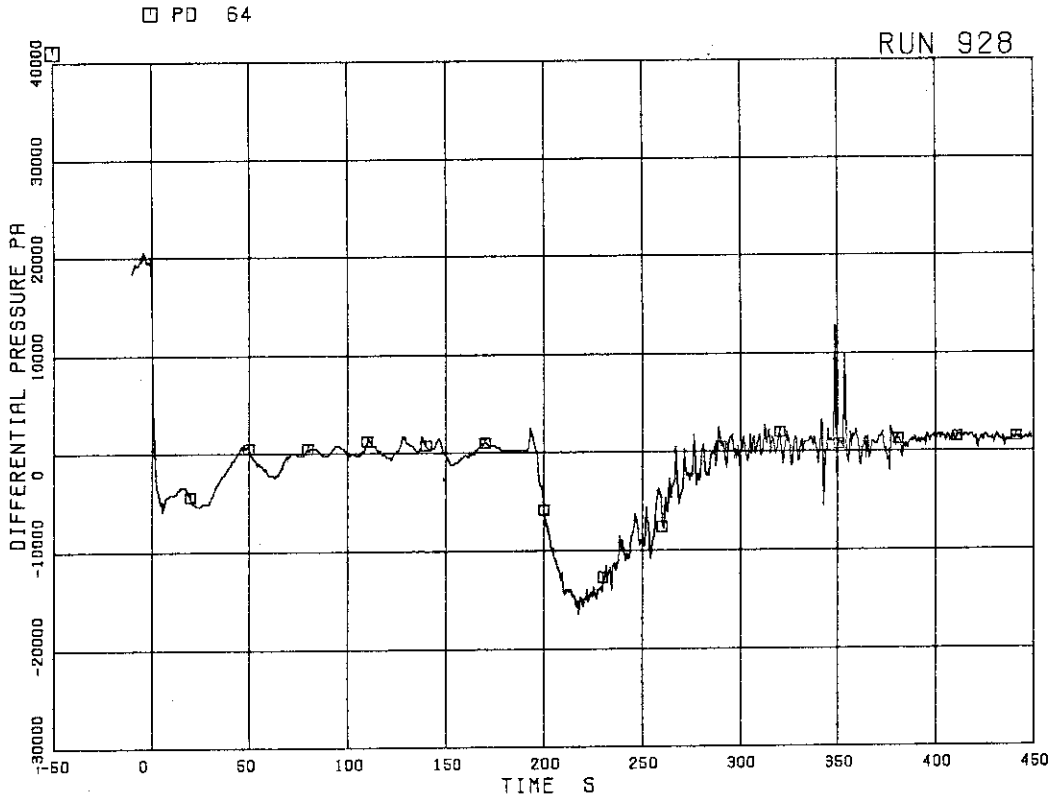


FIG.5. 37 DIFFERENTIAL PRESSURE ACROSS BYPASS HOLE

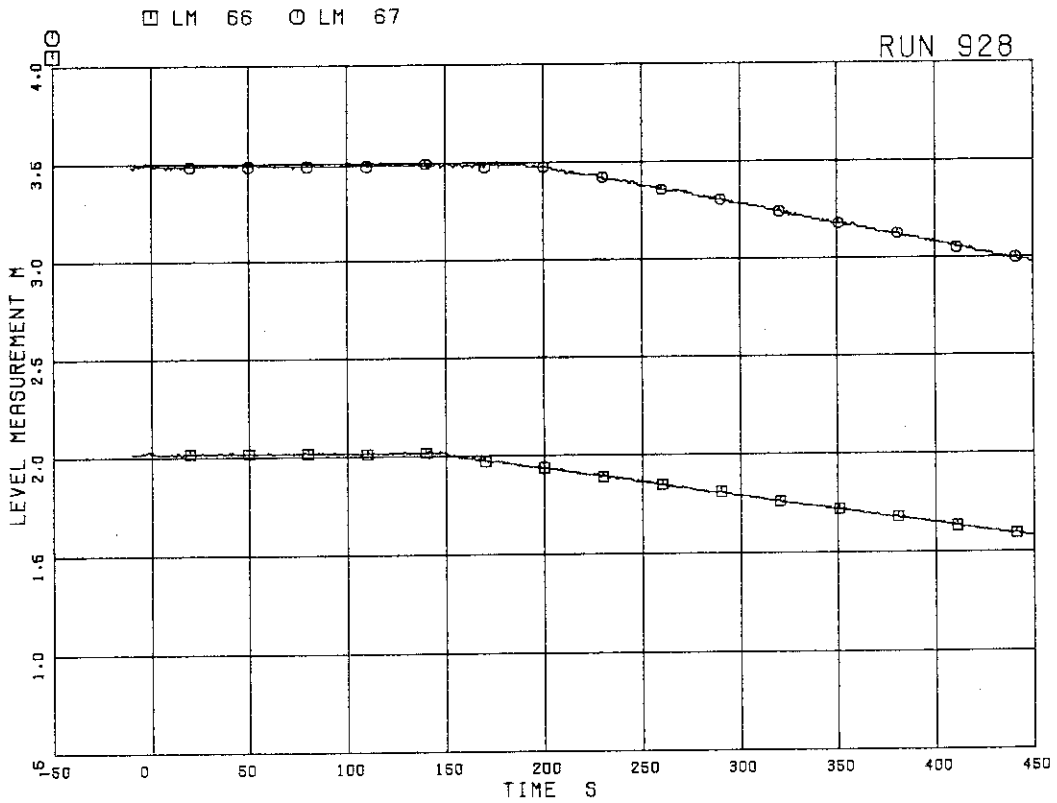


FIG.5. 38 LIQUID LEVELS IN ECCS TANKS

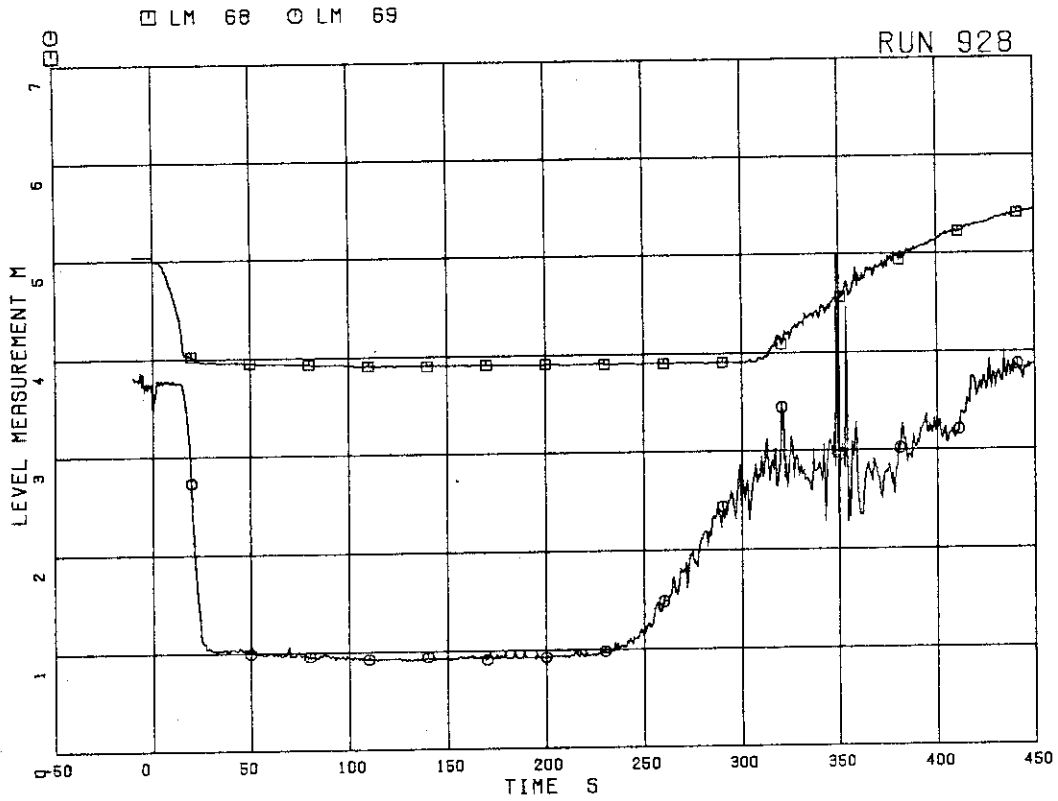


FIG. 5. 39 LIQUID LEVELS IN DOWNCOMER

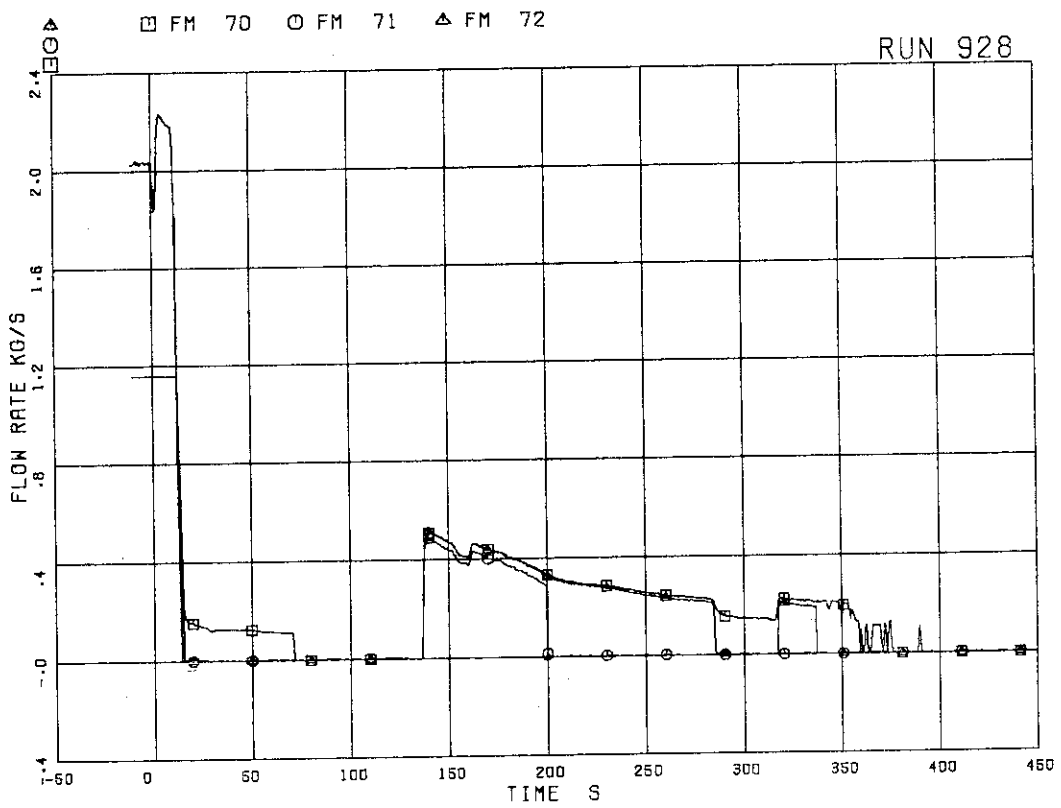


FIG. 5. 40 MASS FLOW RATE IN MSL

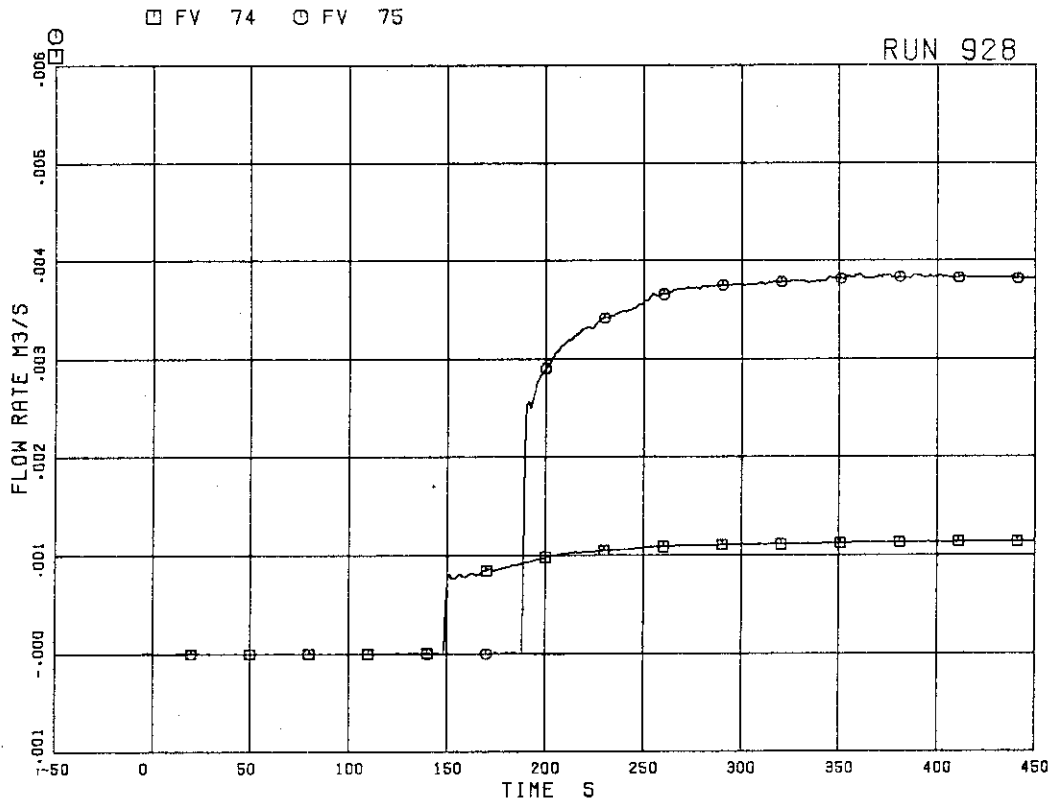


FIG.5. 41 ECC INJECTION FLOW RATE

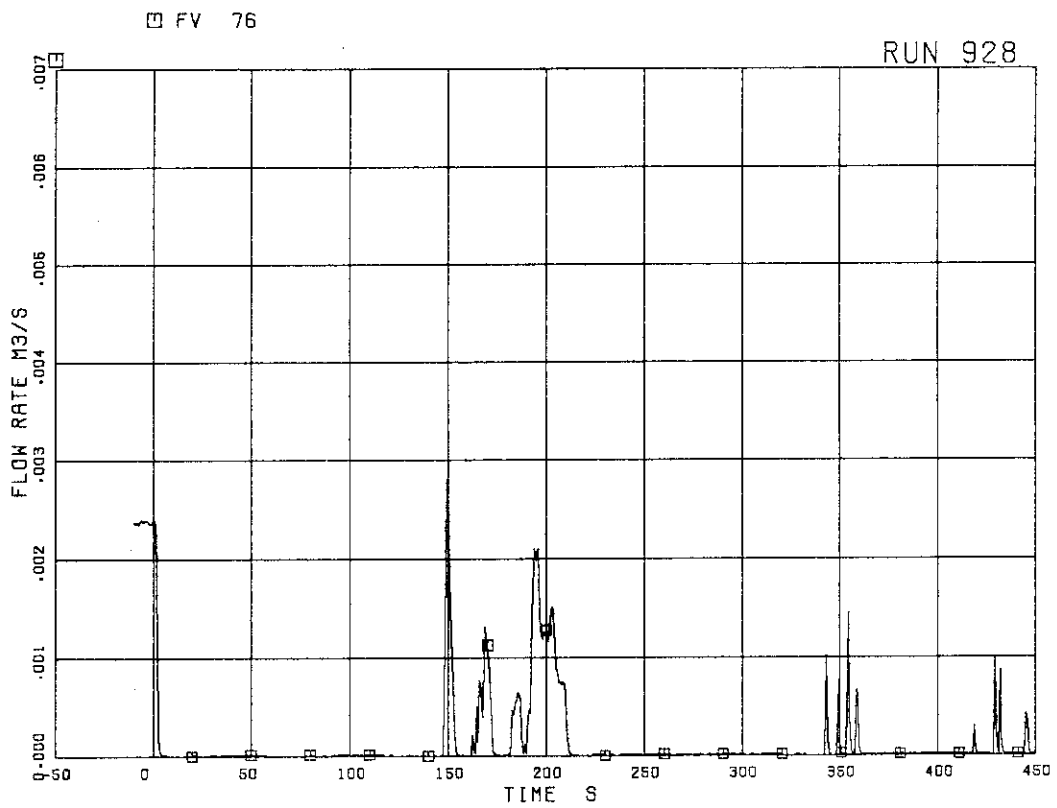


FIG.5. 42 FEEDWATER FLOW RATE

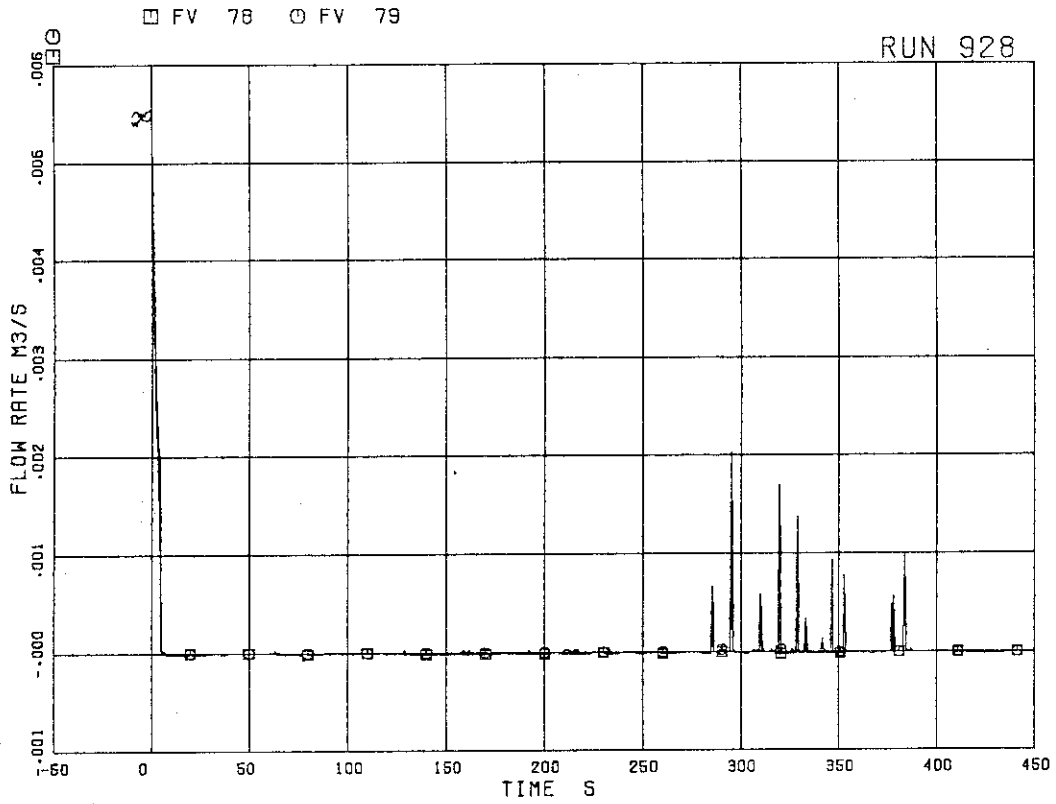


FIG.5. 43 JP-1,2 DISCHARGE FLOW RATE (HIGH RANGE)

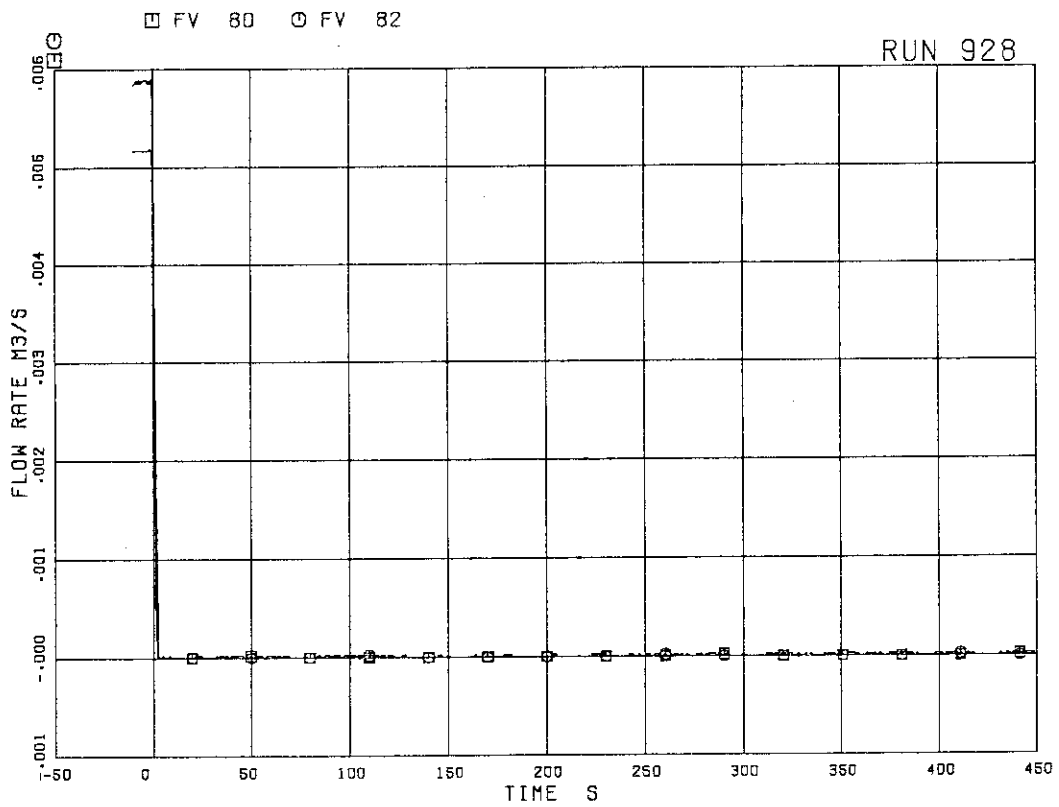


FIG.5. 44 JP-3,4 DISCHARGE FLOW RATE (HIGH RANGE)

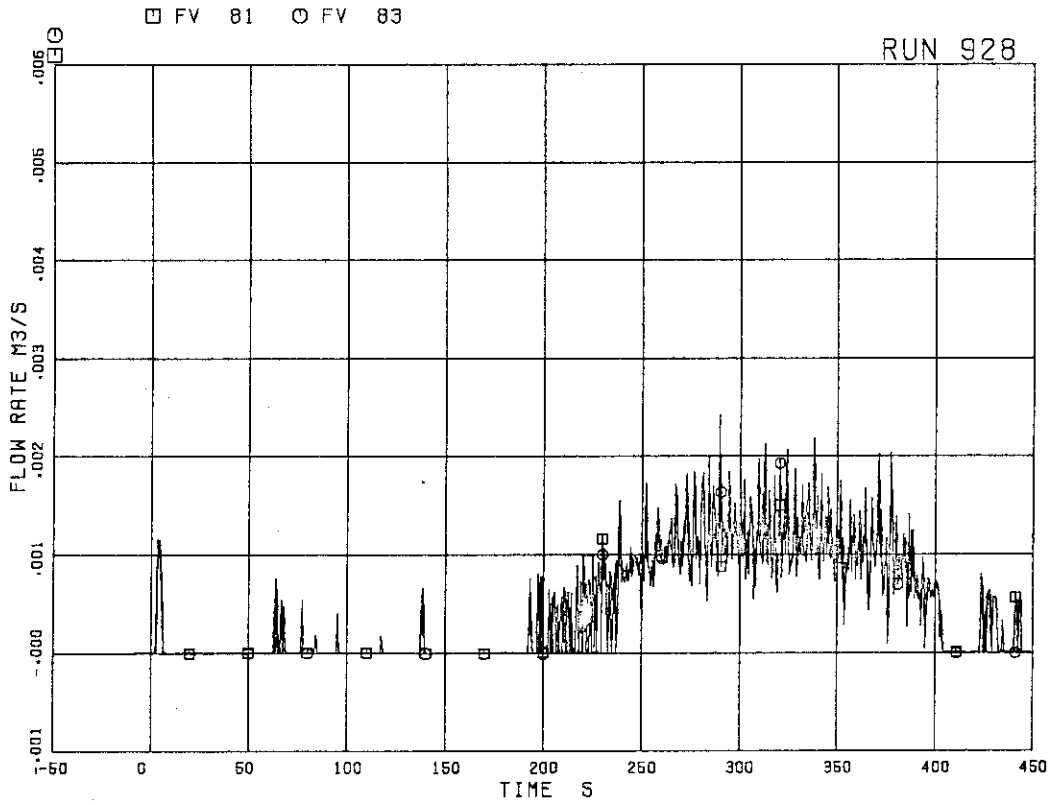


FIG.5. 45 JP-3,4 DISCHARGE FLOW RATE (LOW RANGE)

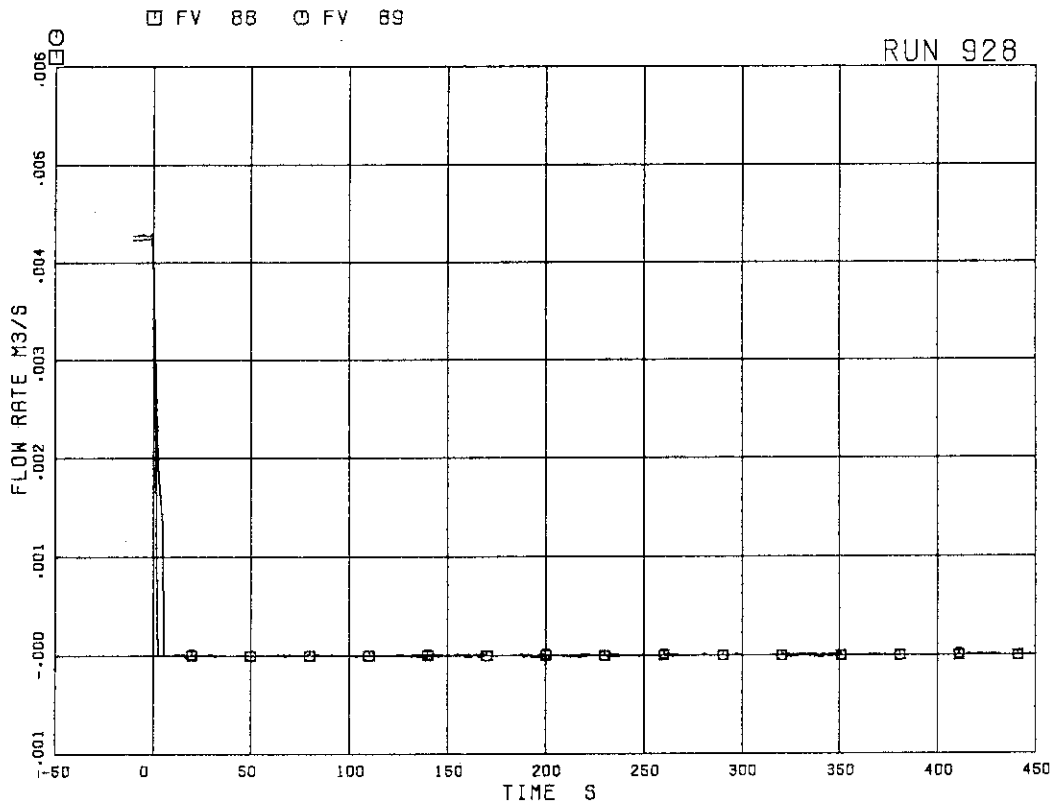


FIG.5. 46 MRP DISCHARGE FLOW RATE

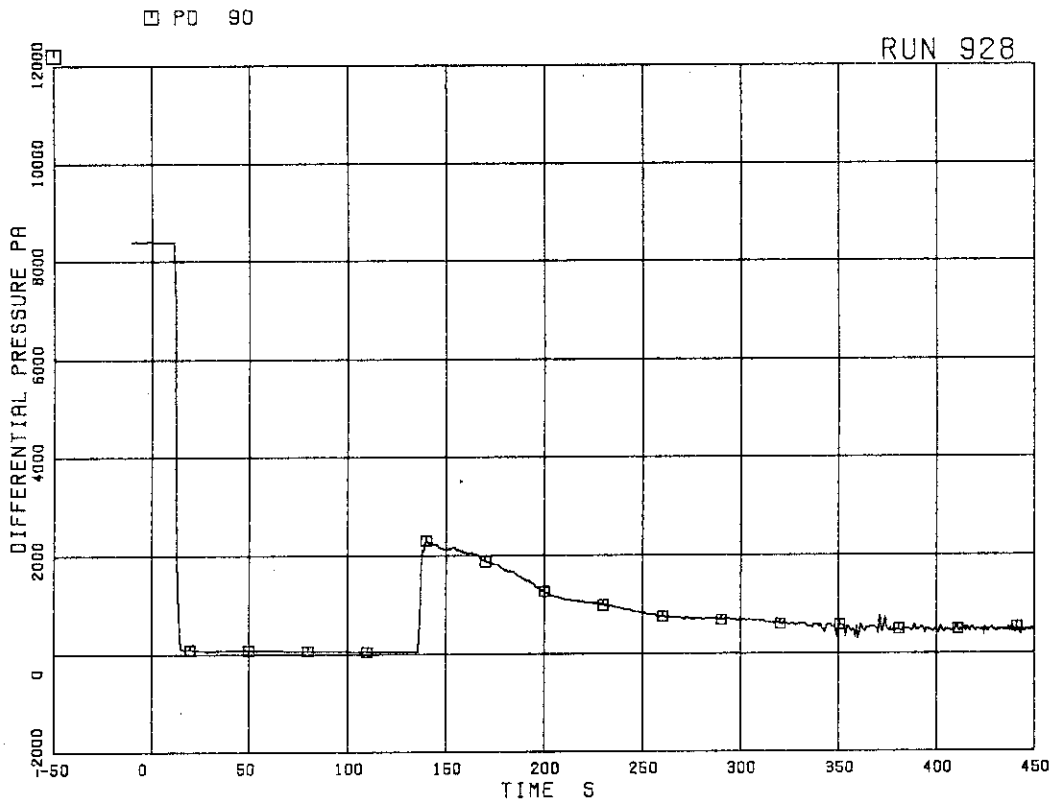


FIG. 5. 47 DIFFERENTIAL PRESSURE ACROSS ORIFICE FLOWMETER F-1

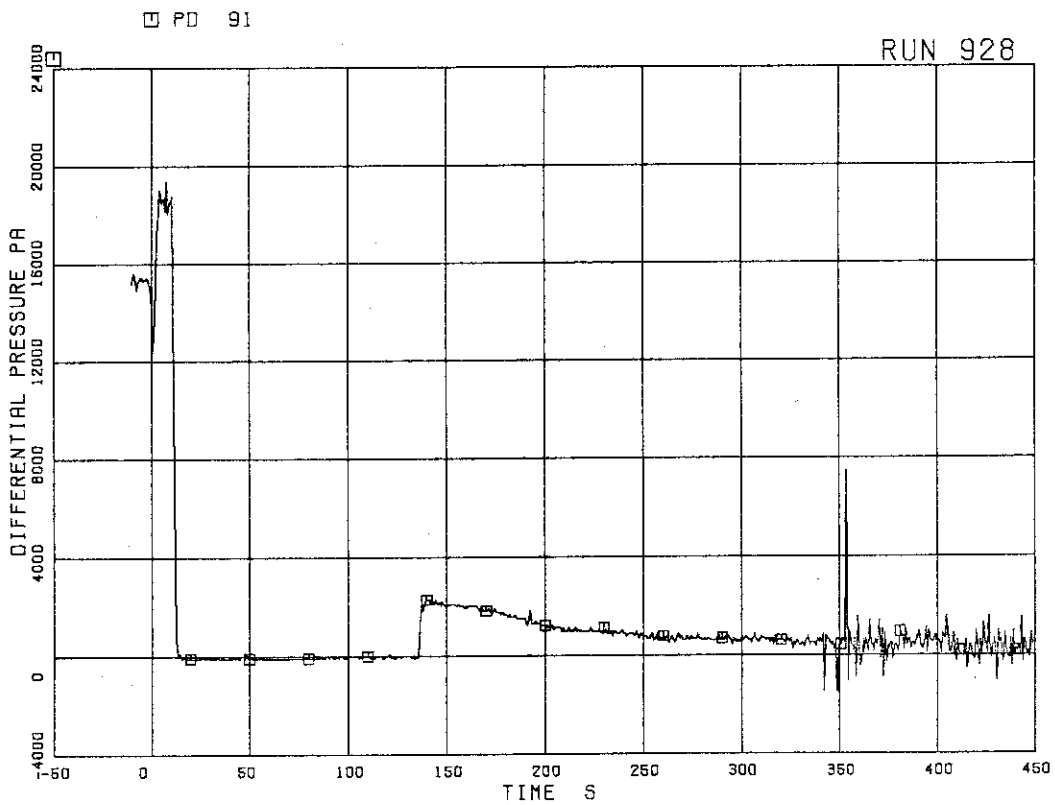


FIG. 5. 48 DIFFERENTIAL PRESSURE ACROSS ORIFICE FLOWMETER F-2



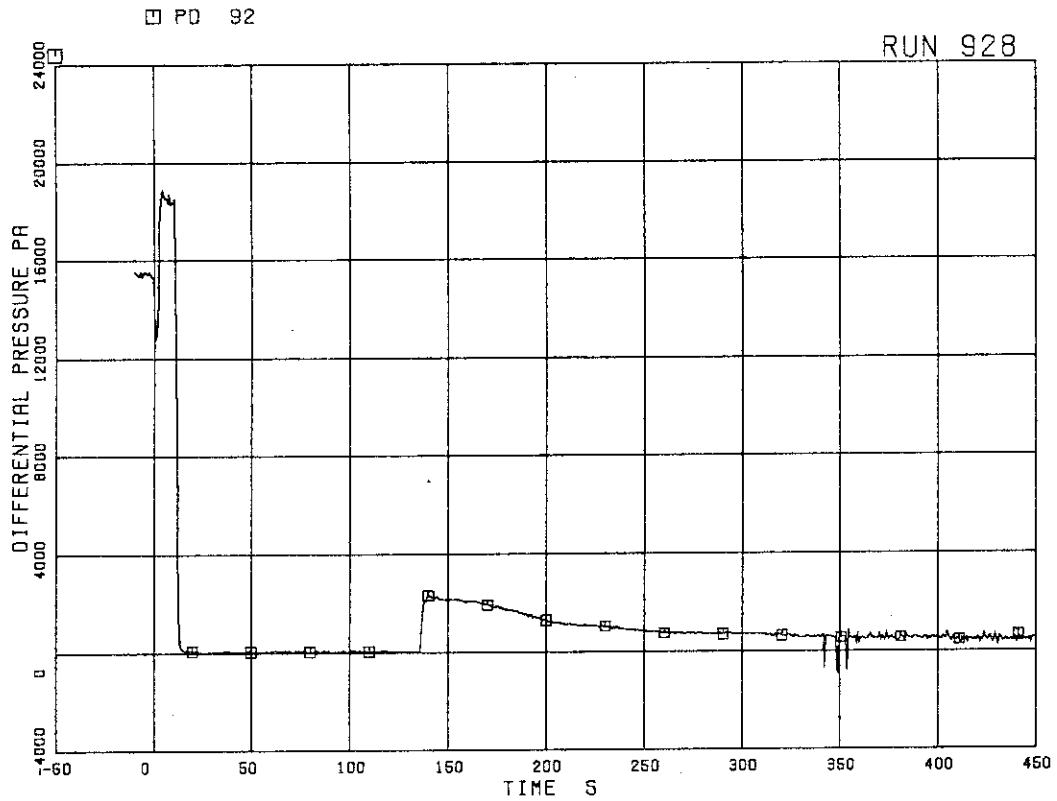


FIG.5. 49 DIFFERENTIAL PRESSURE ACROSS  
ORIFICE FLOWMETER F-3

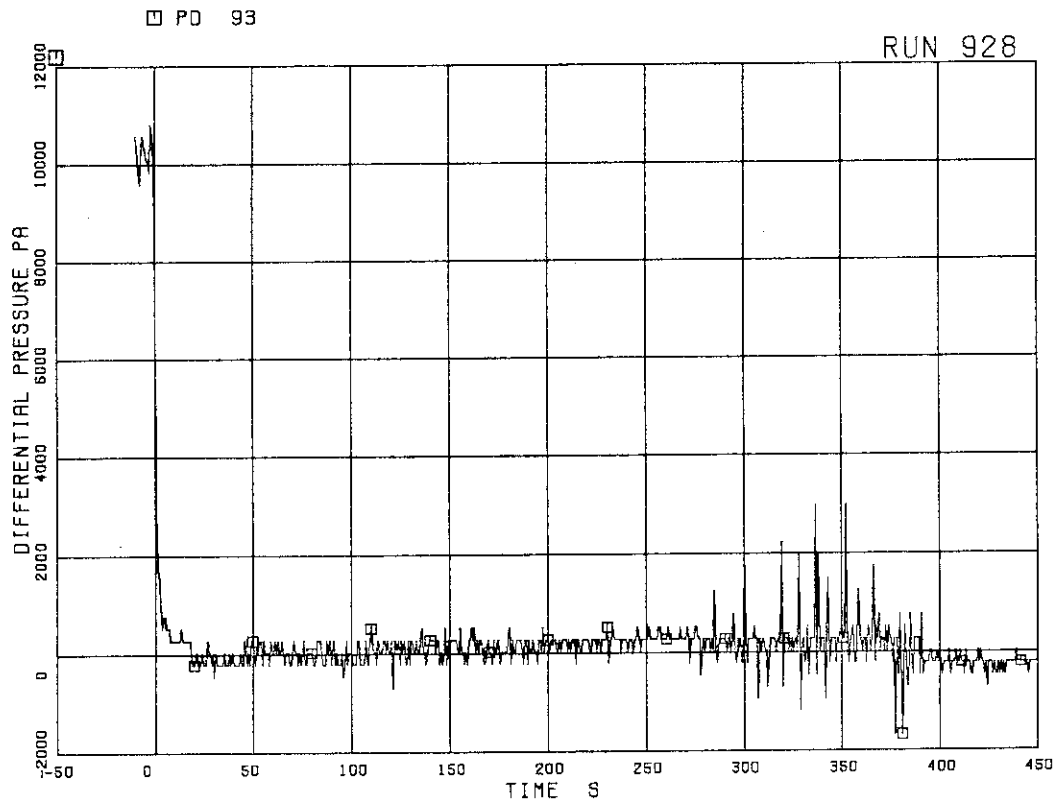


FIG.5. 50 DIFFERENTIAL PRESSURE ACROSS  
VENTURI FLOWMETER F-17

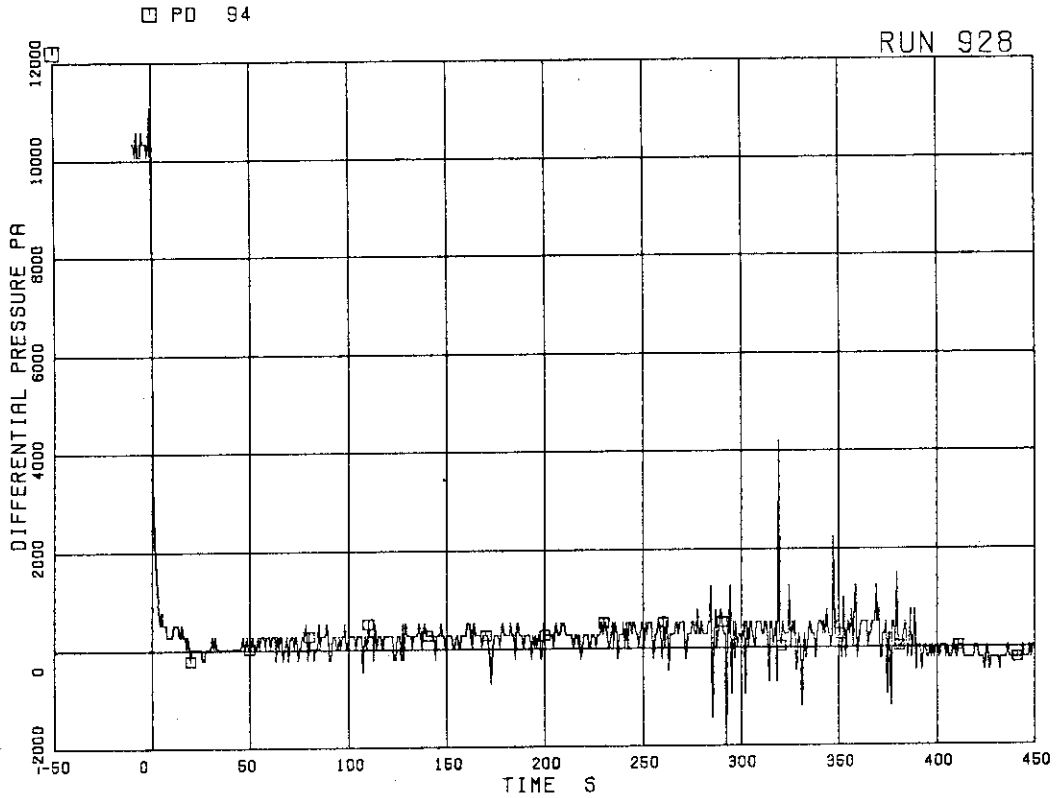


FIG.5. 51 DIFFERENTIAL PRESSURE ACROSS VENTURI FLOWMETER F-18

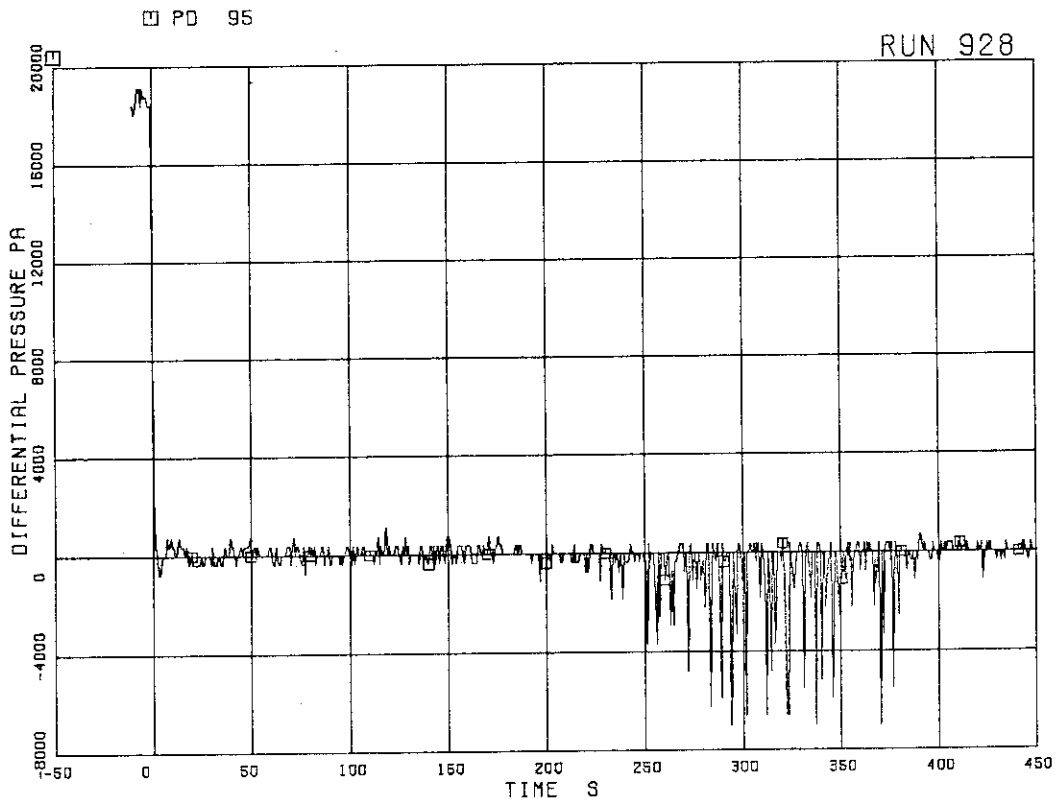


FIG.5. 52 DIFFERENTIAL PRESSURE ACROSS ORIFICE FLOWMETER F-19

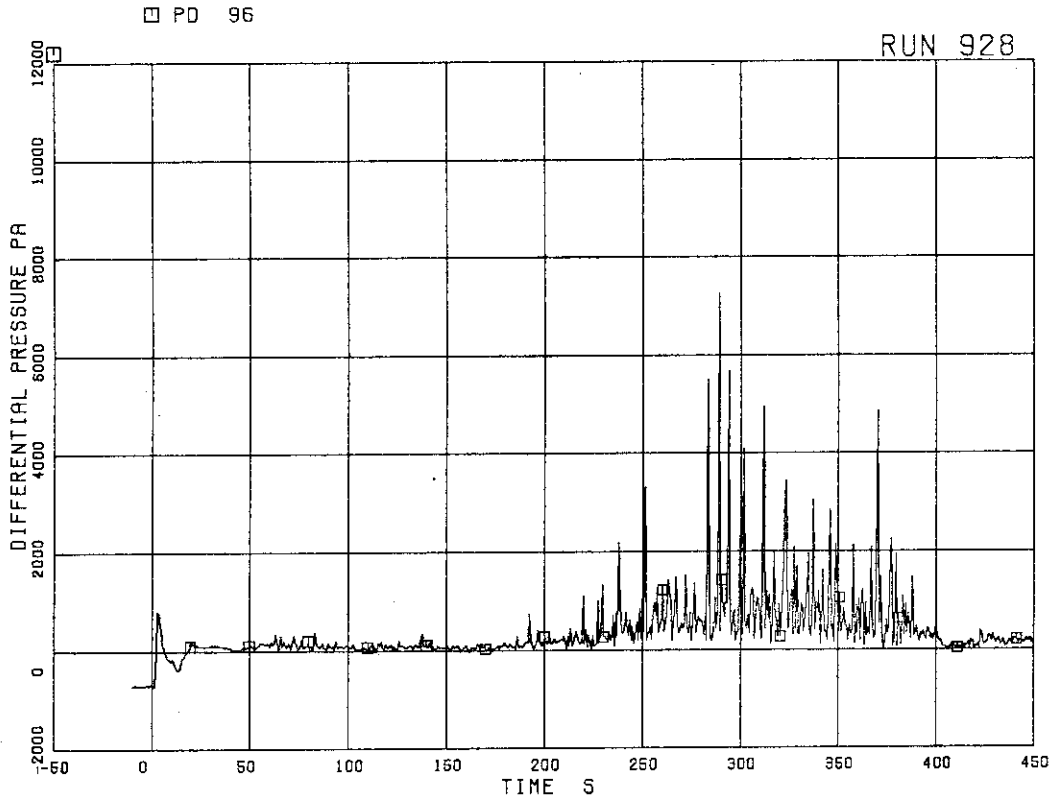


FIG.5. 53 DIFFERENTIAL PRESSURE ACROSS ORIFICE FLOWMETER F-20

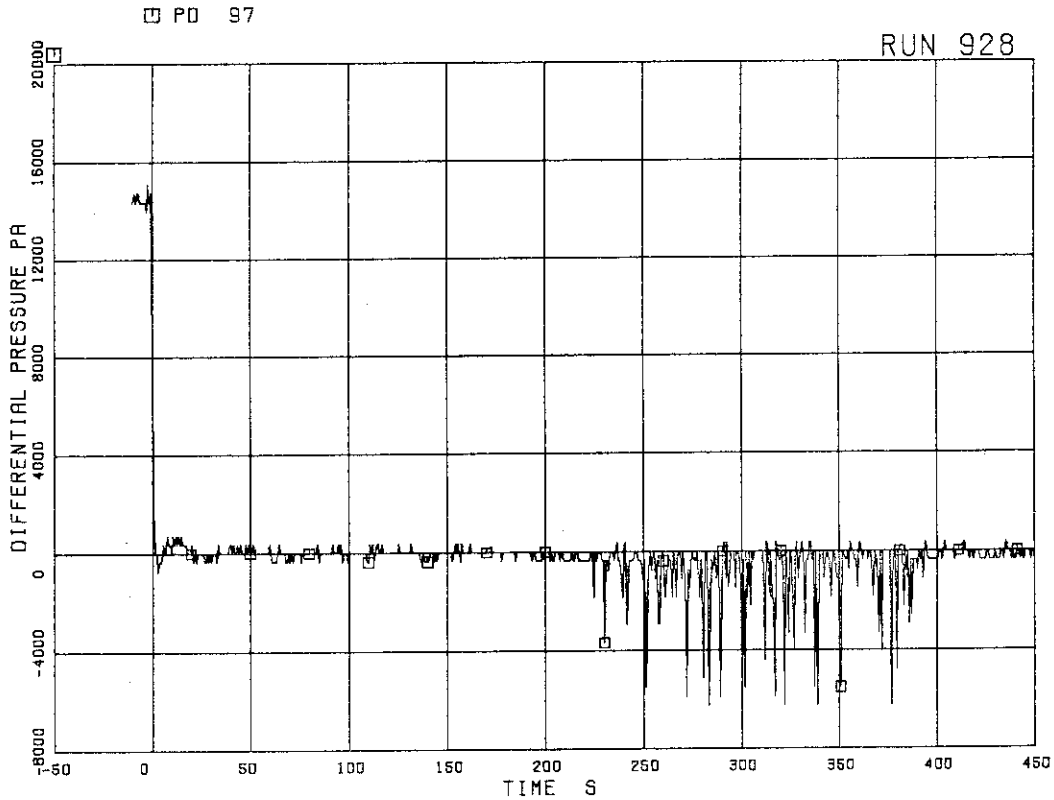


FIG.5. 54 DIFFERENTIAL PRESSURE ACROSS ORIFICE FLOWMETER F-21

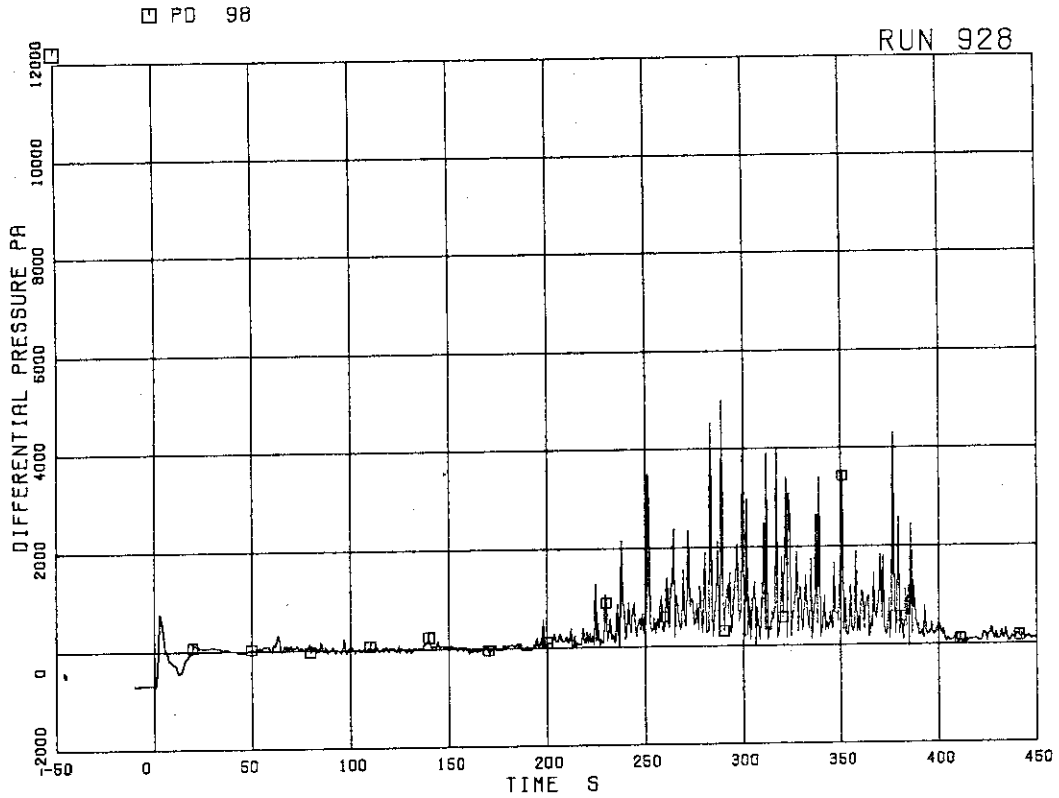


FIG.5. 55 DIFFERENTIAL PRESSURE ACROSS ORIFICE FLOWMETER F-22

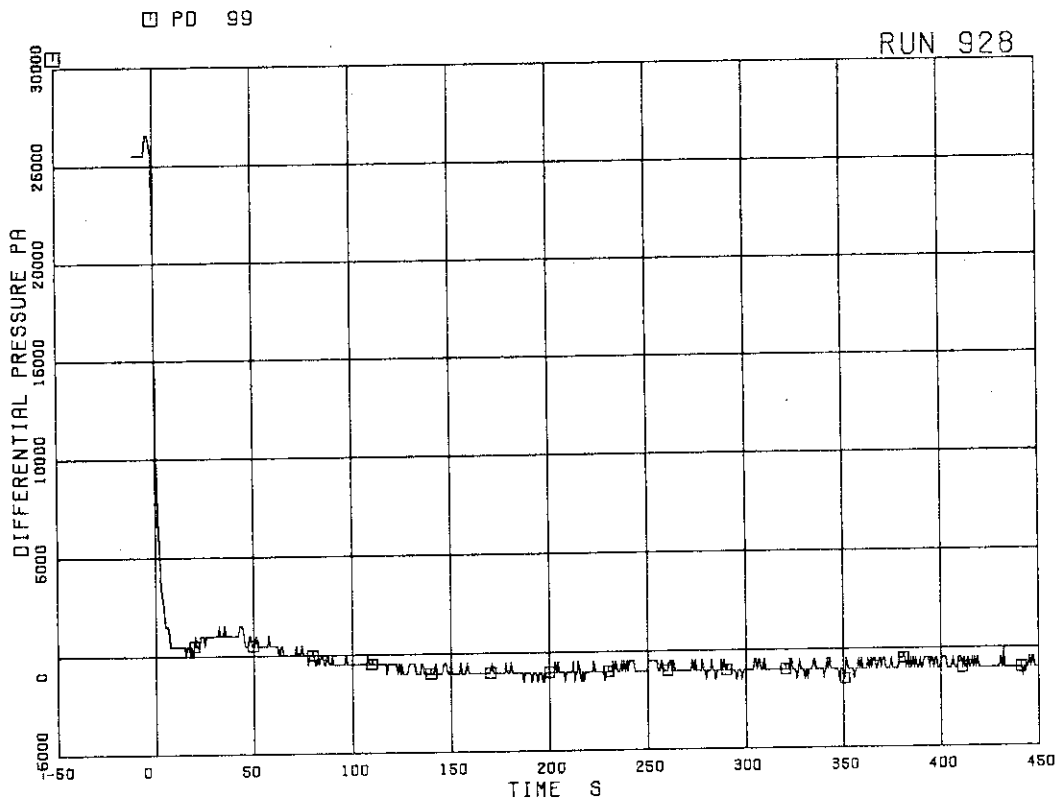


FIG.5. 56 DIFFERENTIAL PRESSURE ACROSS VENTURI FLOWMETER F-27

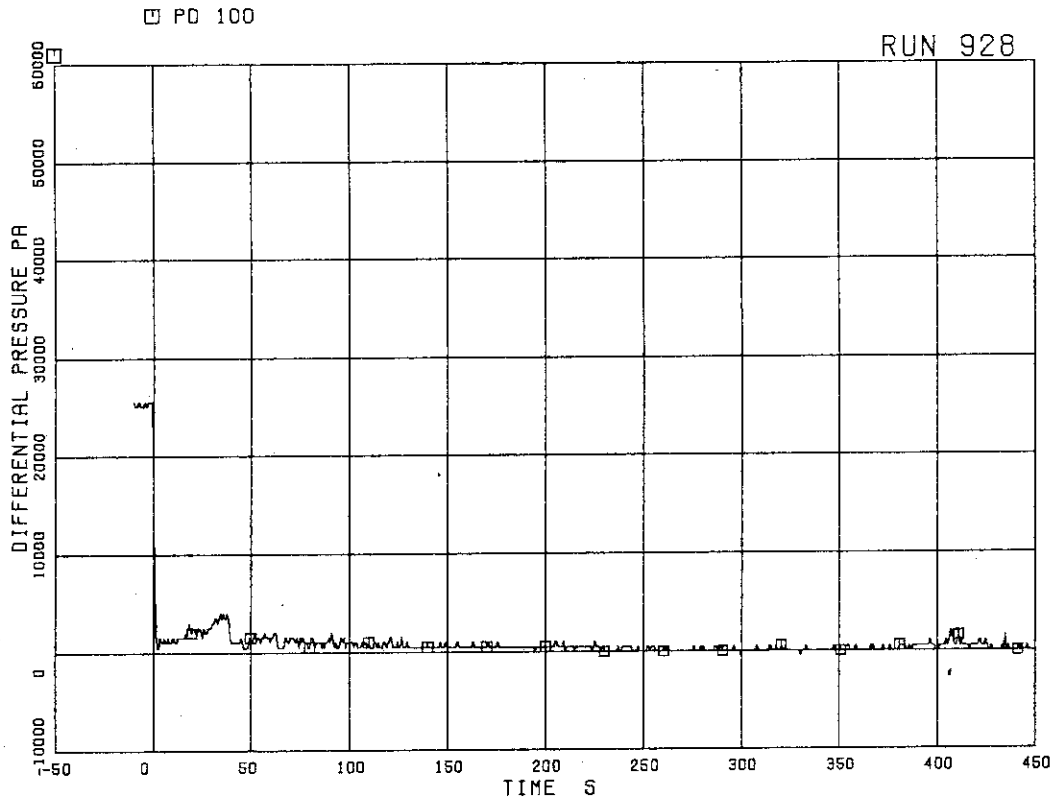


FIG.5. 57 DIFFERENTIAL PRESSURE ACROSS VENTURI FLOWMETER F-28

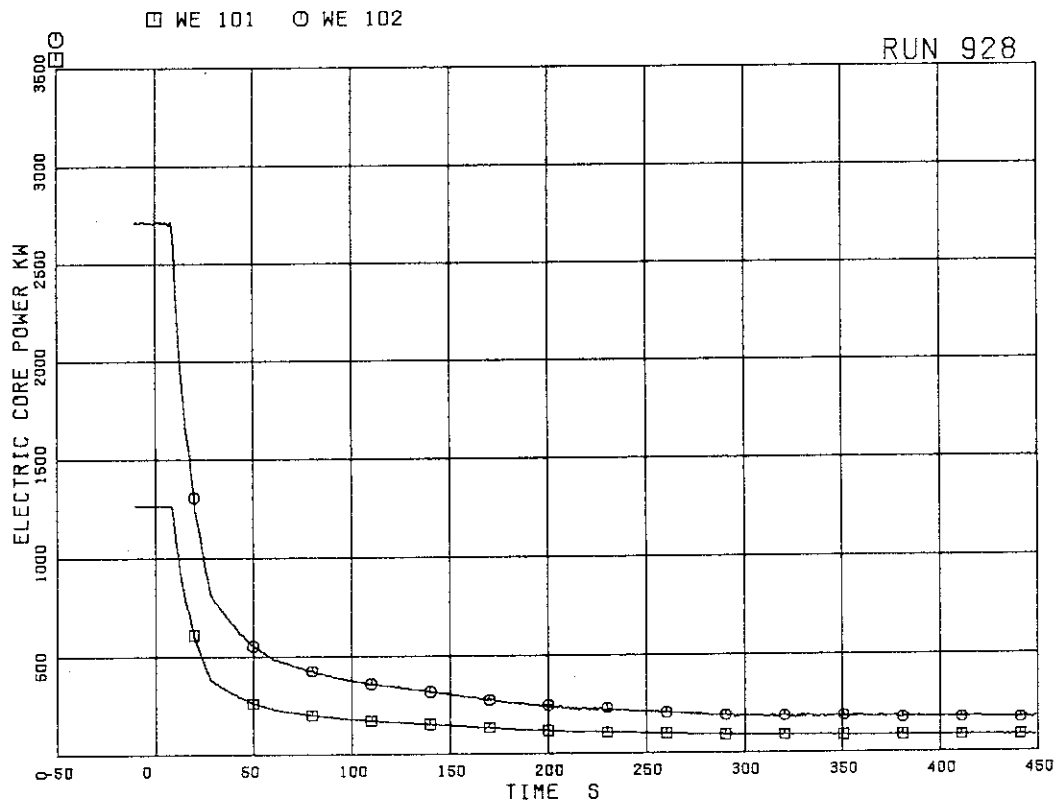


FIG.5. 58 ELECTRIC CORE POWER

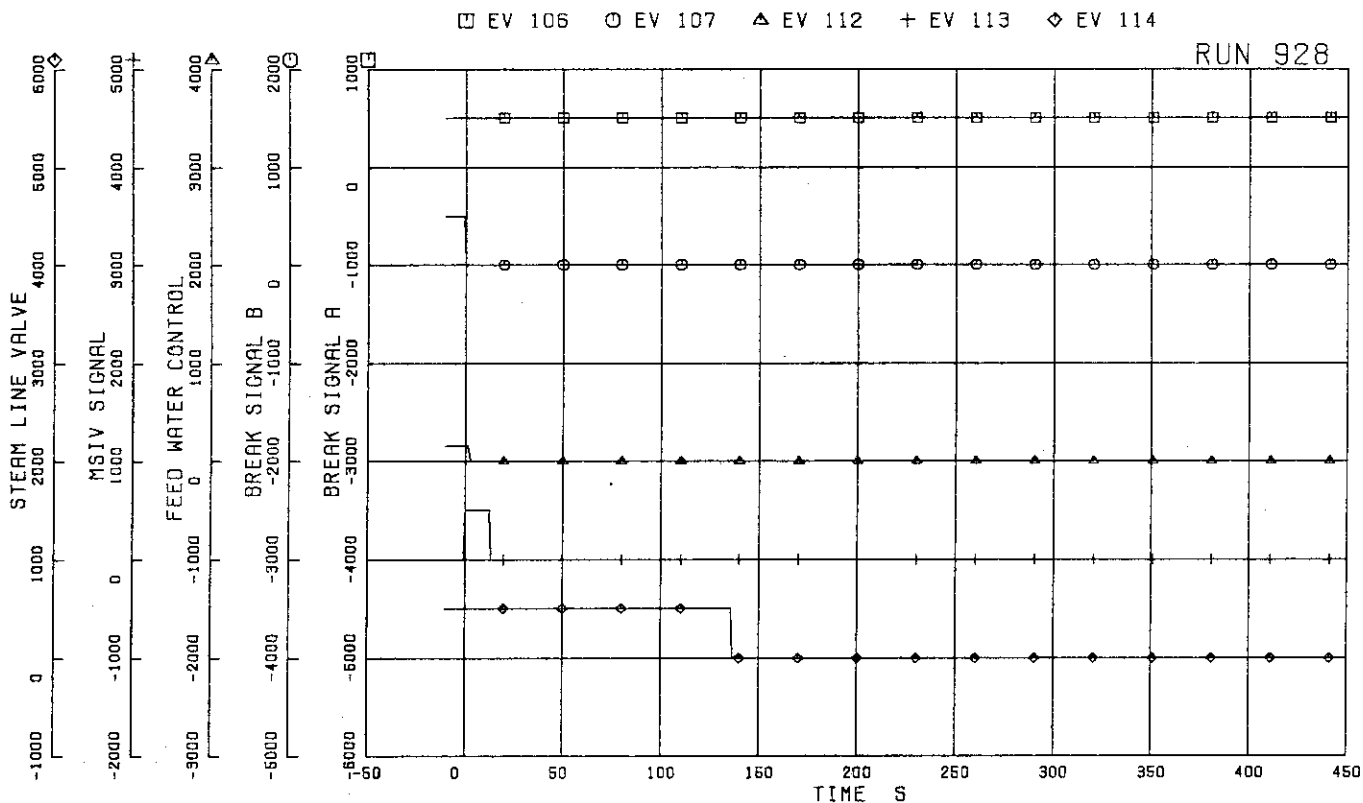


FIG.5. 59 VALVE OPERATION SIGNALS

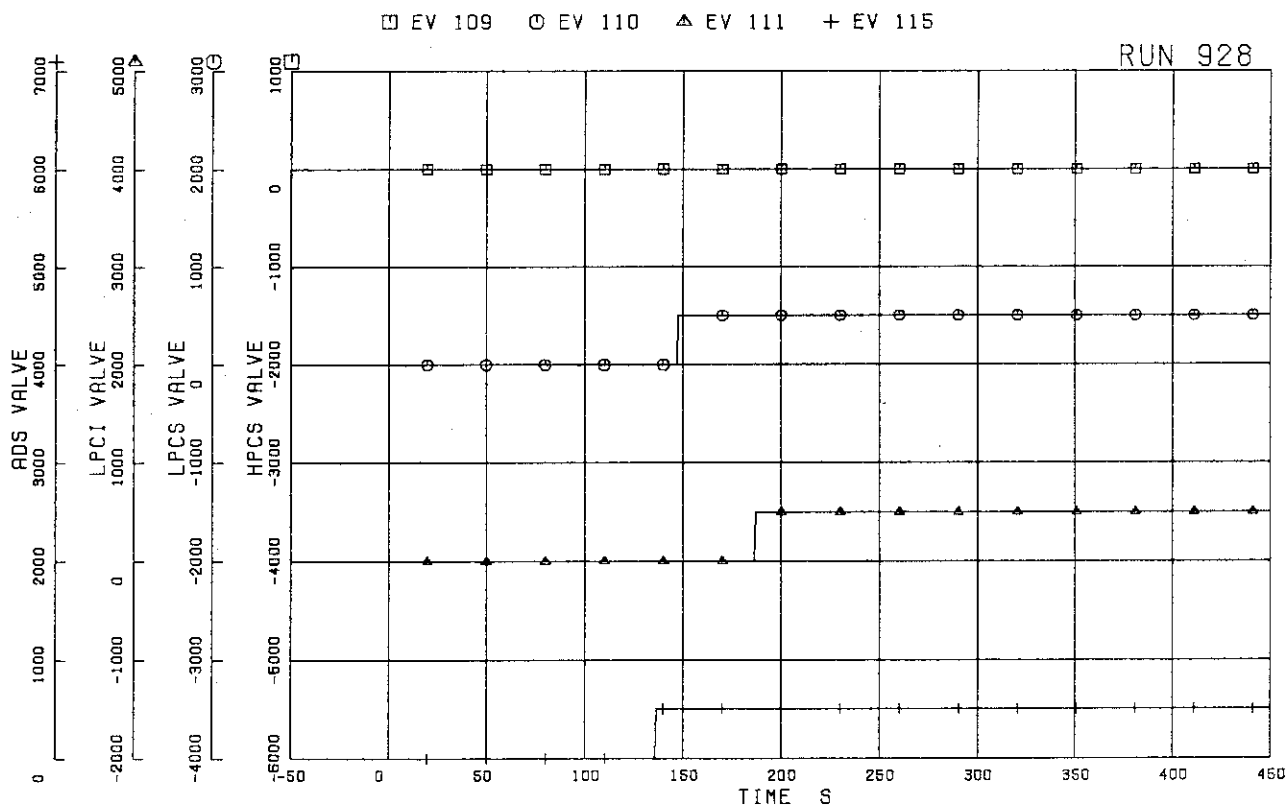


FIG.5. 60 ECCS OPERATION SIGNALS

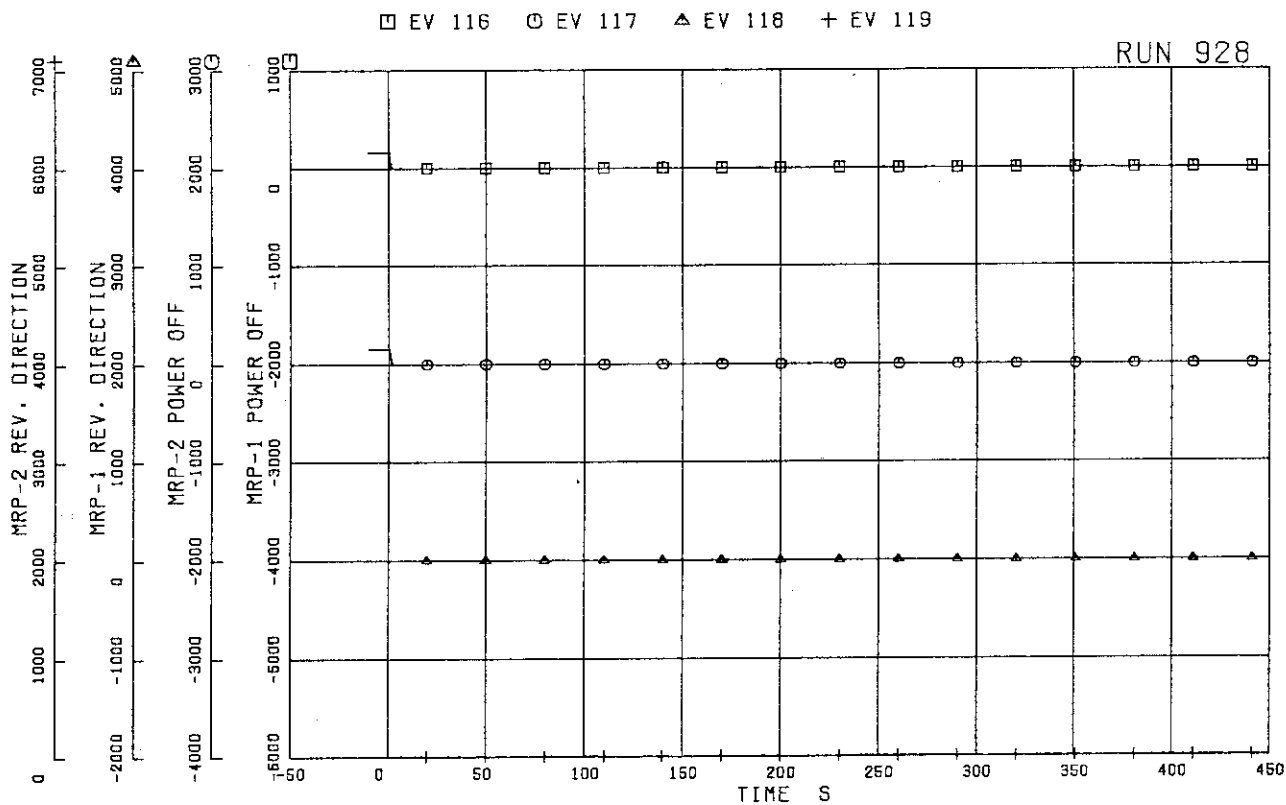


FIG.5. 61 MRP OPERATION SIGNALS

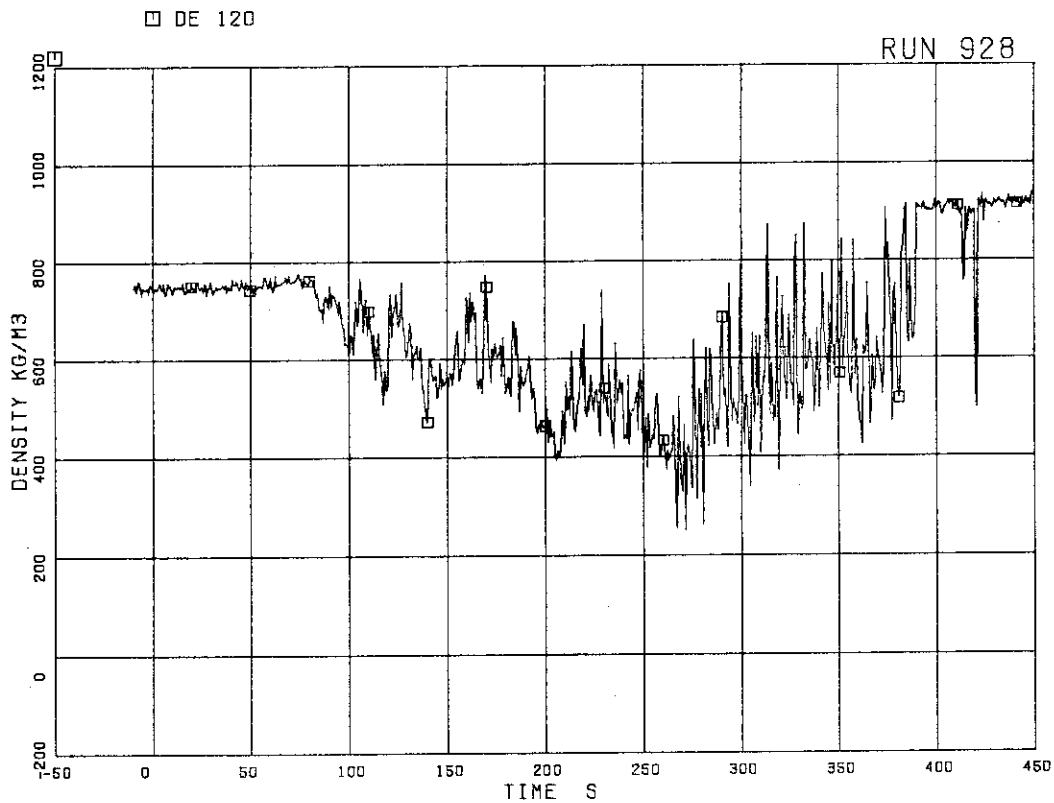


FIG.5. 62 FLUID DENSITY AT JP-1,2 OUTLET, BEAM A

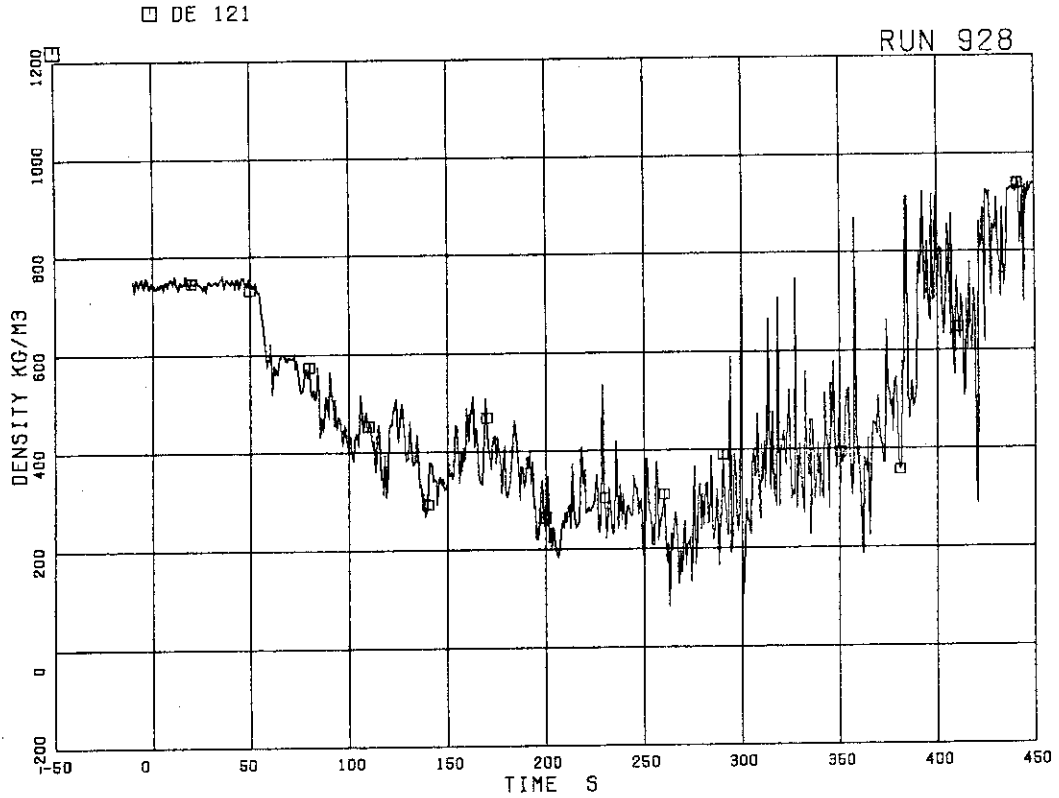


FIG.5. 63 FLUID DENSITY AT JP-1,2 OUTLET, BEAM B

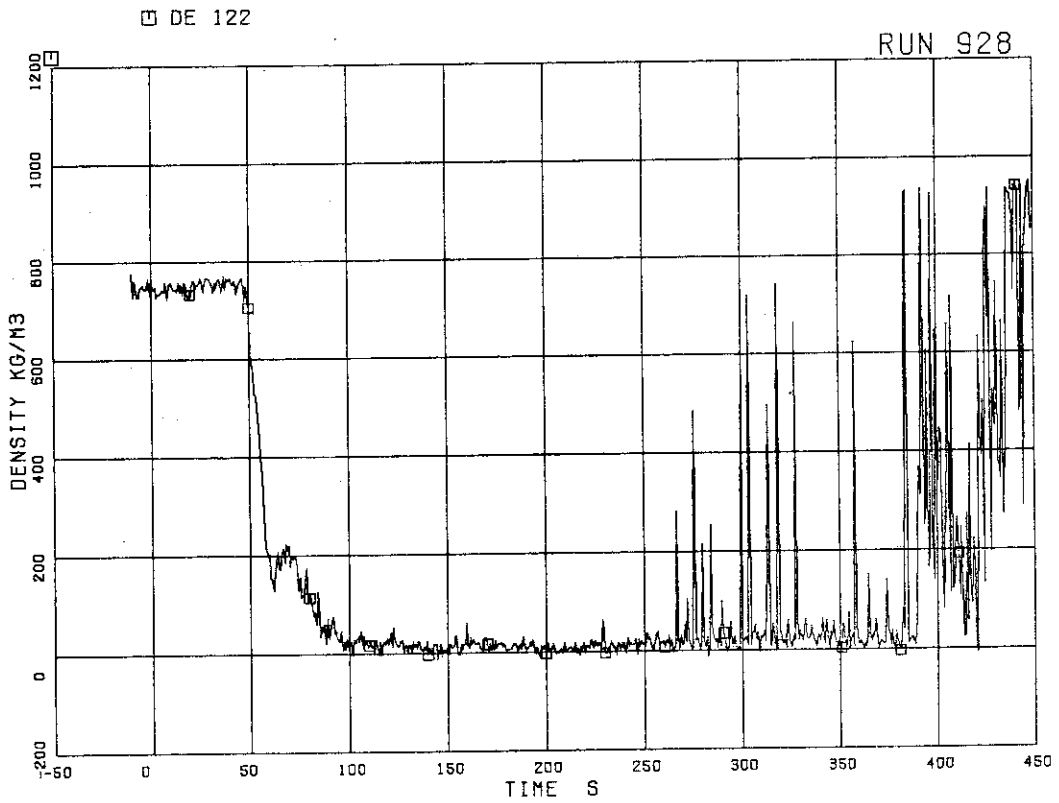


FIG.5. 64 FLUID DENSITY AT JP-1,2 OUTLET, BEAM C



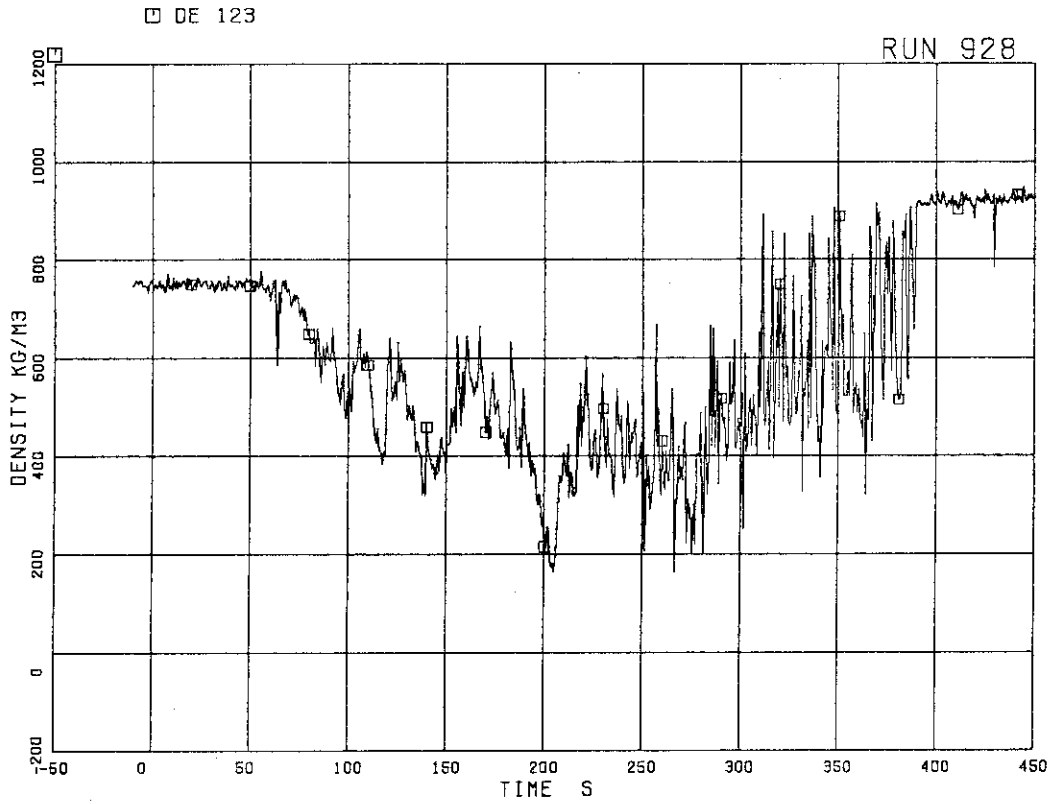


FIG.5. 65 FLUID DENSITY AT JP-3,4 OUTLET, BEAM A

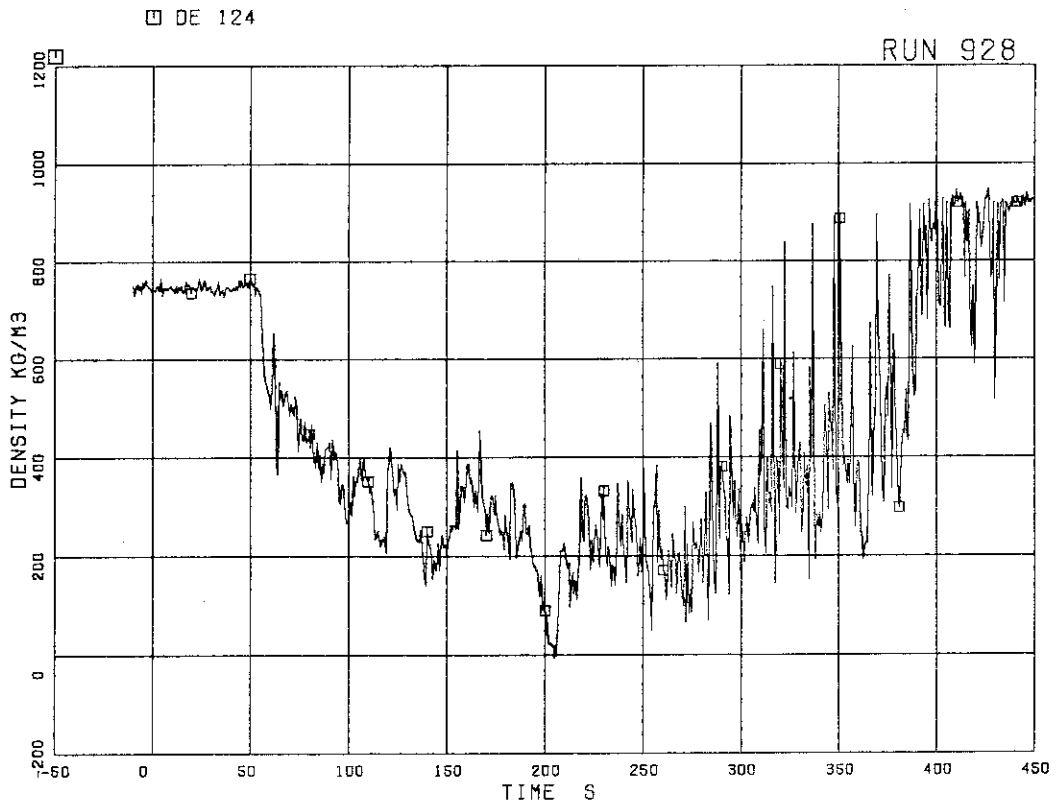


FIG.5. 66 FLUID DENSITY AT JP-3.4 OUTLET, BEAM B

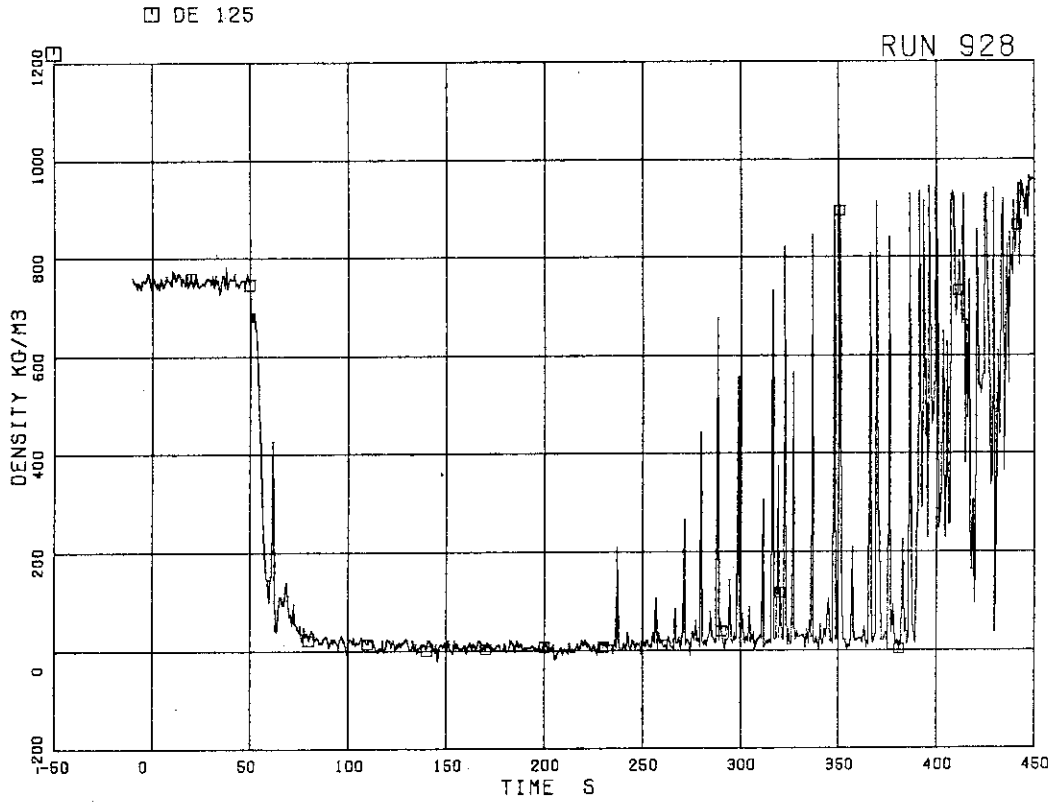


FIG.5. 67 FLUID DENSITY AT JP-3,4 OUTLET, BEAM C

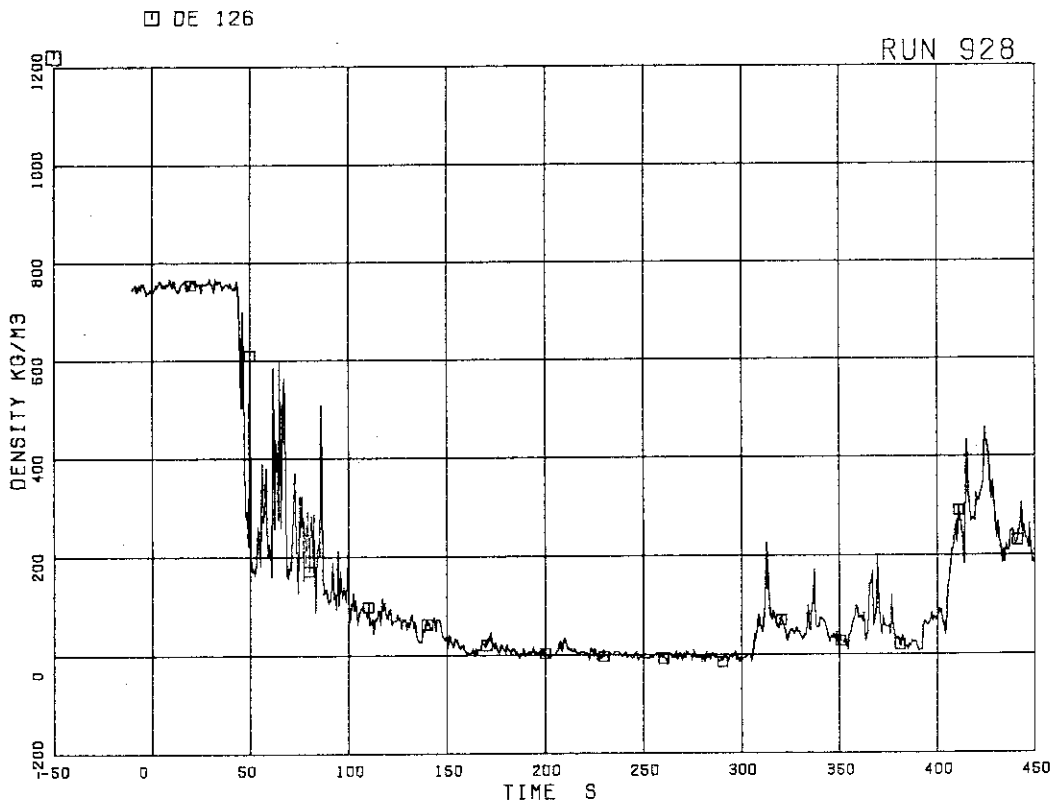


FIG.5. 68 FLUID DENSITY AT MRP SIDE OF BREAK.  
BEAM A

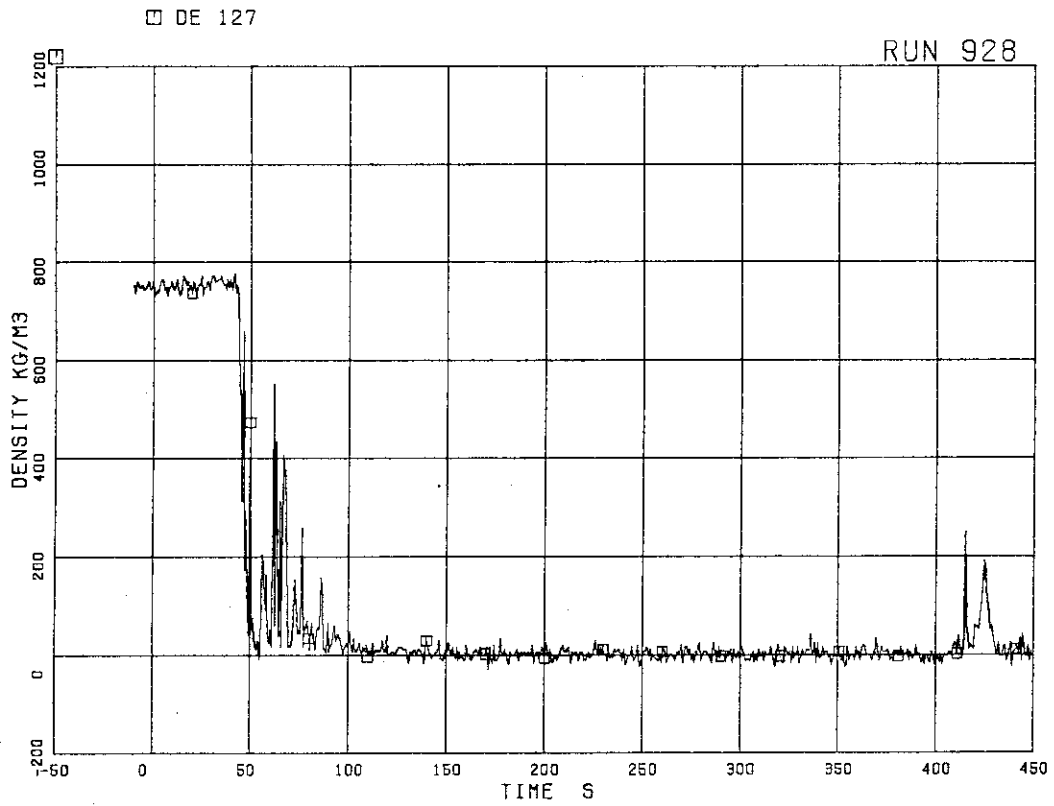


FIG.5. 69 FLUID DENSITY AT MRP SIDE OF BREAK,  
BEAM B

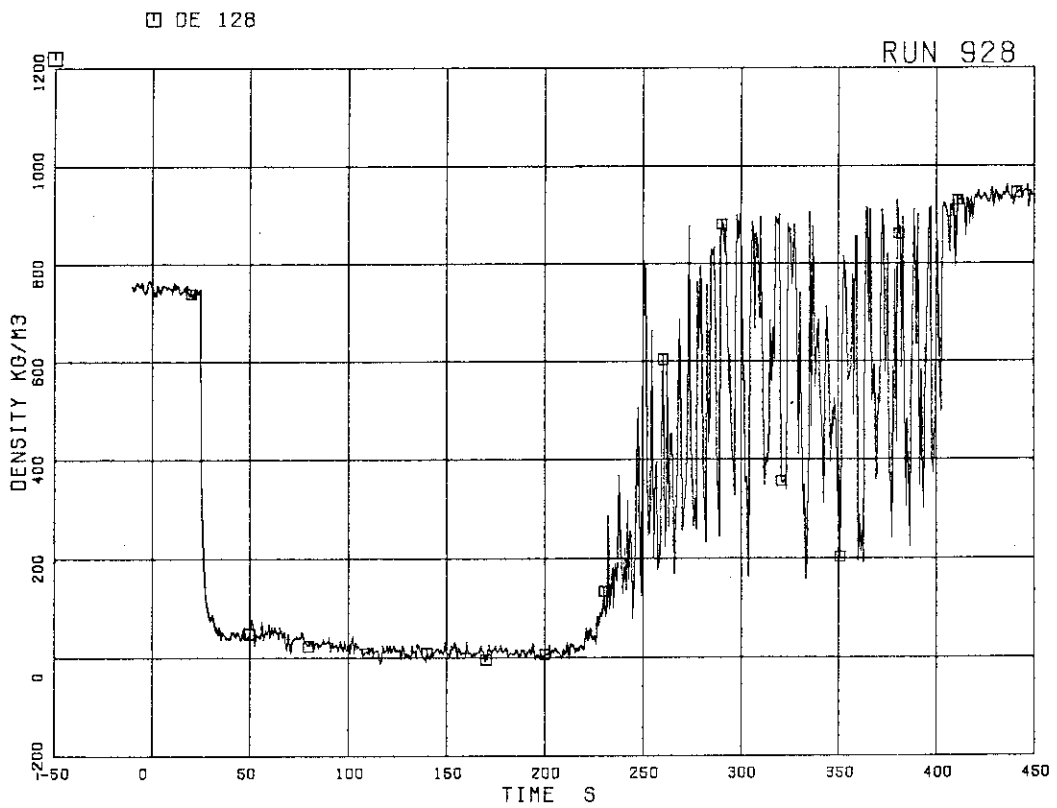


FIG.5. 70 FLUID DENSITY AT PV SIDE OF BREAK,  
BEAM A

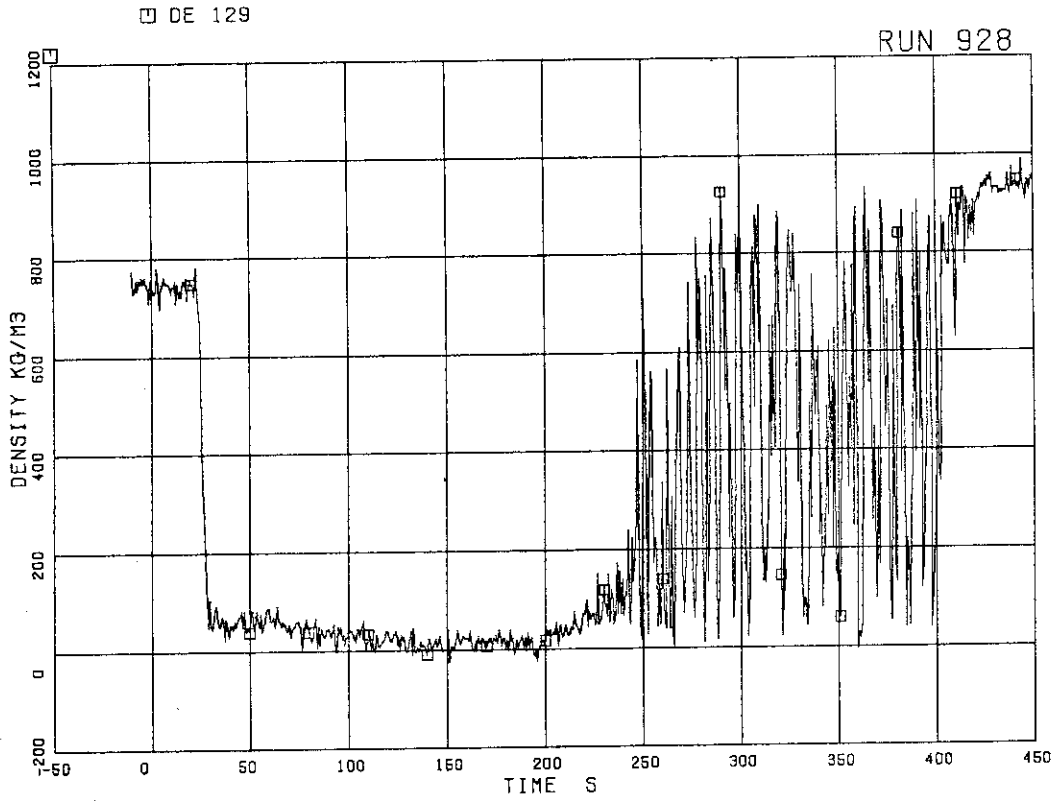


FIG.5. 71 FLUID DENSITY AT PV SIDE OF BREAK,  
BEAM B

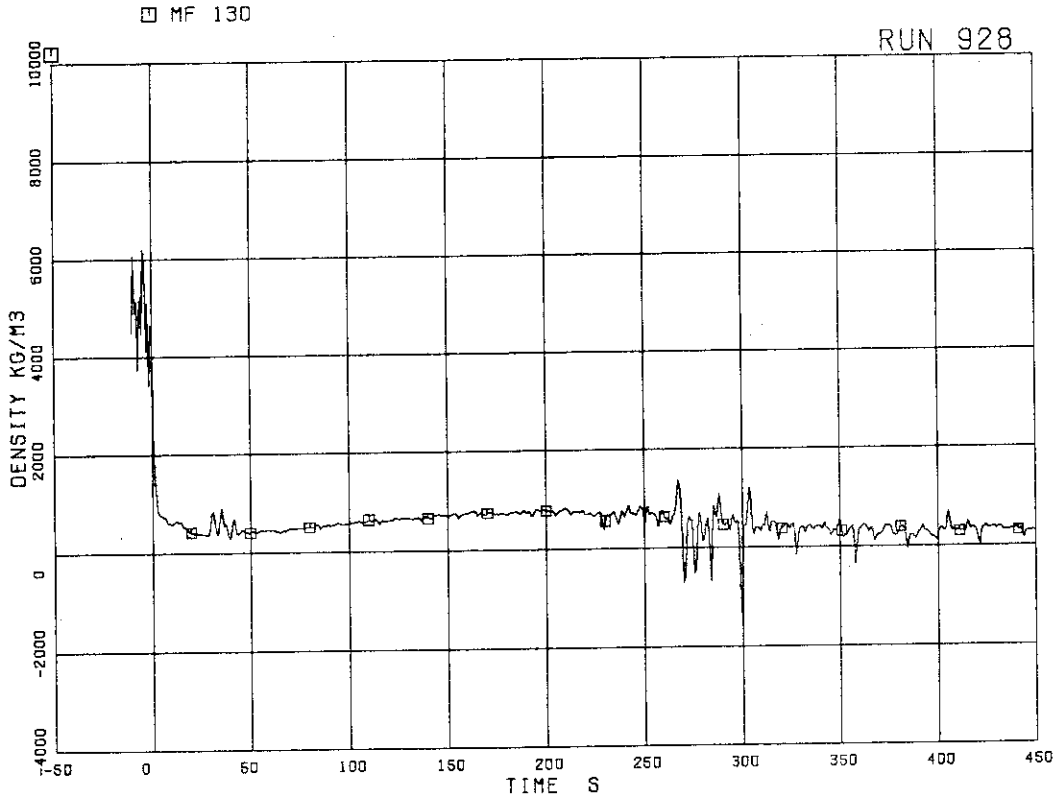


FIG.5. 72 MOMENTUM FLUX AT JP-1,2 OUTLET SPOOL

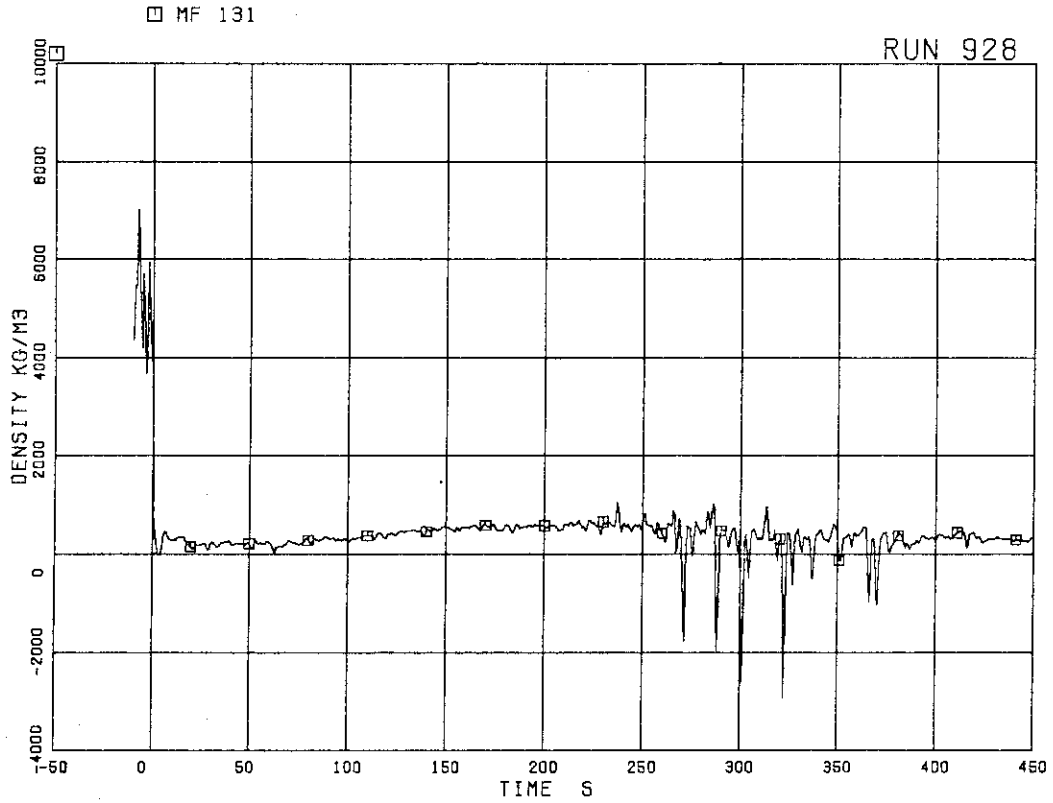


FIG.5. 73 MOMENTUM FLUX AT JP-3,4 OUTLET SPOOL

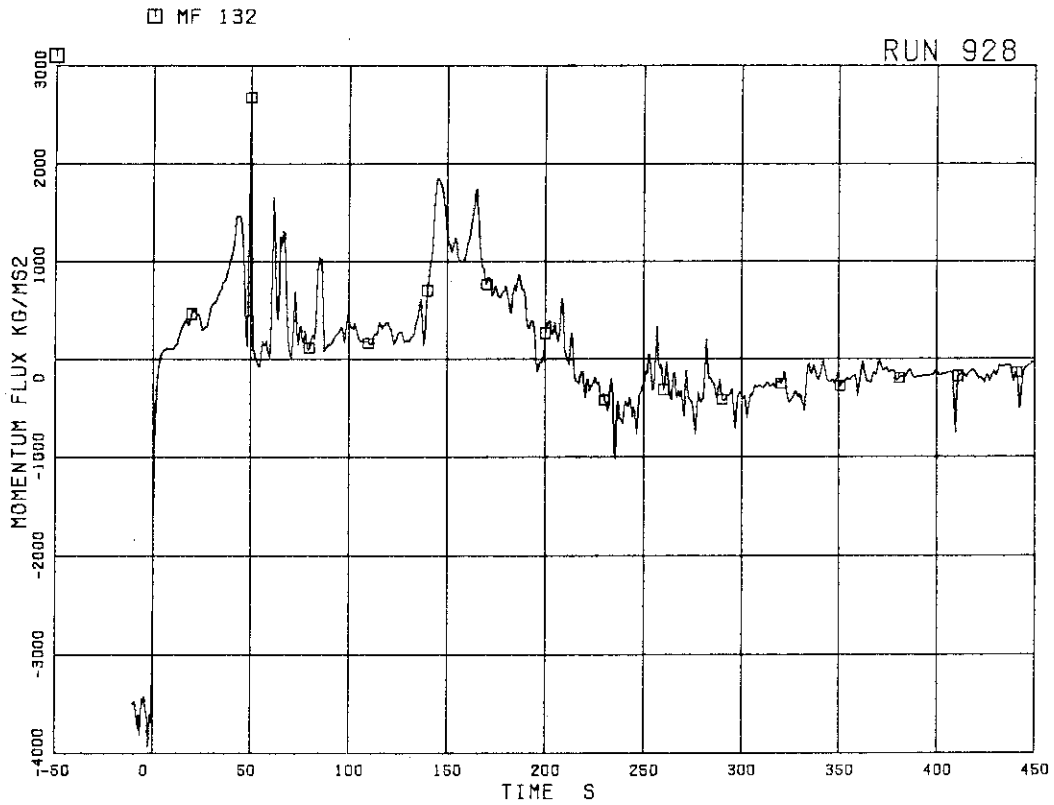


FIG.5. 74 MOMENTUM FLUX AT BREAK A SPOOL PIECE  
(LOW RANGE)

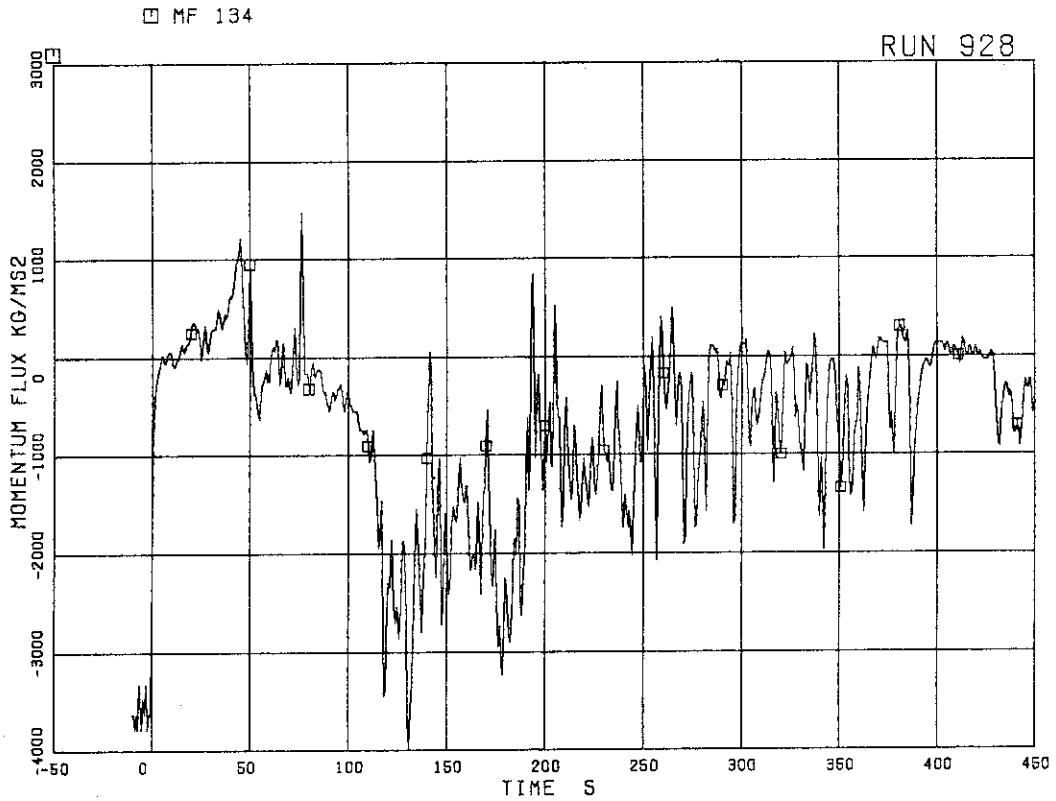


FIG.5. 75 MOMENTUM FLUX AT BREAK A SPOOL PIECE (HIGH RANGE)

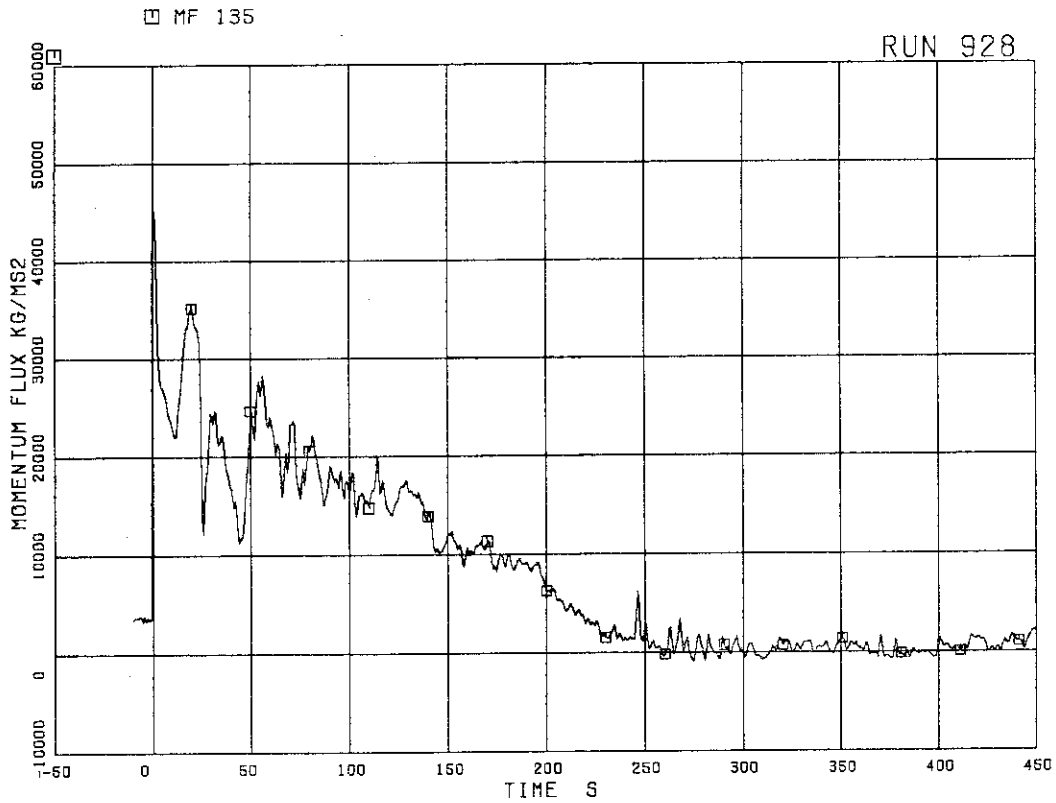


FIG.5. 76 MOMENTUM FLUX AT BREAK B SPOOL PIECE (HIGH RANGE)

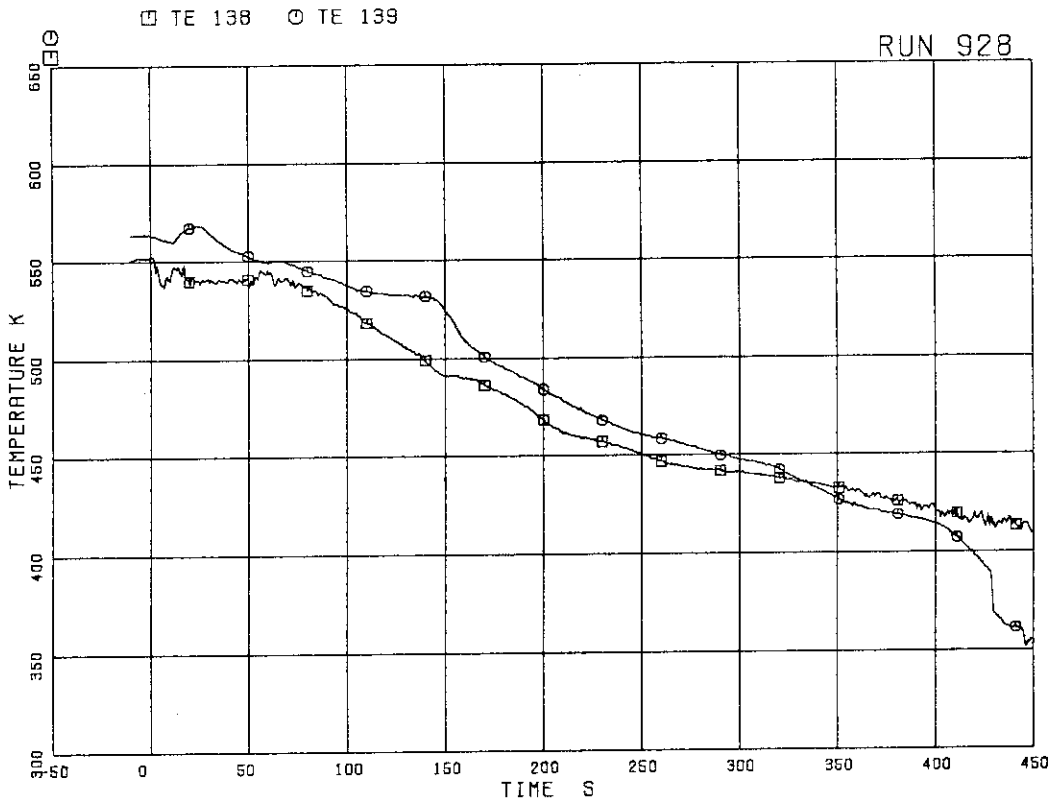


FIG.5. 77 FLUID TEMPERATURES IN LOWER PLENUM AND UPPER PLENUM

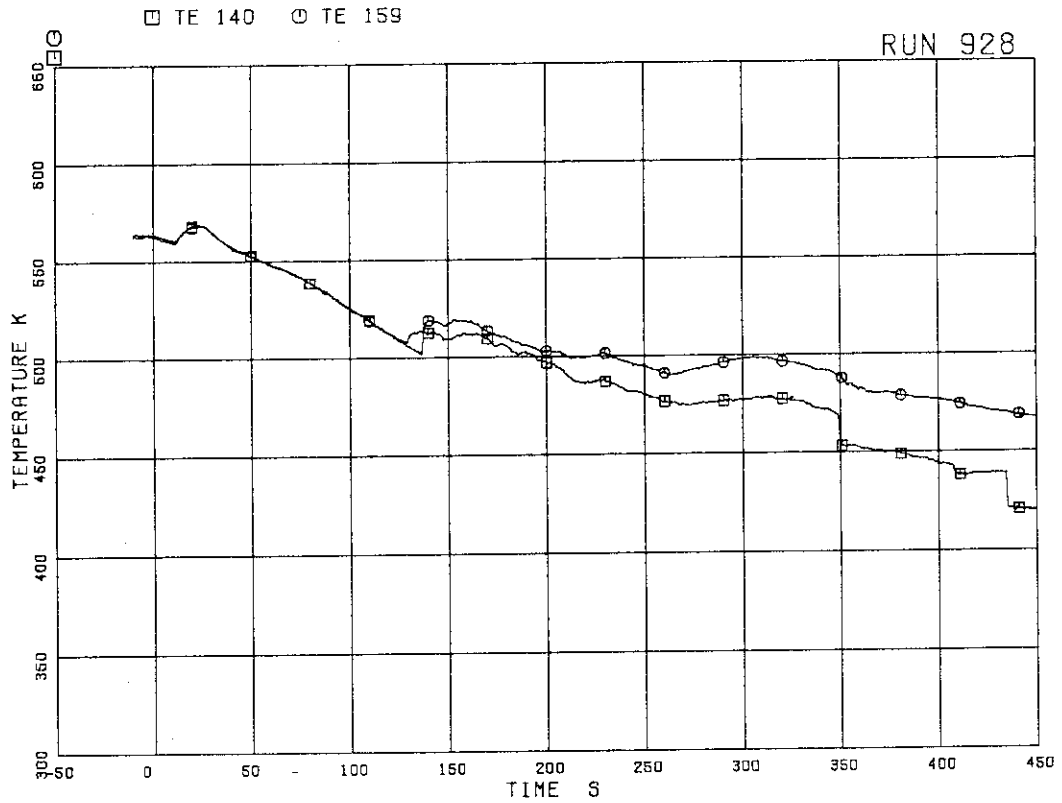


FIG.5. 78 FLUID TEMPERATURES IN STEAM DOME AND MSL

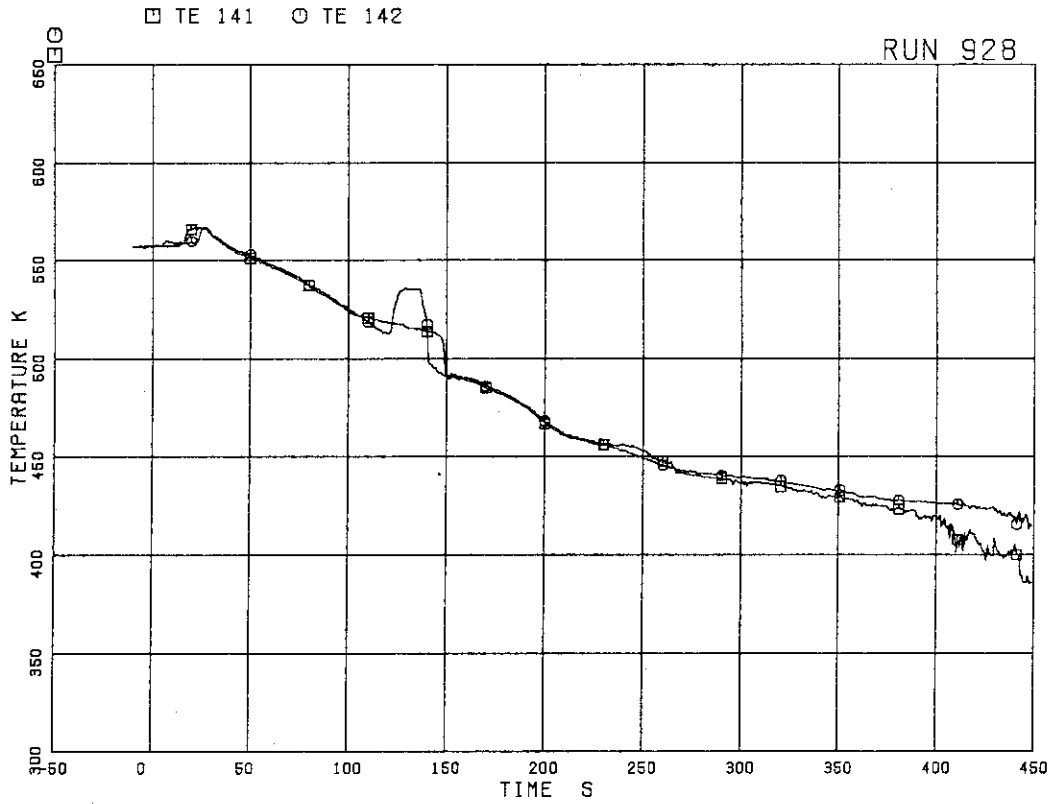


FIG.5. 79 FLUID TEMPERATURES IN DOWNCOMER

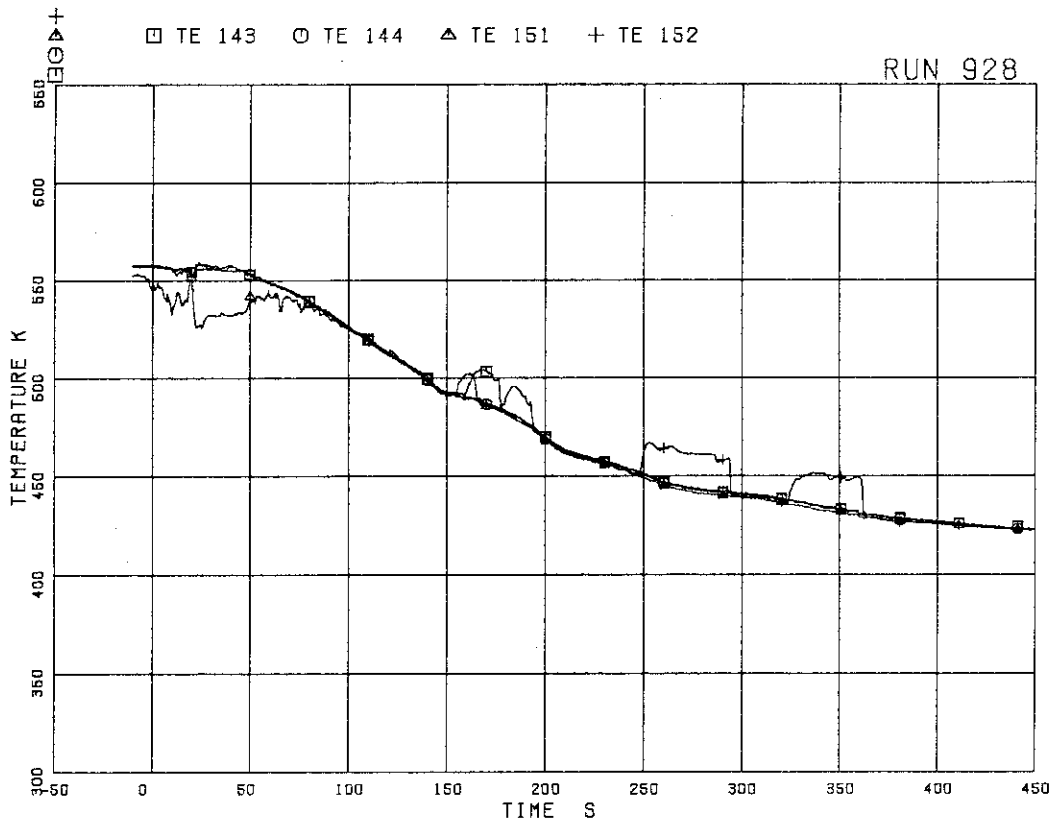


FIG.5. 80 FLUID TEMPERATURES IN INTACT RECIRCULATION LOOP



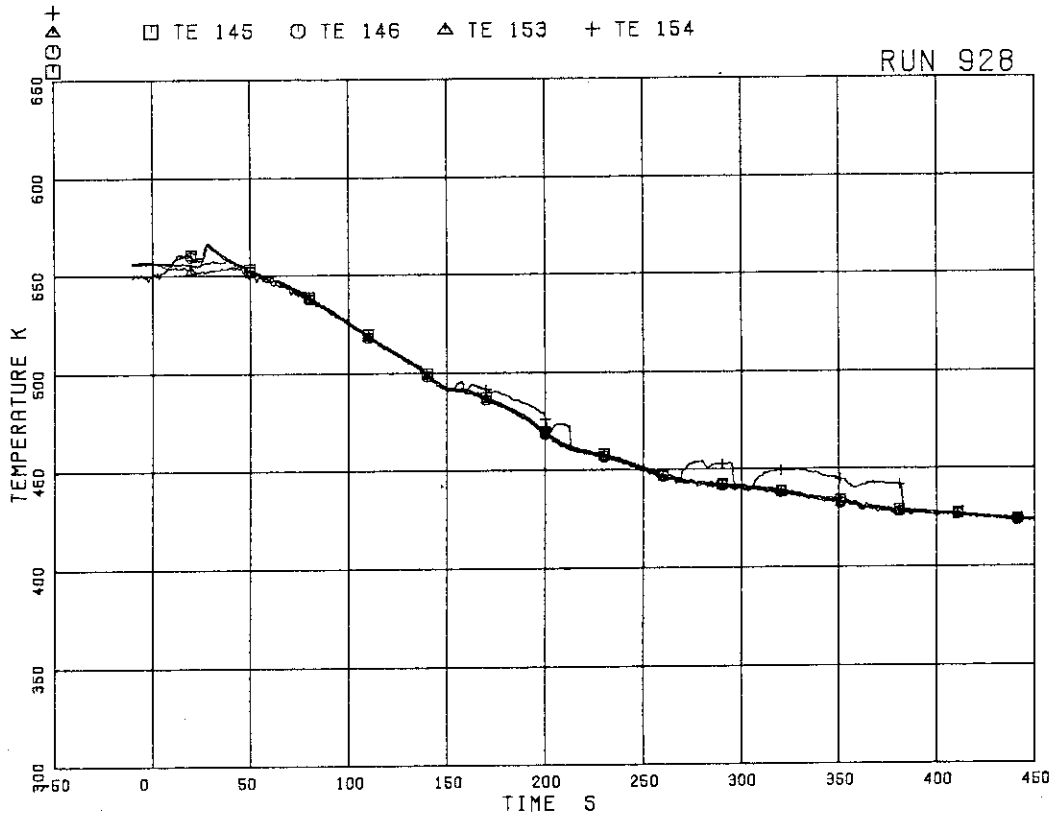


FIG.5. 81 FLUID TEMPERATURES IN  
BROKEN RECIRCULATION LOOP

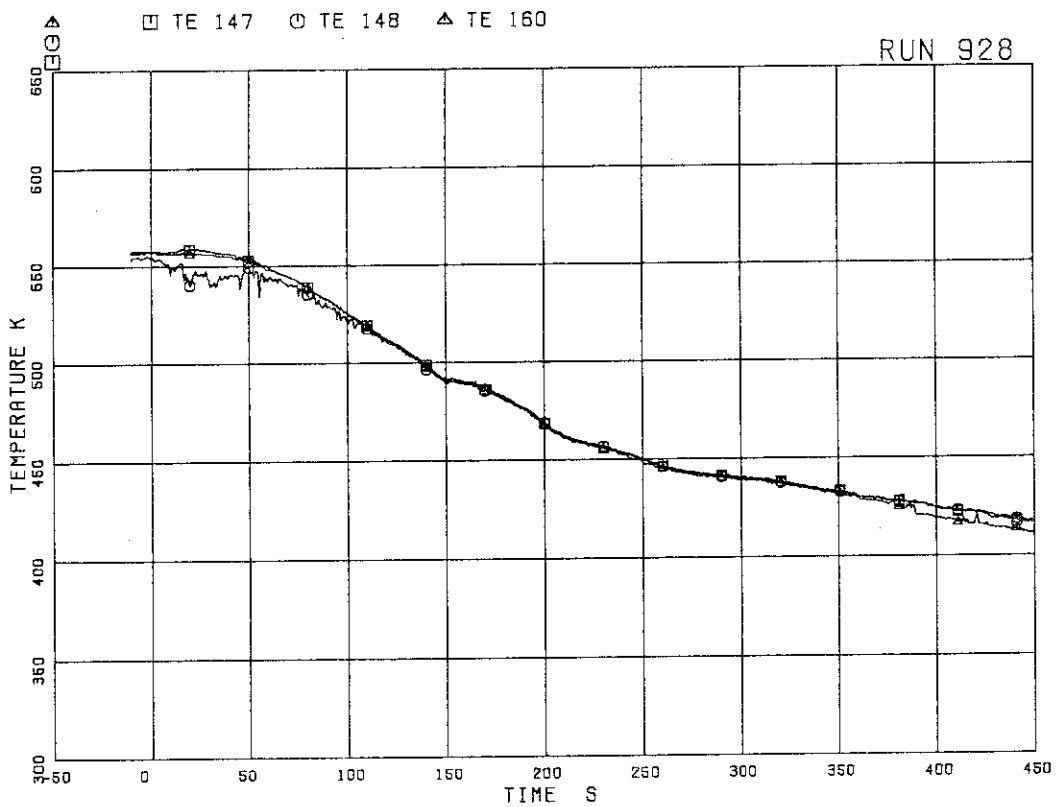


FIG.5. 82 FLUID TEMPERATURES AT JP-1,2 OUTLET

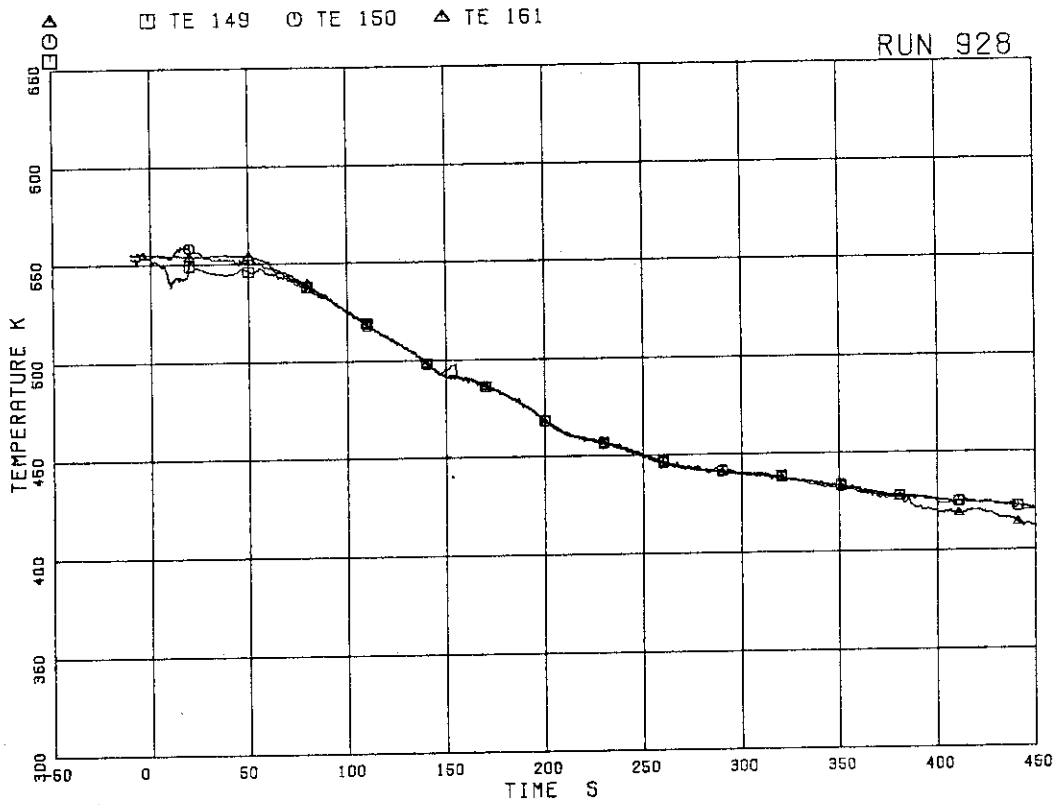


FIG.5. 83 FLUID TEMPERATURES AT JP-3,4 OUTLET

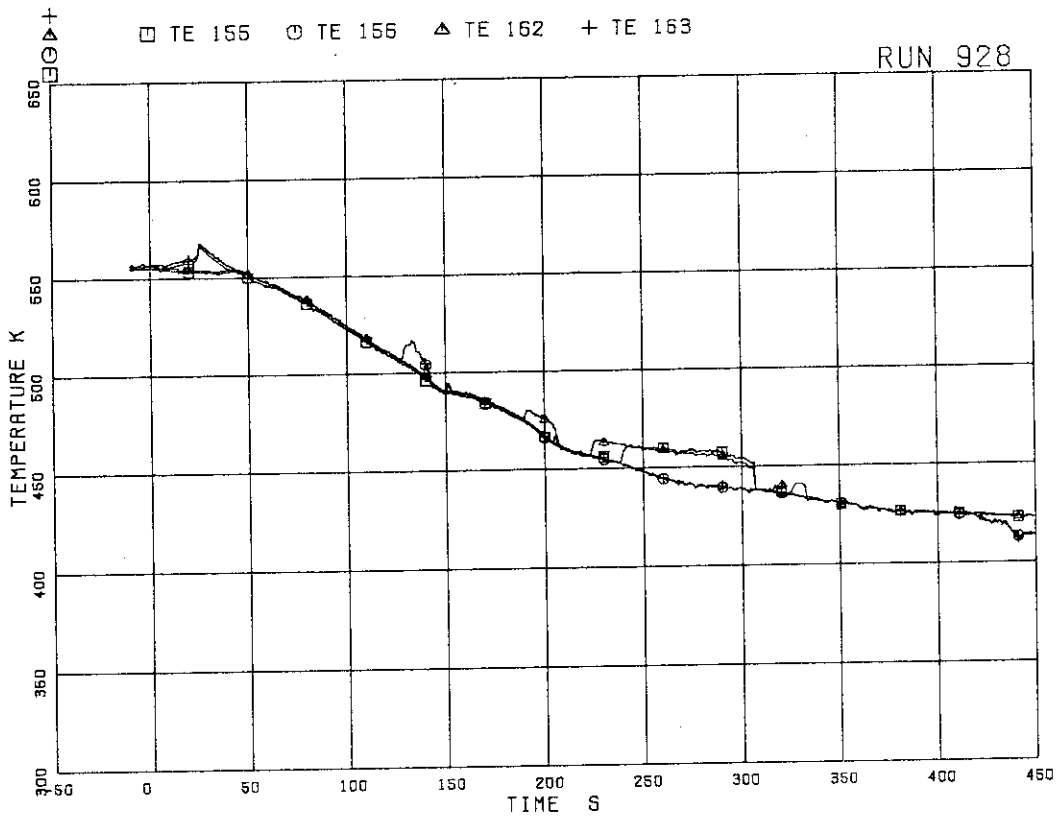


FIG.5. 84 FLUID TEMPERATURES NEAR BREAKS A AND B

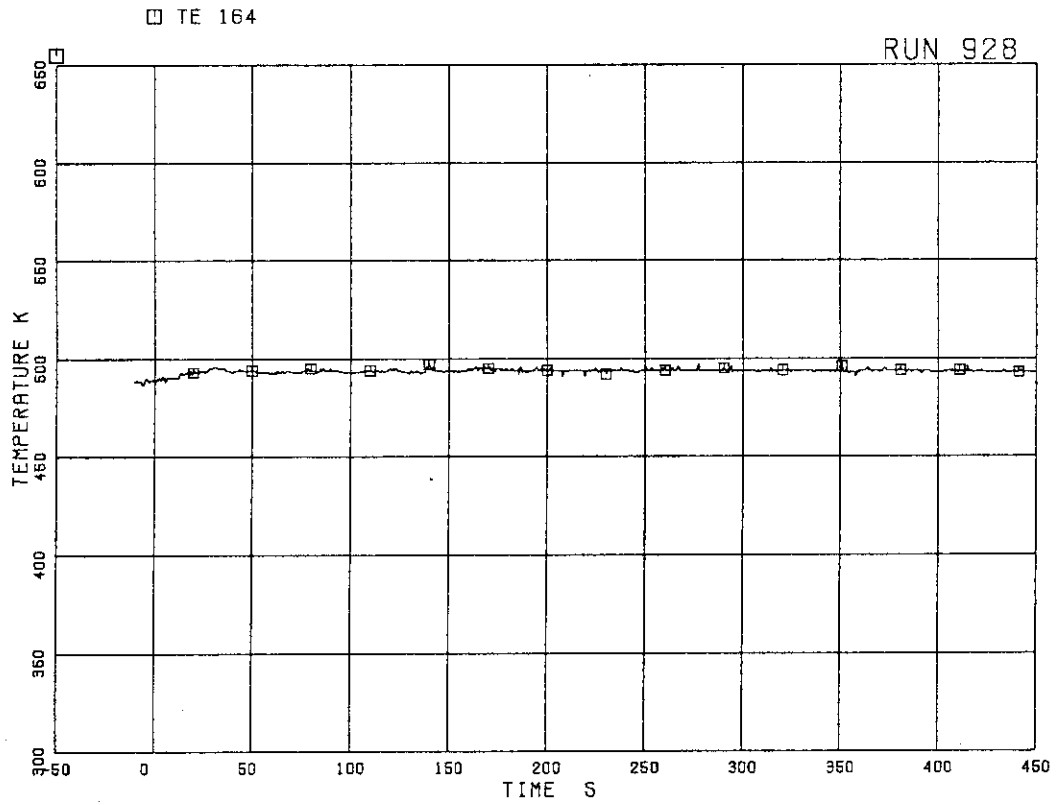


FIG.5. 85 FEEDWATER TEMPERATURE

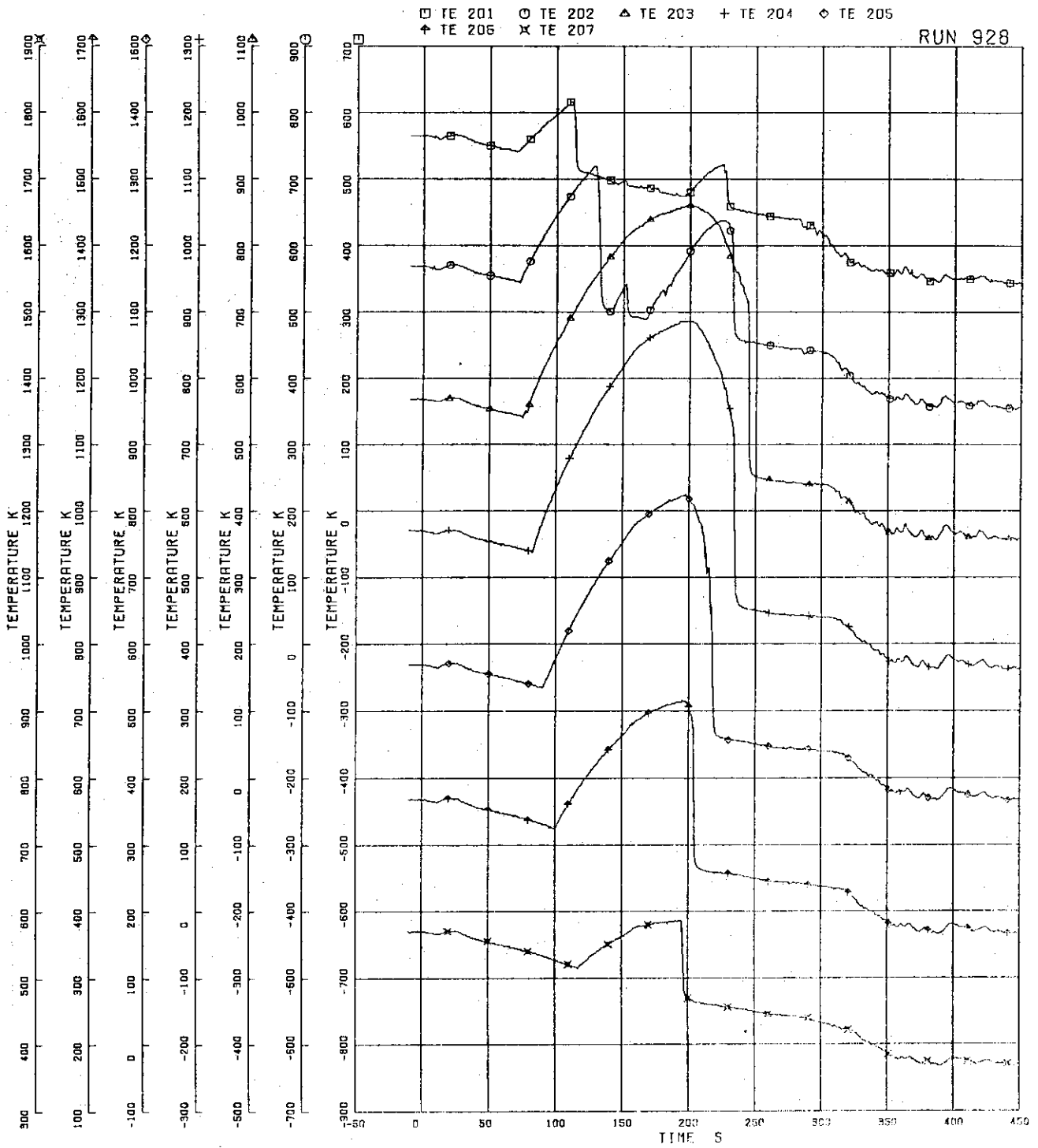


FIG.5. 86 SURFACE TEMPERATURES OF FUEL ROD A11

RUN 928

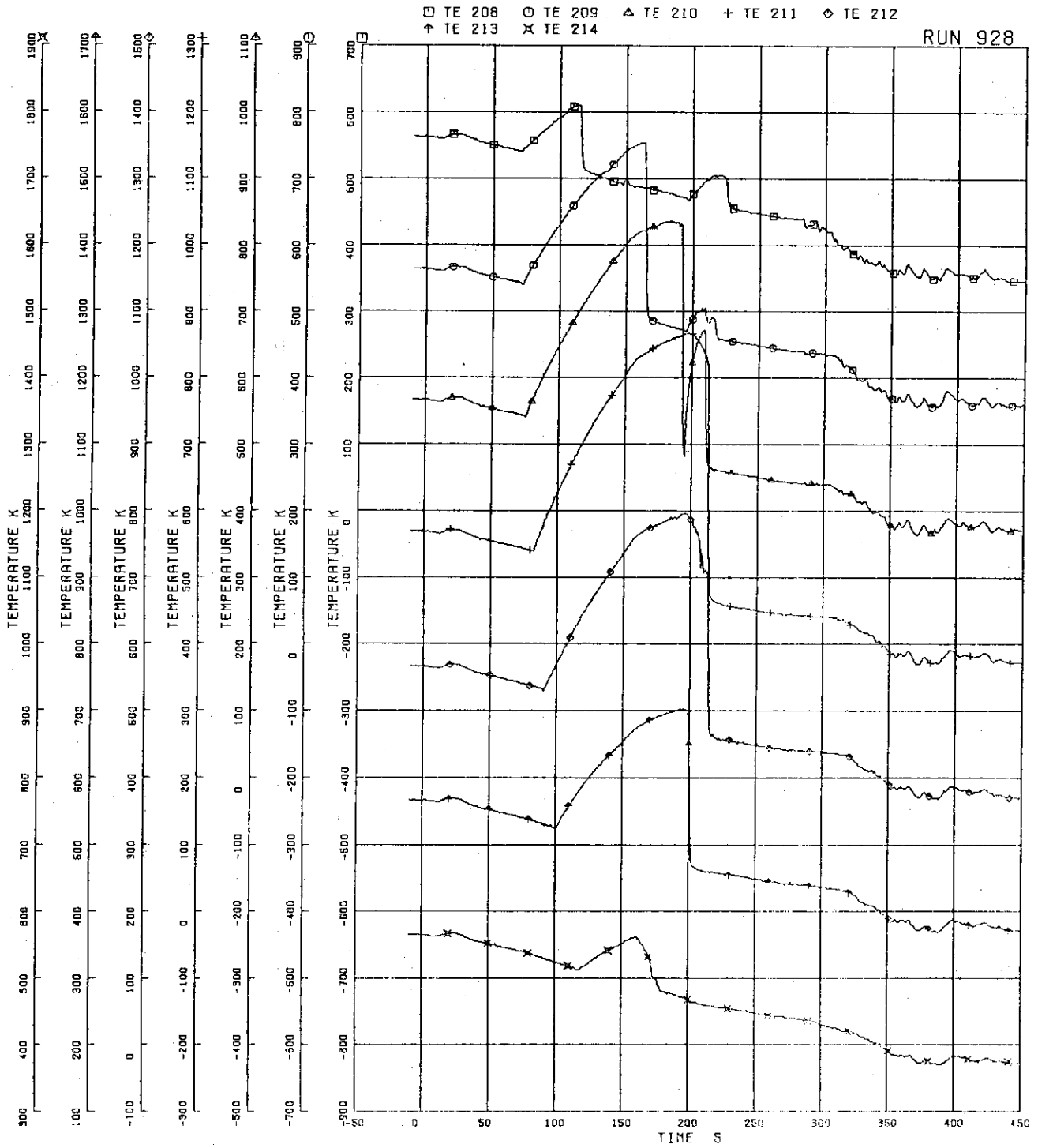


FIG.5. 87 SURFACE TEMPERATURES OF FUEL ROD A12

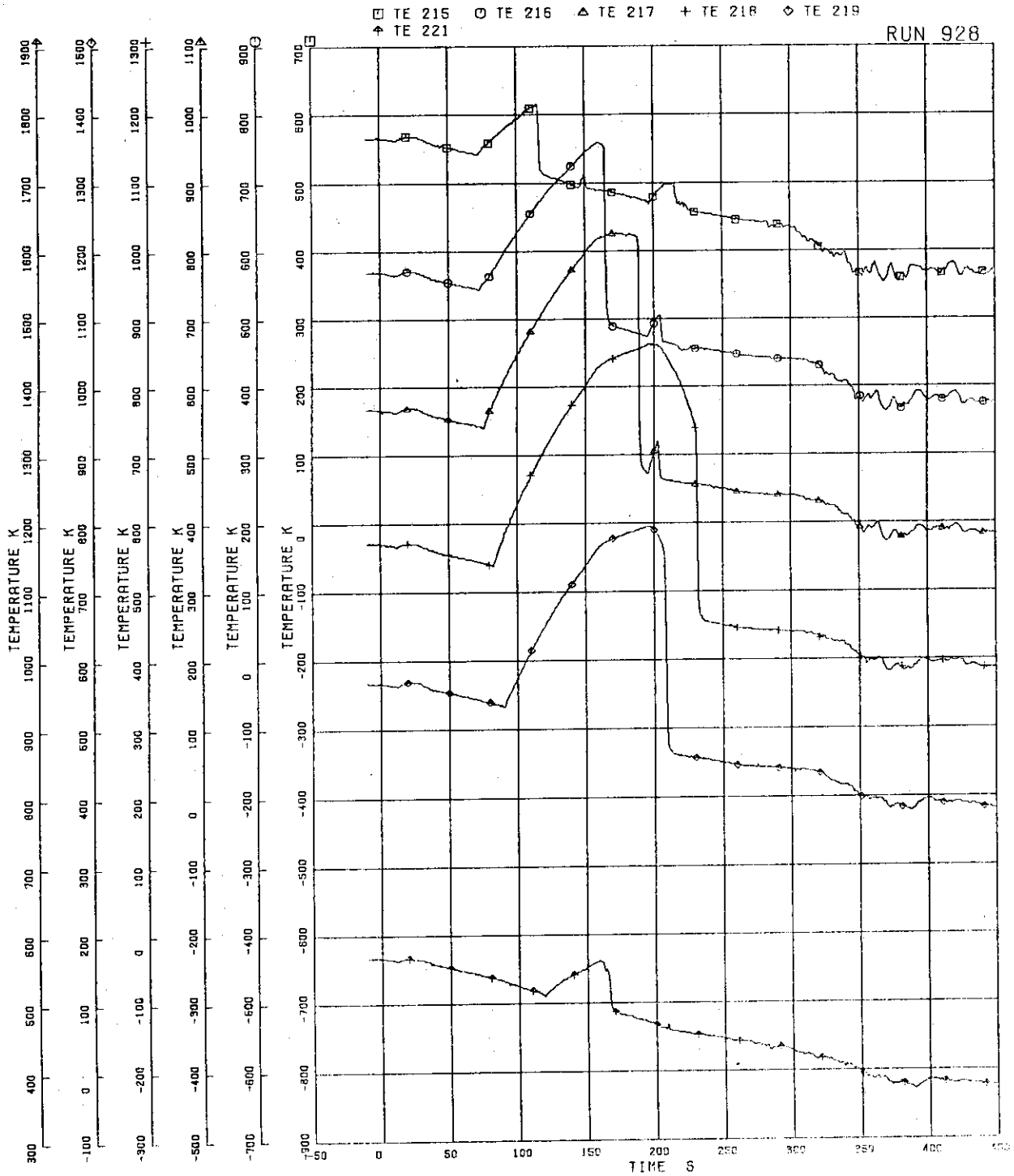


FIG.5. 88 SURFACE TEMPERATURES OF FUEL ROD A13

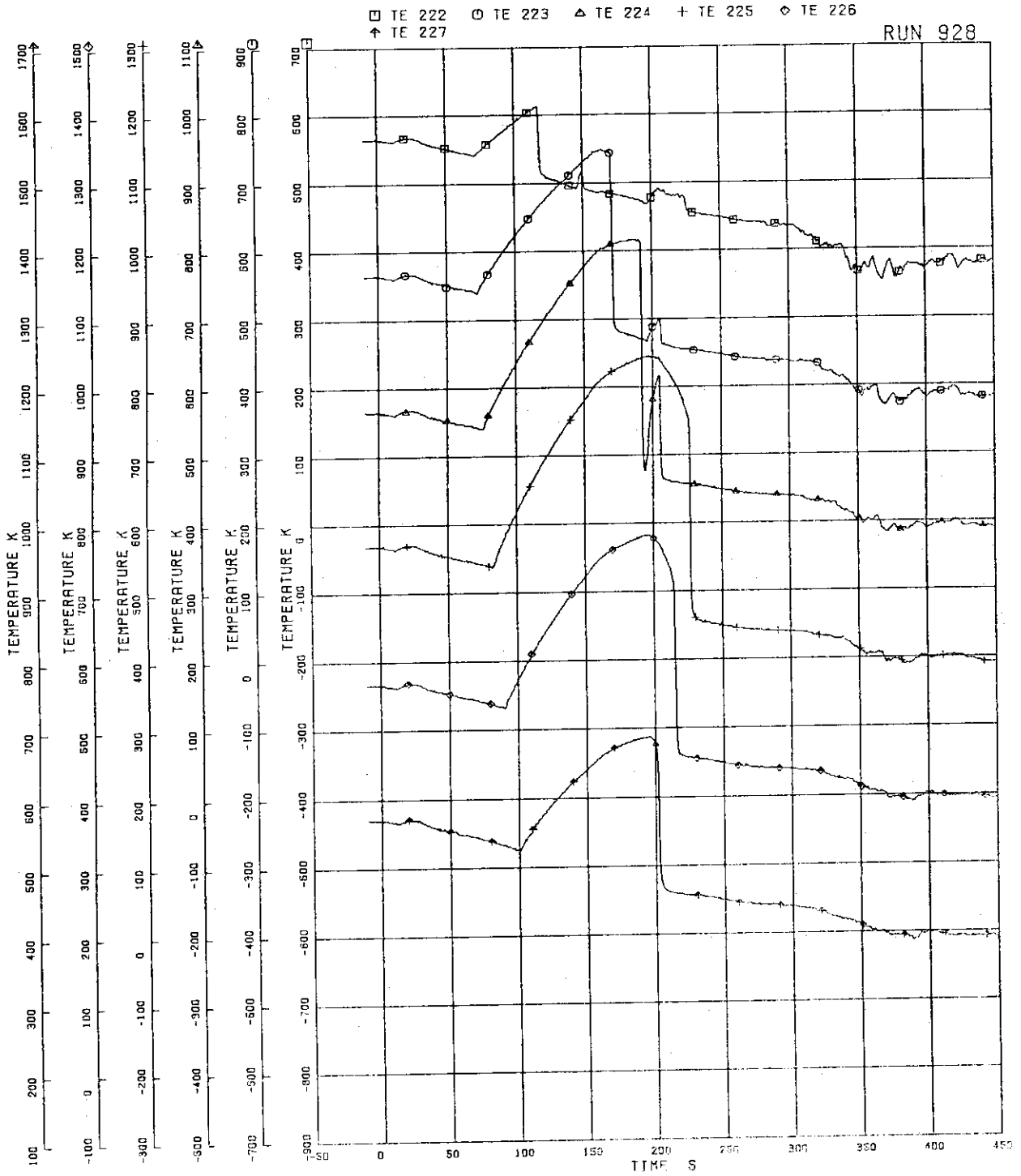


FIG-5. 89 SURFACE TEMPERATURES OF FUEL ROD A14

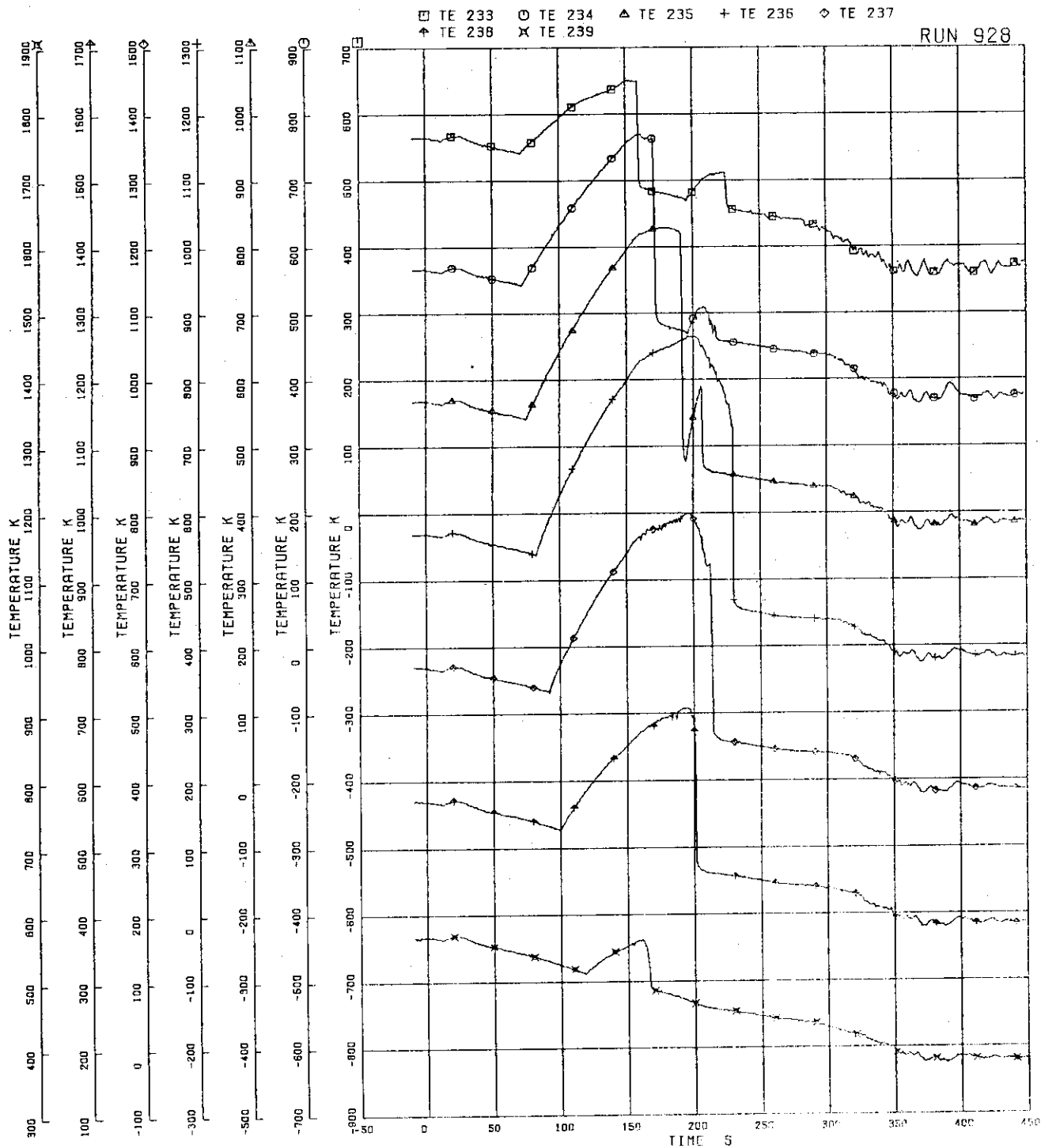


FIG-5- 90 SURFACE TEMPERATURES OF FUEL ROD A22



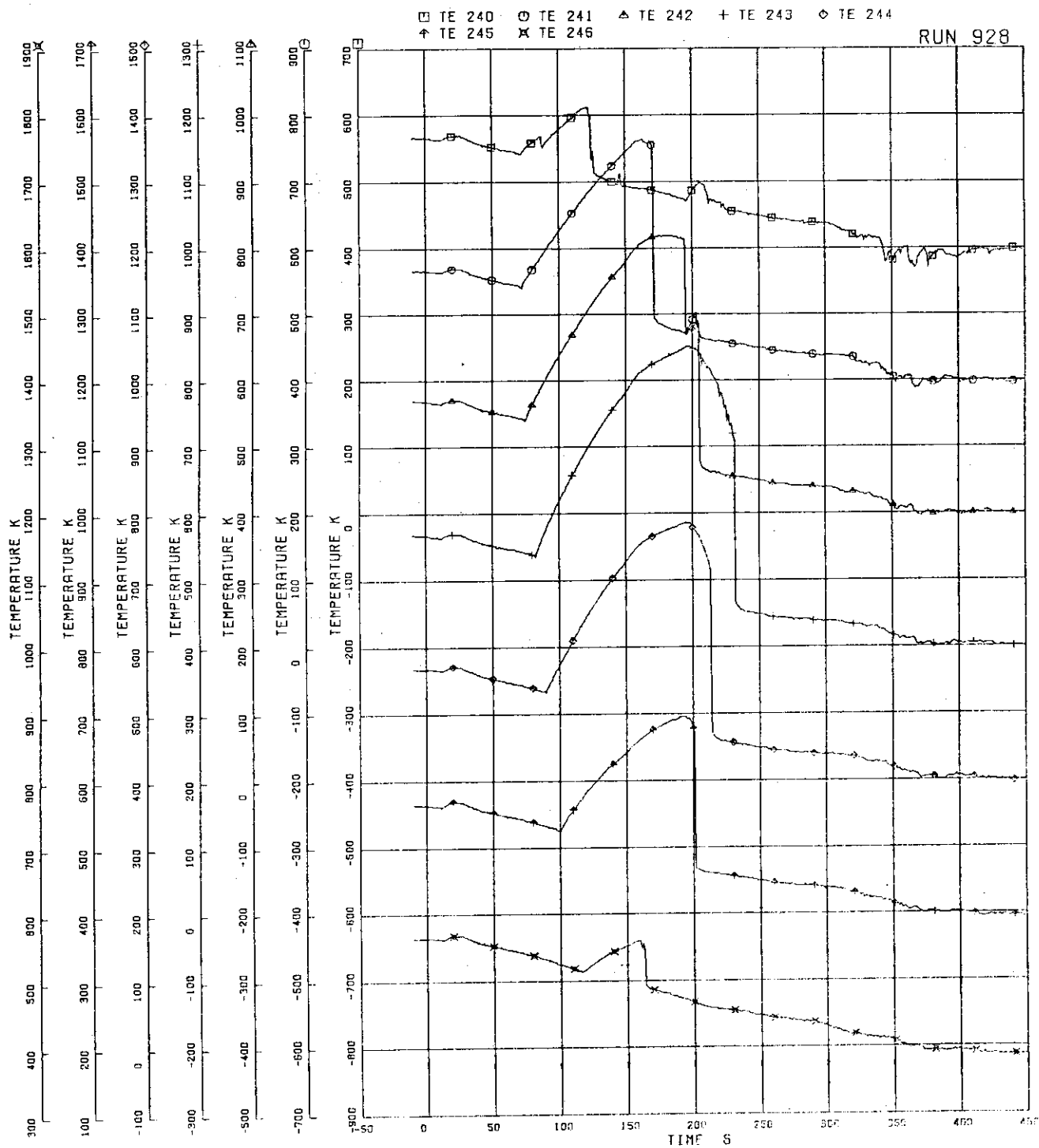


FIG. 5.91 SURFACE TEMPERATURES OF FUEL ROD A24

RUN 928

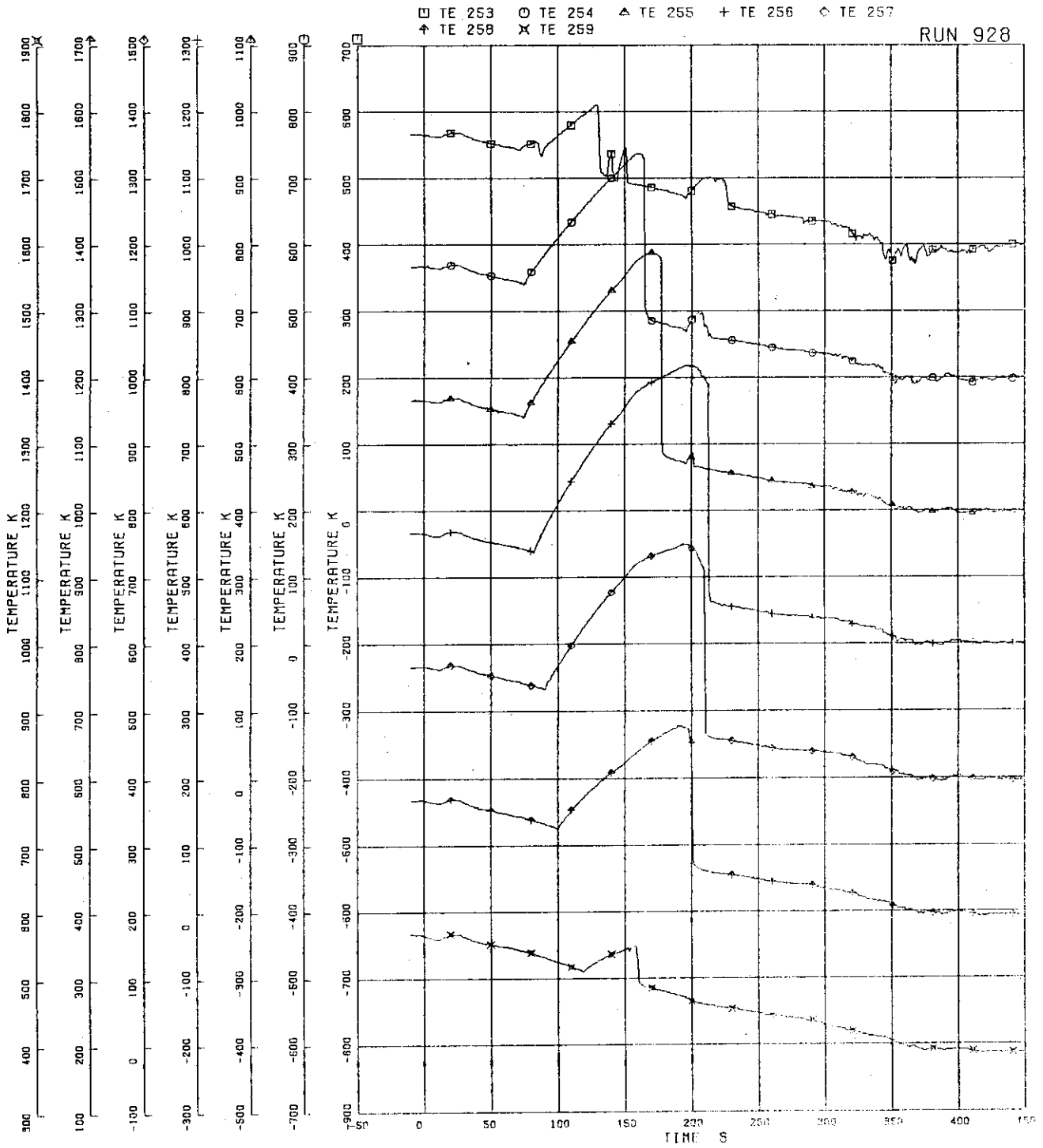


FIG-5. 92 SURFACE TEMPERATURES OF FUEL ROD A33

RUN 928

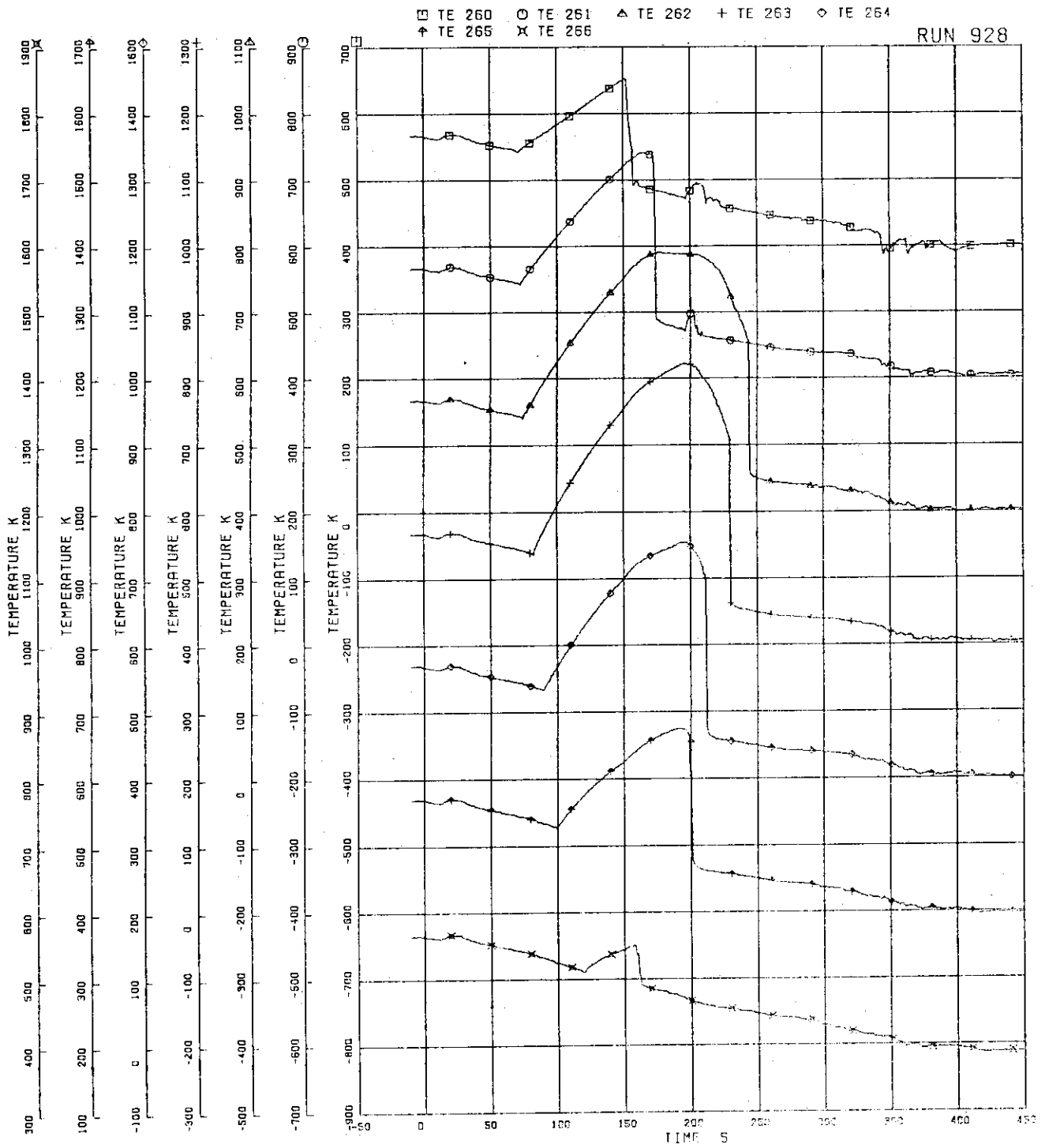


FIG.5- 93 SURFACE TEMPERATURES OF FUEL ROD A34



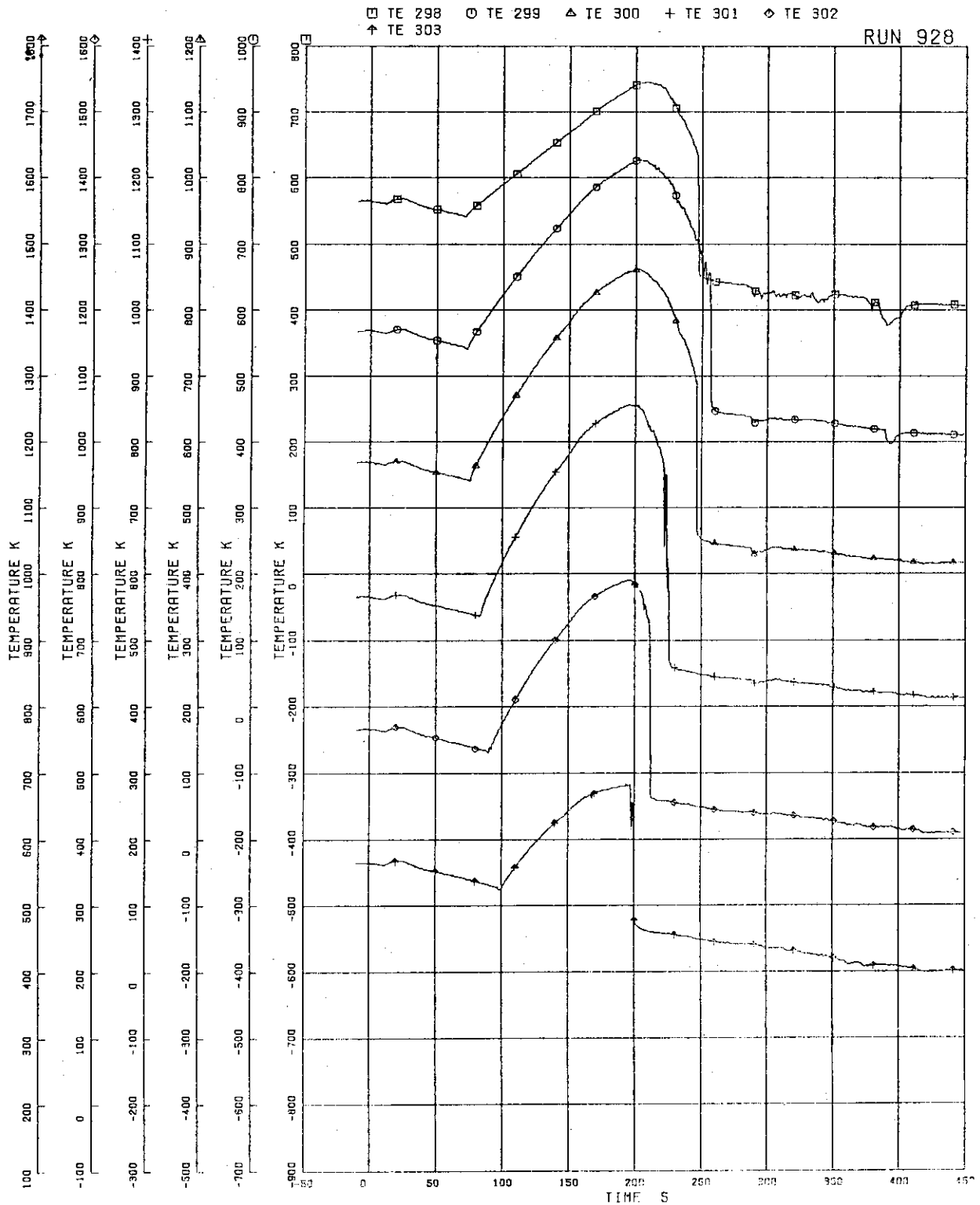


FIG.5- 95 SURFACE TEMPERATURES OF FUEL ROD A77

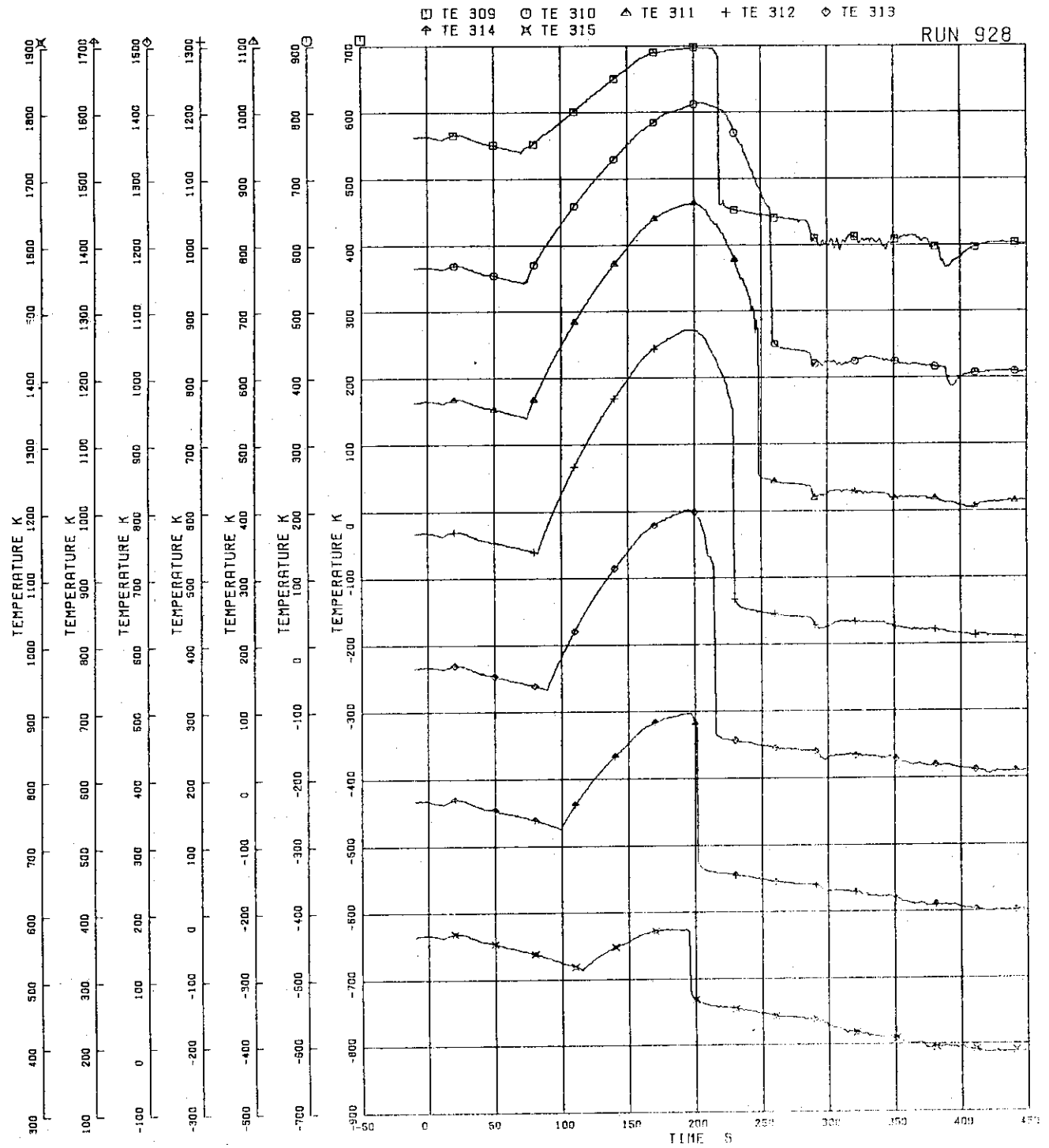


FIG.5- 96 SURFACE TEMPERATURES OF FUEL ROD A85

RUN 928

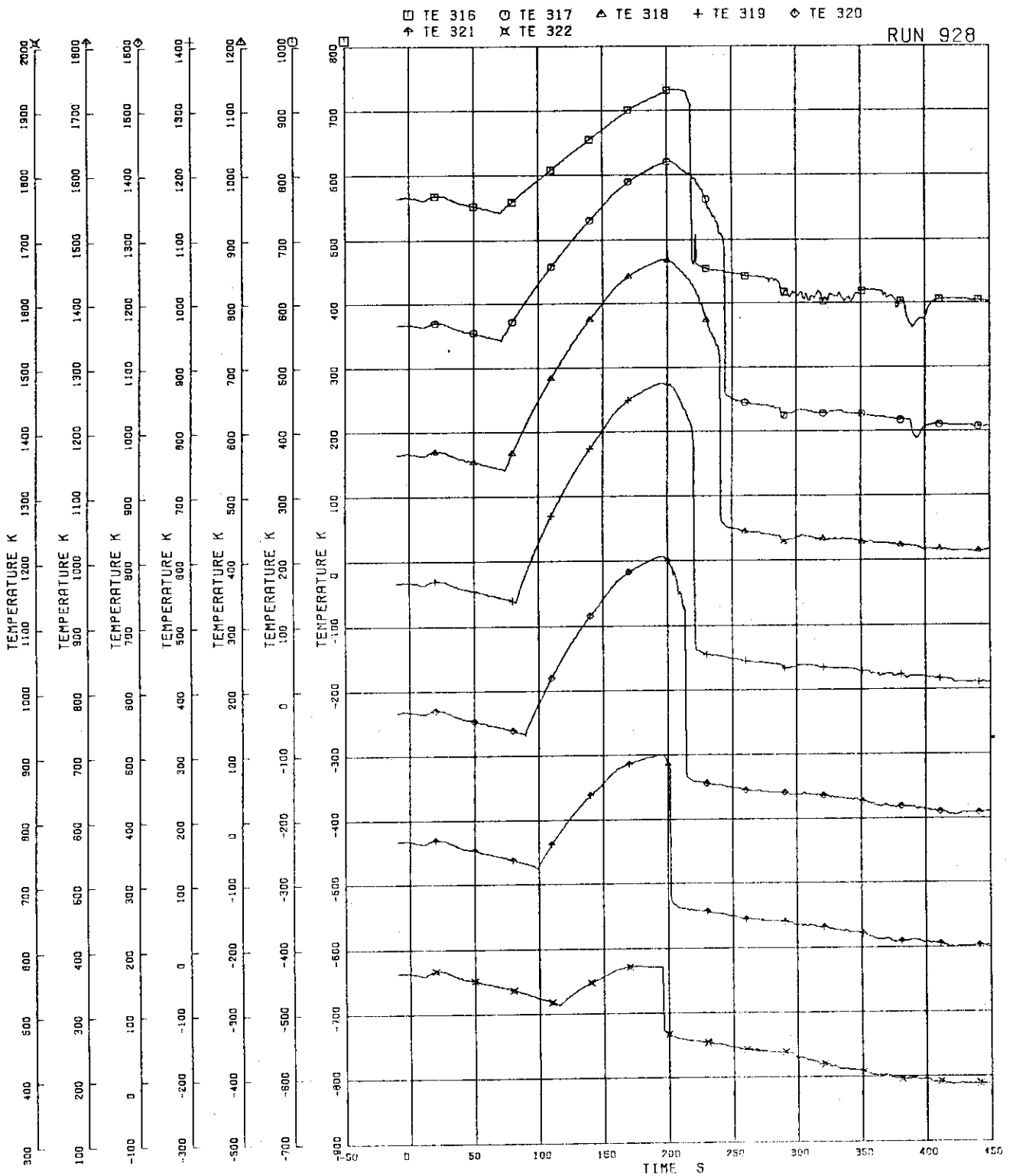


FIG. 5. 97 SURFACE TEMPERATURES OF FUEL ROD A87

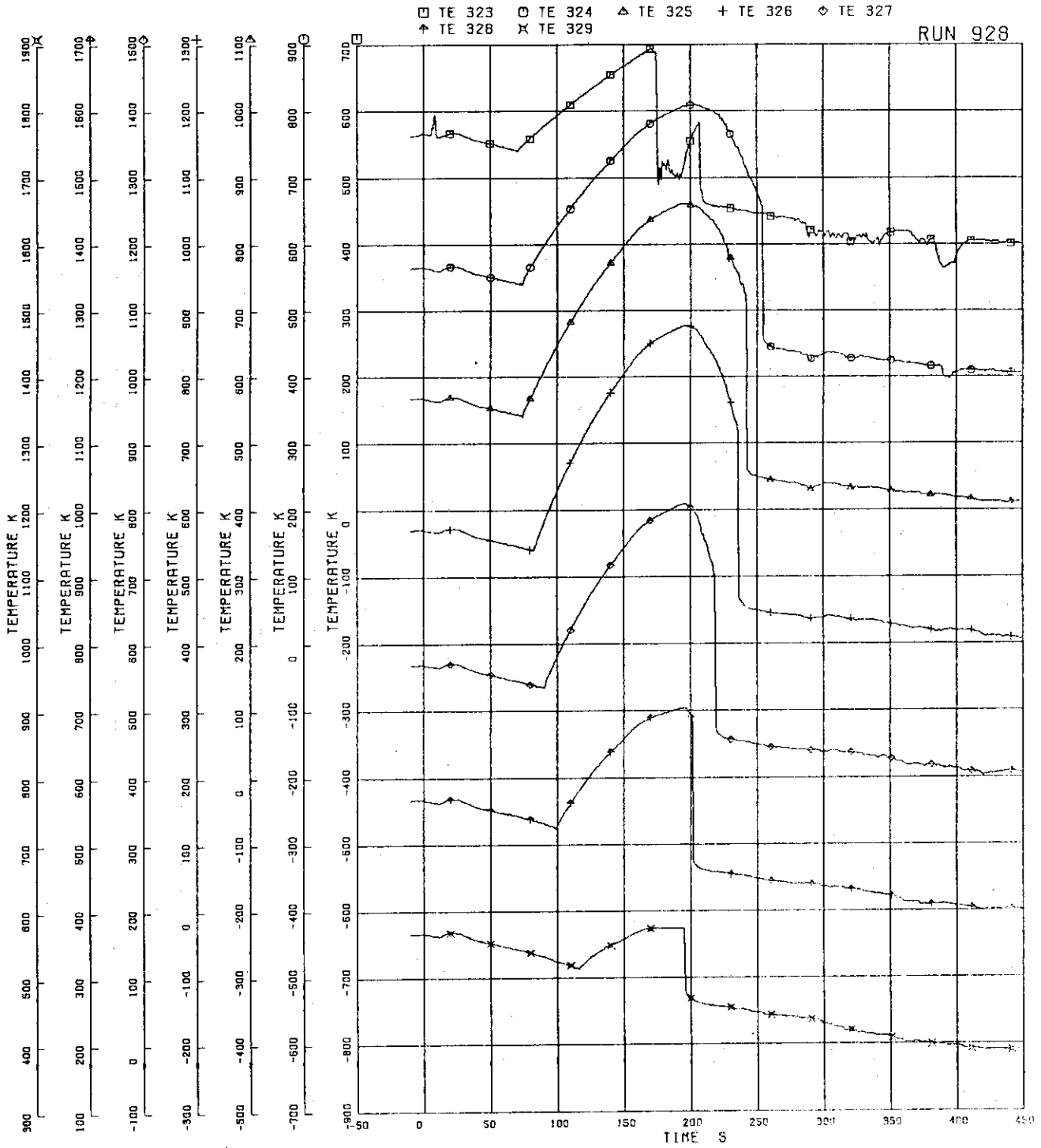


FIG.5. 98 SURFACE TEMPERATURES OF FUEL ROD A88



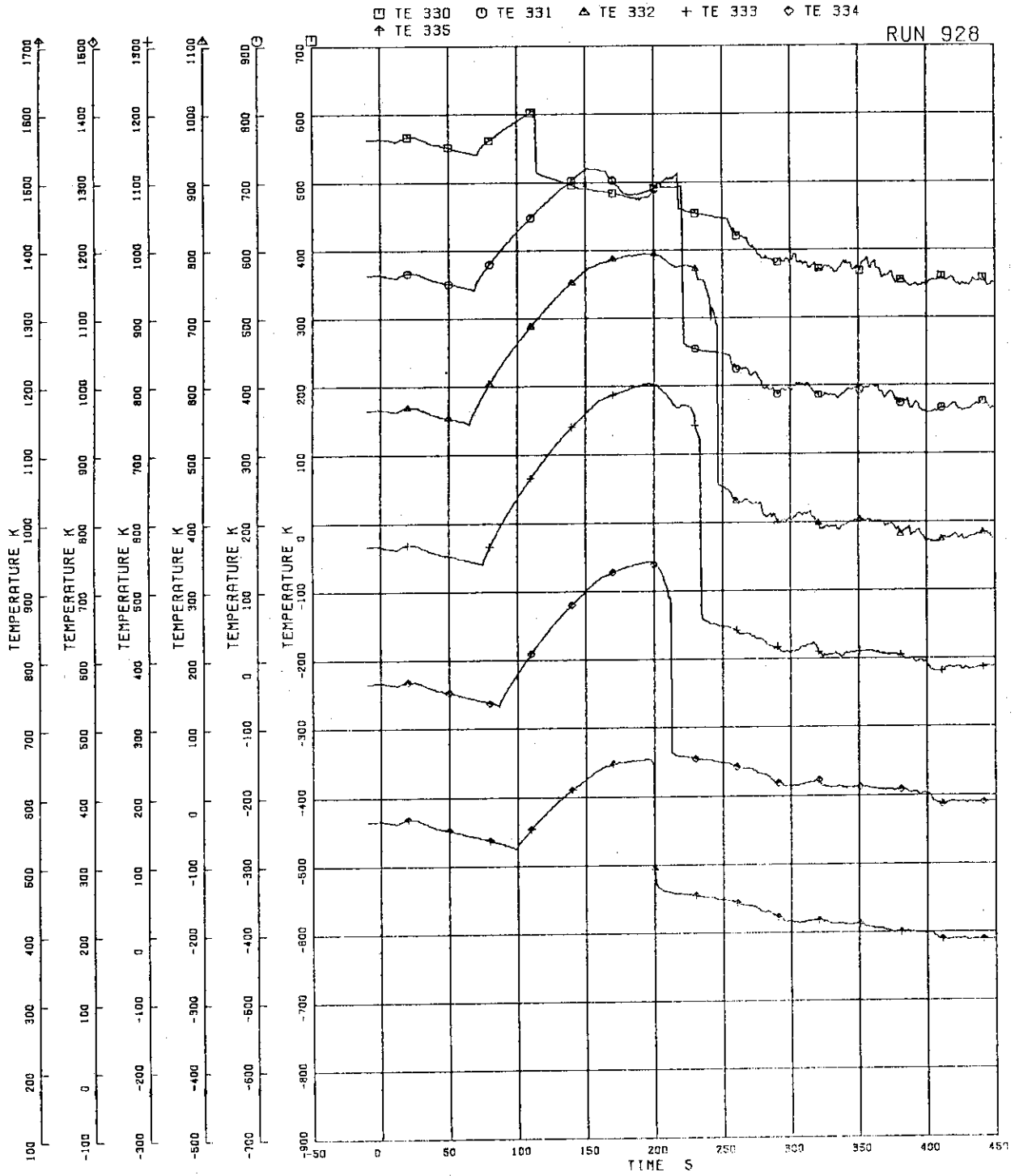


FIG.5. 99 SURFACE TEMPERATURES OF FUEL ROD B11

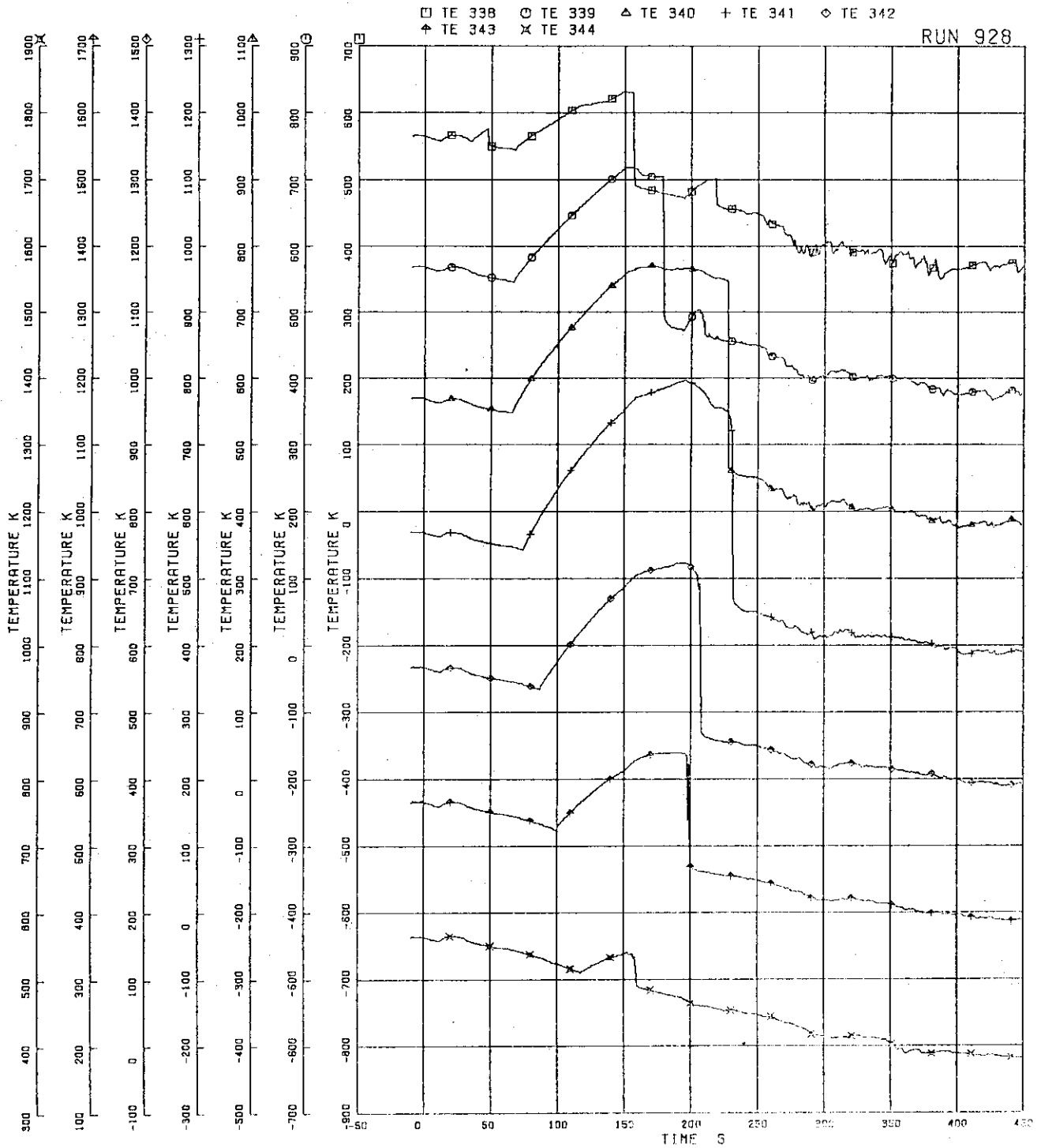


FIG.5.100 SURFACE TEMPERATURES OF FUEL ROD B22

RUN 928

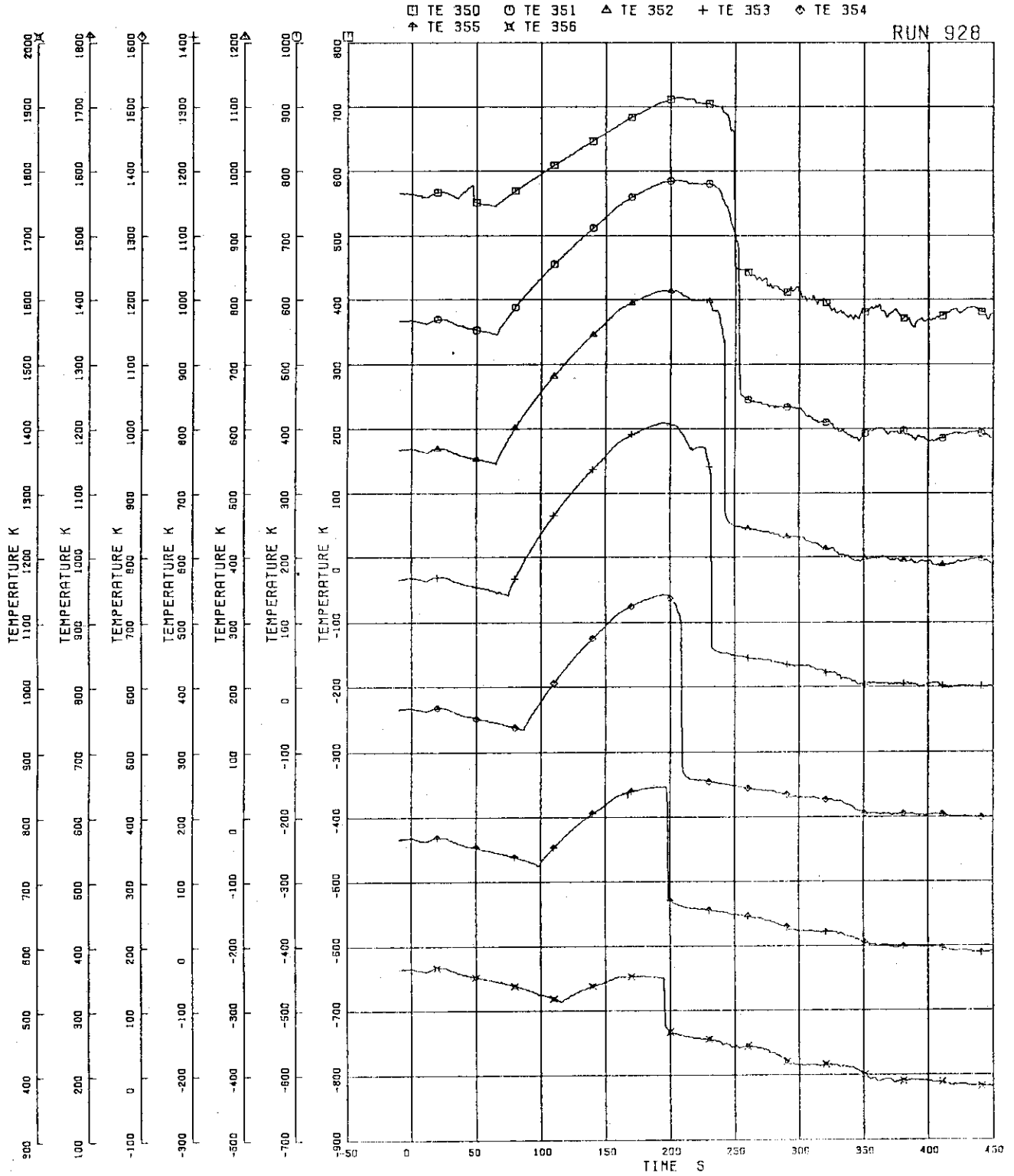


FIG.5.101 SURFACE TEMPERATURES OF FUEL ROD B77

RUN 928

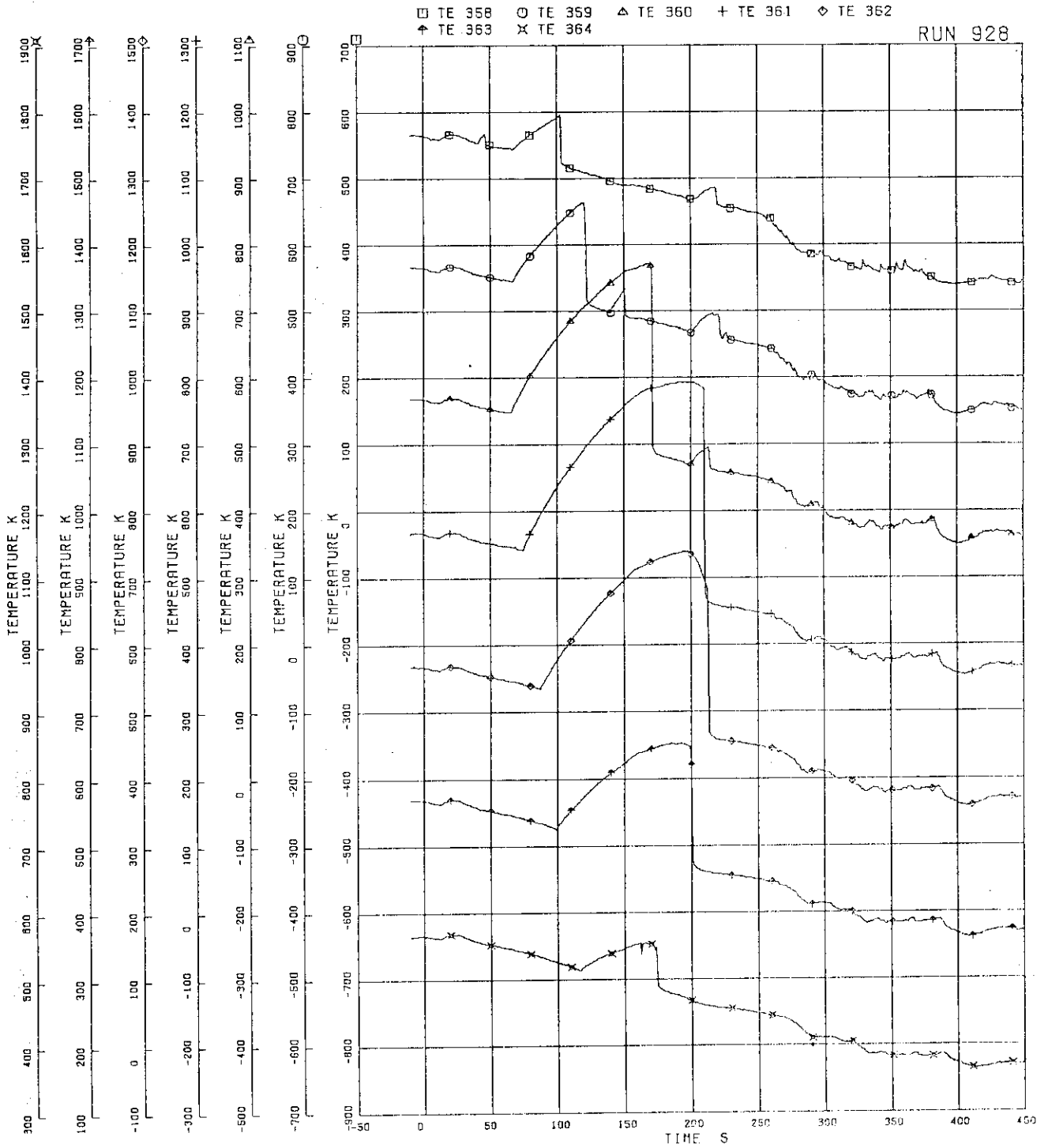


FIG.5-102 SURFACE TEMPERATURES OF FUEL ROD C11

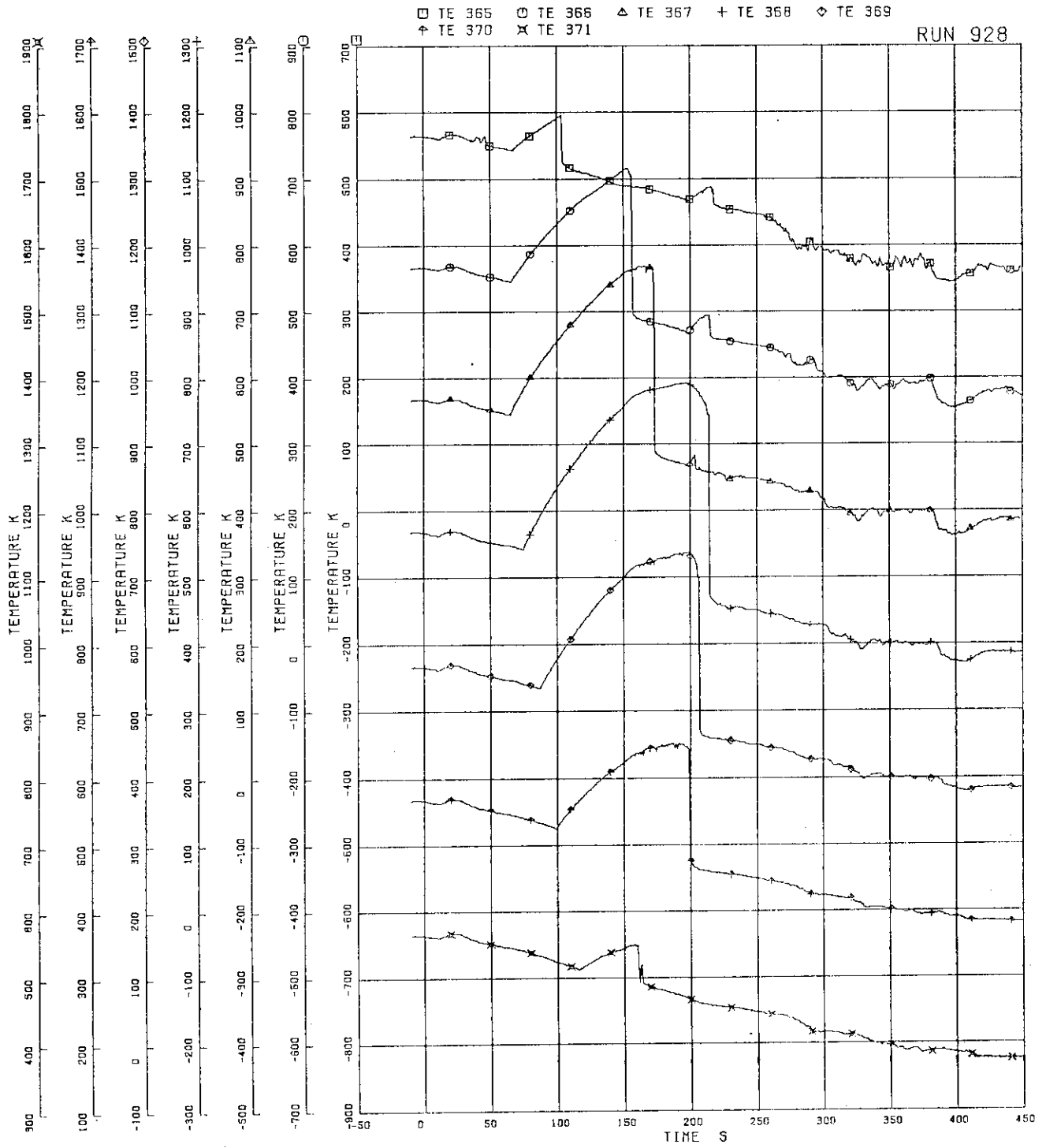


FIG.5.103 SURFACE TEMPERATURES OF FUEL ROD C13

RUN 928

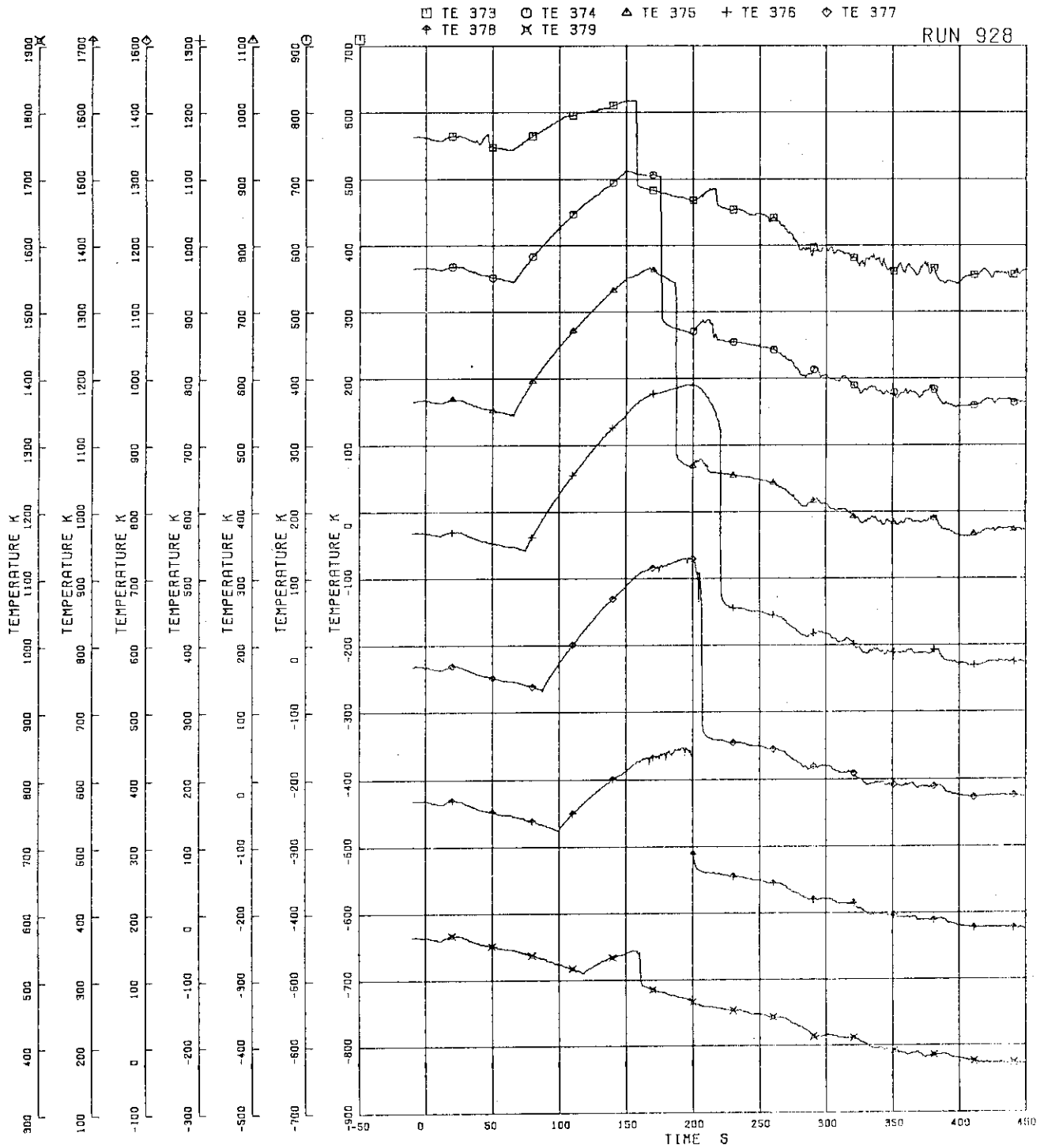


FIG.5-104 SURFACE TEMPERATURES OF FUEL ROD C22

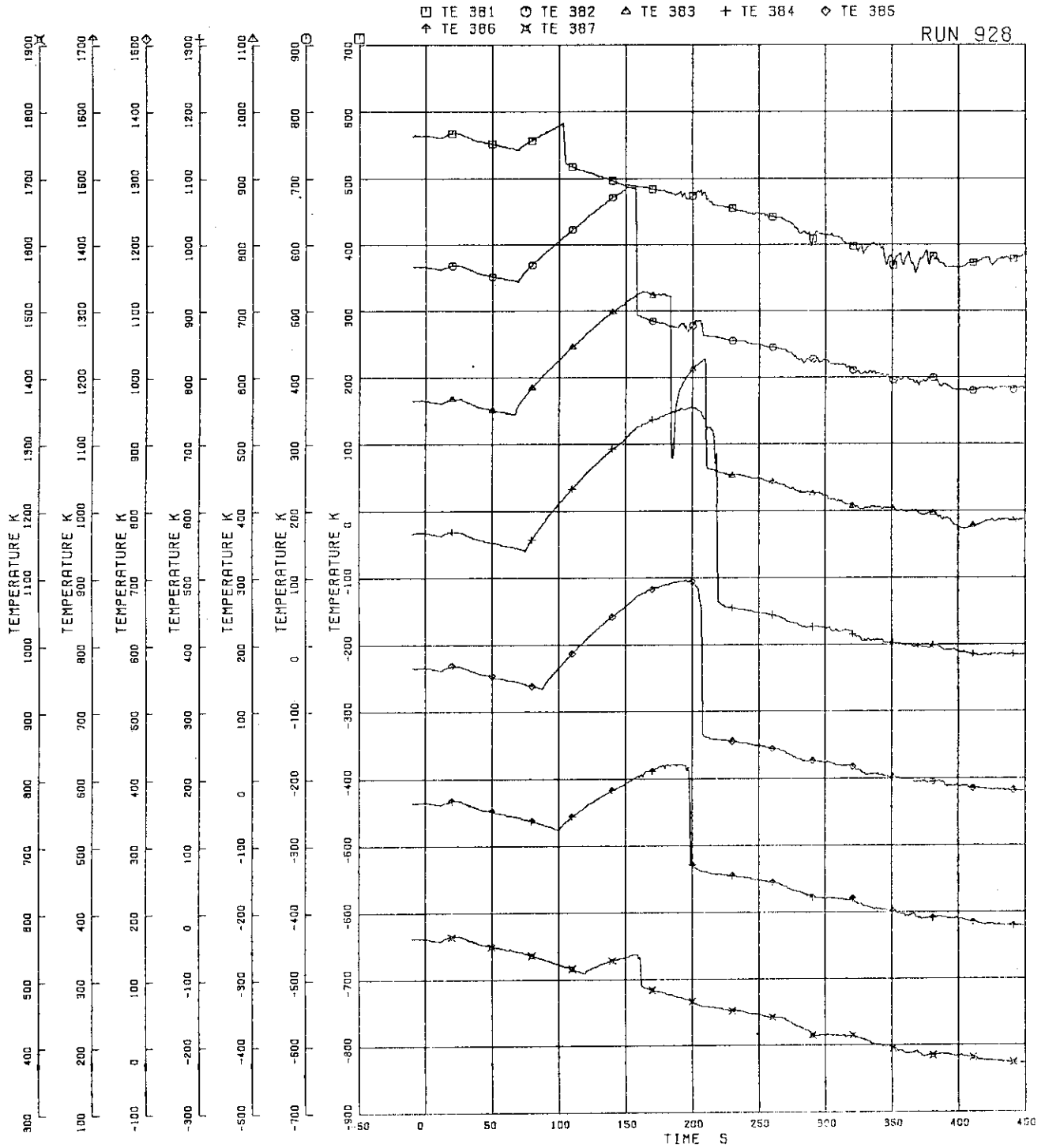


FIG.5.105 SURFACE TEMPERATURES OF FUEL ROD C33

RUN 928

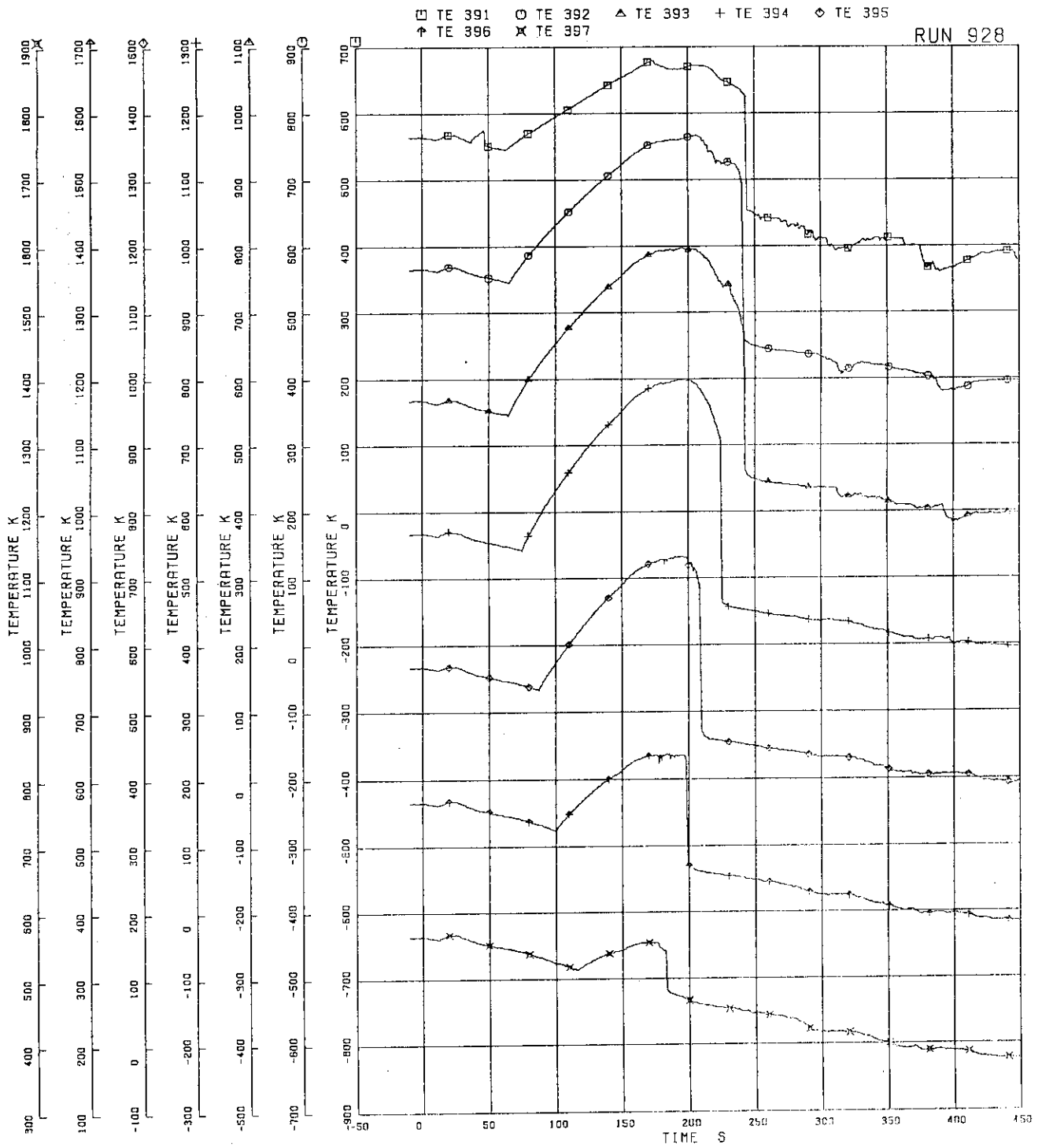


FIG-5.106 SURFACE TEMPERATURES OF FUEL ROD C77



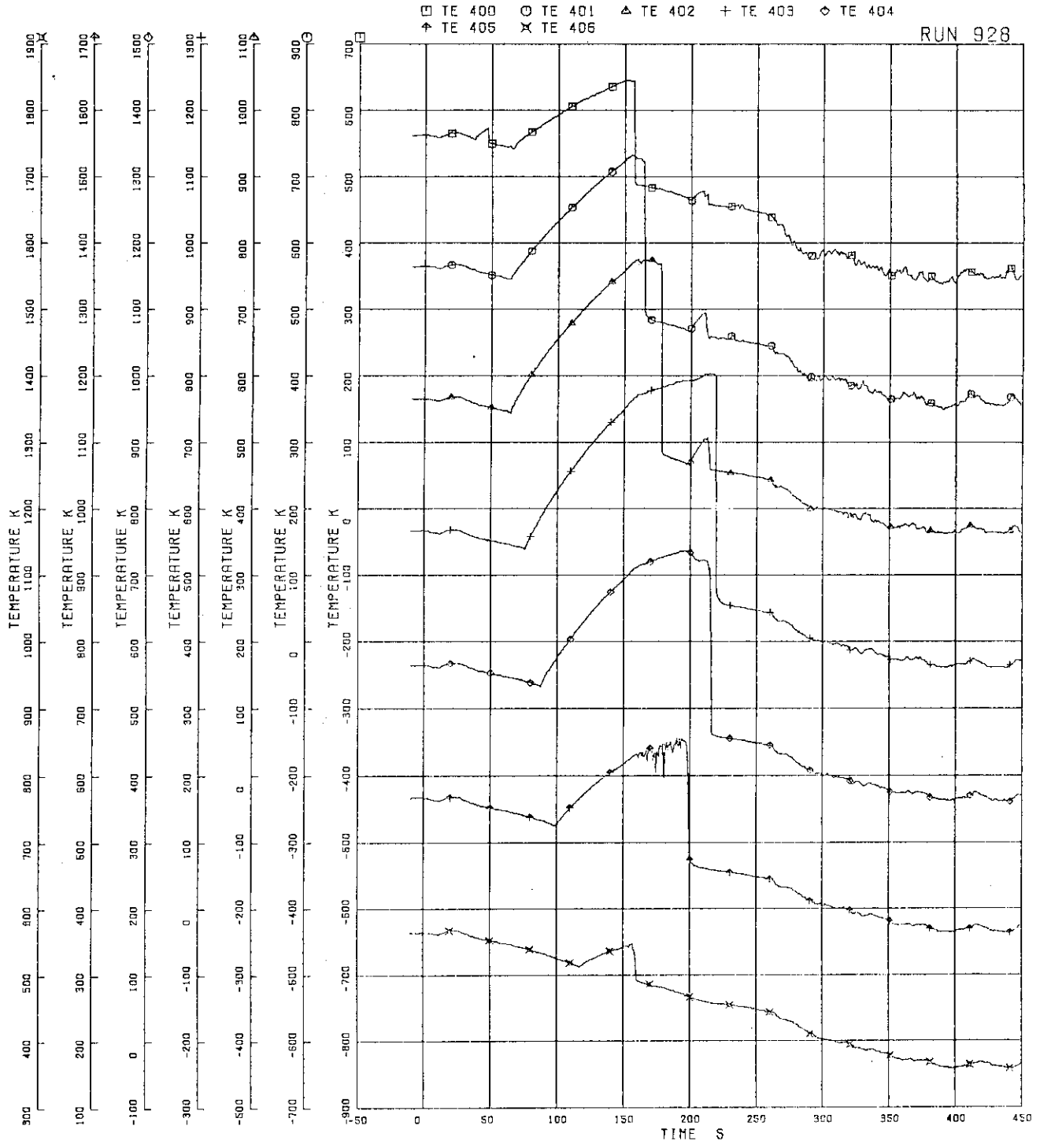


FIG.5-107 SURFACE TEMPERATURES OF FUEL ROD D22

RUN 928

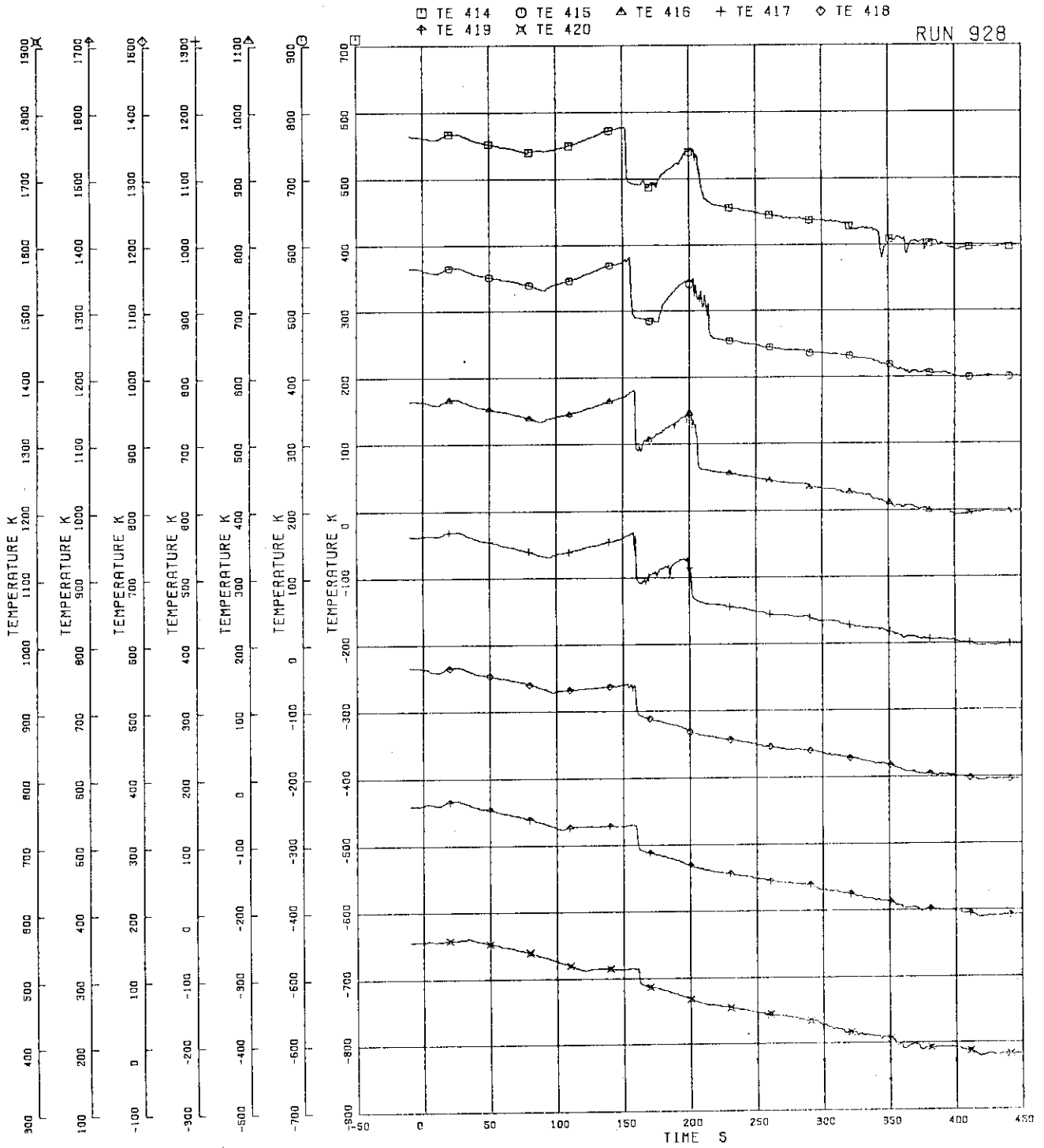


FIG.5-108 SURFACE TEMPERATURES OF WATER ROD SIMULATOR A45

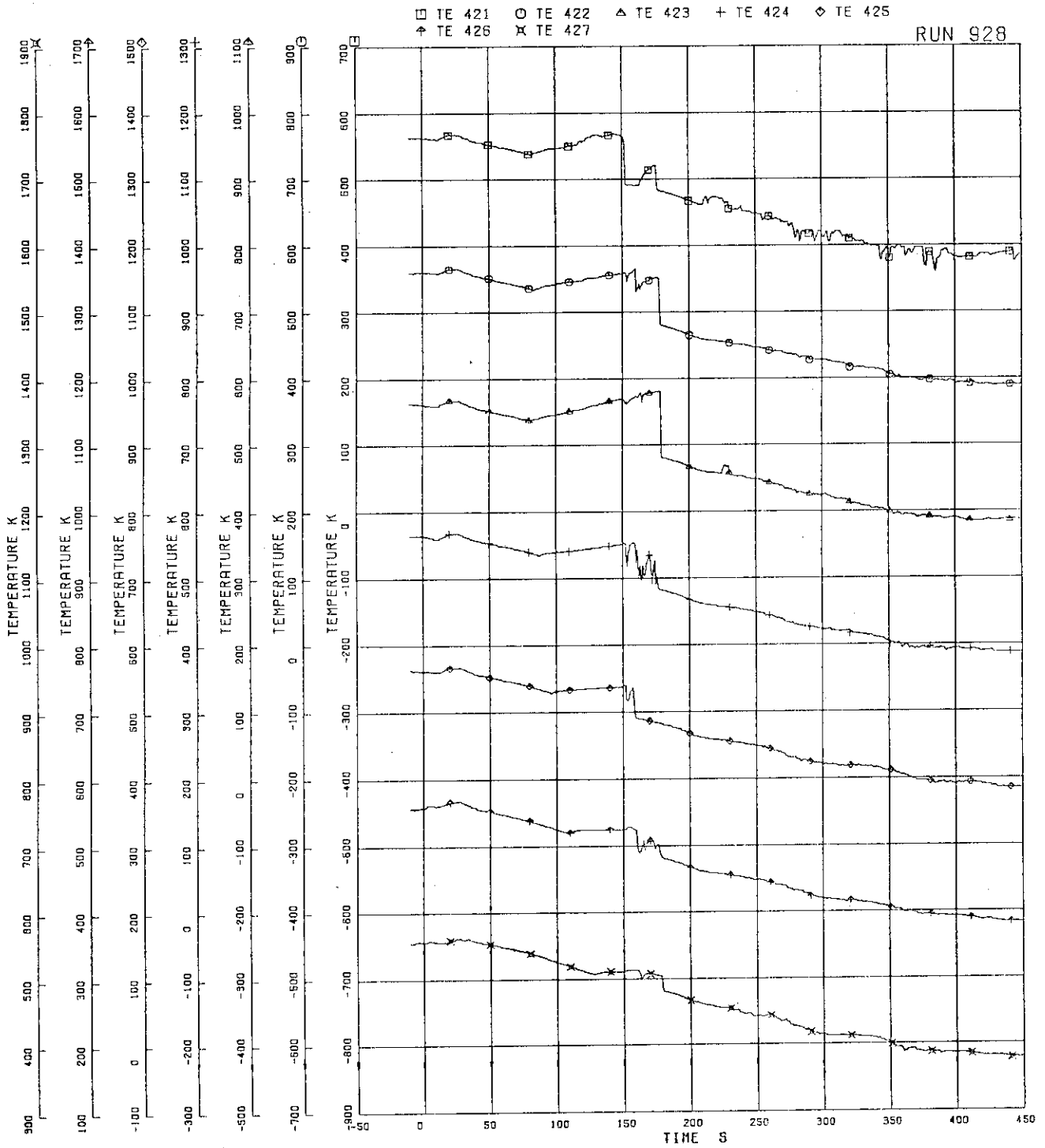


FIG.5.109 SURFACE TEMPERATURES OF WATER ROD SIMULATOR B45

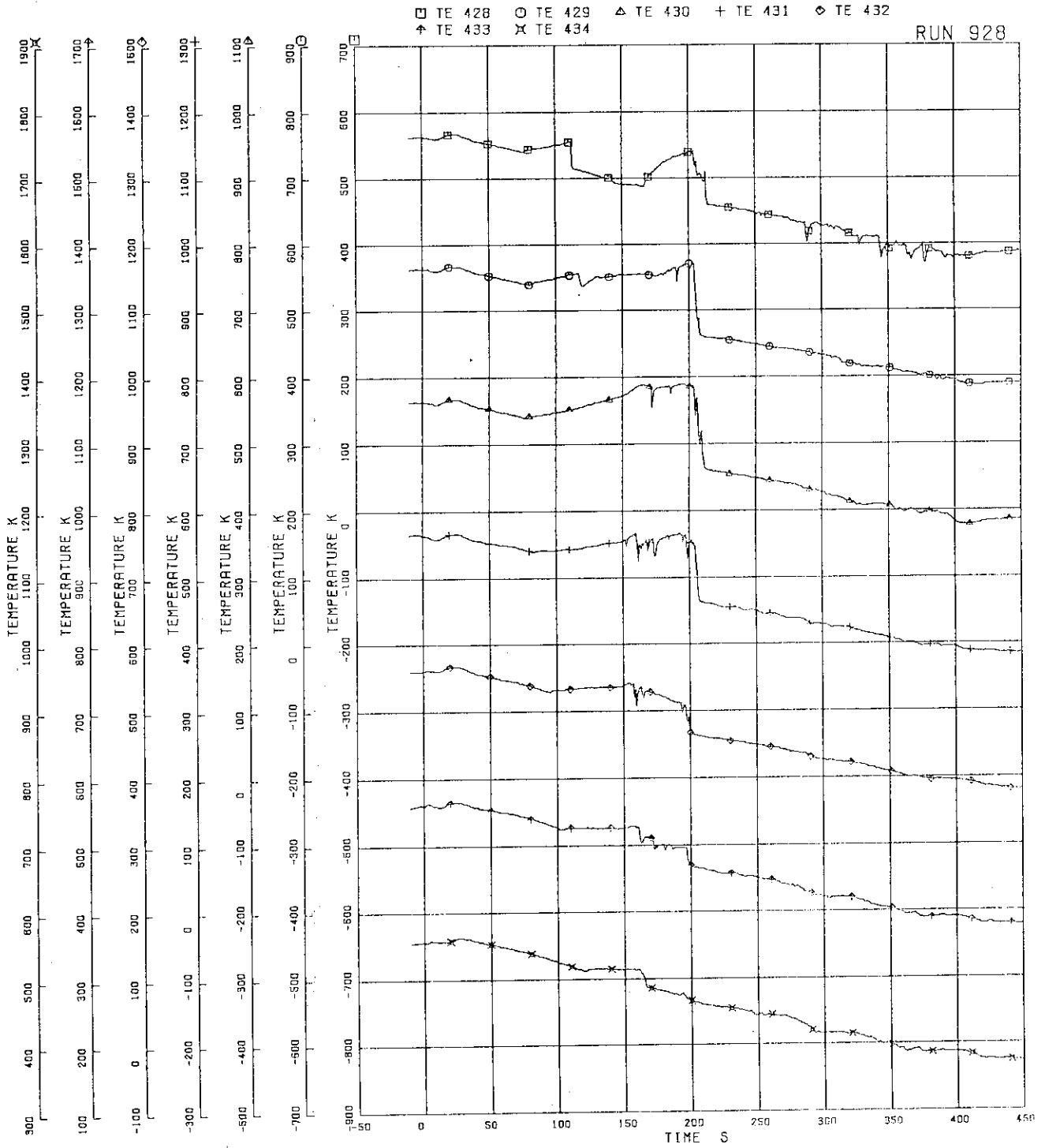


FIG.5-110 SURFACE TEMPERATURES OF WATER ROD SIMULATOR C45

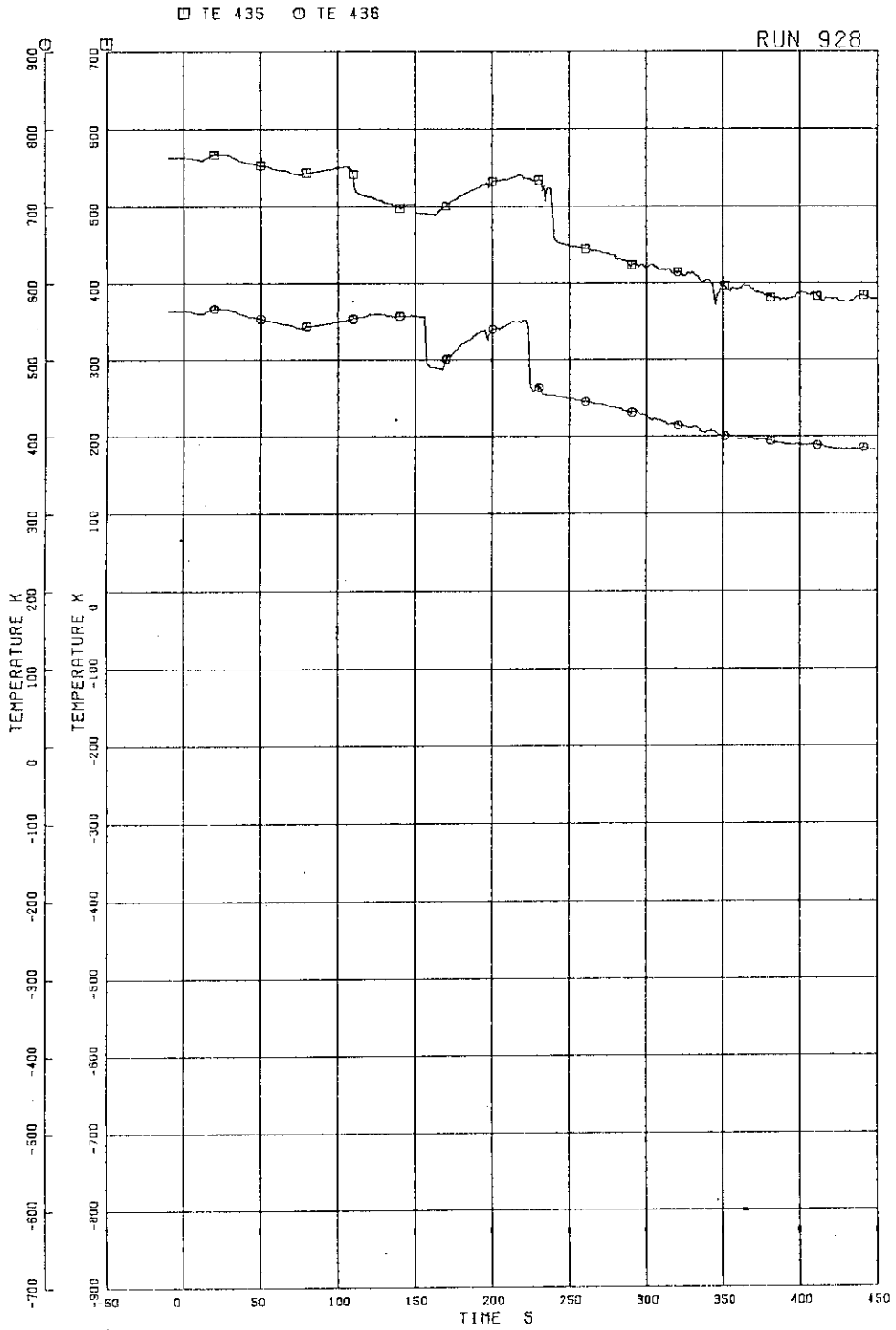


FIG.5.111 SURFACE TEMPERATURES OF WATER ROD SIMULATOR D45

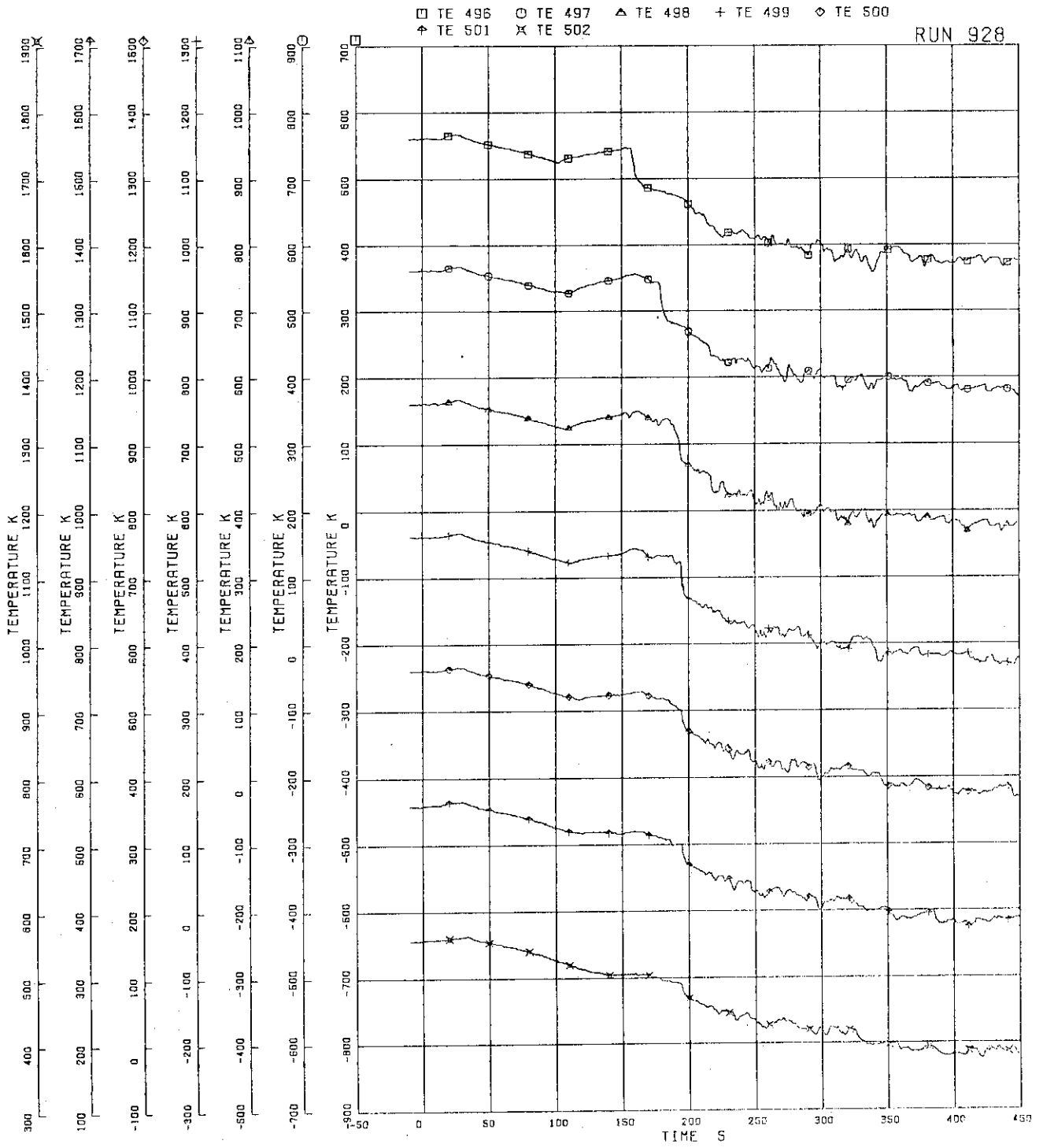


FIG.5.112 INNER SURFACE TEMPERATURES OF CHANNEL BOX A. LOCATION A1

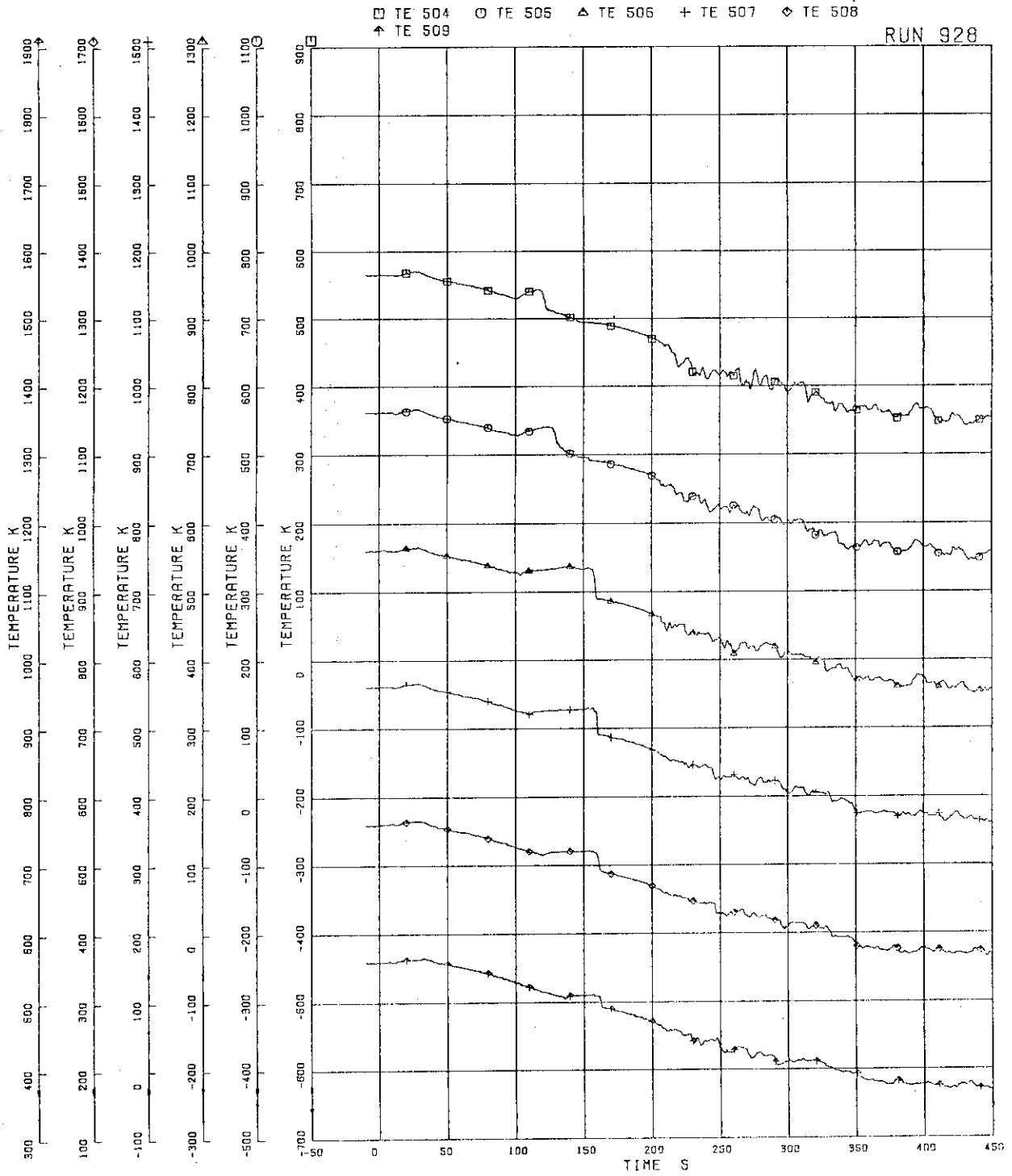


FIG. 5.113 INNER SURFACE TEMPERATURES OF CHANNEL BOX A, LOCATION A2

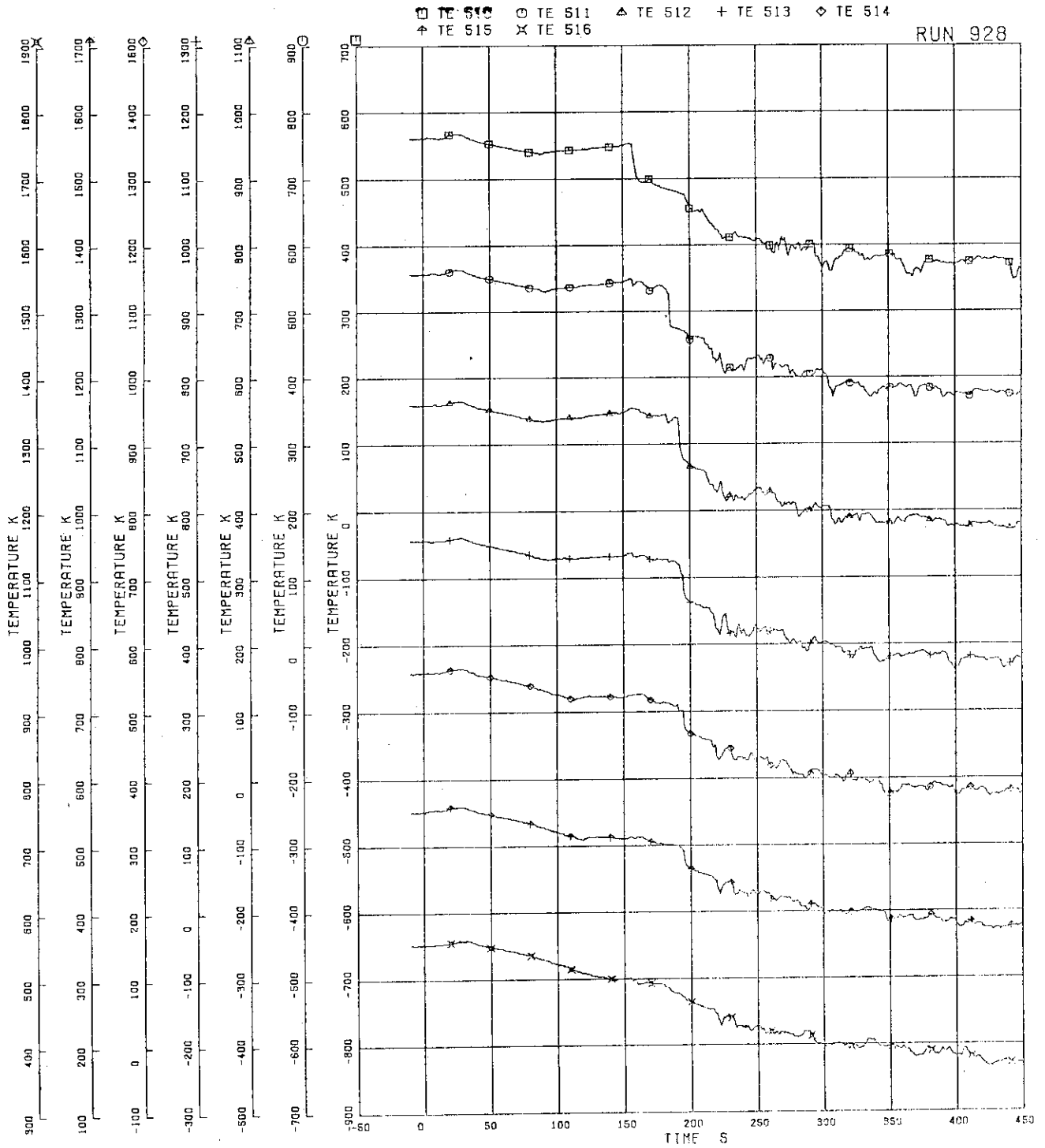


FIG.5-114 INNER SURFACE TEMPERATURES OF CHANNEL BOX B (POSITION 1)



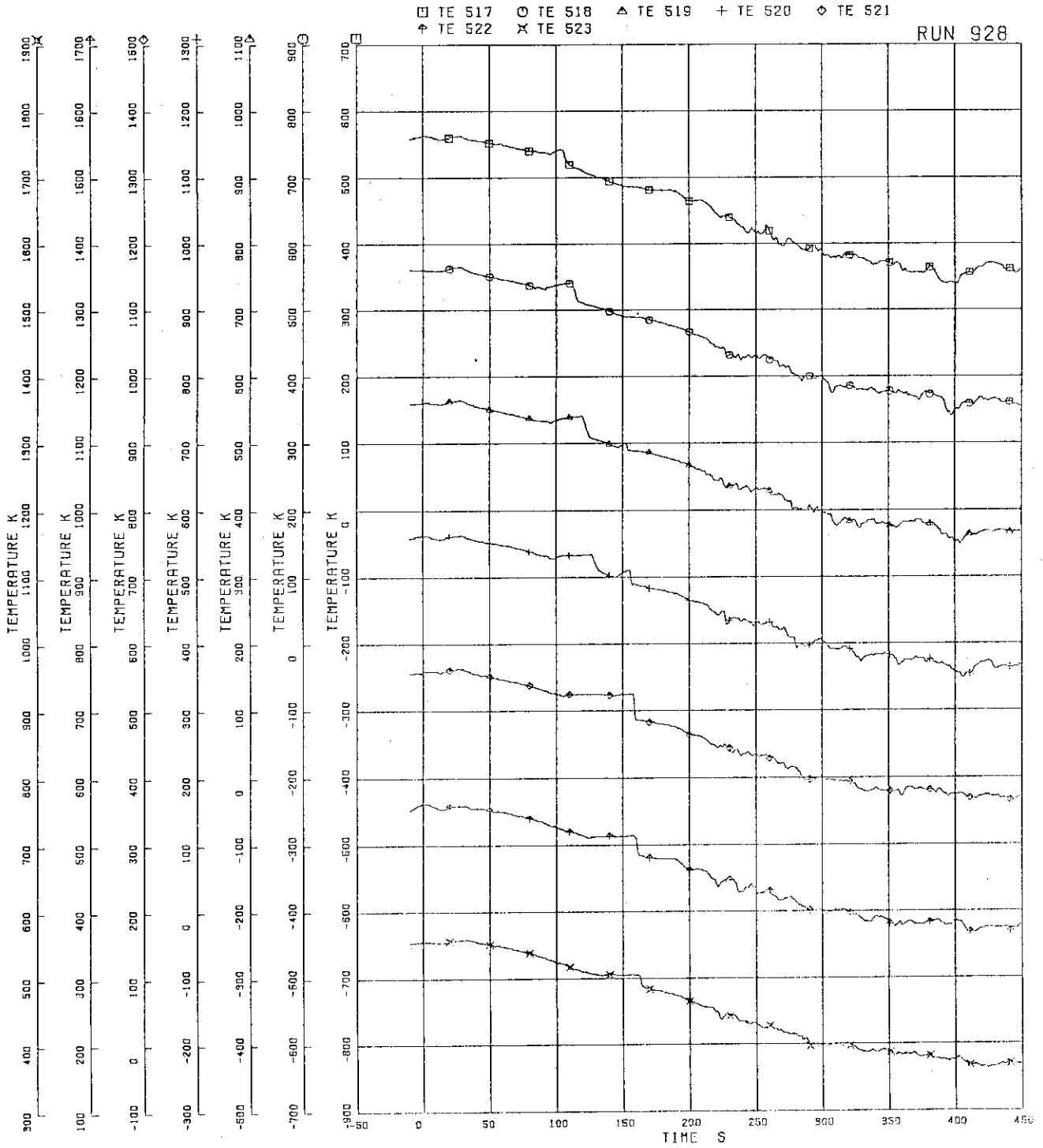


FIG.5.115 INNER SURFACE TEMPERATURES OF CHANNEL BOX C

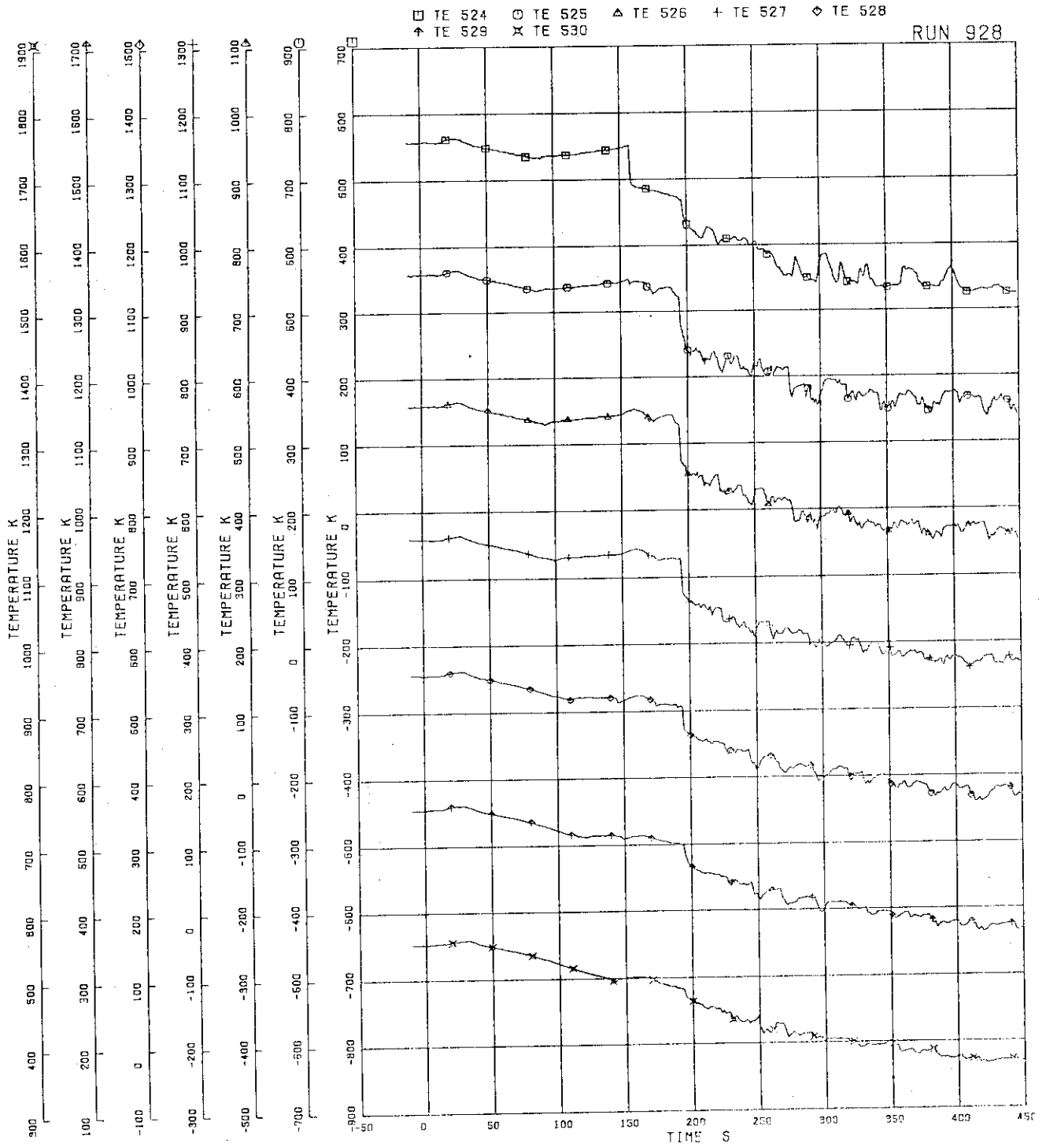


FIG.5.116 INNER SURFACE TEMPERATURES OF CHANNEL BOX D

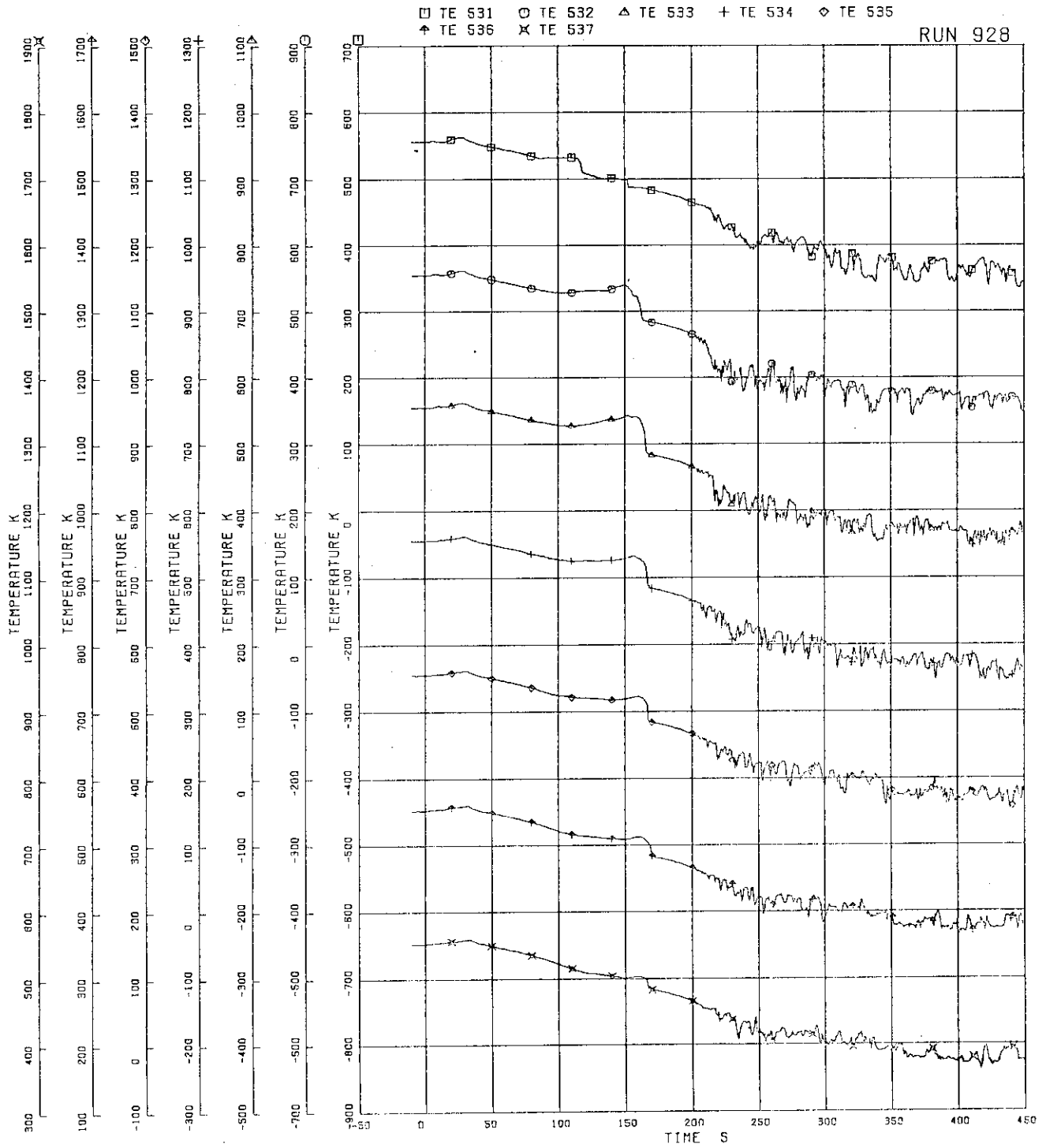


FIG.5-117 OUTER SURFACE TEMPERATURES OF CHANNEL BOX A

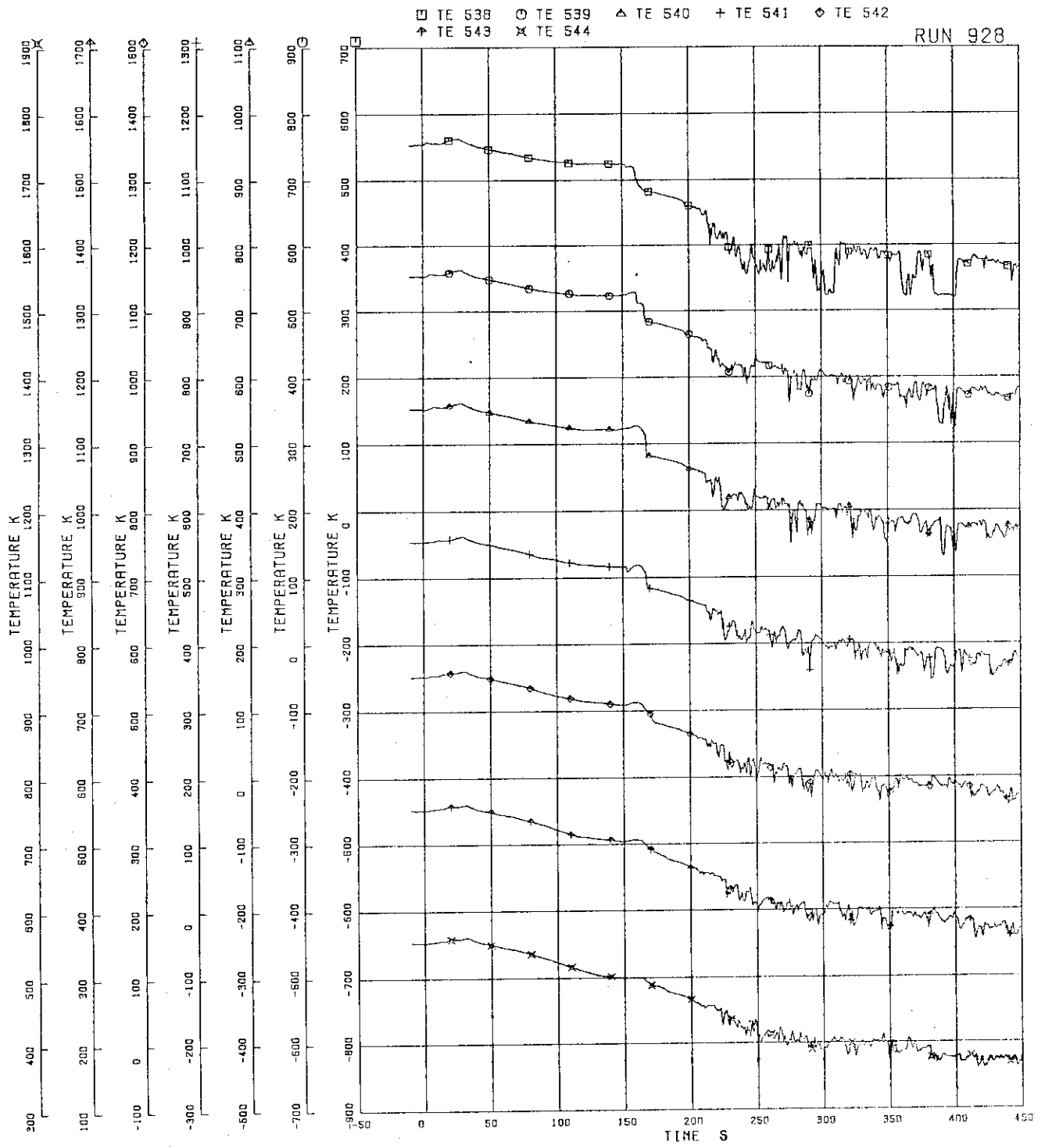


FIG.5-118 OUTER SURFACE TEMPERATURES OF CHANNEL BOX C

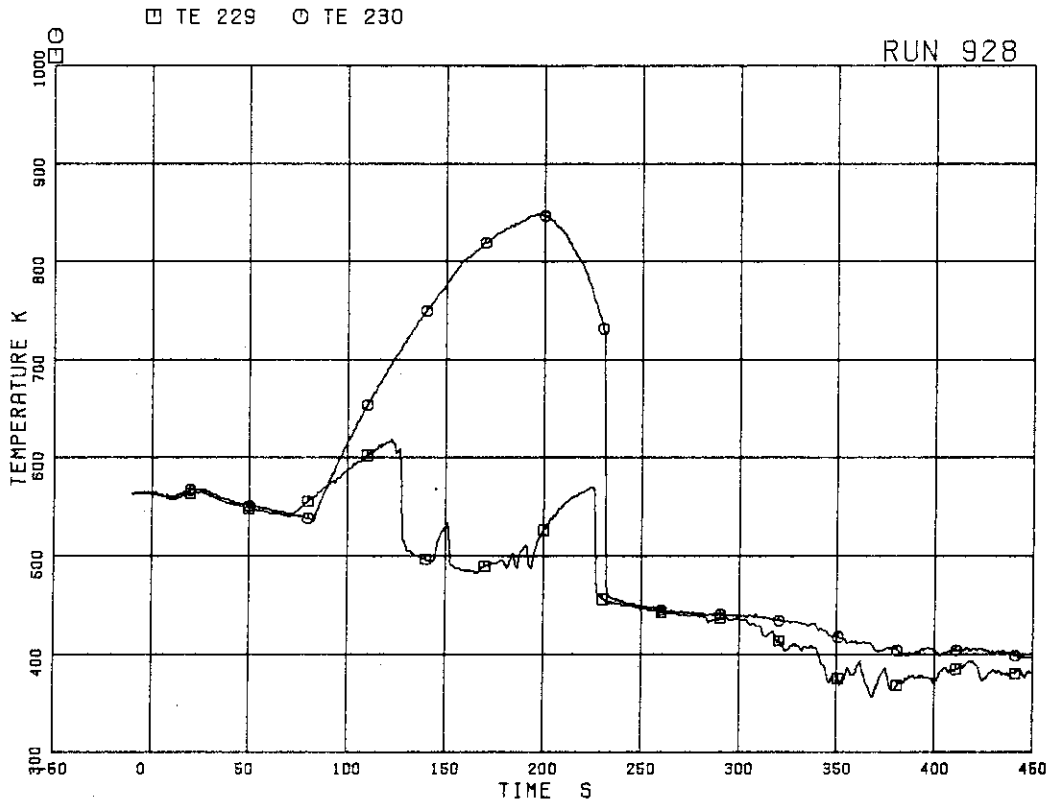


FIG.5.119 SURFACE TEMPERATURES OF FUEL ROD A15 AT POSITIONS 1 AND 4

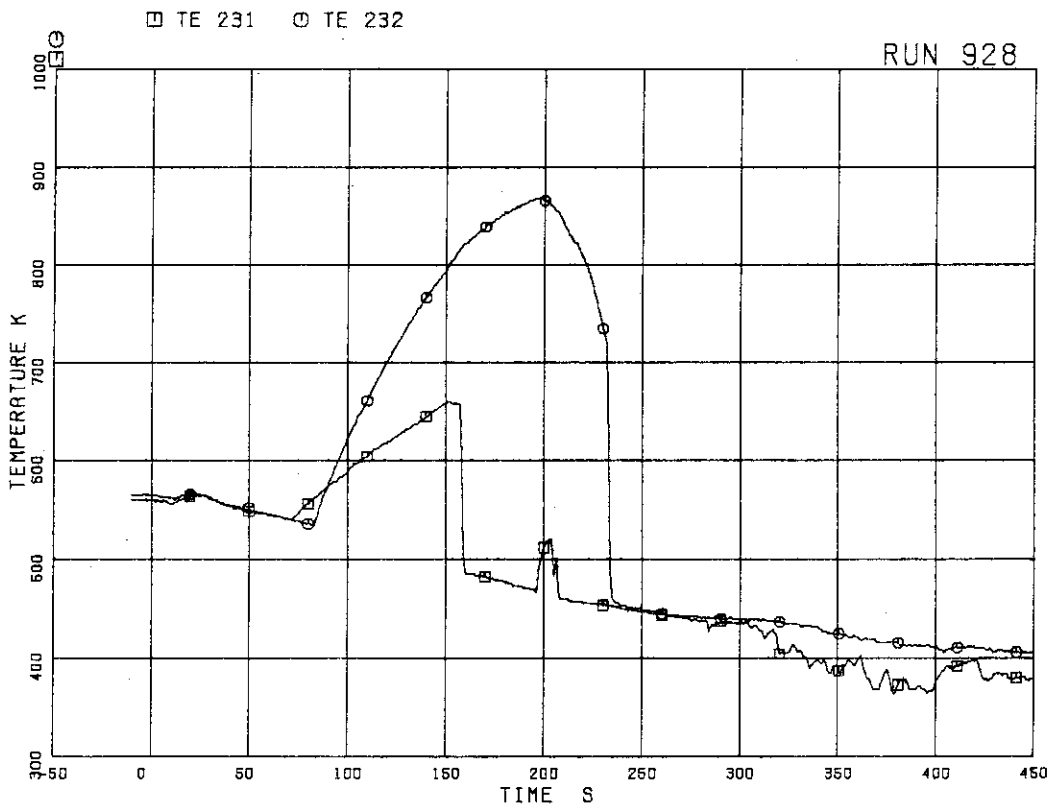


FIG.5.120 SURFACE TEMPERATURES OF FUEL ROD A17 AT POSITIONS 1 AND 4

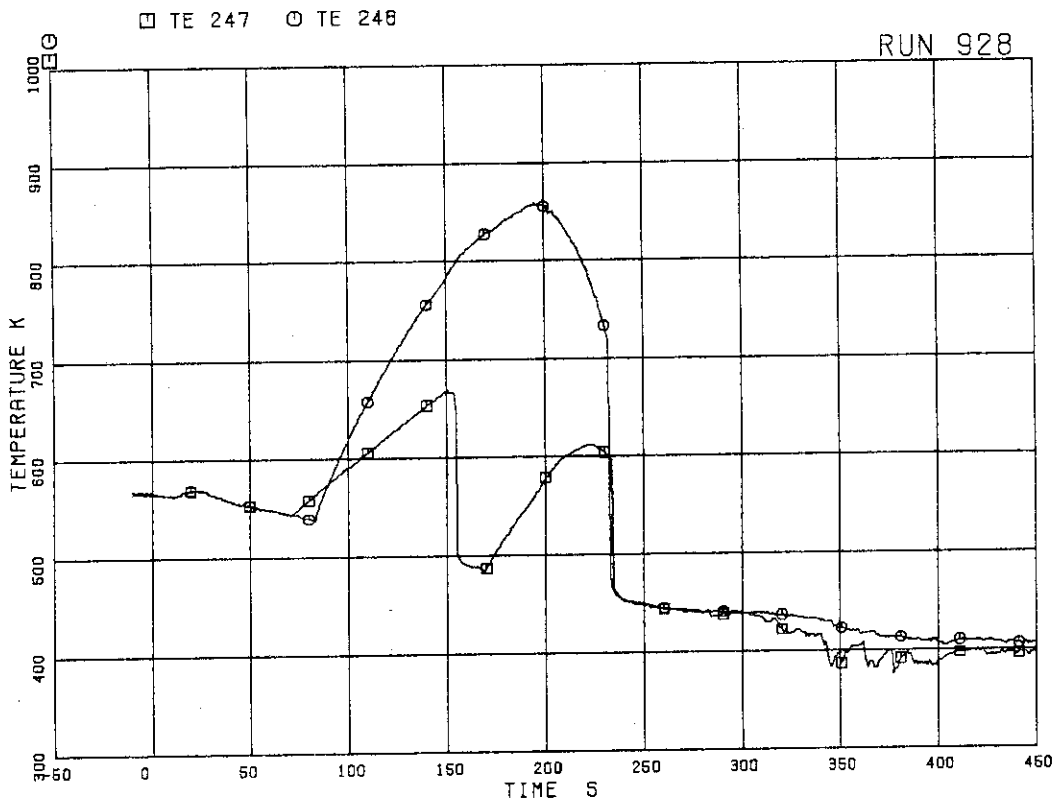


FIG.5.121 SURFACE TEMPERATURES OF FUEL ROD A26 AT POSITIONS 1 AND 4

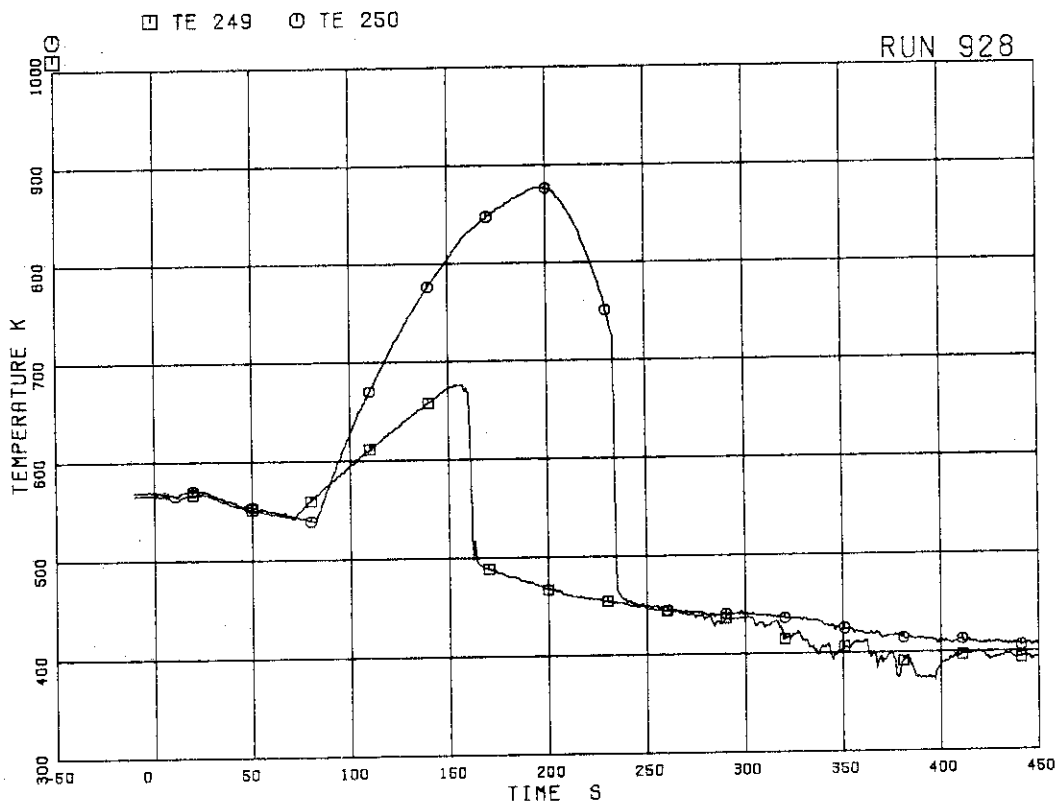


FIG.5.122 SURFACE TEMPERATURES OF FUEL ROD A28 AT POSITIONS 1 AND 4

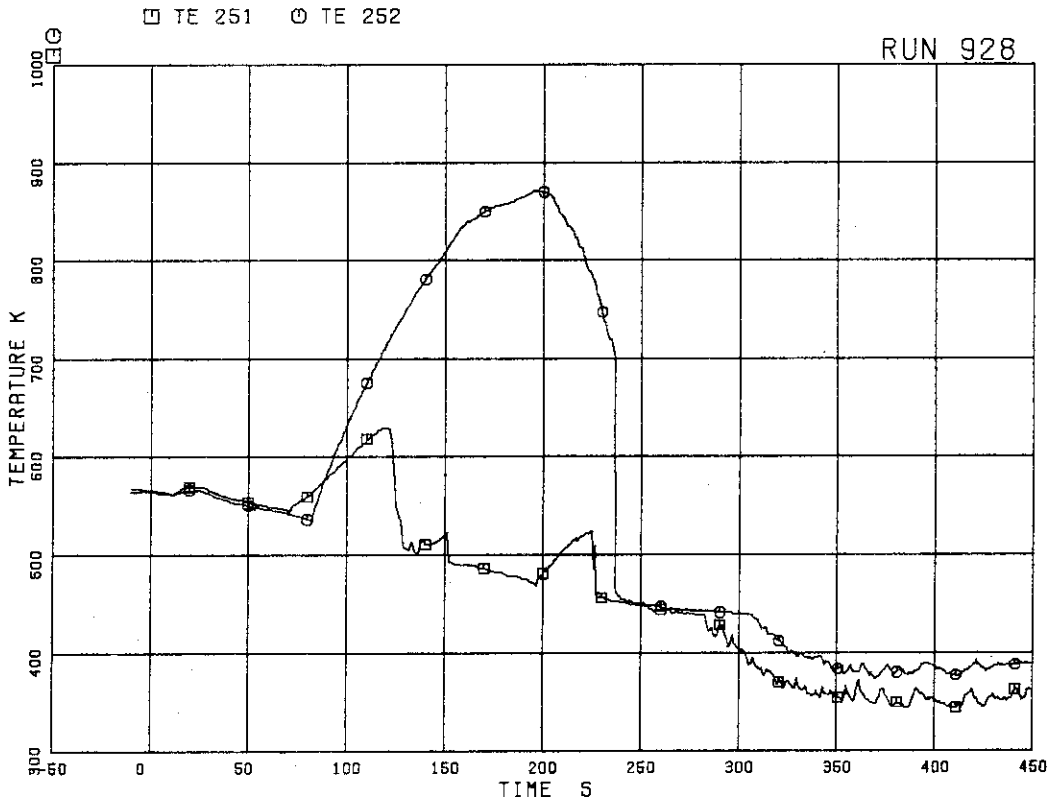


FIG.5.123 SURFACE TEMPERATURES OF FUEL ROD A31 AT POSITIONS 1 AND 4

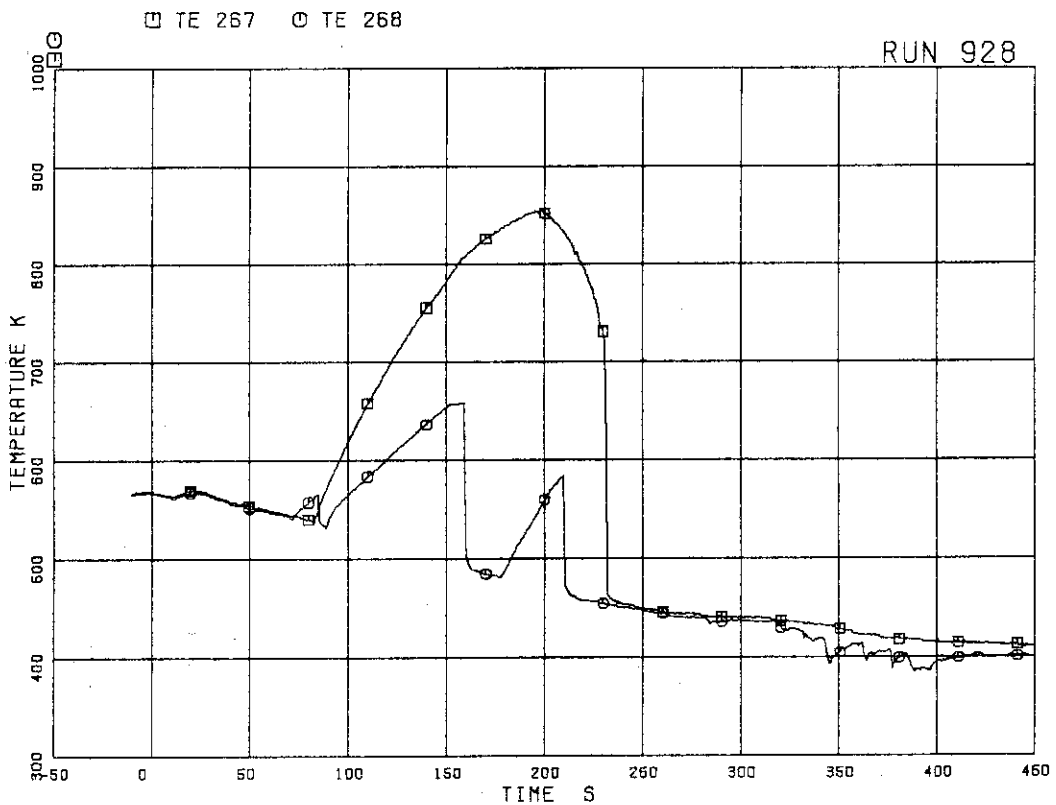


FIG.5.124 SURFACE TEMPERATURES OF FUEL ROD A37 AT POSITIONS 1 AND 4

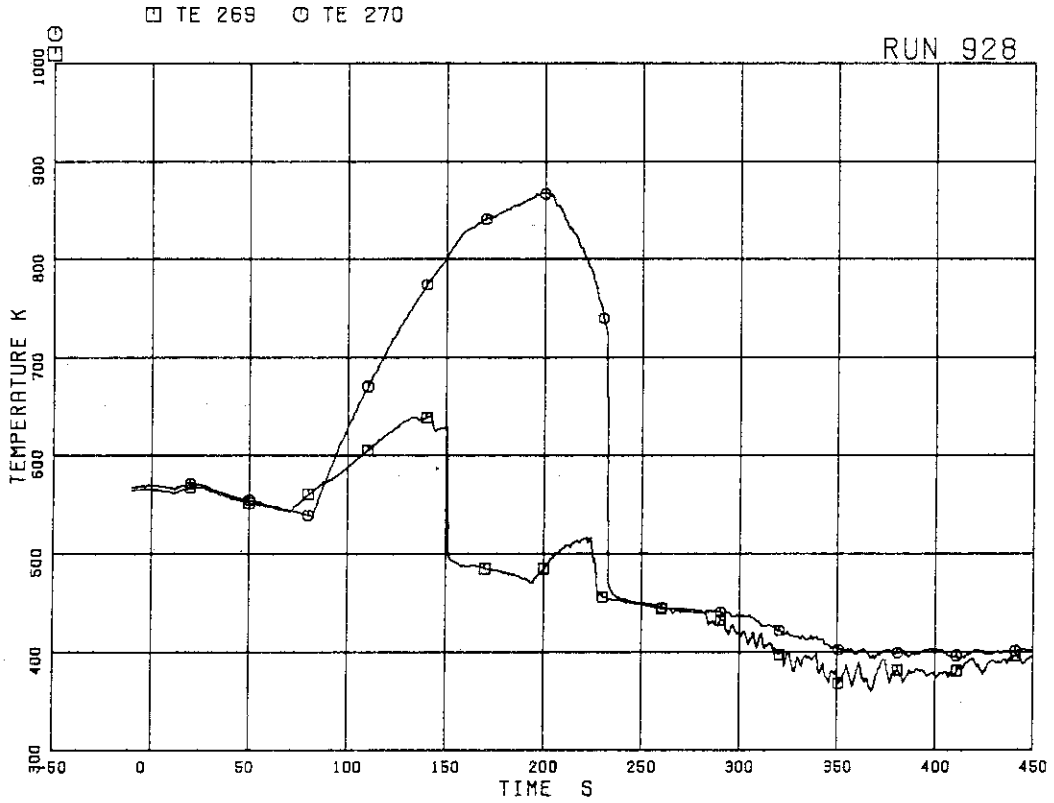


FIG. 5.125 SURFACE TEMPERATURE OF FUEL ROD A42 AT POSITION 1

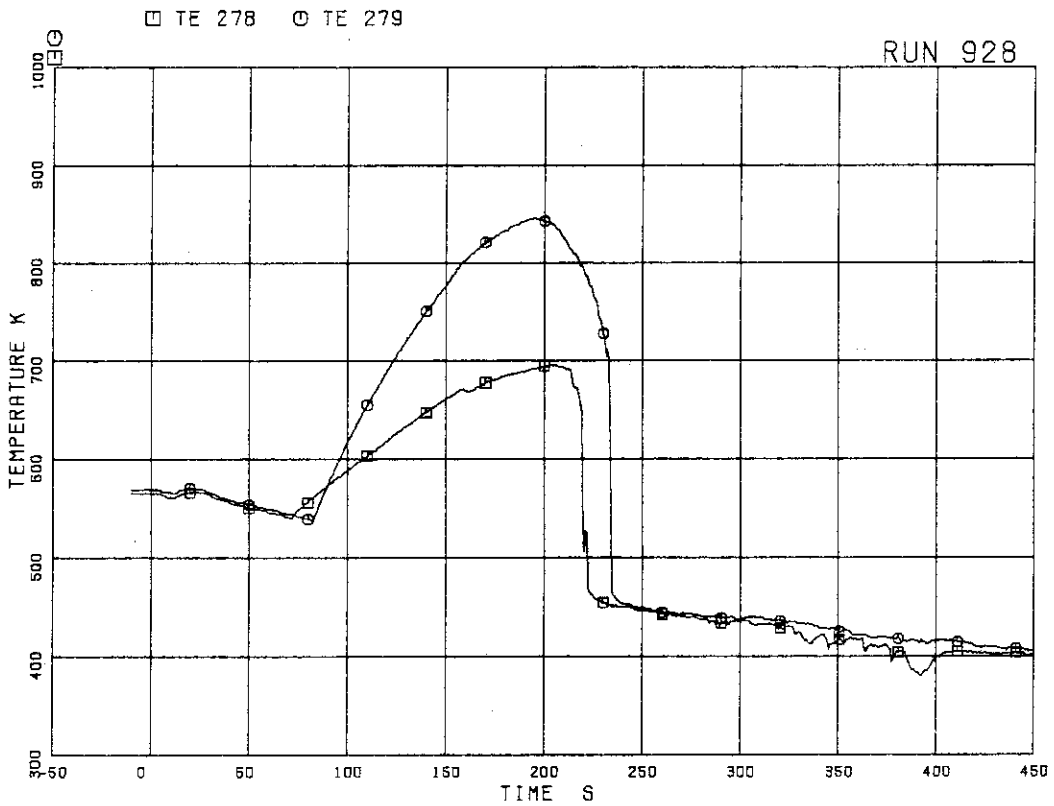


FIG. 5.126 SURFACE TEMPERATURES OF FUEL ROD A48 AT POSITIONS 1 AND 4



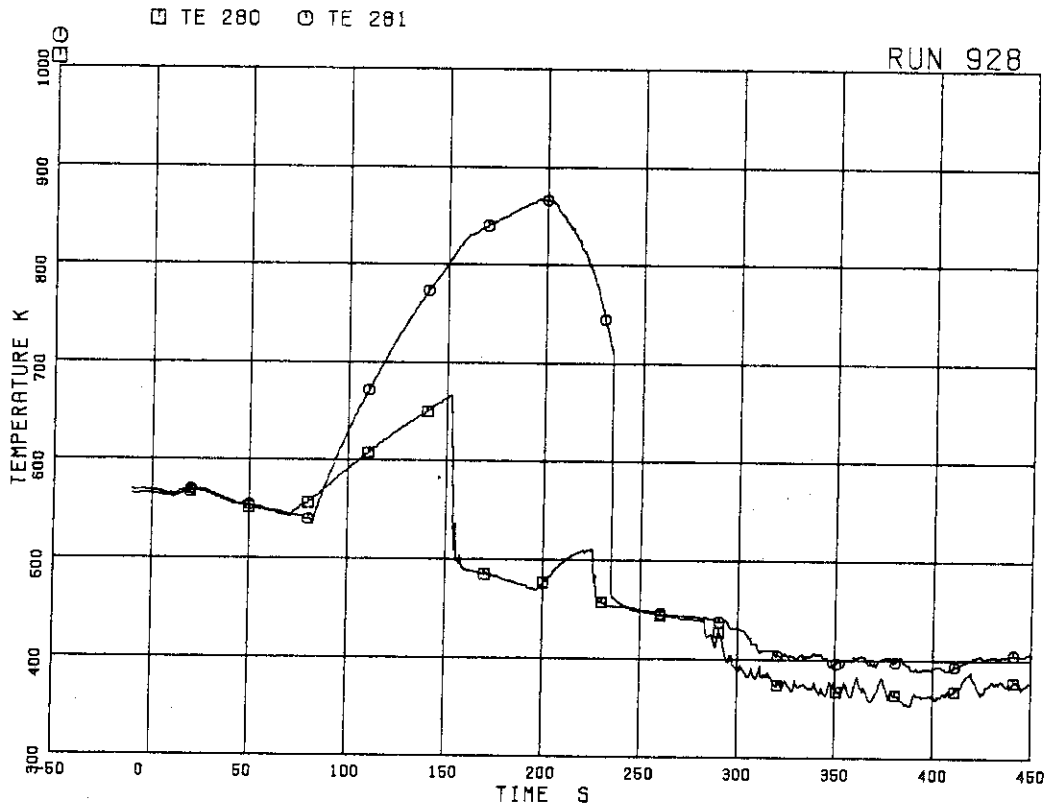


FIG.5.127 SURFACE TEMPERATURES OF FUEL ROD A51 AT POSITIONS 1 AND 4

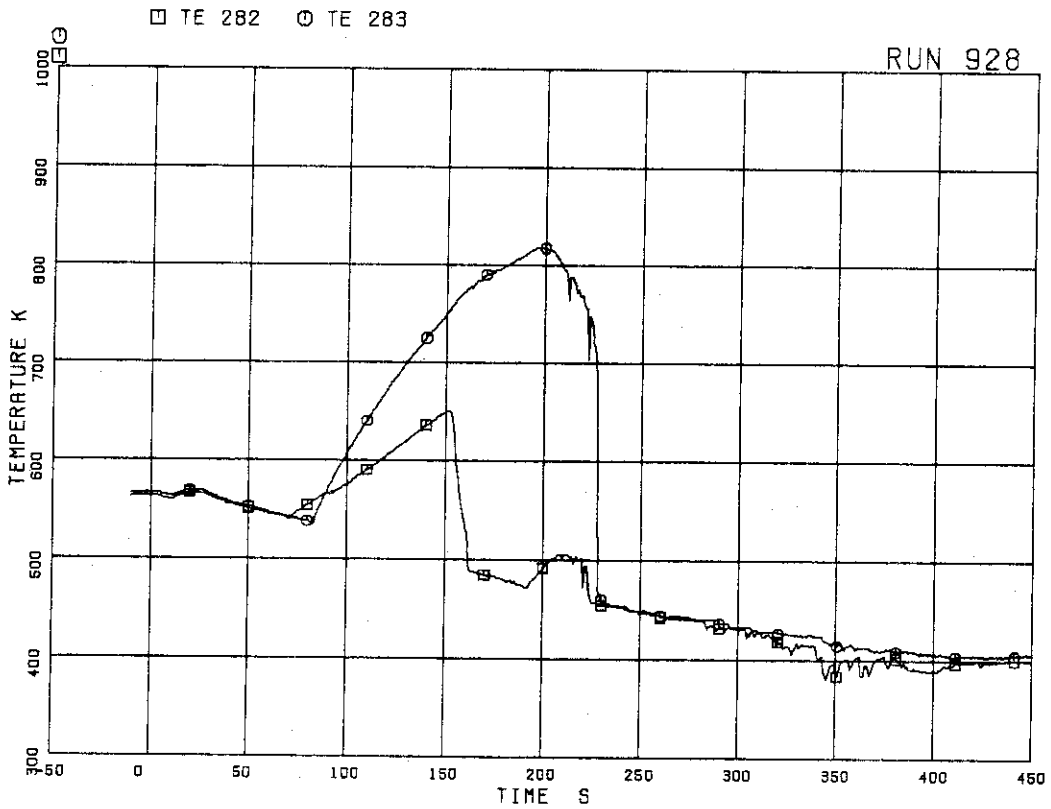


FIG.5.128 SURFACE TEMPERATURES OF FUEL ROD A53 AT POSITIONS 1 AND 4

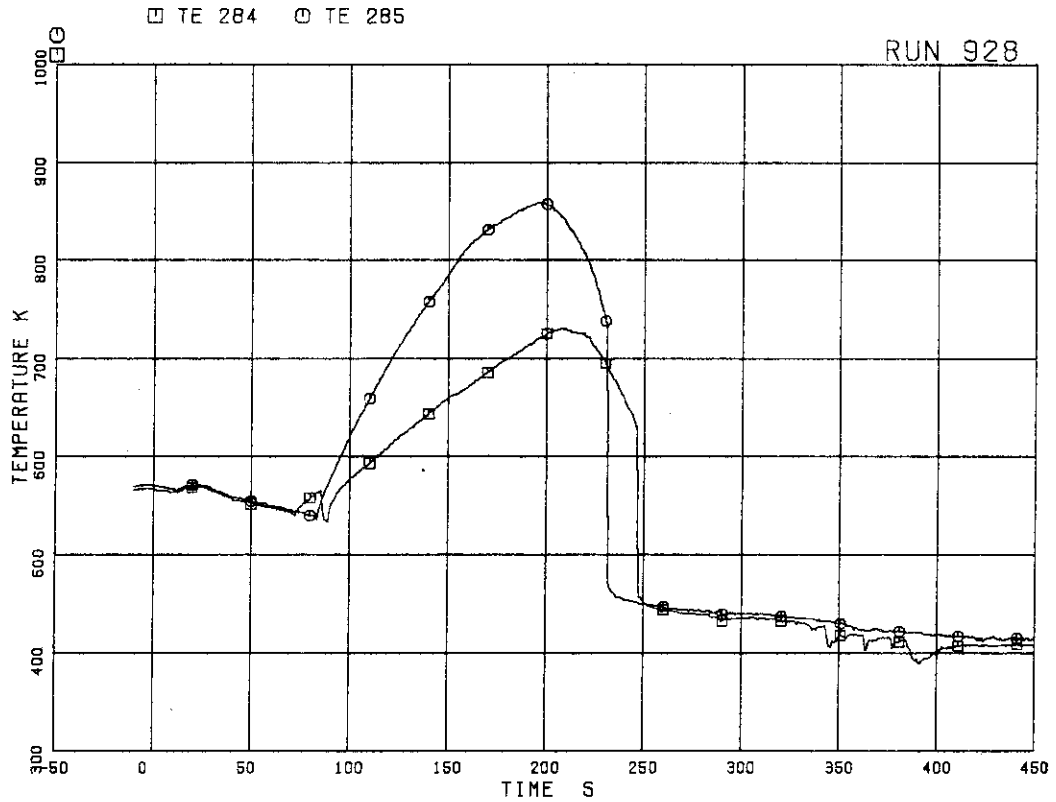


FIG. 5.129 SURFACE TEMPERATURES OF FUEL ROD A57 AT POSITIONS 1 AND 4

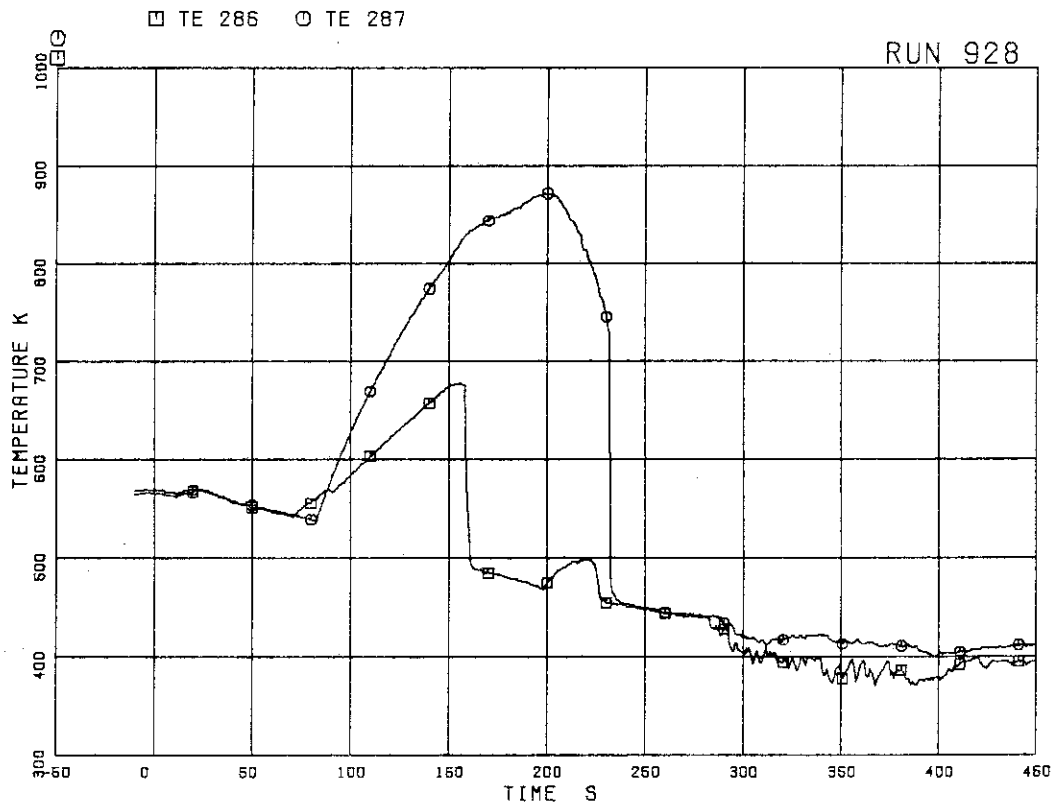


FIG. 5.130 SURFACE TEMPERATURES OF FUEL ROD A62 AT POSITIONS 1 AND 4

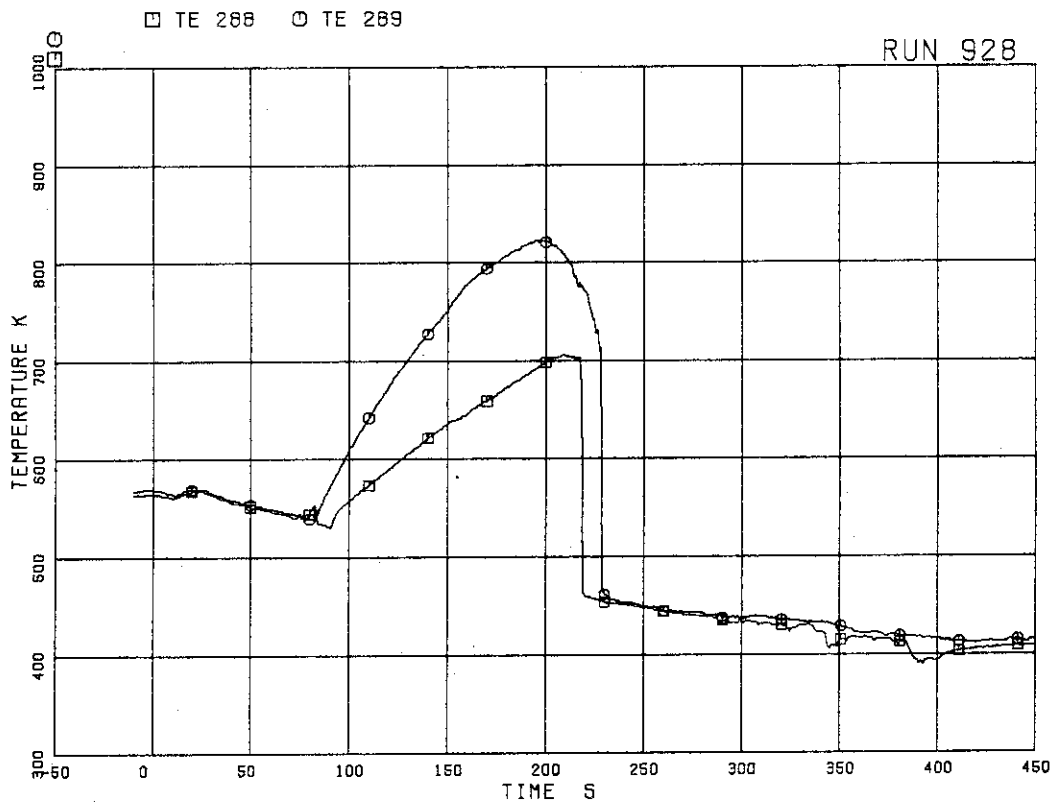


FIG.5.131 SURFACE TEMPERATURE OF FUEL ROD A66 AT POSITION 1

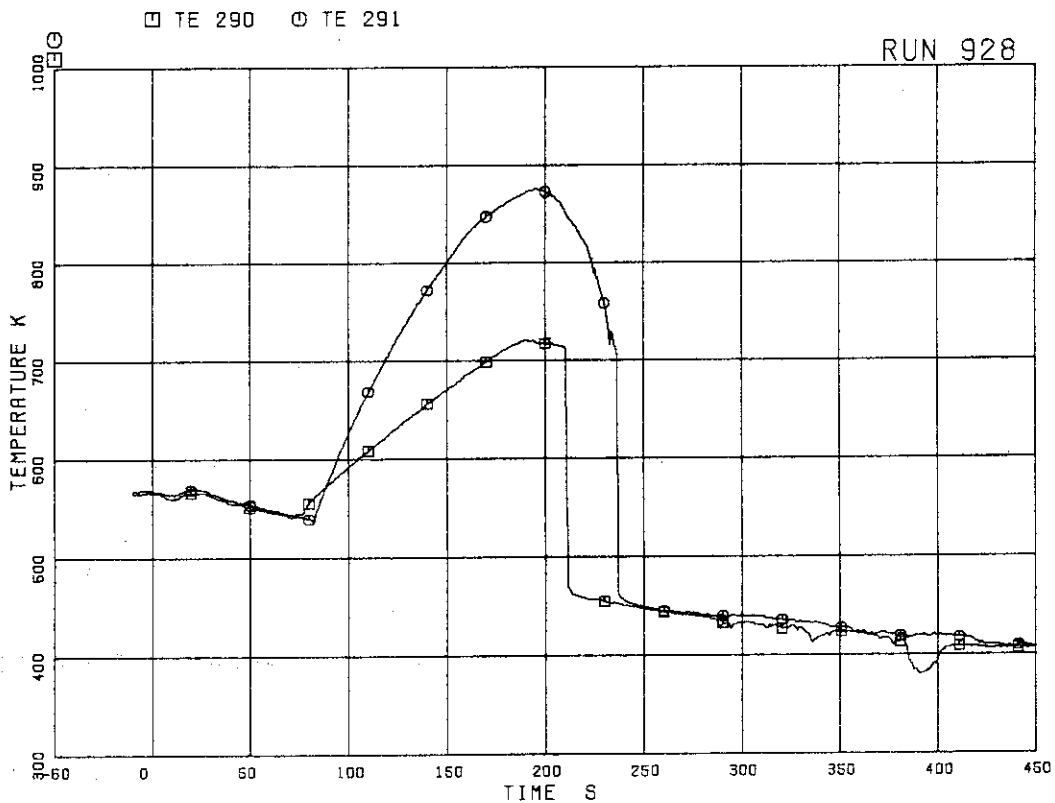


FIG.5.132 SURFACE TEMPERATURES OF FUEL ROD A68 AT POSITIONS 1 AND 4

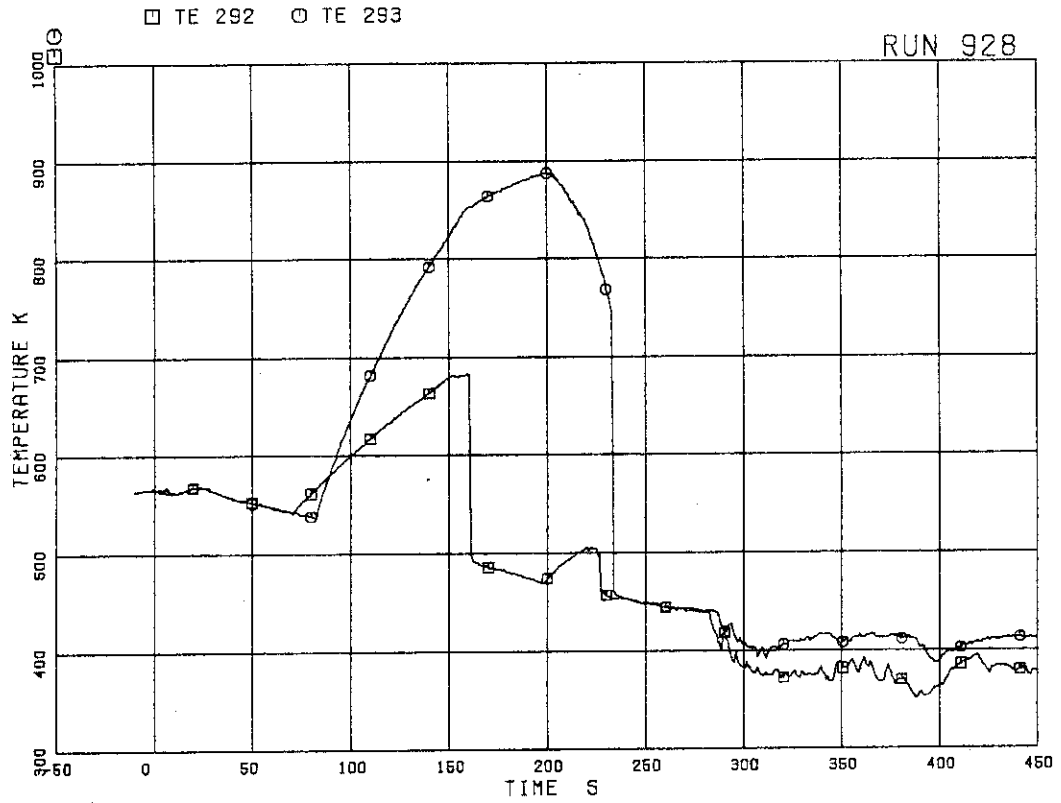


FIG.5.133 SURFACE TEMPERATURE OF FUEL ROD A71 AT POSITION 1

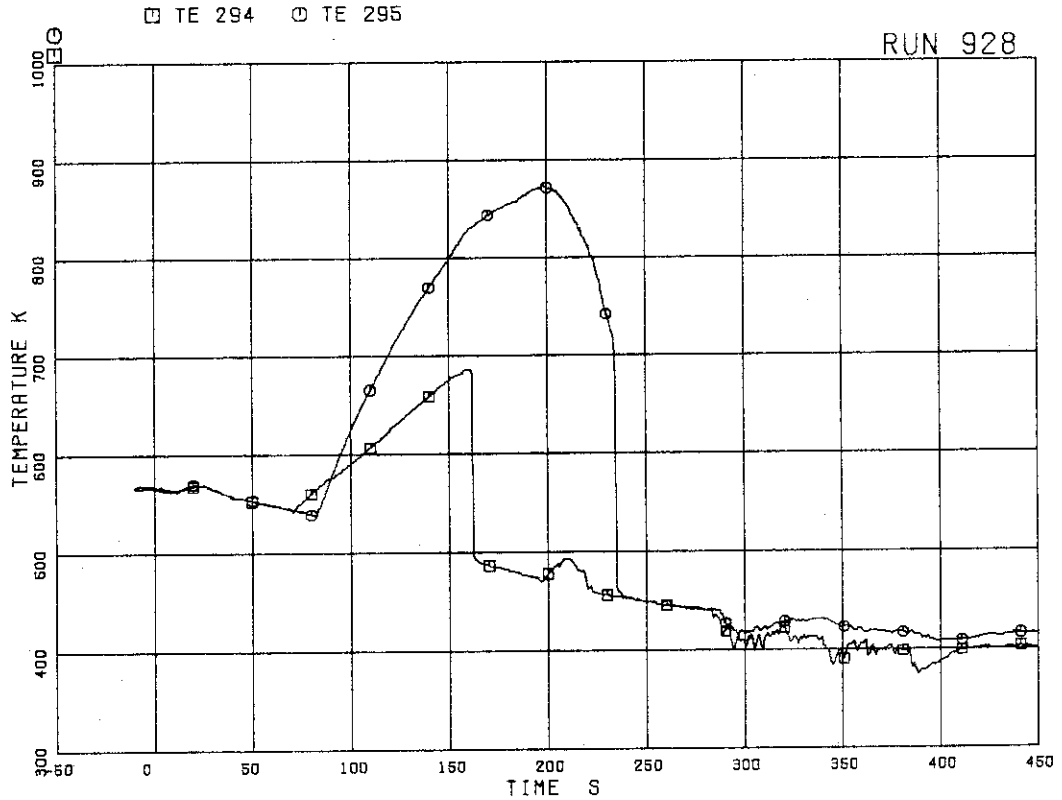


FIG.5.134 SURFACE TEMPERATURES OF FUEL ROD A73 AT POSITIONS 1 AND 4

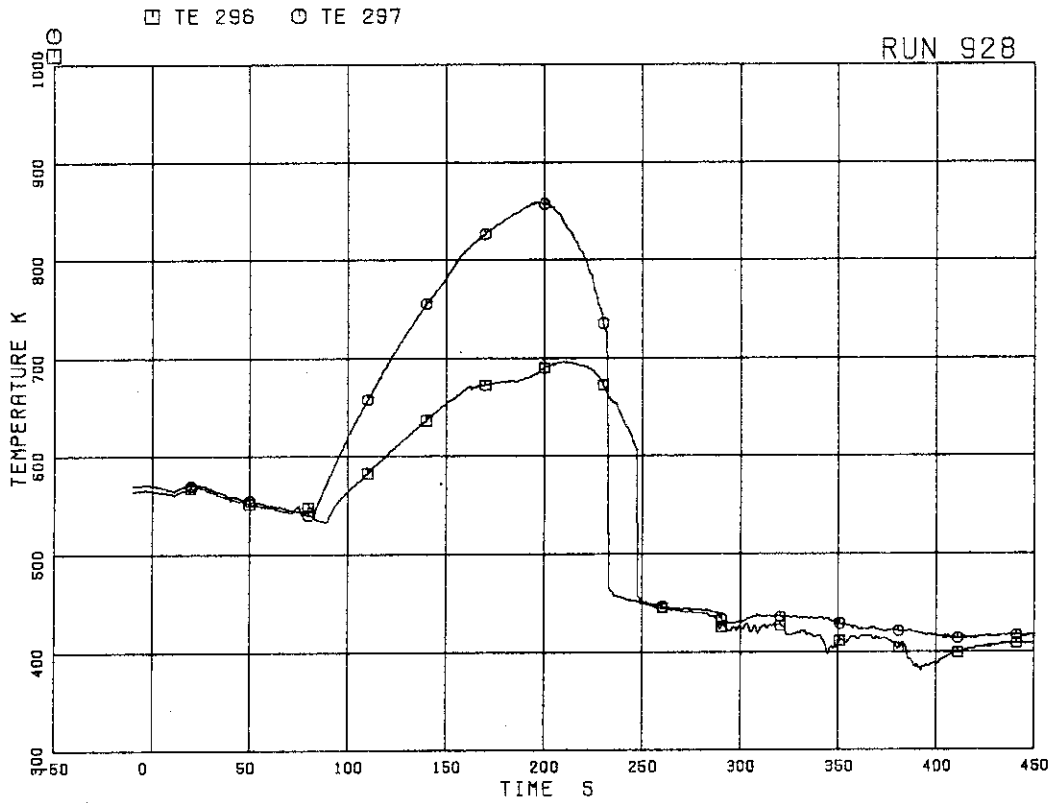


FIG.5.135 SURFACE TEMPERATURES OF FUEL ROD A75 AT POSITIONS 1 AND 4

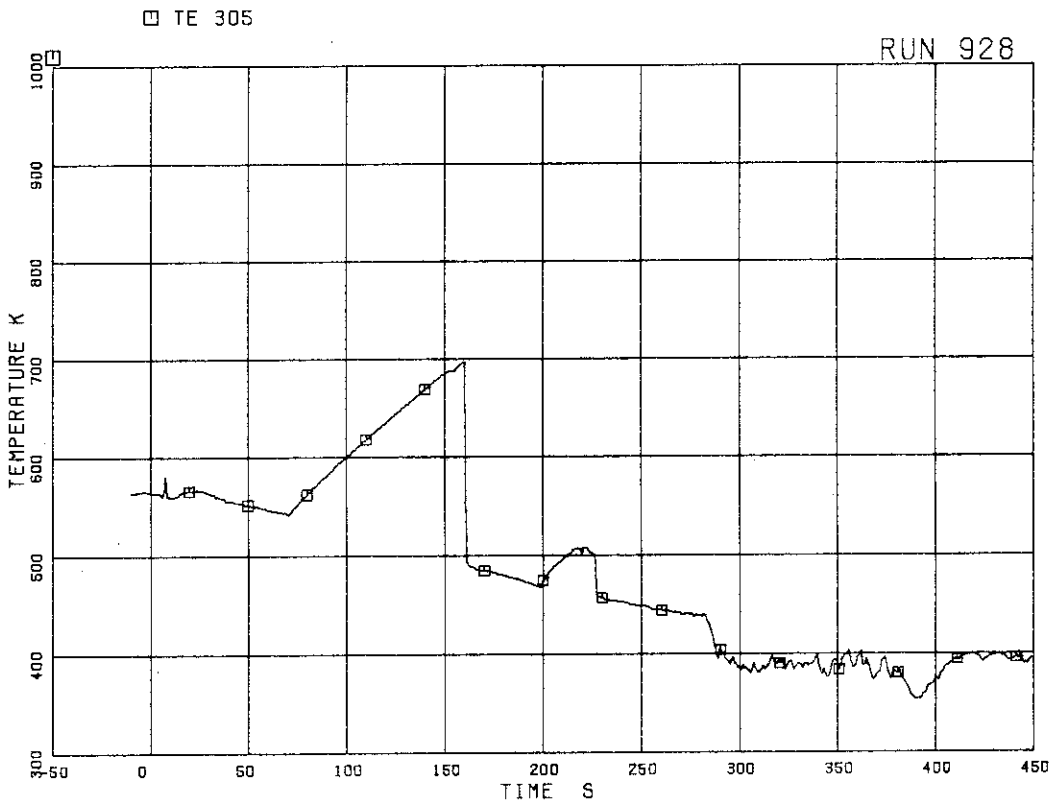


FIG.5.136 SURFACE TEMPERATURE OF FUEL ROD A82 AT POSITION 1

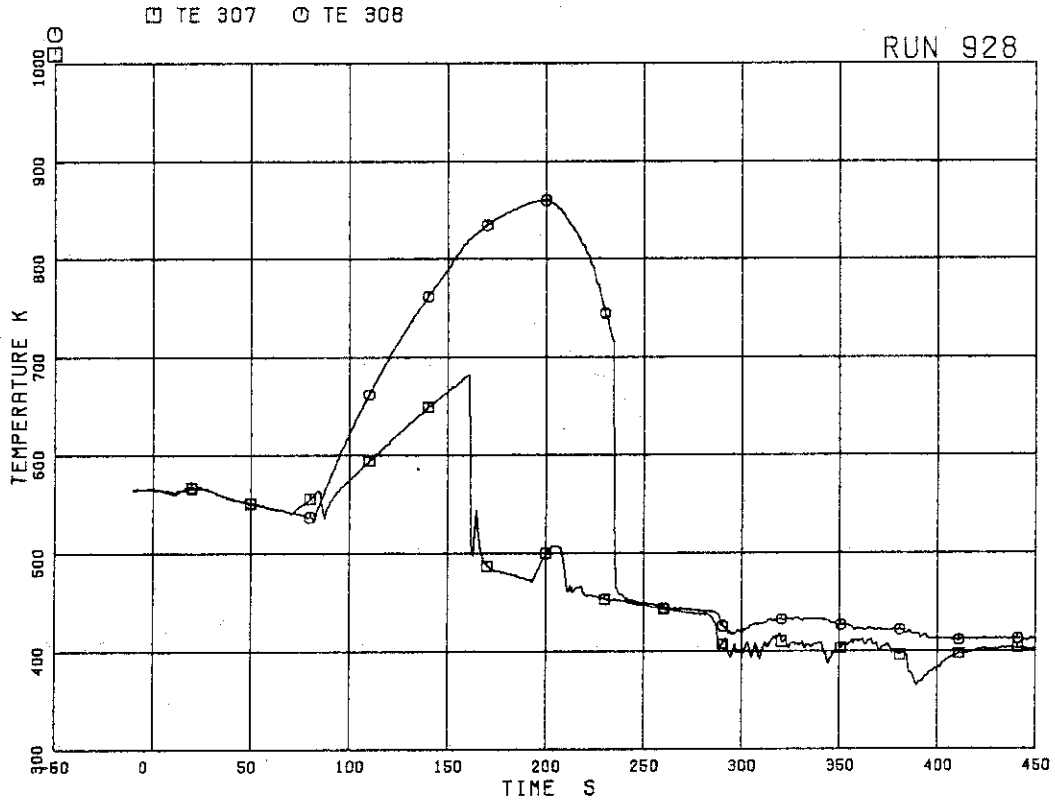


FIG.5.137 SURFACE TEMPERATURES OF FUEL ROD A84 AT POSITIONS 1 AND 4

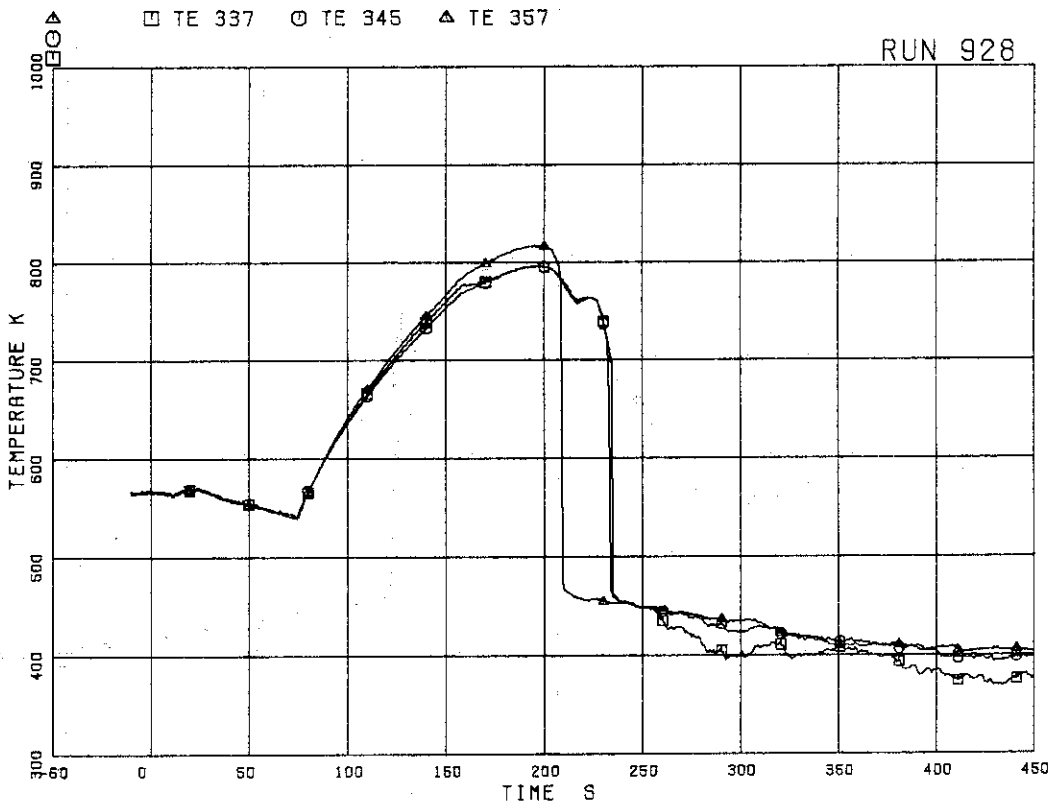


FIG.5.138 SURFACE TEMPERATURES OF FUEL RODS B13, B31, B86 AT POSITION 4

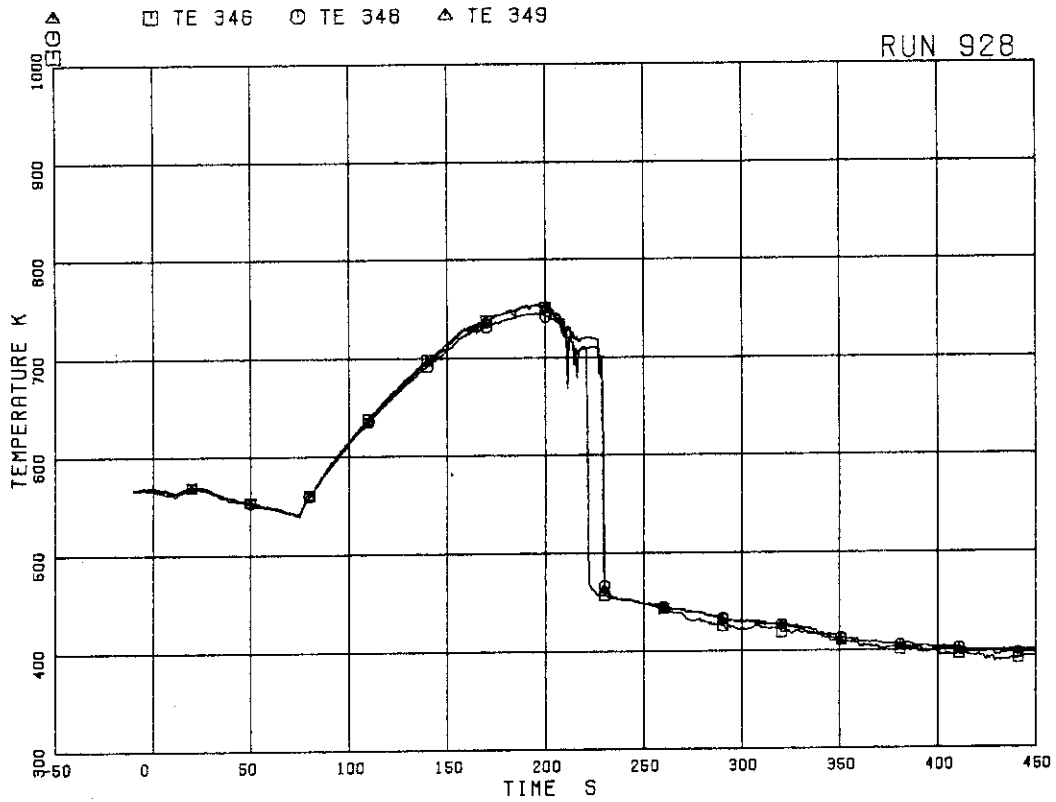


FIG. 5.139 SURFACE TEMPERATURES OF FUEL RODS B33, B53, B66 AT POSITION 4

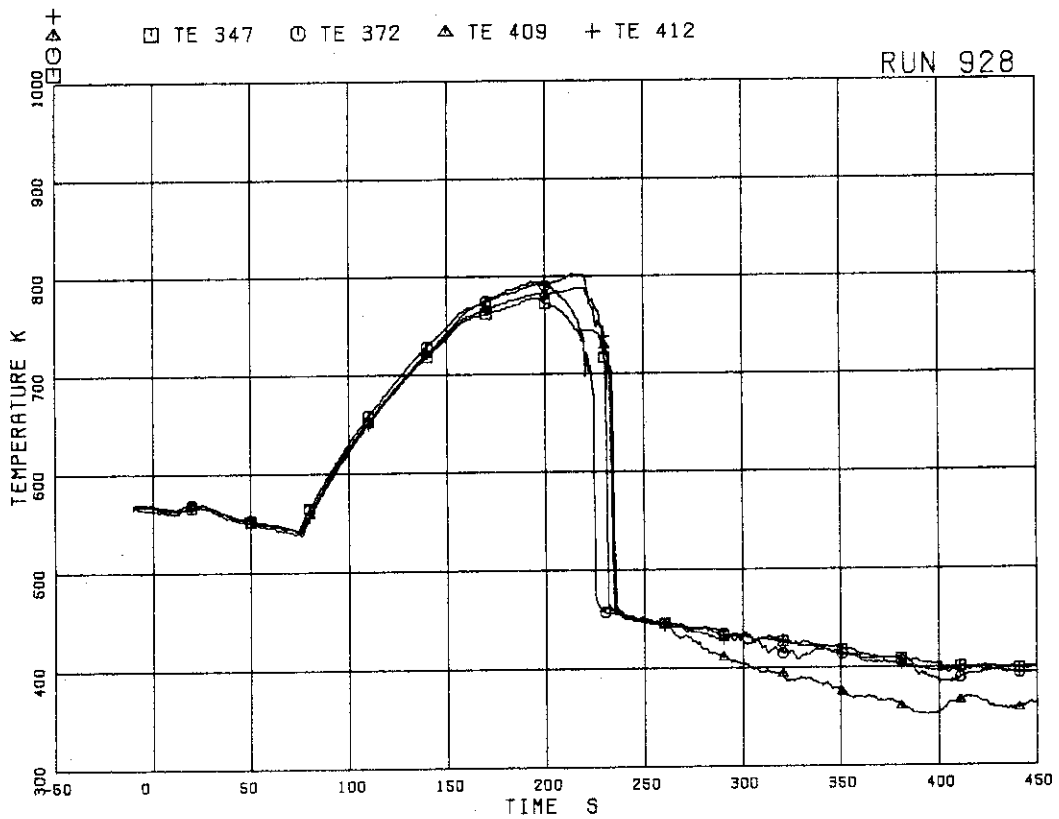


FIG. 5.140 SURFACE TEMPERATURES OF FUEL RODS B51, C15, D51, D77 AT POSITION 4

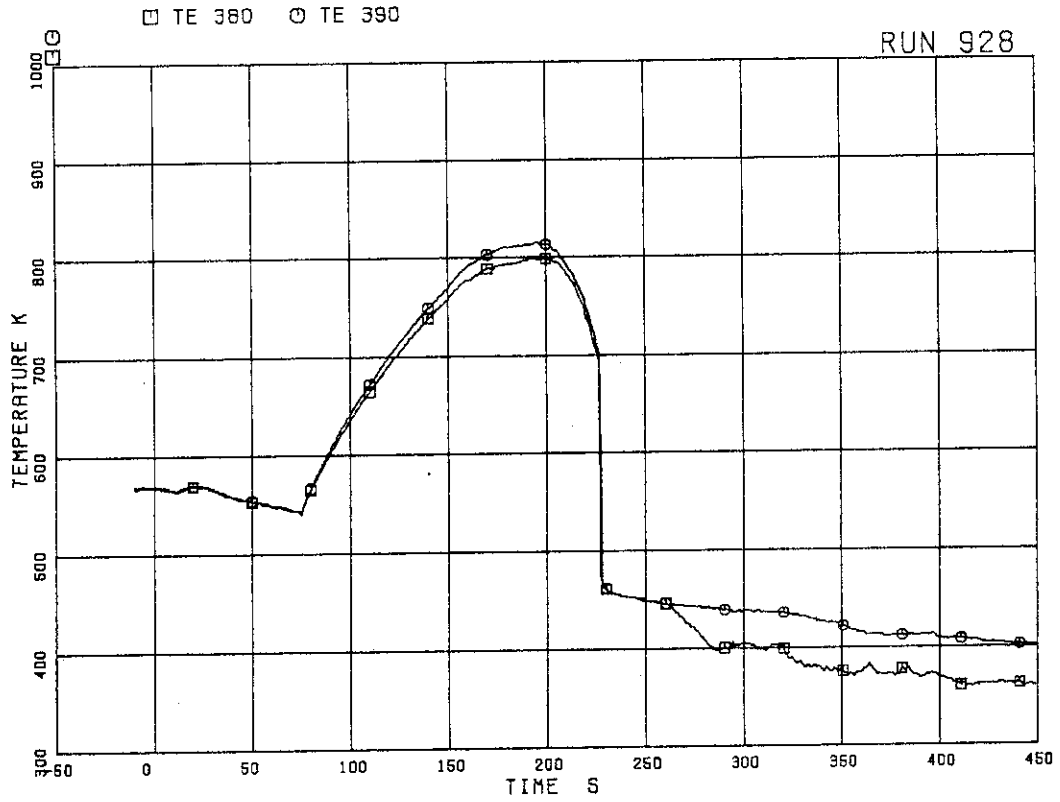


FIG. 5.141 SURFACE TEMPERATURES OF FUEL RODS C31, C68 AT POSITION 4

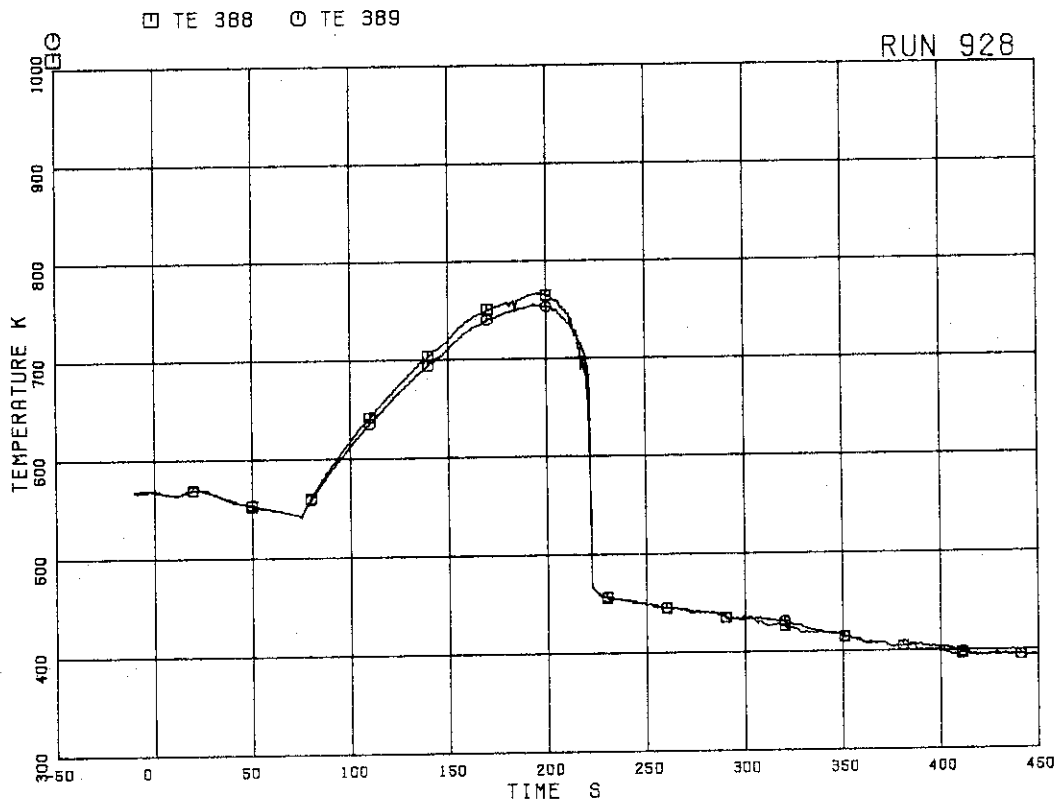


FIG. 5.142 SURFACE TEMPERATURES OF FUEL RODS C35, C66 AT POSITION 4



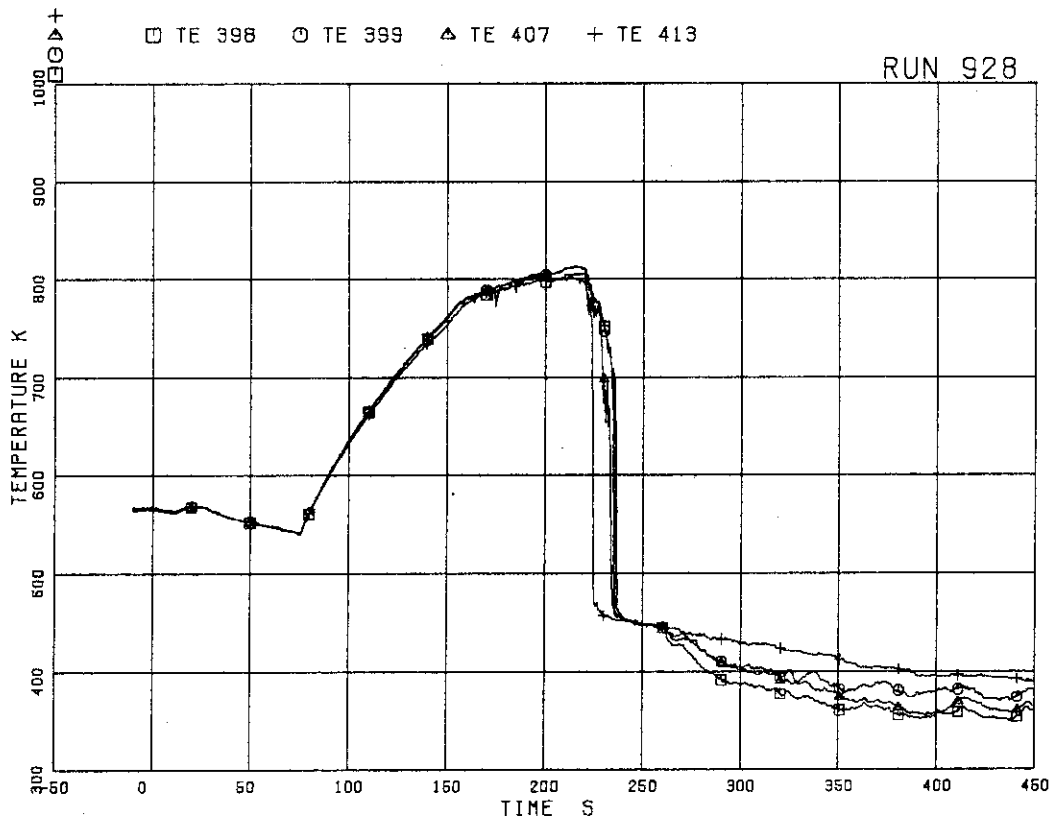


FIG.5.143 SURFACE TEMPERATURES OF FUEL RODS D11,D13,D31,D86 AT POSITION 4

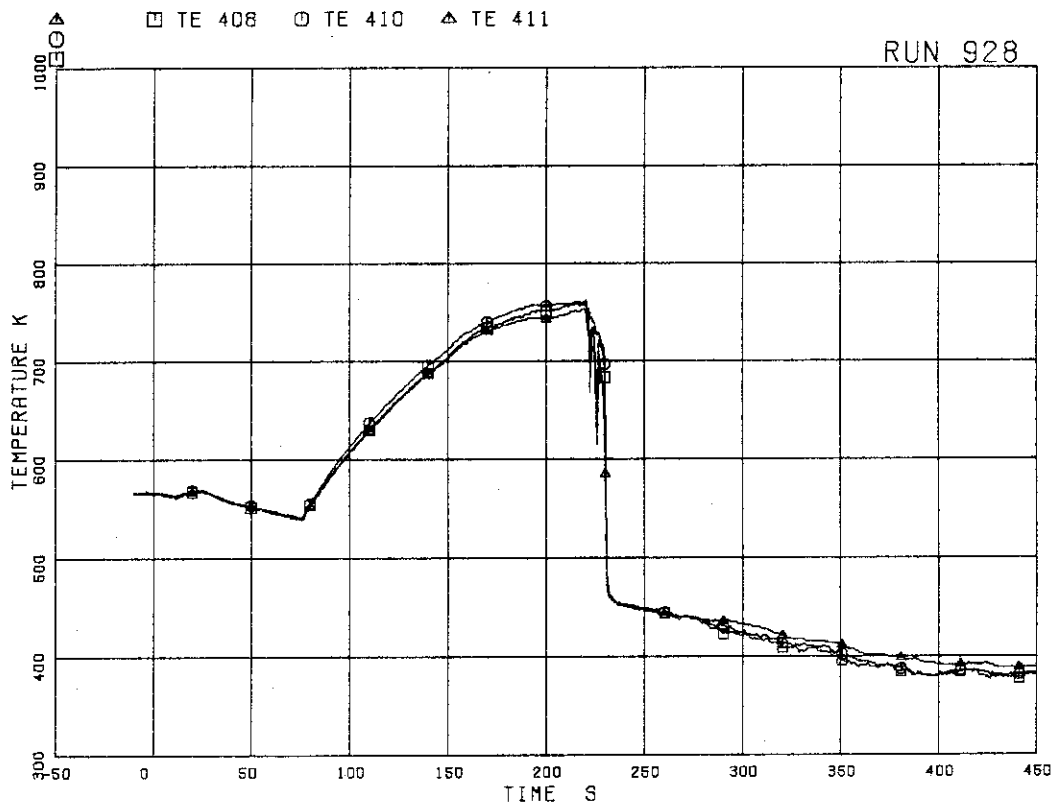


FIG.5.144 SURFACE TEMPERATURES OF FUEL RODS D33,D53,D66 AT POSITION 4

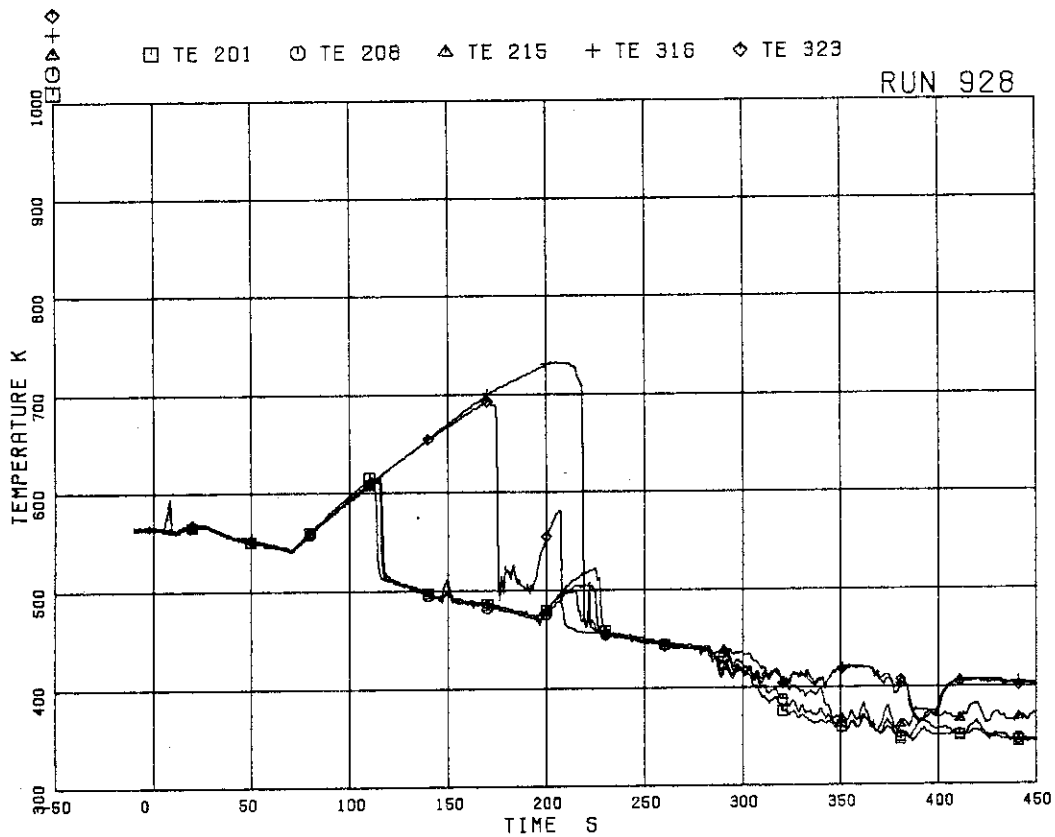


FIG.5.145 SURFACE TEMPERATURES OF FUEL RODS  
A11,A12,A13,A87,A88 AT POSITION 1

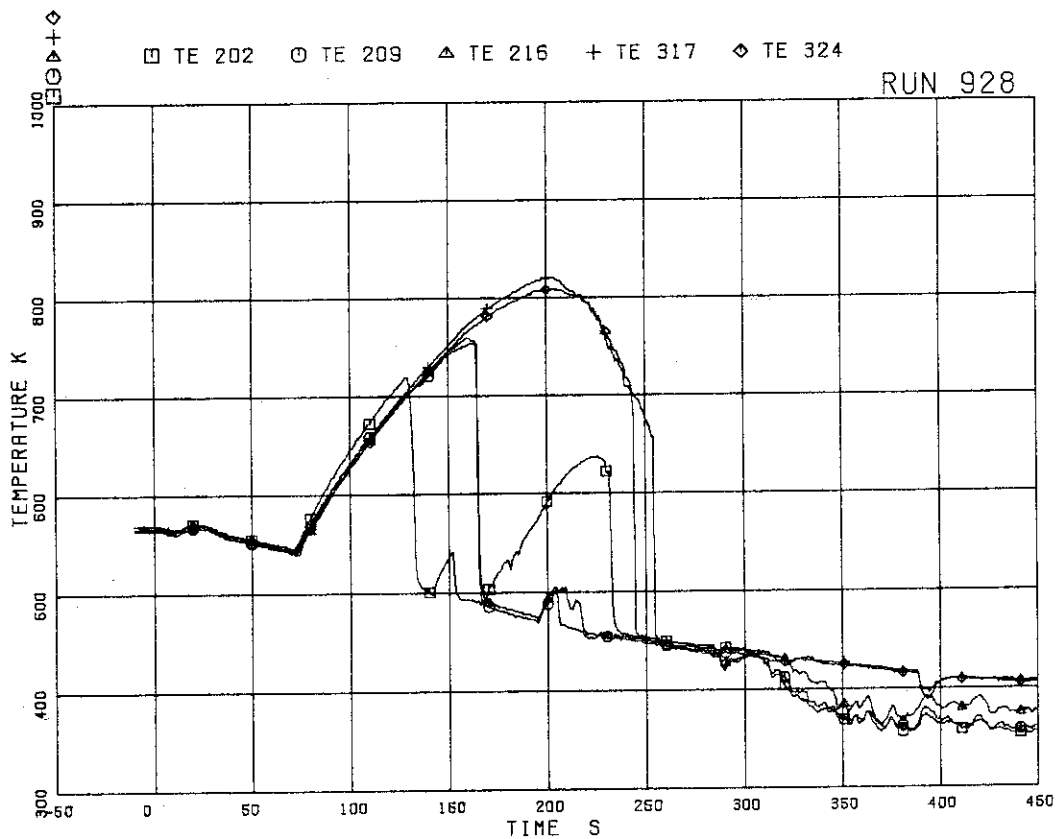


FIG.5.146 SURFACE TEMPERATURES OF FUEL RODS  
A11,A12,A13,A87,A88 AT POSITION 2

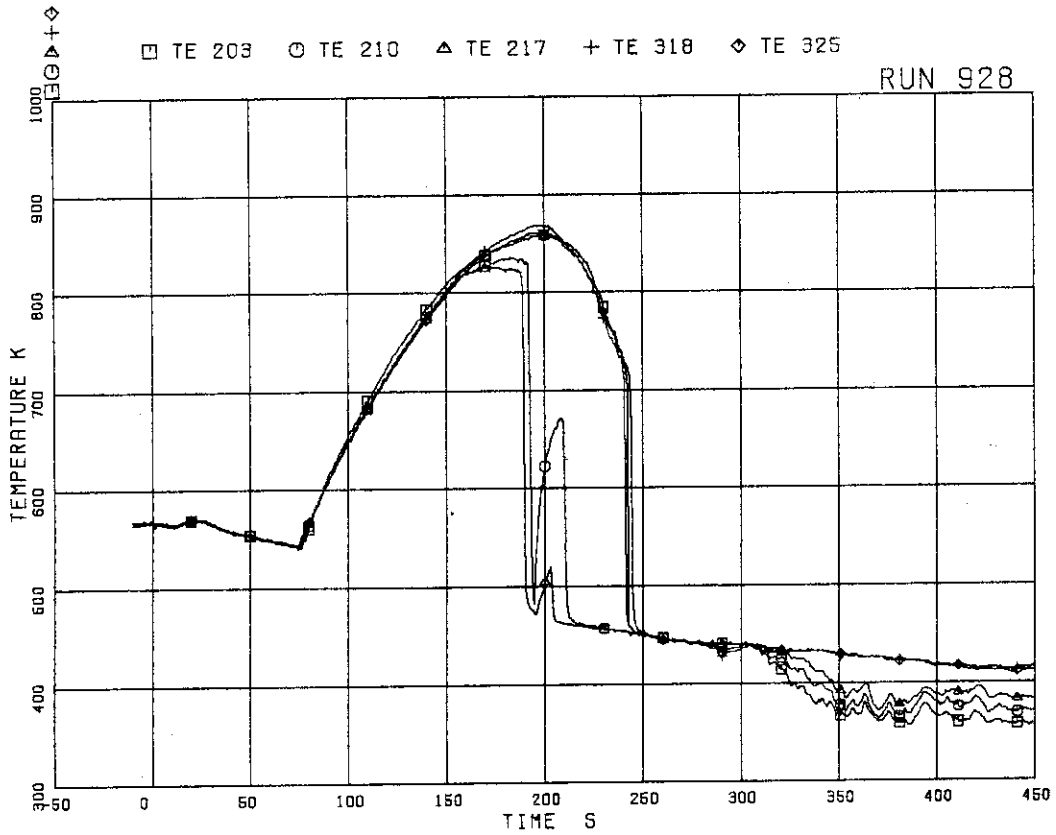


FIG.5.147 SURFACE TEMPERATURES OF FUEL RODS  
A11,A12,A13,A87,A88 AT POSITION 3

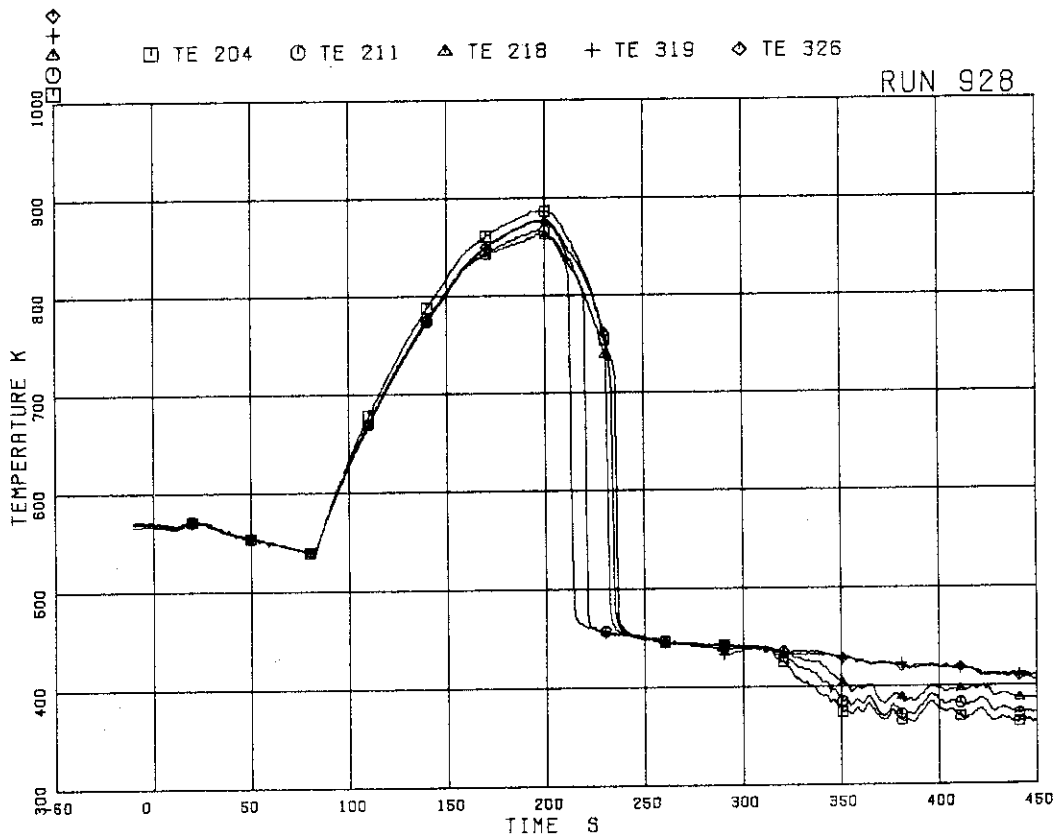


FIG.5.148 SURFACE TEMPERATURES OF FUEL RODS  
A11,A12,A13,A87,A88 AT POSITION 4

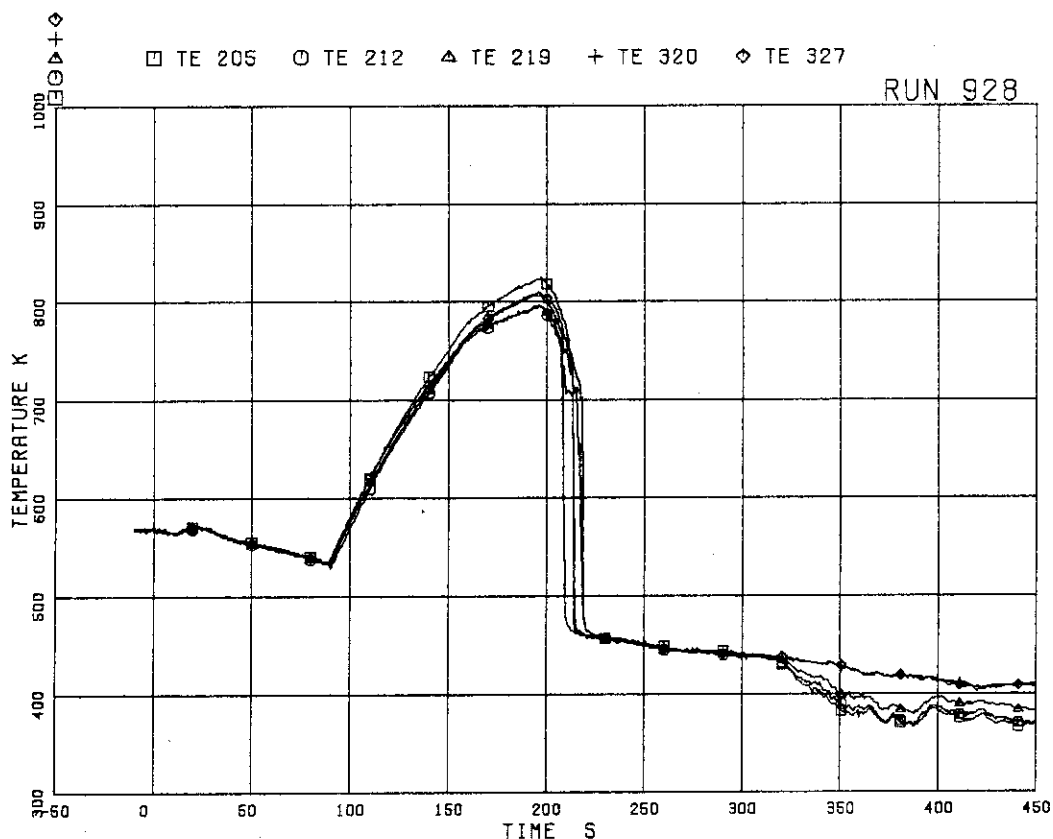


FIG. 5.149 SURFACE TEMPERATURES OF FUEL RODS A11, A12, A13, A87, A88 AT POSITION 5

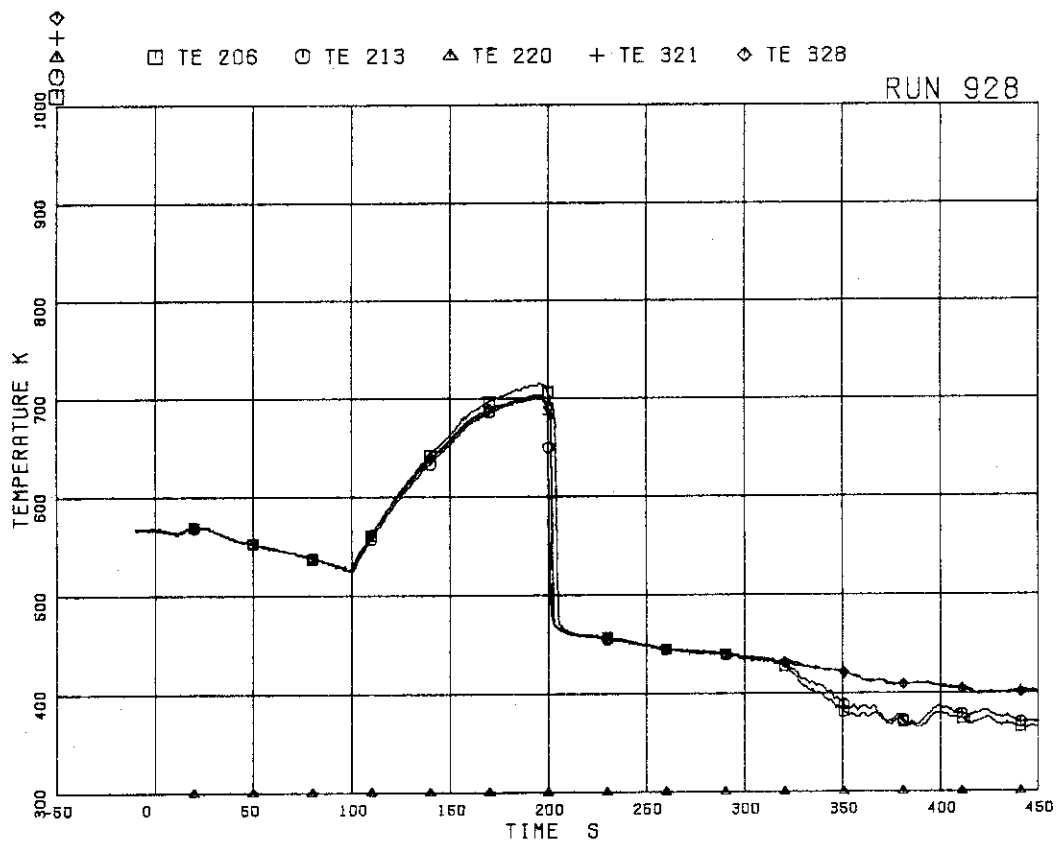


FIG. 5.150 SURFACE TEMPERATURES OF FUEL RODS A11, A12, A13, A87, A88 AT POSITION 6

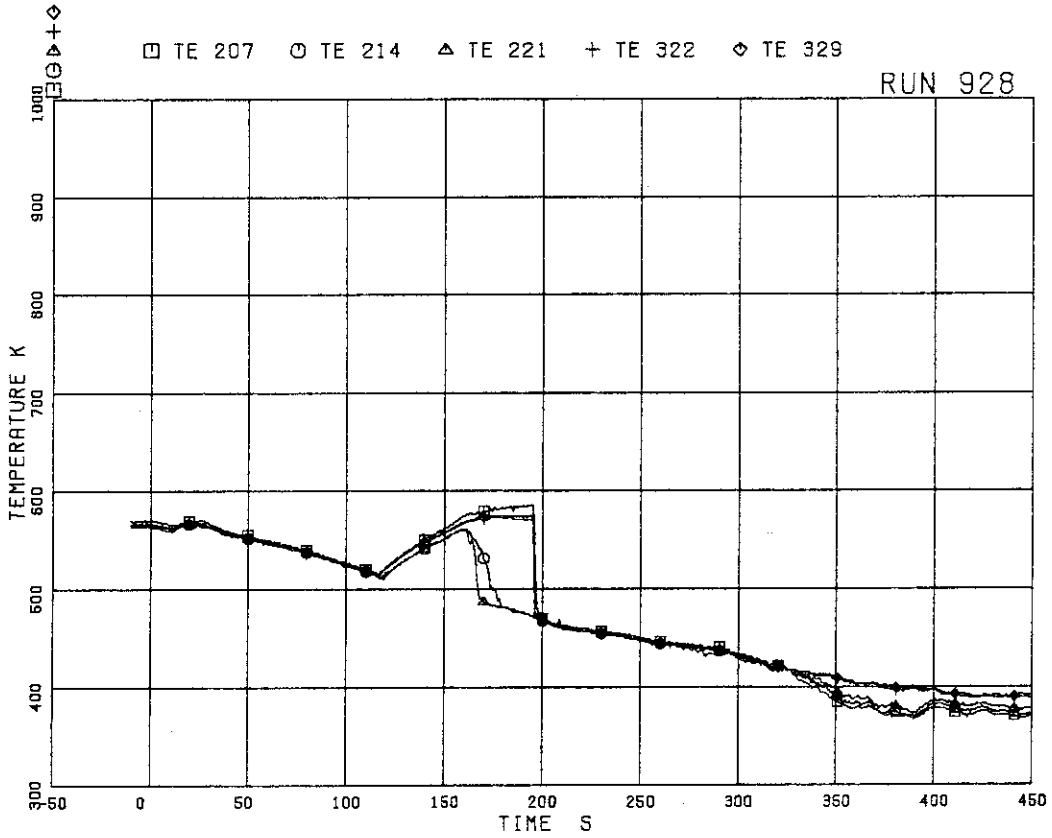


FIG.5.151 SURFACE TEMPERATURES OF FUEL RODS  
A11, A12, A13, A87, A88 AT POSITION 7

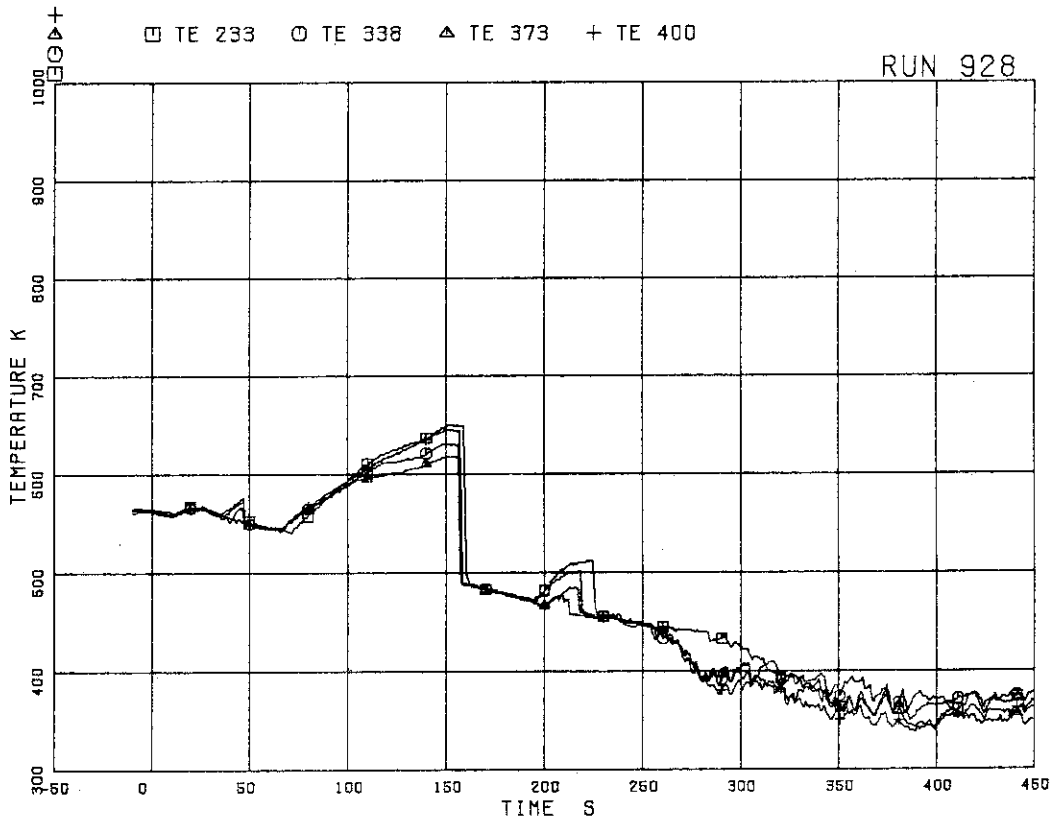


FIG.5.152 SURFACE TEMPERATURES OF FUEL RODS  
A22, B22, C22, D22 AT POSITION 1

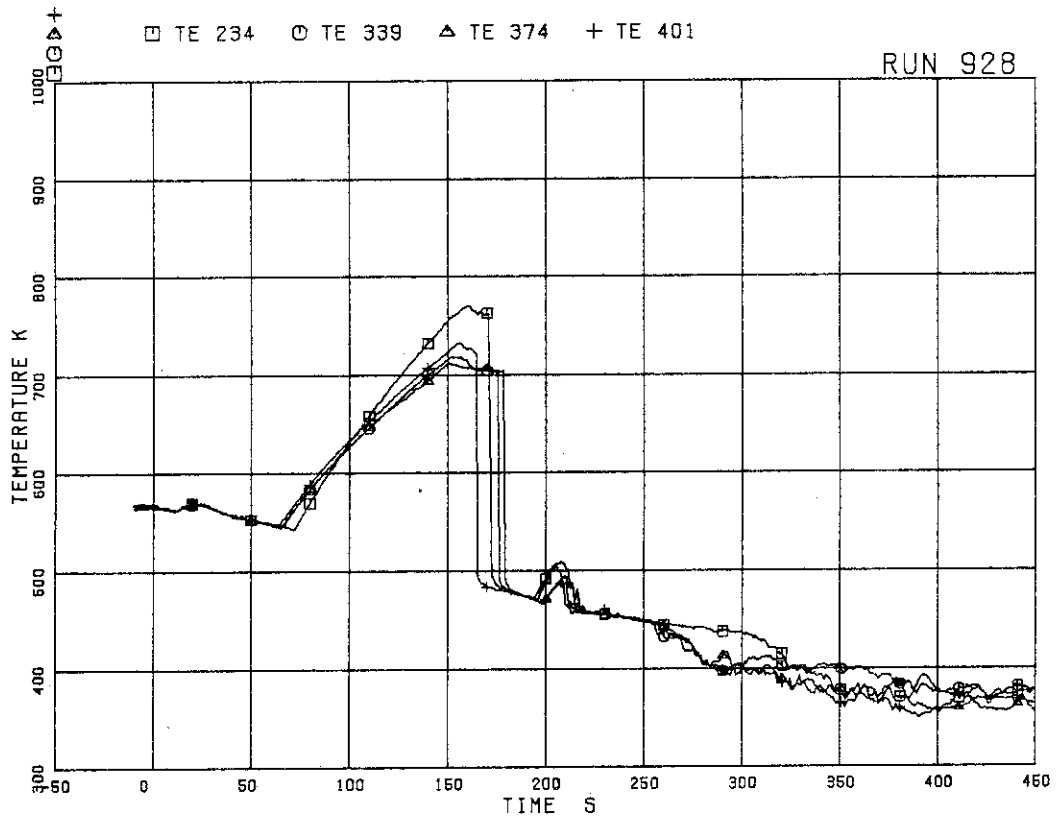


FIG.5.153 SURFACE TEMPERATURES OF FUEL RODS  
A22,B22,C22,D22 AT POSITION 2

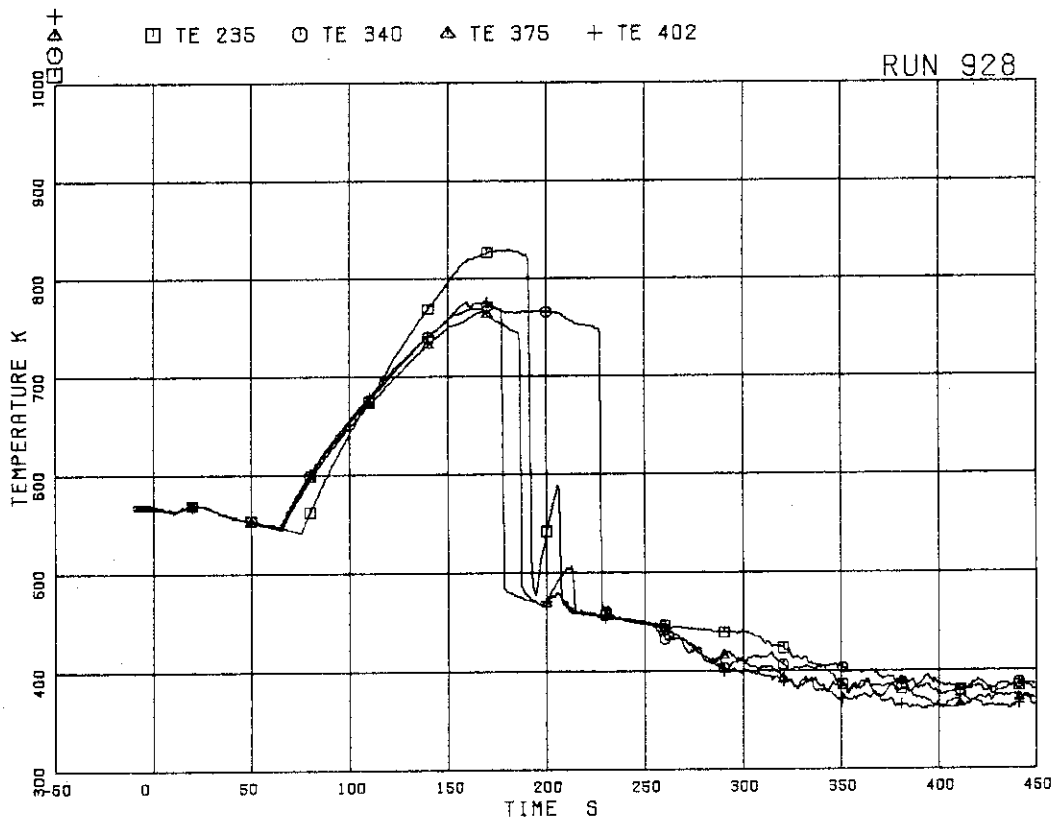


FIG.5.154 SURFACE TEMPERATURES OF FUEL RODS  
A22,B22,C22,D22 AT POSITION 3

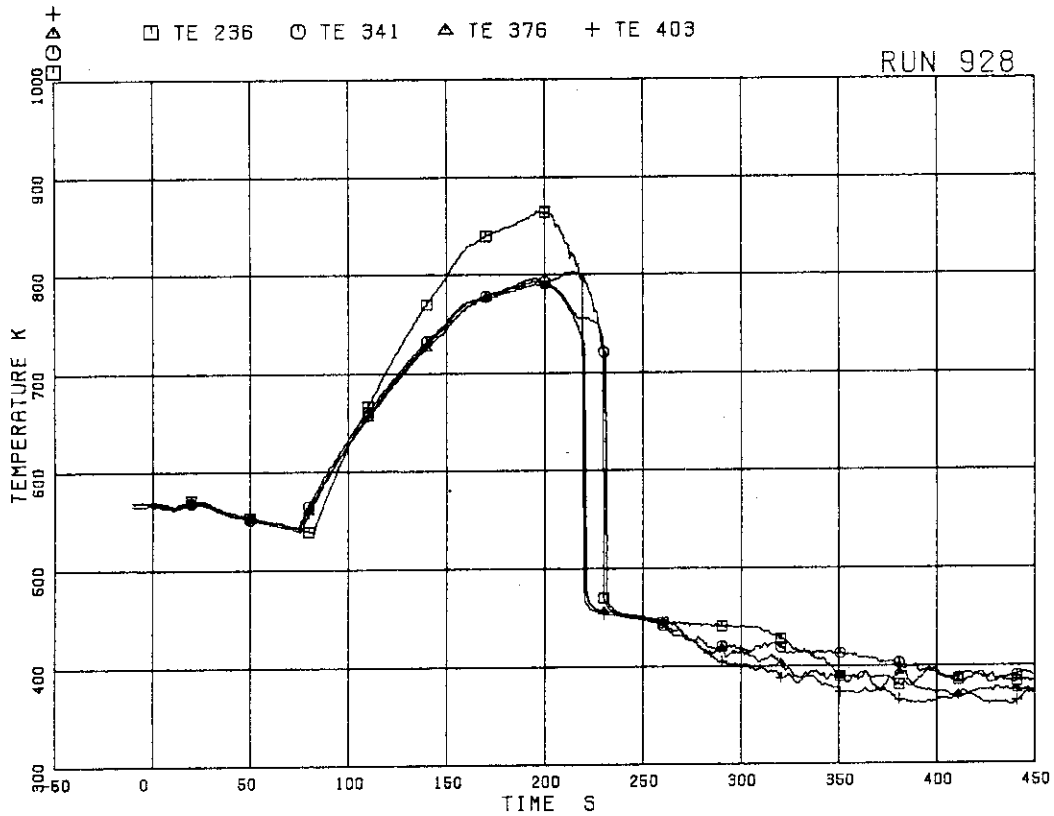


FIG.5.155 SURFACE TEMPERATURES OF FUEL RODS A22,B22,C22,D22 AT POSITION 4

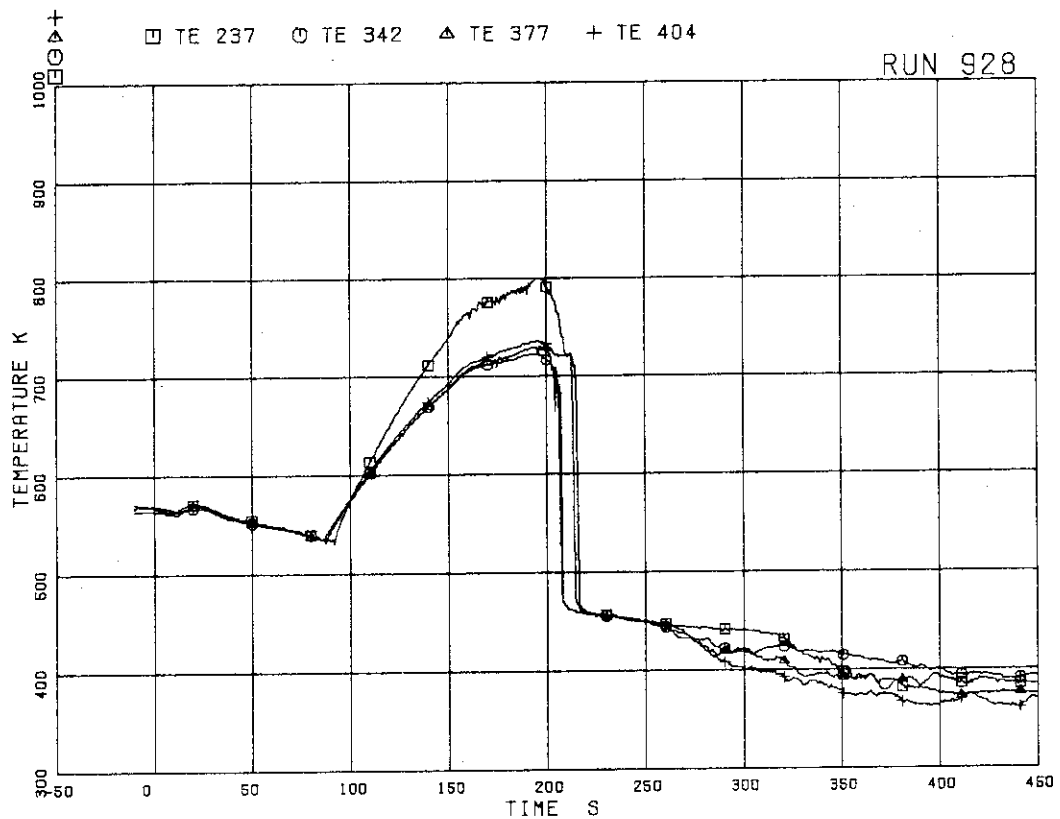


FIG.5.156 SURFACE TEMPERATURES OF FUEL RODS A22,B22,C22,D22 AT POSITION 5

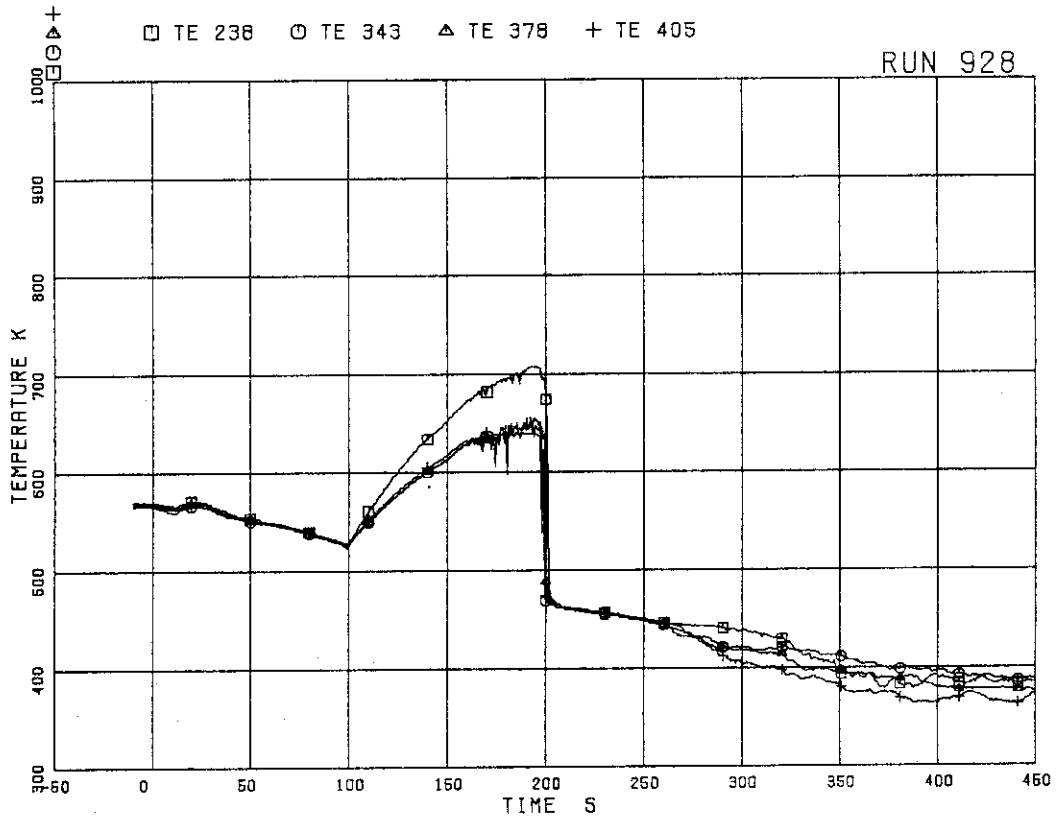


FIG.5.157 SURFACE TEMPERATURES OF FUEL RODS A22,B22,C22,D22 AT POSITION 6

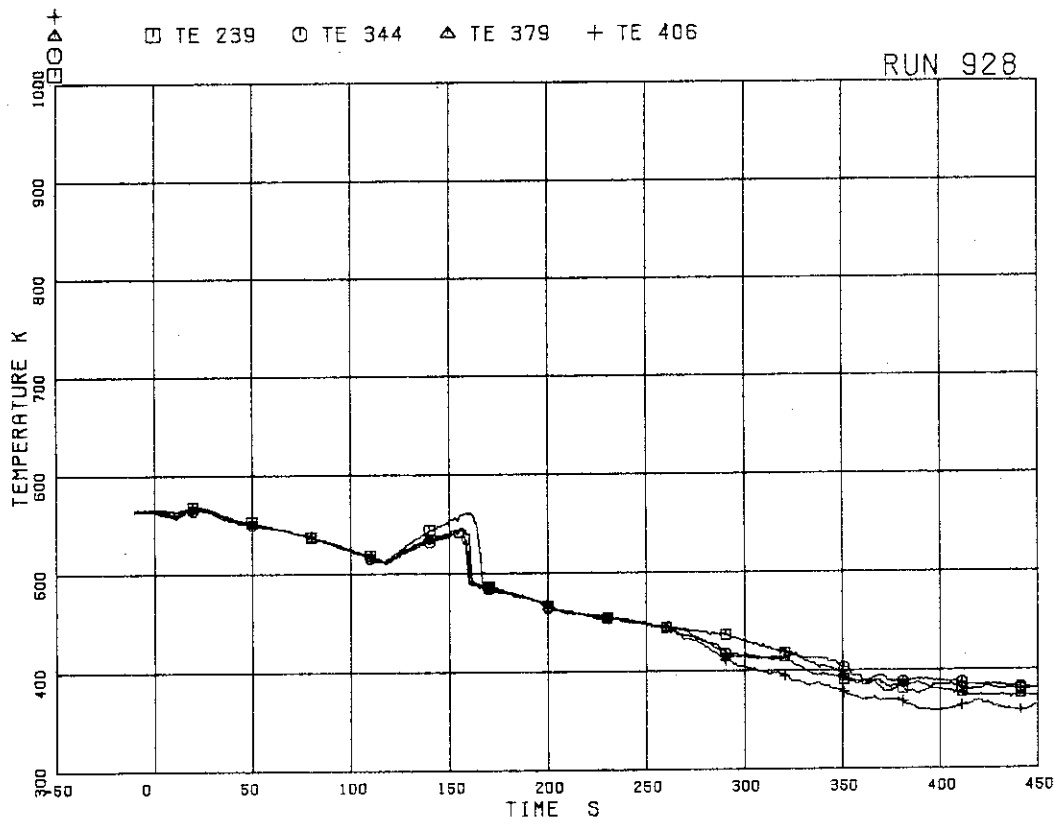


FIG.5.158 SURFACE TEMPERATURES OF FUEL RODS A22,B22,C22,D22 AT POSITION 7



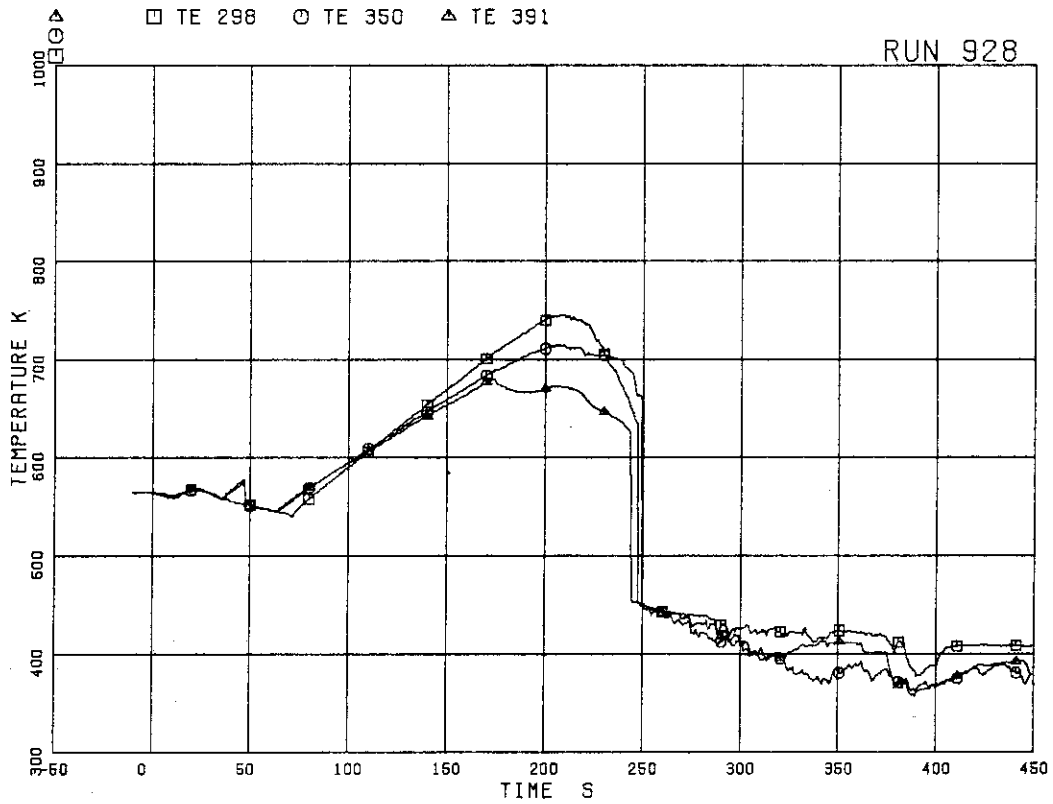


FIG.5.159 SURFACE TEMPERATURES OF FUEL RODS  
A77,B77,C77 AT POSITION 1

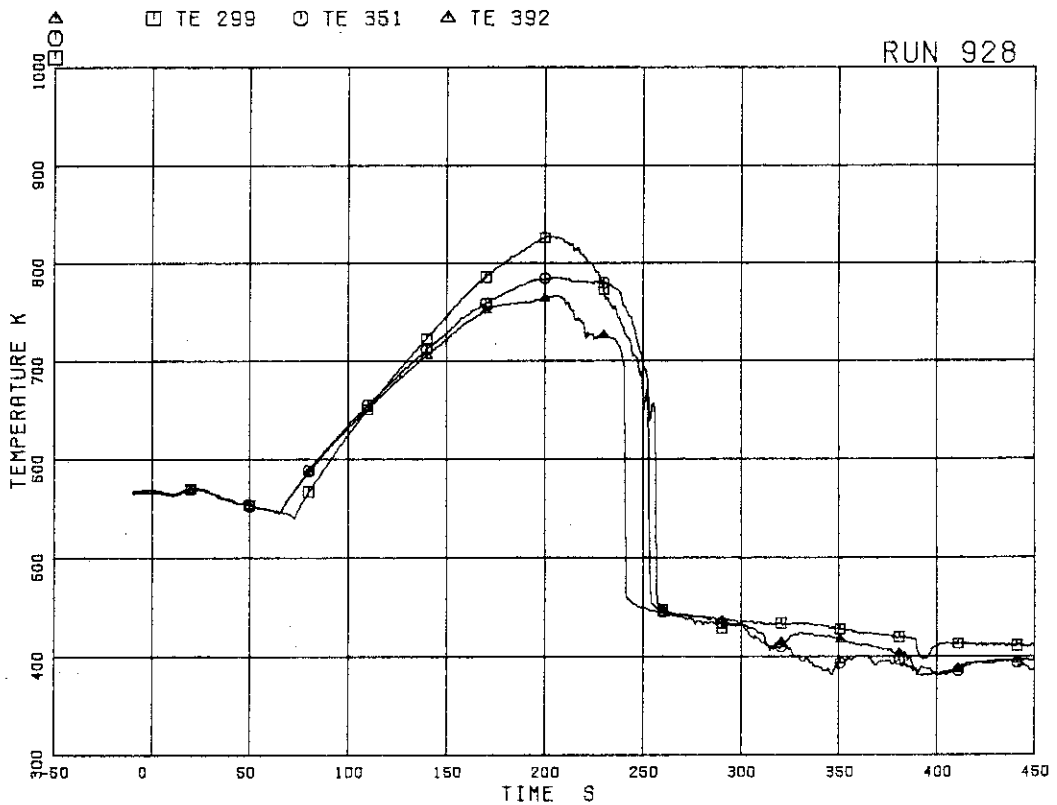


FIG.5.160 SURFACE TEMPERATURES OF FUEL RODS  
A77,B77,C77 AT POSITION 2

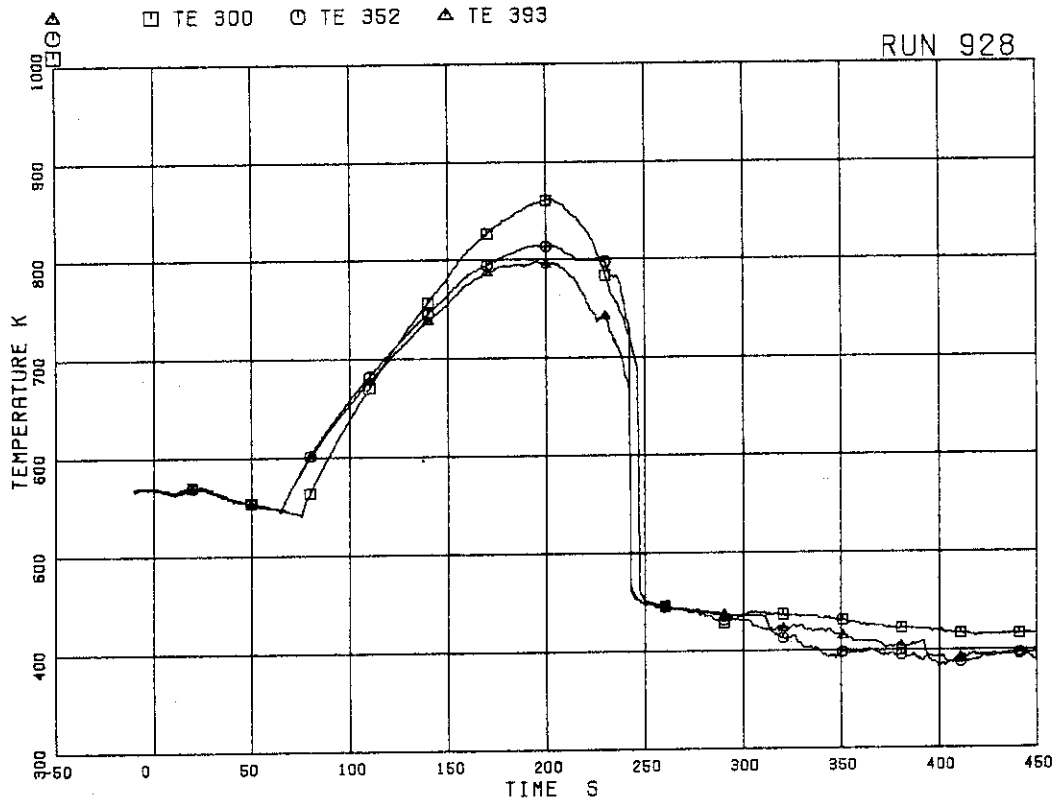


FIG.5.161 SURFACE TEMPERATURES OF FUEL RODS  
A77,B77,C77 AT POSITION 3

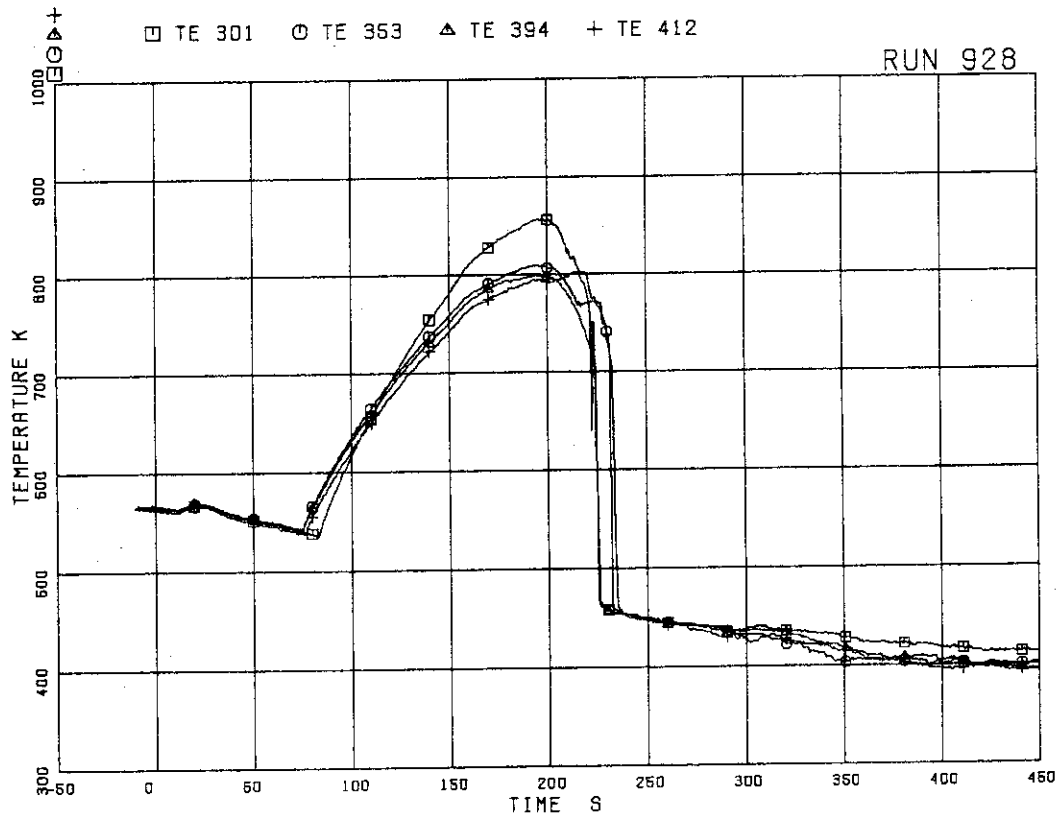


FIG.5.162 SURFACE TEMPERATURES OF FUEL RODS  
A77,B77,C77,D77 AT POSITION 4

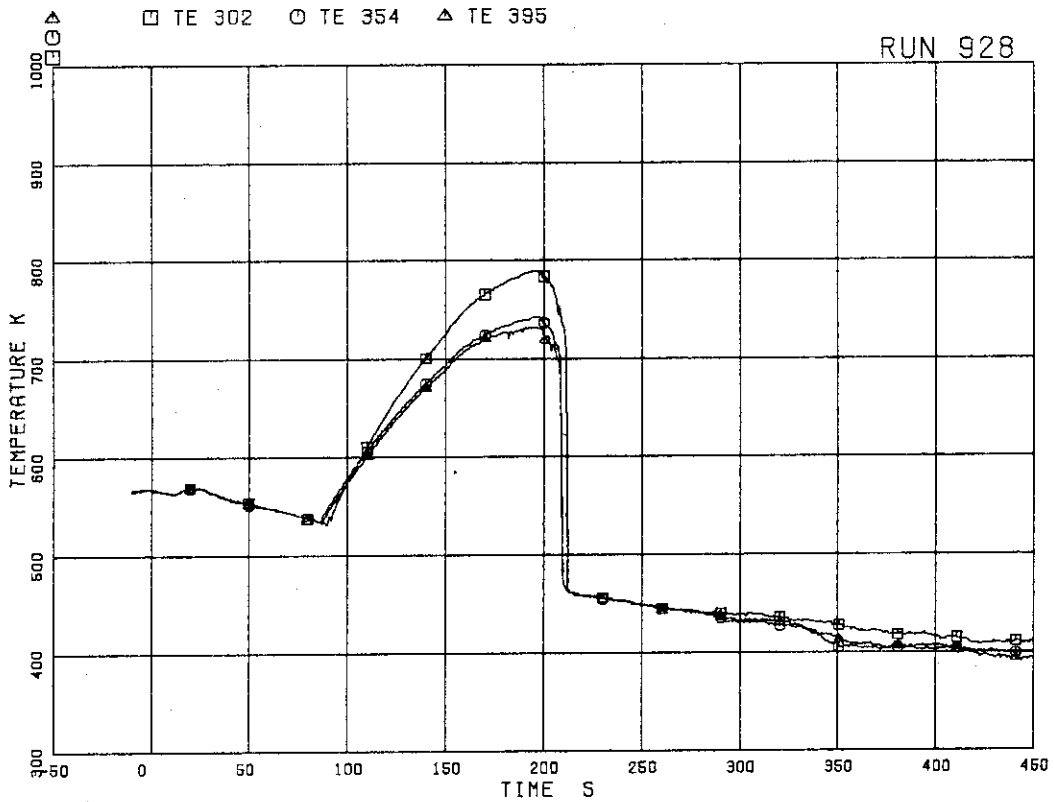


FIG.5.163 SURFACE TEMPERATURES OF FUEL RODS  
A77,B77,C77 AT POSITION 5

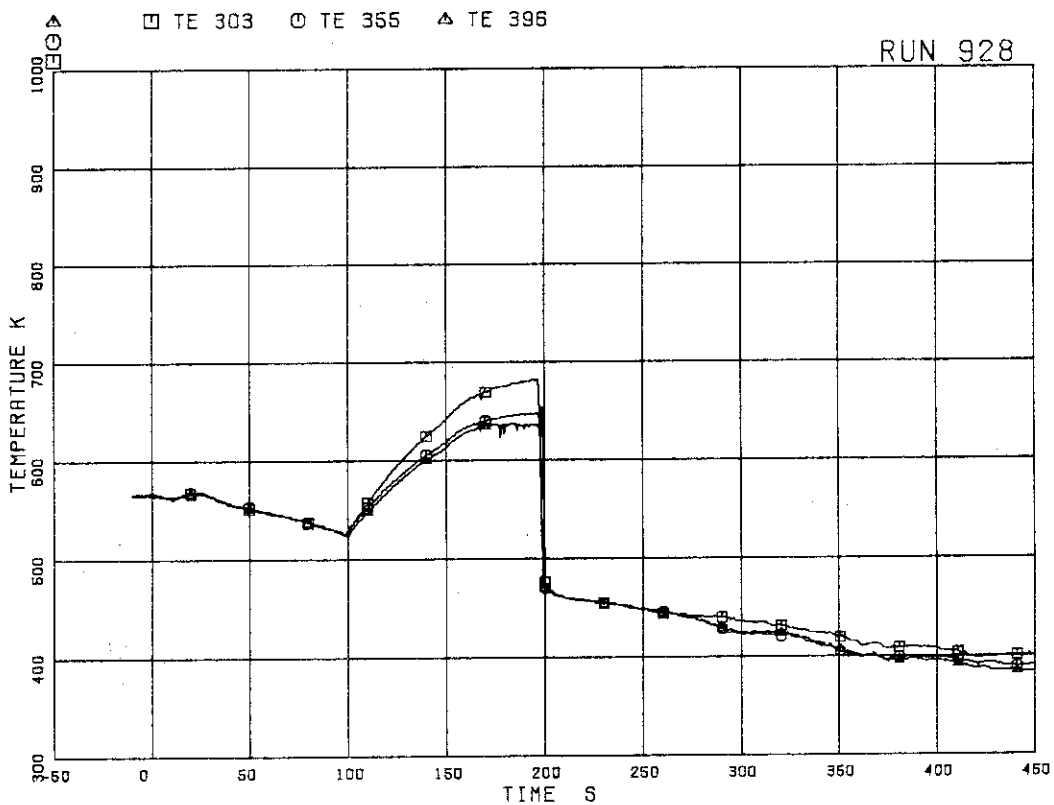


FIG.5.164 SURFACE TEMPERATURES OF FUEL RODS  
A77,B77,C77 AT POSITION 6

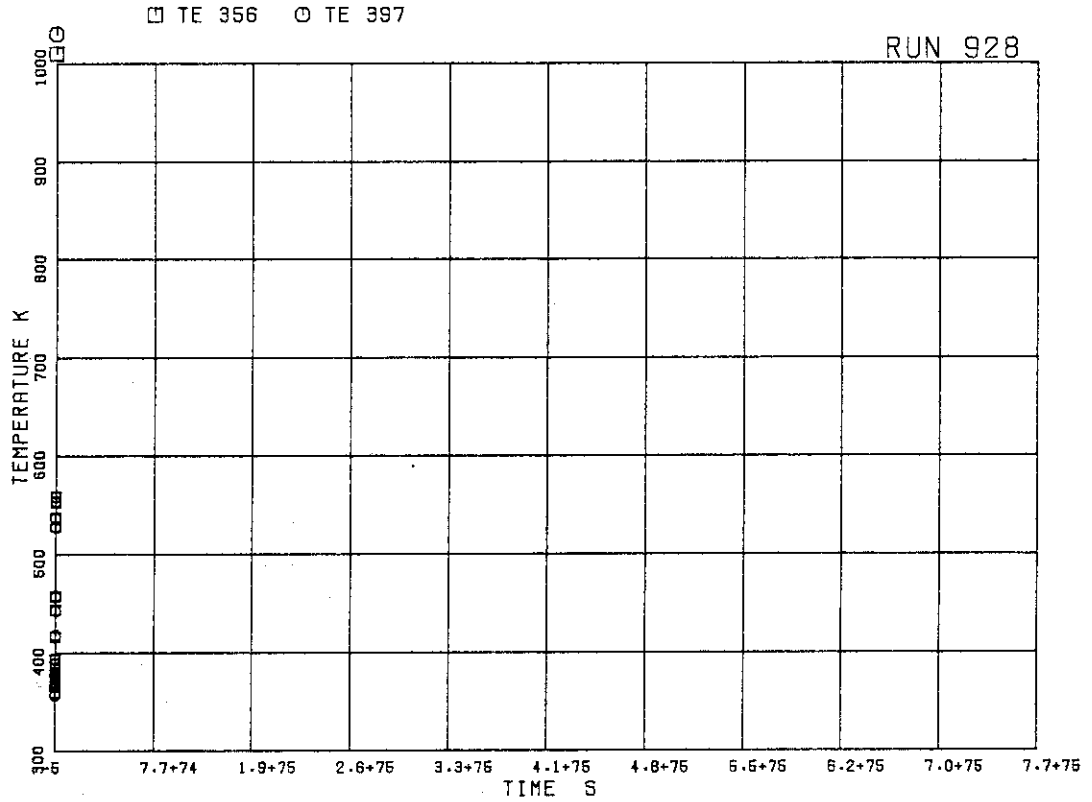


FIG.5.165 SURFACE TEMPERATURES OF FUEL RODS  
B77,C77 RODS AT POSITION 7

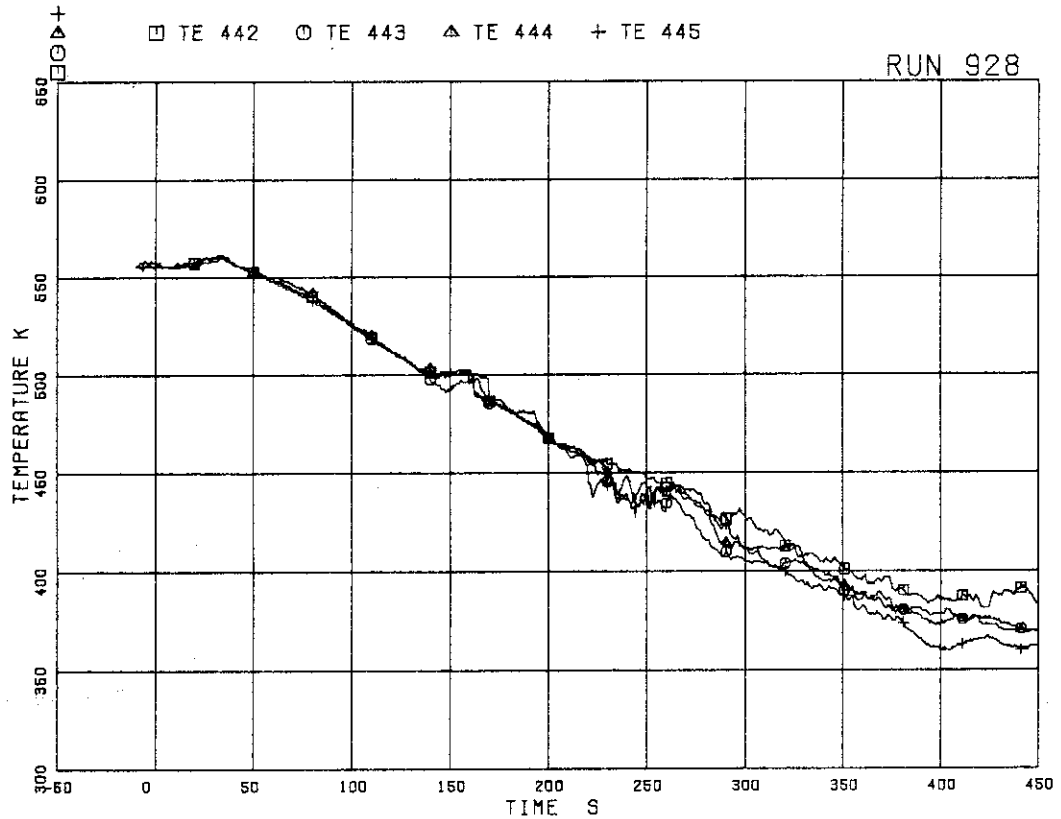


FIG.5.166 FLUID TEMPERATURES AT CHANNEL INLET

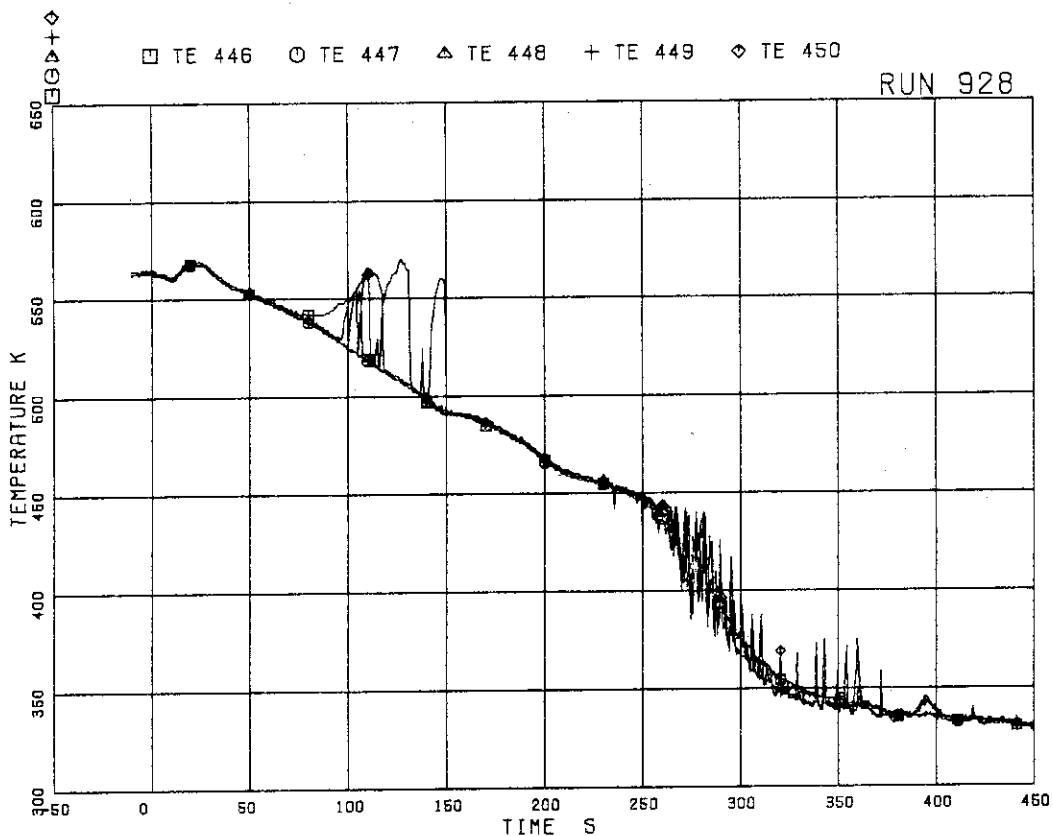


FIG.5.167 FLUID TEMPERATURES AT CHANNEL A OUTLET

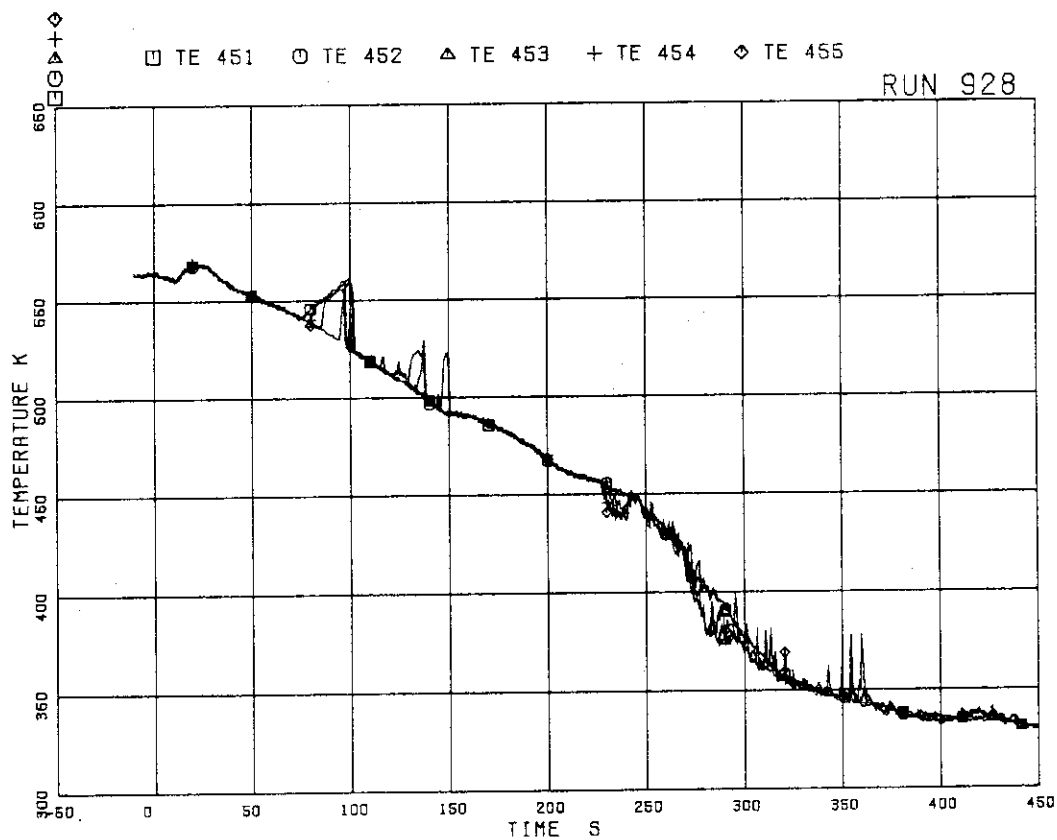


FIG.5.168 FLUID TEMPERATURES AT CHANNEL C OUTLET

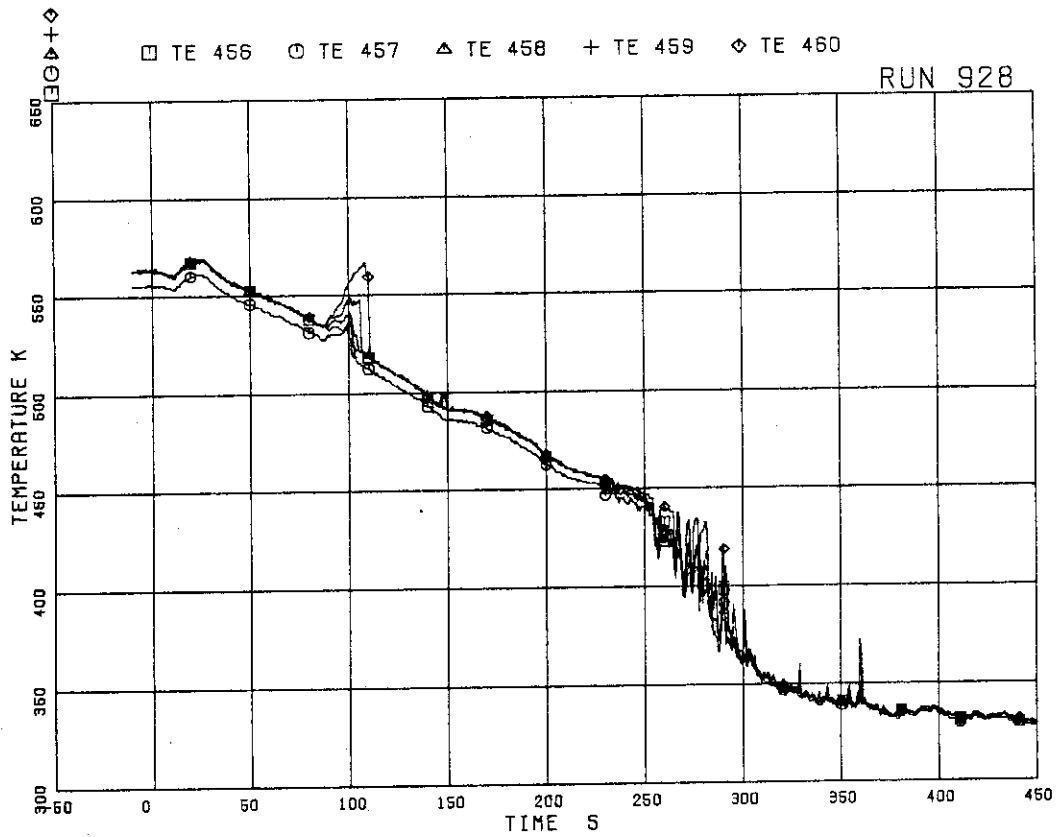


FIG.5.169 FLUID TEMPERATURES ABOVE UTP OF CHANNEL A, OPENINGS 1 TO 5

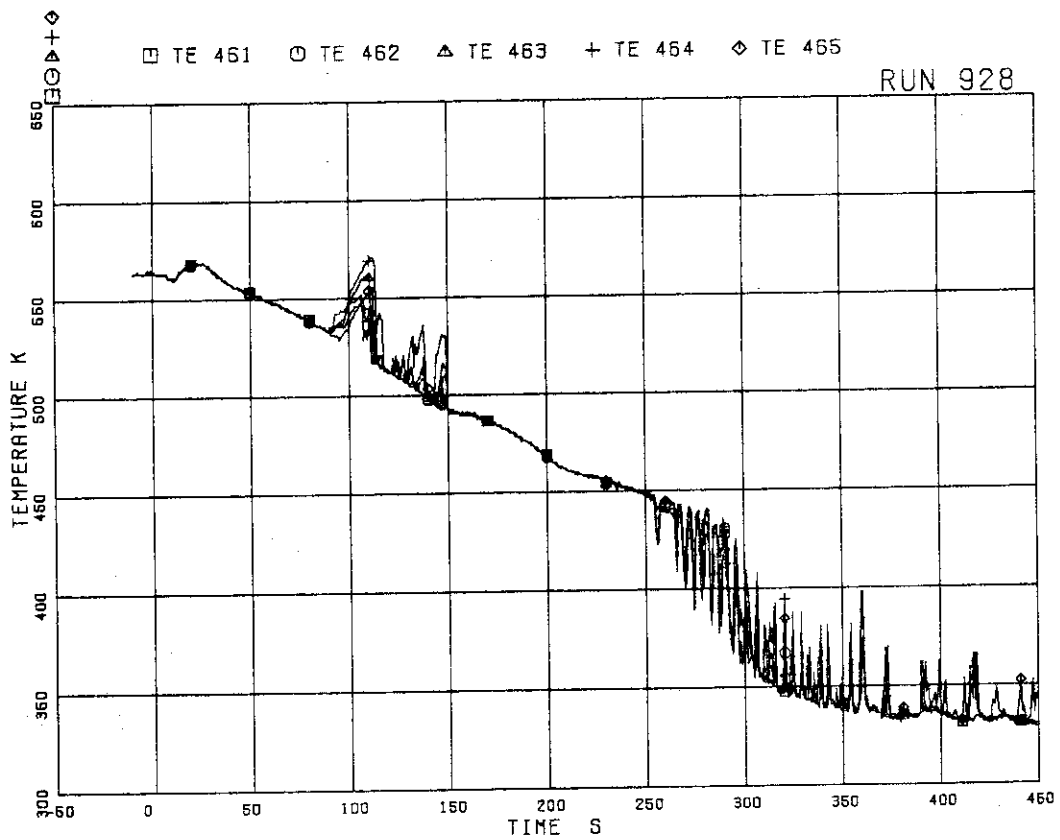


FIG.5.170 FLUID TEMPERATURES ABOVE UTP OF CHANNEL A, OPENINGS 6 TO 10

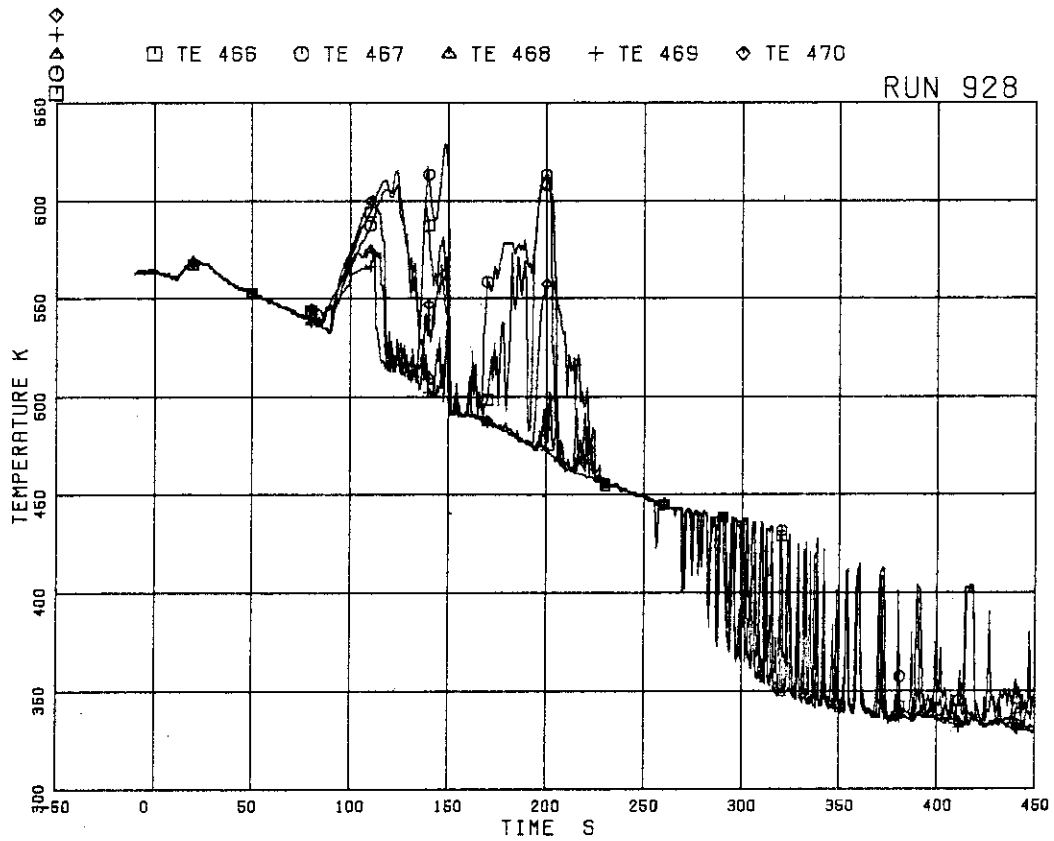


FIG.5.171 FLUID TEMPERATURES ABOVE UTP OF CHANNEL A, OPENINGS 1 TO 5

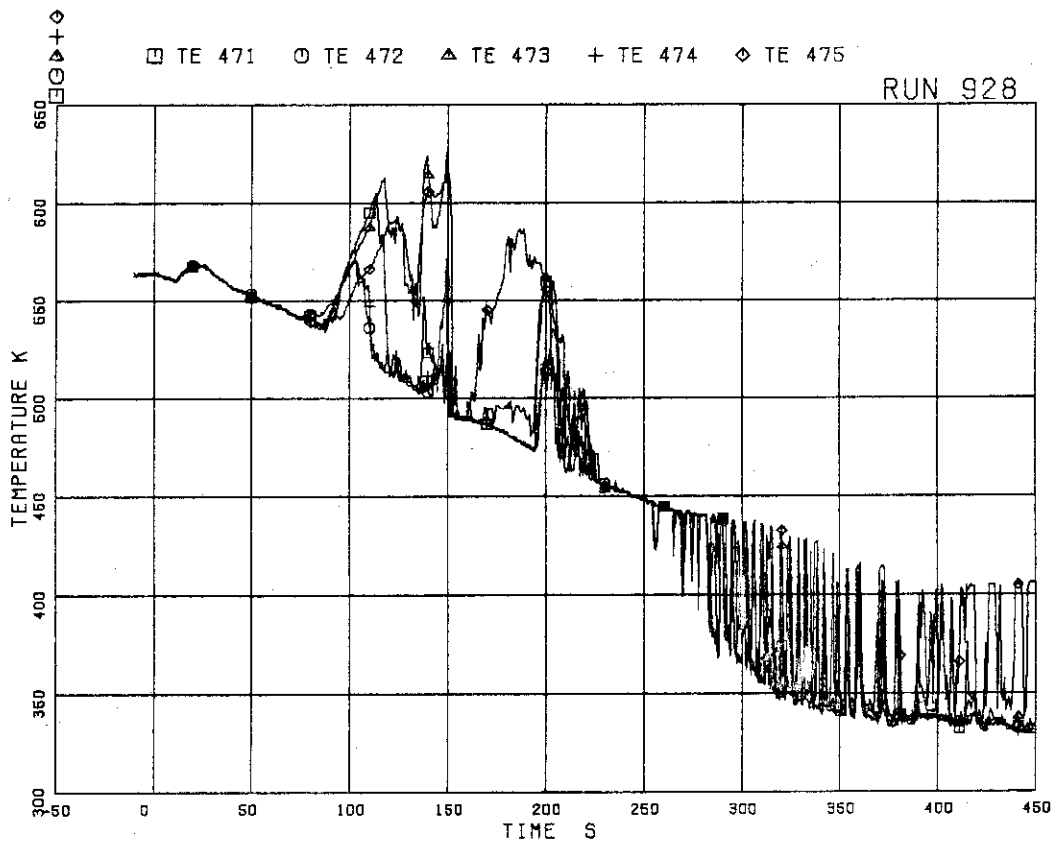


FIG.5.172 FLUID TEMPERATURES ABOVE UTP OF CHANNEL A, OPENINGS 6 TO 10

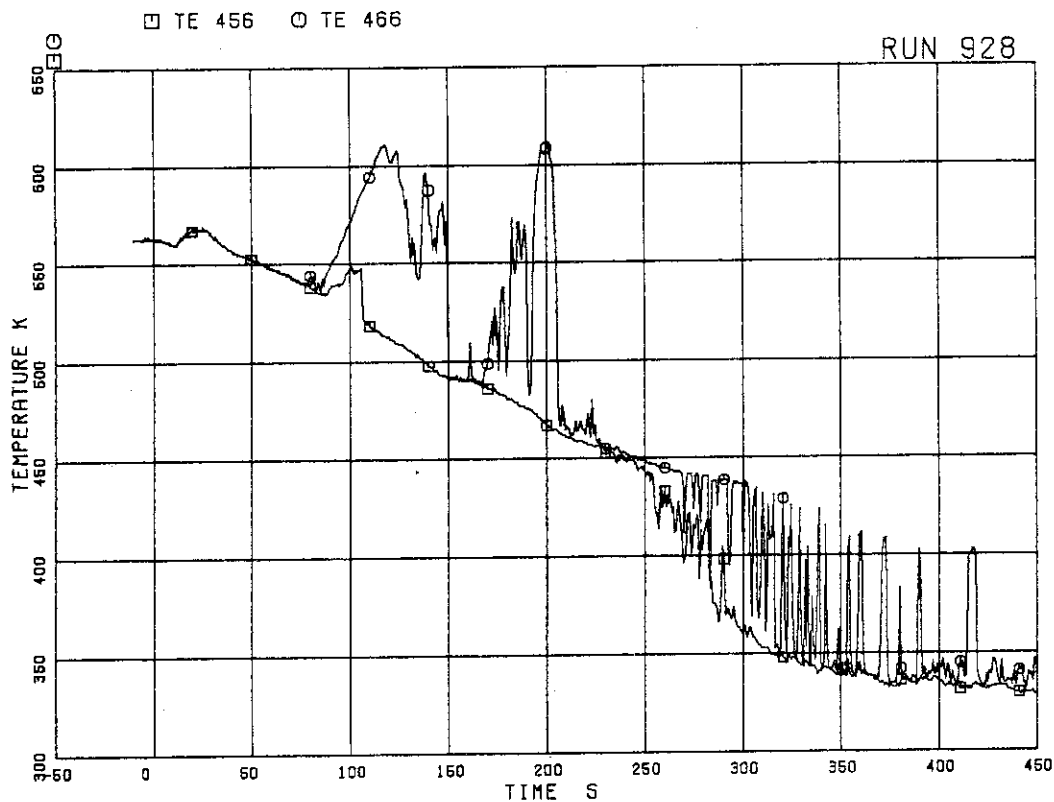


FIG.5.173 FLUID TEMPERATURES AT UTP IN CHANNEL A, OPENING 1

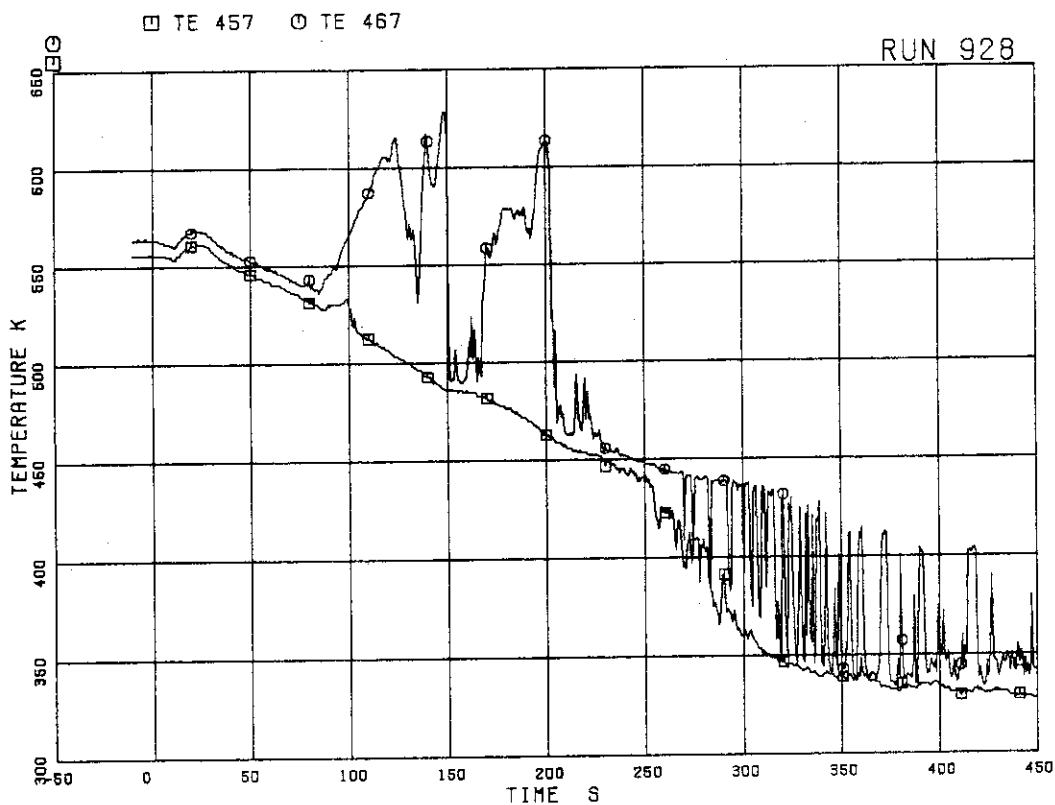


FIG.5.174 FLUID TEMPERATURES AT UTP IN CHANNEL A, OPENING 2



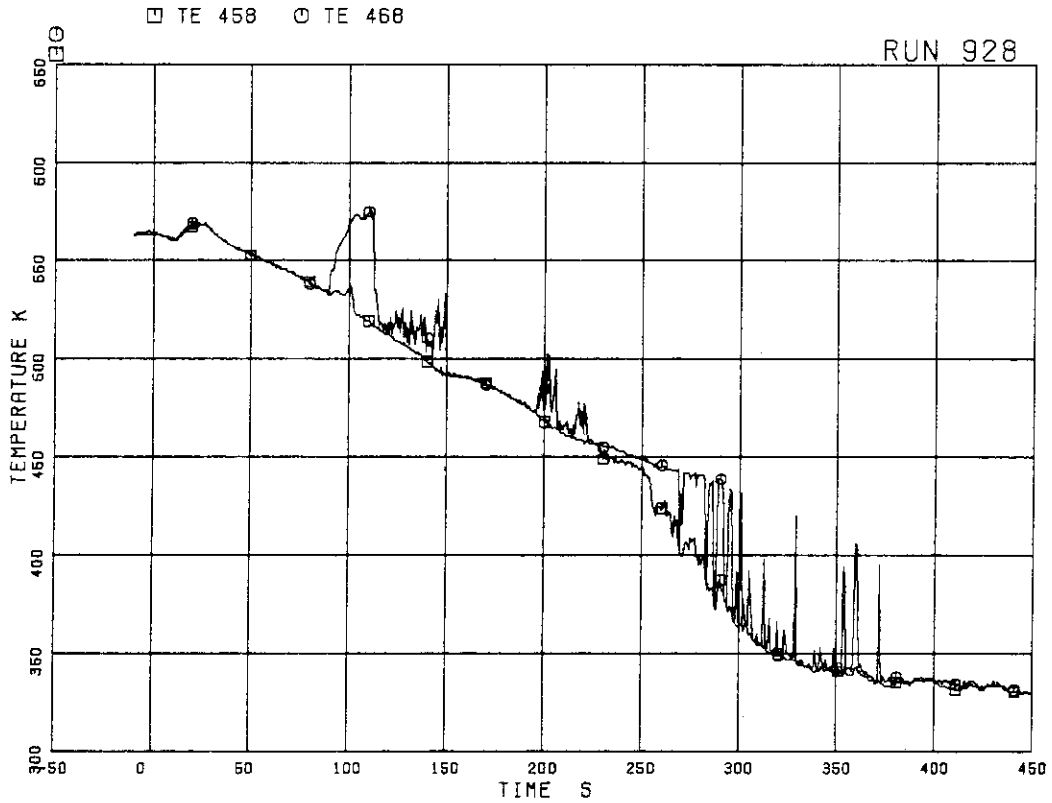


FIG. 5.175 FLUID TEMPERATURES AT UTP IN CHANNEL A, OPENING 3

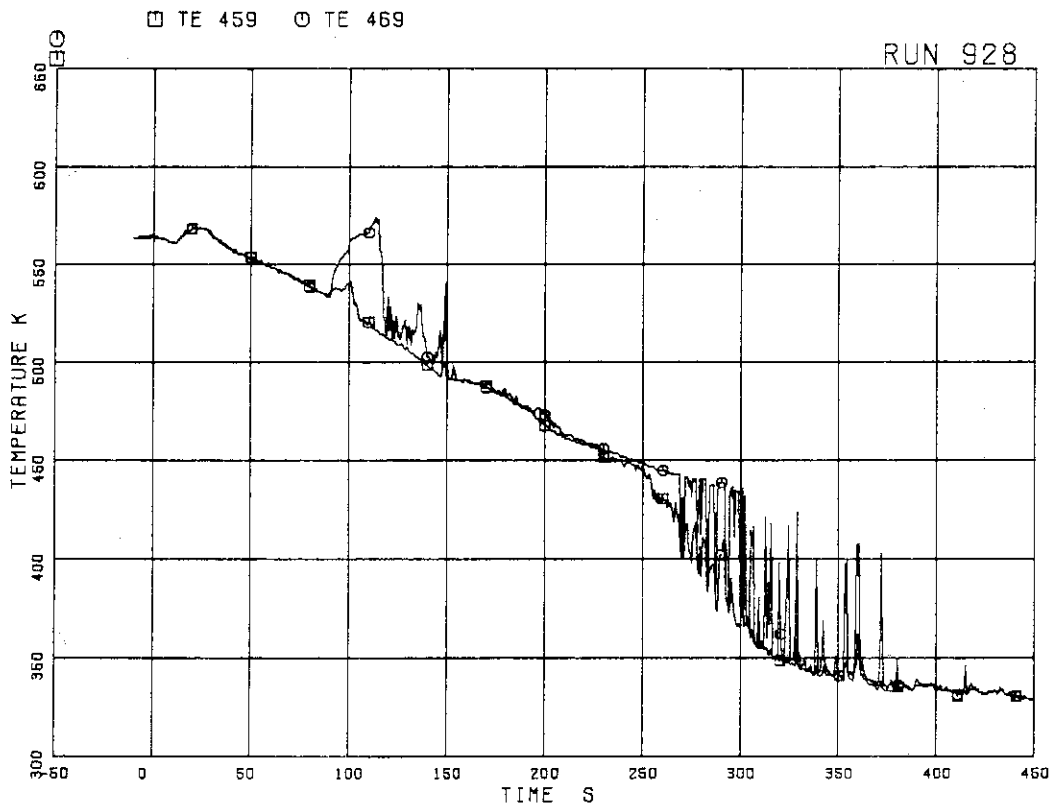


FIG. 5.176 FLUID TEMPERATURES AT UTP IN CHANNEL A, OPENING 4

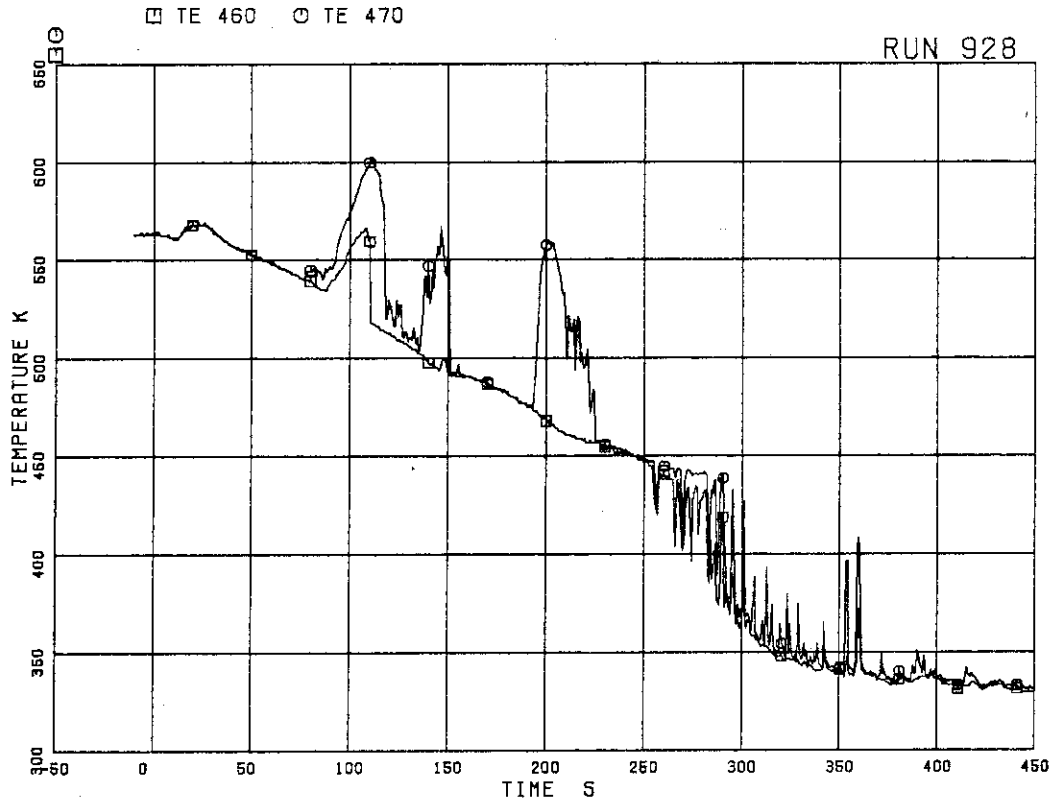


FIG.5.177 FLUID TEMPERATURES AT UTP IN CHANNEL A, OPENING 5

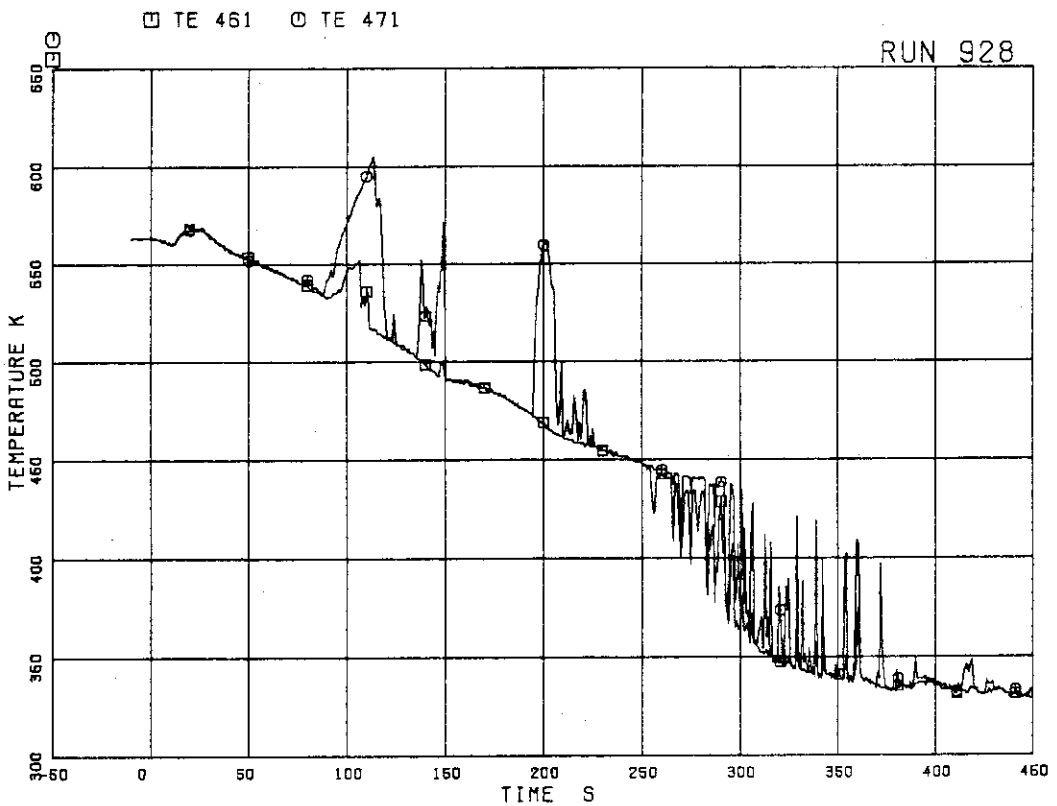


FIG.5.178 FLUID TEMPERATURES AT UTP IN CHANNEL A, OPENING 6

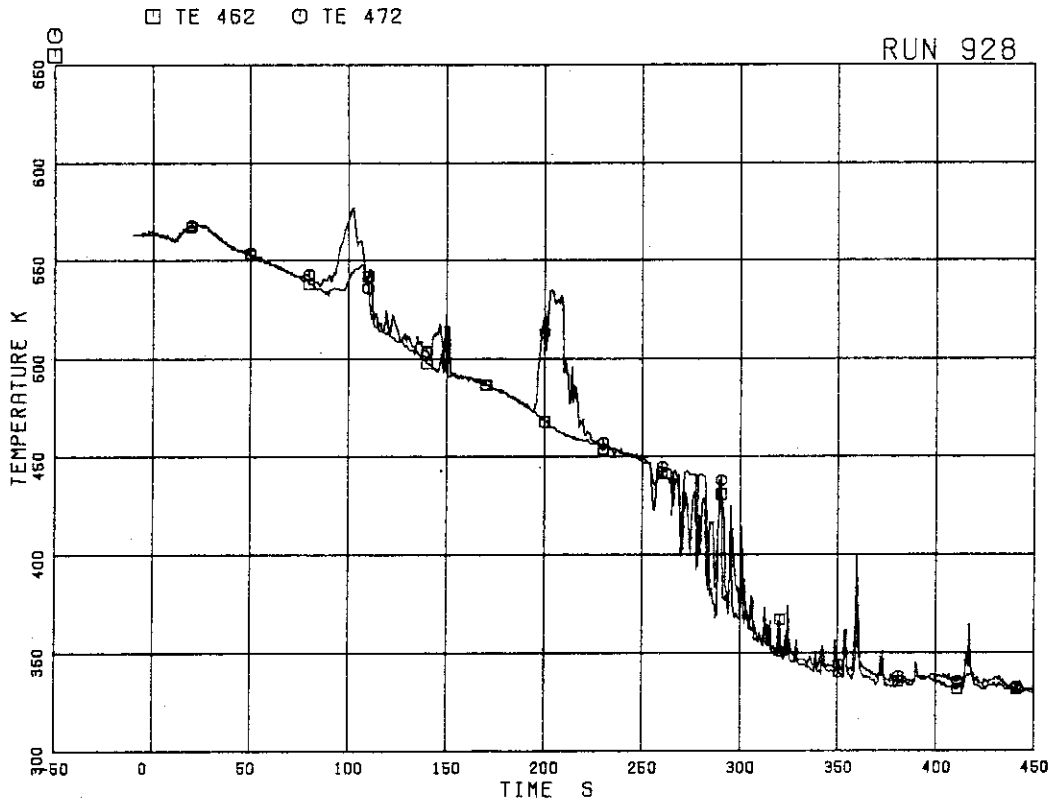


FIG.5.179 FLUID TEMPERATURES AT UTP IN CHANNEL A, OPENING 7

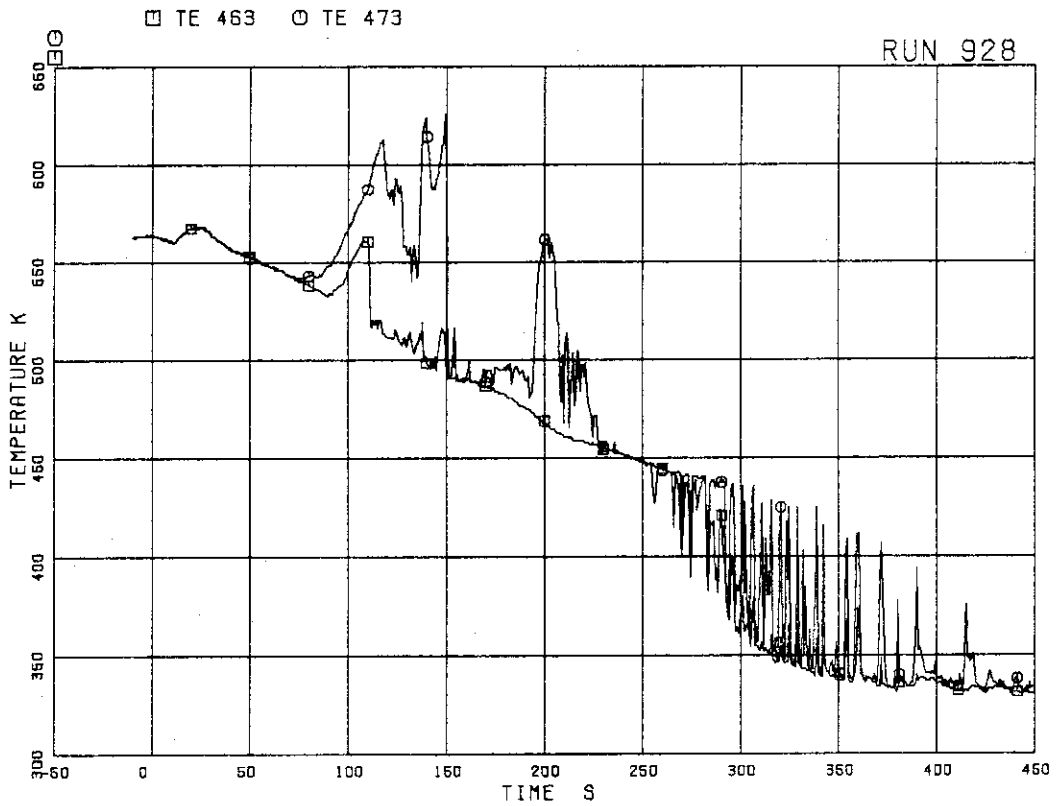


FIG.5.180 FLUID TEMPERATURES AT UTP IN CHANNEL A, OPENING 8

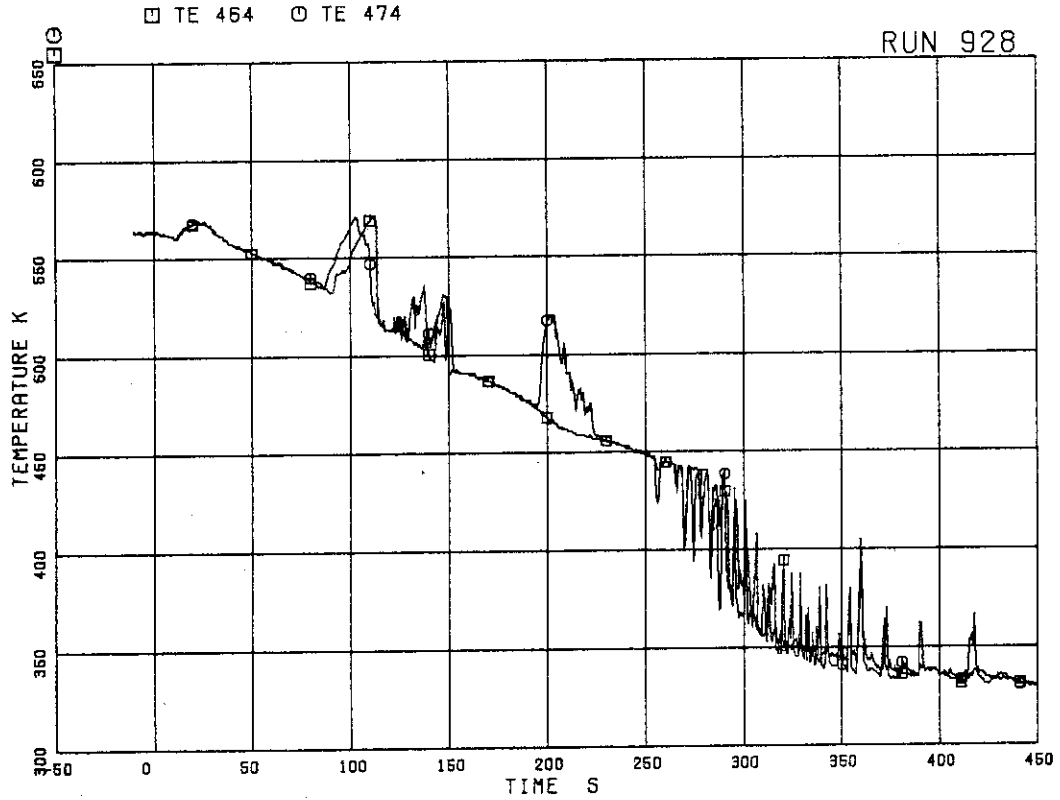


FIG.5.181 FLUID TEMPERATURES AT UTP IN CHANNEL A, OPENING 9

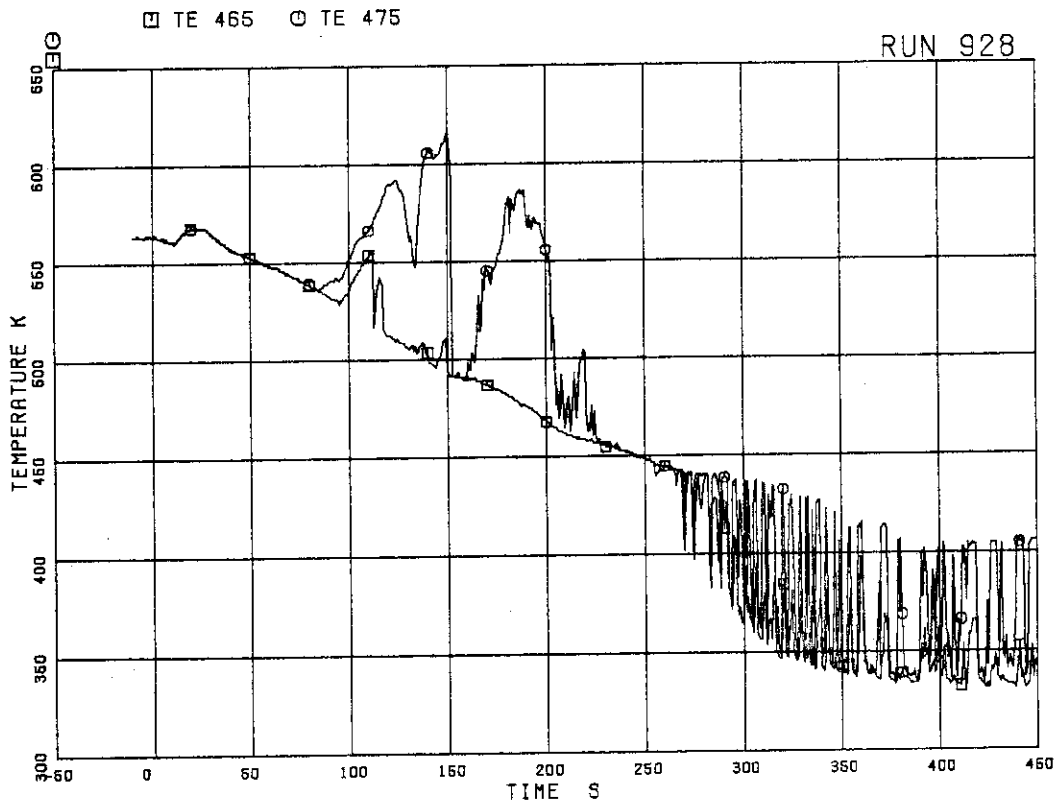


FIG.5.182 FLUID TEMPERATURES AT UTP IN CHANNEL A, OPENING 10

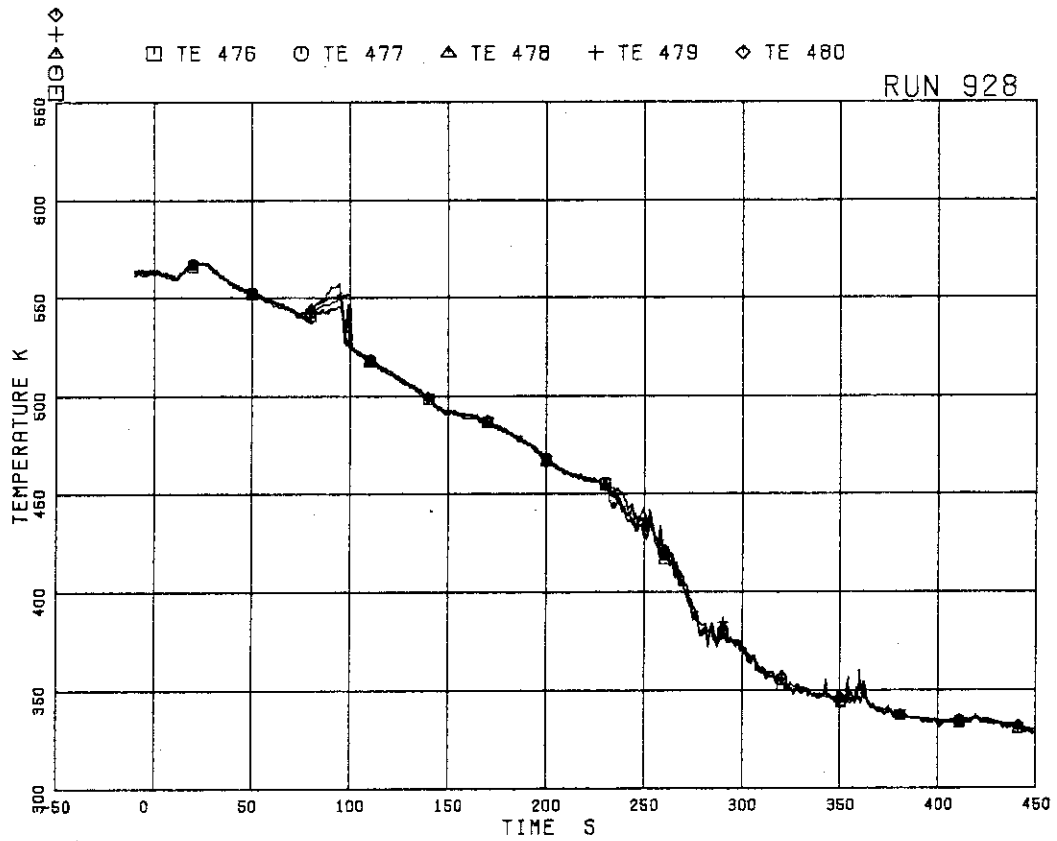


FIG.5.183 FLUID TEMPERATURES ABOVE UTP OF CHANNEL C, OPENINGS 1 TO 5

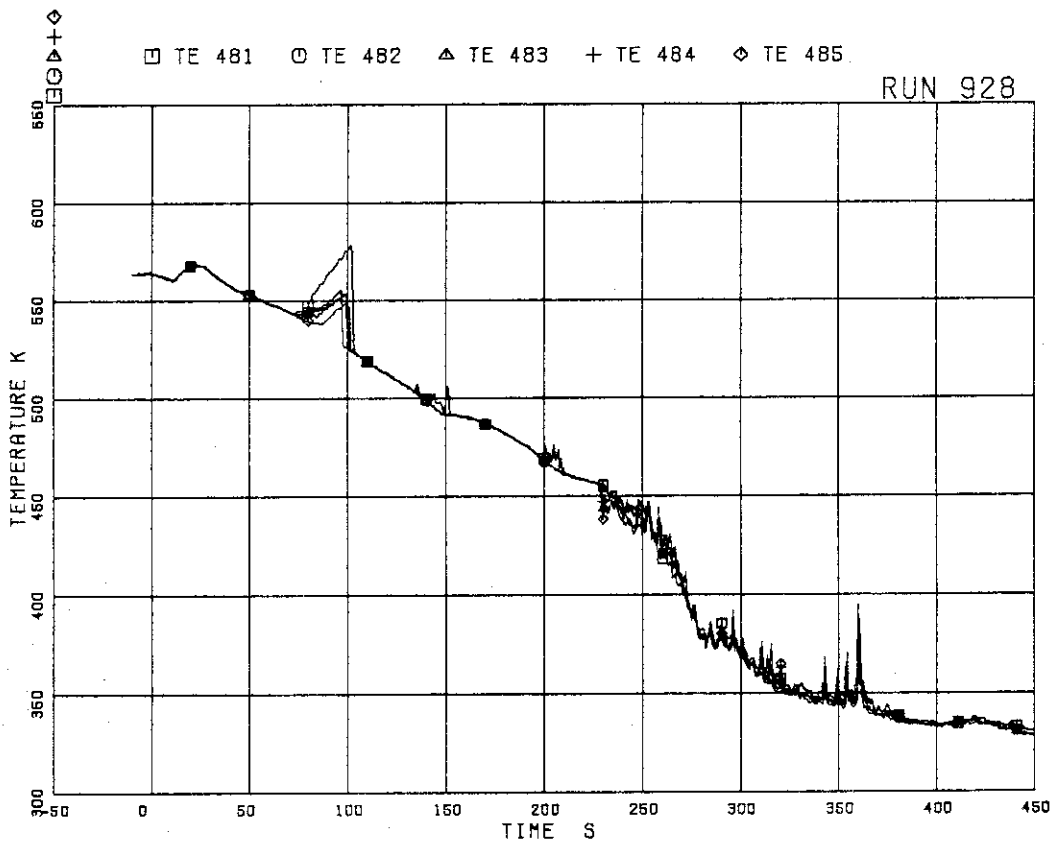


FIG.5.184 FLUID TEMPERATURES ABOVE UTP OF CHANNEL C, OPENINGS 6 TO 10

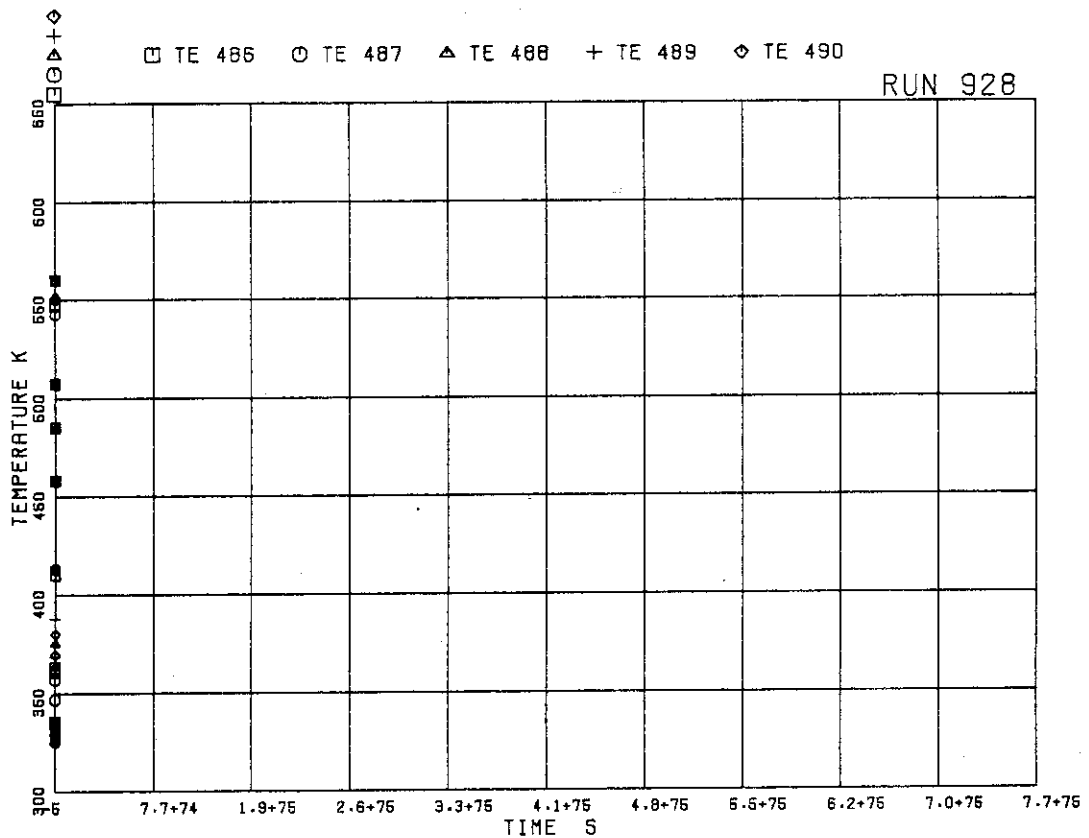


FIG.5.185 FLUID TEMPERATURES BELOW UTP OF CHANNEL C, OPENINGS 1 TO 5

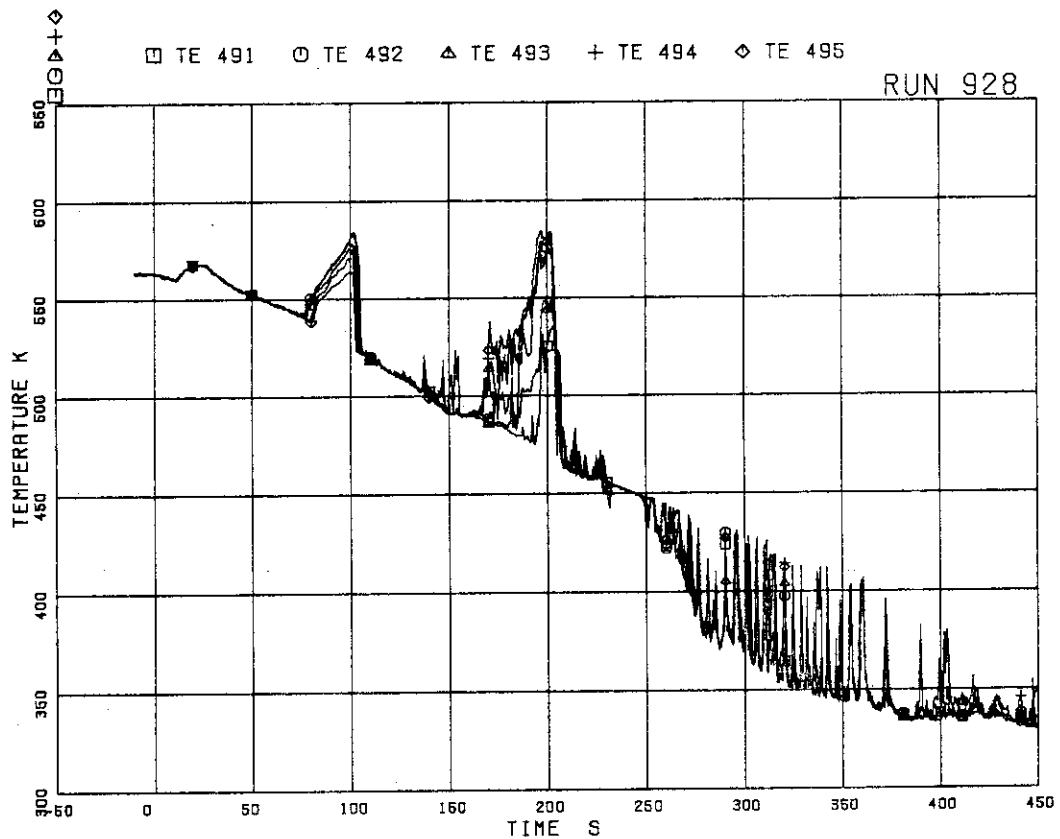


FIG.5.186 FLUID TEMPERATURES BELOW UTP OF CHANNEL C, OPENINGS 6 TO 10

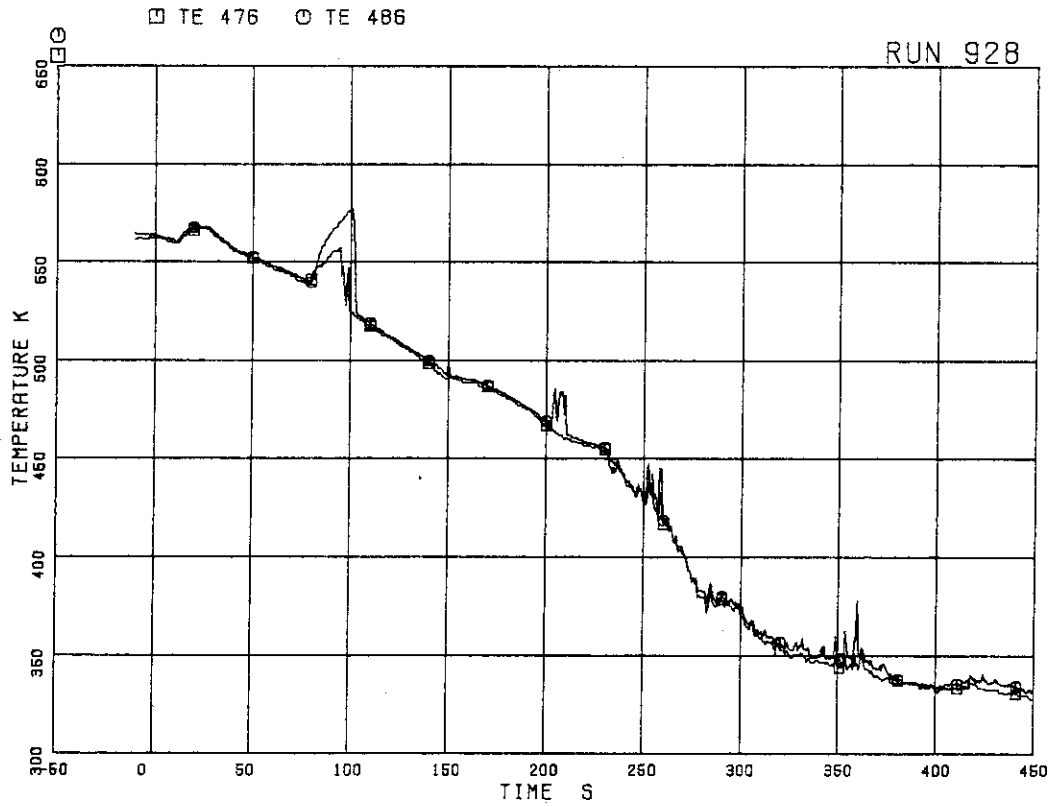


FIG. 5.187 FLUID TEMPERATURES AT UTP IN CHANNEL C, OPENING 1

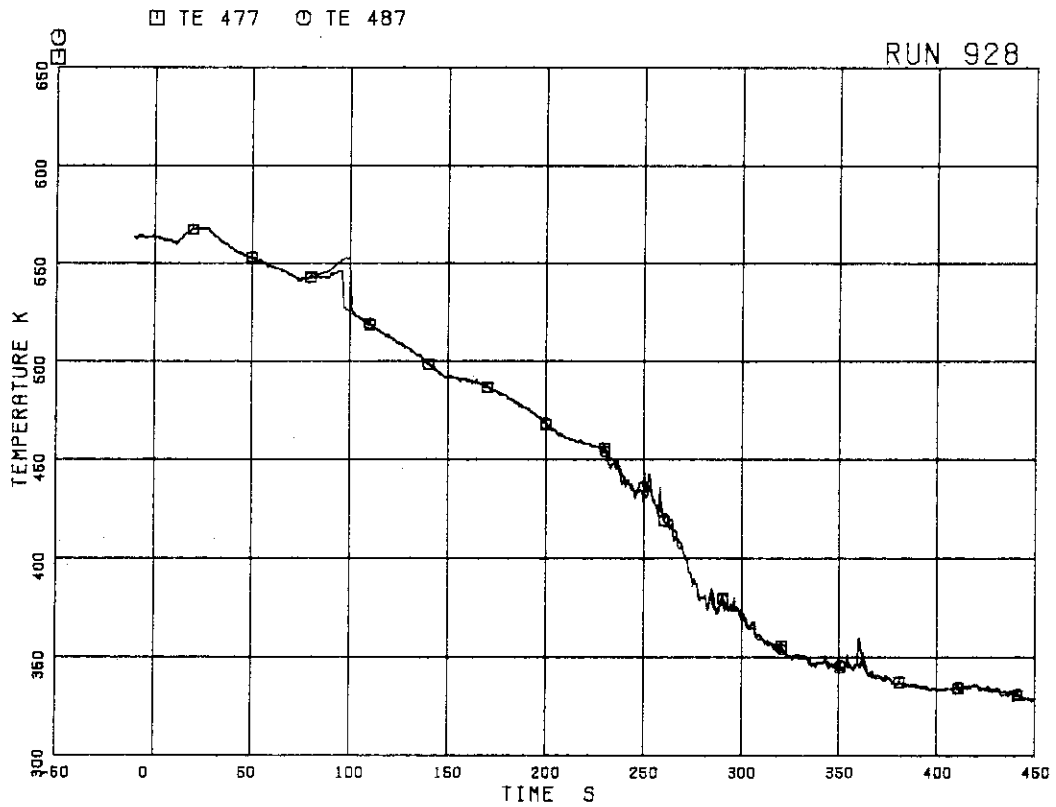


FIG. 5.188 FLUID TEMPERATURES AT UTP IN CHANNEL C, OPENING 2

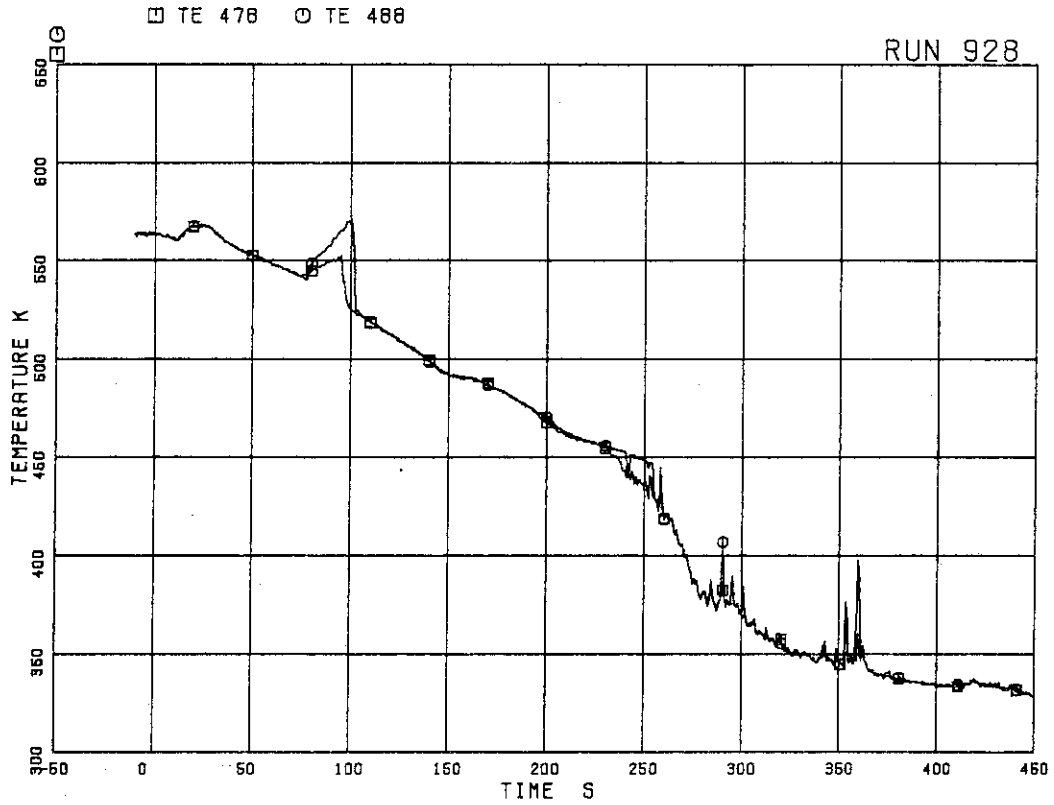


FIG.5.189 FLUID TEMPERATURES AT UTP IN CHANNEL C, OPENING 3

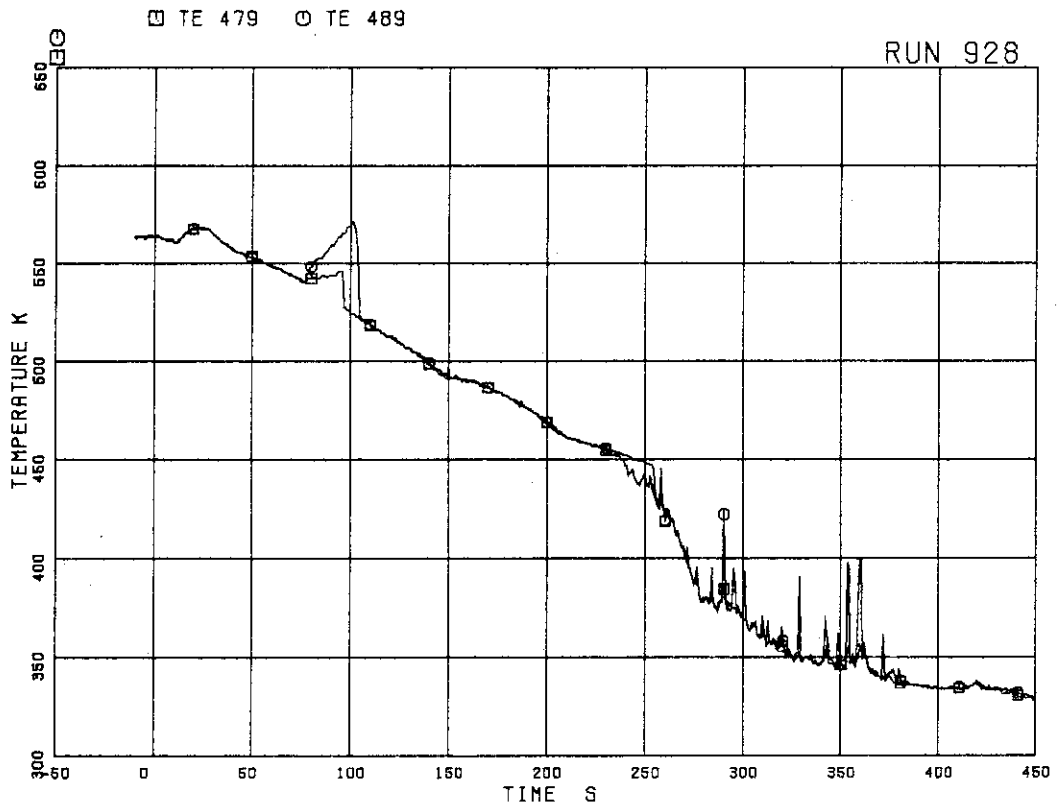


FIG.5.190 FLUID TEMPERATURES AT UTP IN CHANNEL C, OPENING 4



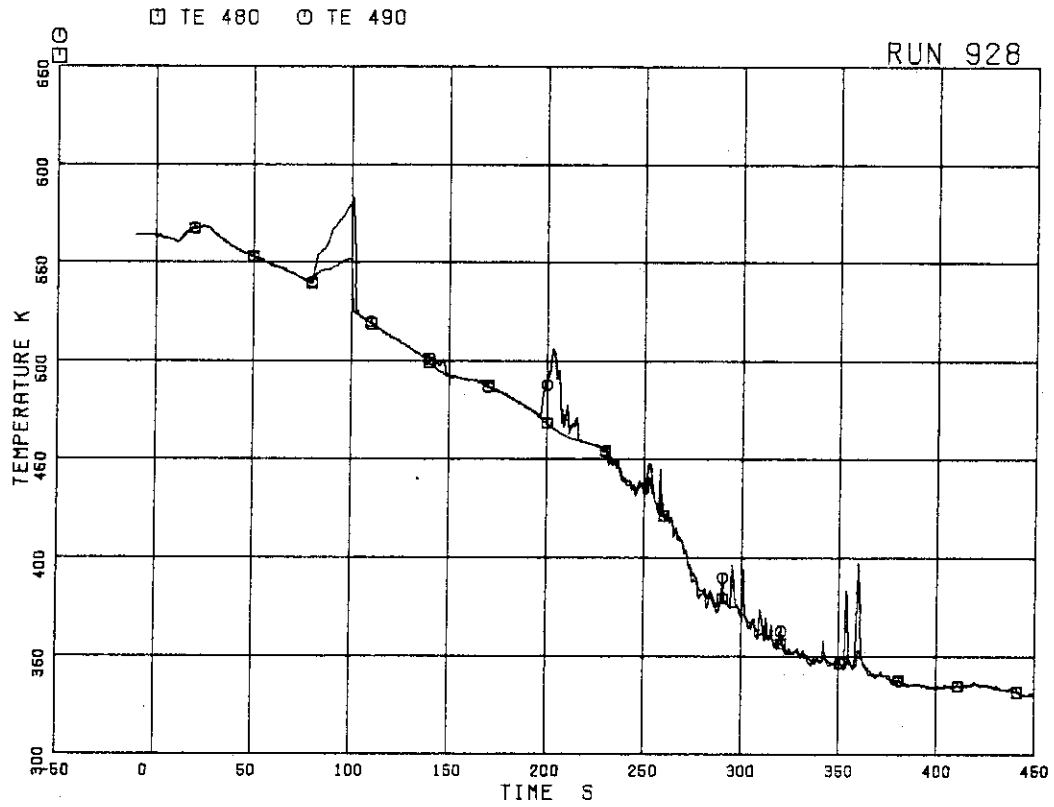


FIG.5.191 FLUID TEMPERATURES AT UTP IN CHANNEL C, OPENING 5

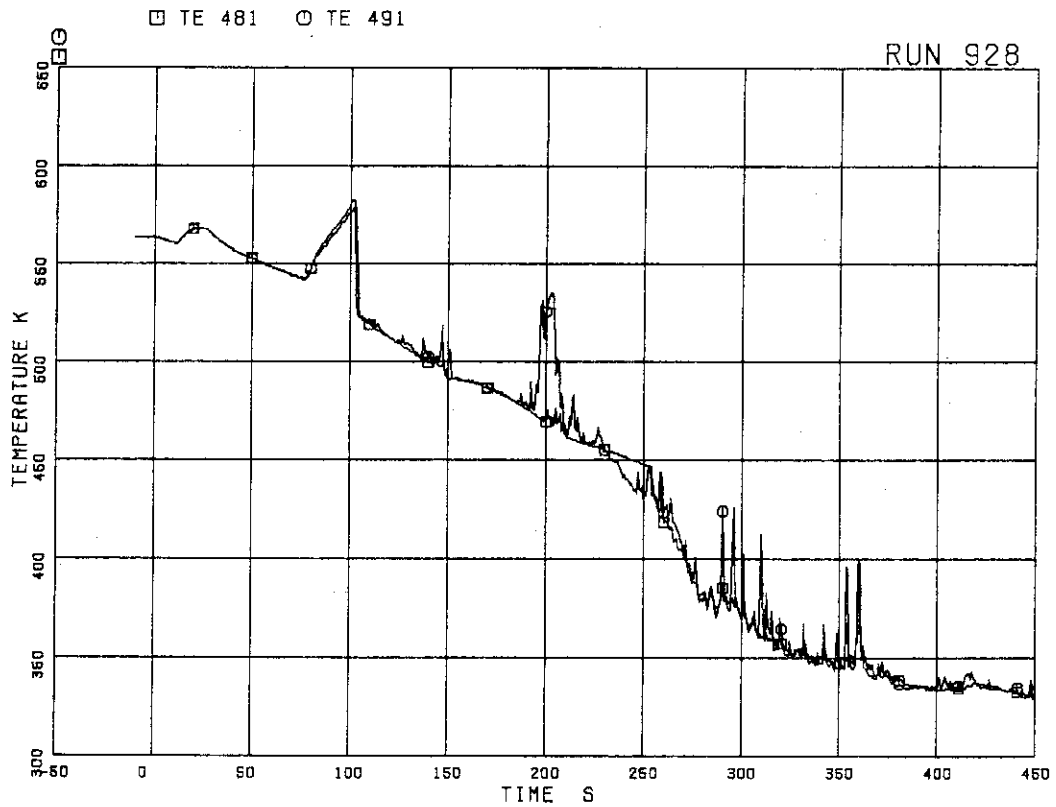


FIG.5.192 FLUID TEMPERATURES AT UTP IN CHANNEL C, OPENING 6

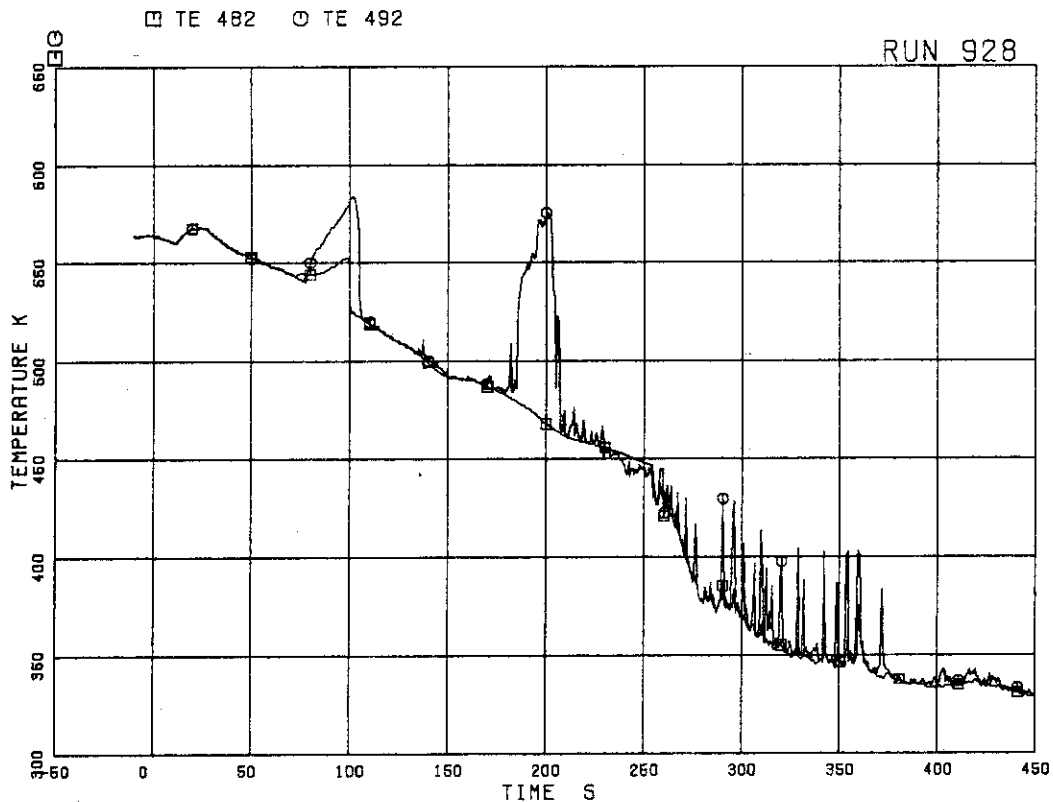


FIG.5.193 FLUID TEMPERATURES AT UTP IN CHANNEL C, OPENING 7

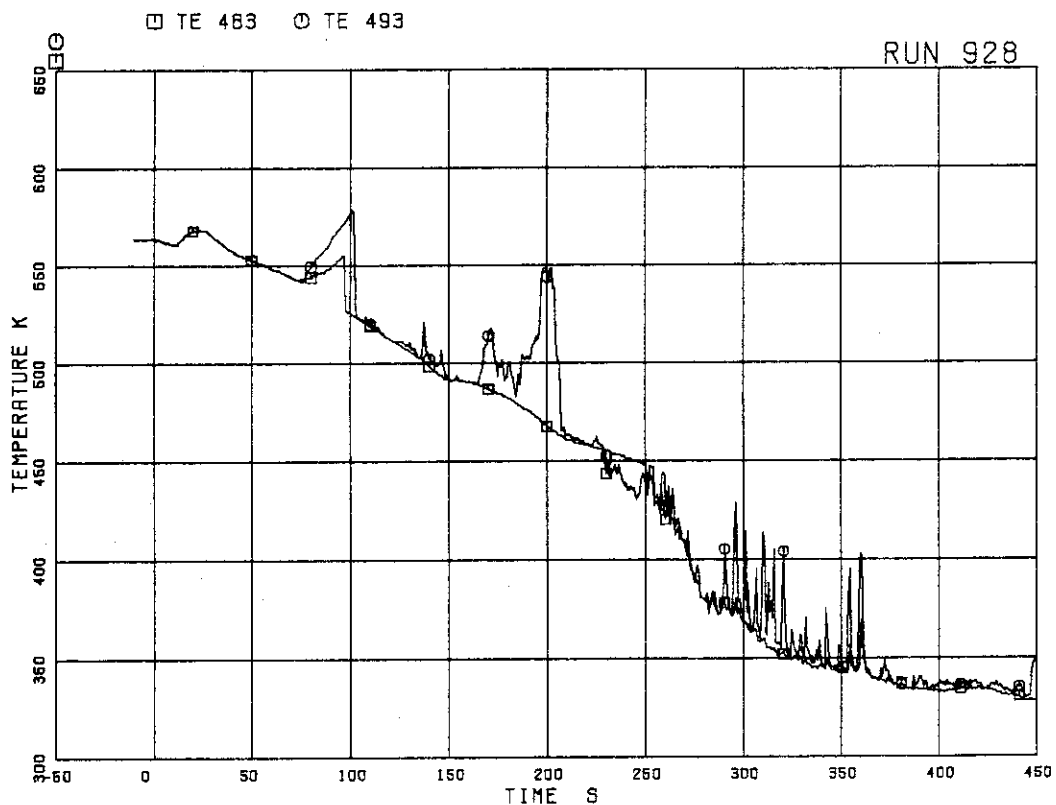


FIG.5.194 FLUID TEMPERATURES AT UTP IN CHANNEL C, OPENING 8

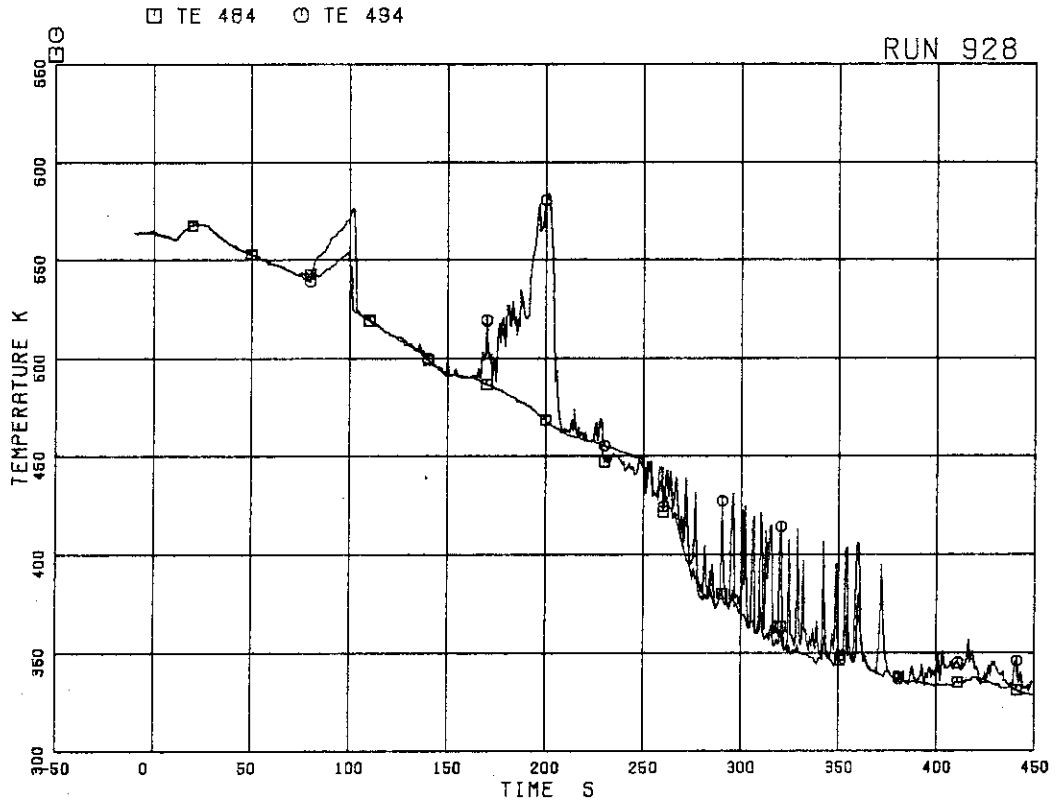


FIG.5.195 FLUID TEMPERATURES AT UTP IN CHANNEL C, OPENING 9

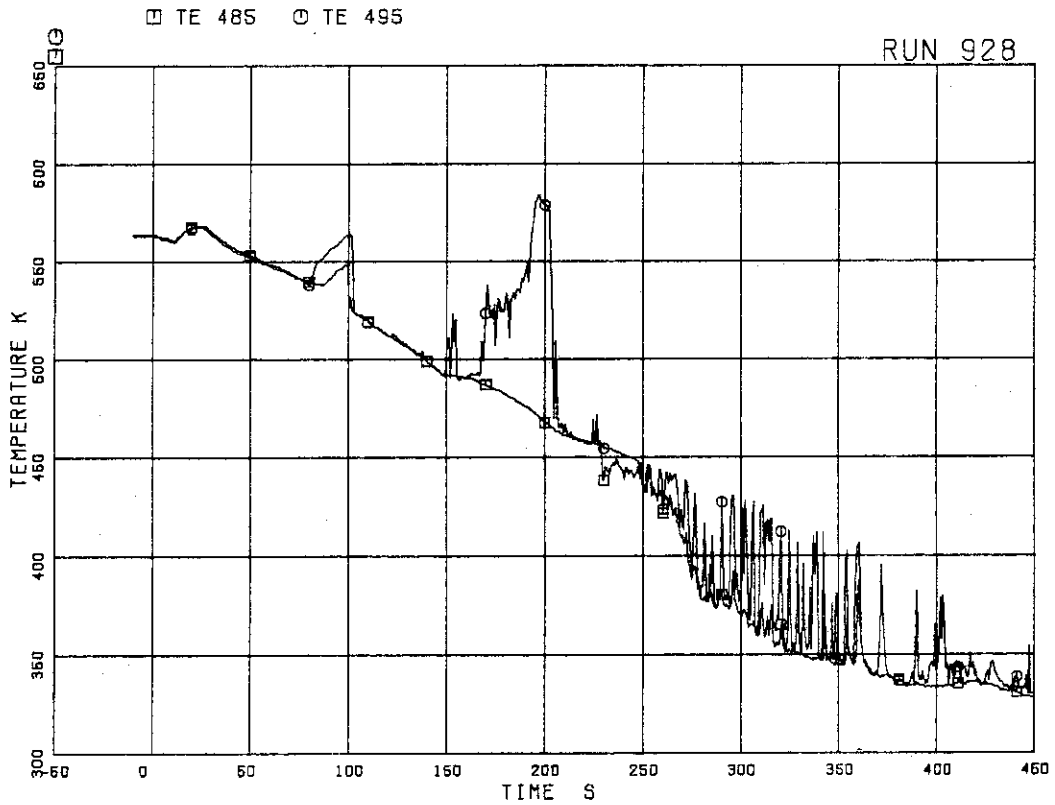


FIG.5.196 FLUID TEMPERATURES AT UTP IN CHANNEL C, OPENING 10

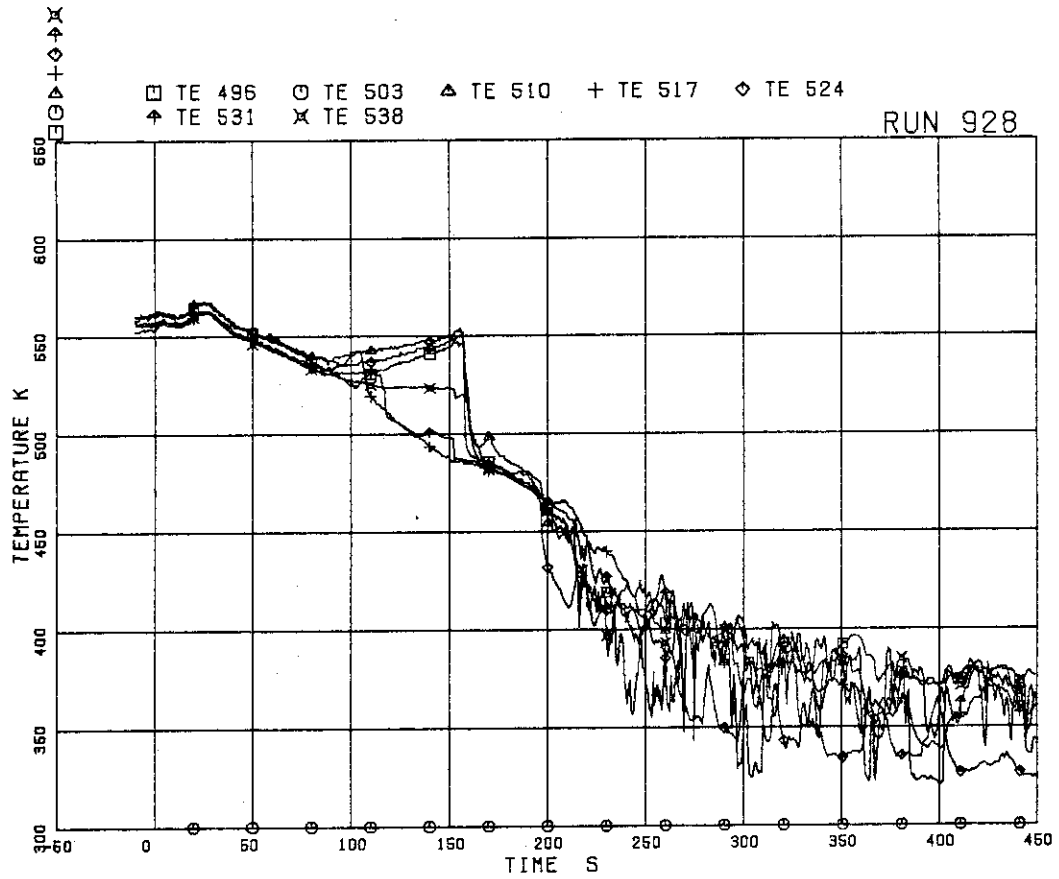


FIG.5.197 INNER AND OUTER SURFACE TEMPERATURES OF CHANNEL BOX AT POS.1

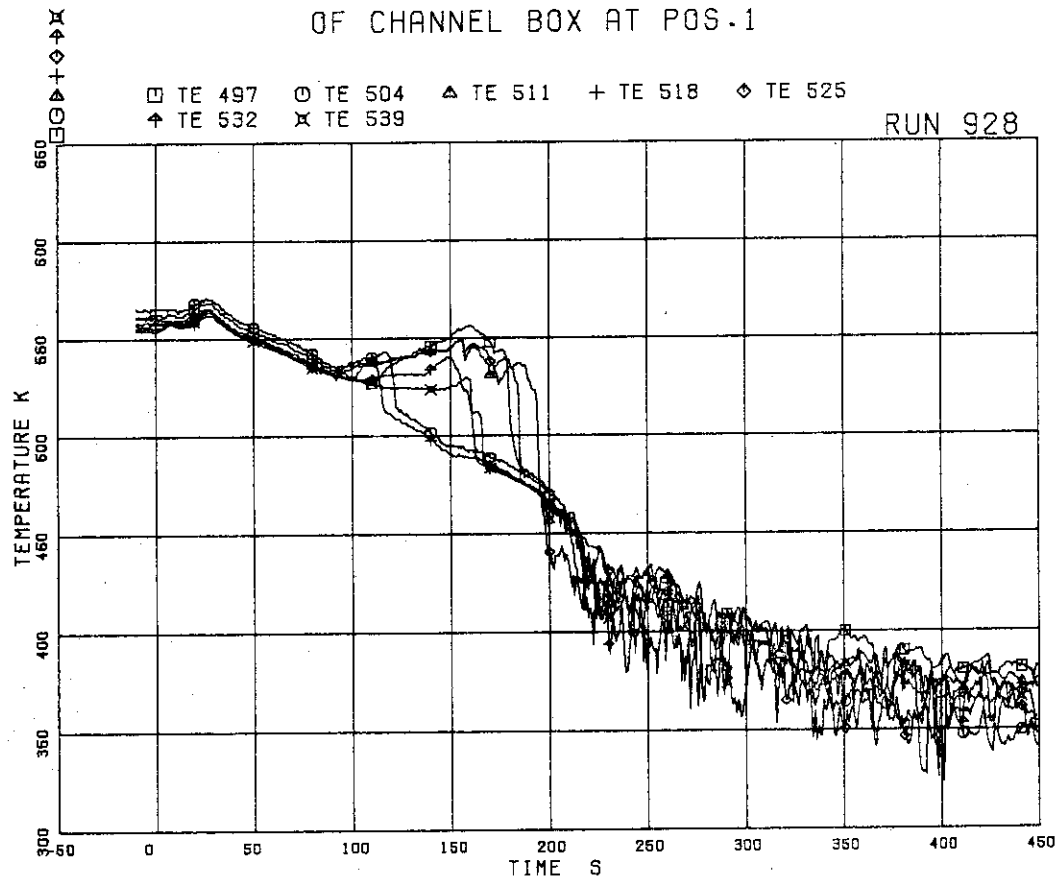


FIG.5.198 INNER AND OUTER SURFACE TEMPERATURES OF CHANNEL BOX AT POS.2

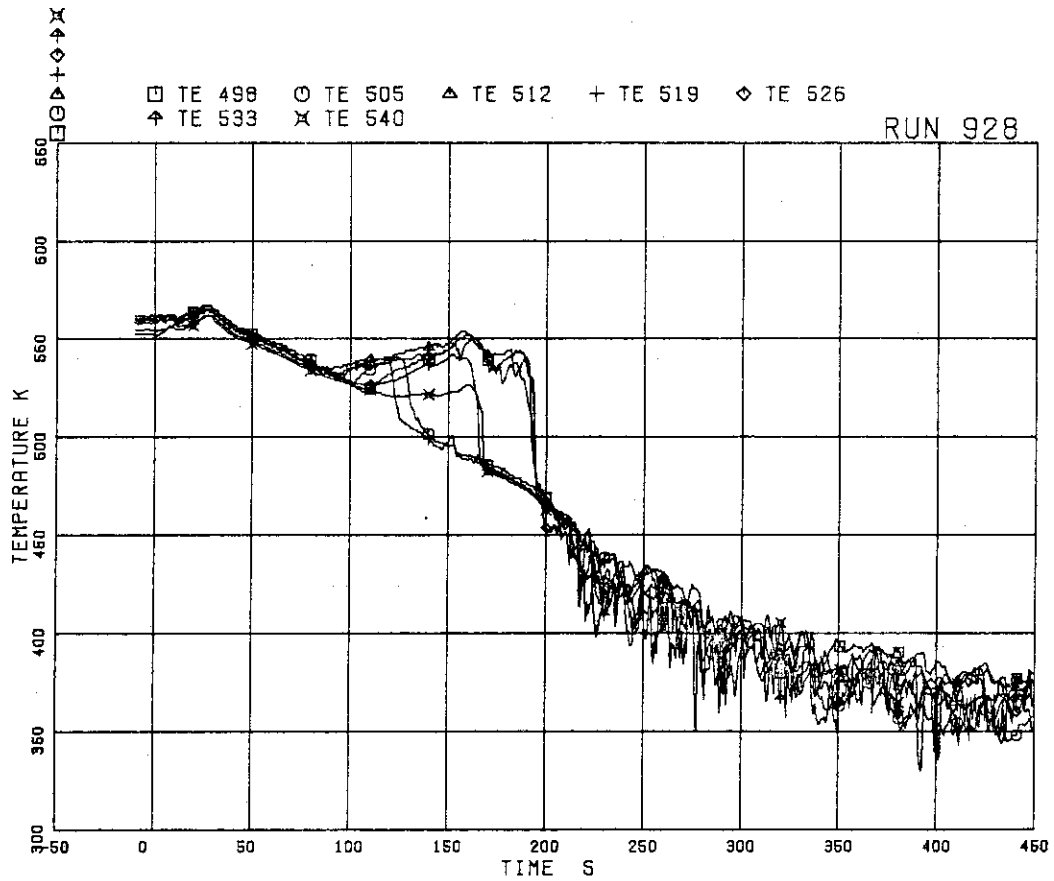


FIG.5.199 INNER AND OUTER SURFACE TEMPERATURES OF CHANNEL BOX AT POS.3

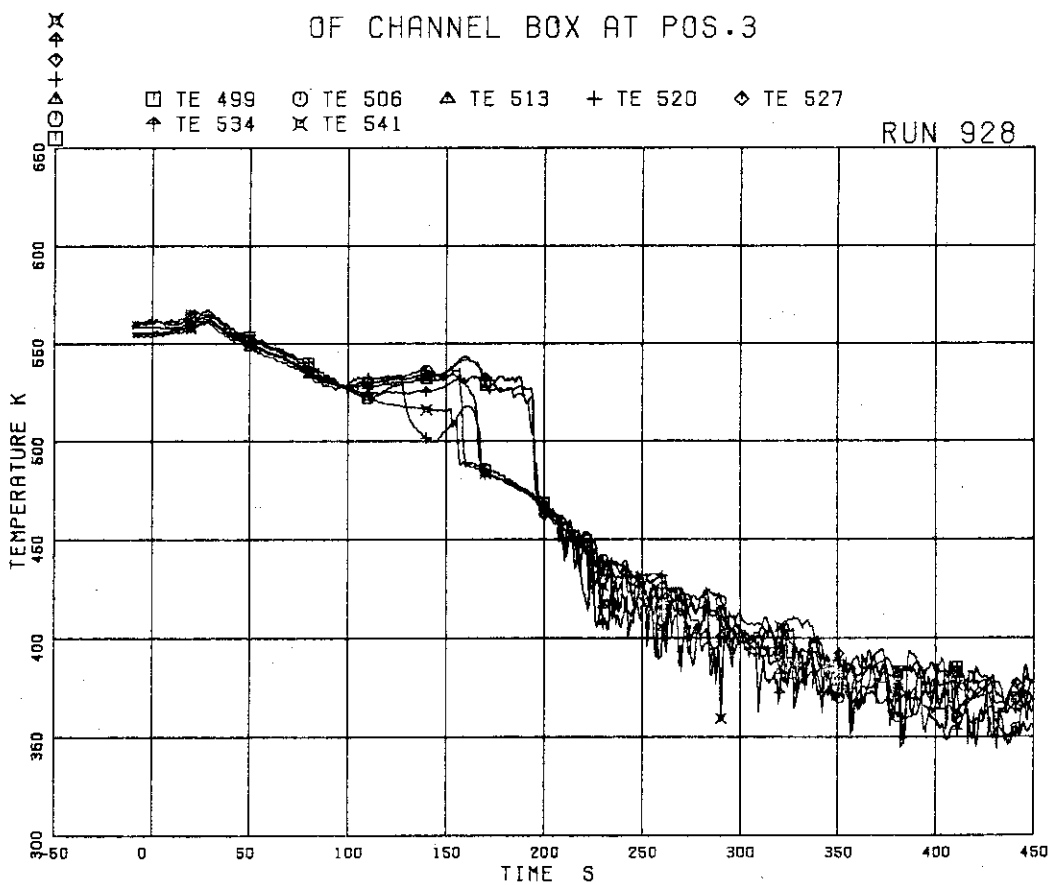


FIG.5.200 INNER AND OUTER SURFACE TEMPERATURES OF CHANNEL BOX AT POS.4

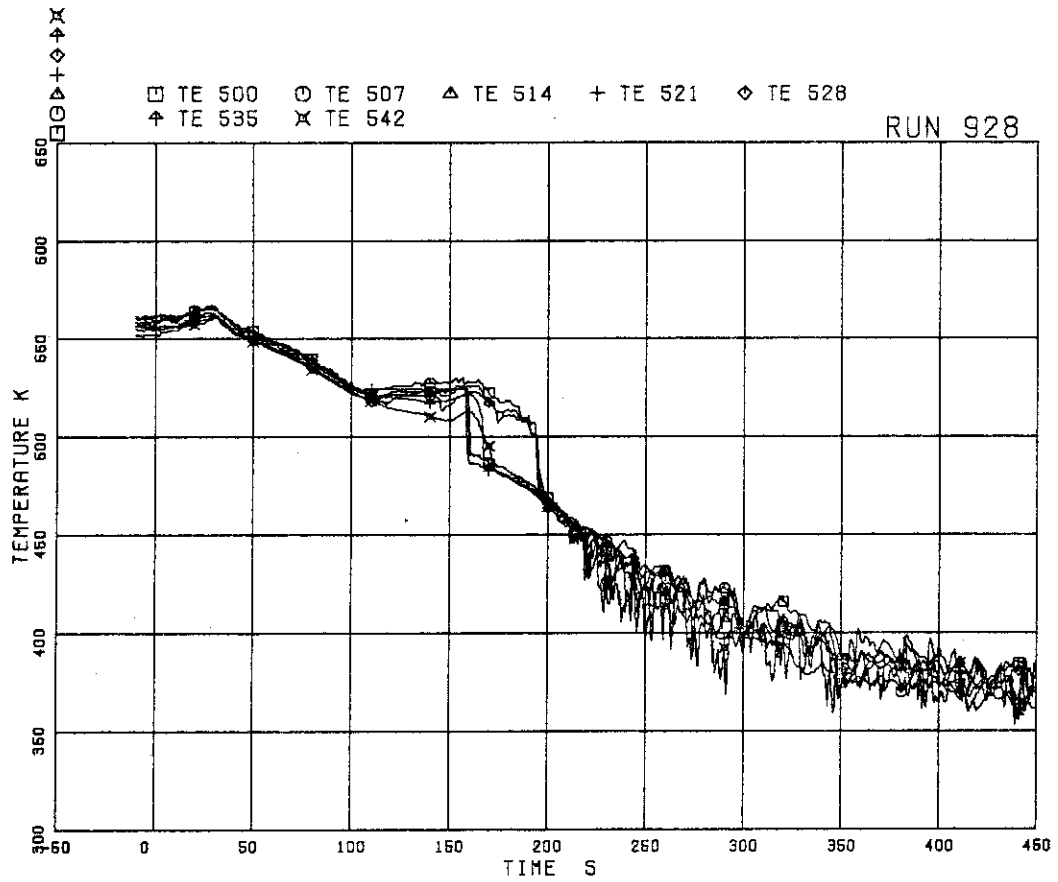


FIG.5.201 INNER AND OUTER SURFACE TEMPERATURES OF CHANNEL BOX AT POS.5

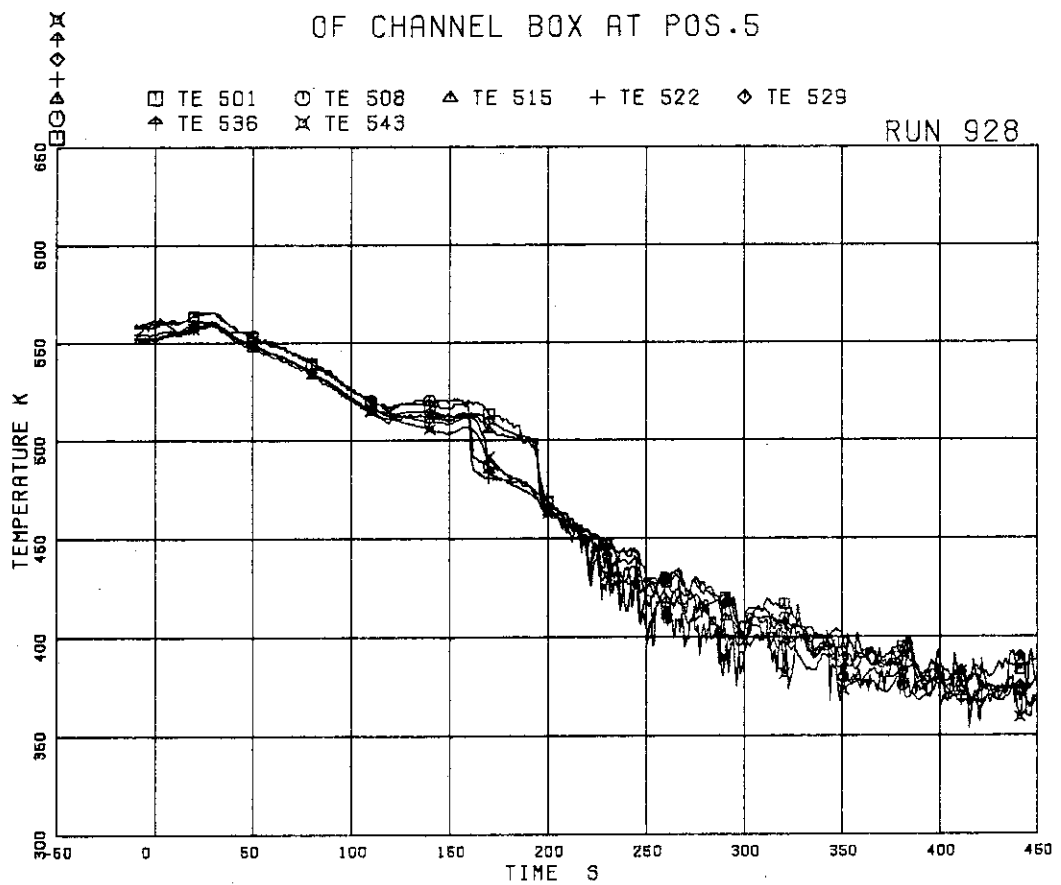


FIG.5.202 INNER AND OUTER SURFACE TEMPERATURES OF CHANNEL BOX AT POS.6

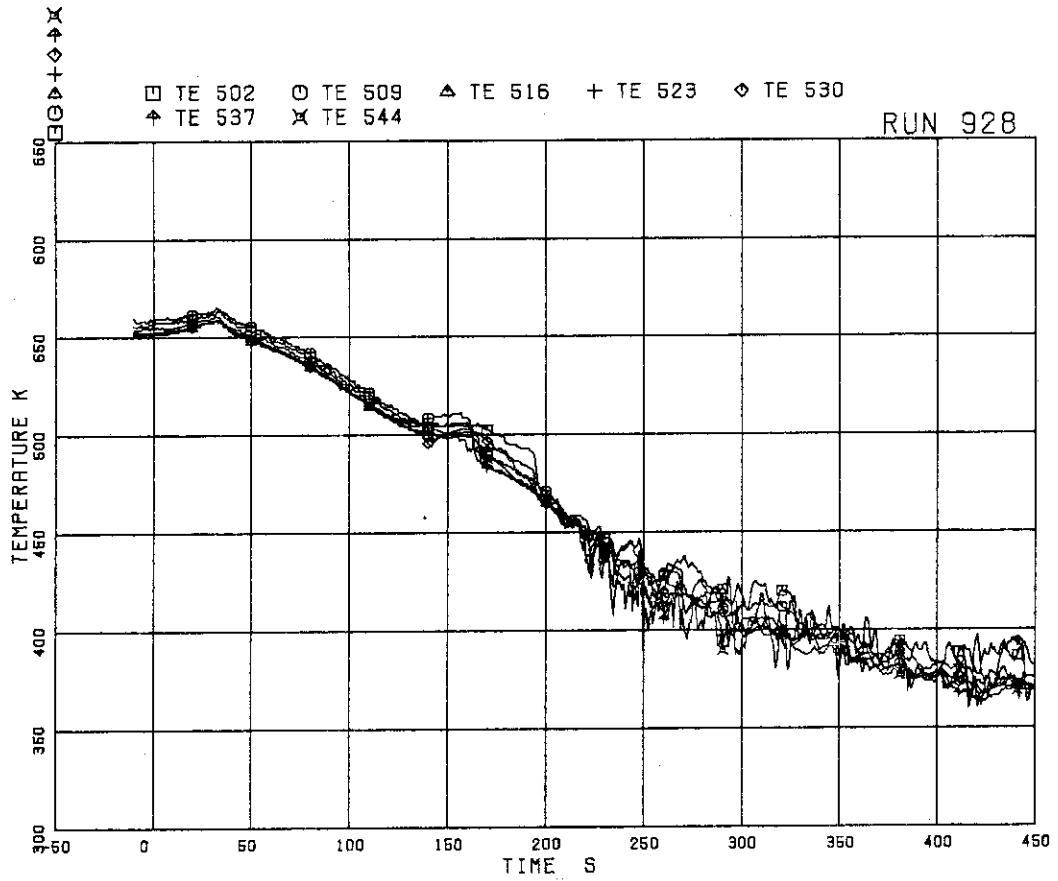


FIG.5.203 INNER AND OUTER SURFACE TEMPERATURES OF CHANNEL BOX AT POS.7

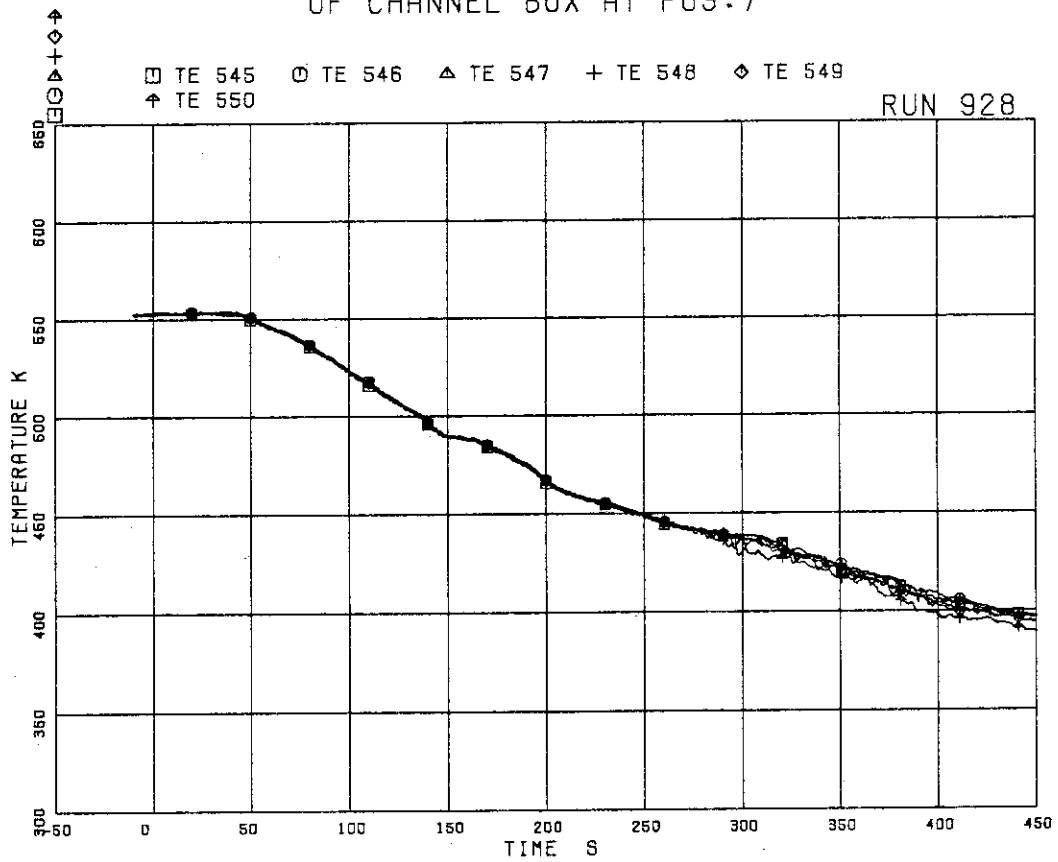


FIG.5.204 FLUID TEMPERATURES IN LOWER PLENUM, CENTER

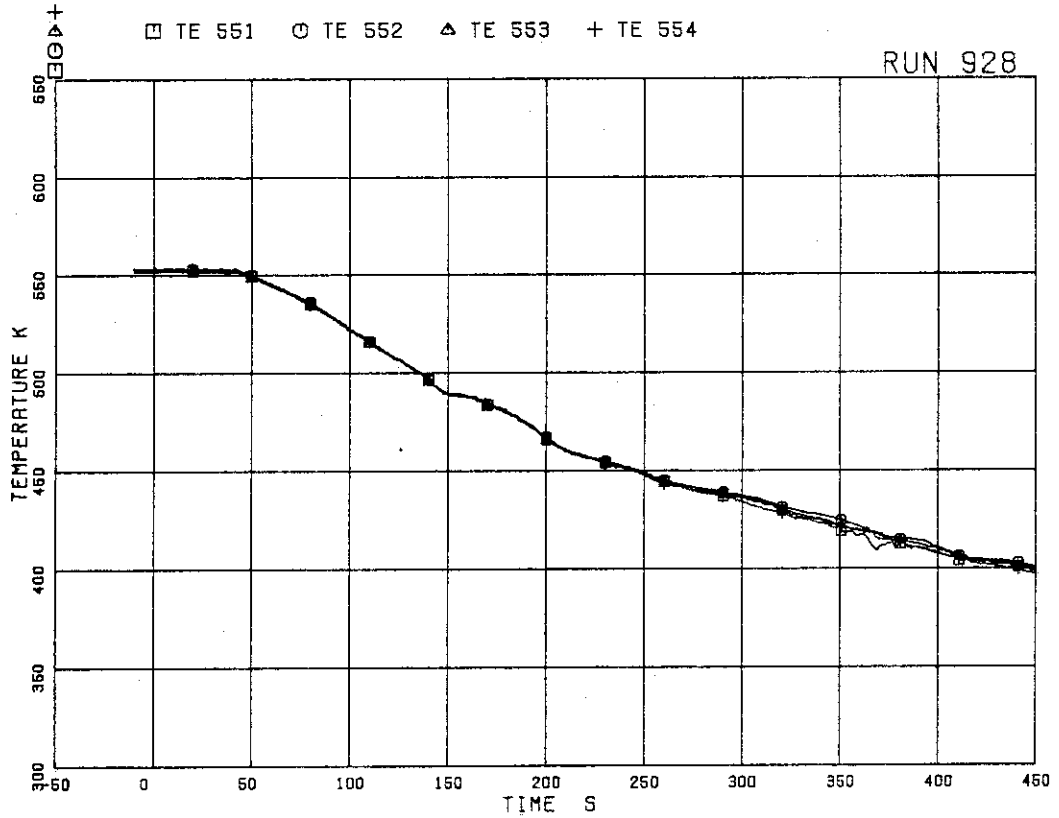


FIG.5.205 FLUID TEMPERATURES IN LOWER PLENUM, NORTH

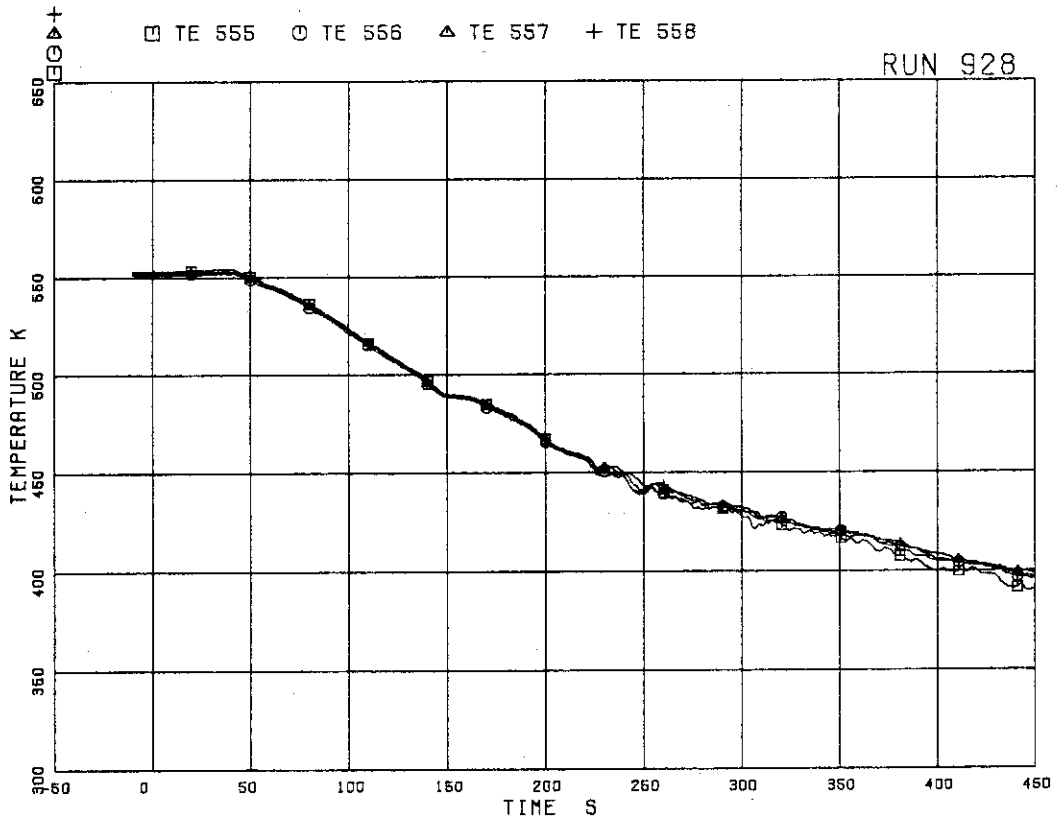


FIG.5.206 FLUID TEMPERATURES IN LOWER PLENUM, SOUTH



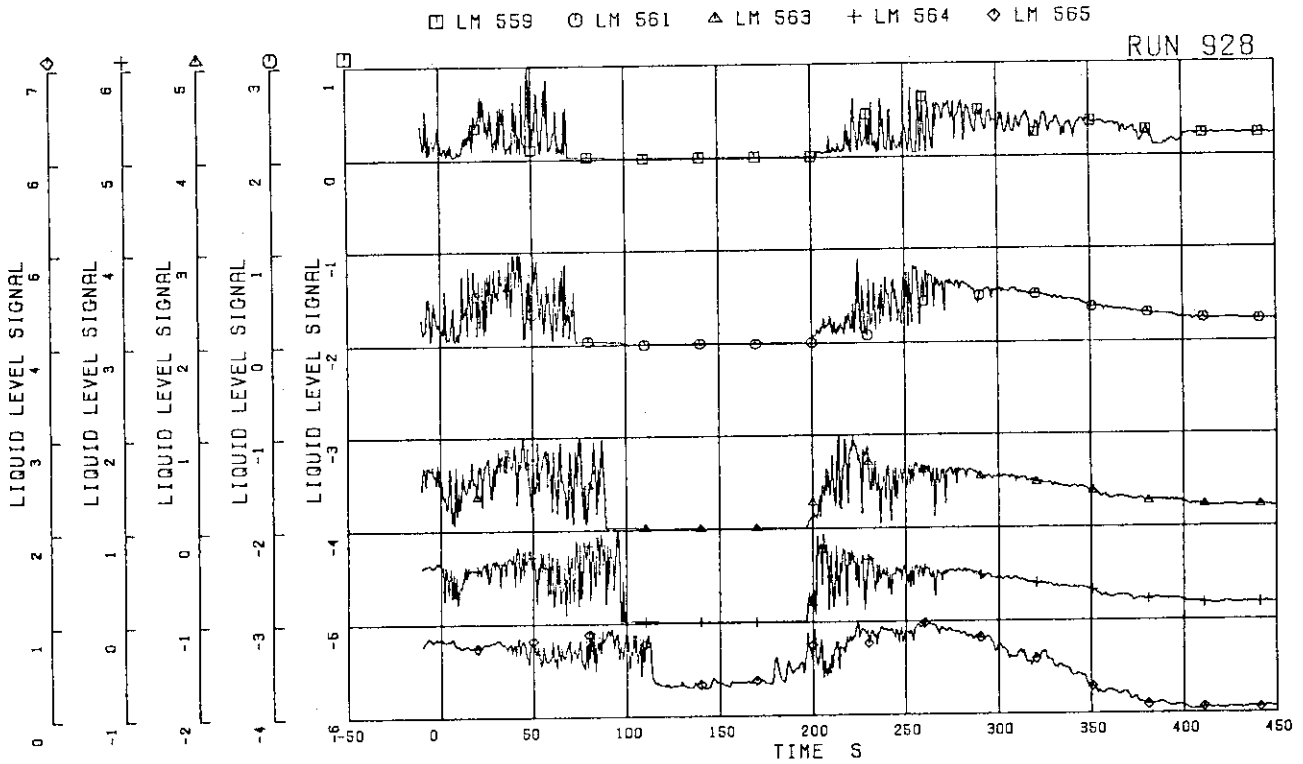


FIG.5.207 LIQUID LEVEL SIGNALS IN CHANNEL BOX A,  
LOCATION A1

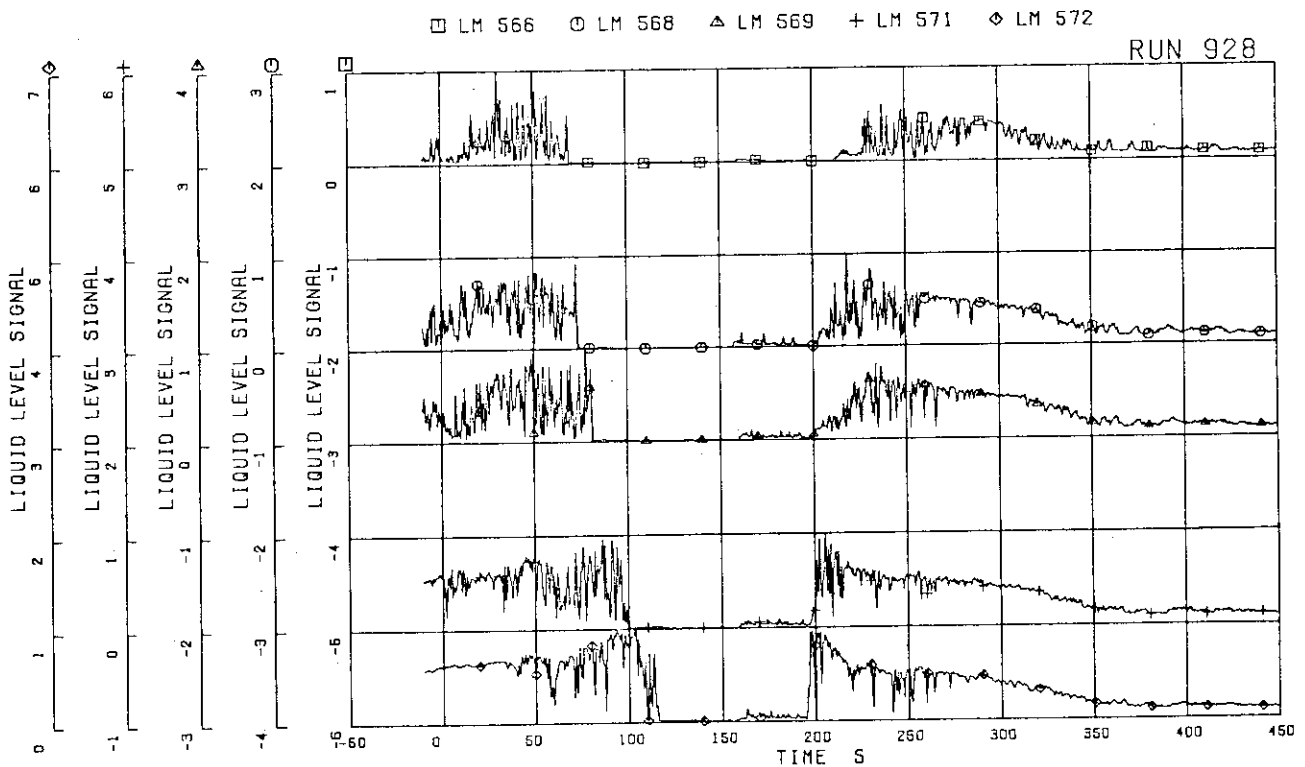


FIG.5.208 LIQUID LEVEL SIGNALS IN CHANNEL BOX A,  
LOCATION A2



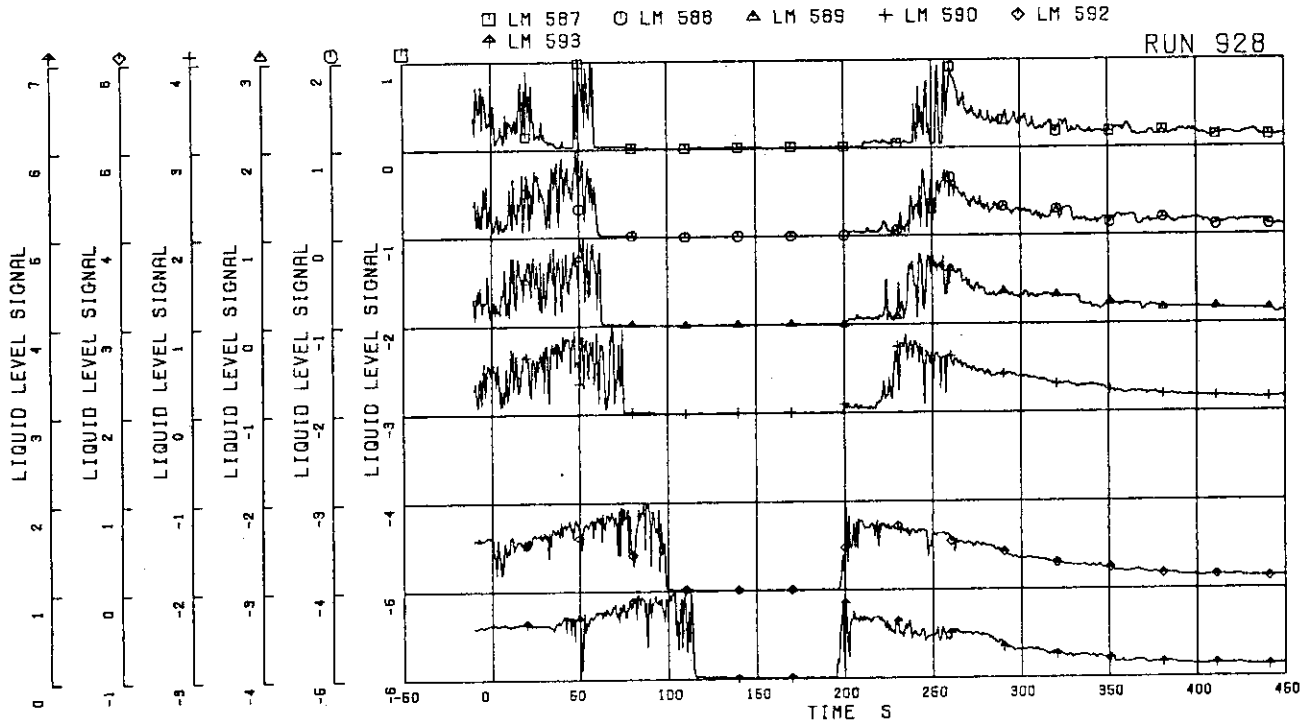


FIG. 5.211 LIQUID LEVEL SIGNALS IN CHANNEL BOX D

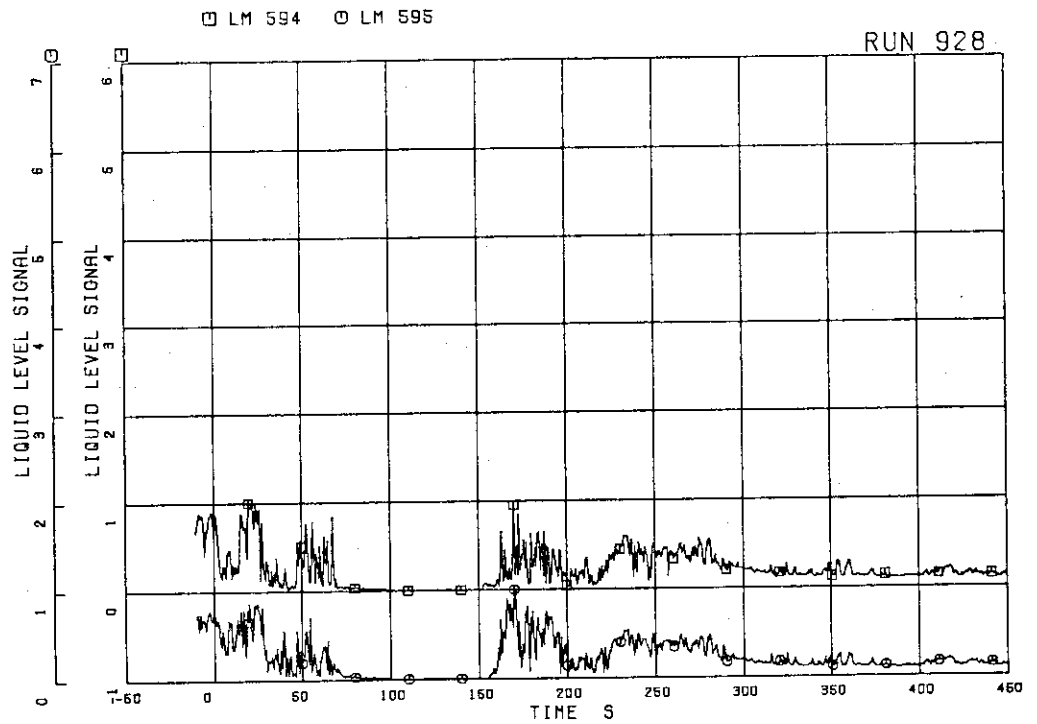


FIG. 5.212 LIQUID LEVEL SIGNALS IN CHANNEL A  
OUTLET LOCATION A1

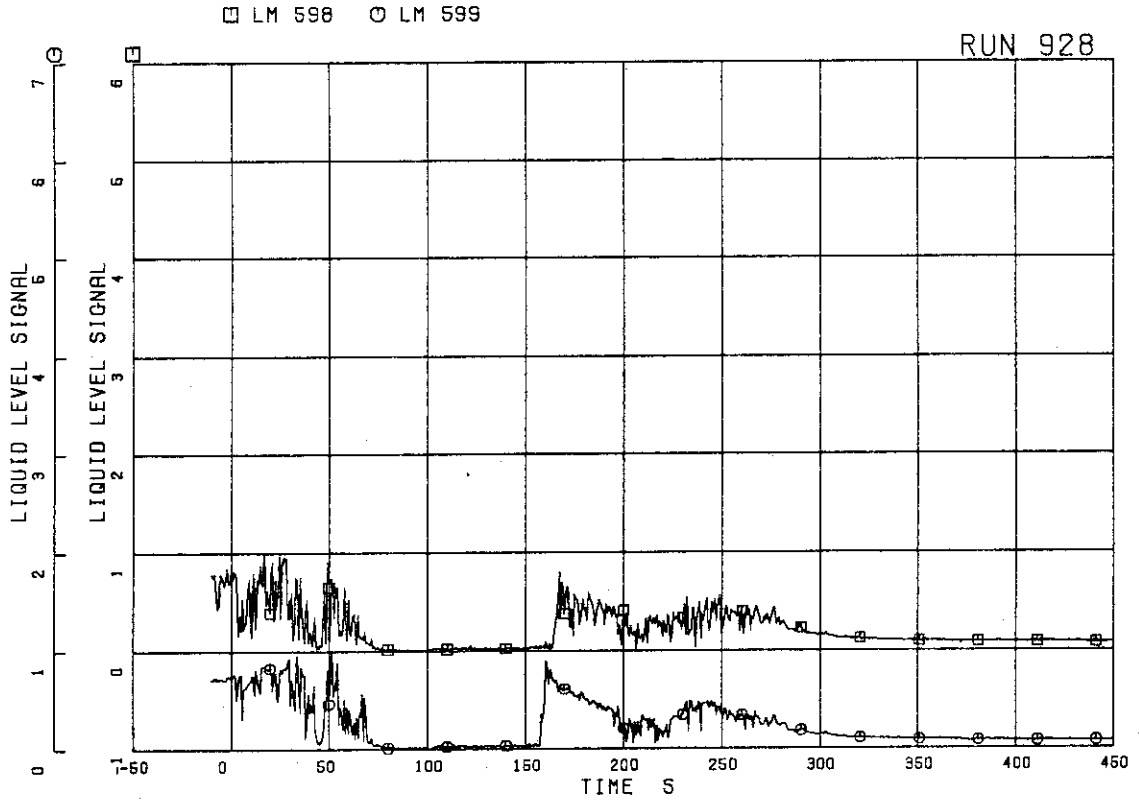


FIG.5.213 LIQUID LEVEL SIGNALS IN CHANNEL A  
OUTLET LOCATION A2

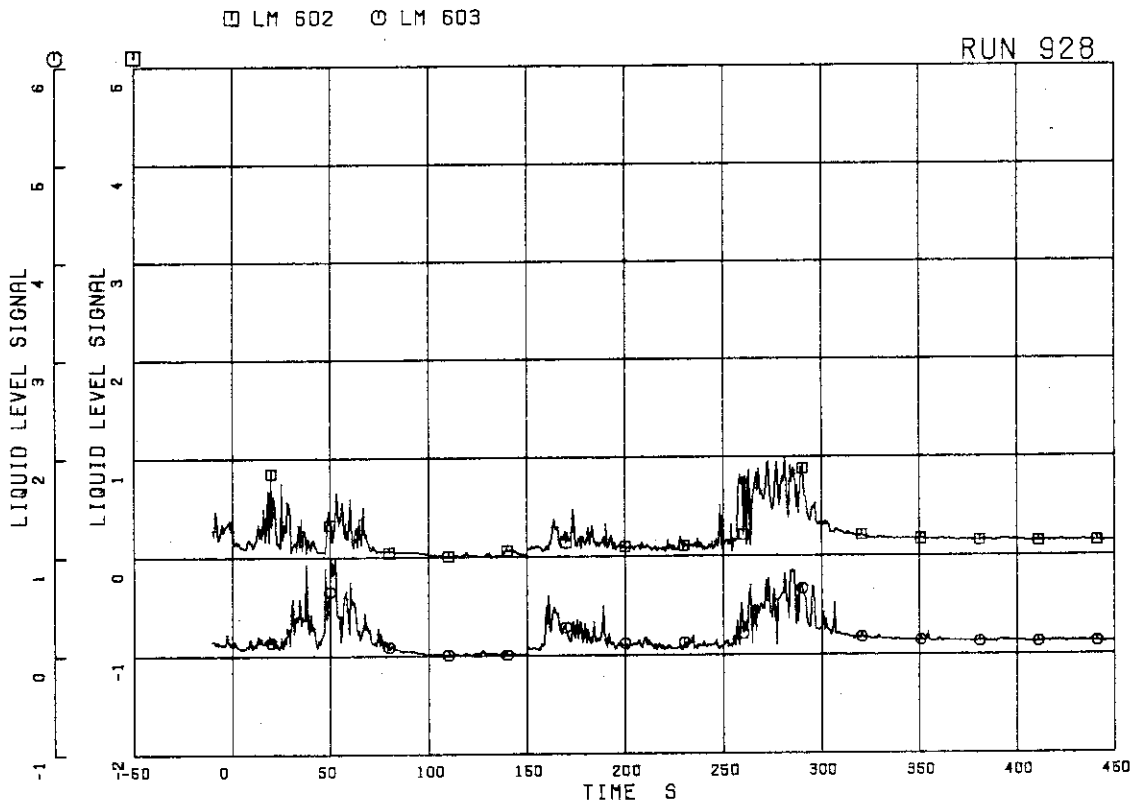


FIG.5.214 LIQUID LEVEL SIGNALS IN CHANNEL A  
OUTLET CENTER

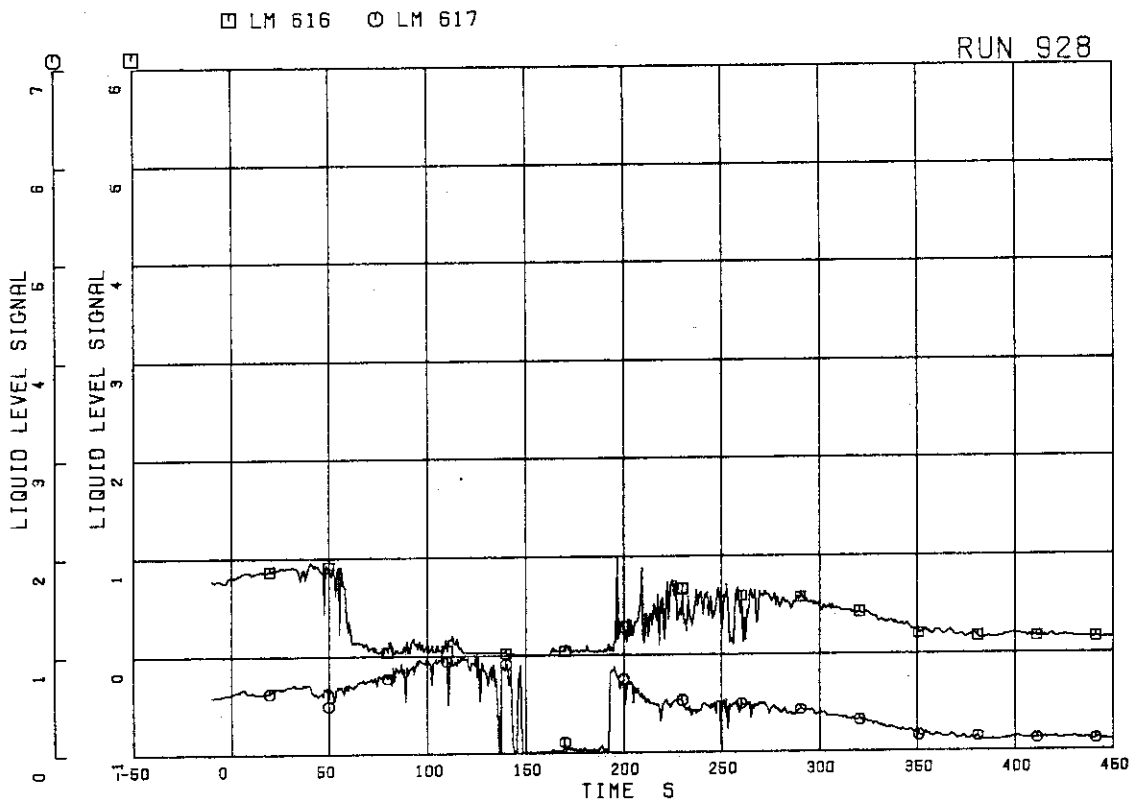


FIG.5.215 LIQUID LEVEL SIGNALS IN CHANNEL A INLET

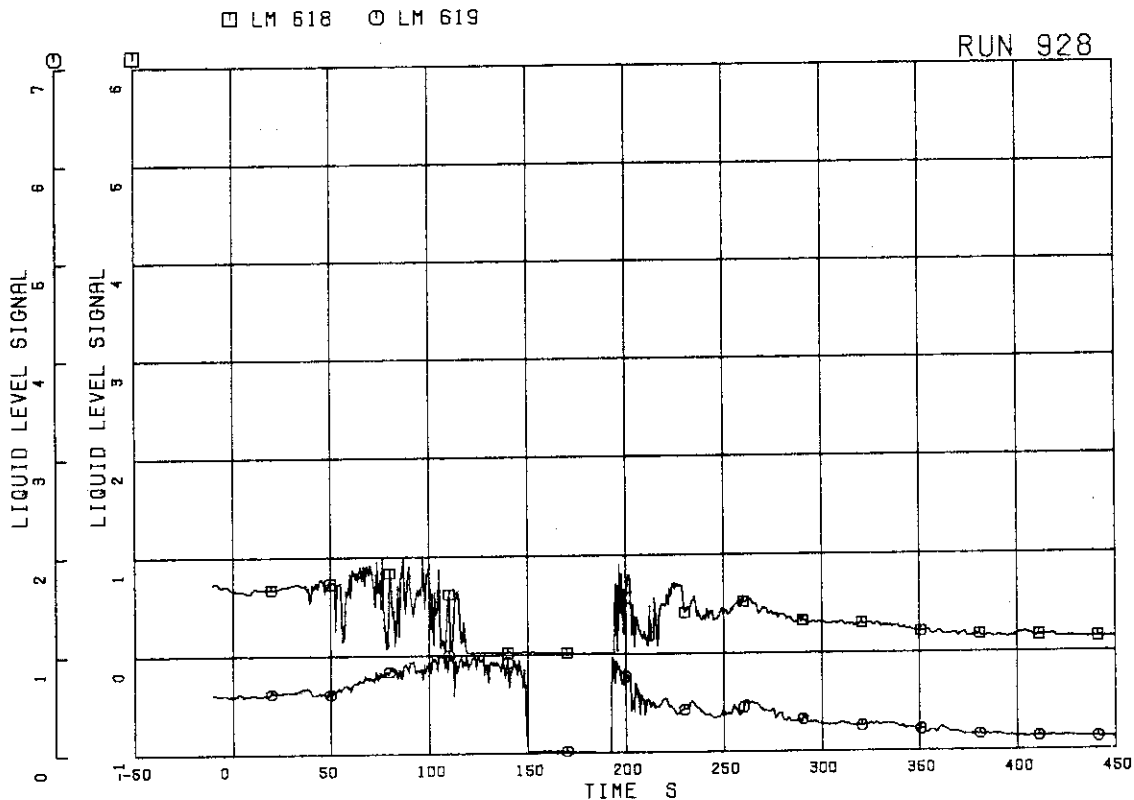


FIG.5.216 LIQUID LEVEL SIGNALS IN CHANNEL B INLET

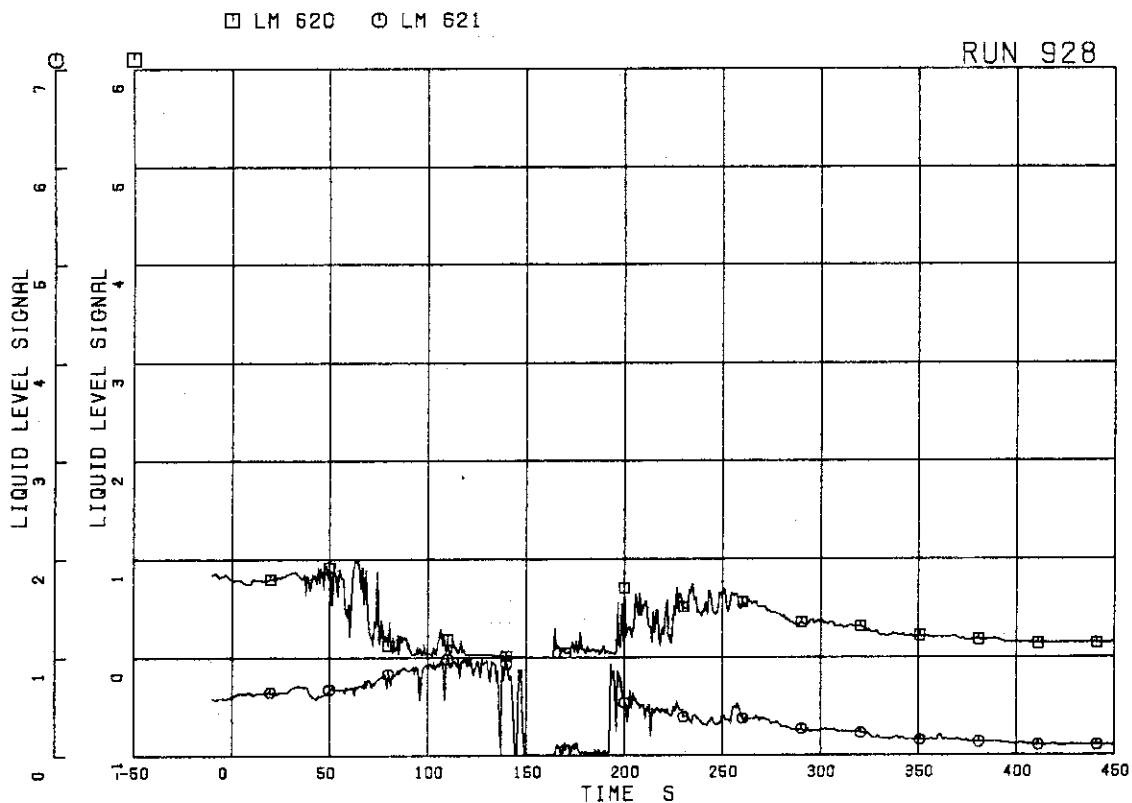


FIG.5.217 LIQUID LEVEL SIGNALS IN CHANNEL C INLET

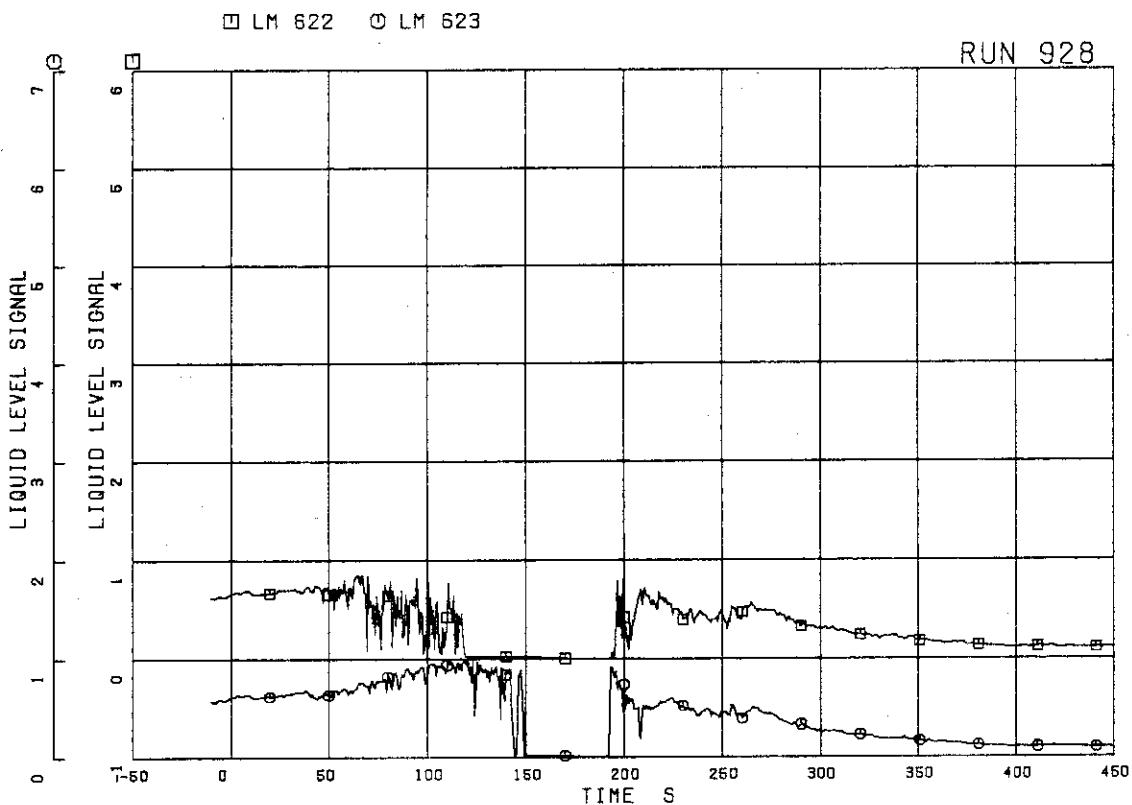


FIG.5.218 LIQUID LEVEL SIGNALS IN CHANNEL D INLET

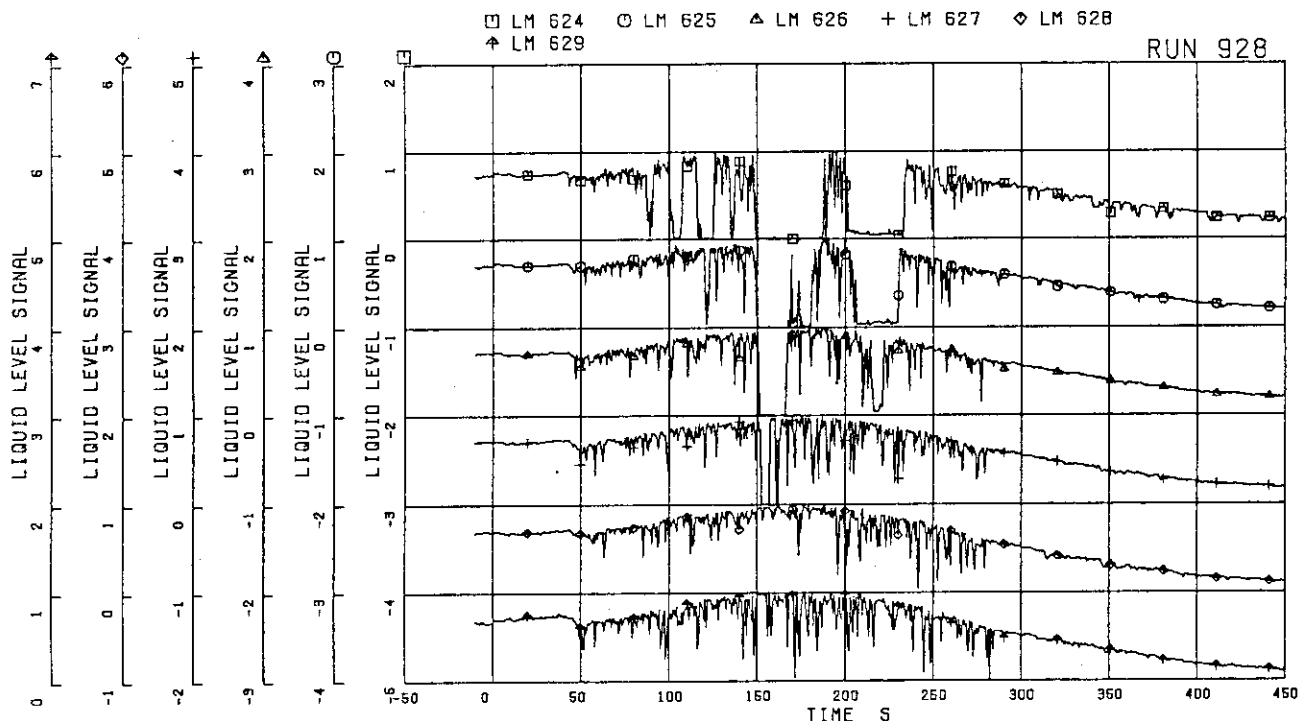


FIG.5.219 LIQUID LEVEL SIGNALS IN LOWER PLENUM, NORTH

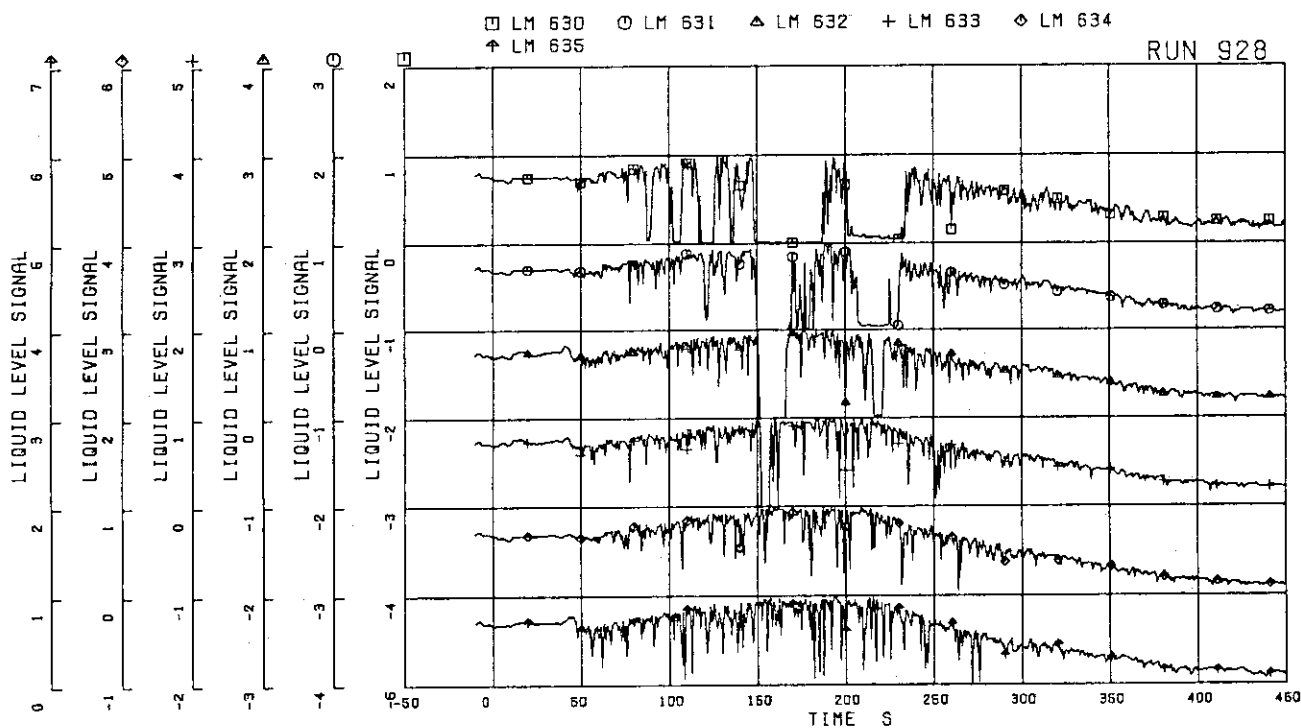


FIG.5.220 LIQUID LEVEL SIGNALS IN LOWER PLENUM, SOUTH

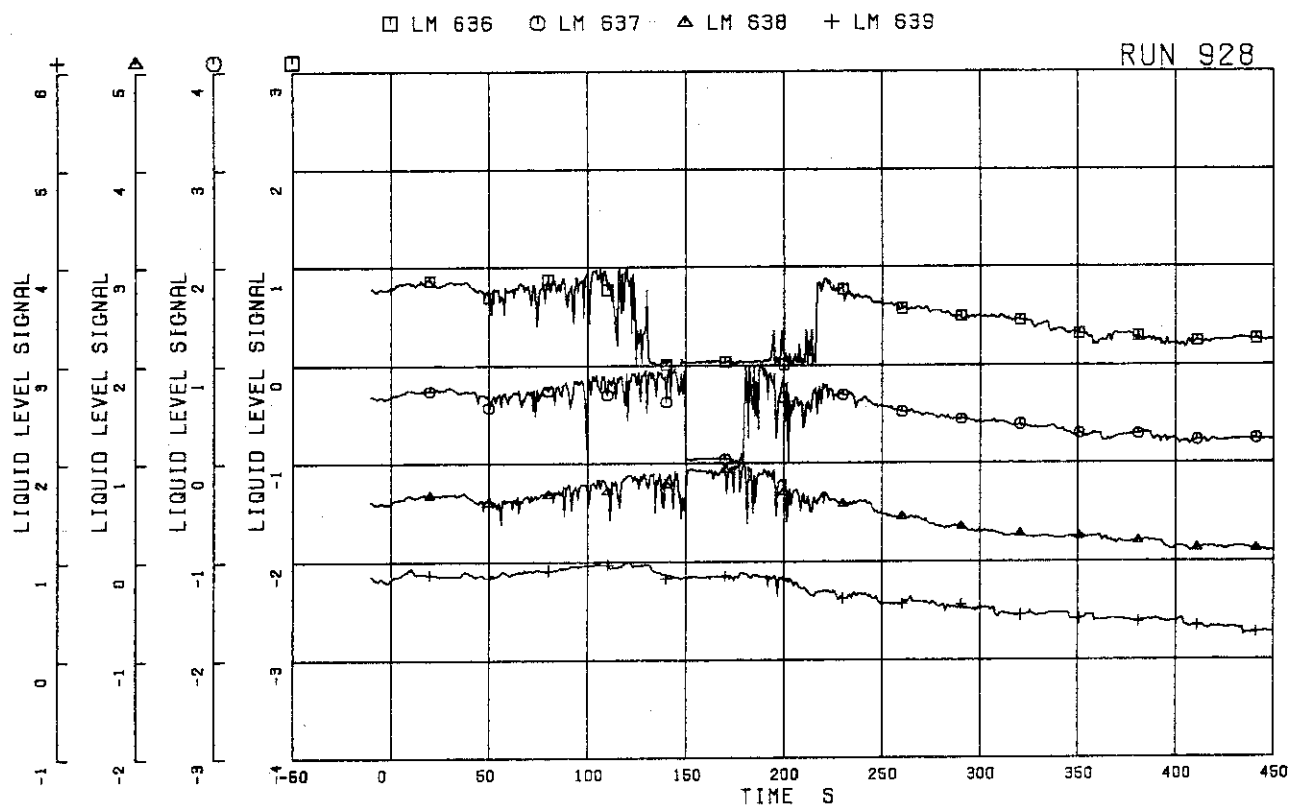


FIG.5.221 LIQUID LEVEL SIGNALS IN GUIDE TUBE, NORTH

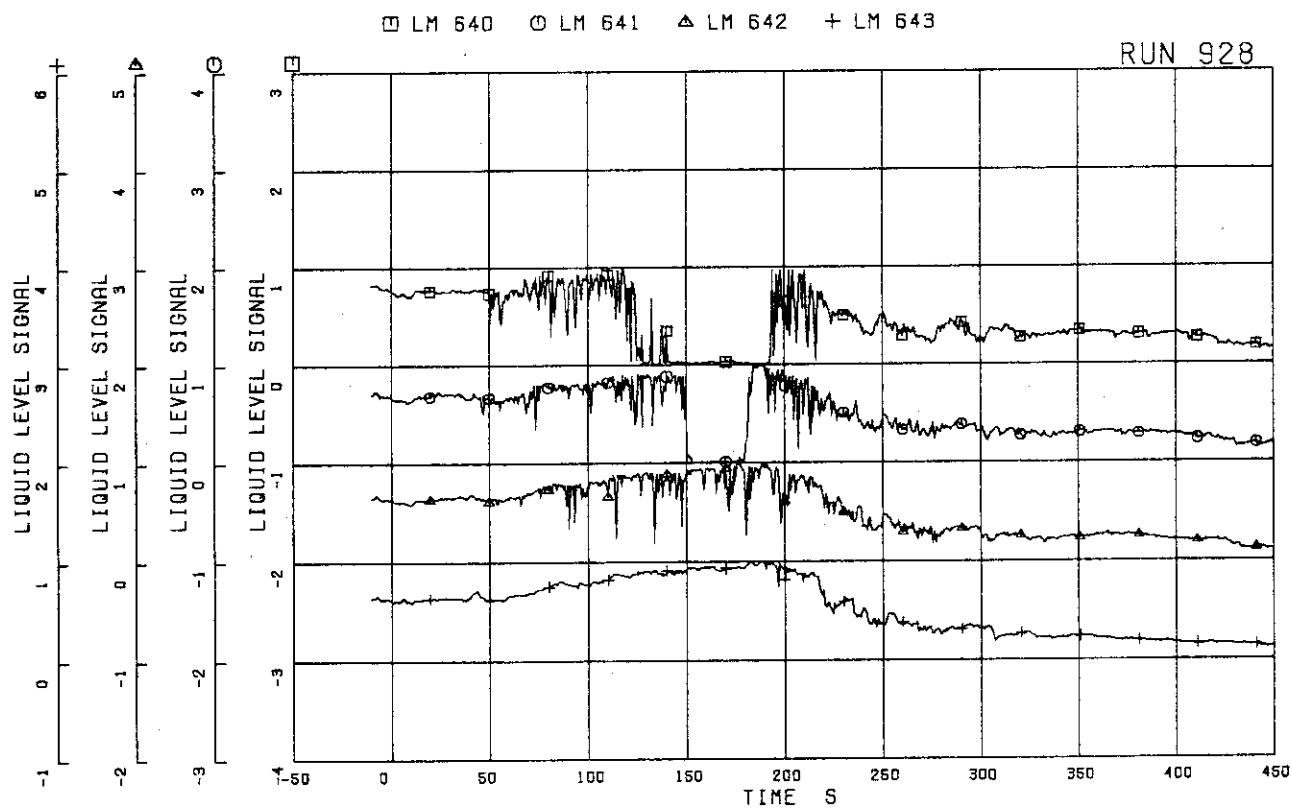


FIG.5.222 LIQUID LEVEL SIGNALS IN GUIDE TUBE, SOUTH



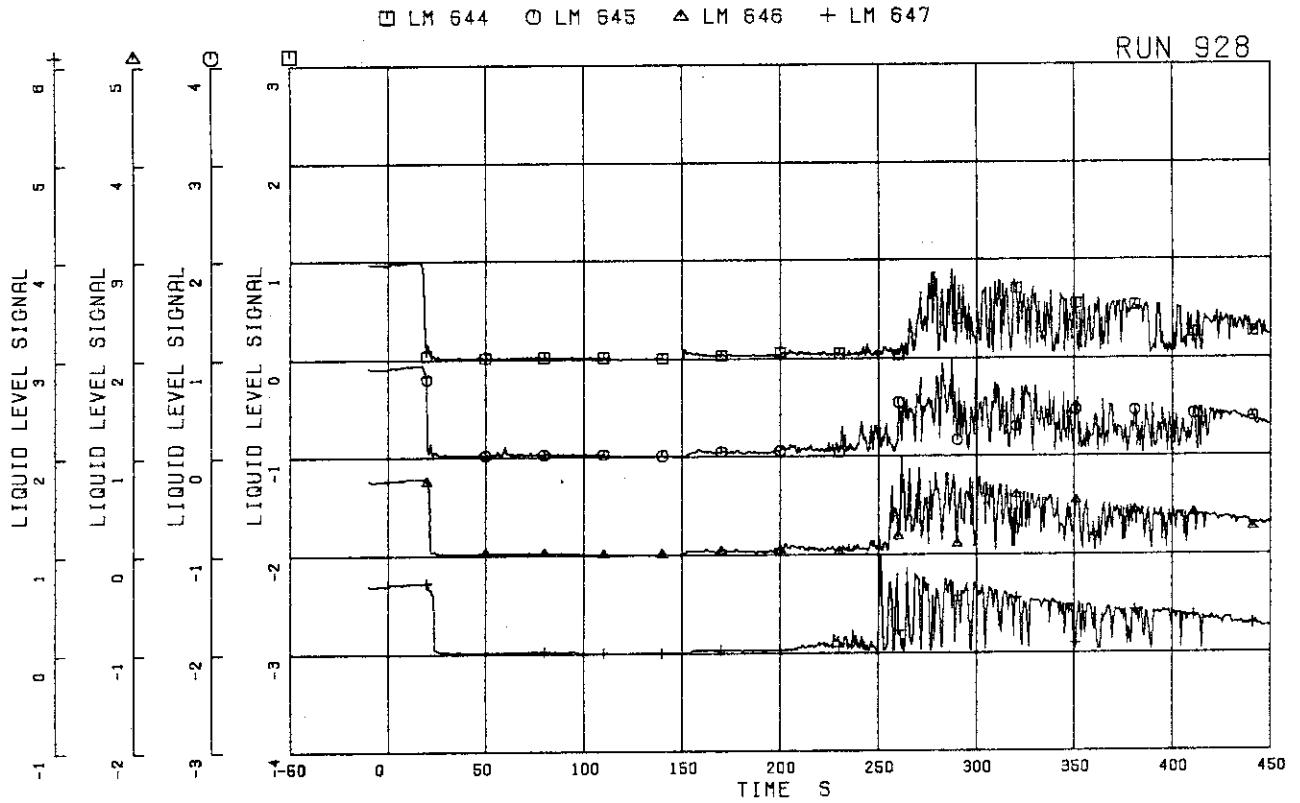


FIG.5.223 LIQUID LEVEL SIGNALS IN DOWNCOMER,  
D SIDE

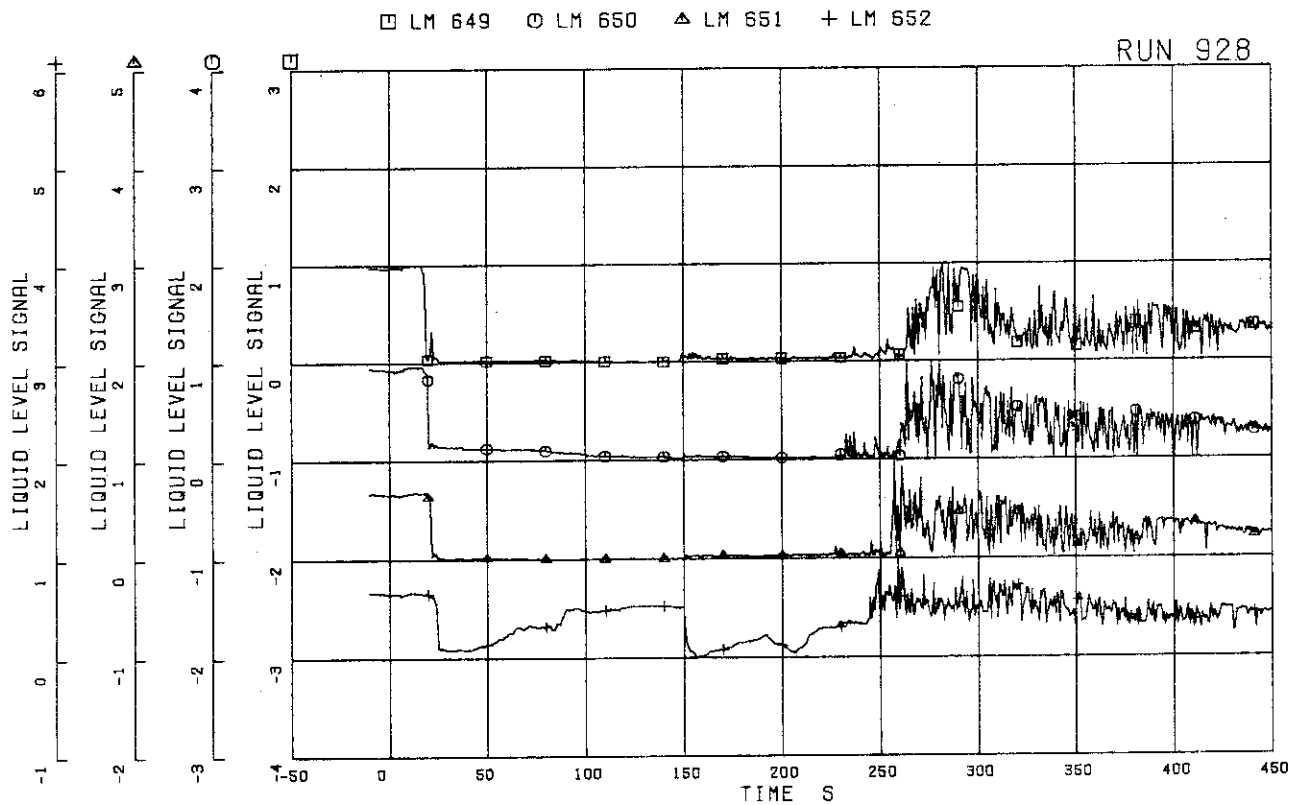


FIG.5.224 LIQUID LEVEL SIGNALS IN DOWNCOMER,  
B SIDE

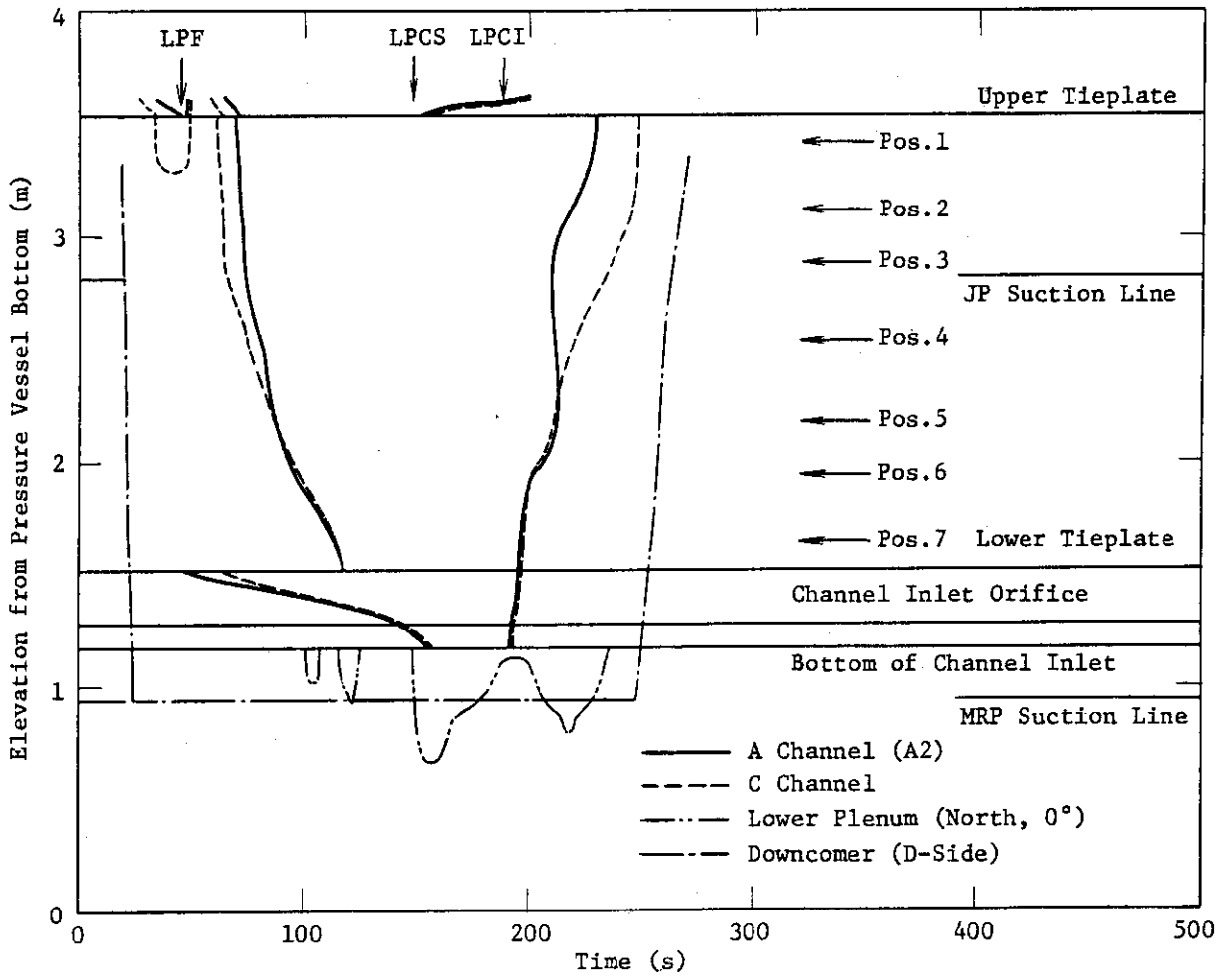


Fig. 5.225 Estimated liquid level in pressure vessel

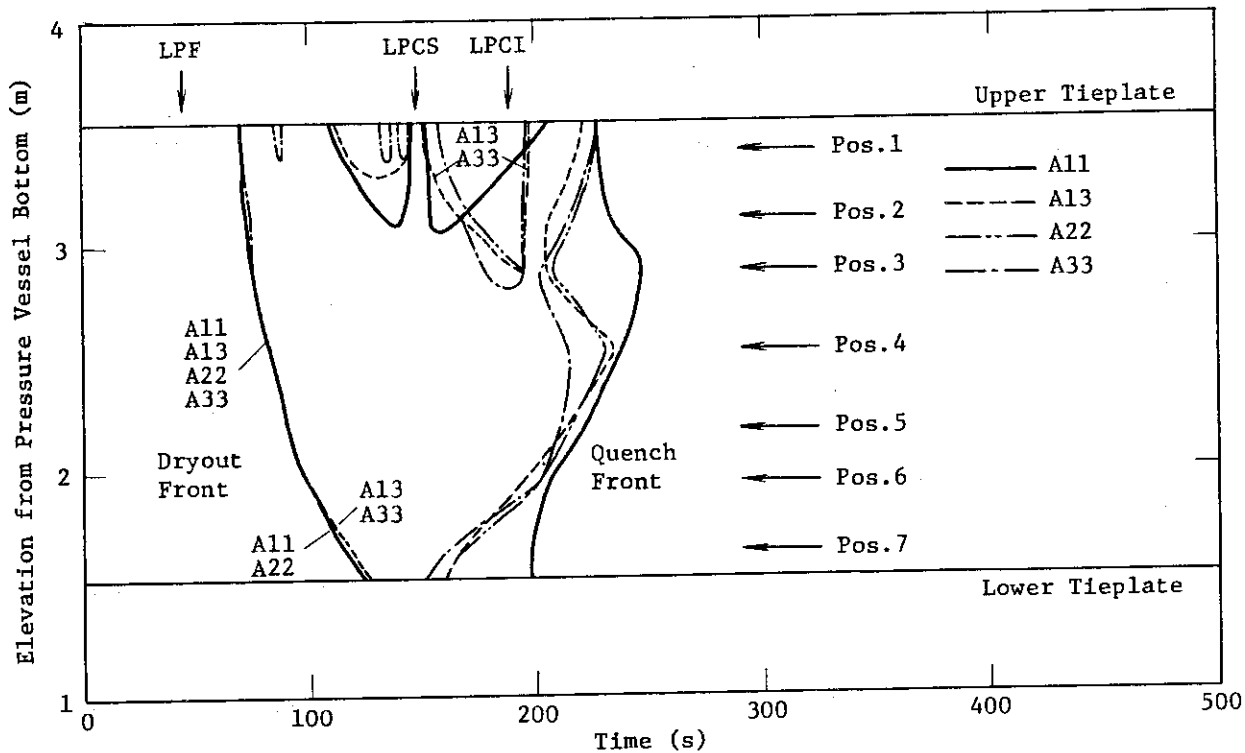


Fig. 5.226 Dryout and quench transients in channel A

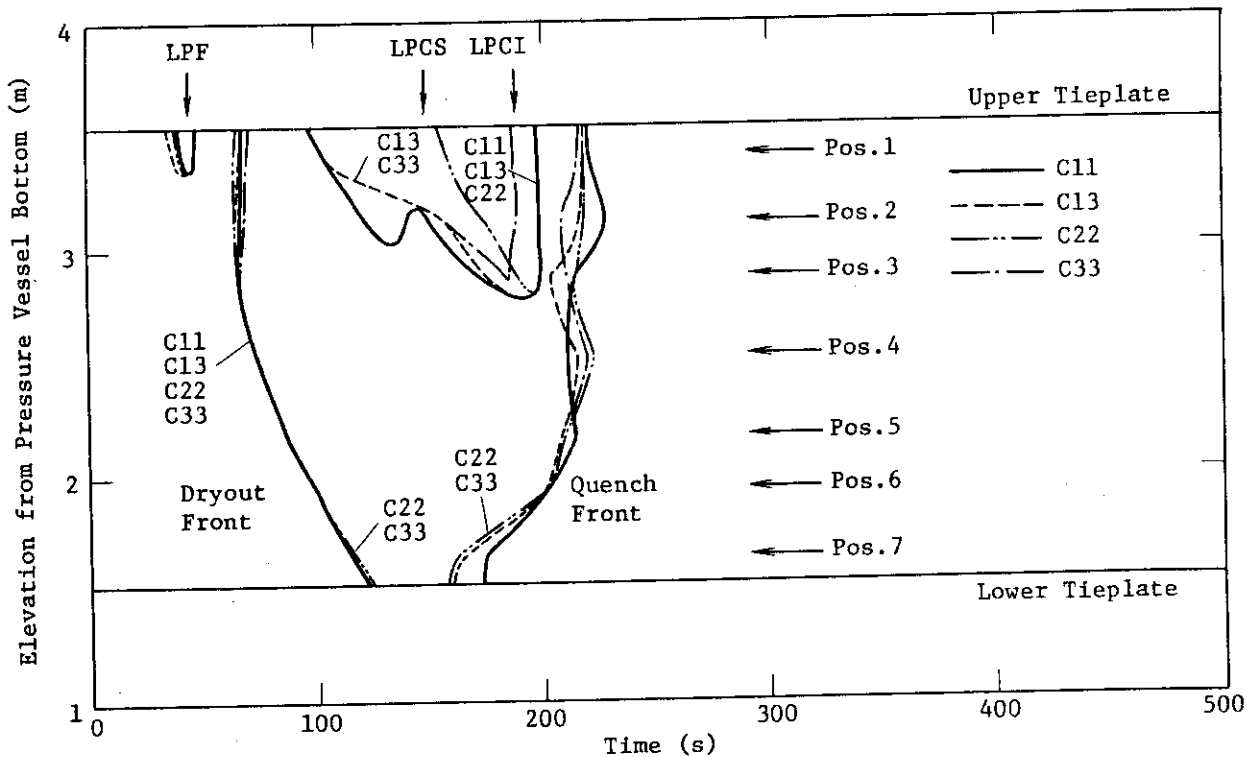


Fig. 5.227 Dryout and quench transients in channel C

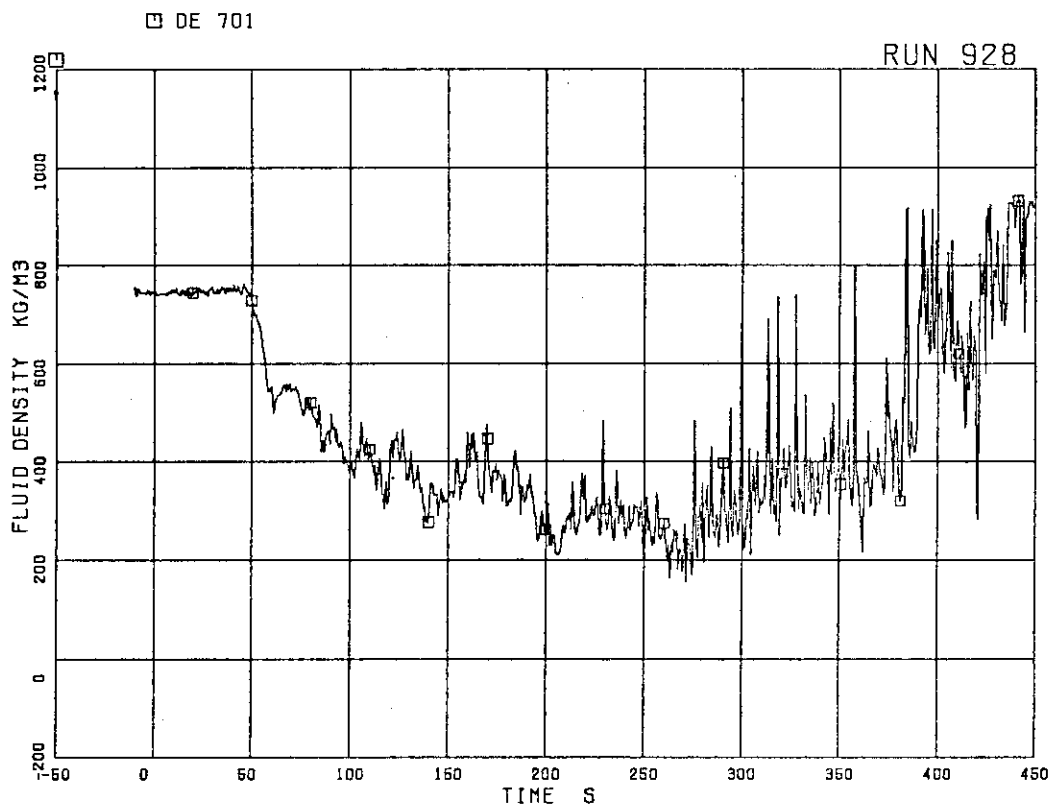


FIG.5.228 AVERAGE DENSITY AT JP-1,2 OUTLET

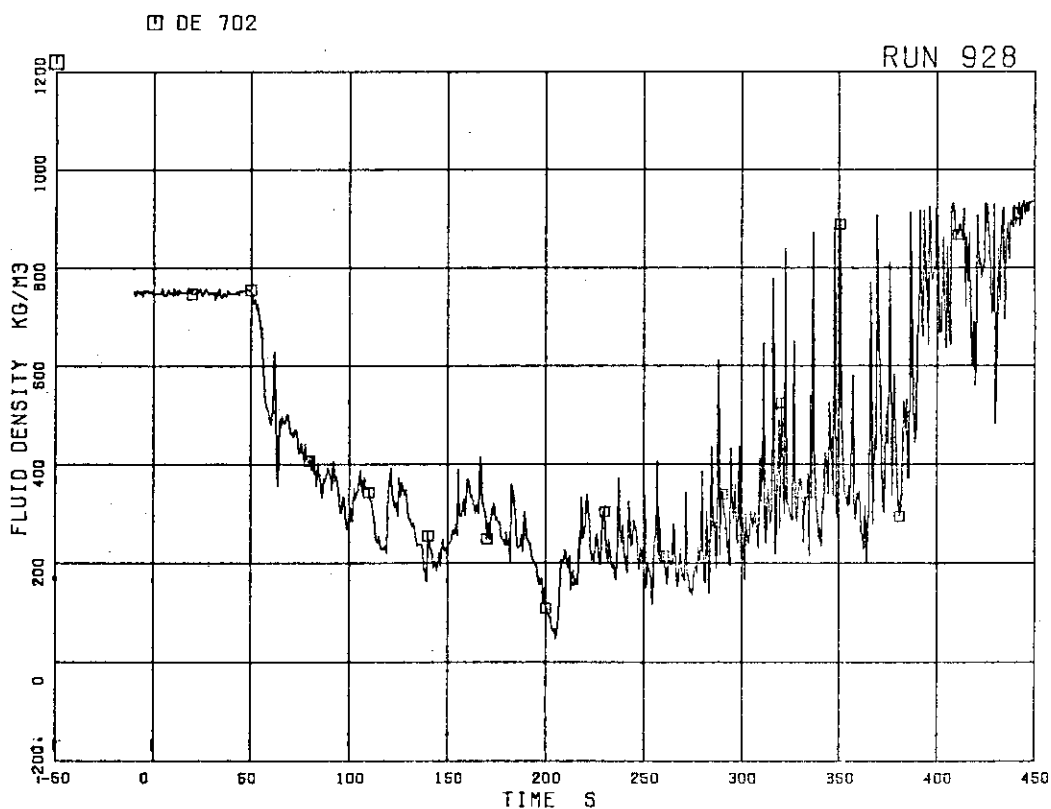


FIG.5.229 AVERAGE DENSITY AT JP-3,4 OUTLET

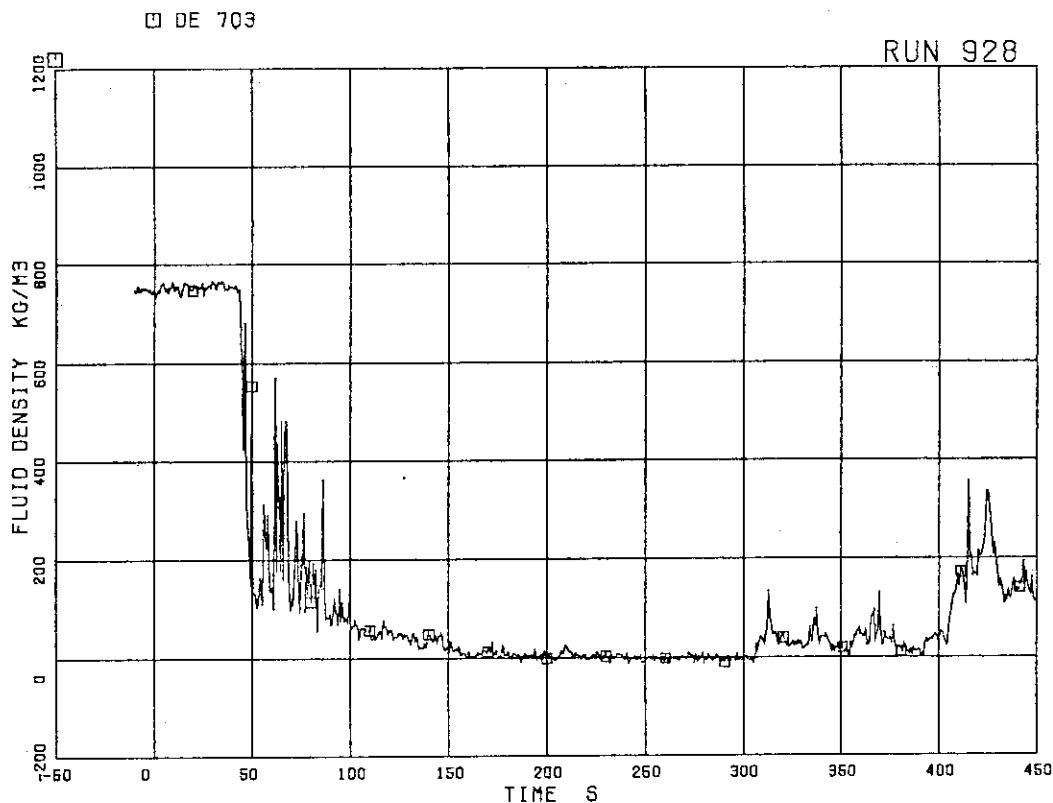


FIG.5.230 AVERAGE DENSITY AT MRP SIDE OF BREAK

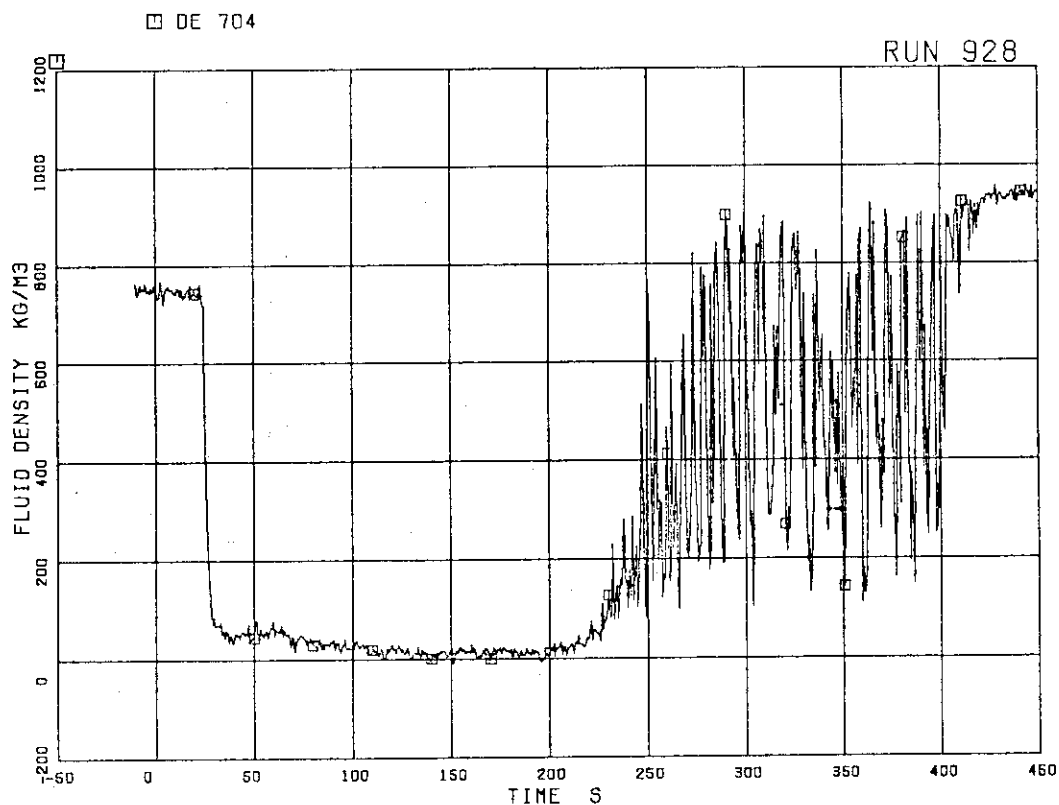


FIG.5.231 AVERAGE DENSITY AT PV SIDE OF BREAK

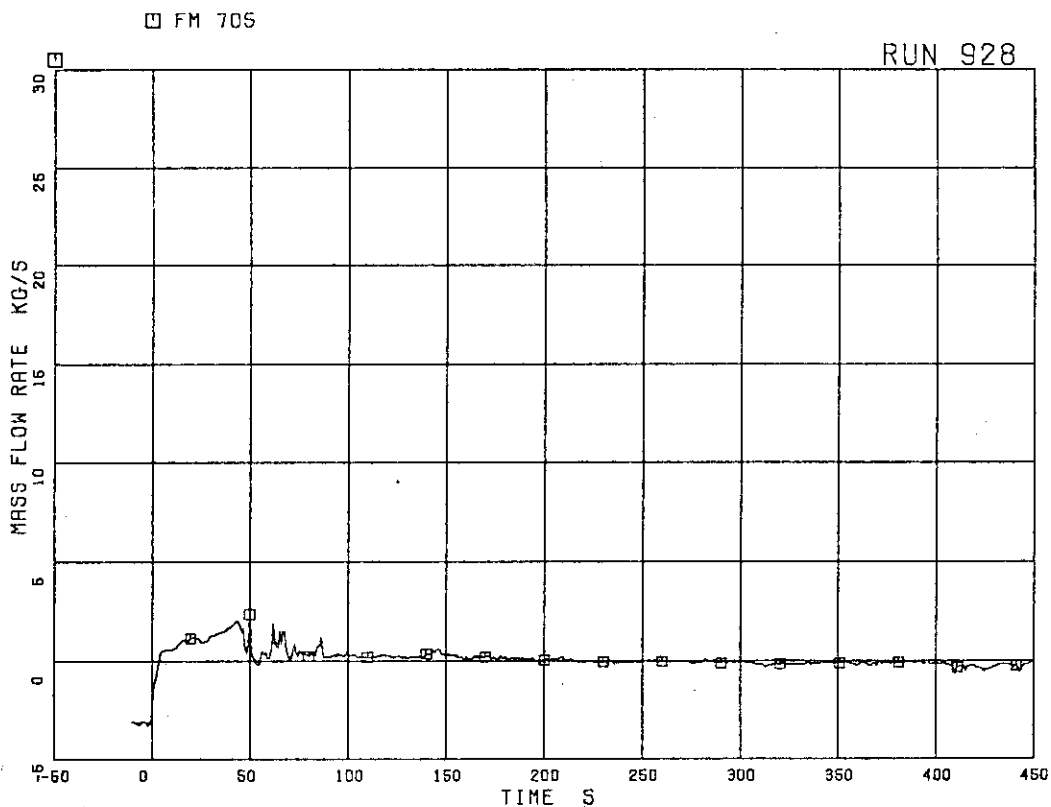


FIG. 5.232 FLOW RATE AT MRP SIDE OF BREAK  
(BASED ON LOW RANGE DRAG DISK DATA)

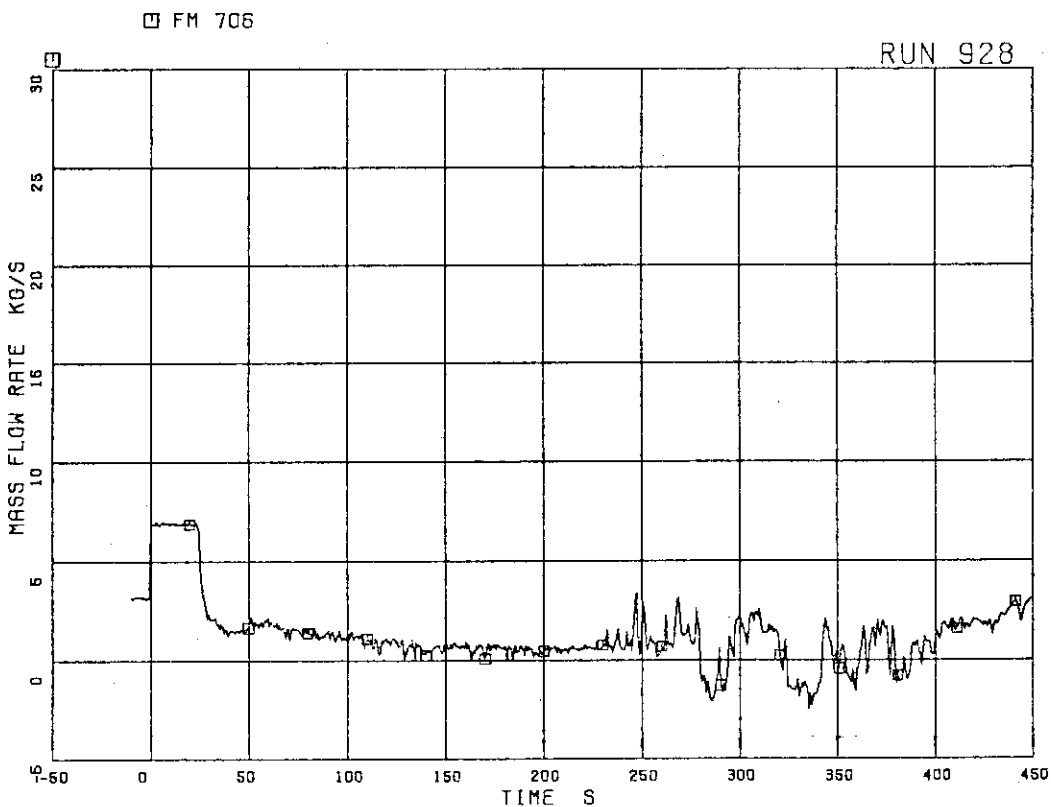


FIG. 5.233 FLOW RATE AT PV SIDE OF BREAK  
(BASED ON LOW RANGE DRAG DISK DATA)

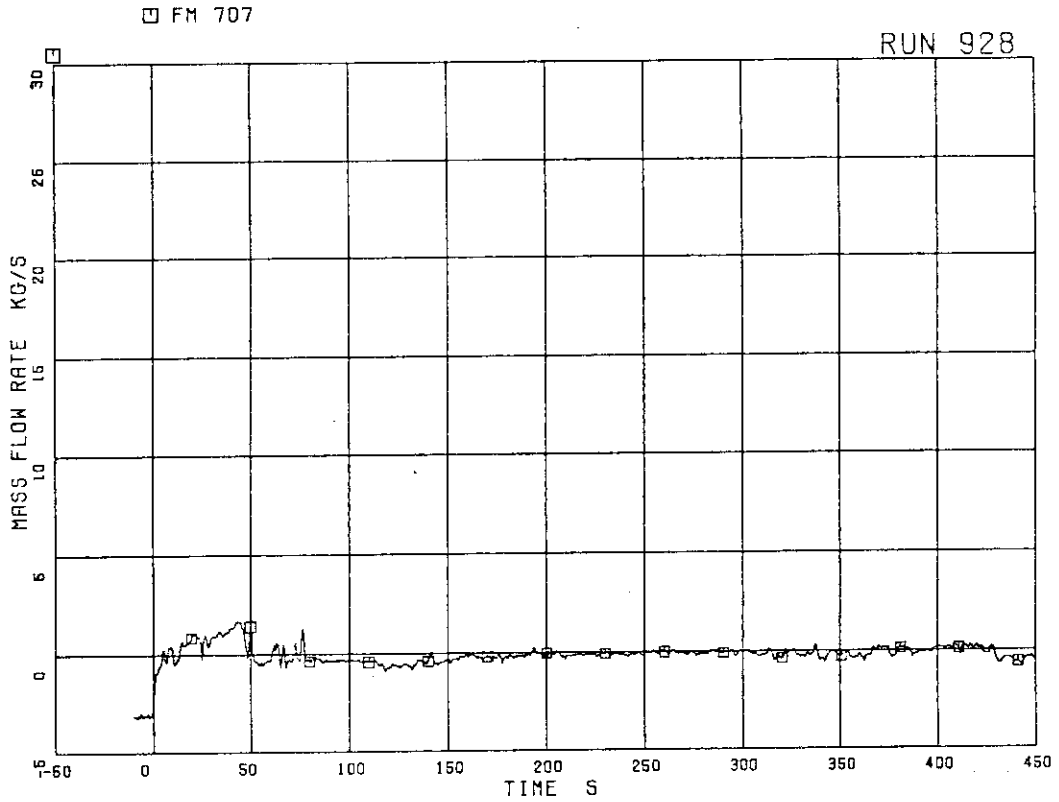


FIG.5.234 FLOW RATE AT MRP SIDE OF BREAK  
(BASED ON HIGH RANGE DRAG DISK DATA)

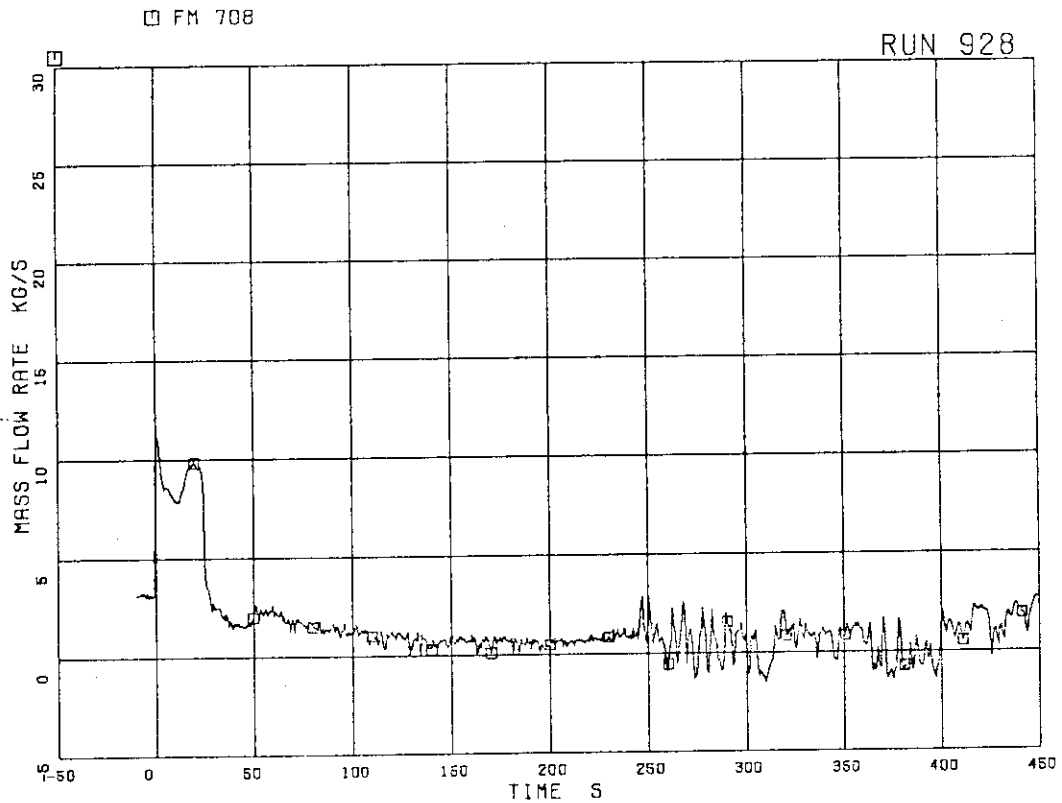


FIG.5.235 FLOW RATE AT PV SIDE OF BREAK  
(BASED ON HIGH RANGE DRAG DISK DATA)

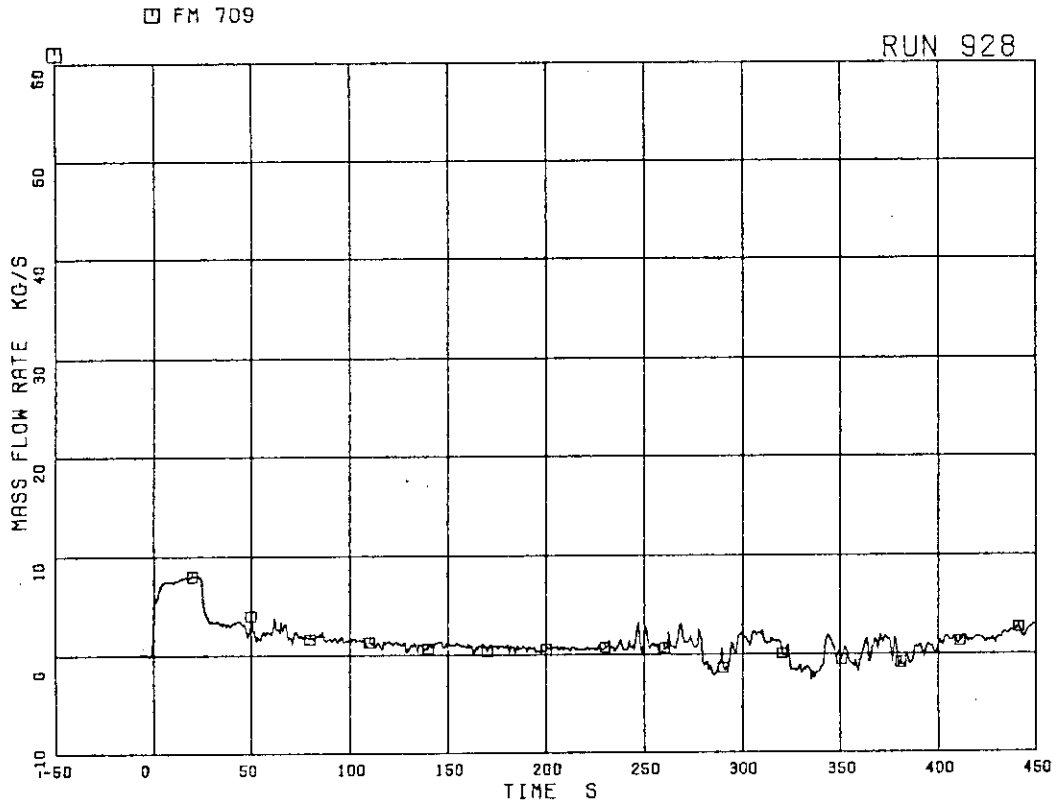


FIG.5.236 TOTAL DISCHARGE FLOW RATE FROM BREAK  
(BASED ON LOW RANGE DRAG DISK DATA)

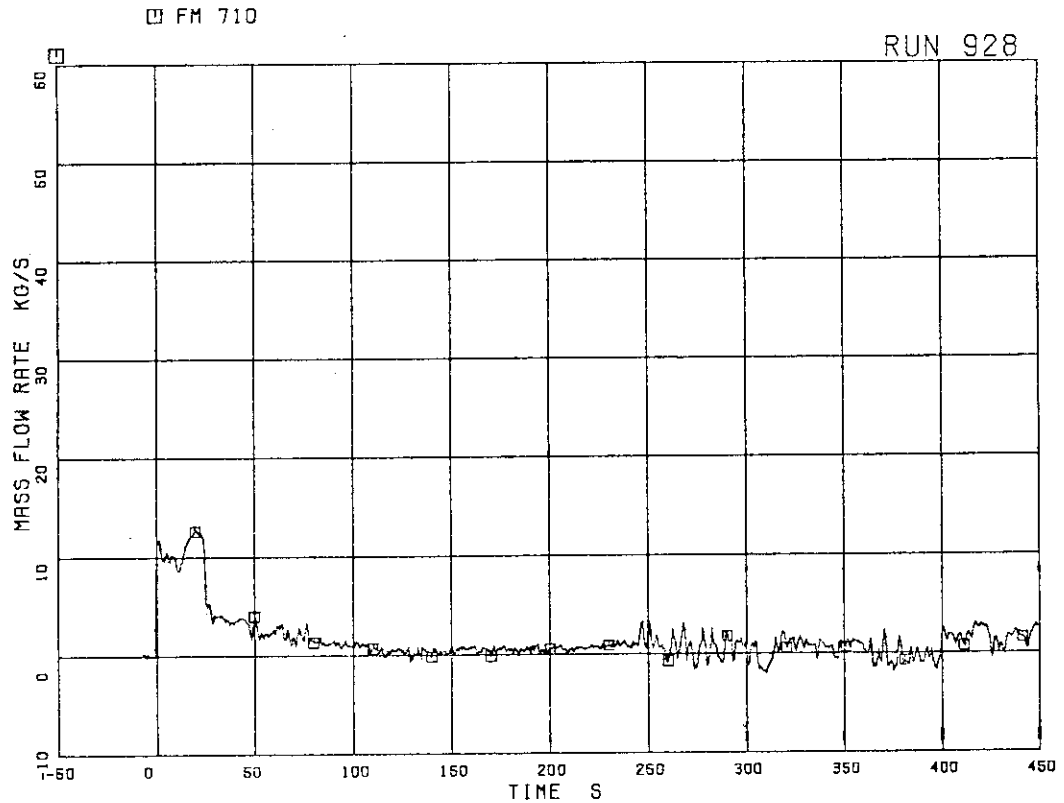


FIG.5.237 TOTAL DISCHARGE FLOW RATE FROM BREAK  
(BASED ON HIGH RANGE DRAG DISK DATA)



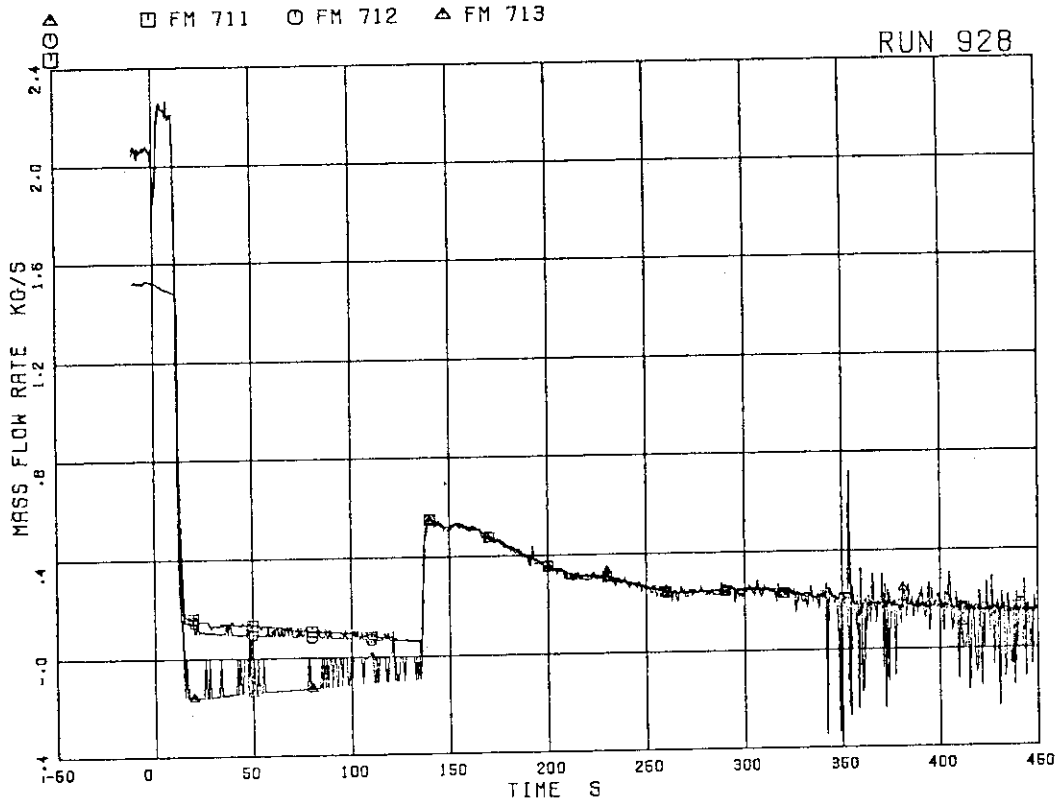


FIG.5.238 STEAM DISCHARGE FLOW RATE THROUGH MSL

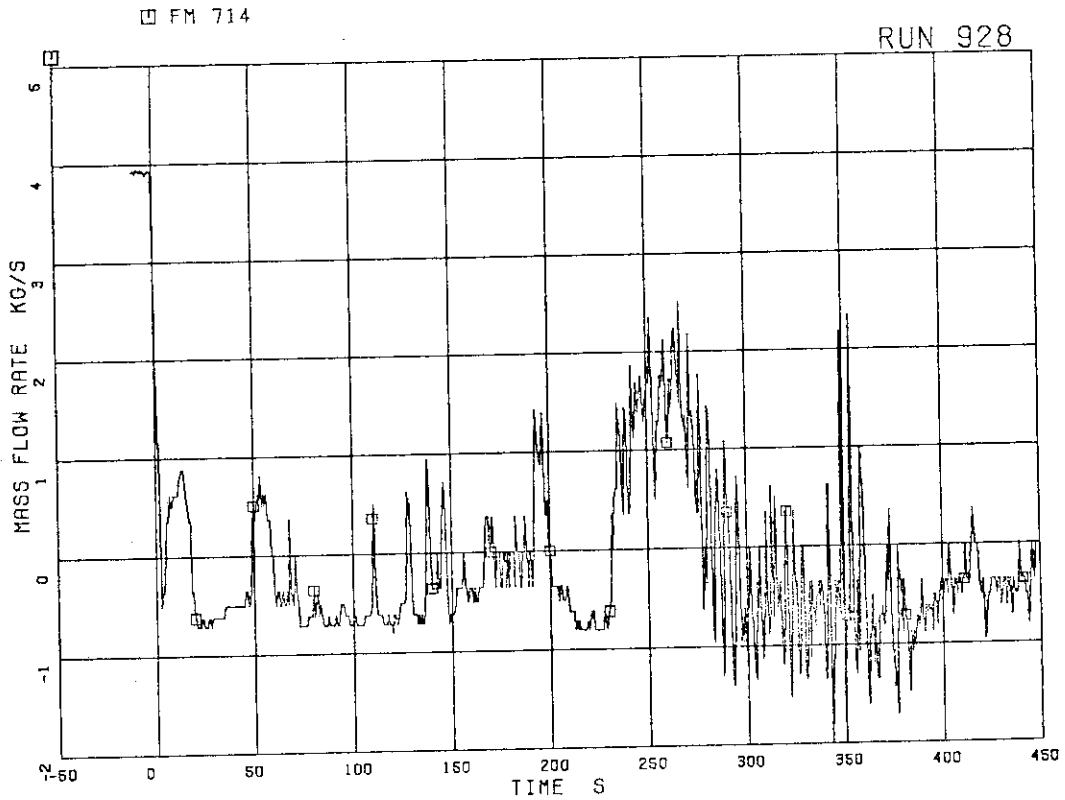


FIG.5.239 FLOW RATE AT CHANNEL A INLET

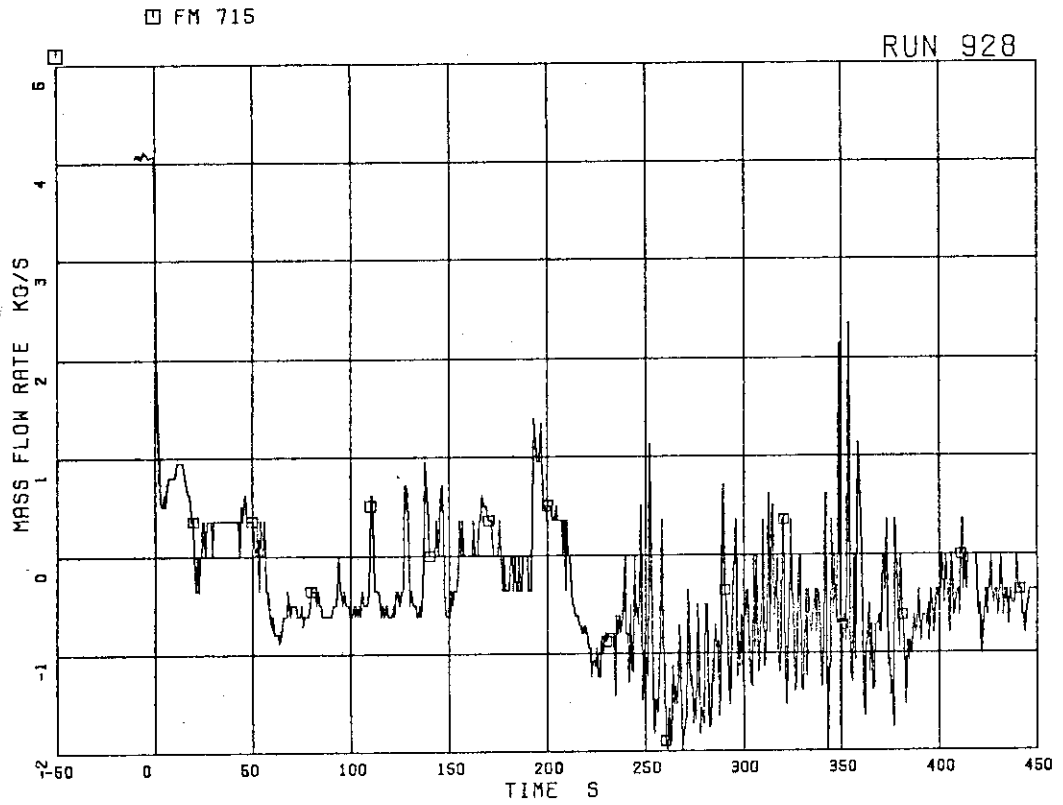


FIG.5.240 FLOW RATE AT CHANNEL B INLET

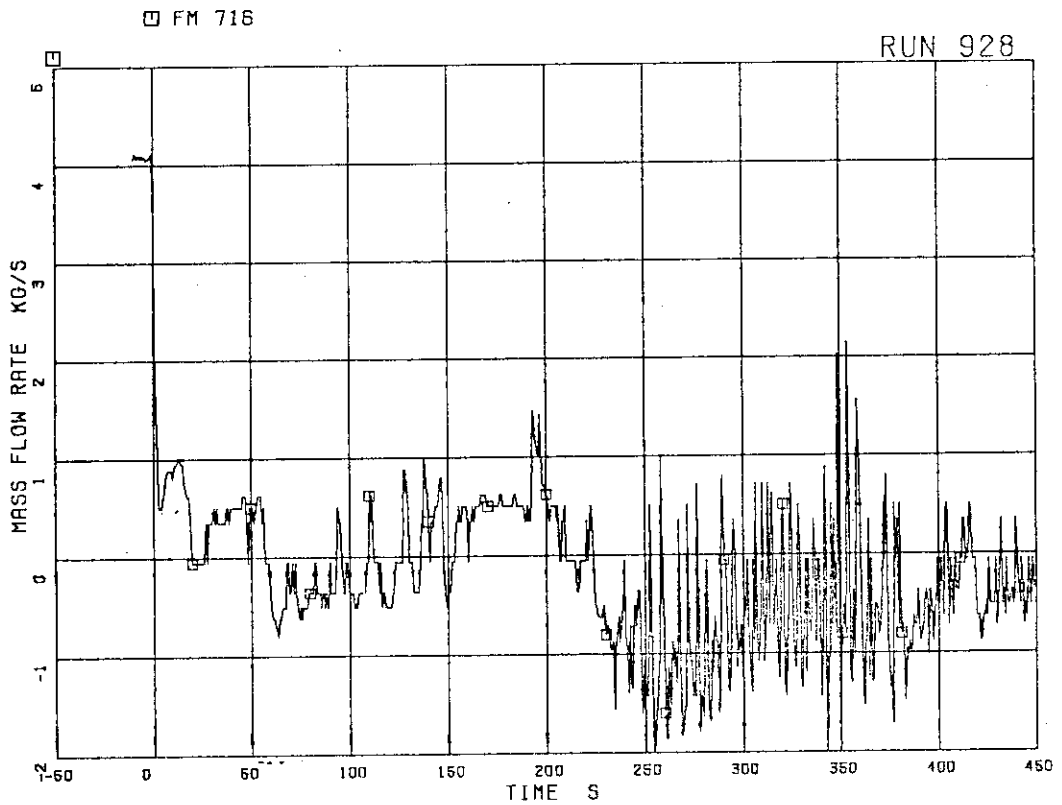


FIG.5.241 FLOW RATE AT CHANNEL C INLET

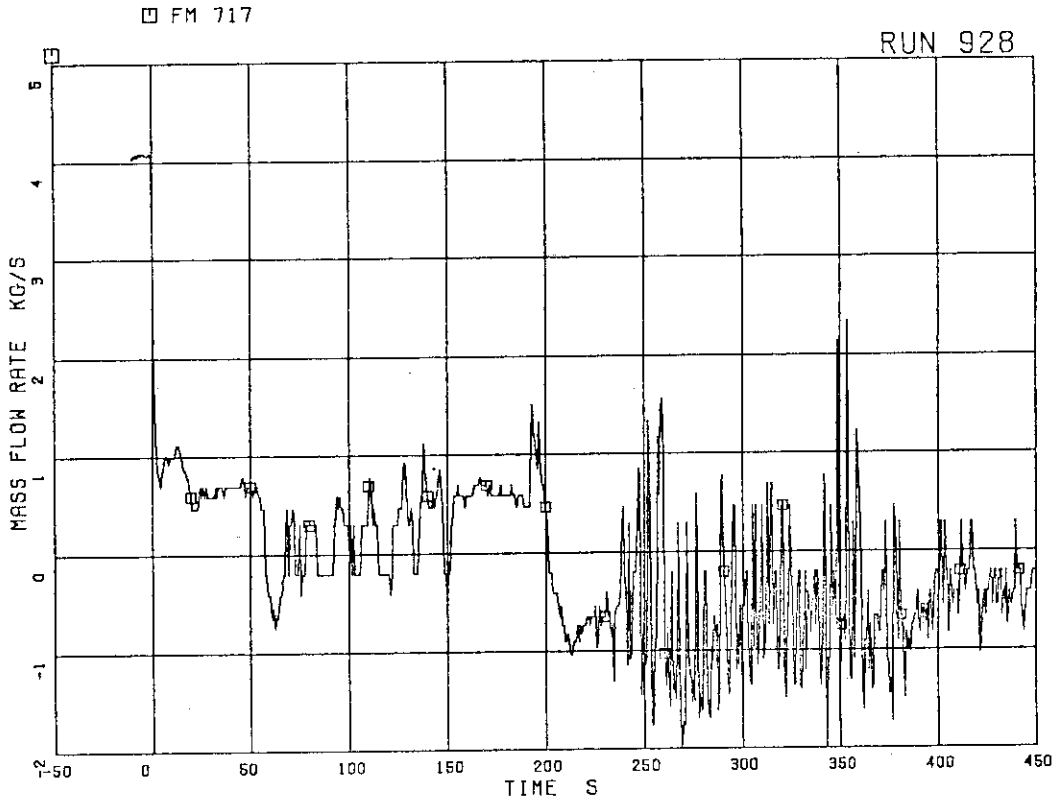


FIG.5.242 FLOW RATE AT CHANNEL D INLET

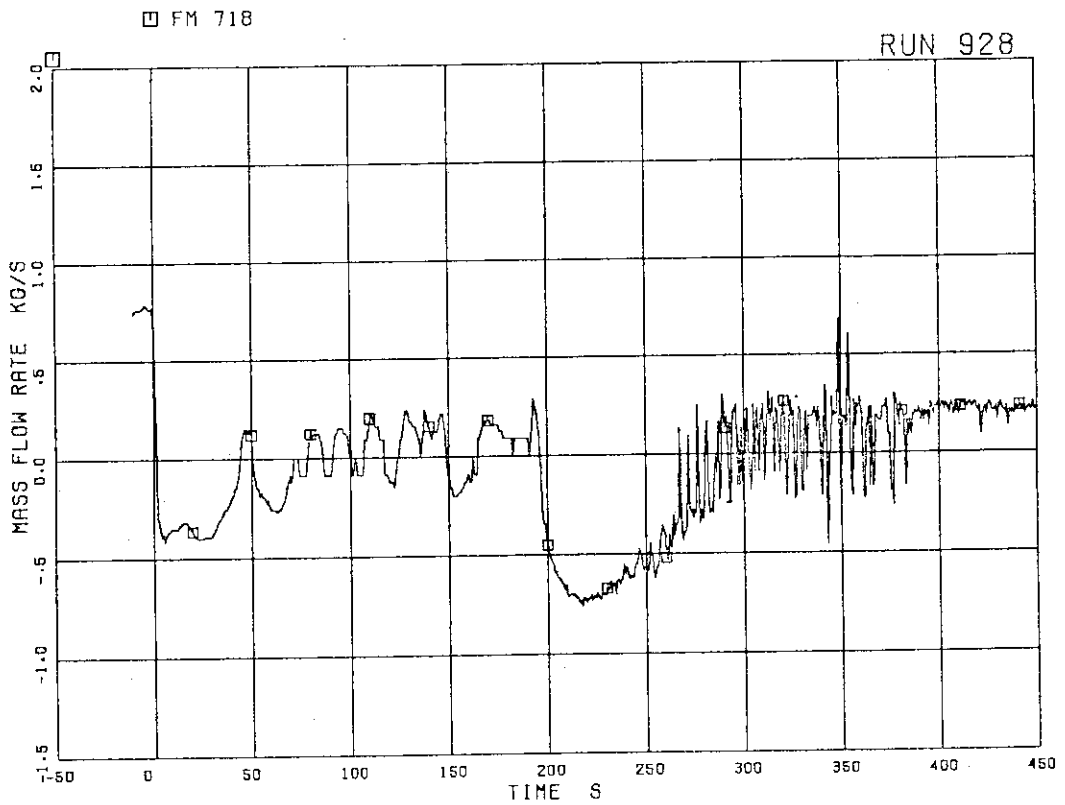


FIG.5.243 FLOW RATE AT BYPASS HOLE

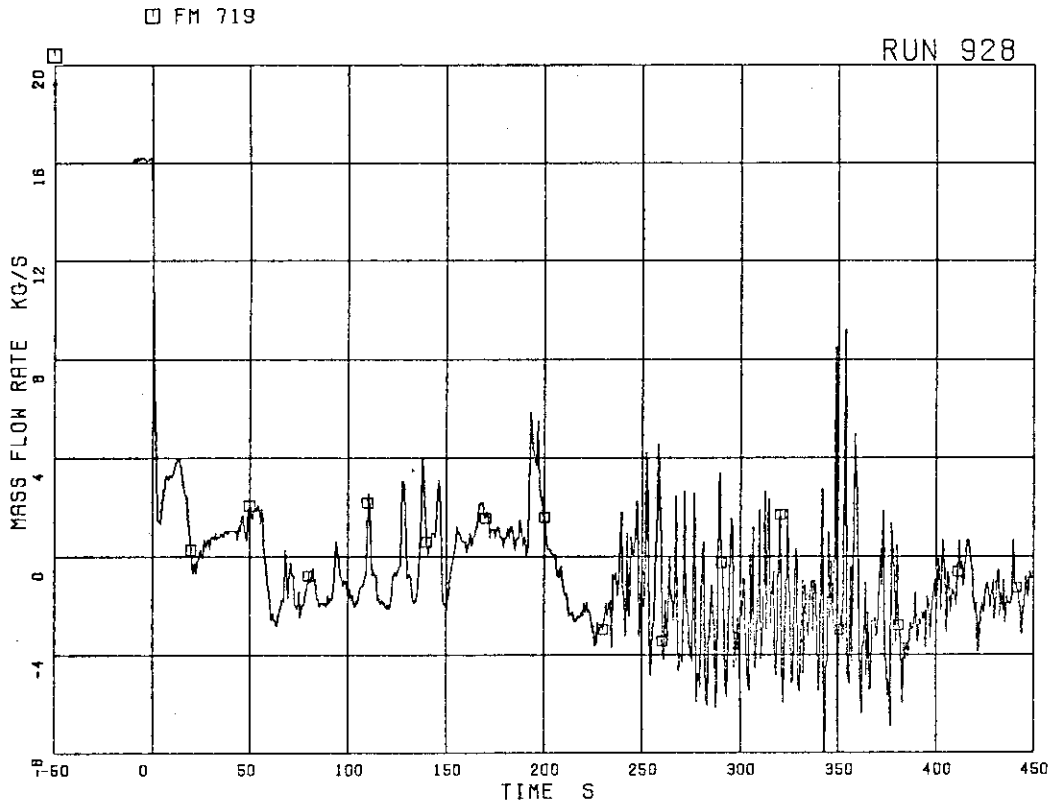


FIG.5.244 TOTAL CHANNEL INLET FLOW RATE

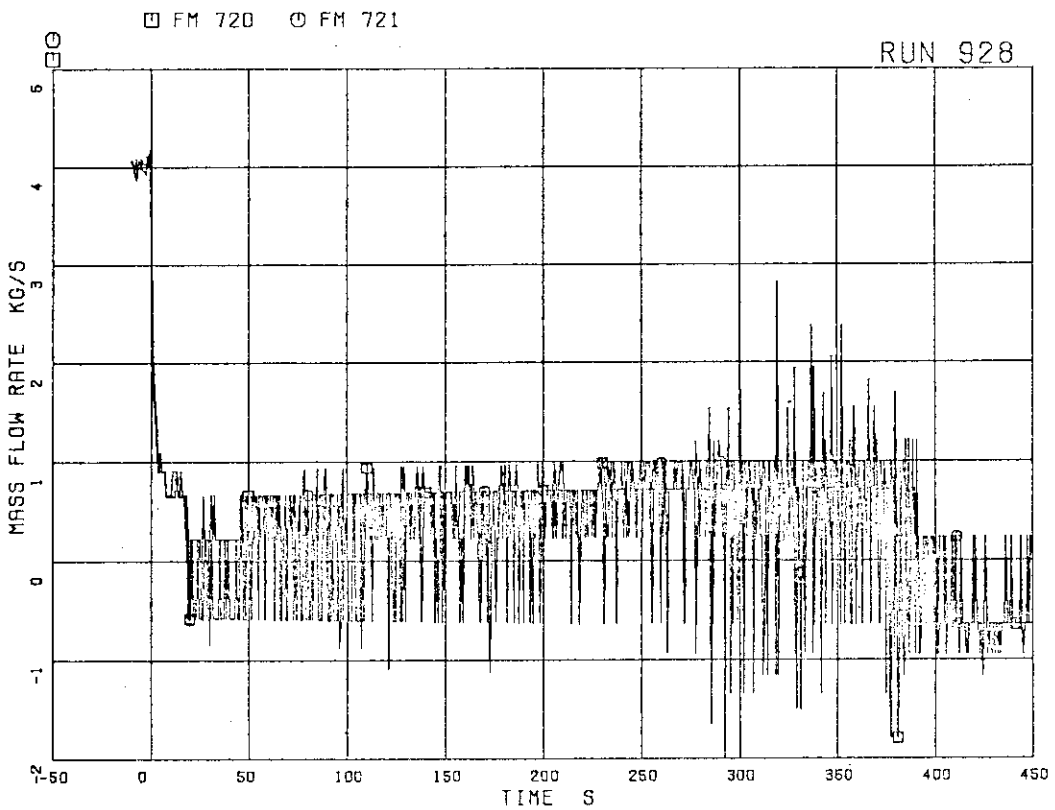


FIG.5.245 FLOW RATE AT JP-1.2 OUTLET  
(HIGH RANGE)

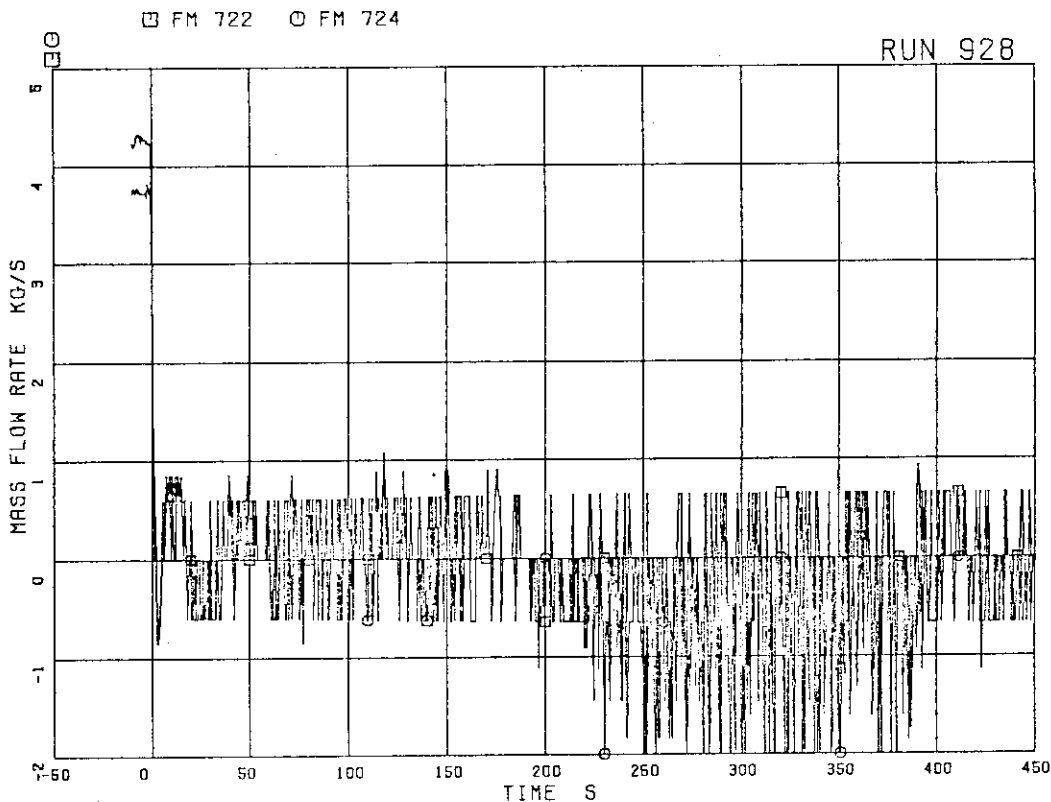


FIG.5.246 FLOW RATE AT JP-3.4 OUTLET  
(HIGH RANGE)

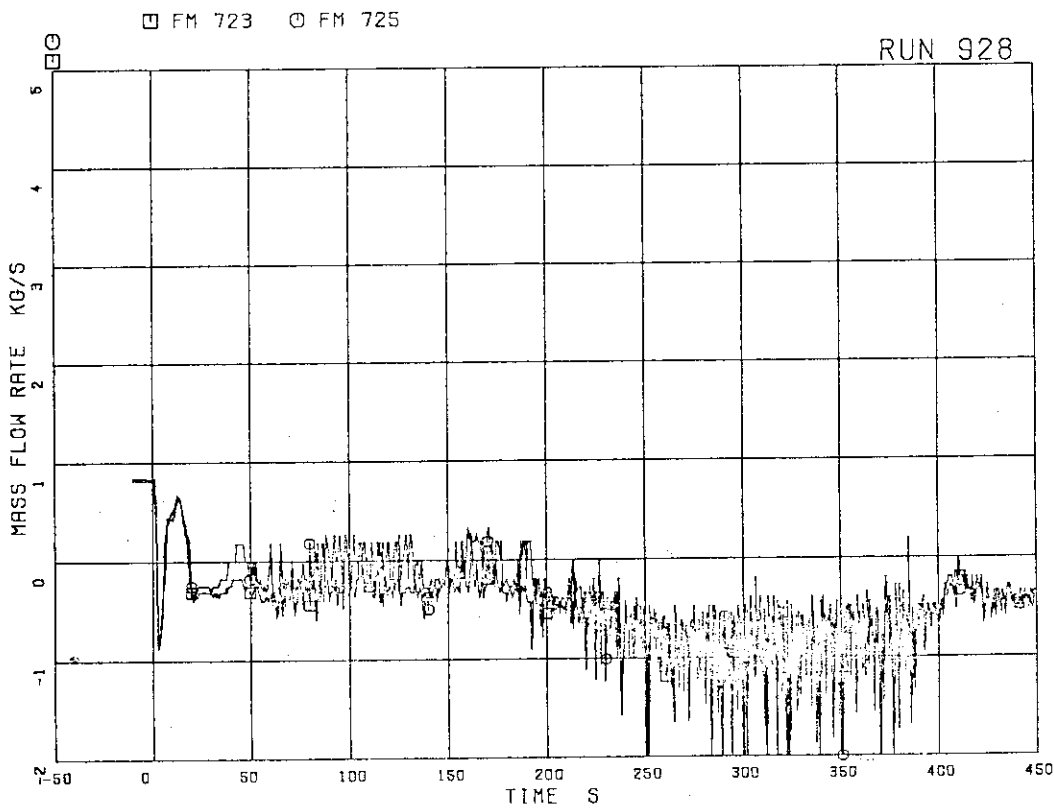


FIG.5.247 FLOW RATE AT JP-3.4 OUTLET  
(LOW RANGE)

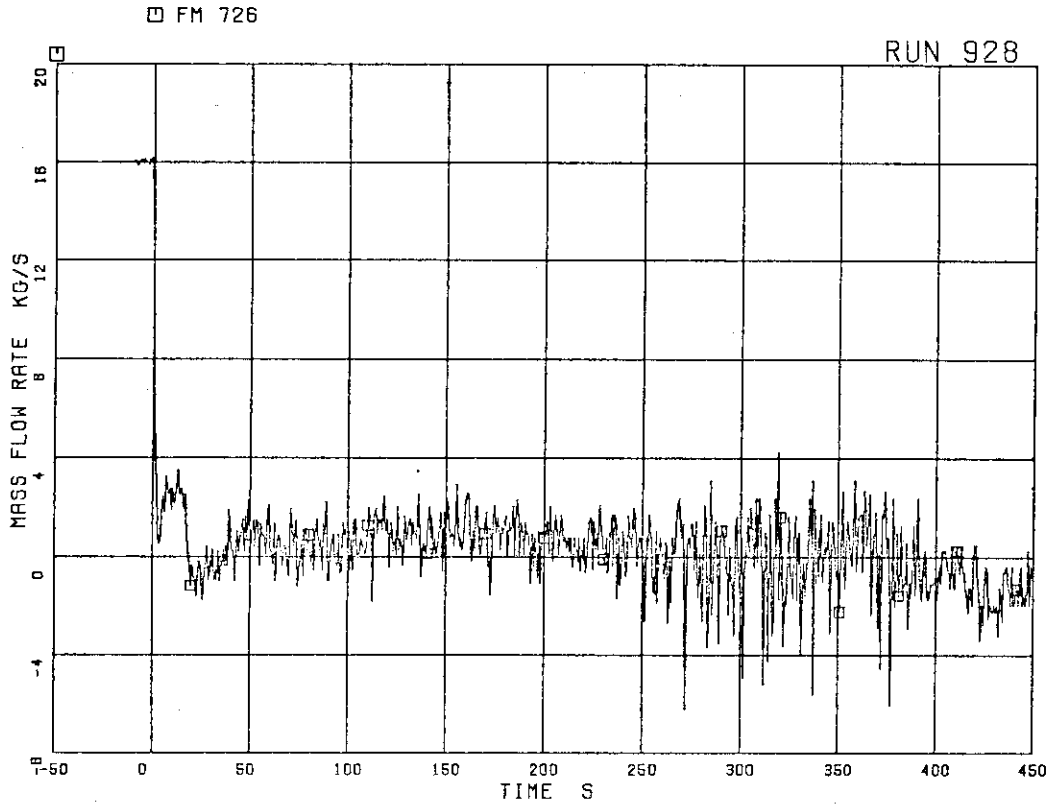


FIG. 5.248 TOTAL JP OUTLET FLOW RATE (HIGH RANGE)

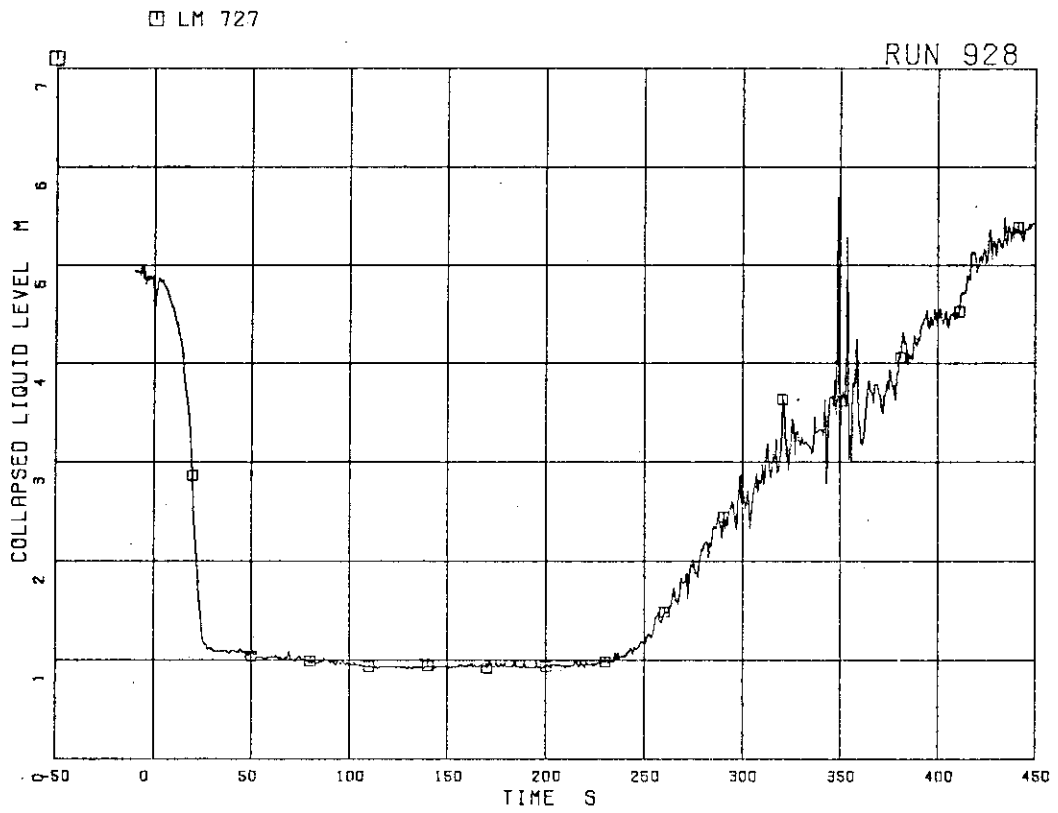


FIG. 5.249 COLLAPSED LIQUID LEVEL IN DOWNCOMER

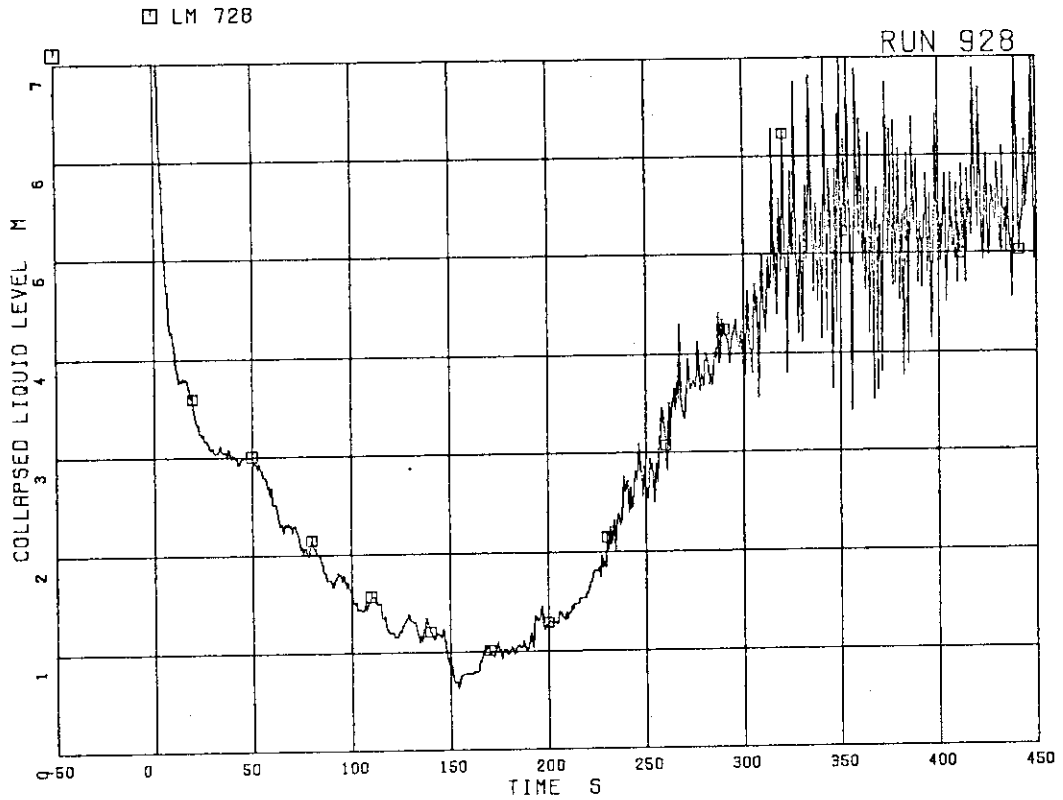


FIG.5.250 COLLAPSED LIQUID LEVEL INSIDE CORE SHROUD

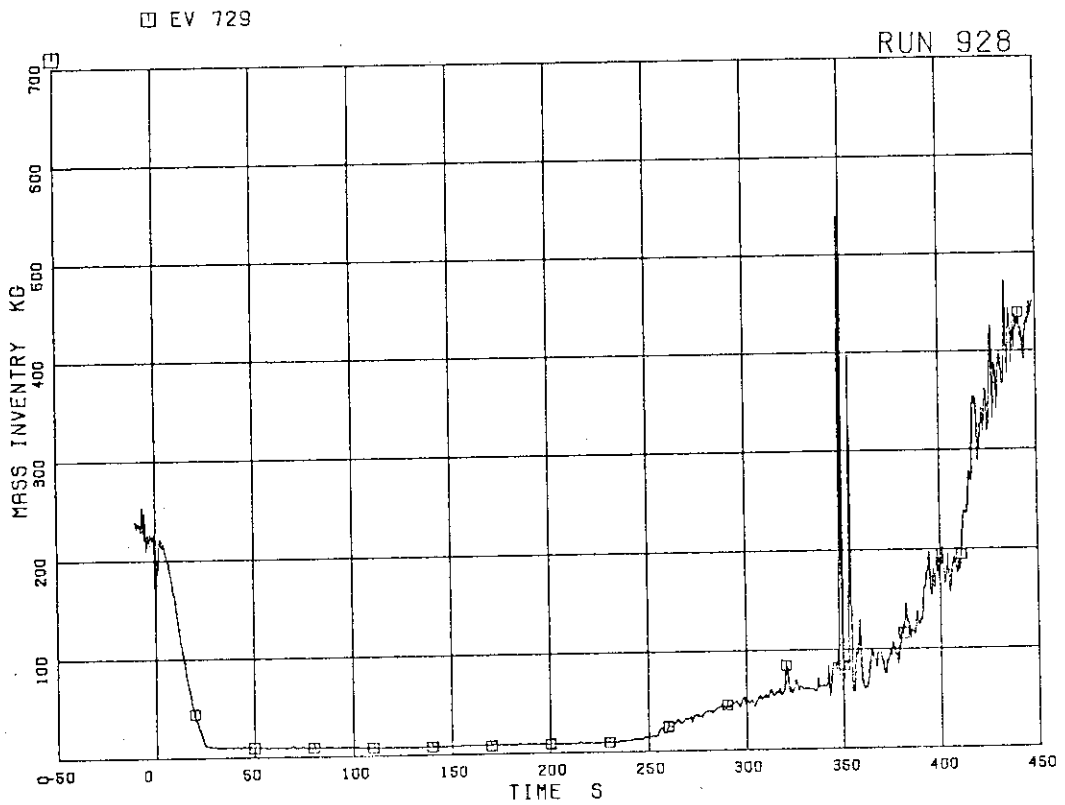


FIG.5.251 FLUID INVENTORY IN DOWNCOMER

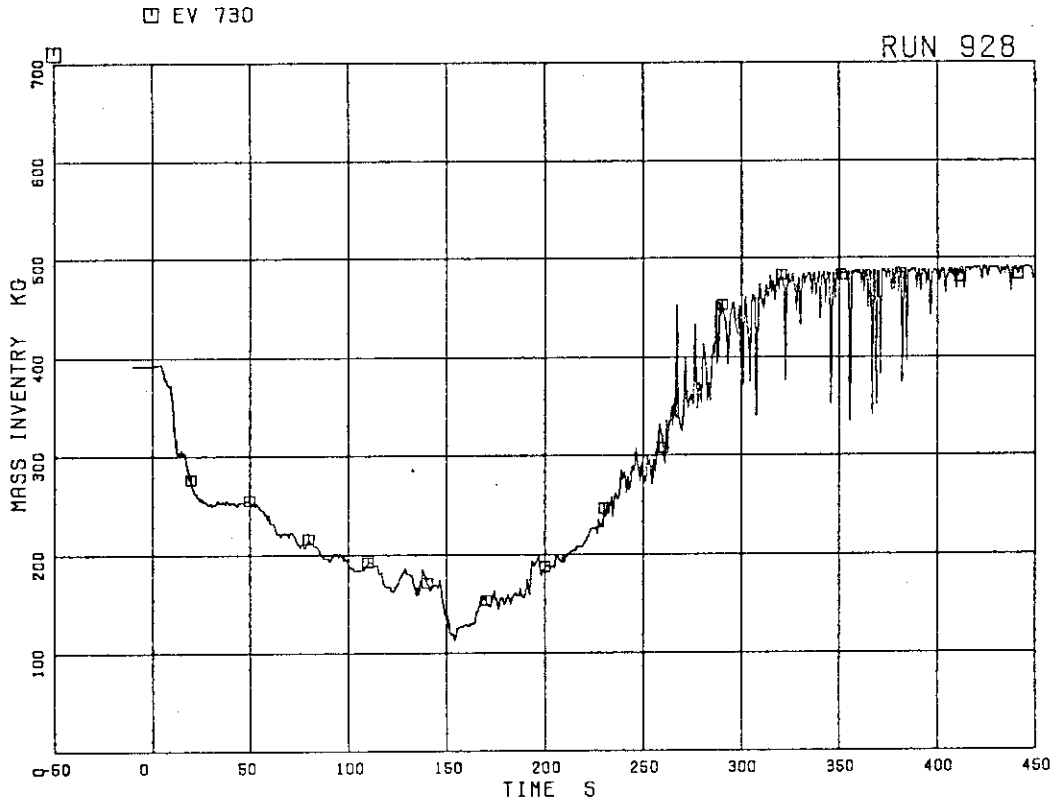


FIG. 5.252 FLUID INVENTORY INSIDE CORE SHROUD

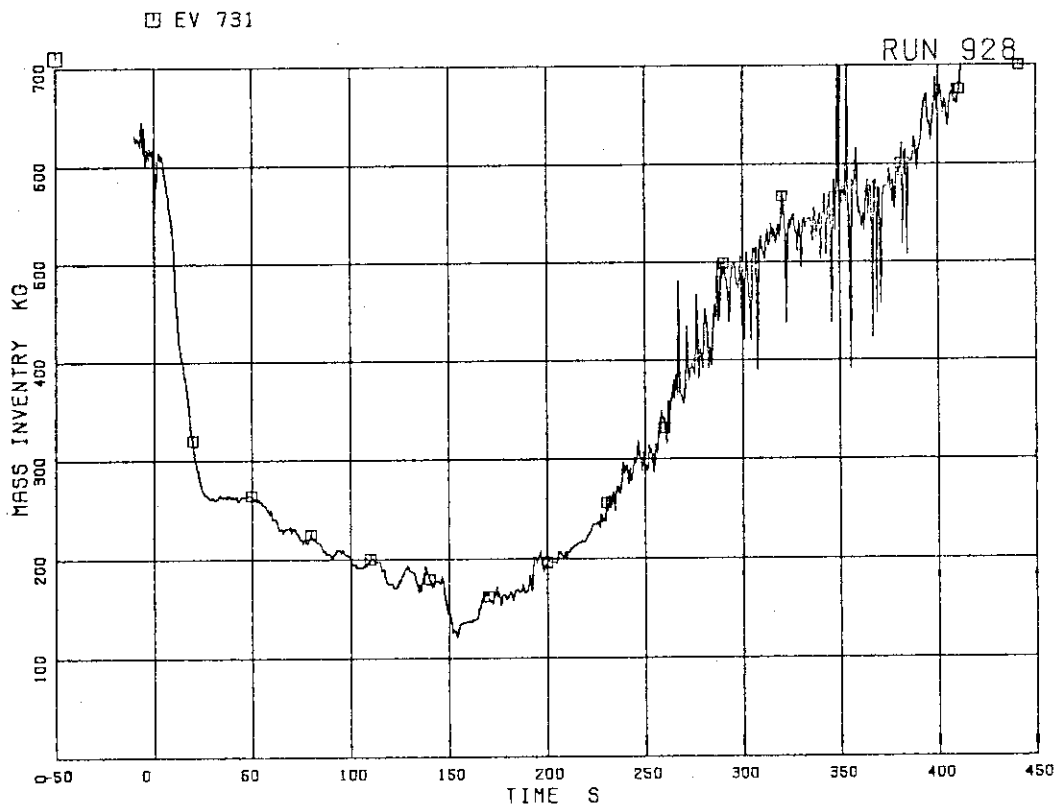


FIG. 5.253 TOTAL FLUID INVENTORY IN PRESSURE VESSEL



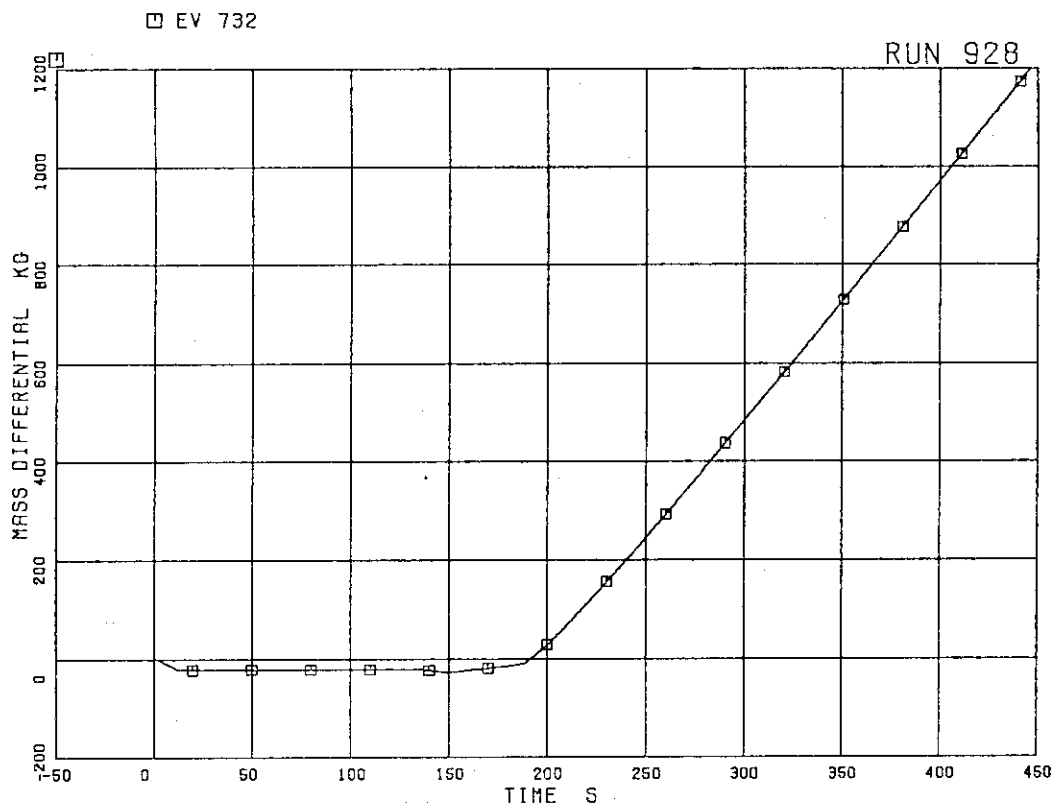


FIG. 5.254 FLUID MASS INCREASE BY ECCS AND FW AND DECREASE BY STEAM DISCHARGE FLOW

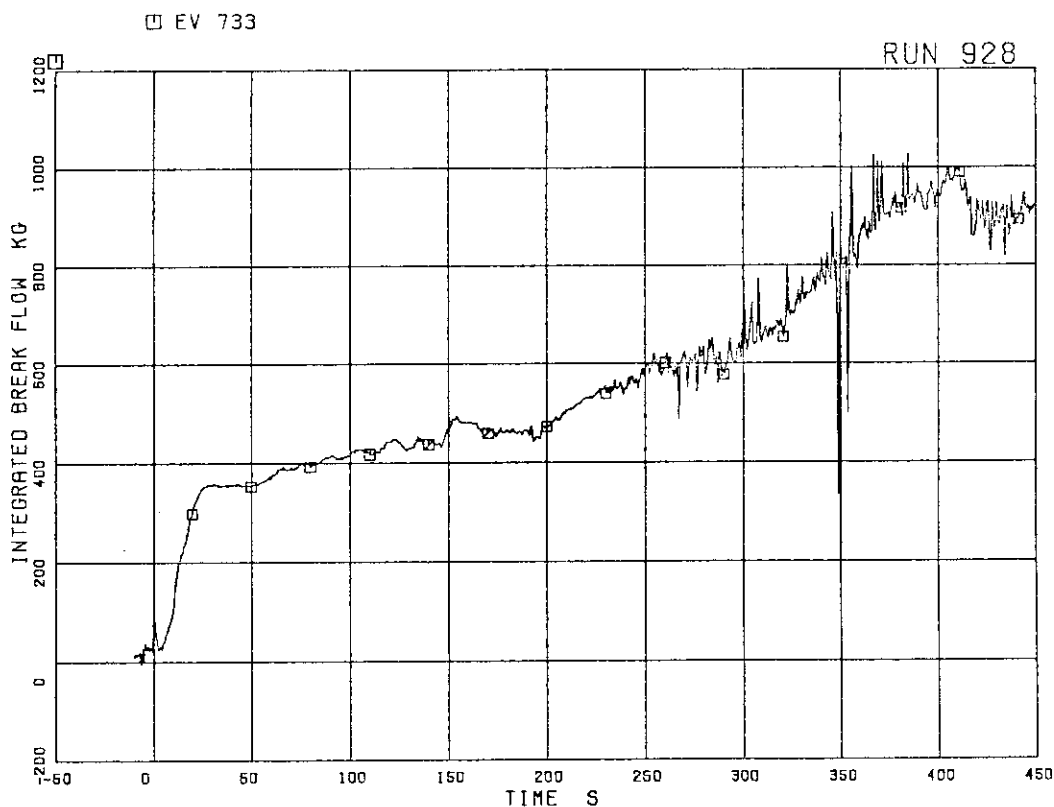


FIG. 5.255 DISCHARGED FLUID MASS FROM BREAK

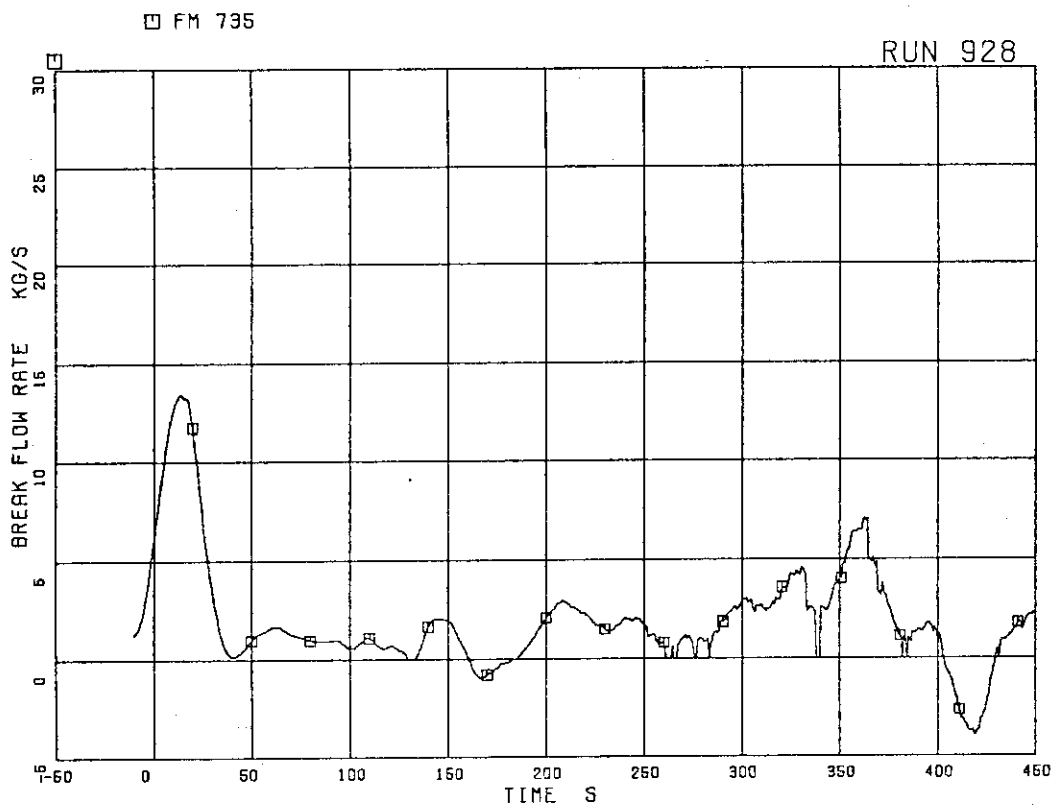


FIG.5.256 DISCHARGED FLOW RATE FROM BREAK

## 6. Test Results and Comparison with those of RUN 916

This section presents interpretation of RUN 928 test data, as well as comparison of RUN 916<sup>(6)</sup>. RUN 916 was the test with a 50% break at MRP suction line using an orifice as a break plane. The effect of break configuration difference can be evaluated by comparing the results of these two tests.

### 6.1 Test Conditions

Table 6.1 compares the initial test conditions and major events in the two tests. The test conditions of the two tests were nearly the same except for break configuration.

### 6.2 System Pressure

The lower plenum pressures in RUNs 928 and 916 are compared in Fig. 6.1. The pressures represent typical system pressure responses in the two tests, respectively. The pressure transients in the two tests show very similar trends: After the initial decrease, the pressure began to recover when MSIV was closed, and to decrease again as the recirculation line was uncovered. The MSIV initiated to close at 12.6 s in RUN 928, 5.1 s later than in RUN 916. The timings of RLU and MSIV closure were later in RUN 928 because downcomer water level decrease rate was slower in RUN 928 than in RUN 916 due to the break flow difference. The lower plenum flashing (LPF) started at 45 s and 38 s in RUNs 928 and 916, respectively, as the system depressurized to the saturation pressure corresponding to the lower plenum fluid temperature. The depressurization rate after LPF in RUN 928 was the same as that in RUN 916, which indicates the break flow rates after RLU in both tests were nearly the same. The feedwater line flashing (FWLF) in RUN 928 occurred later than in RUN 916. After the FWLF initiation the system depressurization rates were decreased in both tests. LPCI and ADS affected the pressure transient little.

### 6.3 Break Flow Rate

The break flow rates in RUNs 928 and 916 are compared in Figure 6.2. The fluid condition upstream of the break was subcooled liquid until RLU and two-phase fluid or single-phase vapor after RLU in the two tests. It is

clearly shown that the subcooled break flow rate in RUN 928 using a nozzle was smaller than that in RUN 916 using an orifice and flow rates after RLU were nearly the same between the two tests. The break flow rates obtained from the measurements with the dragdisks and gamma densitometers include a maximum error of  $\pm 20\%$  in the two phase condition. The break flow rate was also calculated by differentiating the mass inventory with respect to time as shown in Fig.5.256. This estimated flow rate includes the error caused by the mass inventory calculation using the differential pressure data because the differential pressure includes not only the water head but also frictional loss and acceleration loss.

#### 6.4 Coolant Flow Rate

The coolant flow rate through the channel inlet orifices and the bypass hole are calculated from the differential pressure across these flow paths as mentioned in section 5. The total channel inlet flow rate in Run 928, shown in Fig.5.244, is compared with that in RUN 916 in Fig.6.3. The flow rates in the two tests decreased rapidly after break and kept nearly constant value. The flow rate decreased again to nearly zero after the liquid level in the downcomer decreased to the jet pump suction level. The timing of flow decrease was earlier in RUN 916 than in RUN 928 because of a larger break flow rate in RUN 916. After the LPF initiation the flow rate increased temporarily. However, when the flow through the orifice became two phase, the calculated flow rate became incorrect giving only the trend. The flow rates in the two tests showed the downward flow with oscillation after LPF until core inlet dryout. When the liquid level above the channel inlet orifice disappeared, the core inlet flow turned to upward direction. After the FWLF initiation the core flow was reversed to the downward direction temporarily. This is because the rapid steam generation in the feedwater line reduced the system depressurization rate, and reduce the steam generation in the lower plenum. Oscillatory downward flow after 200 s in the two tests was caused by LPCI actuation.

#### 6.5 Liquid Level

Liquid levels in the core and the downcomer in RUNs 928 and 916 are compared in Fig.6.4. These liquid levels are estimated from signals obtained from the conductivity probes installed in the pressure vessel.

The downcomer water level in RUN 916 decreased faster than that in RUN 928 because of difference in the subcooled break flow rate.

The core liquid level behaviors showed the same trend between RUNs 928 and 916. The liquid levels in the two tests began to drop at 68 s in RUN 928 and at 61 s in RUN 916 from the upper tieplate as LPF moderated. The whole core dryout occurred in both tests. When LPCI was actuated, the core reflooding started. The core uncover duration was nearly the same between the two tests.

CCFL was observed at both of the upper tieplate and the channel inlet orifice. The CCFL at core inlet orifice affected the core mixture level behavior. The core mixture level began to rise before the lower plenum was completely filled with water in both tests.

#### 6.6 Fuel Rod Surface Temperature

Dryout and quenching behaviors in channels A and C in RUN 928 are shown in Figs. 5.226 and 5.227. These behaviors were estimated from the fuel rod surface temperature histories. The mixture levels in channels A and C are also presented in Figs. 5.226 and 5.227, respectively. The dryout behaviors corresponded closely to the mixture level in the channel box. The dryout front followed the falling liquid level. The quench occurred from core top by LPCS actuation and from core bottom by core mixture level rise. They are called top-down quench and bottom-up quench, respectively.

In RUN 928 the peak cladding temperature (PCT) was 888 K and was occurred at 198 s at midplane of A71 rod in the peak power channel A as shown in Fig. 6.5. The PCT in RUN 916 was 917 K and occurred at 190 s at midplane of the fuel rod A82 in the peak power channel A. The PCTs were nearly the same in RUNs 928 and 916.

Table 6.1 Comparison of Initial Conditions and Major Events in RUN 928 and RUN 916

Parameter	I	RUN 928	I	RUN 916
Break Diameter	I	18.5 mm	I	18.5 mm
Break Configuration	I	Nozzle	I	Orifice
Core Power	I	3.962 MW	I	3.963 MW
Steam Dome Pressure	I	7.36 MPa	I	7.32 MPa
Core Inlet Flow	I	16.4 kg/s	I	16.5 kg/s
Lower Plenum Subcooling	I	9.4 k	I	11.2 K
PCT	I	888 K	I	917 K
	I	(A17 Pos.4 198s)	I	(A82 Pos.4 190s)
Events	I	Time after break	I	s
Feedwater Stop	I	1.4 - 3.4	I	1.6 - 3.2
MSIV Closure	I	12.6 - 16.2	I	7.5 - 12.2
LPF initiation	I	45	I	38
ADS Actuation	I	136	I	131
LPCS Actuation	I	147	I	143
FWLF Initiation	I	148	I	142
LPCI Actuation	I	186	I	183
Whole core quench	I	245	I	255

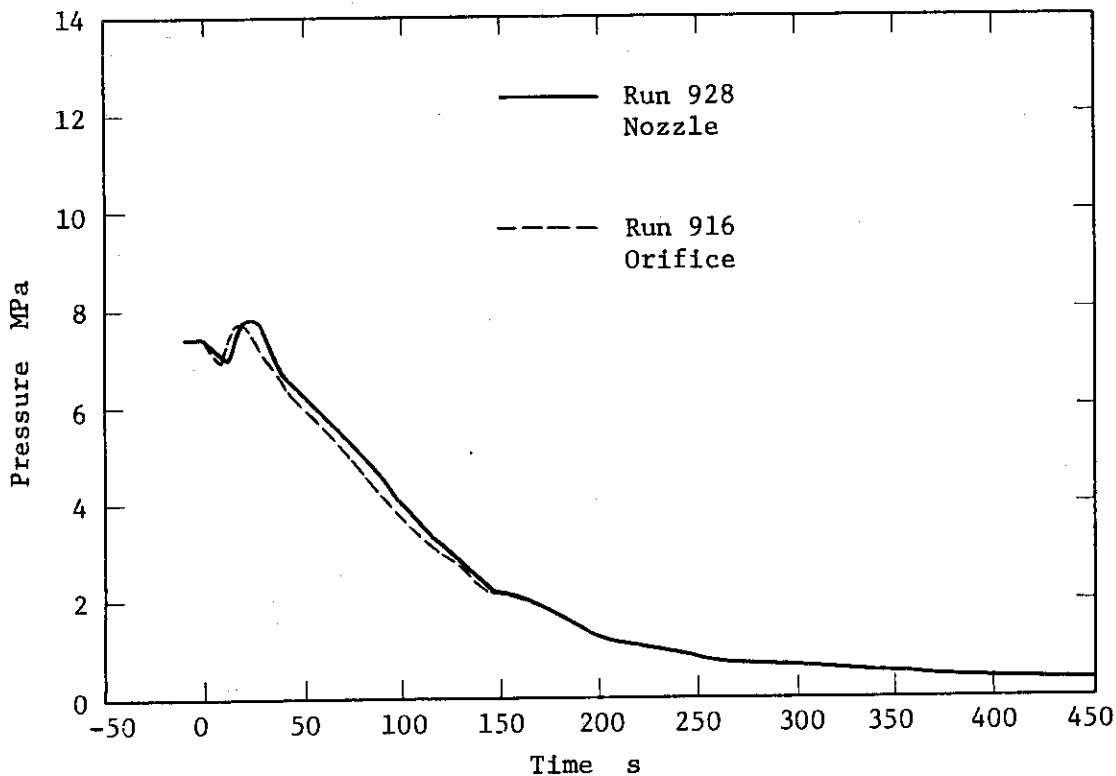


Fig. 6.1 Lower plenum pressures

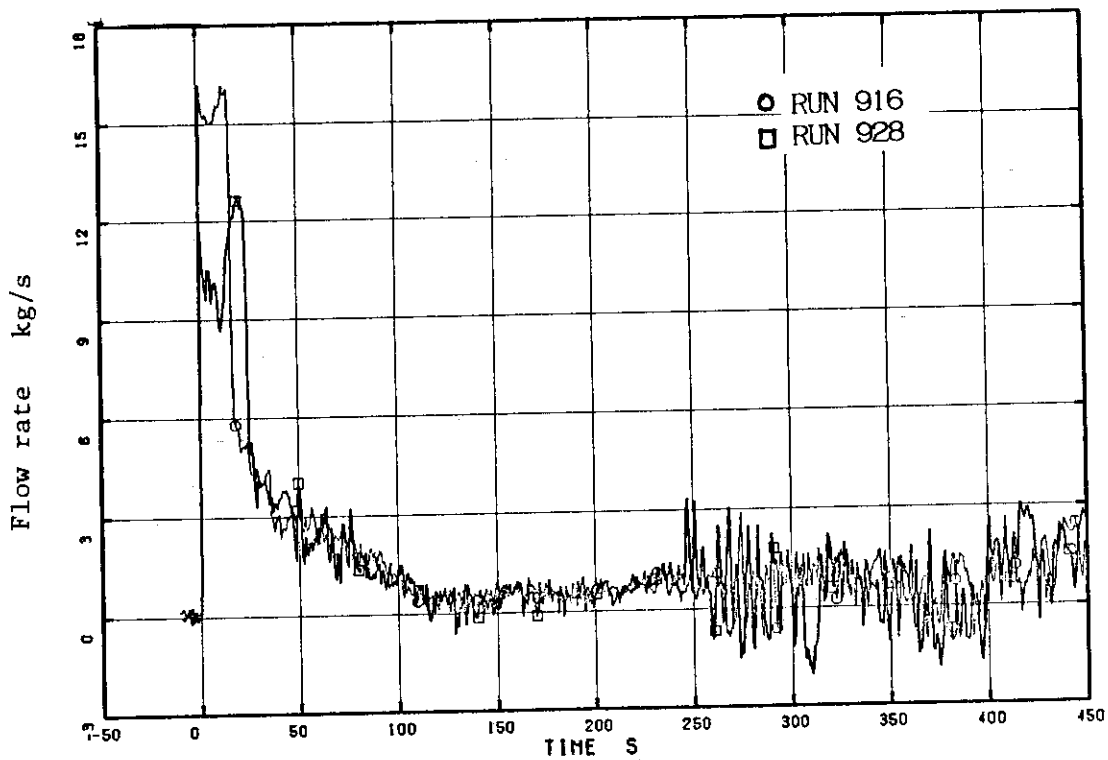


Fig. 6.2 Break flow rates

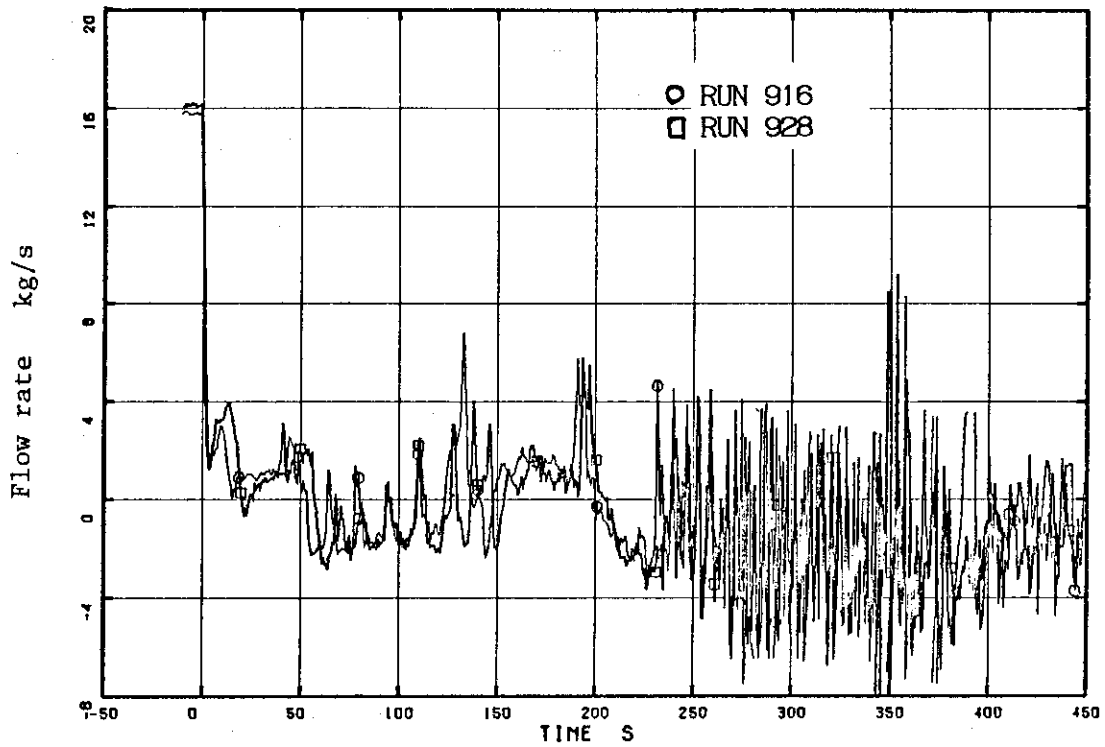


Fig. 6.3 Total channel inlet flow rates

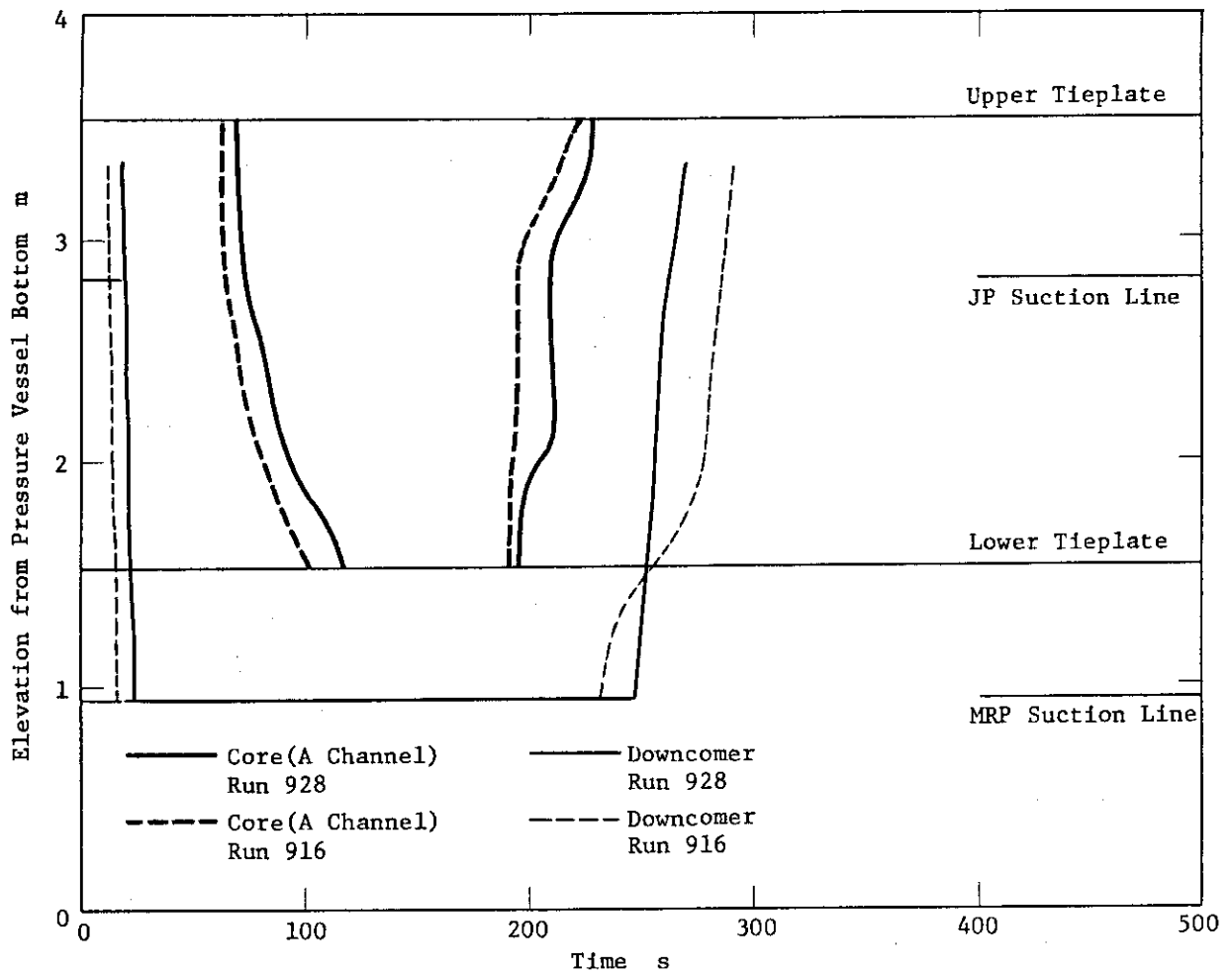


Fig. 6.4 Mixture levels in the pressure vessel



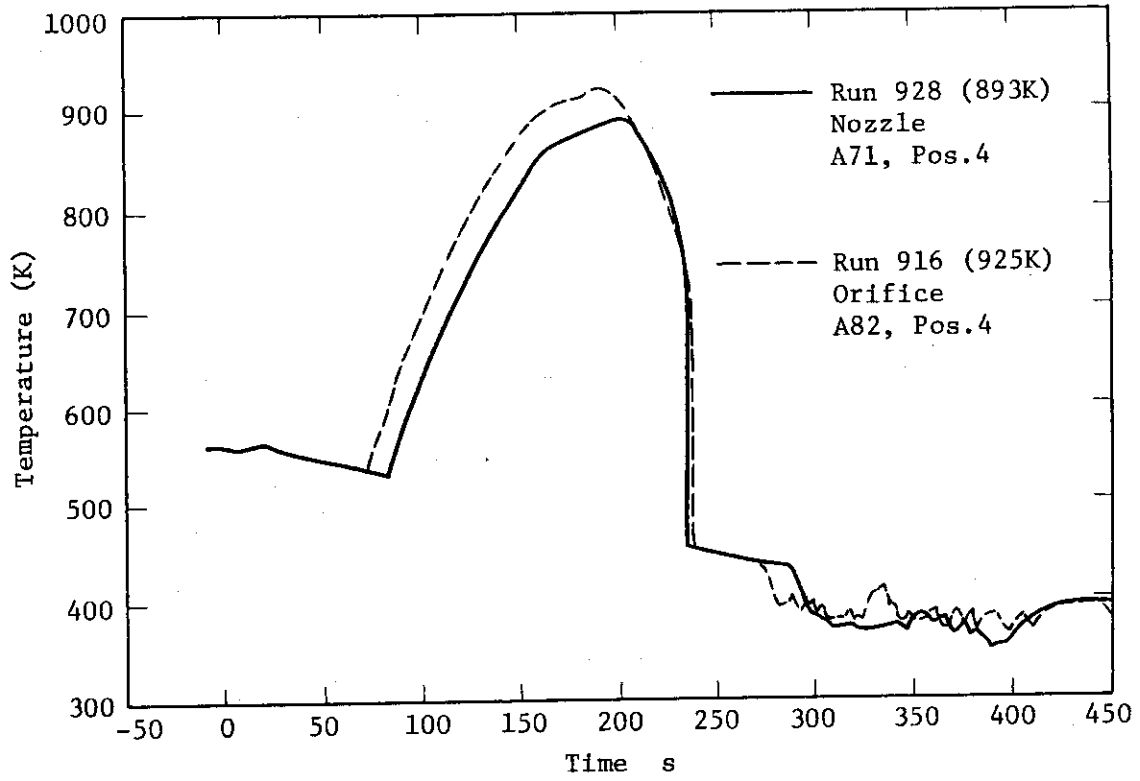


Fig. 6.5 Peak cladding temperatures

## 7. Conclusions

In this report, all the available test data obtained in a 50% break LOCA test RUN 928 were presented with information on the ROSA-III test facility, instrumentation and the test procedure. The explanations of the test results were also given.

RUN 928 was a 50 % break LOCA test at the recirculation pump suction line without HPCS actuation, and conducted as one of the break configuration sensitivity tests. A long throat nozzle was used as a break plane. From evaluation of the test results of RUN 928 and comparison between the test results of RUN 928 and RUN 916 which was a 50% break test using an orifice as a break plane, the following conclusions were obtained :

- (1) The fundamental thermal-hydraulic phenomena during a 50% break LOCA at a recirculation pump suction line have been clarified.
- (2) The PCT in RUN 928 was 888 K and observed at midplane of the A71 rod in the high power channel at 198 s after break. All fuel rods were quenched after the LPCI actuation and the effectiveness of ECCS for core cooling has been confirmed.
- (3) There were strong correlations between the mixture level transients in the core and the fuel rod surface temperature transients.
- (4) The break flow difference caused by the configuration difference was observed only in the subcooled break flow condition. The subcooled break flow rates through the orifice was much larger than those through the nozzle.
- (5) Two-phase or single phase vapor break flow rate was affected little by the break configuration difference.
- (6) The effects of the subcooled break flow difference on the other system behaviors were not significant. Because the duration of subcooled break flow was relatively short comparing with the whole LOCA transient time.

## Acknowledgment

The authors are grateful to Mr.M.Shiba for discussions and suggestions and H. Asahi, T. Odaira, T. Takayasu, S. Sekiguchi, Y. Kitano and T. Numata of Nuclear Engineering Corporation for their assistance in conducting the experiment and K. Yamano, Y.Hirano and K. Hiyama of Information System Laboratory Corpotation for preparing the data plots.

## References

- (1) ANODA, Y., et. al., "ROSA-III System Descripton for Fuel Assembly No. 4", JAERI-M 9363 (1981).
- (2) SOBAJIMA, M., et. al., "Instrumentation and Data Processing for ROSA-III Test" (in japanese), JAERI-M 8499 (1979).
- (3) ABE, N., et. al., "Electric Power Transient Curve for ROSA-III Tests", JAERI-M 8728 (1980).
- (4) "General Electric Standard Safety Analysis Report, BWR/6", DOCKET-STN-50531-22, General Electric Company.
- (5) "BWR Blowdown Emergency Core Cooling Program, Preliminary Facility Description Report for the BT/ECCIA Test Phase", GEAP-23592, NRC-2 (1977).
- (6) Yonomoto, Y., et. al., "ROSA-III 50 % Break Integral Test RUN 916 (Break Area Parameter Test )", JAERI-M 85-109 (1985).

## Acknowledgment

The authors are grateful to Mr.M.Shiba for discussions and suggestions and H. Asahi, T. Odaira, T. Takayasu, S. Sekiguchi, Y. Kitano and T. Numata of Nuclear Engineering Corporation for their assistance in conducting the experiment and K. Yamano, Y.Hirano and K. Hiyama of Information System Laboratory Corpotation for preparing the data plots.

## References

- (1) ANODA, Y., et. al., "ROSA-III System Descripton for Fuel Assembly No. 4", JAERI-M 9363 (1981).
- (2) SOBAJIMA, M., et. al., "Instrumentation and Data Processing for ROSA-III Test" (in japanese), JAERI-M 8499 (1979).
- (3) ABE, N., et. al., "Electric Power Transient Curve for ROSA-III Tests", JAERI-M 8728 (1980).
- (4) "General Electric Standard Safety Analysis Report, BWR/6", DOCKET-STN-50531-22, General Electric Company.
- (5) "BWR Blowdown Emergency Core Cooling Program, Preliminally Facility Description Report for the BT/ECCIA Test Phase", GEAP-23592, NRC-2 (1977).
- (6) Yonomoto, Y., et. al., "ROSA-III 50 % Break Integral Test RUN 916 (Break Area Parameter Test )", JAERI-M 85-109 (1985).